# Proteomic Analysis of Ocular Surface Components by use of HPLC based Mass Spectrometric Strategies

Dissertation

zur Erlangung des Grades

„Doktor der Naturwissenschaften“

am Fachbereich Biologie der

Johannes Gutenberg-Universität

in Mainz

von

Sebastian Funke

geboren in Iserlohn

Mainz, 15.09.2014

Dekan:

1. Berichterstatter:

2. Berichterstatter:

Tag der mündlichen Prüfung: 20.04.2015

# Annotation

**Parts of the thesis have been published in international journals and/or presented on international conferences**

**Publications related to the thesis**

**Funke, S.**, Azimi, D., Wolers, D, Grus, F. H, Pfeiffer, N. 2012. Longitudinal analysis of taurine induced effects on the tear proteome of contact lens wearers and dry eye patients using a RP-RP-Capillary HPLC-MALDI TOF/TOF MS approach. *Journal of Proteomics* 75: 3177-3190

Bell, K., **Funke, S.**, Pfeiffer, N., and Grus, F.H. 2012. Serum and antibodies of glaucoma patients lead to changes in the proteome, especially cell regulatory proteins, in retinal cells. *PLoS One* 7(10): e46910

Bell, K., Gramlich, O. W., Von Thun Und Hohenstein-Blaul, N., Beck, S., **Funke, S.**, Wilding, C.; Pfeiffer, N., Grus, F. H. 2013. Does autoimmunity play a part in the pathogenesis of glaucoma? *Progress in Retinal and Eye Research* 36: 199-216

Von Thun Und Hohenstein-Blaul, N., **Funke, S.**, Grus, F.H. 2013. Tears as a source of biomarkers for ocular and systemic diseases. *Experimental Eye Research*. 117: 126-137

Boehm, N., **Funke, S.**, Wiegand, M., Wehrwein, N., Pfeiffer, N., and Grus, F.H. 2013. Alterations in the tear proteome of dry eye patients--a matter of the clinical phenotype. *Investigative Ophthalmolology & Vision Science* 54(3): 2385-2392

Perumal, N., **Funke, S.**, Pfeiffer, N., Grus, F. H. 2014. Characterization of lacrimal proline-rich protein 4 (PRR4) in human tear proteome. *Proteomics* 00: 1-12

Bell, K., Wilding, C., **Funke, S.**, Pfeiffer, N., Grus, F. H. 2014. Protective effect of 14-3-3 antibodies on stressed neuroretinal cells via the mitochondrial pathway. *BMC Neuroscience*, submitted

Perumal, N., **Funke, S.**, Wolters, D., Pfeiffer, N., Grus, F. H. 2014. Upregulation of lacrimal proline-rich protein 4 (PRR4) in human reflex tear proteome. *Proteomics*, submitted

**Funke, S.**, Beck, S., Lorenz, K., Kotterer, M., Wolters, D., Pfeiffer, N., Grus, F. H. 2014. Analysis of the effects of preservative-free tafluprost on the tear proteome. *Opthalmology*, submitted

**Publications related to the thesis (in preparation)**

**Funke, S**., Bell, K., Wilding, C., Wolters, D., Pfeiffer, N., Grus, F. H. Taurine effects on the conjunctival cell proteome.

**Funke, S.**, Bechter, L., Perumal, N., Wolters, D., Pfeiffer, N., Grus, F. H. Proteomic analysis of glaucomatous human trabecular meshwork.

**Funke, S**., Perumal, N., Gabelt-Scheurich, S., Gramlich, O., Beck, S., Boehm, N., Wolters, D., Pfeiffer, N., Grus, F. H. Proteomic mass spectrometric analysis of the human glaucomatous retina.

**Funke, S.,** Perumal, N., Scieranski, M., Beck, S., Pfeiffer, N., Grus, F. H. Proteomic investigation on the tear proteome of glaucoma patients with dry eye sensation.

**Funke, S**., Perumal, N., Gabelt-Scheurich, S., Mwiiri, F. K., Wolters, D, Gerbig, C., Weiler, L., Pfeiffer, N., Grus, F. H. In depth mass spectrometric analyis of the porcine retina proteome.

Perumal, N., **Funke, S**., Wolters, D., Pfeiffer, N., Grus, F. H. Identification of human tear fluid biomarkers in different dry eye disease subgroups using label-free quantitative proteomics.

**Poster presentations on international conferences**

**Funke, S**., Azimi, D., Pfeiffer, N., Grus F. H. 2011. Taurine induced effects on the tear proteome of dry eye patients and contact lens wearers using a RP-RP-2D-capillary-LC-MALDI-TOF/TOF MS approach. 6680-D1167. Fort Lauderdale, USA. *ARVO Visionary Genomics World Conference 2011*

Perumal, N., **Funke, S.**, Boehm, N., Peiffer, N., Grus, F. H. 2011. Defining proline rich proteins (PRPs) distribution in tear proteome. 6681-D1168. Fort Lauderdale, USA. *ARVO Visionary Genomics World Conference 2011*

Wolters, D., **Funke, S.,** Grus, F. H., Pfeiffer, N. 2012. Post transcriptional modifications in mass spectrometry based proteomics data. P8. Obergurgl, Austria. *ARVO Optic Nerve Degeneration and Ageing Conference 2012.*

Wilding, C., Bell, K., **Funke, S.**, Pfeiffer, N., Grus, F. H. 2012. Gamma synuclein antibody effects on mitochondrial apoptosis pathways. P2. Obergurgl, Austria. *ARVO Optic Nerve Degeneration and Ageing Conference 2012.*

Wilding, C., Bell, K., **Funke, S.**, Beck, S., Peiffer, N., Grus, F. H. 2013. Protective effect of GFAP antibody on RGC5 cells via actin cytoskeleton pathways. 432-A0163. Seattle, USA. *ARVO Life Changing Research World Conference 2013*

**Funke, S.**, Wolters, D., Weiler, L., Mwiiri, F. K., Bell, K., Wilding, C., Peiffer, N., Grus, F. H. 2013. In depth analysis of retinal proteins using a combinatory HPLC based mass spectrometric platform. 698-D0255. Seattle, USA. *ARVO Life Changing Research World Conference 2013*

Bell, K., Wilding, C., **Funke, S.**, Peiffer, N., Grus, F. H. Changes in antibodies from glaucoma patients lead to changes in apoptosis pathways of neuroretinal cells. 1605-D0032. Seattle, USA. *ARVO Life Changing Research World Conference 2013*

Perumal, N., **Funke, S.**, Pfeiffer, N., Grus, F. H. Characterization and post-translational modifications of proline-rich protein 4 (PRP4) in basal and reflex tear proteome of human. 2453-D0058. Seattle, USA. *ARVO Life Changing Research World Conference 2013*

Perumal, N., **Funke, S.**, Pfeiffer, N., Grus, F. H. 2013. Significant up-regulation of proline-rich protein 4 (PRR4) in human reflex tear proteome. St Malo, France. *EuPA Conference 2013*

**Funke, S.**, Lorenz, K., Kotterer, M., Beck, S., Wolters, D., Pfeiffer, N., Grus, F. H. 2014. Analysis of the effects of Taflotan® sine on tear protein profiles. 1474-C0113. Orlando, USA. *ARVO Leading Eye and Vision Research World Conference 2014*

Perumal, N., **Funke, S.**, Wolters, D., Pfeiffer, N., Grus, F. H. 2014. In depth protein profiling and identification of tear fluid biomarkers in different subgroups of dry eye disaese: Proline-rich protein 4 (PRR4) as apotential biomarker for aqueous-deficient dry eye syndrome. 2002-B0301. Orlando, USA. *ARVO Leading Eye and Vision Research World Conference 2014*

Wilding, C., Bell, K., **Funke, S.**, Pfeiffer, N., Grus, F. H. 2014. Participation of ERP57 in the pro-survival potential of GFAP antibodies on RGC5. 2438-B0137. Orlando, USA. *ARVO Leading Eye and Vision Research World Conference 2014*

Perumal, N. , **Funke, S.**, Pfeiffer, N., Grus, F. H. 2014. Identification of human tear fluid biomarkers in different dry eye disease subgroups using label-free quantitative proteomics. Madrid, Spain. *13th Human Proteome Organization World Congress,* accepted

**Oral papers on international conferences**

**Funke, S.**, Beck, S., Boehm, N., Pfeiffer, N., Grus, F. H. 2012. Retinal biomarkers in glaucoma. O063. Berlin, Germany. *ISER XX Biennial Meeting of the International Society for Eye Research Conference 2012*

**Funke, S.**, Wolters, D., Bell, K., Wilding, C., Pfeiffer, N., Grus, F. H. 2012. Protein modifications and ageing. Obergurgl, Austria. *ARVO Optic Nerve Degeneration and Ageing Conference 2012.*

**Funke, S.**, Bell, K., Wilding, C., Perumal, N., Pfeiffer, N, Grus, F. H. 2013. Mass spectrometric based strategies to recover and characterize proteins from retinal sample species. Obergurgl, Austria. *Optic Nerve Conference 2013*

Wilding, C., Bell, K., Beck, S., **Funke, S.**, Pfeiffer, N., Grus, F. H. 2013. GFAP antibodies interact with ERP57 on the cell membrane of RGC5 cells and have prosurvival potential against oxidative stress. Obergurgl, Austria. *Optic Nerve Conference 2013*

**Research prices**

Sicca-Förderpreis des Ressorts Trockenes Auge und Oberflächenerkrankungen im Berufsverband der Augenärzte Deutschlands 2013. Taurine induced effects on tear film and ocular surface revealed by mass spectrometric based proteomics. Berlin, Germany. *111$^{th}$ DOG Excellent Vision-Vision of Excellence Conference 2013*

## Aknowledgements

First, I would like to thank my supervisor for the opportunity to realize the thesis in the *Experimental Ophthalmology* lab of the University Medical Center Mainz and for his help, support and scientific experience he shared with me. I also thank my co-supervisor for his support.

Furthermore, I would like to thank my collegues for their contribution to the realization of this work.

Special thanks go to my wife and families for their help and support over the past years.

# Table of Content

# 1 Purpose

The ocular surface is a complex functional unit, not completely understood, ecspecially focusing on the proteome. Dry eye disease as a multifactorial disorder directly impacts the status of the ocular surface encircling tear film and cellular components, reflected by quantitative and qualitative changes in the proteome. Therefore, in this work, an intensive proteomic characterization of ocular surface components with special focus on tear film and ocular surface epithelial cells should be realized. Beside explorative analysis of the ocular surface proteome, two therapeutic strategies should be determined, encircling the influence of taurine eye drops on the tear film proteome of dry eye patients and contact lens wearers as well as the influence on the ocular surface of primary open angle glaucoma (POAG) patients switching from a common topical anti-glaucoma medication (Xalatan®) to a preservative-free formulation (Taflotan® sine) in terms of ocular surface complications. Accordingly, for “in depth” proteomic analysis of ocular surface components, HPLC based mass spectrometric workflows should be developed, optimized and compared. Results should provide a detailed proteomic view to the ocular surface and uncover underlying mechanism and potentials in the two focused therapeutic interventions, taurine and Taflotan® sine appliance.

# 2 Introduction

## 2.1 Mass spectrometry (MS) based proteomics

Proteomics first drafted by the groups of Wilkins and Wasinger (Wasinger *et al.*, 1995, Wilkins *et al.*, 1996a) referring to “PROTein complement of the genOME” (Apweiler *et al.*, 2009, Kraj and Silberring, 2008, Wilkins *et al.*, 1996b) describes the analysis of all proteins in living systems (Guerrera and Kleiner, 2005). Displaying high dynamics, (Kettman *et al.*, 2001) (Fig.1) a highlighted aim in proteomic science is the illumination of molecular changes in the course of a disease with the aim to find specific disease-related proteins indicating early diagnosis, molecular targeting or monitoring of therapeutic success (Etzioni *et al.*, 2003, Kraj and Silberring, 2008, Lescuyer *et al.*, 2007, Rifai *et al.*, 2006). MS evolved as the proteomic method of choice starting up from the 1980s demonstrating sensitivity and accuracy towards proteomic investigations (Mann *et al.*, 2001b). Generally, the first step of a proteomic workflow is to extract proteins or peptides from their sample source using various homogenization and extraction techniques (Chertov *et al.*, 2004, Cox and Emili, 2006, Ferro *et al.*, 2000, Goklen and Hatton, 1987, Holmquist and Carlson, 1977, Kushnirov, 2000, Molloy *et al.*, 1999, Naoe *et al.*, 1999, Naoe *et al.*, 1998, Selber *et al.*, 2004). Thus, for MS prior to protein/peptide ionization complexity reduction is mandatory to avoid masking effects by high abundant components (Granger *et al.*, 2005) and to reduce ion suppression provoked by salts, detergents and coextracted contaminants (Annesley, 2003, Hirabayashi *et al.*, 2007, Jessome and Volmer, 2006, Piwowar *et al.*, 2009, Remane *et al.*, 2010b, Wang *et al.*, 2003). Therefore, MS compatible fractionation (Issaq, 2001, Issaq *et al.*, 2005) or depletion (Bjorhall *et al.*, 2005, Magagnotti *et al.*, 2010) strategies have been developed. After sample processing, components are ionized and introduced to MS instruments showing a common fundamental design consisting of ion source, optics, mass analyzer and data processing electronics (Guerrera and Kleiner, 2005, Yates *et al.*, 2009). In case of proteomics soft ionization with low internal intensities leading to low ion fragmentation is usually coupled to mass analyzers (Daniel *et al.*, 2002, Pappin *et al.*, 1993).The two main soft ionization techniques are matrix assisted laser desorption ionization (MALDI) developed by Karas and Hillenkamp (Karas and Hillenkamp, 1988), in parallel by Tanaka and collegues (Tanaka *et al.*, 1988) and electrospray ionization (ESI) invented by Fenn and collegues (Fenn *et al.*, 1989, 1990) (Fig 2). MALDI features analyte co-crystallization with UV-absorbent small organic acids (Bird *et al.*, 2002, Canas *et al.*, 2007) and high vacuum pulsed laser evaporation leading to matrix and analyte desorption (Bahr *et al.*, 1992, Erra-Balsells and Nonami, 2003, Koubenakis *et al.*, 2004). The matrix transfers and receives protons and is believed to absorb energy as well as to isolate analytes from each other (Canas *et al.*, 2007). Usually, MALDI generates singly charged ions in the form [M+H]+ or [M-H]+ (Karas *et*

*al.*, 2000b, Yates *et al.*, 2009). In contrast ESI features ionization by application of high voltage (2-6kV) to a soluble analyte passing a narrow capillary which leads to the formation of an electrically charged spray, Taylor cone (Yates *et al.*, 2009) resulting in micro-drop evaporation and release of multiply charged analyte ions (Fenn *et al.*, 1990, Whitehouse *et al.*, 1985, Yates *et al.*, 2009). However, ESI and MALDI have different properties, ionization characteristics, sensitivity values and compatibilities. Importantly, MALDI is used in the off-line mode decopling sample processing and MS analysis (Baessmann *et al.*, 2005, Mitulovic and Mechtler, 2006, Murray, 1997, Rejtar *et al.*, 2002, Stevenson and Loo, 1998) with respect to some exceptions (Brivio *et al.*, 2002, Musyimi *et al.*, 2005, Musyimi *et al.*, 2004, Preisler *et al.*, 1998). In contrast ESI is an on-line technique (He, 2000, Wang *et al.*, 2006, Xiang *et al.*, 1999). Pulsed MALDI sources are usually combined with time-of-flight (TOF) analyzers discriminating ions based on their time of flight in a field-free tube (Guerrera and Kleiner, 2005, Yates, 2000). In contrast continuous ESI sources are commonly coupled to ion traps (Guerrera and Kleiner, 2005). Due to their complementary character, MALDI and ESI are proposed to be used in combination (Bodnar *et al.*, 2003, Mo and Karger, 2002, Stapels and Barofsky, 2004, Stapels *et al.*, 2004). Regarding mass analyzers two fundamental instrument types exist: scanning/ion beam instruments [TOF, quadrupol (Q)] and traps [ion trap (IT), Orbitrap, *Fourier* transform ion cyclotron resonance (FT-ICR)] (Yates et al. 2009). Accordingly ion separation corresponds to time of flight, quadrupol electric field selection, selective ion ejection from a three-dimensional trapping field (Mann *et al.*, 2001a) and orbital ion trapping (Scigelova and Makarov, 2006). Generally two types of information are obtained by MS, accurate mass and amino acid sequence (Yates, 2000). To achieve information on the amino acid sequence, parent ions entering the mass analyzer can be further fragmented using different techniques, e.g. post source decay (PSD), collision induced decay (CID), high energy C-trap dissociation (HCD), electron capture dissociation (ECD) (Mo and Karger, 2002, Olsen *et al.*, 2007, Suckau *et al.*, 2003) or electron transfer dissociation (ETD) (Mikesh *et al.*, 2006, Syka *et al.*, 2004). The fragments can be measured with higher resolution e.g. in TOF/TOF analyzers (Medzihradszky *et al.*, 2000) or in hybrid instruments like QTOF or Orbitrap analyzers (Hardman and Makarov, 2003, Hu *et al.*, 2005). Method selection strongly depends on the technical features of a mass analyzer. PSD is a common technique in MALDI TOF/TOF MS/MS workflows (Medzihradszky *et al.*, 2000) featuring the metastable fragmentation of peptides by single or double cleavage of the peptide backbone (Suckau *et al.*, 2003). CID commonly features trap instruments inducing similar fragmentation at the N-O peptide bond leading to the generation of *b*- and *y*-ions with respect to amino acid side chains (Papayannopoulos, 1995, Schlosser and Lehmann, 2000) by collision with gas molecules such as argon or helium (Hoteling *et al.*, 2003). However, beside the heterogeneity of mass analyzers and fragmentation workflows, in this work special focus is

laid on two instrument types: a MALDI-TOF/TOF and an ESI LTQ Orbitrap hybrid instrument. The application of both approaches towards the ocular surface proteome in association to dry eye related phenomena and potential therapeutic approaches were addressed in particular. Advantages, limitations and also the complementary character of both techniques were also examined.

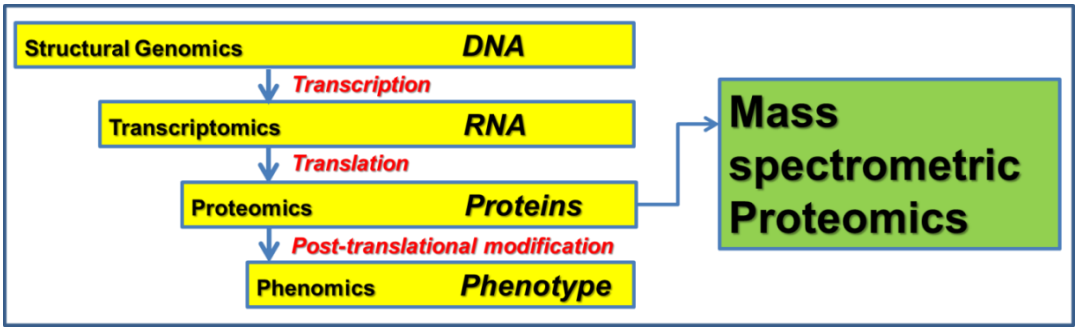


**Fig 1** Hierarchical principle of proteomics science linked to mass spectrometry (illustrated according to Kraj and Silberring 2008).

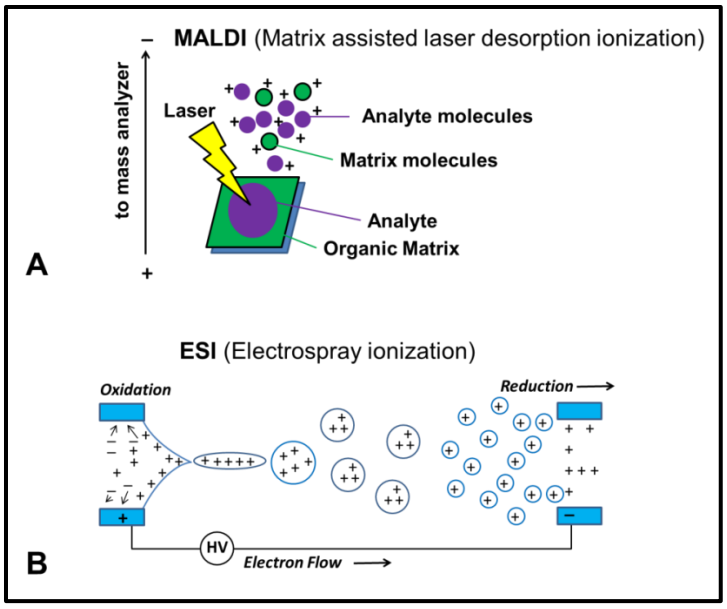


**Fig 2** Soft ionization principles for MS based proteomics; A. MALDI: After analyte/matrix cocrystallization analyte molecules are ionized and vacuum evaporated by laser beam and enter the mass analyzer. B: ESI: Analyte solution passes an electric field leading to Taylor cone formation, charged droplet release and multiply charged analyte ion transfer to the mass analyzer (illustrated according to Kraj and Silberring 2008; www.intechopen.com).

## 2.2 Bottom Up (BU) *vs.* Top Down (TD)

Two major MS proteomic categories coexist: “Top Down” (TD) and “Bottom Up” (BU). TD means the MS introduction of sample ions derived from intact non-digested components (Reid and McLuckey, 2002), whereas in BU proteins are first enzymatic digested followed by MS analysis. Accordingly, the categoric definition refers to the entities introduced to an

analyzer, which is in agreement with the majority of researchers (Capriotti *et al.*, 2011, Reid and McLuckey, 2002) based on the concept of McLafferty and collegues (Kelleher *et al.*, 1999). However, there is growing confidence that a combination of both approaches will be most effective (Mo and Karger, 2002). Regarding TD a clear benefit of MALDI is the high analysis speed and contaminant robustness playing a predominant role in fast and direct experiments of crude sample materials and the possibility of storage and reanalysis (Frohlich and Arnold, 2006, Mukhopadhyay, 2005). In both approaches, there is a certain need of sample precleaning and purification to increase sensitivity, especially regarding low abundant components (Kraj and Silberring, 2008) desirable for their potential to predict health status or treatment success (Chertov *et al.*, 2005, Veenstra *et al.*, 2005). Regarding fractionation and separation methods applicable to recover low abundant intact peptides/proteins there is still a lack of development in the proteomics research field (Capriotti *et al.*, 2011). Therefore, several complexity reducing TD approaches have been addressed, e.g. solvent precipitation (Chertov *et al.*, 2004, Chertov *et al.*, 2005), filter size exclusion (Berven *et al.*, 2007, Wang *et al.*, 2003), subcellular fractionation (Cox and Emili, 2006, Huber *et al.*, 2003, Jiang *et al.*, 2004, Stasyk and Huber, 2004), liquid-liquid extraction (Du *et al.*, 2007, Kjellstrom and Jensen, 2003) or depletion of predominant proteins (Chromy *et al.*, 2004, Fratantoni *et al.*, 2010, Fu *et al.*, 2005, Yocum *et al.*, 2005). Regarding TD the special focus of the clinical proteomic biomarker research in the last decade was on solid phase extraction (SPE) methods, e.g. agarose/polyacrylamide bead based affinity chromatography (Cuatrecasas, 1970a, b, Nishikawa and Bailon, 1975), magnetic beads (Ketterlinus *et al.*, 2005, Rehm, 2006, van Hagen, 2008), which were successfully used to determine the human proteomic profiles of body fluids like serum (Baumann *et al.*, 2005, Jimenez *et al.*, 2007a), plasma (Zhang *et al.*, 2004b), saliva (Wu *et al.*, 2009b), urine (Fiedler *et al.*, 2007), cerebrospinal fluid (Jimenez *et al.*, 2007b) and tear fluid (Sekiyama *et al.*, 2008). A common TD strategy is surface enhanced laser desorption ionization (SELDI) ProteinChip® technology providing component enrichment on surface modified metal chips (Hutchens and Yip, 1993, Issaq *et al.*, 2002, Tang *et al.*, 2004). In spite of its promising use for proteomic analysis of body fluids (Issaq *et al.*, 2003, Jr *et al.*, 1999, Paweletz *et al.*, 2001, Petricoin *et al.*, 2004) SELDI was contrary discussed regarding reproducibility (Baggerly *et al.*, 2004, Bons *et al.*, 2006), robustness (Gast *et al.*, 2009) and sensitivity (Neuhoff *et al.*, 2004). Beyond technical aspects, high costs regarding single-use chips are disadvantageous (Rehm, 2006). In contrast, Callesen and colleagues reviewed the MALDI and SELDI platform regarding *m/z* peak biomarker candidate establishment in ovarian cancer and reported high reproducibility across different research groups and pre-fractionation methods (Callesen *et al.*, 2012, Callesen *et al.*, 2008) which gives new input to the debate of SELDI application to clinical TD proteomics. However, sensitivity and reproducibility of the mentioned approaches is very low

compared to the abilities of high pressure liquid chromatography (HPLC). The use of LC MALDI for TD proteomic profiling is limited to a few publications. Wall et al. described a TD LC MALDI approach for the proteomic mapping of whole *E.coli* cell lysates whereby they first collected LC fractions in solution followed by a transfer to MALDI tragets (Wall *et al.*, 1999). Koomen and colleagues investigated on the intact low molecular weight human serum proteome <5500 *m/z* by use of a LC MALDI TOF approach (Koomen *et al.*, 2005). Hu et al. used LC MALDI for oral cancer biomarker screening of saliva samples (Hu *et al.*, 2007). Thus, in contrast to bead or chip based approaches regarding ocular sample species there is still a lack of publications highlighting TD LC MALDI proteomics. Furthermore, most of the reported studies refer to in-solution fraction collection and direct on target collection approaches automated by robotic units have been attempted (Mukhopadhyay, 2005). Beside TD approaches to get a deeper view to the proteome BU workflows are a promising toolbox for clinical research. BU experiments focus on complex enzymatic peptide mixtures (Duncan *et al.*, 2010) challenging for MS performance due to contaminants, ion suppression and masking effects (Annesley, 2003, Gumerov *et al.*, 2002, Gustavsson *et al.*, 2001, Remane *et al.*, 2010a, Sjodahl *et al.*, 2005). Therefore, like in TD prefractionation, methods have to be integrated at protein level, at peptide level or at both stages. One usual strategy is to fractionate proteins in the first dimension by one-dimensional (1D) or two-dimensional (2D) gel electrophoresis followed by targeted digestion of molecular weight areas, gel lanes or single spots (Fountoulakis and Langen, 1997, Rosenfeld *et al.*, 1992). In contrast, multidimensional protein identification technology (Mudpit) highlights the gel-free digestion and fractionation of complex protein extracts by use of multidimensional HPLC systems (Chen *et al.*, 2006, Kislinger *et al.*, 2005, McDonald *et al.*, 2002). In fact, peptides generally cope better with chromatography and MS than proteins regarding solubility, ionization and fragmentation (Duncan *et al.*, 2010). Despite its lab intensive character, a certain advantage of gel-based systems is the effective removal of contaminants through electrophoresis (Lu and Zhu, 2005) taking advantage of the reproducibility of precast gels (Berkelman *et al.*, 2010, Herbert *et al.*, 2001). Furthermore, the gel technology itself allows quantification, for example realized by scanning densitometry (Claeys *et al.*, 1995, Ng *et al.*, 2000b) as well as control steps for method development. In summary, strategy selection, BU or TD strongly depends on research questions and sample type. The evaluation of both strategies for the analysis of ocular components is featured in this work.

## 2.3 MALDI-TOF-(TOF) MS (/MS)

MALDI-TOF MS provides ion mass-to-charge ratio recording flight time in a field-free vacuum adjusted metal tubing of specific length (Domon and Aebersold, 2006) after source ionization considering faster travel of low *m/z* than high *m/z* molecules (Rehm, 2006). Resolution of

TOF analyzers is limited but can be increased with tubing elongation (Schiller *et al.*, 2007). By coupling two TOF analyzers in tandem, PSD or CID fragments can be interpreted with higher resolution (Medzihradszky *et al.*, 2000). In these approaches a whole sample MS spectrum is generated in the first run, whereas in a follow-up run parent peaks corresponding to a mass list of the MS spectrum as well as their fragments are selected by a voltage dependent ion gating occurring in the precursor ion selector (PCIS) due to their flight time (Rehm, 2006, UltraflexTOF/TOFOperatorManual, 2001). Resolution is additionally increased by an “electrostatic mirror”, the reflector (Schiller *et al.*, 2007), which turns on ions compensating for small differences in their initial kinetic energies due to adsorbed initial laser energy (Aebersold and Mann, 2003, Rehm, 2006). This consequently results in higher resolution generating *Gaussian* shaped peak pattern allowing exact mass determination of isotopic peaks in MS/MS spectra (Suckau *et al.*, 2003). MS spectra can be used for simple peptide mass fingerprinting (PMF) via data bases, whereas MS/MS spectra give more additional information on the amino acid sequence in more complex samples (Kraj and Silberring, 2008, van Hagen, 2008). However, since the reflector works only for ions within a specific energy potential range, the analytic performance is usually limited to small components <4000 Da (Rehm, 2006) (UltraflexTOF/TOFOperatorManual, 2001). Decreased ion transmission to the detector in the reflector mode (Hortin, 2006) is the main reason for the analysis of intact peptides or proteins in the instruments linear mode without reflector. Accordingly, the drawback of lower resolution in the linear mode is balanced by its advantage of higher sensitivity. In this work, an Ultraflex II MALDI-TOF/TOF MS instrument was used (Fig. 3A). The instrument was developed by Suckau and coworkers and features a special “LIFT” technique (Fig. 3B) to select and fragment peptide ions overcoming the adjustment of different reflector potentials acuiring full fragment ion spectra within one single scan by kinetic energy adaption between parent ion and fragment ions (Rehm, 2006, Suckau *et al.*, 2003) (UltraflexTOF/TOFOperatorManual, 2001). First, parent ions and PSD fragments are selected by use of PCIS. Then, their kinetic energy levels are raised in the LIFT chamber, consisting of four electrodes building three chambers, by a two-step 19kV potential increase. Thereby, energy levels of parent ion and fragments are adapted to a difference of less than 30% and can for this reason be simultaneously reflected allowing their simultaneous detection in a single scan (Suckau *et al.*, 2003, UltraflexTOF/TOFOperatorManual, 2001). Whereas the Ultraflex series was successfully applied for protein profiling and/or identification in numerous proteomic studies of various cancer forms (de Noo *et al.*, 2006, Ebert *et al.*, 2006, El Ayed *et al.*, 2010, Feuerstein *et al.*, 2005, Freed *et al.*, 2008, Gamez-Pozo *et al.*, 2009, Groseclose *et al.*, 2008, Huang *et al.*, 2006, Kojima *et al.*, 2008, Lemaire *et al.*, 2007, Mustafa *et al.*, 2007, Oppenheimer *et al.*, 2010, Villanueva *et al.*, 2004), the implementation to ocular proteomic studies encircling pseudoexfoliation (Hardenborg *et al.*,

2009, Joachim *et al.*, 2007a), glaucoma (Brust *et al.*, 2008, Grus *et al.*, 2008, Joachim *et al.*, 2007b, Joachim *et al.*, 2009, Joachim *et al.*, 2008, Joachim *et al.*, 2010) or eye surface diseases (Acera *et al.*, 2011, Kramann *et al.*, 2011) is still expandable. In this work the instrument is used as for TD as well as for BU analysis.

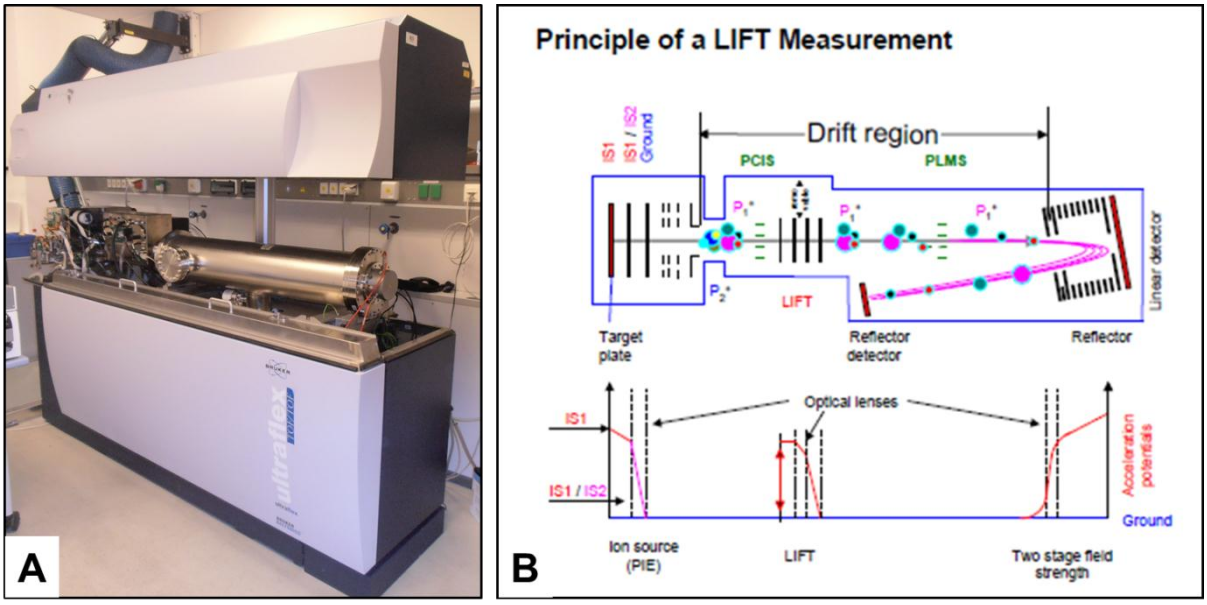


**Fig 3** Principle of the Ultraflex II MALDI TOF-TOF MS instrument; A: Panorama view of the instruments interieur containing MALDI source at the left side and flight tube on the right side of the machine; B: Ions passing the flight tube are compensated for kinetic enegy differences by the reflector leading to increased resolution. Kinectic energy differences of precursor masses and corresponding fragment ions are approximated to each other in a LIFT chamber allowing their simoultan detection.

## 2.4 LTQ-Orbitrap XL MS

The LTQ Orbitrap XL is a “hybrid” instrument combining a linear ion trap (LTQ) with an orbitrap analyzer (Fig. 4). Development and proof-of-principle of the orbitrap analyzer was realized by Makarov (Makarov, 2000) following establishment six years later by Makarov and collegues (Makarov *et al.*, 2006a, Makarov *et al.*, 2006b). In the hybrid instrument the LTQ is used to accumulate ions and transfer them via a linked quadrupol c-shaped ion trap (C-trap) to the orbitrap analyzer (Hager, 2004, Scigelova and Makarov, 2006). The orbitrap itself consisting of an inner and outer electrode generates a quadro-logarithmic electrostatic potential to trap introduced ions, oscillating harmonically in axial direction while orbiting around a central electrode whereby the oscillating frequency (50-150 kHz for 200-2000 *m/z*) corresponds to their *m/z* values and can be determined after *Fourier* transformation (Makarov, 2000, Makarov *et al.*, 2006a, Makarov *et al.*, 2006b, Marshall and Hendrickson, 2008, Scigelova and Makarov, 2006, Yates *et al.*, 2009). Highlights of the orbitrap analyzer are its high resolution (max.150.000), high mass accuracy (2-5 ppm), high dynamic range

(>103) and a *m/z* range of 6000 (Scigelova and Makarov, 2006, Yates *et al.*, 2009). Actually, instrumental mass deviation can be decreased to <1 ppm by the introduction of “lock-mass” background signals for internal calibration (Olsen *et al.*, 2005, Scheltema *et al.*, 2008). Usually, the LTQ Orbitrap workflow features ion fragmentation in the LTQ ion trap allowing multiple fragmentation levels (MSn) and generates full MS scans in the orbitrap taking advantage of the speed (3-5 spectra/s) and sensitivity of the ion trap considering the mass accuracy and resolution of the orbitrap (Scigelova and Makarov, 2006, Yates *et al.*, 2009). Moreover, ion trap and orbitrap work in parallel since the initial orbitrap high resolution spectrum is used to select precursors for fragmentation in the ion trap while high resolution orbitrap measurement is still in progress (Scigelova and Makarov, 2006). For fragmentation CID, HCD, ECD or in modified machines ETD can be choosen and combined in experimental designs. Numerous studies in different proteomic fields, especially cancer proteomics (Kim *et al.*, 2012, Kosanam *et al.*, 2011, Lu *et al.*, 2009, Saratsis *et al.*, 2012, Whelan *et al.*, 2009, Zeng *et al.*, 2011) have been done since its commercial introduction in 2005. Nevertheless, the number of opthalmological studies run on the LTQ Orbitrap XL is still limited (Bennett *et al.*, 2011, de Souza *et al.*, 2006, Galiacy *et al.*, 2011, Srinivasan *et al.*, 2012). In this work the instrument is used for a BU workflow for the analysis of the ocular surface.

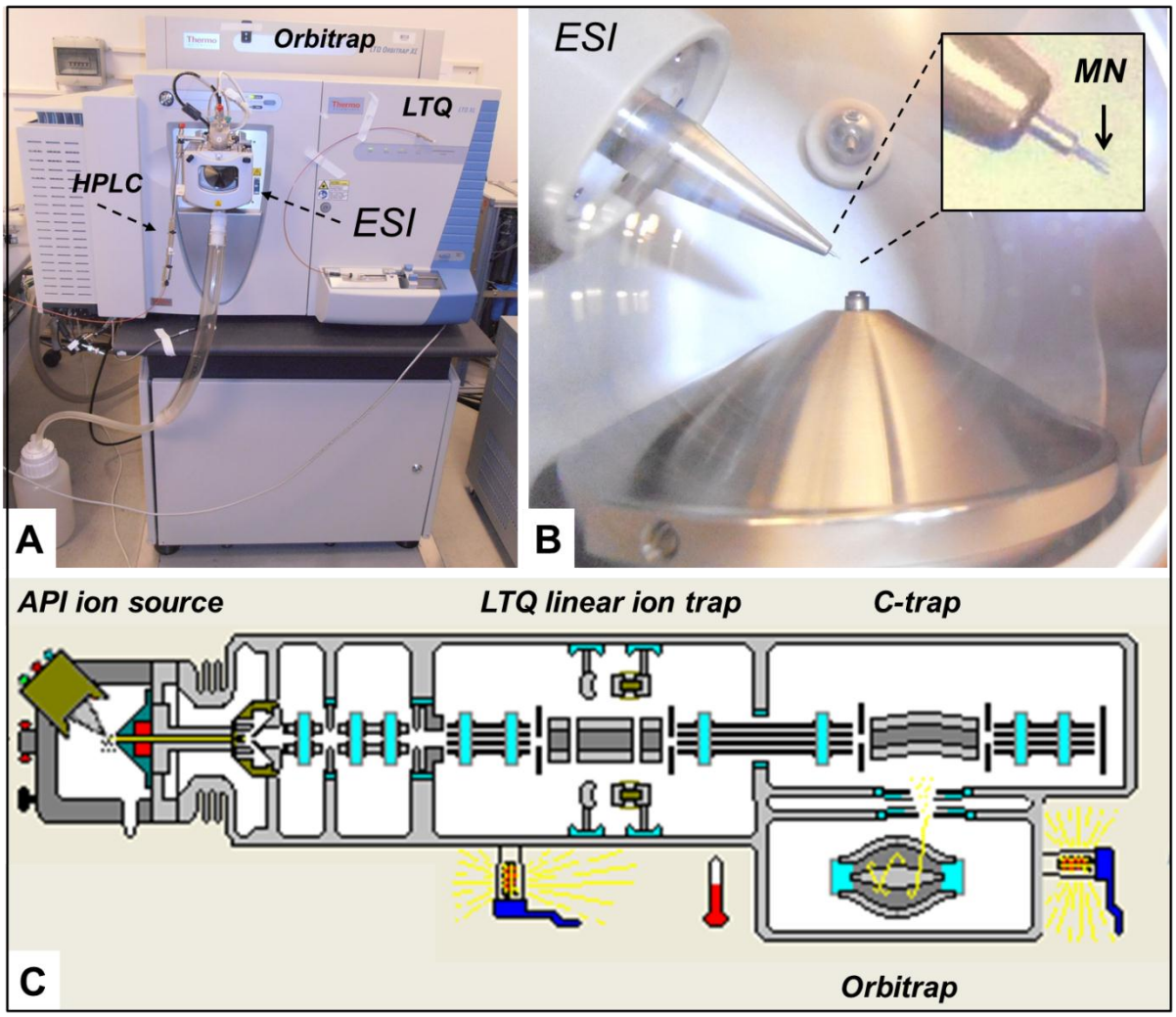


**Fig 4** Principle of the LTQ Orbitrap XL instrument in LC ESI mode; A: Overview of the hybrid machine consisting of linear ion trap (LTQ) and orbitrap analyzer also indicating HPLC column system and ESI source; B: Detailed view of the ESI source featuring nozzle with integrated ESI metal needle (zoom view, arrow) and cone representing the heated capillary as mass analyzer entrance; C: Scheme of the hybrid instrument featuring ion trap for ion selection and fragmentation, C-trap for ion transfer and orbitrap for accurate mass analysis.

## 2.5 HPLC in mass spectrometry

HPLC approaches were developed to fractionate and purify samples by use of cylindric tubing stationary phases encircling various retention modes (reversed phase, normal phase, size-exclusion, ion exchange, affinity) (Issaq, 2001, Mitulovic and Mechtler, 2006) based on porous, non-porous or superficial porous bead-shaped (Kirkland, 2000) or monolithic materials (Barroso *et al.*, 2003, Maruska *et al.*, 2007, Zou *et al.*, 2002a) prior to MS (Kraj and Silberring, 2008) (Examples of basic HPLC principles are given in Fig. 5). Reversed phase (RP) approaches separating molecules based on their hydrophobicity are very common in proteomics since most buffers are MS compatible (Yates *et al.*, 2009). Column parameters, e.g. inner diameter (ID), length, particle size, pressure, flow rate and capacity characterize the system directly affecting MS sensitivity (Rozing *et al.*, 2004). Column ID categories range

from “preparative” (> 10 mm) over “narrow(small)-bore” (4 mm ≥ ID ≥ 2.1 mm) to “open tubular” (< 25 µm) (Rozing, 2003). However, in proteomics “microbore” (2.1 mm ≥ ID ≥1 mm), “capillary” (1 mm ≥ ID.≥ 100 µm) and “nanobore” (100 µm ≥ ID ≥ 25 µm) are of common interest (Rozing, 2003) due to sensitivity increase by ID and flow rate scale-down (Frohlich and Arnold, 2006). Accordingly, microbore columns demonstrate a higher performance than “semi-preparative” columns (Bhown *et al.*, 1986, Bowermaster and Mcnair, 1983) and were early proposed for direct MS coupling (Garcia and Barcelo, 1993) allowing appropriate flow rates between 50 and 1000 µl/min (Rozing, 2003). Nevertheless, in MALDI experiments ID and corresponding flow rates are not as crucial as in ESI workflows since fractions are collected off-line allowing complete solvent evaporation and analyte concentration on the target plate. In contrast, in on-line ESI approaches, column ID and flow rate will directly affect sample concentration introduced to the analyzer favoring down-scaled flow rates regarding ion formation (Karas *et al.*, 2000a). Despite increased sensitivity of nanobore systems (Mitulovic and Mechtler, 2006), disadvantages on the pratical side addressing risk of column blocking, overloading, decreased column life times, consequent need for advanced sample pre-cleaning steps, extended analysis times due to nano flow rates, challenging pressure and dead volumes, advanced nano pump systems or split systems and higher costs have to be mentioned (Noga *et al.*, 2007). The use of HPLC techniques combined with gel-based or orthogonal chromatographic approaches linked to MS allowed the proteomic analysis of several ophthalmological relevant sample species like e.g. lens (Grey and Schey, 2009, Hoehenwarter *et al.*, 2005, Shearer *et al.*, 2008, Ueda *et al.*, 2002, Wilmarth *et al.*, 2009), optic nerve tissue (Bhattacharya *et al.*, 2006), optic nerve head astrocytes (Rogers *et al.*, 2012), microglia (Glanzer *et al.*, 2007), vitreous humour (Gao *et al.*, 2008, Kim *et al.*, 2007b, Ouchi *et al.*, 2005, Yu *et al.*, 2008), aqueous humor (Chowdhury *et al.*, 2010, Duan *et al.*, 2008, Funding *et al.*, 2005), sclera (Frost and Norton, 2007, 2012) and cornea (Dyrlund *et al.*, 2012, Galiacy *et al.*, 2011, Karring *et al.*, 2006, Karring *et al.*, 2005, Thompson *et al.*, 2003).Despite overall growing research attemps in ocular proteomics, there is still a high degree of necessity to use HPLC based methods for a more detailed basic appreciation of the eye surface realized in the present work. Accordingly, a brief introduction to achievements and limitations in ocular surface proteomics is given in the following chapters.

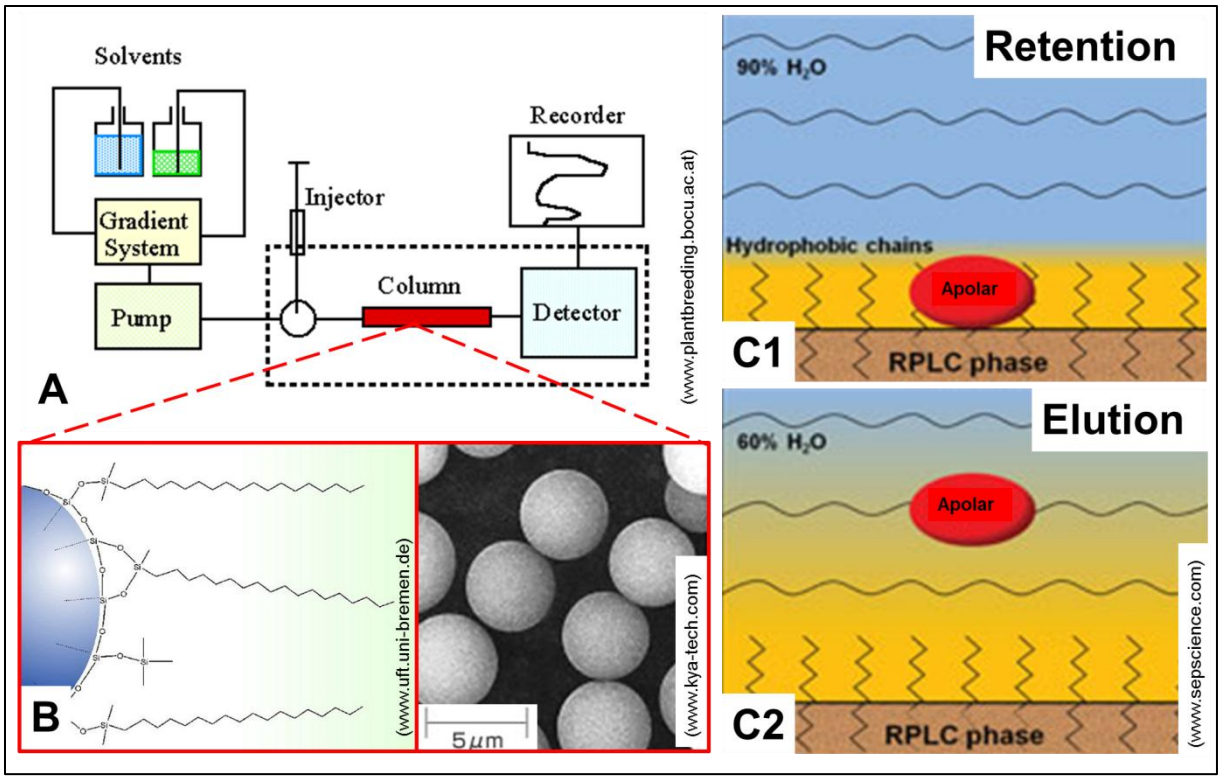


**Fig 5** Principles of HPLC; A: Basic HPLC system buildup, in case of LC MS; detection and recording is realized by the MS instrument; B: Interior of a RP column system featuring the stationary phase consisting of microspheres with a funtionalized alkyl chain surface for protein/peptide capture; C: Basic principle of RP retention facilitating component retention on the stationary phase under aqueous condition (C1) and component elution with increasing solvent portion of the mobile phase (C2).

## 2.6 Ocular surface proteomics

To realize the role of ocular surface proteomics, it is important to understand morphology and function of the eye surface encircling cornea, conjunctiva and tear film, as a direct environmental exposed organ, sensitive towards external and manipulative factors. The transparent, vessel-poor and immune-priviliged six layer cornea (Dua *et al.*, 2013, Lang, 2008) contributes mainly to image focusing, whereas the conjunctiva is discriminated from the cornea by the *Limbus corneae* and represents a vessel and gland-rich mucous layer (Lang, 2008). Furthermore, estratified, wet surfaced corneal and conjunctival epithelia (Gipson and Argueso, 2003) are covered by the tear film (Kampik, 2002) protecting the integrity of sclera, cornea and conjunctiva as a functional unit, important for image focusing (Kampik, 2002, Tiffany, 2008) (Fig 6). The tear film consisting of three layers, outermost lipid layer, aqueous layer and mucus layer (Wolff, 1946, 1954) provides numerous functions: light refraction, eyelid lubrication, conjunctiva/cornea lubrication, nutrition, white blood cell access, outwash of foreign materials and antimicrobial defense (Davidson and Kuonen, 2004). The meibomian glands' secreted lipid layer (McCulley and Shine, 1997) is built by two sub layers [apolar lipid (meibomian oil layer) and a polar lipid sub layer (Shine and McCulley, 2003)],

which are both associated to lipophil proteins like lipocalins (Glasgow *et al.*, 1995). Tear lipids are bound to proteins and protein-lipid interactions providing the functional integrity to the lipid layer protecting against fluid evaporation from the ocular surface (Bron *et al.*, 2004, Craig and Tomlinson, 1997). Tear mucins and also non-mucin proteins are known to lower tear surface tension assisting to spread the precorneal tear film (Lemp, 1973) for viscosity and stability control (Gouveia and Tiffany, 2005, Schoenwald *et al.*, 1997). The aqueous phase secreted by the lacrimal glands (Tiffany, 2008) includes electrolytes, amino acids, sugars, peptides and proteins (Dunson, 1970) highlighting gel-building mucins and glycoproteins (Holly and Lemp, 1977), which provide an optimal consistence of the tear fluid (Davidson and Kuonen, 2004). Beside pathogen defense by antimicrobial peptides (Haynes *et al.*, 1999), corneal nutrition is the predominant function of the aqueous layer (Chen *et al.*, 1997, Iwata, 1973). The glycocalyx consists mainly of glycoproteins and sol-building mucins, which are secreted by corneal epithelia while some mucin groups are membrane associated (Gipson, 1994, Gipson and Inatomi, 1998). Ocular glands, tear fluid and protein composition have been studied in several species like dog (Barrera *et al.*, 1992, Berger and King, 1998, de Freitas Campos *et al.*, 2008), cat (Petznick *et al.*, 2012, Petznick *et al.*, 2011), horse (Deeg *et al.*, 2006, Martin *et al.*, 1997, Parma *et al.*, 1987), camel (Chen *et al.*, 2011b, Shamsi *et al.*, 2011), rabbit (Zhou *et al.*, 2007), dolphin (Tarpley and Ridgway, 1991, Young and Dawson, 1992), crocodile (Dunson, 1970, Rehorek *et al.*, 2005, Schmidtnielsen and Fange, 1958) and frog (Nowack and Wohrmann-Repenning, 2010). However, regarding the tear proteome the most intensive studies were applied on humans. Using MS, de Souza and collegues reported 491 proteins encircling numerous proteases and protease-inhibitors (de Souza *et al.*, 2006), for example cystatin S demonstrated to inactivate cysteine proteinases (Barka *et al.*, 1991, Ghiso *et al.*, 1988). Zhou et al. could increase sensitivity, identifying 1543 tear proteins using a LC ESI Triple TOF 5600 system (Zhou *et al.*, 2012). Also, by targeted proteomic analysis of meibomian gland fluid 90 proteins have been revealed (Evans *et al.*, 2003, Tsai *et al.*, 2006). In fact, tear fluid is predominated by a small subset of high abundant proteins providing 70-80% of the whole protein content (Azzarolo *et al.*, 2004) including lysozyme, lactoferrin and lipocalin (Sack *et al.*, 2001). Furthermore, ceruloplasmin, Zinc-α-2-glycoprotein, secretory IgA, IgG, albumin and glycoproteins are detectable in moderate concentrations (Davidson and Kuonen, 2004, Green-Church and Nichols, 2008, Tiffany, 2008). In addition, tear proline-rich proteins have been characterized (Fung *et al.*, 2004). Most of the abundant tear proteins display antimicrobial activity like lysozyme (Jensen and Gluud, 1985, Selinger *et al.*, 1979), lipocalin (Fluckinger *et al.*, 2004), cystatine (Stoka *et al.*, 1995), secretory phospholipase A2 (Qu and Lehrer, 1998) and lactoferrin (Broekhuyse, 1974, Flanagan and Willcox, 2009, Jensen and Gluud, 1985, Selinger *et al.*, 1979). Deeper functions have been proposed for certain proteins, e.g. lipocalin including immunomodulation

(Flower, 1996). A correlation between tear proteomic composition and the health status (Antoine *et al.*, 2010) has been demonstrated for ocular disorders, especially dry eye (Grus and Augustin, 1999, Grus *et al.*, 2005b, Li *et al.*, 2005, Versura *et al.*, 2010, Zhou *et al.*, 2009c), meibomian gland disease (Tong *et al.*, 2011), pterygium (Zhou *et al.*, 2009a) and glaucoma (Aho *et al.*, 2002, Pieragostino *et al.*, 2013, Pieragostino *et al.*, 2012, Roedl *et al.*, 2007, Roedl *et al.*, 2008), ocular affected Sjögren´s syndrome (Caffery *et al.*, 2008, Tomosugi *et al.*, 2005b) or systemic diseases like cancer (Evans *et al.*, 2001, Lebrecht *et al.*, 2009, Streckfus *et al.*, 2006). There are many external factors that can influence the ocular surface including anti-glaucoma medication (Malvitte *et al.*, 2007, Wong *et al.*, 2011), use of contact lenses (Glasson *et al.*, 2006, Li *et al.*, 2005) and lens care solutions inducing proteomic changes (Green-Church and Nichols, 2008, Grus *et al.*, 2005a, Zhao *et al.*, 2009). In accordance, the tear proteome represents a rich source of markers to evaluate the ocular health status (von Thun Und Hohenstein-Blaul *et al.*, 2013) with special focus on cornea and conjunctiva (Macri and Pflugfelder, 2000, Pisella *et al.*, 2000). In terms of dry eye disease, several proteins are already proposed as “biomarkers”. Despite numerous descriptions of the term (Hakansson, 2007, Strimbu and Tavel, 2010), a biomarker is commonly defined as “a characteristic that is objectively measured and evaluated as an indicator of normal biological processes, pathogenic processes, or pharmacologic responses to a therapeutic intervention” (BiomarkersDefinitionWorkingGroup, 2001). Accordingly, biomarker proteins can be used in targeted monitoring to evaluate the ocular surface status (de Paiva *et al.*, 2013) encircling conjunctival impression cytology, immunocytological procedures, tear film glycomics, lipidomics and proteomics (Deschamps and Baudouin, 2013). In fact, tear proteins have been proposed as dry eye biomarkers including S 100A8, S100A9, lipocalin-1, secretory phospholipase A2, metalloproteinase 9, proline-rich protein 4, mammaglobin B and mucins as well as several cytokines and chemokines (Aluru *et al.*, 2012, Boehm *et al.*, 2013, Corrales *et al.*, 2011, Enriquez-de-Salamanca *et al.*, 2012, Kramann *et al.*, 2005, Zhou *et al.*, 2009b). However, there is still need for more investigation to explain tear proteomic changes related to ocular surface complications and to obtain a deeper view to the ocular surface proteome, especially under therapeutic condition. Therefore, in this work a HPLC based MS platform should be developed allowing in depth analysis of the ocular surface with special focus of topical appliance of taurine and Taflotan® sine.

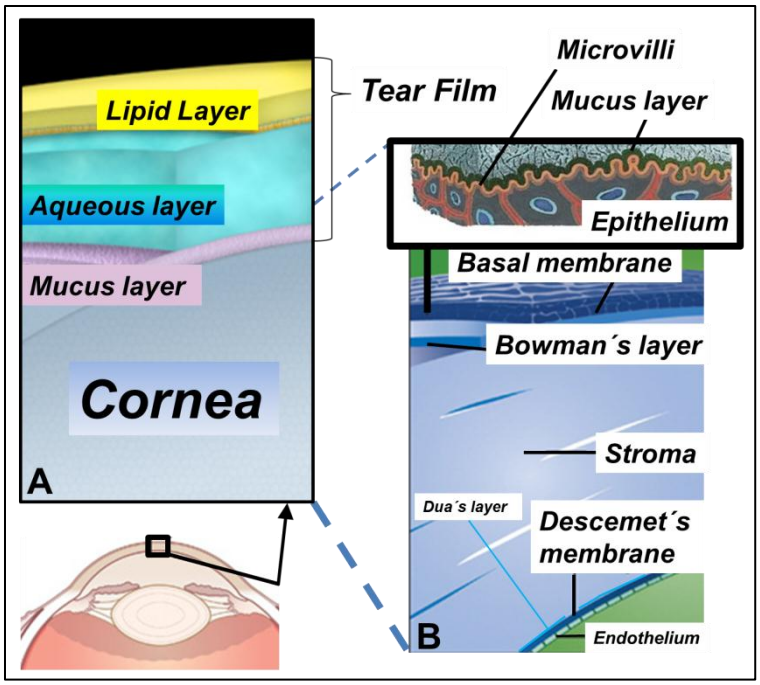


**Fig 6** Constitution of A: Human tear film and B: Human cornea. The cornea epithelium containing microvilli entering the mucus layer are highlighted. (illustrated in accordance to Cornea research foundation of America: www.cornea.org; A. www.eyecalm.org, B. Morgan 2010, La Croix 2010)

## 2.7 Dry Eye: Causes and consequences

Directly affecting the ocular surface, dry eye disease also known as dry eye syndrome or keratoconjunctivitis sicca, is defined as a multifactorial disease complex in accordance to the International Dry Eye Workshop 2007 (Lemp and Foulks, 2008) (Fig. 7) with prevalences ranging from 7% (USA) over 11% (Spain) and 21% (China) to 33% (Taiwan, Japan) (Gayton, 2009, Jie *et al.*, 2009, Viso *et al.*, 2009). Dry Eye disease is characterized by various symptoms like ocular fatigue (Toda *et al.*, 1993), foreign body sensation, photophobia, burning (Lemp, 1995), irritation and blurred vision (Tutt *et al.*, 2000). Symptoms are correlated with tear film dysfunction, decreased cornea/conjunctiva lubrication (Rolando and Zierhut, 2001), tear film instability and hyperosmolarity resulting in a damage of the ocular surface (Lemp, 2008, Peng *et al.*, 2013, Sweeney *et al.*, 2013, Tomlinson *et al.*, 2006, Tomlinson *et al.*, 2010). Moreover, inflammatory processes are common dry eye features (Baudouin, 2001, Lemp, 2008). Regarding the manifestation of dry eye disease cornea, conjunctiva, accessory lacrimal glands, meibomian gland, tear film, lacrimal gland and nervous innervations build a functional unit and dysfunction in one or more components lead to dysbalances resulting in inflammatory processes and ocular surface damage (Stern *et al.*, 1998, Stern *et al.*, 2004) The tear film is one functional trigger point since excessive tear evaporation and/or reduced tear (Johnson and Murphy, 2004). Consequently, the disease manifests in a decline of image quality and vision (Goto *et al.*, 2002, Tutt *et al.*, 2000) and

affects patients daily life quality (Deschamps *et al.*, 2013, Kim *et al.*, 2011, Li *et al.*, 2012, Miljanovic *et al.*, 2007, Miljanovic *et al.*, 2004, Nelson *et al.*, 2000, van Landingham *et al.*, 2013). Several risk factors have been documented, e.g. arthritis (McCarty *et al.*, 1998, Moss *et al.*, 2000), diabetis (Barcaroli *et al.*, 1997, Seifart and Strempel, 1994) (Barcaroli *et al.*, 1997, Kaiserman *et al.*, 2005), caffeine consumption, high-density lipoprotein cholesterol ratio (Moss *et al.*, 2000), smoking (Thomas *et al.*, 2012), use of video display terminals (Blehm *et al.*, 2005, Schlote *et al.*, 2004, Tsubota and Nakamori, 1993, Uchino *et al.*, 2013, Von Stroh, 1993) and general diet (Miljanovic *et al.*, 2005). Thereby, female gender, progressed age (Schaumberg *et al.*, 2003) as well as an ethnic bias have been reported as prevalences (Lee *et al.*, 2002) (Foong *et al.*, 2007, Lavanya *et al.*, 2009) (Guo *et al.*, 2010, Tran *et al.*, 2013). Furthermore, contact lens wearing was documented to induce dry eye with controverse findings regarding gender prevalence (Chalmers and Begley, 2006, Fonn *et al.*, 1995, Hikichi *et al.*, 1995, Mackie, 1985, Nichols and Sinnott, 2006, Young *et al.*, 2011). Hormonal changes (Rocha *et al.*, 2013, Sullivan, 2004, Sullivan *et al.*, 2002) and viral infections (Alves *et al.*, 2013, Kamoi and Mochizuki, 2012, Lemp, 2008, Lestari *et al.*, 2013) are validated as further risk factors. Moreover, clinical surgery like LASIK (laser in situ keratomileusis) (Donnenfeld *et al.*, 2003, Huang *et al.*, 2012, Toda, 2007, Toda *et al.*, 2001) can lead to dry eye and other eye diseases like macular edema or diabetic retinopathy (Manaviat *et al.*, 2008, Najafi *et al.*, 2013) were proposed for prevalence. Regarding ocular disorders topical medications represent risk factors for ocular surface complications since ophthalmic formulations commonly contain antimicrobial preservatives (Barkman *et al.*, 1969, Messmer, 2012, Olson and White, 1990, Tu *et al.*, 2013), also able to realize intraocular penetration (Messmer, 2012). Various preservatives are in use (Herrero Vanrell, 2007) displaying toxic qualities (Gasset *et al.*, 1974). Former used preservatives like neoplycine, cocaine and phospholine iodid lead to morphological changes of the ocular surface indicated by loss of peripheral microvilli and complete corneal layers (Pfister and Burstein, 1976). Quaternary ammoniums (Lapiere and Thunus, 1967), displaying a wide range of antimicrobial properties (Caillier *et al.*, 2009) are common in ophthalmic solutions (Herrero Vanrell, 2007). Among these chemicals, benzalkonium chloride (BAC) (Fig. 8) is widely distributed in eye drop formulations (Messmer, 2012). Especially, topical application of BAC containing intraocular pressure (IOP) reducing agents in anti-glaucoma therapy (Fig. 8) is known to elevate the risk of ocular surface complications in POAG patients (Arici *et al.*, 2000, Dejong *et al.*, 1994, Erb *et al.*, 2008, Jandrokovic *et al.*, 2013, Noecker, 2001, Nordmann *et al.*, 2003, Steven and Cursiefen, 2013) with a prevalence of 42% (Stewart *et al.*, 2011) leading to “medication induced dry eye” (Fraunfelder *et al.*, 2012). De facto, long-term BAC utilization had been reported to alter the ocular surface (Arici *et al.*, 2000, Cho *et al.*, 2011, Yalvac *et al.*, 1995) supported by dose-dependent BAC toxicity on epithelia demonstrated by

in-vitro and in-vivo studies (Baudouin *et al.*, 2007, Becquet *et al.*, 1998, Liang *et al.*, 2008, Whitson *et al.*, 2006, Yee *et al.*, 2006). In fact, BAC was found to lead to membrane damage of cornea epithelia while also rupturing tight junctions (Pfister and Burstein, 1976) and increasing corneal permeability (Ramselaar *et al.*, 1988). Tripathi and coworkers could demonstrate that 0.01% BAC caused cessation of cell movement, cytokinesis and mitosis followed by complete cell degeneration within 2-8 h (Tripathi *et al.*, 1992). Apoptotic processes were supported for lower BAC concentrations, whereas higher concentrations were reported to induce necrosis (Debbasch *et al.*, 2001). In accordance, BAC associated morphological and anti-proliferative changes on cells have been reported for glaucoma therapeutics (Seibold *et al.*, 2013). Moreover, in vivo studies showed negative BAC induced effects on tear fluid production (Kuppens *et al.*, 1995) and stability (Baudouin and de Lunardo, 1998, Wilson *et al.*, 1975). Most toxic effects are due to the chemical nature of BAC displaying detergent-like features, binding and altering the cellular membrane, inducing toxic processes in cells, e.g. through interaction with cellular proteins and precipitation of enzymes (Furrer *et al.*, 2002, Grant and Acosta, 1996, Herrero Vanrell, 2007). BAC induced declined membrane integrity leads to decreased viability in rabbit corneal cells (Georgiev, 2011). Strong BAC lipid interactions could be monitored and also perturbation of the tear film lipid layer has been observed (Georgiev, 2011). Besides, BAC was found to display inflammatory potential beyond toxicity, reflected by tolerance breakdown (Galletti *et al.*, 2013) and sensitizer and histamine releaser activity in allergic reactions (Weston and Assem, 1994). Accordingly, latanoprost containing BAC caused increase in eosinophiles in glaucoma patients (Costagliola *et al.*, 2001). In confidence inflammation was found to occur on conjunctival epithelial cells administred in the course of topical antiglaucoma monotherapy using latanoprost, betaxolol and timolol (Cvenkel and Ihan, 2002). However, there is still a need to investigate on proteomic ocular surface changes in the course of glaucoma medication. Monitoring of proteomic changes of the tear film can help to objectively estimate the health status of the ocular surface in POAG sicca patients building a fundament for new therapeutic strategies. Tear proteomic changes in POAG sicca, non-glaucoma sicca and contact lens wearers should be focused on in this work. Therefore, as a toolbox HPLC based MS methods should be developed for the detailed investigations on the ocular surface proteome.

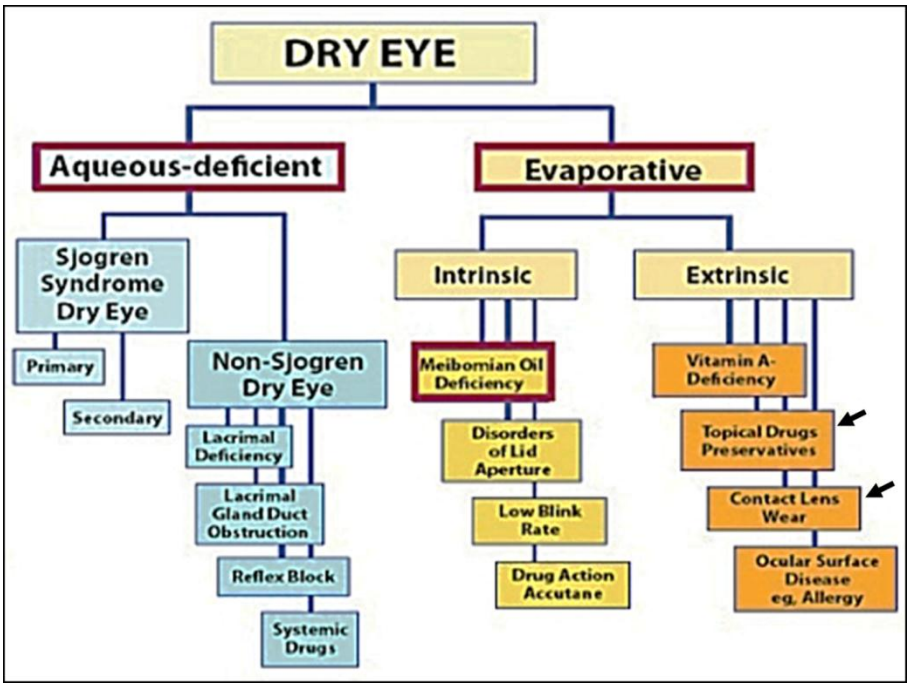


**Fig 7** Classification of dry eye syndrome pathologies based on the concept of the 2007 Dry Eye Workshop (DEWS) (Lemp 2007). The arrow highlighted dry eye forms are especially focused on in the present work.

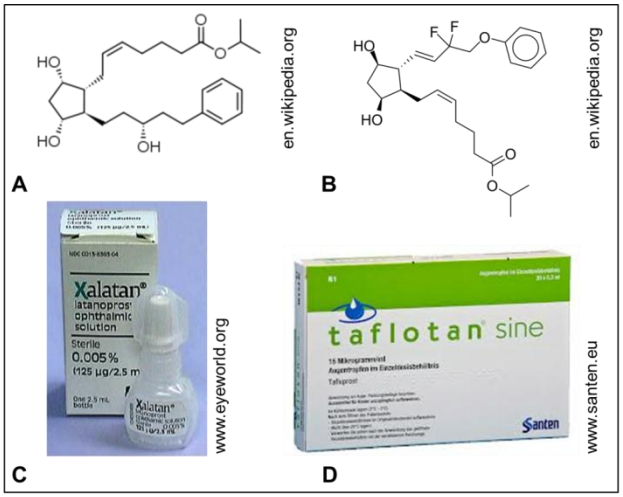


**Fig 8** Prostaglandine related IOP reducing agents and commercial formulations used in POAG glaucoma therapy; A. Latanoprost; B: Tafluprost; C: Xalatan® (Pfizer) containing 0.005% latanoprost and 0.02% BAC; D: Preservative-free Taflotan® sine (Santen) containing 0.0015% tafluprost.

## 2.8 Therapeutic management with special focus on Taflotan® sine and taurine

According to the complex character of dry eye disease, new therapeutic strategies have to be addressed. Thereby, special focus is on “medication induced” dry eye (Fraunfelder *et al.*, 2012) in POAG therapy. Consequently, therapeutic key features should address preservative, especially BAC reduction, in topical formulation. Horsley & Kahook reported beneficial effects on the ocular surface in glaucoma patients switching from latanoprost (0.02% BAC) to *sof*ZIA™ medication indicated by an amendment in ocular surface disease

index (OSDI), corneal staining and tear break-up time (TBUT) (Horsley and Kahook, 2009). Because BAC displays toxic potential in very low concentrations (Furrer *et al.*, 2002), a complete avoidance of this preservative most likely is the aim for long term application. Nevertheless, common prostaglandine analogue formulations contain preservatives, e.g. latanoprost, travoprost or bimatoprost (Liu and Mao, 2013). In contrast tafluprost (AFP-168), the latest prostaglandin $F_{2\alpha}$ derivate (Takagi *et al.*, 2004), as the first IOP lowering agent available in a preservative-free formulation, evidenced promising results regarding effectivity and tolerability (Hamacher *et al.*, 2008, Hommer *et al.*, 2010, Hos *et al.*, 2013). In comparison to preservative-containing formulations tafluprost exhibited very low or no apoptotic/necrotic/oxidative effects revealed in IOBA-NHC cells (Brasnu *et al.*, 2008). Local tolerability was evaluated to improve up to 86% after a medical switch from preservative-based medication to tafluprost in a large patient cohort of 2123 patients (Erb *et al.*, 2011). Uusitalo and collegues reported that tafluprost compared to latanoprost showed comparable results revealed from a study encircling 533 glaucoma patients (Uusitalo *et al.*, 2010). In confidence Janulevičienė and coworkers showed an equal IOP lowering effect but a higher ocular tolerability indicated by lower tear osmolarity levels for tafluprost compared with BAC containing latanoprost (Januleviciene *et al.*, 2012). Tafluprost available under the trade name Taflotan® sine (Santen Pharmaceutical Co., Ltd.), is in use in glaucoma therapy, but objective indicators for the effect of Taflotan® sine on the ocular surface are still missing and no detailed proteomic examination has been realized so far. Despite the preservative focused strategy in “medication induced dry eye” additional therapeutic strategies generally adressing dry eye had been proposed including tear secretagogues (Koh *et al.*, 2013, Nakamura *et al.*, 2012, Nichols *et al.*, 2004), anti-inflammatory topical therapeutics (McCabe and Narayanan, 2009, Mrukwa-Kominek *et al.*, 2007, Pflugfelder, 2003, 2004) like cyclosporine, tetracycline, doxycycline, corticosteroids, vitamin A topical utilization (Calonge, 2001, De Paiva *et al.*, 2006, Kim *et al.*, 2009a, Kobayashi *et al.*, 1997, Perry *et al.*, 2008, Yang *et al.*, 2006), cytokines (Pflugfelder *et al.*, 2013), anakinra (Vijmasi *et al.*, 2013), coumarin 18 (Govek *et al.*, 2010) and the utilization of artificial tears (Sindt and Foulks, 2013). However, there is still need to discover new drugs and to obtain a deeper understanding of proposed agents in dry eye therapy (Aquavella, 2013, Dogru *et al.*, 2013, Gadaria-Rathod *et al.*, 2013, Skalicky *et al.*, 2013). Thereby, topical or oral appliance of small receptor interacting molecules like CF101 (Avni *et al.*, 2010), essential fatty acids (Kokke *et al.*, 2008, Rashid *et al.*, 2008), peptides (Li *et al.*, 2013, Peral *et al.*, 2008, Sosne *et al.*, 2012) amino acids (Aragona *et al.*, 2013, Peral *et al.*, 2008) are among the future components for dry eye management. Regarding amino acids special focus is on taurine (Fig. 9), which was proposed as a promising agent in preventive medicine (Birdsall, 1998, Chesney, 1985, Kendler, 1989) and is still under investigation for its therapeutic potential facing ocular disorders (Ripps and

Shen, 2012). Taurine is a multifunctional zwitterionic, sulfonated, non-proteinaceous ß-amino acid (Huxtable, 1992, Redmond *et al.*, 1998, Wright *et al.*, 1986) derived from methionine and cysteine metabolism (Brosnan and Brosnan, 2006, Redmond *et al.*, 1998) and is present in high concentration in tissues of algae and animals (Jacobsen and Smith, 1968). Also, in mammalian species taurine has been documented for various tissues (Awapara *et al.*, 1950), with high concentrations in ocular tissues (Heinamaki *et al.*, 1986) including lens, iris ciliar body (Gupta and Mathur, 1983, Heinamaki *et al.*, 1986, Reddy, 1967, Reddy, 1970) and retina (Lake and Verdonesmith, 1989, Orr *et al.*, 1976, Pow *et al.*, 2002, Rassin *et al.*, 1978, Sturman *et al.*, 1978, Voaden *et al.*, 1977). Especially, on the ocular surface, high taurine abundance had been reported encircling cornea, conjunctiva and tear film (Nakatsukasa *et al.*, 2011, Pescosolido *et al.*, 2009, Reddy, 1967). Beyond metabolic functions including nutrition (Tesseraud *et al.*, 2009, Wu, 2009), more specialized features are associated to taurine, e.g. vitamin transport (Petrosian and Haroutounian, 2000) and osmoregulation (Gupta and Mathur, 1983, Lange, 1963, Thurston *et al.*, 1980, Uchida *et al.*, 1991). De facto, taurine was found to display anti-toxic cytoprotective features in host tissues (Dawson *et al.*, 2002, Lerdweeraphon *et al.*, 2013, Pasantes-Morales and Cruz, 1985, Saad and Al-Rikabi, 2002, Timbrell *et al.*, 1995, Venkatesan *et al.*, 1997, Waterfield *et al.*, 1994, Wettstein and Haussinger, 1997). Most of these effects are due to the ability of taurine to prevent oxidative stress and peroxidative damage (Cozzi *et al.*, 1995, Endo *et al.*, 2002, Mahalakshmi *et al.*, 2003, Nakamori *et al.*, 1993a, Pasantes-Morales and Cruz, 1984) by its membrane interacting and stabilizing features (Koyama *et al.*, 1996, Lopez-Colome and Pasantes-Morales, 1981, Pasantes-Morales and Cruz, 1985). Confidently, the amino acid has been demonstrated to protect plasma/mitochondrial and ER membranes under stress condition (Ye *et al.*, 2013) facilitating the interaction with lipids and proteins (Sebring and Huxtable, 1986), stabilizing proteins, especially membrane proteins from denaturation (Arakawa and Timasheff, 1985, Nandhini and Anuradha, 2003, Ye *et al.*, 2013). Interestingly, osmolytes like taurine have been lately proven to protect lysozyme as a major tear protein representative (Bruzdziak *et al.*, 2013). Antioxidative effects of taurine have been intensively studied (Nakamori *et al.*, 1993a), whereby protective effects exceed effectivity of vitamin C and E (Rodriguez-Martinez *et al.*, 2004). Regulation of $Ca^{2+}$ uptake, $Ca^{2+}$ATPase, generation of peroxide and superoxide anions in mitochondria (Chang *et al.*, 2004) as well as inhibition of consequent oxidative damage could be demonstrated for various tissues and organisms, e.g. for rat spermatozoa (Alvarez and Storey, 1983), rat liver (Kerai *et al.*, 1998), rat mesangial cells (Trachtman *et al.*, 1993), rat liver cells (Kerai *et al.*, 1998), plasma, liver and aorta of rabbits (Balkan *et al.*, 2002), hamster bronchioles (Gordon *et al.*, 1986) and human lymphoblastoid cells (Pasantesmorales *et al.*, 1984). Regarding ocular tissues, taurine was documented to prevent lipid peroxidation in rod outer segments (Pasantes-Morales, 1982,

Pasantes-Morales and Cruz, 1985), photoreceptors (Keys and Zimmerman, 1999) and diabetic precataractous lens (Kilic *et al.*, 1999, Mitton *et al.*, 1999, Obrosova and Stevens, 1999). Beside the ability of stabilizing proteins and membranes, taurine prevents uncontrolled protein modification, e.g. nonenzymatic glycosylation which plays a role for a proteomic functional decrease in aging and disease (Rattan, 1996, Soskic *et al.*, 2008). Szwergold could demonstrate that taurine has the ability to prevent generation of a sugar-protein "Schiffbase", which represents the initial step in glycation (Szwergold, 2005, 2006). Confidently, taurine was demonstrated to inhibit glycation of lens proteins (Devamanoharan *et al.*, 1997), to counterstrike glucose-induced apoptosis (Di Wu *et al.*, 1999), to prevent sugar induced cataracts in rabbits (Malone *et al.*, 1993) and retinal glial cell apoptosis in rats (Zeng *et al.*, 2010). In fact, anti-apoptotic effects of taurine have been intensively studied (Verzola *et al.*, 2002) evidencing taurine to inhibit the formation of the Apaf-1/Caspase-9 apoptosome (Takatani *et al.*, 2004), to inhibit the *m*-calpain and caspase-3 mediated cascade (Sun and Xu, 2008) and to reduce *Bcl-2* (Wu *et al.*, 2009a). Furthermore, taurine can modulate cellular pathways by modulation of protein phosphorylation (Lombardini, 1985, Lombardini *et al.*, 1996, Mollerup and Lambert, 1996) and receptor binding, e.g. triggering GABA (Bureau and Olsen, 1991, Louzada *et al.*, 2004) and insulin receptors (Maturo and Kulakowski, 1988) reflecting the wide range of molecular taurine trigger points. Moreover, immunomodulative functions (Kim, 2006, Marcinkiewicz and Kontny, 2012, Redmond *et al.*, 1998, Schuller-Levis and Park, 2003) due to chloramine generation (Marcinkiewicz *et al.*, 1995, Verdrengh and Tarkowski, 2005) have been reported for the molecule. In fact, taurine chloramine release by activated granulocytes and monocytes during oxidative burst (Arnitz *et al.*, 2006) has been widely demonstrated (Schuller-Levis and Park, 2004). Taurine levels decrease in ocular tissues in the course of aging (Baskin *et al.*, 1977) explaining a correlation between aging, oxidative damage, taurine avaibility and disease (Malone *et al.*, 1990, Militante and Lombardini, 2004, Yildirim *et al.*, 2007). In confidence with these findings protective effects of taurine are known for various disorders including arterial calcionosis (Yamauchitakihara *et al.*, 1986), pancreatitis (Akay *et al.*, 2013), closed head injury (Sun *et al.*, 2013), diabetes (Kim *et al.*, 2007a), heart diseases (Franconi *et al.*, 1985, Wojcik *et al.*, 2010), renal injuries (Chiba *et al.*, 2002, Wang *et al.*, 2008), including bladder and kidney injuries (Sener *et al.*, 2005) and neuronal injuries like Alzheimer´s disease (Louzada *et al.*, 2004). Special interest was on ocular disorders indicating taurine´s regenerative potential in goldfish retina (Lima *et al.*, 1993), its role in retinal ganglion cell survival in glaucoma models (Froger *et al.*, 2012, Gaucher *et al.*, 2012) and its beneficial performance regarding diabetic cataracts (Hsu *et al.*, 2012, Kilic *et al.*, 1999). Actually taurine showed high performance in epithelial woundhealing (Degim *et al.*, 2002, Dincer *et al.*, 1996) and derivates like taurine bromamine have been found effective for the management of epithelial inflammation

(Marcinkiewicz, 2009, 2010, Marcinkiewicz and Kontny, 2012), which is promising for ocular surface disorder management. Taurine application has been found beneficial for the prevention of oxidative damage of the ocular surface (Koyama *et al.*, 1996, Nakamori *et al.*, 1993b) and topical *N*-chlorotaurine performed well in bacterial conjunctivitis therapy (Nagl *et al.*, 2000, Teuchner *et al.*, 2005). Regenerative features of taurine have been proposed for the formation of protective polymer-based ocular surface films (Kedik *et al.*, 2011) and for the application in eye drops in case of ocular surface damage (Koyama *et al.*, 1996). Up to date, taurine has been included in food supplemental oral spray, numerous eye drop formulations and in AMO Complete Moisture Plus® contact lens cleaning solution indicating a regenerative effect on the tear film of contact lens wearers referring to MS tear protein profiles shifting towards profiles of healthy control subjects (Grus *et al.*, 2005a). This finding could be validated for conjunctival cells incubated with different contact lens solutions, whereby cells incubated with AMO Complete Moisture Plus® have been found to show less signs of apoptosis, necrosis and proteomic alterations (Bell *et al.*, 2012a). Since taurine is the main ingredient of this lens care solution taking advantage of the molecules ability to increase the buffer capacity towards alkaline influence (Hansen *et al.*, 2010, Watanabe *et al.*, 2006), it is proposed to be responsible for the observed beneficial effects on the ocular surface (Grus *et al.*, 2005a). However, no study of longitudinal topical effects of taurine in terms of ocular surface disorders have been realized so far and little is known about the influence on the ocular surface proteome. Accordingly, the identity of taurine target proteins need to be investigated on, which is part of the present work. In summary, two therapeutic strategies and their impact on the ocular surface should be contemplated in this work by use of LC MS proteomics: the topical use of taurine and Taflotan® sine.

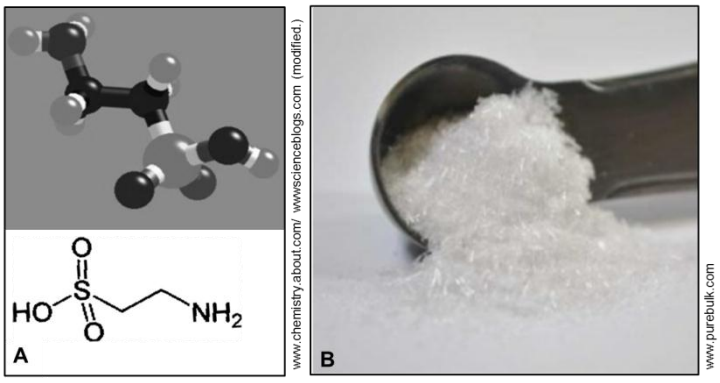


**Fig 9** A: Taurine (2-aminoethanesulfon acid, $C_2H_7NO_3S$) molecule; B: Purified, crystallized taurine

# 3 Material & Methods

## 3.1 Training samples

For LC MS method development RGC5 neuroretinal mouse (*Mus musculus*) cells (Van Bergen *et al.*, 2009, Wood *et al.*, 2010) (Fig. 10), established in the *Experimental Ophthalmology* lab were used. Despite their discussed biological status the cell line was intensively characterized (Crabb *et al.*, 2010, Kim *et al.*, 2009b, Yang and Tezel, 2005) providing a proper proteomic reference for method development purposes. Moreover, material can be easily obtained in the research group. Cell culture was realized due to a standardized protocol of the *Experimental Ophthalmology* including transfer of $N_2$ frozen cells to DMEM/FCS [10%], penicillin/streptomycin [1%], L-alanin-L-glutamine [4%] at 5% $CO_2$/ 37°C, thawing and incubation (2 days/37°C). Cells were monitored in a *Neubauer* chamber by use of a Nikon Eclipse TS 100 phase contrast microscope and 45000 cells were transferred for cultivation. Cell pellets were recovered by dissolving (DPBS/2 mM EDTA/Protease inhibitor) and centrifugation (300 g/4°C/ 20 min). Washed pellets were stored at -80°C. Cell lysis buffer volume was adjusted to the cell pellet weight with a reference ratio of of 0.06 g pellet to 100 µl lysis buffer (0.1% *n*-dodecyl-*ß*-maltoside). Cells were disrupted by freeze/thawing (5x, 20°C *vs* -80°C), lysis buffer and sonication (ice bath/1 min). Resulting homogenates were centrifuged (1500 g/4°C/10 min). Pellets were repeatly lysed. Finally, supernatants (S1, S2) were combined and filtered through an Acrodisc GHP filter (13 mm x 0.45 µm). 10 µl were used for protein concentration assay while 30 µl filtrate aliquots were stored at -80°C. As substitute simillary processed extracts of bovine retinae (*Bos taurus*) obtained from the local slaughterhouse (Robert-Bosch-Str. 23, 55232 Alzey, Germany) were used.

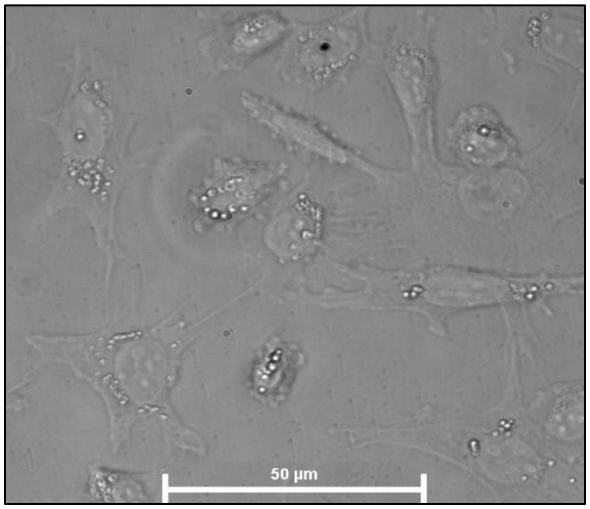


**Fig 10** Microscope image of RGC5 cells used in this work for method development

## 3.2 Study samples

For proteomic characterization and taurine treatment studies, non-transfected spontaneous immortalized IOBA conjunctival cells (IOBA-NHC; IOBA-University of Valladolid, Spain) derived from human conjunctiva were used as ocular surface epithelia model (Fig. 11). Cells have been characterized as a human conjunctiva model at the *University Institute of Applied Ophthalmobiology* (IOBA) and were defined as preserved epithelial cells (Diebold *et al.*, 2003). Gene expression was documented to differ from primary conjunctival cells, but was found to be more suitable for e.g. drug and cosmetic ocular surface studies than alternative conjunctival cell lines, e.g. ChWK (Tong *et al.*, 2009) explaining their frequent use in ocular surface studies (Benito *et al.*, 2013, Brasnu *et al.*, 2008, Li *et al.*, 2009). However, there is still a lack of sensitive proteomic investigations on NHC-IOBA cells. The cells were maintained in DMEM/HAM's F12 1:1, 10% FCS, insulin [1 µg/ml], EGF [1 µg/ml], hydrocortisone [5 µg/ml]). Preparation workflow corresponds to the described RGC5 workflow.

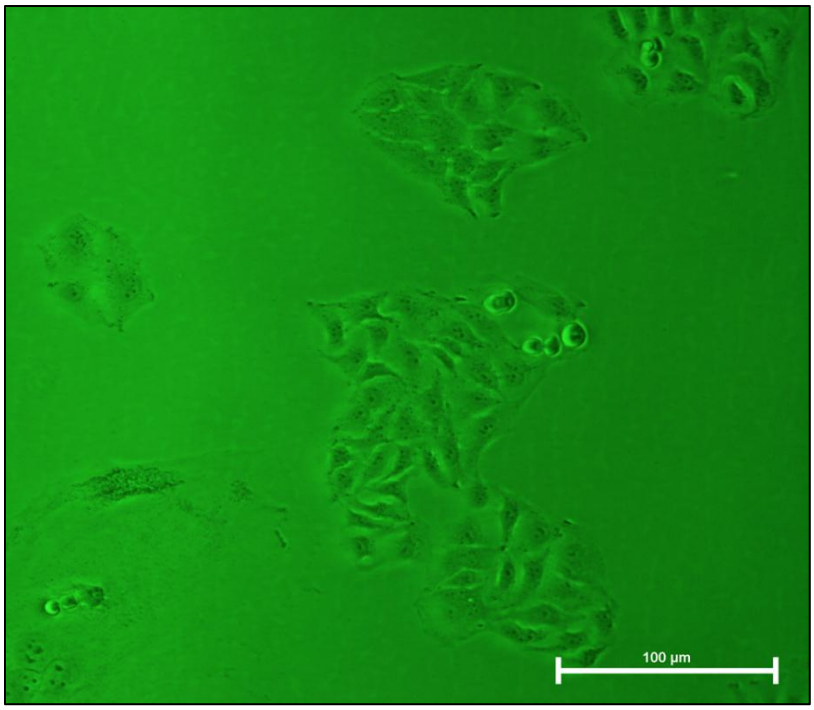


**Fig 11** Microscope image of NHC-IOBA cells, human immortalized conjunctival cells used as an ocular surface culture model.

### 3.2.1 Tear fluid

Tear fluid was sampled by two methods, glass micro capillary tubes and Schirmer strips (Wright and Meger, 1962). Due to their diagnostic purpose strips are common in clinical routine (Whitcher, 1987). Regarding strip collection in this work Tear Test ophthalmic strips were adjusted to the eye lid without cornea anaesthesia and left for 5 min in the eye. For

sample analysis, each strip was soaked in 300 µl DPBS and tear proteins were extracted overnight on a KS250 basic Intellimixer at 4°C. Regarding capillary tears, tear fluid was collected by use of Ringcaps® Duran® disposable micro pipettes with ring mark. In both methods resulting samples were stored at -80°C until use. Prior to use, samples had been adjusted to -20°C and then to 4°C to allow a gentle adjustment of proteins to avoid freeze/thawing protein loss effects as much as possible. Taflotan® sine study sample collection and taurine study sample collection were supported by members of the lab staff.

## 3.3 Sample preparation

### 3.3.1 Intact sample processing

Protein amount estimation was realized by use of the Pierce® BCA Protein assay and a Multiscan Ascent scanner according to the protocol of the manufactor. Freshly thawed sample aliquots for TD LC MALDI analysis were adjusted to 3 µg/µl final concentration due to 15 µg maximum column capacity and 5 µl injection volume (3 µg/µl x 5 µl = 15 µg) with running buffer A (4% ACN, 0.1% TFA). 40 µl sample volume were prepared for each LC run. The samples were transferred to V-bottom 96 well plates for automated sample injection.

### 3.3.2 SDS-PAGE

Since a direct MS analysis is crucial in BU proteomic approaches due to high complexity, 1D SDS PAGE invented by Lämmli (Laemmli, 1970) was used to fractionate proteins corresponding to their molecular weight prior to LC MS analysis. Usually, form, charge and mass influence migration of a protein through a polyacrylamide gel network (Schagger and von Jagow, 1987). Anionic SDS detergent binds to hydrophobic regions (Löffler, 2003) provides negative charges and faciliates denaturation. Consequently, electronical field migration through the gel meshwork is directly proportional to the protein mass, whereby smaller proteins migrate faster than higher mass proteins (Löffler, 2003). However, the qualitative output depends on various factors, e.g. the maximum gel loading capacity (van Hagen, 2008). Therefore, protein load should not impede migration, but consider MS sensitivity. Based on RGC5 extracts, a protein load of 80 µg was estimated optimal for ESI and MALDI experiments. Above 80 µg protein lanes clearly smeared due to overloading effects. In contrast, if available, at minimum 20 µg protein should be separated per lane to fit the MS dynamic range. Samples encircling RGC5 or IOBA-NHC lysates and tear fluid were mixed with NuPAGE LDS sample buffer (+/- reducing agent). Corresponding samples were heated (10 min/90°C) and run on NuPage 12% Bis-Tris, 10-well prepared minigels (100 V/10 min - 150 V) in the XCell SureLock™ system using MES or MOPs buffers. SeabluePlus 2 prestained protein standard was used as molecular weight reference. Reproducibility was

tested using replicate aliquots of test samples. Gels were fixed and stained overnight using the Novex Colloidal Blue staining kit according to the manual of the manufactor. For documentation gels were recorded by use of a DCP-9042 CDN benchtop scanner with a resolution of 1200 x 1200 dpi as *tif*-data assisted by Photoshop C53 extended version.

### 3.3.3 In-gel digestion

The procedure was based on a modified protocol of Shevchenkov et al. (Shevchenko *et al.*, 2006) considering ESI/MALDI optimizations. In case of LC MALDI experiments, a gel lane of interest was divided into 15 slices, which allows one lane to be positioned on a 386 spot target. In case of LC ESI a gel lane was divided into 17 slices. The lane division was decided corresponding to the CBB protein signal abundance. Mass area slices were cut into equally small pieces, destained (50% ACN, 50% 100 mM Ambi, 10 min) and dehydrated (100% ACN). Dried gel pieces were saturated with trypsin solution (200 µl reaction buffer, 1300 µl 20% ACN/10 mM Ambi) ([15 ng/µl], 60-100 µl/slice) and incubated over night (37°C). Digestion was quenched by a pH shift by addition of 10 µl 0.1% TFA. Supernatants were transferred to fresh 0.5 ml tubes and peptides were extracted with appropriate amount of extraction buffers on a Unimax 1010 shaker at 700 rpm. In case of LC MALDI, prior to analysis, combined supernatants and peptide extracts of each slice were filtered through GHP Acrodisc 13 mm x 0.45 µm pre-HPLC syringe filters followed by vacuum concentration (30°C) in a Concentrator 5301 instrument. LC MALDI destinated samples were equilibrated with 20 µl running buffer A (1% MeOH, 1% ACN 0.05% TFA), whereas LC ESI samples were equilibrated with 20 µl 0.1% TFA. In case of LC ESI analysis, sonication resolubilized peptides were SPE purified once again to reduce background signals due to the less contaminant robust character of ESI systems (Kraj and Silberring, 2008).

### 3.3.4 Solid phase extraction (SPE)

Because SPE tips had been demonstrated to generate more accurate results than magnetic beads (Tiss et al. 2007) ZIPTIP® C18 pipette tips (15 µm, 200 Å) were used. 10 µl peptides were bound by 20 binding cycles on the C18 resin followed by a 0.1% TFA wash step followed by 10 µl duplicate elution (50% ACN, 0.1% TFA). The tip was once again rinsed with pure ACN, equilibrated with 0.1% TFA and binding cycles were repeated. Resulting aliquots were combined leading to a 40 µl peptide sample corresponding to each slice digest. Duplicate ZIPTIP® purification was used to exceed the resin saturation limit of 5 µg protein (UserGuideforRPZipTipPipetteTipsforSamplePreparation, 2007) since approximately 4-10 µg protein load (1 lane = 80 µg/17 slices = 4.7 µg/slice; ~4-10 µg/slice) was provided per gel slice with respect to protein distribution pattern. Lyophilized peptides were stored at -80°C until use. For LC ESI analysis peptides were resolubilized (20 µl 0.1% TFA, ice

bath/sonication/10 min) followed by transfer to V-bottom 96 well plates for automated sample injection.

### 3.3.5 Microbore-RP-HPLC for MALDI Top Down (TD) analysis

For direct MALDI TD ocular sample analysis employing the Ultraflex II linear mode, a microbore column (0.8-2 mm Id) (Kraj and Silberring, 2008) was chosen achieving a higher robustness in comparison to capillary and nano approaches (0.05-0.8 mm Id), but exceeding performance of common analytical (2-10 mm Id) and semipreparative columns (10-100 mm Id) (Kraj and Silberring, 2008). However, care had to be taken for column blocking regarding direct analysis of crude samples. Accordingly, microbore should balance robustness and sensitivity. For gradient elution, a Rheos Allegro pump system was used. Furthermore a PAL HTS robot was programmed for automated sample injection and on target fractionation (Fig. 13). Eluting peptides were deposited on 386 MTP polished/matt steel MALDI targets by use of 75 µm ID fused silica tubing. A Prosphere P-HR 4 µm microbore column (150 x 1 mm) was used as analytical column directly coupled to a Security Guard™ cartridge system with an RP1 (4x2 mm) filter inlet (Fig. 12). The guard column should allow direct injection of crude "dirty" samples. Even if the cartridge was developed for columns with IDs >2 mm and was widely used with good suitability for these systems (Halquist and Karnes, 2011, Ireland *et al.*, 2006, Lichtenthaler *et al.*, 2005, Woodward *et al.*, 2009), it was not used in a TD LC MALDI workflow. In fact, the guard column was documented to work well as a trapping column (Boernsen, 2000) in terms of column-switching system and was actually found to perform excellent in direct combination with the 1 mm ID system in this work. The split-free flow rate was adjusted to 20 µl/min and 15 s injection times enabled a 5 µl injection volume. A start delay of 14.25 min. was set prior to fraction deposition. The spotting frequency was 3 s for each fraction approximating 1 µl/spot. Spots were dried and 2 µl matrix (18 mg CHCA, 60% ACN, 2% TFA) was applied on each spot. The matrix composition and spotting technique was found optimal considering homogen crystal formation and signal generation. Matrix spotting automation was realized on a Sun Collect MALDI spotter. Since the manufactor´s spotting needle (50 µm ID) was found to exhibit a low degree of robustness, a custom-built adapter in combination with a Tecan steel teflon-coated spotting tip was adjusted to the robot showing reproducible and robust performance resulting in homogeny spots and low carry-over effects (Fig. 14). The HPLC fractionation method was optimized by use of retina lysates from 240 over 120 to finally 92 fractions collected for each sample run. Running buffer A were prepared as follows: A= 4% ACN/0.1% TFA, B= 96% ACN/0.1% TFA). The gradient was programmed as follows: 0-12 min: 90-30% A, 12-16: 30-0% A, 16-21: 0% A, 21-25: 0-100% A, 25-35:100% A. Optimizations and monitoring were realized by the 2D-gel view generator Survey Viewer version 1.1 tool. Finally, the reproducibility of the system was

determined by comparing elution behavior of reporter *m/z* peaks monitored between replicate runs as well as comparison of fraction profiles between sample runs. To assess system sensitivity, the number of detected WarpLC compounds was ascertained and compared to the literature. Also unfractionated samples were measured in parallel and resulting profiles were compared to HPLC processed samples. The microbore HPLC method should allow the analysis of ocular cell species and should finally be transferred to tear samples.

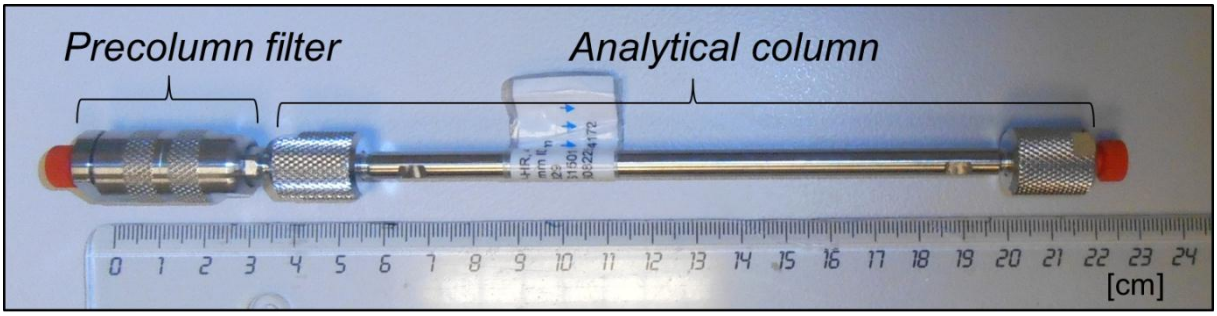


**Fig 12** Microbore column system for TD LC MALDI consisting of a Security Guard™ cartridge with a RP1 filter (4x2 mm) connected to a microbore analytical Prosphere P-HR 4µm column (150 x 1 mm)

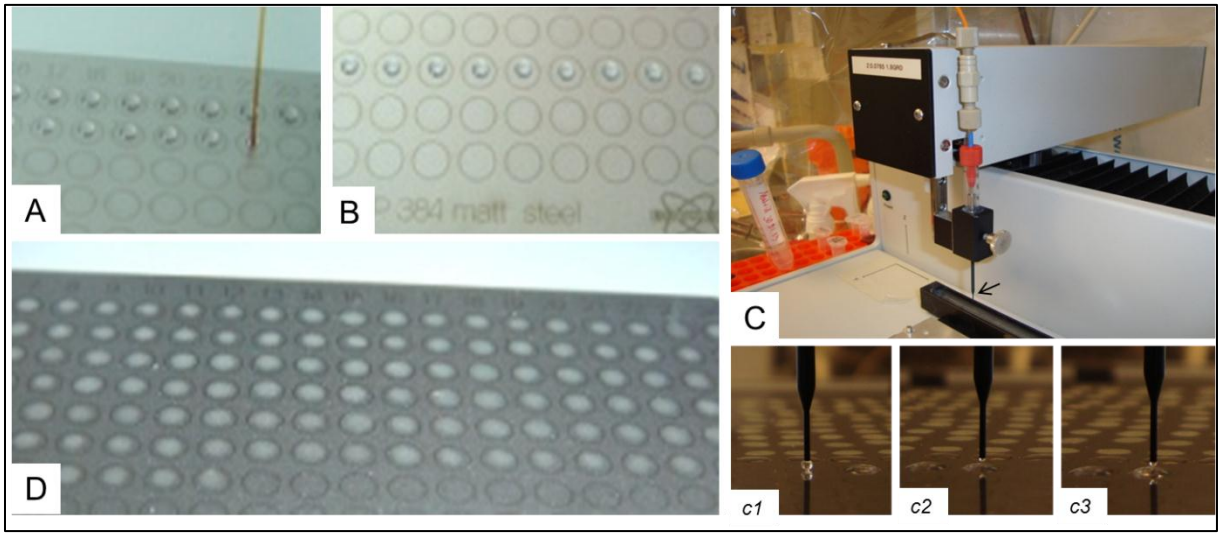


**Fig 13** TD LC MALDI Sample preparation; A: Direct on target sample fractionation realized by a PAL HTS robot connected to the column system leading to B: accurate fraction deposits; C. Matrix spotting by use of a customized Tecan Teflon coated needle unit (arrow) integrated on a Sun Collect robot station allowing accurat matrix deposition on dried analyte fractions (*c1-c3*) leading to D:homogen analyte/matrix spots.

### 3.3.6 Capillary-RP-RP-HPLC (for MALDI)

For BU MALDI analysis the Ultraflex II and the Rheos Allegro Pump system were employed. The system performs optimal gradient mixing in a flow rate range between 20 µl to 1000 µl/min according to the manual of the manufacturer. Accordingly, flow rates <20 µl/min lead to declined reproducibility of the gradient. Another disadvantage is the extended time period

the gradient needs to reach the column head, probably causing diffusion effects and decreased performance. For optimal conditions, a pre-column flow splitting strategy was established. Thereby, the flow split should consider the pump´s optimal gradient range and should leave the analytical column with low flow rate. As mechanical split system an M-472 graduated micro-split valve was used. The micro-split valve was selected due to a pressure resistance >200 bar. The challenge in flow splitting refers to the column system, which creates high pressure. Consequently, without appropriate waste port backpressure all solvent will flow out of the waste port failing to pass the split port and without entering the column. Therefore, appropriate backpressure adjustment is a challenging step. Accordingly, for optimal pump flow splitting different splitter graduation settings and pump flow rates have been tested. In consequence, the adjustment of the split flow rate exclusively by the splitter graduation was found to be unsuitable for accurate fine regulation of the split stream. Hence, reproducible adjustment was successfully achieved only in a small setting window confident with manual splitter inspection, which supports the splitter to work preliminary as a shut-off valve with distinct limitation in split ratio adjustment. Consequently, as a counteracting splitting strategy, peek tubings with varying IDs were connected to the waste port to generate appropriate backpressure at a fixed graduation setting which was also documented for comparable splitter models (Kozerski *et al.*, 2003, Rogatsky *et al.*, 2009). The use of peek tubings for backpressure adjustment is an economic strategy to down-scale common HPLC systems to capillary or nano dimension (Aguilar, 2004, Moritz, 2007, Profrock, 2010, Yi *et al.*, 2003, Zhang *et al.*, 2004a). Therefore, variations of peek tubing length and pump flow rates were combinatorial determined for backpressure genearation and capillary flow rate setting. A combination of a 1/16” OD x 0.10” ID x 5 ft PEEK$^{TM}$ tubing under a pump flow rate of 300 µl/min was found to work optimal resulting in a split flowrate of 7.8 µl/min, matching the capillary range. Hence, 300 µl/min pump flow had been documented for most systems to guarantee suitable pump function and solvent portioning (Chervet *et al.*, 1996). Split flow rate reproducibility was tested by time assays monitoring different mobile phase compositions passing through a 20 µl defined capillary tube. The splitting system was connected to the injection valve by combination of 1/16” OD x 0.0025” ID and 1/16” OD x 0.007” PEEK$^{TM}$ tubings connected by use of a stainless steel NanoTight$^{TM}$ union (10-32 to 10-32, 0.007” thru-hole) to allow an easy reinstallation of the microbore system or other systems (Fig. 14). All tubings and connectors were capillary compatible to avoid dead volumes in the system. Accordingly, the 6-port valve outlet was connected to the column system by use of a 1/16”OD x 0.005 ID PEEK$^{TM}$ tubing. Tubings were connected by use of 10-32 PEEK$^{TM}$ fingertight fittings. Since the present instrumentation did not allow column switching and peptide trapping, the design of cationic/anionic exchange and reversed phase as common 2D-HPLC strategies for BU analysis (Link, 2002) was not possible. To counteract this

drawback the idea was to develop a column system which displays slightly different retention properties achieving proper orthogonality under identical RP solvent conditions in an online-system. Thereby, the combination of C18 with a phenyl stationary phase was the key point of the concept since there is growing evidence for the efficiency of combinatory RP-RP strategies in BU proteomics (McQueen and Krokhin, 2012). In fact, Gilar and colleagues showed that a RP-RP combination under different pH conditions performs higher orthogonality than a SCX-RP combination (Gilar *et al.*, 2005). Actually, alkyl residues, especially C18, are commonly used to retain peptides, whereas RP materials like cyanopropyl ligands and phenyl materials offer additinal selectivity (Aguilar, 2004). Consequently, the idea was to combine RP materials taking advantage of slightly selectivity differences for peptides. To realize this concept a RP-RP-capillary column system was developed, which consisted of a 30 x 0.5 mm BioBasic® C18 precolumn connected to a 100 x 0.5 mm BioBasic® Phenyl analytical column combined with a 150 x 0.5 mm Jupiter® 4 µ Proteo analytical column. To avoid gel particles and contaminants to enter the column system the whole system was protected by an A 316 0.5 µm online precolumn filter. All system parts were directly connected via Onyx® column couplers to minimize dead volumes and rediffusion (Fig.15). Consequently, the column phases including the C18 pre-column refer to RP but differ in selectivity properties. Regarding the gradient conditions running buffer A consisted of 98% water, 1.94% ACN, 0.06% MeOH and 0.05% TFA. Running buffer B consisted of 95% ACN, 3 % MeOH, 2% water and 0.05% TFA. For each gel slice a 60 min gradient was run (0-5 min: 100% A, 5-45 min: 0-80% D, 45-47 min: 80-100% D, 47-49 min: 100% D, 49-58 min: 0% A-100% A, 58-60 min: 100% A). The addition of MeOH was found to improve the selectivity of the phenyl phase towards aromatic residues (Yang *et al.*, 2005)(www.restec.com). Elimination of sample carry over effects, which play a critical role in LC-MS based experiments (Burton *et al.*, 2008, Mitulovic and Mechtler, 2006, Vu *et al.*, 2013), was achieved by running equilibration gradients of 12 min between samples by 80% ACN injection also maintaining sample loop and valve port clearance. For automated sample injection and on target fractionation, the PAL HTS robot was programmed. Eluting peptides were deposited with a frequency of 40s/spot on 386 MTP polished steel MALDI targets. Thereby, each gel slice extract was fractionated over 24 spots on the target. Accordingly, one target corresponded to one sample lane consisting of 15 gel slices. CHCA based matrix was applied on dried fractions as already described. Representative “reporter ions” eluting in replicate runs were monitored to evaluate retention time (RT) reproducibility. Finally, the method should be used for the sensitive analysis of tear samples.

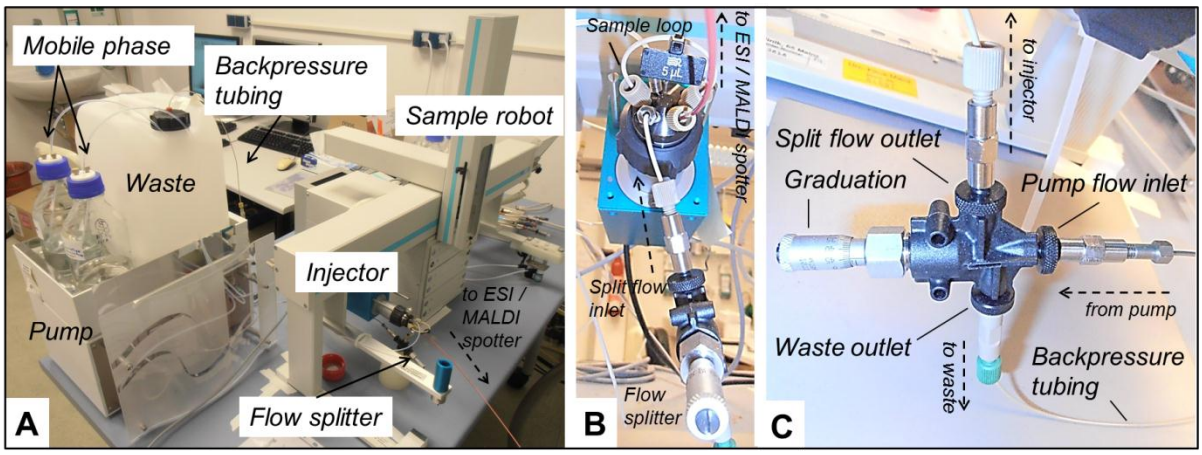


**Fig 14** A: Overview of the capillary HPLC system developed for the ESI/MALDI BU application consisting of an Rheos Allegro HPLC pump and PAL HTS sample robot, which can be used also to fractionate eluting samples direct on MALDI targets; B: Precolumn split system using a M-472 (for MALDI) or a P-470 (for ESI, shown) microsplitting valve to downscale high pump flow rates to capillary flow rates between 7-10 µl/min; C: Detailed view of the microsplit system.

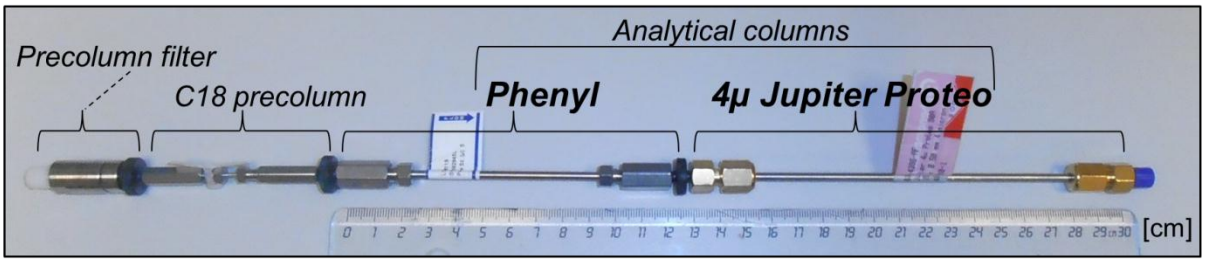


**Fig 15** RP-RP column system developed for MALDI BU analysis of tear fluid. The system consists of two online coupled stationary capillary (0.5 mm ID) RP phases, phenyl and 4µ Jupiter Proteo material, which provide slight differences in retention properties. Actually the C18 precolumn additionally contributes to orthogonal phase selectivity.

### 3.3.7 Capillary-RP-HPLC (for ESI)

For ESI experiments the identical split system described for the MALDI system was used with slight modifications, instead of the M-472 the P-470 splitter was used which comes with a 10-32 split port instead of a 6-32 split port, allowing easier installation. As column system only a 1D HPLC strategy was used consisting of a 30 x 0.5 mm BioBasic® C18 precolumn connected to a 150 x 0.5 mm BioBasic® C18 analytical. The whole system was protected by use of an A 316 0.5 µm online precolumn filter (Fig. 16). Like in the MALDI setup, all components were directly connected via Onyx® column couplers and also mobile phase composition was identical to the LC MALDI approach. Since the flow rate was influenced by different backpressure condition due to the ESI needle, system settings could not been directly transferred from the MALDI setup. The pump flow rate was reduced from 300 to 200 µl/min resulting in a flow rate of ~ 6.7 +/- 0.03 µl/min (*N*= 20 measurements), whereby different gradient settings were tested. The challenge was to find a compromise between

sensitivity and analysis time which should allow lab routine integration. Therefore, a first workflow using 80 min gradient per slice corresponding to 17 gel slices per lane was developed determining reproducibility and sensitivity running RGC5 lysates (*N*= 8). Quantitative (number of identified proteins) as well as qualitative reproducibility (protein identification congruency) were determined. During a sequence after each slice run 30 min washing runs injecting 80% ACN were used to counterstrike carryover effects. However, washing runs were eliminated to reduce total analysis time without affecting the performance remaining washing runs between different sample subjects (eg. control, treatment). In the end of a sequence the system was equilibrated to 80% solvent for column storage. To economize analysis time, the 80 min peptide elution pattern was inspected using two different gradient optimization strategies. At first, a proportional economization of the gradient was tested for its sensitivity; secondly, a targeted reduction of the elution area was applied taking main peptide elution areas of chromatograms into consideration. For optimization, RGC5 gel mass area replicates (1/17 lane) were used. In parallel, a different strategy was tested to economize analysis time decreasing the number of slices per gel lane in various steps. To determine the reproducibility of the LC ESI workflow, as already mentioned, quantitative and qualitative parameters were analyzed. Reproducibility of sensitivity was realized by quantitative comparative component analysis including number of CID precursor masses, CID fragment ions and resulting protein hits, considering two different scoring strategies (relaxed= MASCOT ion score $p<0.05$, stringent= peptide score<30). Qualitative comparative analysis revealed overlap in CID precursors, fragments and proteins focusing on technical replicates (n= 6) corresponding to representative RGC5 gel mass areas (*N*= 8). Moreover, the RT reproducibility was examined monitoring the RT of representative reporter ions observed in all replicates of a certain gel mass area. Finally, the LC ESI approach should be applied to ocular surface samples encircling tear fluid and conjunctival cells.

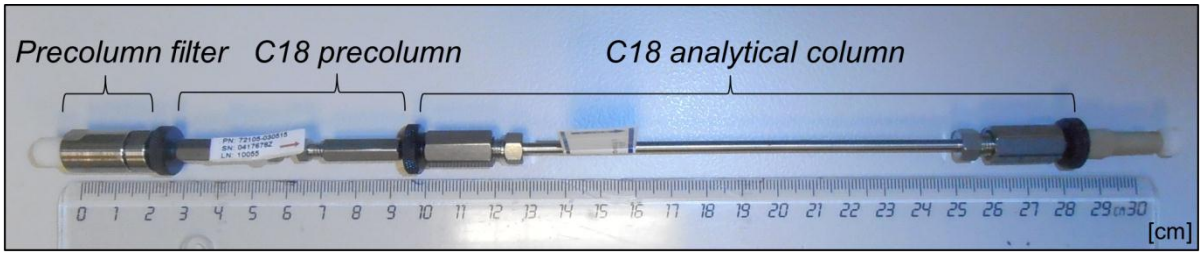


**Fig 16** HPLC capillary column system (0.5 mm ID) employed for ESI BU analysis of ocular surface sample species.

### 3.3.8 MALDI-TOF/TOF MS/MS

#### 3.3.8.1 Linear mode for Top Down (TD) MS (microbore HPLC)

For TD LC MALDI analysis, the Ultraflex II instrument was used. The instrument was equipped with a nitrogen laser under control of MarathonControl software. Samples were measured in the MS linear mode controlled by Flex Control/Flex Analysis under priority of WARP-LC software. For Flex Control adjustment, the pulsed ion extraction was set to 100 ns and the linear detector gain was adjusted 38x with 0.10 sample rate and highest electronic gain. Matrix clusters were suppressed up to 1000 Da implementing a blast of 10 shots with 75% laser power (LP) for background suppression. For signal recording 600 shots in 60 shot steps with 25% LP were found to give the best results balancing intensity and resolution. Laser shots were fired without fuzzy logic on each spot using a hexagon raster focusing on masses between 1000 and 17000 Da (S/N>3; resolution>100). The system was calibrated using the protein calibration standard I for reference.

#### 3.3.8.2 Reflector mode for Bottom Up (BU) MS (capillary RP-RP HPLC)

For fraction analyis the Ultraflex II instrument was used taking advantage of the instrument´s TOF/TOF MS/MS concept using the described control software platform. The instrument was run scanning a range of 900-3700 *m/z* to record precursor masses. Thereby, 500 shots in 50 shot steps from ten different spot positions were applied for each fraction without fuzzy logic. MS peaks were detected using the *SNAP* (Sophisticated Numerical Annotation Procedure) algorithm, which detects monoisotopic masses in raw reflector MS spectra recognizing a component´s isotopic distribution by a non-linear fit function (FlexAnalysis2.4OperatorManual, 2005). Based on detected peaks a WARP-LC compound list was generated. Thereby, the WARP-LC algorithm represents an intelligent concept linking MS to chromatography (WARP-LC1.1UserManual, 2006), whereby peptides that had once been fragmented are excluded for further fragmentation, which increases the probability of low abundant peaks to be selected for analysis. The strategy economizes shots, sample and time while providing higher sensitivity. It is important to note that each laser shot during fragmentation physically eliminates sample components, which means that multiple fragmentation cycles corresponding to a particular peptide reduce the chance to identify low abundant coeluting peptides in a fraction. Confidently, chromatographic effects like peak shifting and smearing are taken into consideration (Berger, 1993, Castells and Castells, 1998, Conder, 1982, Fraga *et al.*, 2001). Furthermore, compound list settings are used as MS/MS precursor selection filter. To account for chromatographic blur, peaks of similar *m/z* value considering 100 ppm mass tolerance were defined as identical compound if they were separated by less than 3 fractions (S/N>10, intensity>700), which provided best results for

efficient overall fragmentation in preexperiments. Compounds occurring in more than 90% of an analysis were defined as background and excluded from precursor selection. A maximum of 70 MS/MS measurements was allowed for each spot during a WARP-LC run. The system was calibrated using the peptide calibration standard for reference and internally by autodigestive trypsin signals. Limits of the system were also considered by monitoring the accuracy of peak detection and fragmentation efficiency.

### 3.3.9 ESI LTQ Orbitrap XL MS

#### 3.3.9.1 Spray system

For spray generation, a 75 µm ID silica-fused tubing was used, which displayed fast performance decline. Microscopic inspection of the tubing tip indicated corrosive surface damage leading to spray inaccuracy, instability and electrical circuits (Fig. 17). Corresponding spray fluctuations were found to lead to noozle droplet adhesion causing a whole breakdown of the spray and analysis. Therefore, the needle system was substituted by a low flow metal needle for API 2 probes appropriate for the capillary flow range. Actually, by use of the metal needle a small sensitivity decline was recognized, however stability and reproducibility of the system was distinctly improved which represents the main argumentation for installation of the metal needle. Thereby, the spray voltage was ~4.2 kV, spray current ~0.9 µA, capillary voltage ~44 V, capillary temperature ~ 275°C and tube lens was ~125 V. The ESI probe coordinates were adjusted to position B defining the depth of the probe noozle in the probe chamber and graduation 1.1 which describes the accurate distance of the needle to the ESI cone. However, events of needle blocking in case of the metal needle have been recognized by corrosive particles of unknown origin, which brings need for periodical maintenance of the needle system (Fig 17). Also the heated ion transfer capillary was frequently cleaned by use of methanol and sonication.

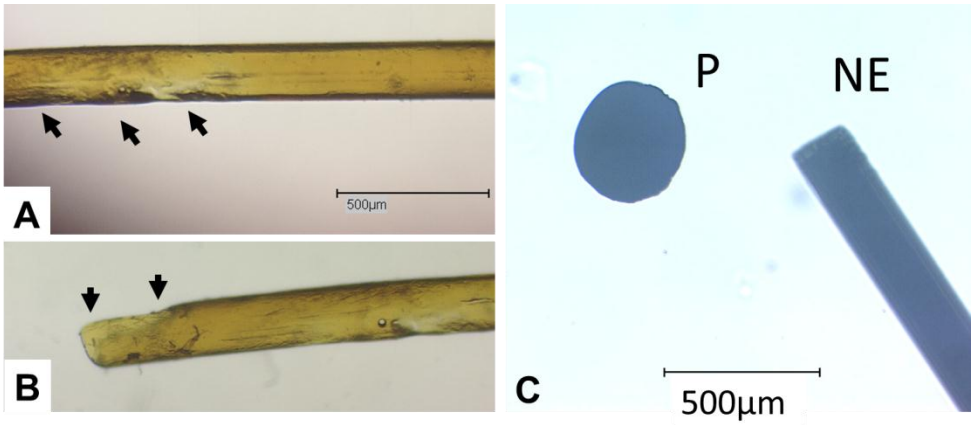


**Fig 17** A/B: Corrosive modifications at the ESI fused silica tubing outlet after several measurements (indicated by arrows) leading to spray instability; C.: Corrosive particle (P) blocking the inlet of the ESI metal needle end (NE) resulting in decreased analysis performance.

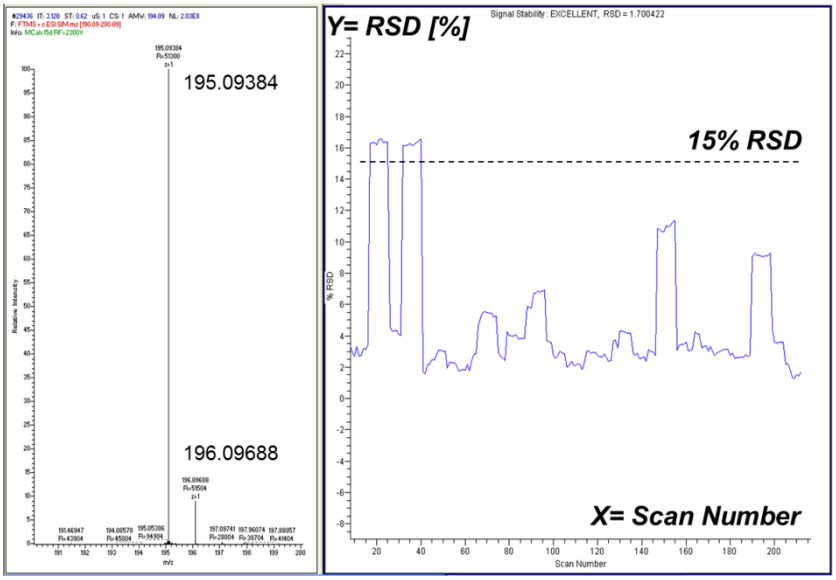


**Fig 18** Spray stability test indicating high stability with *RSD*<10% during test measurements focusing on reporter masses 195.094 and 196.097 *m/z* after installation of a low flow metal ESI needle.

### 3.3.9.2 MS settings

The coordination between MS, sample robot and HPLC was realized using XCalibur® related contact closure signaling. For Orbitrap MS a range of 300–2000 *m/z* in the instruments positive mode was focused on. The maximum injection times were set to 50 ms for ion trap (LTQ/ITMS) and 500 ms for orbitrap (FTMS) analysis. For LTQ peptide fragmentation, CID was used with helium as collision gas (normalized collision energy= 35, activation time= 30ms, activation Q= 0.25). The top five centroid detected monoisotopic peaks (charge state=2, intensity≥ 500) were selected within an isolation width of 2 *m/z* for fragmentation in each scan event. Data acquiring time was adapted to the length of the gradient (finally 50min). The complete instrument was semi-automatically calibrated weekly using Pierce® LTQ ESI positive ion calibration mix corresponding to five components: caffeine (195 *m/z*), MRFA (524 *m/z*) and Ultramark components (1322, 1422 and 1522 *m/z*). For internal real time calibration a 445.120025 *m/z* ambient air background peak corresponding to polydimethylcyclosiloxane (PCM) was used according to the mass lock calibration strategy (Lee *et al.*, 2011, Olsen *et al.*, 2005). Optimal LTQ settings for dynamic exclusion and resolution were determined using RGC5 lysate replicates (1/17 lane), referring to number of identified proteins and score values leading to 90 s dynamic and 30 s repeat duration. Since a resolution >30000 was shown to result in a protein identification rate decline, 30000 was set for analysis. Also the dynamic range of the system was tested by dilution of RGC5 (80

µg) standard digest (Fig. 19). Finally, optimal MS settings corresponding to 50 min HPLC gradients were used for the analysis of tear fluid and conjunctival cell studies.

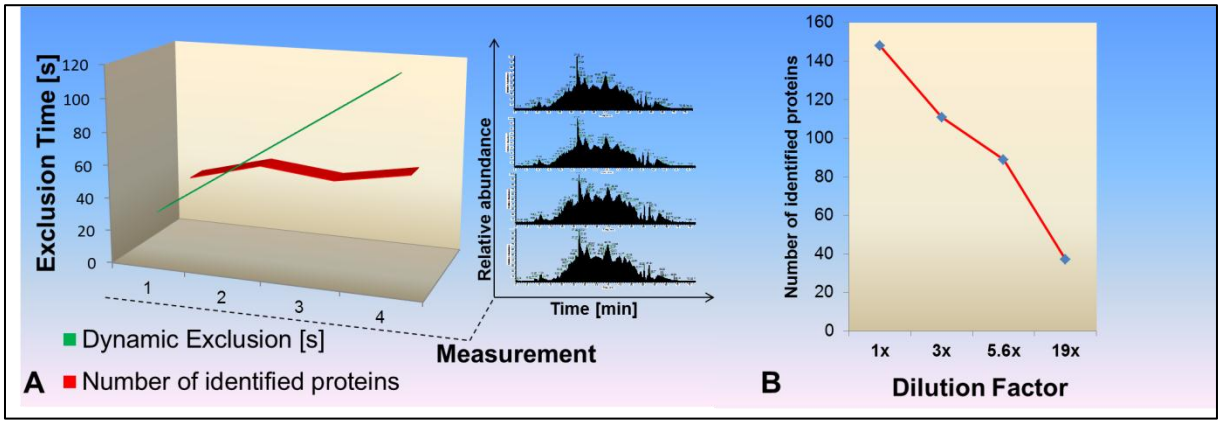


**Fig 19** A: Influence of dynamic exclusion duration on the number of identified proteins showing a slight positive correlation; B: Correlation between sample dilution and sensitivity

### 3.3.10 Data processing & Protein identification

#### 3.3.10.1 Linear Microbore LC-MALDI Top Down (TD) analysis

Raw MS spectra were manually inspected and optimal processing and peak detection was realized in FlexAnalysis. Spectra were *Savitzky Golay* smoothed (Gorry, 1990, Savitzky and Golay, 1964) with an optimum width of 30 and 3 cycles balancing noise reduction and sensitivity (Fig. 20) followed by *Convex Hull* baseline substraction (Fung and Enderwick, 2002, Ilina *et al.*, 2010) and *Centroid* peak detection (S/N≥17, *m/z* width= 9, 80% percent height, 0.2% rel. intensity) (Blais and Rioux, 1986, Yang *et al.*, 2009) (Fig. 21). Optimal processing and peak detection were automated using a FlexAnalysis method script in the batch processing mode (Fig. 22).

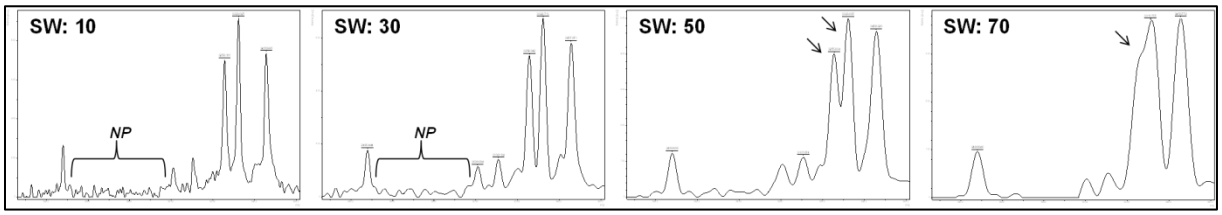


**Fig 20** Influence of smoothing width (SW) settings on spectrum quality in linear MALDI MS spectra; whereas noise peaks (NP) are suppressed at SW 70 also distinct peaks (arrows) merged and could not be resolved. An optimal balance between noise reduction and resolution was found at SW 30.

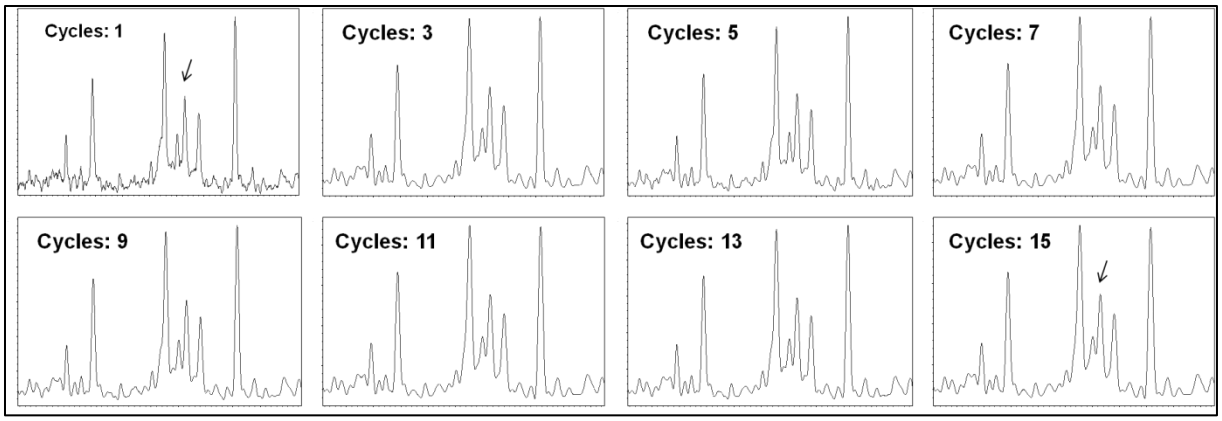


**Fig 21** Influence of smoothing cycles on linear MALDI MS spectra. No clear changes on distinct peaks (example indicated by arrow) were found after 3 smoothing cycles.

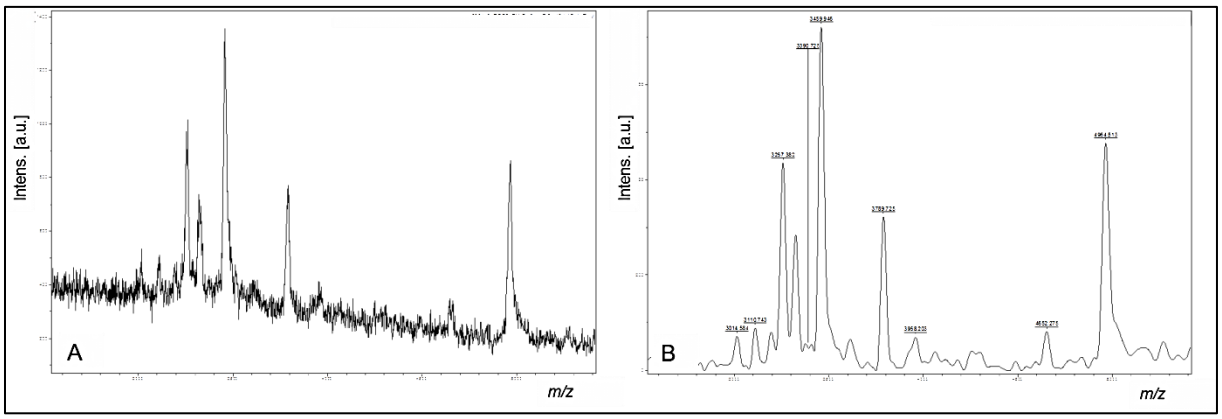


**Fig 22** Automated batch mode processing featuring noise reduction and peak detection with implemented optimal settings; A: Raw linear MALDI MS spectrum; B. Processed spectrum allowing accurate peak detection.

### 3.3.10.2 Reflector Capillary LC-MALDI Bottom Up (BU) analysis

For protein identification, combined MS/MS spectra corresponding to a particular experiment were transferred to MASCOT as *mgf* files and searched against the SwissProt version 57.8 database (SwisProt_111101, 519348 sequences; 183273162 residues). Depending on the sample origin *Homo sapiens* (tears, NHC-IOBA) (20359 sequences) or *Mus musculus* (RGC5) (16409 sequences) were set as taxonomy, trypsin as enzyme and one missed cleavage was allowed. Charge state was adjusted to 1+ and mass tolerance was set 100 ppm for MS precursors and 0.8 Da for MS/MS fragments. To achieve most stringent results protein queries were run either under *MUDPIT* scoring conditions (if queries/entries>0.001; after any taxonomy filter, www.matrixscience.com) with a significance threshold of $p<0.05$ for protein identification. Additionally, only those proteins that were based on unique peptide sets were documented to avoid redundant protein entries.

#### 3.3.10.3 Capillary LC-ESI Bottom Up (BU) analysis

All MS/MS spectra of a particular experiment were combined by use of the Proteome Discoverer® version 1.1. The resulting *msf* file containing all experimental data was MASCOT searched against the SwissProt as described for MALDI. ESI protein identification settings were realized in a Proteome Discoverer® script featuring a precursor mass range of 150 to 2000 Da (charge= 1-4, S/N ≥6), trypsin as enzyme (1 allowed missed cleavage), 20 ppm mass tolerance for precursors and 0.8 Da for fragments. Moreover, ammonia-loss (N-term C), oxidation (H/W, M) and phosphorylation (S/T, Y) were selected for variable modifications and carbamidomethyl (C) was set as fixed modification.

### 3.3.11 Protein quantification and statistics

In case of LC MALDI BU analysis semi quantitative protein level estimation was carried out by use of a modified version of the in-house developed *P2M* software platform (Tschoerner, 2008), whereby MS and MS/MS spectra were imported directly from Flex Analysis following normalization of MS spectra according to the mean total ion current (TIC) ($Intensity_{MS}$ x $mean TIC_{\Sigma MS}/TIC_{MS}$). Spectra with a minimum factor of 0.1 or maximum factor of 10 were categorized as “low quality” and excluded from analysis. To allow comparison of protein levels between all samples, a protein that failed to be identified in some of the samples was extrapolated regarding the intensity value at the corresponding *m/z* position with a tolerance of 0.3 Da. Since proteins can smear over several gel slices, a “Blur” function considering drifting proteins in gels was implicated with a tolerance of +/- 1 slice. All sub experiment files were merged in one Excel *csv* summary file and transferred to Statistica version 8/10. Moreover all normalized peptide levels, which contributed to the identification of a particular protein, were summarized for the protein. Protein levels were then used for statistical protein level determination. In case of LC ESI experiments, a further optimized *P2M* workflow was established (Wolters, 2011, Wolters, 2012) featuring *raw* files and Proteome Discoverer® result *mgf* file containing protein and peptide information for TIC normalization. Thereby, each particular peptide corresponding to an identified protein is searched with a tolerance between 0.02-0.05 Da considering experimental quality in all samples of the experiment that should be compared. Moreover a RT shift algorithm had been implemented in the software, which scans spectra for peptides within the RT range, where the pepide was primarily identified. Normalized peptides were summarized for each particular identified protein and transferred to a final Excel *csv* file for statistical analysis of protein levels in Statistica.

### 3.3.12 Protein functional annotation analysis

To determine origin, function and implementation of ocular surface proteins two different software solutions were used. Cytoscape version 2.8.3 with integrated BINGO 2.44 plugin

(www.cytoscape.org), which enables gene ontology annotation of proteins, was used for the taurine tear study, whereas for the Taflotan® sine study additionally the Ingenuity® (www.ingenuity.com) IPA® tool system was used. Beside software based analysis, data has also been inspected manually by literature search.

### 3.3.13 Ocular surface studies

#### 3.3.13.1 Taurine tear study design

The study was realized by use of the LC MALDI BU workflow focusing on capillary tears monitoring three age-matched groups (*N*= 4 individuals/group): two contact lens wearer groups (soft daily lens use >2 years), one applying 0.05% taurine eye drops (CL_Taurine, 25.5+/−1.29 years); the other for control physiological NaCl solution (CL_NaCl, 25+/−0.82 years) and a third taurine drops using a group of sicca patients (S_Taurine, 24.75+/−3.86 years). Dry eye was diagnosed in the clinical ambulance by use of a Schirmer test II (BST<10 mm) and subjective dry eye ocular discomfort. Study exclusion criteria for probands were: Diabetis mellitus and/or eye diseases/medication probably influencing inflammatory processes or tear production. Accordingly, all participants were asked to avoid topical therapeutics during the study period and informed consent was obtained prior to the study. All protocols were approved by the institutional ethics committee and were conformed to the provisions of the *1964 Declaration of Helsinki*. Individual tear samples were collected once a week (at study onset; after 3 days; after 1, 2, 4 and 5 weeks) from the left or right eye. Furthermore, tears of an additional group encircling healthy non-contact lens wearers (*N*= 8) were examined for verification. Individual tear samples of each group and time point were adjusted to 12 µg of total protein and pooled referring to time points. Accordingly, tear pools of each experimental group per time point (e.g. S_Taurine_3days) contained 48 µg total protein. Four gels were run in parallel (100 V, MES) encircling 18 lanes (18 time points/group pools) and one additional lane referring to the healthy non-contact lens wearer pool divided each in 15 slices/lane. Gel fixation, staining, in-gel digestion, peptide extraction and LC MALDI sample preprocessing were carried out as already described for LC MALDI BU analysis. Accordingly, tryptic peptides were fractionated by use of the developed capillary RP-RP LC MALDI system. Since each slice extract was fractionated over 24 spots on a MALDI target, one target corresponded to one sample lane (group tear pool per time point). In summary 19 study targets were prepared (3 groups x 6 time points + 1 reference group) and analyzed following the described LC MALDI BU protocol. Protein identification was realized by creation of a *mgf* file containing MS/MS spectra of all 19 sub experiments (Fig. 23). Followed by the described *Homo sapiens* MASCOT/SwissProt search protocol with the exception that no fixed modification was selected since samples have not been reduced, also no variable modification was allowed considering *MUDPIT* scoring and p<0.05 for protein

identification. After *P2M* transfer, normalized protein sum intensities were analyzed over the study period in Statistica using a linear regression model for the three experimental groups.. Proteins (scores≥35) were selected by their $R^2$ values. $R^2$ values≥0.5 in at least one of the groups qualifies the focused protein for further examination. Moreover, non-linear effects were determined by use of *Kruskal-Wallis* analysis regarding protein level medians over the whole study period of a particular protein. Therefore, regarding a particular protein, intensity levels of all time points of the taurine treatment groups (CL_Taurine, S_Taurine) were normalized to the start point level of the control group (CL_NaCl) to eliminate initial group specific differences not associated with the treatment. Normalized levels were used for *Kruskal-Wallis* followed by *post hoc* analysis. Moreover, a functional annotation analysis using Cytoscape was realized with candidate proteins. In addition, data were compared to the literature.

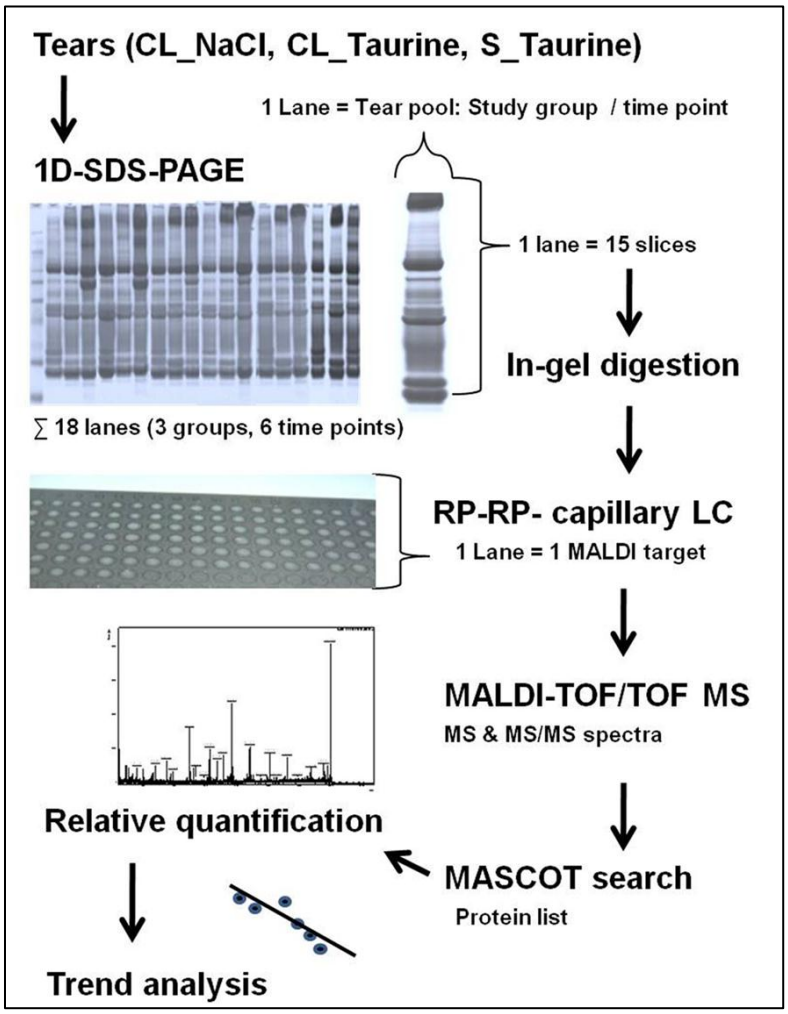


**Fig 23** Study design of the longitudinal taurine tear study illustrating tear gels of 3 study groups and 6 time points (the additional reference sample, lane #19 is not shown). Samples were analyzed by the developed RP-RP LC MALDI BU workflow (Funke *et al.*, 2012).

### 3.3.13.2 Taurine conjunctival cell study design

To monitor taurine effects on stressed conjunctival cells (IOBA-NHC), cells were prepared in 24well plates for two stress conditions: staurosporine (30000 cells, 0.25 µM/5 h) and $H_2O_2$ (40000 cells, 20 mM/1 h). Cell viability was examined by crystal violet assay and reactive oxygen species (ROS) level by DCFH-DA ROS assay, both performed in duplet for each taurine concentration. Moreover, each experiment was repeated four times. For LC ESI MS analysis 50000 cells/dish were seeded to pool for proper protein amount (taurine= 3xdishes/concentration; control= 3xdishes). Taurine solutions were freshly prepared in cell buffer featuring 3h cell incubation for each concentration: 100, 50, 20, 4, 2, 1, 0.5, 0.2, 0.05 mM inferred from the literature (Das *et al.*, 2011, Franconi *et al.*, 1985, Jong *et al.*, 2012, Muhling *et al.*, 2002, Pan *et al.*, 2010, Pan *et al.*, 2012, Pasantes-Morales, 1982, Weiss *et al.*, 1982, Wu *et al.*, 1999) followed by cell harvest, lysis and protein extraction, BCA assay, SDS PAGE and LC ESI MS. For the first experiment 6 gel lanes (50, 20, 4 mM; 3x control) were run, for the second experiment two duplicate lanes (2x 0.05 mM, 2x control) were run in parallel to monitor gel reproducibility. For the first experiment all lanes (*N*= 6), for the second experiment one taurine (0.05mM) and one control lane were prepared for LC ESI MS. Also, all samples were group randomized and measured ($\Sigma$ *N*= 6) in the first experiment. Corresponding *raw* files of three samples (4 mM, 50 mM taurine; control) were combined for quantification. For the second experiment, each sample lane was measured in duplicate to additionally counteract technical bias, whereby *raw* files of all runs were combined. SwissProt corresponding normalized proteins were quantified using the described *P2M*/Statistica workflow. Statistical analysis was realized using a minimum 2fold level alteration threshold in confidence with the literature (Blagoev *et al.*, 2004, Choe *et al.*, 2005, Friedman *et al.*, 2004, Leal *et al.*, 2012, Mann and Kelleher, 2008, Molloy *et al.*, 2003, Ohlmeier *et al.*, 2004, Old *et al.*, 2005, Wilkins, 2006) for potential taurine responding protein candidates. Conjunctival proteome characterization was done by Cytoscape and literature screening. The complete workflow is depicted below (Fig. 24).

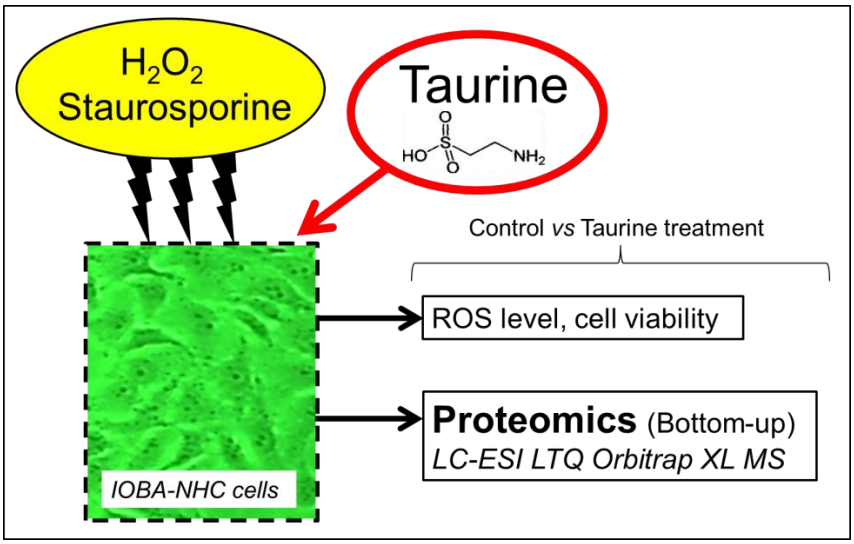


**Fig 24** Study design of the taurine conjunctival cell study: IOBA-NHC cells were stressed with staurosporine or peroxide and incubated with different taurine concentrations followed by ROS and cell viability estimation and proteomic analysis of taurine treated cells by the LC ESI BU approach.

### 3.3.13.3 Taflotan® sine tear study design

The study was realized by use of the developed LC ESI workflow. Thereby, a group of POAG patients, who switched from the topical use of preservative-containing latanoprost (Xalatan®, application≥6 month) to preservative-free tafluprost (Taflotan® sine) because of ocular surface discomfort symptoms, were focused on. Patients were diagnosed POAG in the clinical ambulance due to optic disc glaucomatous appearance and visual field. Moreover, only patients who displayed $IOP_{baseline}$≤22 mmHg and clinical dry eye parameters (BST<10 mm, TBUT<10 s) reporting subjective ocular surface discomfort, e.g. irritation or burning, have been included in the study. Informed consent was taken from all study participants prior to study onset and all protocols had been approved by the local ethics committee corresponding to the *1964 Declaration of Helsinki*. Also, clinical parameters were recorded longitudinally including TBUT, BST, visual acuity and *superficial punctate keratitis* (SPK). Moreover, subjective life quality parameters referring to the *ocular surface disease index* (OSDI) (Schiffman, 2001) were documented. Regarding tear proteomic analysis at first longitudinal pattern changes should be monitored after the switch in a pilot POAG patient cohort by LC ESI MS BU explorative determination followed by microarray validation of MS derived candidate proteins and preselected dry eye markers in comparison to healthy subjects. For explorative LC ESI MS BU analysis Schirmer proteins were concentrated by 3K MWC spin filters recovering proteins ≥3 kDa by centrifugation (14000 g/30 min/4°C). To estimate filter effects, raw and filtered aliquots of a test tear pool (*N*= 20) were compared and filtrates were inspected for the occurrence of components ≤3 kDa by SDS PAGE, moreover evaluating dynamic range and suitability for MS analysis. A protein amount of 45 µg/lane was found optimal addressing MS sensitivity. A first batch of patients (*N*= 7) was recruited for

explorative MS analysis. However, samples corresponding to 4 weeks were missing in the sample set for two patients and a high protein content variance was found challenging for representative pooling and follow-up microarray (MA) analysis. Moreover, only three patients of the first batch were found to contribute enough protein over the remaining time points. Consequently, exclusively three patients (*N*= 3; 2 females, 1 male, 66 +/- 16 years) were monitored over four time points (0, 2, 12, 24 weeks +/- 1 week) in the explorative MS analysis. Accordingly, 15 µg protein/patient at a particular time point was pooled resulting in a sample pool of 45 µg/time point. Time point corresponding pools were analyzed by the developed LC ESI MS BU workflow. Peptide extracts corresponding to time point samples were run in duplet during LC ESI analysis. The "original run" SwissProt protein list was completed by proteins exclusively reported in the "replicate run" list ($p<0.05$ MASCOT ion score, score≥30) in a combined *mgf* file for *P2M* quantification. Finally, normalized protein levels were transferred to Statistica for time pattern analysis averaging duplicate time point intensities for each identified protein analyzing dynamic intensity pattern by linear regression at first instance. To screen for protein candidates, which potentially respond in the course of time, only those proteins were selected as candidates, which significantly fit the linear model ($p<0.05$) or display $R^2 \geq 0.9$. Thus, non-linear effects were examined by polynomial regression analysis. Thereby, only proteins displaying a significant fit to the polynomial model were selected as candidates. Additionally, a level increase or decrease was taken into consideration. Consequently, proteins which describe a distinct concave or convex shape in their time pattern without a clear slope direction were excluded from further analysis. Additionally, a fold change cluster method according to the "optimal matching" algorithm (Gabadinho *et al.*, 2011) was applied to the data to record non-linear approximately time dependent regulation pattern of proteins. Thereby, the *TramineR* package of the *R-project* was used. For pattern alignment three categories have been generated. The category "decrease" defined a minimum fold decrease of 0.5 of the protein intensity from a time point intensity value to the intensity value of the previous time point, whereas "increase" defined a minimum fold increase of 2 in the same manner and "equal" defined no change. The 2fold change value has been selected as significance threshold in consistence to the literature as already mentioned. Accordingly, 4 clusters have been calculated for the whole protein list. In a final approach the protein list was screened for already documented dry eye marker proteins and the time pattern of those "a priori" defined markers was screened with a lower linear regression threshold of $R^2 \geq 0.5$ to ascertain regulation tendencies in suspective dry eye proteins. Accordingly, linear, polynomial, fold change clustering and "a priori" selection were used to generate a final candidate list for Ingenuity® analysis and manual literature screening. In the second part of the study, MS observed tear dynamic pattern changes were validated by MA analysis using a higher number of subjects and comparing POAG patients

(*N*= 16, 70 +/-10 years, 11 females, 5 males) with age-matched healthy controls without any ocular disorders (*N*= 15, 11 females, 4 males, 51 +/- 10 years) over five time points (0, 2, 4, 12, 24 weeks +/- 1week) for POAG and over three time points (0, 4, 24 weeks/+/-1 week) for healthy subjects. Thereby, commercial available antibodies against selected representative MS derived candidate proteins, dry eye associated preselected markers and cytokines were immobilized on nitrocellulose slices and incubated with fluorescent labeled longitudinal tear protein samples. For analysis, a sciFLEXARRAYER MA spotter equipped with a piezo driven spotting unit (100-500 pl/drop) and a 428$^{TM}$ array laser scanner equipped with a green and red laser for fluorophor excitation (532/635 nm) were employed. MA preparation followed a laboratory-established workflow (Boehm et al. 2011, 2012; Bohm et al.2011). Accordingly, 1 nl commercial antibodies was applied per spot on Oncyte Avid 6.5mm x 6.5mm nitrocellulose slides in triplicate and incubated with 7.5 µg of fluorescent labeled (Cy5 Alexa Fluor 647) tear protein of each individual and time point to generate a longitudinal intensity pattern for each subject. Proteins, which could not been spotted properly, were excluded from further analysis. Spots were scanned in preview with 20 and 50 µm and for quantification with 10 µm resolution. Quantification was realized by use of ImaGene® version 5.5 exporting median spot and background signals to Statistica and difference was calculated between both signal median values. Negative difference values were excluded from the list, which contained triplicate antibody response intensities for each patient. Mean intensities encircling all group individuals (POAG *vs* Control) were calculated for each time point and each candidate. For regression analysis, only tendencies were focused on. To obtain a more accurate impression, if the mean intensity level of a certain protein converges from POAG to control, a time point comparison was operated. For that purpose, the mean of all time point intensities of the Control group was compared to the mean intensity of the initial and final time point of the POAG group estimating the confidential degree of the “POAG to Control level approximation” by t-test. A highly confidential approximation should therefore show significant intensity differences between the initial time point of the POAG group compared to the mean value encircling all time points of the Control group, but displaying non-significant differences between the final time points of the POAG group compared to the overall control group level. A brief overview on the study workflow is illustrated in Fig. 25.

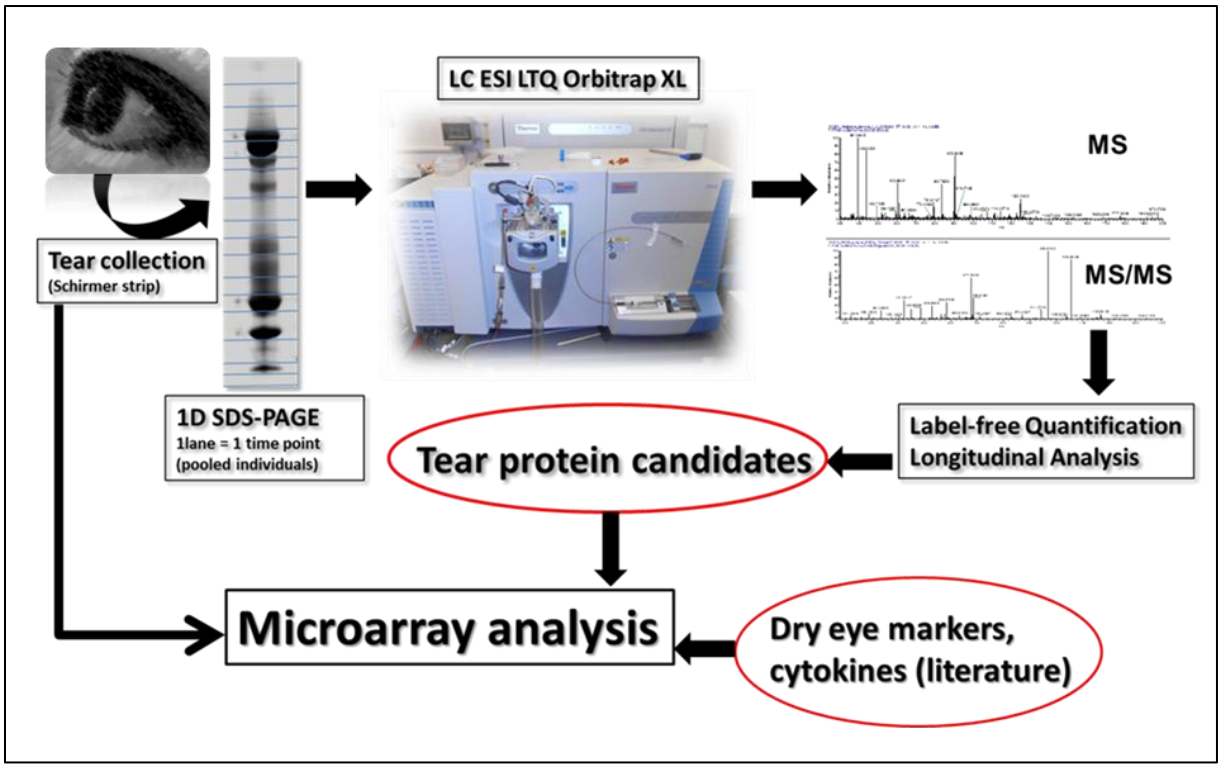


**Fig 25** Study design of the Taflotan® sine tear film study: Schirmer tear samples from POAG patients were processed by the LC ESI BU workflow following statistical analysis of longitudinal protein pattern dynamics. Results were validated by use of MA analysis in a larger patient cohort including POAG patients and healthy controls. (Funke *et al.*, 2014)

# 4 Results

## 4.1 Microbore-RP-HPLC (for MALDI)

The developed column system was found appropriate for direct fractionation of crude samples without further sample pretreatment indicated by succesfull retaining of contaminant particles by the Security Guard™ cartridge (Fig. 26). Defined isolated fractions could be deposited on MALDI targets displaying low sample carry-over and homogene crystallization (Fig. 27). Regarding MS output, the method generates “high quality” linear MS spectra regarding *m/z* peak pattern of selected LC fractions (Fig. 28). Furthermore, high separation efficiency of the LC system could be achieved (Fig. 29). Compared to non-fractionated samples, an elaborative purification benefit could be registered for the HPLC prepared samples which resulted in a distinct increase of peak intensities (Fig. 30). Regarding training samples, the method showed a high level of run-to-run reproducibility (Fig. 31, 32). Retention deviation was estimated <12 s on average for a 3 s fraction deposition frequency monitored for selected reporter peaks 2481, 4962 and 6275 *m/z* based on first component detection (Fig. 33). The spotting time could be adjusted to a high degree of speed counting 4 min 36 s for each LC run. During training set runs, the HPLC running time for each run was 35 min and the complete HPLC running time of 24 samples including equilibration runs and automated matrix spotting could be recorded (92x24x35= 7782 min + 24 x 10 Dummy runs= 240 min + 92 x 24 x 10 s matrix spotting/spot= 368 min) <6 days (139.8 h). The linear MS measuring rate using 50 hz laser frequency was set to approximately 44 s/spot. Accordingly, the study encircling analysis of all 6 study targets could be finished in approximately 27 h. In summary, the total analysis time including HPLC fractionation, matrix spotting and MALDI TOF MS did not exceed 7 days for 24 samples. Therefore, high quality MS pattern could be generated and the overall sensitivity of the approach prior to normalization was estimated by 856 RGC5 WARP-LC compounds corresponding to a mean number of 960 peaks detected in each LC run (*N*= 24). However, identification of exemplary reporter components 3789, 4279, 6648, 7208 and 8567 *m/z* detected in all samples was challenging. Direct fractionation of masses >4000 Da is critical in MALDI MS (Nilsen *et al.*, 2011) and even direct fractionation of peaks below this threshold was found problematic due to decreased reflector sensitivity. Only 3789 *m/z* could be detected by reflector analysis (Fig. 34), however, failing to reach threshold abundance for successful fragmentation. For this reason, an alternative strategy in reference to a comparable workflow (Boehm *et al.*, 2013) was chosen to clarify protein identities including ZIPTIP® C18 fractionation (2-40% ACN in 2% steps) of intact lysates, 1D SDS PAGE, intact protein extraction from the gel mass range of interest, MALDI linear reanalysis and in-gel digestion of the corresponding gel mass range for MALDI/LC ESI MS/MS analysis (Fig. 35, 36A). Despite reporters 3279, 4279 and 8567 *m/z* could be

redetected in linear MS spectra corresponding to ZIPTIP® fractions (Fig. 35) only 8567 *m/z* could be successfully gel-extracted in its intact form, reprofiled in the MALDI linear mode (Fig. 36B) most likely corresponding to ubiquitin (gel area B: ESI: polyubiquitin B; score= 114; gel area C: ESI: polyubiquitin B; score= 365; MALDI: ubiquitin-40s ribosomal protein S27a; score= 134; polyubiquitin B; score= 102). Confidently, literature screening supported the observed correspondence of 8567 *m/z* to ubiquitin in MALDI (Niu *et al.*, 1998, Sanders *et al.*, 2008) and ESI spectra (Ebeling *et al.*, 2000, Scalf *et al.*, 2000). Regarding CNS, ubiquitin was identified as a peak at 8565 *m/z* in brain tissue sections (Pierson *et al.*, 2004) and at 8588 *m/z* in R28 cells by SELDI-TOF-MS (Brust *et al.*, 2008) supporting the finding. The reporter 6648 *m/z* was found to refer most likely to cytochrome C oxidase, which was detected as the predominant protein in corresponding gel areas (area A: ESI: cytochrome C oxidase subunit 5a; score= 132; area D: ESI: cytochrome C oxidase subunit 7a2; score= 69; area A: MALDI: cytochrome C oxidase subunit 7c; score= 58). Despite the failure for intact linear reprofiling, the attribution of the component to cytochrome C oxidase was supported by the literature according to MALDI brain studies (Bruand *et al.*, 2011, Hanrieder, 2011, Pierson *et al.*, 2004). Despite two clarified reporter compounds, several other proteins could be identified in the focused mass range including profilin, 10 kDa heat shock protein, thioredoxin, galectin, 40s ribosomal protein S21/28, protein S100 A6 and ATP synthase protein 8 (gel areas A, B, C, D) and keratines (gel areas E, F). For the remaining reporter compounds only literature matching attemps could be realized attributing 4279 *m/z* most likely to a ß-amyloid polypeptide form exhibiting molecular weights of 4.2/4.3 kDa producing signals in the range of 4-5 kDa (LeBlanc, 1995, Lippa, 1993, McGowan, 2005, Rohner, 2005). The candidate marker at 3789 *m/z* most likely indicates calcitonin gene related protein neuropeptide (Goodman and Iversen, 1986, Jonhagen *et al.*, 2006, Kuwayama and Stone, 1987, Simon *et al.*, 2003), highly abundant in rodent CNS (Silverman and Kruger, 1989, Skofitsch and Jacobowitz, 1985) and also reported for tear fluid (Tsuji, 2012) as a peak of 3785 *m/z* (Mulvenna *et al.*, 2000). In summary, reporter mass identification was challenging leading to likely identification of ubiquitin and cytochrome C oxidase and critical records for ß-amyloid peptide and calcitonin gene-related protein. Despite low protein identification performance, the LC microbore method was employed for the analysis of tear fluid, however with low success yielding clearly less intact signals compared to cell lysates, most likely due to the less complex nature of tear fluid in the small to medium proteome range compared to cell samples. Consequently, TD approach was found to enable fast, reproducible and robust analysis of crude sample materials, e.g. cell materials, but contrary it was hampered by insufficient sensitivity towards tear samples and performance was also decreased by difficult, intensive follow-up steps considering the risk of uncertain protein identification.

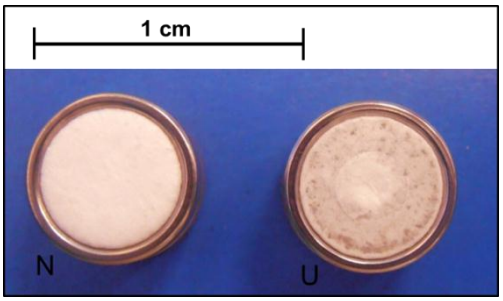


**Fig 26** Succesful retainment of contaminent particles of crude RGC5 test lysates by the direct coupled Security Guard$^{TM}$ cartrige indicated by contaminant spots on the filter RP1 resin (right) in comparison to a fresh filter (left).

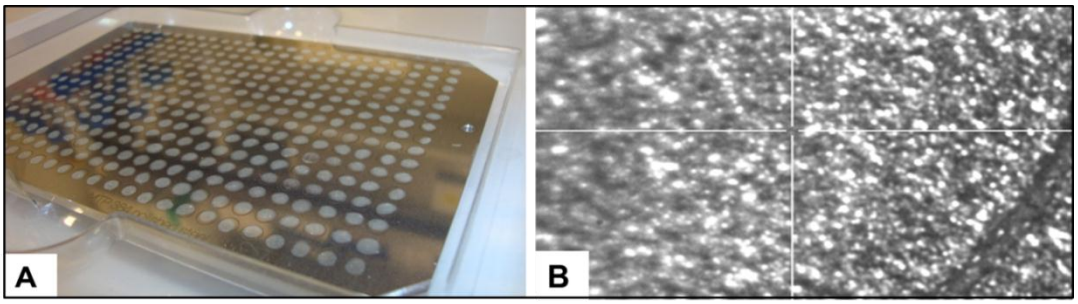


**Fig 27** Microbore fractions after automated matrix application resulting in A: distinct separated spots displaying B: homogeny crystal distribution allowing accurate representative measurements.

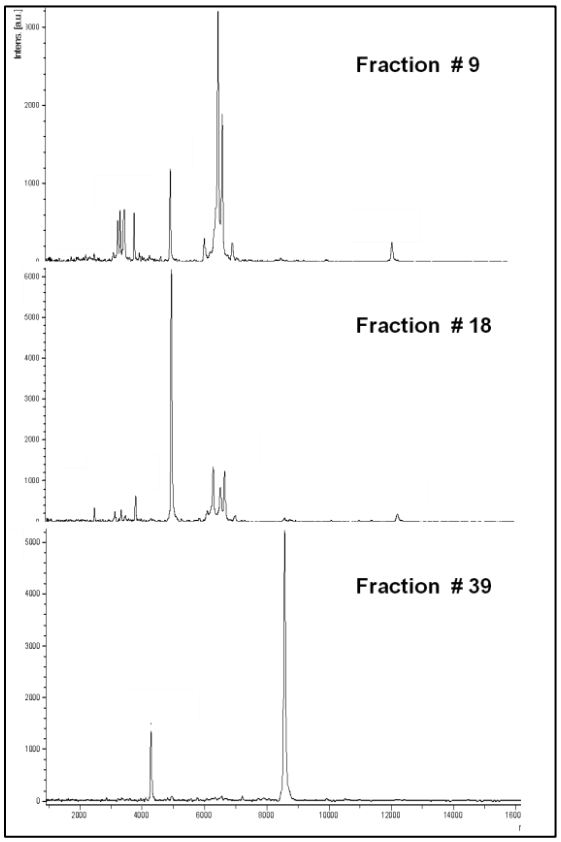


**Fig 28** Exemplary high qualitative linear microbore MS spectra corresponding to selected microbore LC MALDI TD fractions of crude RGC5 test sample lysates.

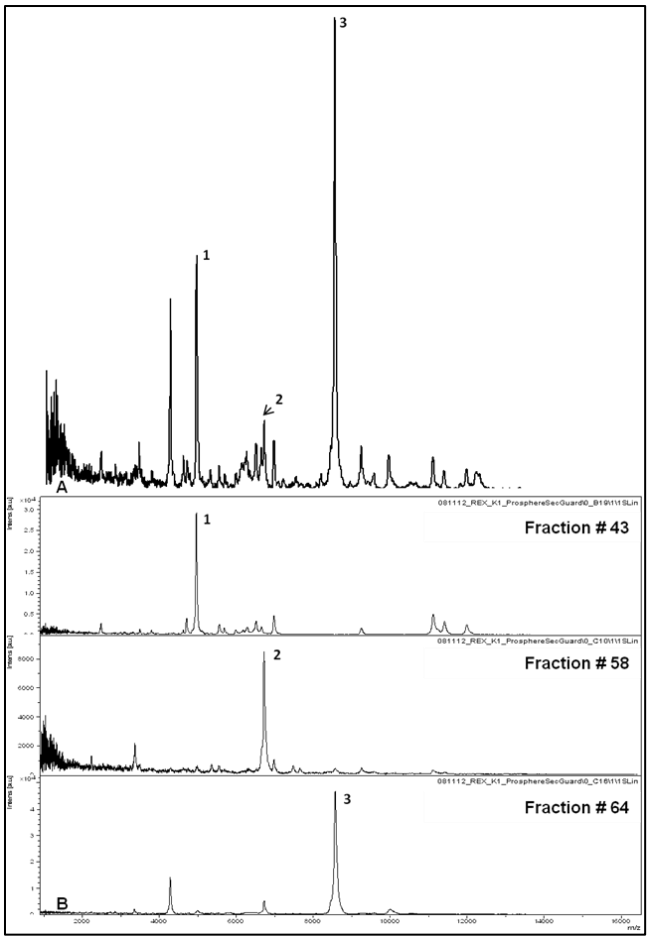


**Fig 29** Separation efficiency of the microbore LC MALDI TD approach indicated by three reporter peaks; A: Purified RGC5 sample without fractionation showing the three reporter peaks with noise background; B: Efficient separation of the three reporter peaks in three defined fractions by microbore HPLC.

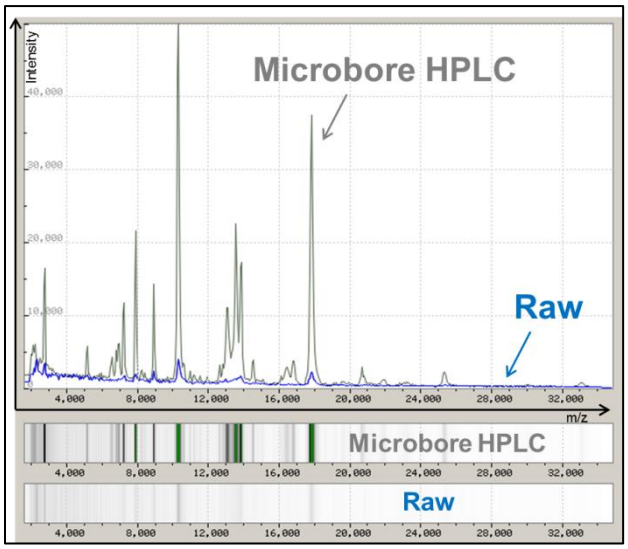


**Fig 30** Linear MALDI sensitivity increase obtained by microbore HPLC: Whereas the analysis of raw unfractionated RGC5 test samples showed only low intense peaks (blue MS spectrum) by use of microbore LC high intensity values for peak species could be obtained indicated in a merged HPLC run spectrum corresponding to 92 fractions (grey). The difference is also illustrated in the gel-like view below.

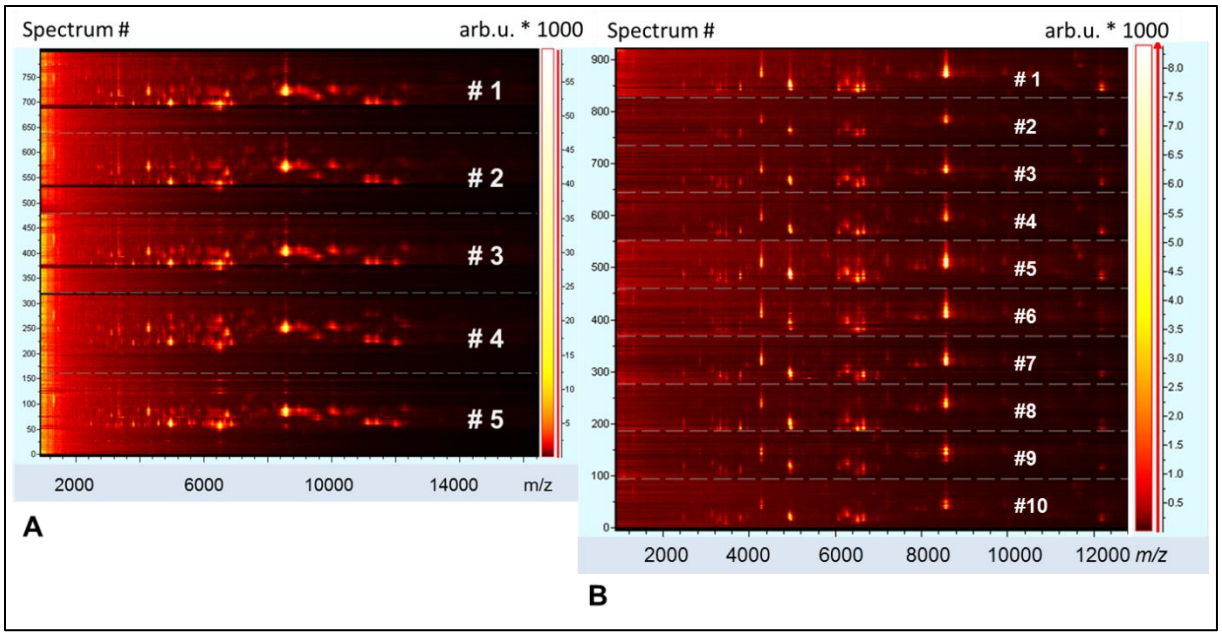


**Fig 31** Survey View of run-to-run reproducibility corresponding to A: 120 fractions/sample (retina sample replicates; *N*= 5) and to B: 92 fractions/sample (RGC5 samples; *N*= 10) showing high congruency in signal pattern.

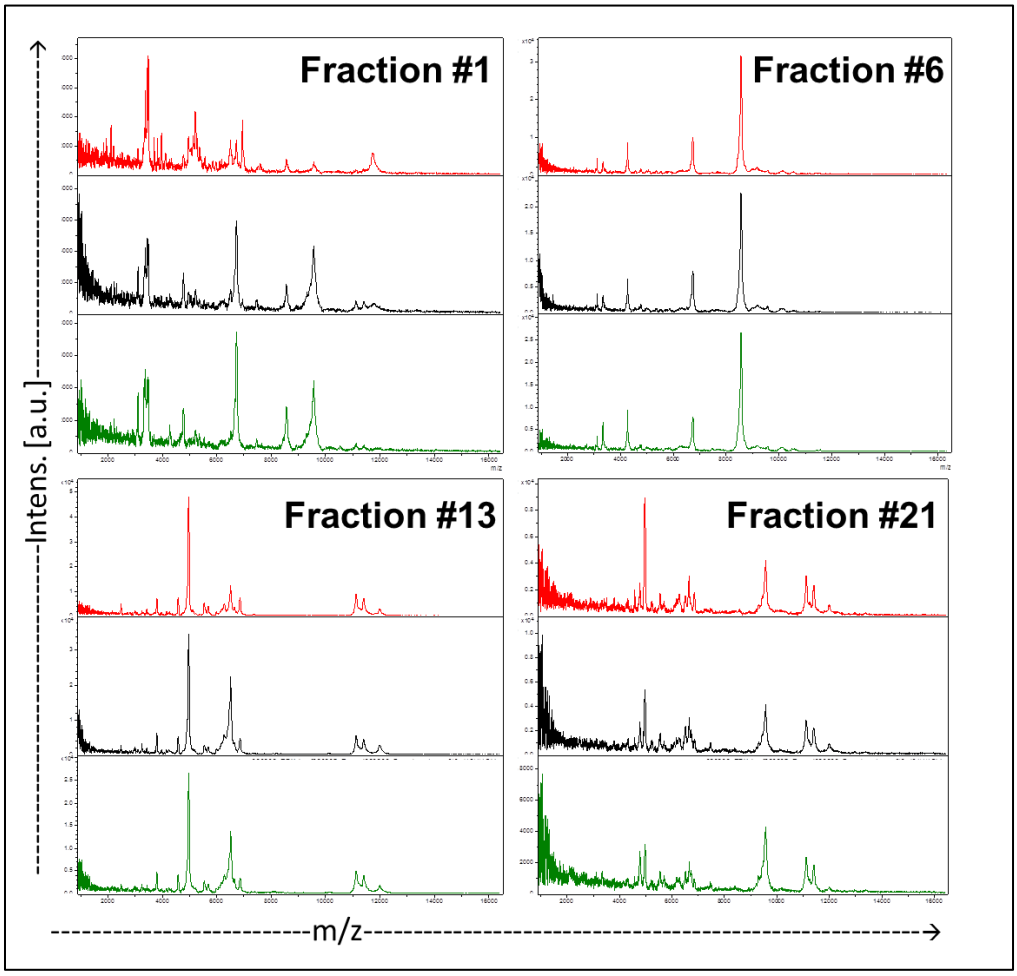


**Fig 32** Run-to-run reproducibility indicated by linear MS spectra corresponding to exemplary fractions of three similar processed retina samples showing high congruency in peak pattern.

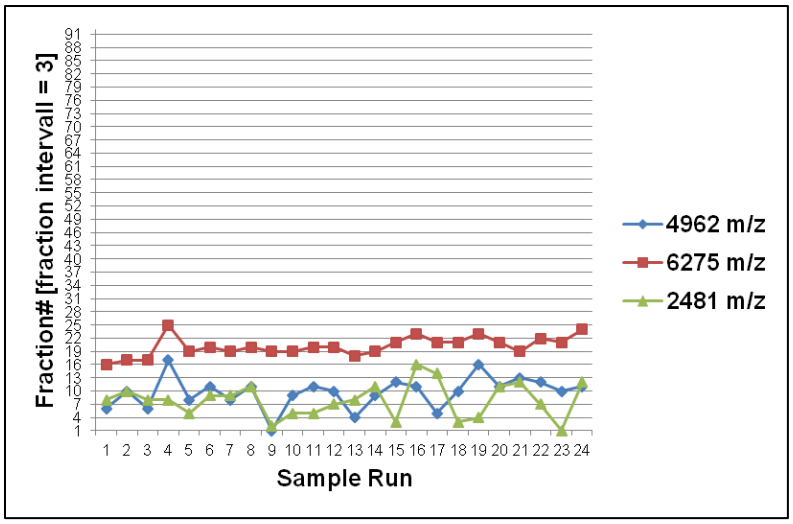


**Fig 33** Retention time (RT) reproducibility indicated by three reporter peaks detectable in RGC5 test sample runs (N= 24) showing a low degree of fraction shift (<12 s for 3 s/fraction).

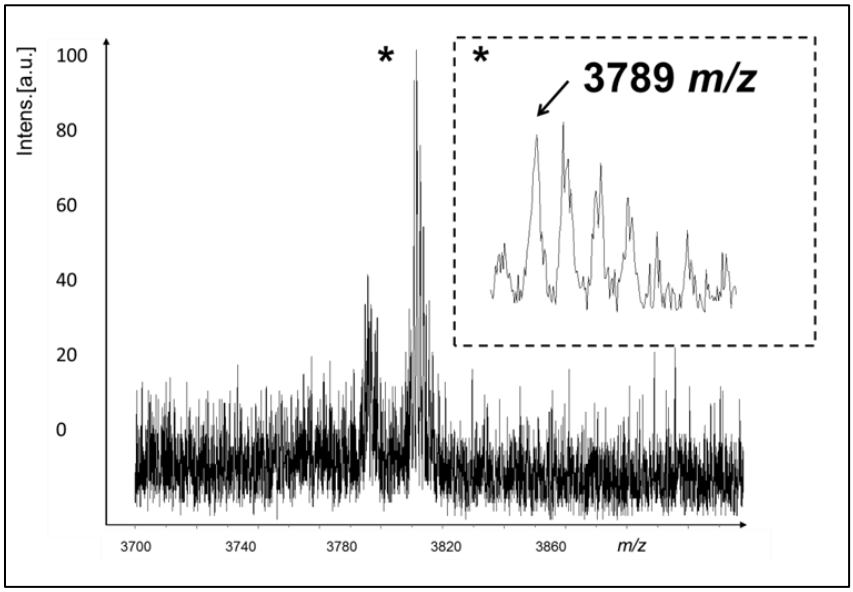


**Fig 34** Redetection of reporter peak 3789 m/z in the reflector mode: Despite the successful monoisotopic peak recognition (asterisk), the intensity was too low for fragmentation and MS/MS related identification.

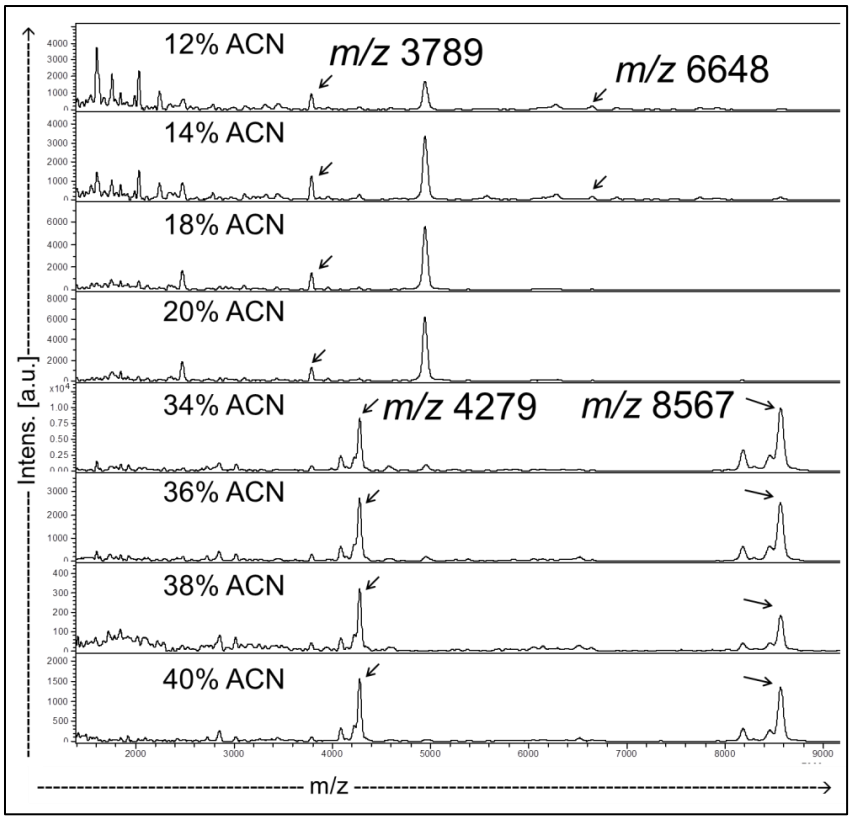


**Fig 35** Purification of four exemplary reporter masses by use of ZIPTIP® C18 2% ACN step purification for follow-up identification. The four components could be captured between 12-40% ACN.

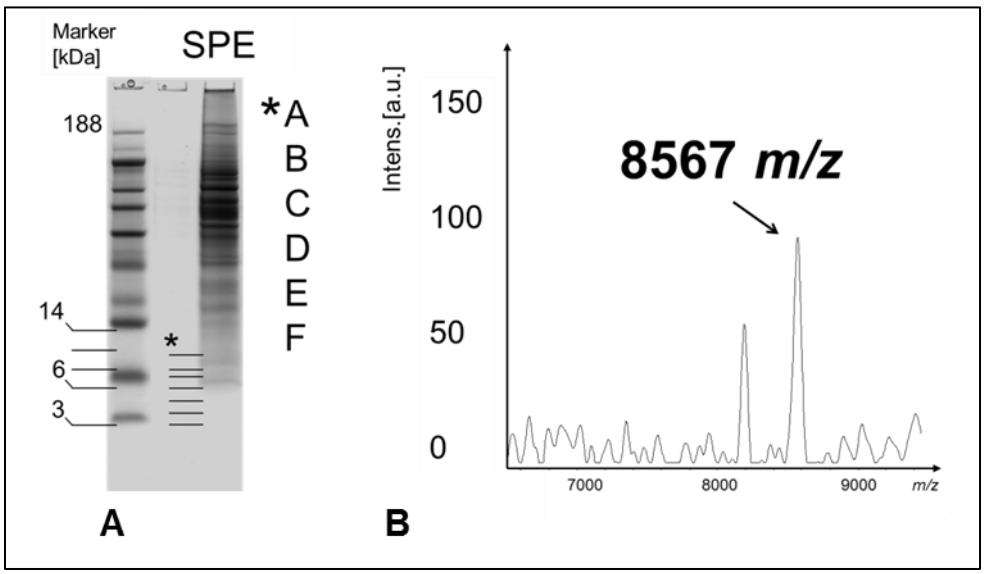


**Fig 36** Reprofiling and follow-up identification attempts of selected reporter peaks; A: ZIPTIP C18 purified 12-40% fraction (SPE) with focused mass regions (asterisk: A-F) between 14 and 3 kDa for reporter reprofiling by intact extraction, linear MALDI reprofiling, in-gel-digestion and identification by MALDI/ESI MS/MS analysis; B: Only reporter 8567 m/z could be successfully reprofiled with low intensity after gel intact extraction in the MALDI linear mode.

## 4.2 Capillary-RP-RP-HPLC (for MALDI)

For initially performance evaluation of the workflow, training samples were focused on. In case of cell lysates (*N*= 12), the combination of two sample pools lead to the detection of 13246 tryptic WARP-LC compounds. Thereby, 8180 MS/MS measurements lead to the identification of 294 proteins under stringent *MUDPIT* scoring conditions using SwissProt database. Compared to common proteomic strategies focusing on RGC5 cells used as test reference in this work, the sensitivity of the developed gel-based LC MALDI workflow was found comparable to the literature regarding approximately 300 (Yang and Tezel, 2005), 400 (Kim *et al.*, 2006, Tezel *et al.*, 2005, Zhang *et al.*, 2008) and 1000 detectable 2D gel protein signals (Kanamoto *et al.*, 2009). Using 2D gels followed by MALDI TOF MS Kim et al. reported 318 significant protein matches in RGC5 lysates (Kim *et al.*, 2009b). Also a 2D-nano-HPLC MALDI TOF/TOF MS/MS shotgun workflow focusing on lysates generated from in vivo rat retinal ganglion cells resulted in the identification of 268 proteins (Crabb *et al.*, 2010). In confidence with these studies, the present workflow showed an appropriate sensitivity also taking the stringent scoring strategy into consideration. Moreover the approach was proven suitable for lower amounts of material since 1D instead of 2D SDS PAGE was used as first fractionation dimension, which also simplified protein selection from the gel since instead of single spots whole mass regions were selected. Therefore, the workflow was also more economic regarding analysis time and laborative effort and was found suitable for the analysis of study tear samples. Accordingly, regarding capillary tear fluid by use of the developed workflow, a combinatory database search including 5535 MS/MS spectra obtained from two capillary sample pools including individual tears (*N*= 8), lead to the detection of 5640 peptide compounds and 90 significantly identified proteins using stringent *MUDPIT* scoring conditions. Inspection of raw data showed high qualitative MS spectra corresponding to LC fractions and also high qualitative MS/MS fragment spectra could be recorded (Fig. 37). Regarding the output of a large tear sample set, the taurine study was focused on. Single gel lanes in the tear study showed 3425 WARP-LC compounds, which were detected on average across all experiments (*N*= 19 lanes) leading to the identification of 267 significant unique tear proteins under stringent scoring condition (Fig. 38). In comparison, using 2D SDS PAGE 63 (Ananthi *et al.*, 2008) and 243 (Herber *et al.*, 2001) capillary tear protein spots have been detected which fits well with the results of the present study. Using SELDI-TOF MS 56 protein peaks in a range of 1500-20000 *m/z* (Tomosugi *et al.*, 2005a) and >1000 below 50000 *m/z* (Grus *et al.*, 2005b) have been described. Referring to protein identifications, only few works based on gel or MALDI techniques provide comparable results. For example, 30 capillary tear proteins have been identified by N-terminal Edman sequencing from 2D gels (Molloy *et al.*, 1997). Moreover high reproducibility of the HPLC system monitoring elution behavior of three different mass region

reporter peaks detected across investigated samples could be documented. Accordingly, a fraction shift of +/−0.8 fractions focused on a reporter ion 1792.92 *m/z* found in HPLC runs of the slice #9, a fraction shift of +/−0.9 fractions referring to ion 1400.73 *m/z* found in chromatographic runs corresponding to slice #13 and a shift of +/−0.8 fractions related to ion 2849.88 *m/z* detected in runs of slice #3 could be documented. Moreover, peptides showed a high degree of purity since CBB could be retained from MS analysis. In fact, an additional aromatic selectivity of the system could be supported by the effective retention of CBB traces originated from roughly destained test samples during method development. Thereby, CBB signals indicated by a deep blue staining of the spot matrix surface were detected in the final fractions of RGC5 test samples corresponding to higher solvent condition and reflecting a strong retention of the component on the stationary phase (Fig. 39). Regarding the measurement protocol, several limitations of the MALDI system could be revealed. Differences in sample and matrix spotting could lead to crystal caldera formations challenging homogeny analysis leading to quality differences in the MS output. Another drawback is the high number of unassigned MS/MS spectra in database searches also reported in the literature (Kapp *et al.*, 2005, Katz *et al.*, 2007, Ning *et al.*, 2010), which could be due to database records or to analysis limitations, encircling spectrum quality and peak detection tenacity. Regarding the *SNAP* algorithm, it was found in some cases, that a misleading peak in near neighborhood of the real monoisotopic peak was selected as parent mass precursor, which can lead to inaccuracies in fragmentation and MS/MS pattern assignment. Besides, post-processing of MS/MS spectra regarding smoothing and noise reduction increased the MS/MS annotation rate, thereby increasing also the number of scores of already identified hits. However, this approach was evaluated as highly time consuming and therefore not suitable for large datasets.

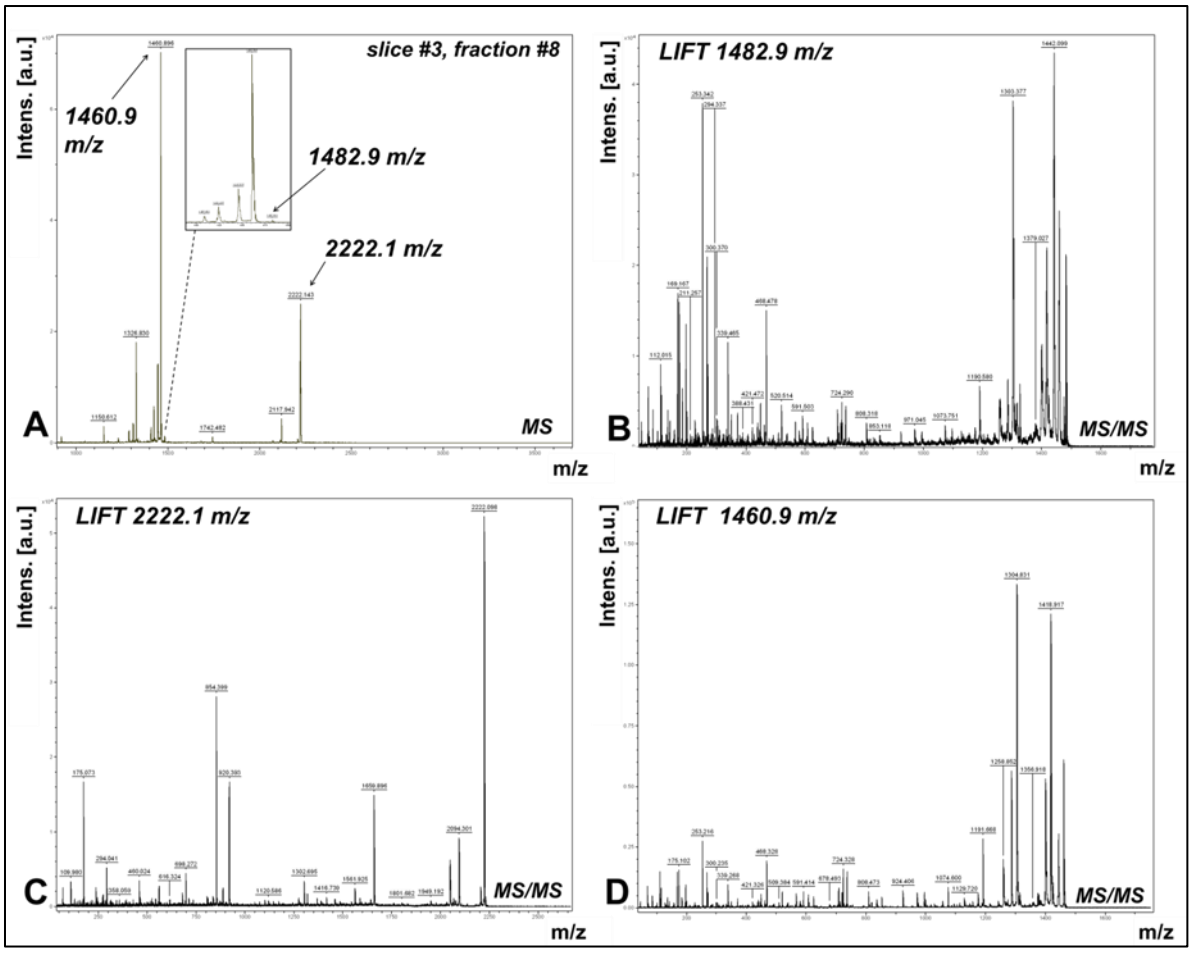


**Fig 37** Performance of the capillary RP RP LC MALDI BU approach; A: Detection and resolution of three exemplary masses showing low (1482.9 *m/z*, zoom view), medium (2222.1 *m/z*) and high intensity (1460.9 *m/z*); leading to B-D: high qualitative fragment MS/MS spectra.

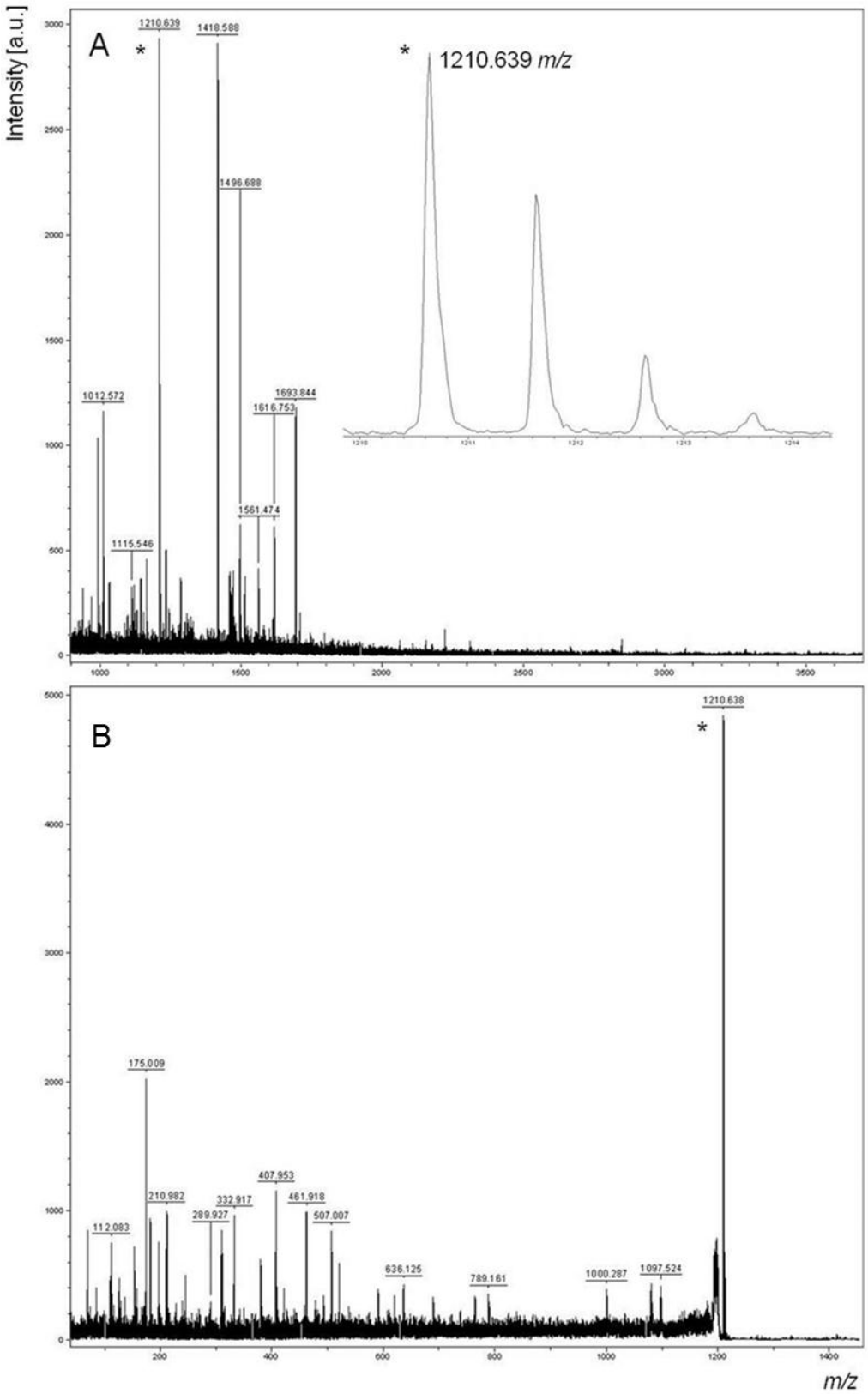


**Fig 38** Exemplary succesful protein identification for proline-rich protein 4 (PRP4) by fragmentation of A: high resolution precursor 1210.639 m/z (asterisk, zoom view) leading to B: high qualitative MS/MS spectrum allowing identification of PRP4 (Funke *et al.*, 2012)

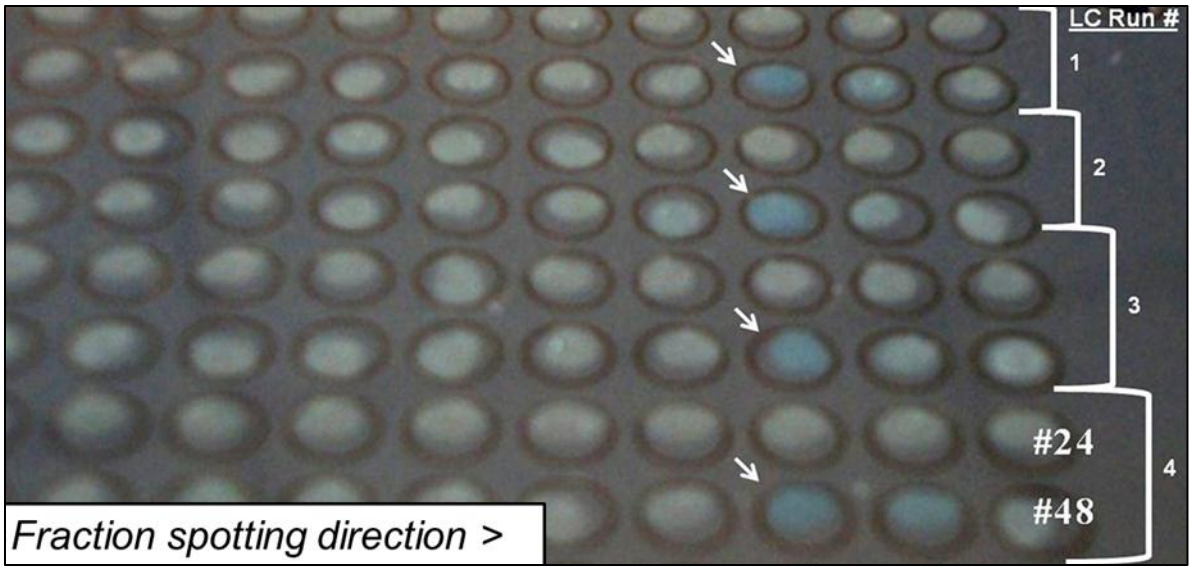


**Fig 39** Strong CBB retention indicated by strong reproducible blue crystal staining in final fractions (indicated by arrows) of 48 fraction training sample test runs supporting additional aromatic selectivity of the developed capillary RP RP HPLC system (Funke *et al.*, 2012)

## 4.3 Capillary-RP-HPLC (for ESI)

Employing the 80 min LC ESI gradient, the total processing period for one gel lane corresponding to one sample was calculated to ~1.3 days (17 x 80 min gradient + 17 x 30 min washing run= 1870 min= 31.17 h). To reduce the analysis time, at first washing runs have been eliminated. De facto, after chromatographic inspections, no distinct signs of carryover were found. The intensive chromatographic inspection of representative replicate RGC5 slice digests (1/17 lane, mass area #2, #4) (Fig. 40) showed, that predominantly peptides eluting from 20 to 40 min of the 80 min gradient area contributed to significant protein identification (Fig. 41). Taking a system dead volume of ~1.6 min (tubing: 0.005" ID, 0.127 µl/cm, 86 cm length; flow rate 6.7 µl/min= 0.127 x 86 = 10.922 µl; 10.922µl/6.7 µl/min= 1.6 min) into consideration, most likely the elution profile reflected the observation, that mainly hydrophobic peptides favored for ionization in ESI MS, which is in confidence with the literature (Stapels *et al.*, 2004). Adjustment of the starting mobile phase composition to 15% B saved analysis time and increased sensitivity in case of the 80 min gradient. An optimization in 5 min steps referring to the main elution area between 20 and 40 min of the reference 80 min gradient (Fig. 42) showed a distinct sensitivity decrease below 35 min, whereas from 80 to 35 min a slight decline could be observed. In accordance, the range between 40 and 80 min was focused on for further optimization (Fig. 42). The proportional adaption of this "optimum gradient range" in 10 min-steps resulted in a significantly linear increasing number of protein identifications for both, relaxed and stringent scoring strategies (MASCOT ion score $p<0.05$: $R^2= 0.98$, $p= 0.0112$; peptide score≥30: $R^2= 0.99$, $p= 0.0052$). Consequently, as a compromise between analysis time and sensitivity, the optimized 50 min gradient was selected as study setting which lead to a total analysis time of ~0.6 days per

sample (lane) (17x50 min [analytical gradient] + 1x 30 min [washing run] = 880 min= 14.67 h) representing a 54% reduction of analysis time. The final optimized 50 min LC ESI workflow showed a reproducible efficient peptide elution pattern with the majority of masses observed between 10 and 40 min RT (Fig. 44) and a high chromatographic congruency of technical replicates of corresponding gel mass areas indicated by inspection of TIC chromatograms (Fig. 45). A high RT reproducibility inferred from time monitoring of reporter ions (n= 20) observable in all technical replicates (*N*= 6) of investigated gel mass areas (*N*= 8, M1-8) (Fig. 43) could be demonstrated. Thereby, the mean *CV* was 0.62% (*SD*= 0.57%) with a minimum *CV* value of 0.15% for reporter peak 1067.00 *m/z* observed at 34.02 min mean RT in all replicates of gel mass area M6 (Fig. 46A) and a maximum *CV* value of 2.37% for reporter peak 544.33 *m/z* observed at 16.65 min mean RT in all replicates of gel mass area M2 (Fig. 46B). The reproducibility values of the system fits well with observations reported by the literature for comparable systems reporting a range of 0.17-4.5% *RSD* (Duan et al. 2009) and 0.1-2.6% *RSD* (Dunn *et al.*, 2008). Furthermore, high analysis accuracy observing most of high scoring masses with an error of approximately 2-4 ppm (Fig. 47) could be achieved. Also, a reproducibility of quantitative sensitivity was determined with a *CV* of 1.94% regarding the number of CID fragmented precursor ions, which means that in replicate runs nearly identical numbers of peptides have been detected. Thereby, the qualitative overlap of CID precursors was 21% in all replicates, after outlier extraction increasing to 57% in 4/6 of the samples. The analysis of CID fragment congruency lead to a heterogenic image of fragmentation since the overlap of investigated precursors showed a mean value of 22% with a *SD* of 28% with a maximum value of 64% and minimum value of 0% depending on estimated precursor ions (Fig. 48). These observations conclude a relatively high congruency in precursor detection and selection but a lower degree of precursor fragmentation control. Resulting consequences for protein characterization were investigated on in the next steps. The sensitivity of the initial 80 min workflow towards RGC5 samples (*N*= 8) was estimated with a mean of 1521 +/- 128 proteins (MASCOT ion score, $p<0.05$) and 633 +/- 72 proteins using the more stringent scoring strategy (peptide ion score >30) decreasing only slightly in the optimized 50 min gradient workflow (Fig. 49, 50). Regarding the qualitative reproducibility analysis, a congruency of 33% in all samples to 76% corresponding to half of the sample set was observed in cell samples under relaxed scoring condition. Additionally, a congruency of 49% in all samples to 88% in half of the sample set using more stringent condition could be determined regarding the different cell samples run on different days on different gels focusing on the 80 min gradient method. The optimized 50 min gradient workflow resulted in a mean overlap of 52% in all technical replicates (*N*= 6) to 76% overlap in 4/6 of replicates encircling all investigated gel mass areas (*N*= 8) under relaxed scoring condition. By use of more stringent scoring the overlap was increased to 63% in all replicates and 88%

congruency observed in 4/6 of the replicates (Fig. 51). Thereby, the observed reproducibility values were in confidence to the values inferred from the literature (Crabb personal communication 2013, Mezhoud *et al.*, 2008, Tabb *et al.*, 2010, Zhang *et al.*, 2005). In summary, the results emphasize the robust performance potential of the developed workflow with drawbacks in fragmentation control. Compared with the literature the optimized gel-based LC ESI workflow showed a high degree of sensitivity and was found to distinctly exceed gel-based as well as MS related protein detection approaches and was therefore employed for the examination of conjunctival cells and tear fluid studies.

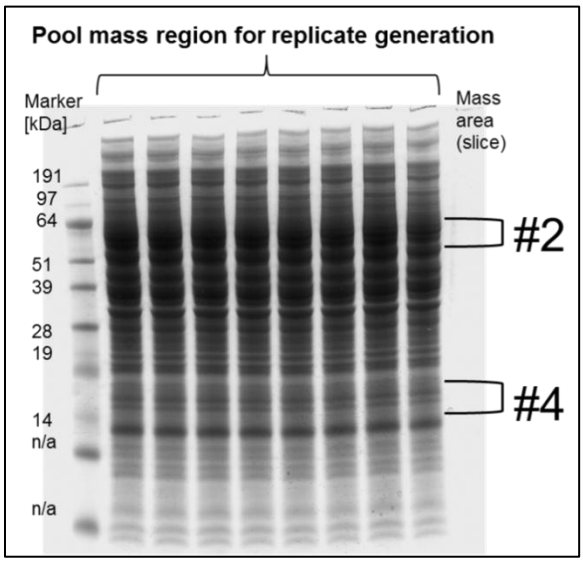


**Fig 40** Training sample replicate gel for method development containing 80 µg RGC5 lysate/lane; mass area #2 and #4 were depicted pooled, digested and processed and split tp identical replicates immediately befor LC ESI MS analysis.

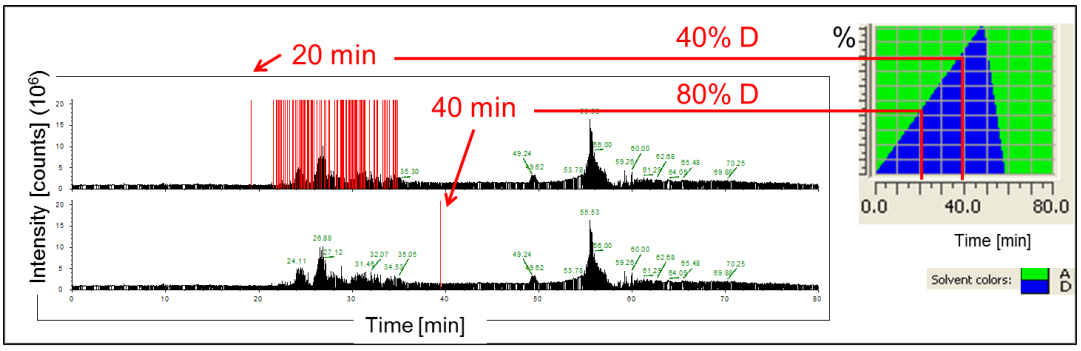


**Fig 41** Chromatographic view of the initially developed 80 min HPLC gradient indicating the RT range containing spectra, which contributed to successful protein identification. Proteins were identified between 20 and 40 min. RT, which represents 40-80% running buffer B. The chromatographic inspection was used as reference for follow-up gradient development.

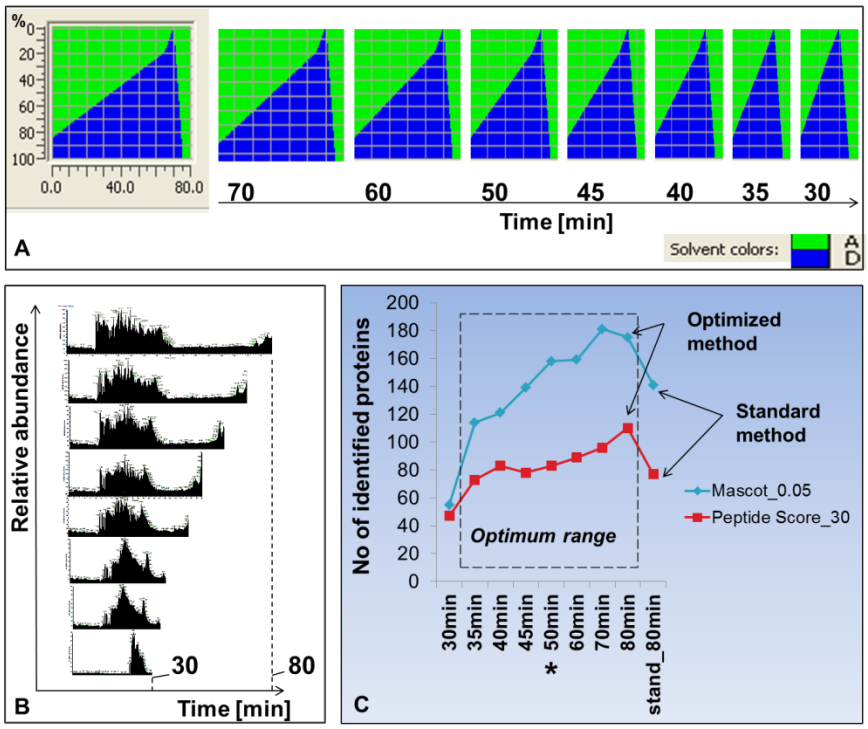


**Fig 42** LC ESI gradient development; A: Stepwise gradient adaption (5 min steps) to reduce analysis time; B: chromatograms corresponding to adapted gradients showing a distinct elution signal decline correlating with decreased gradient time; C: Sensitivity obtained in the course of gradient adaption and optimization, whereby an optimized 50 min gradient was selected as final optimum method (asterisk) due to a compromise between sensitivity and analysis time.

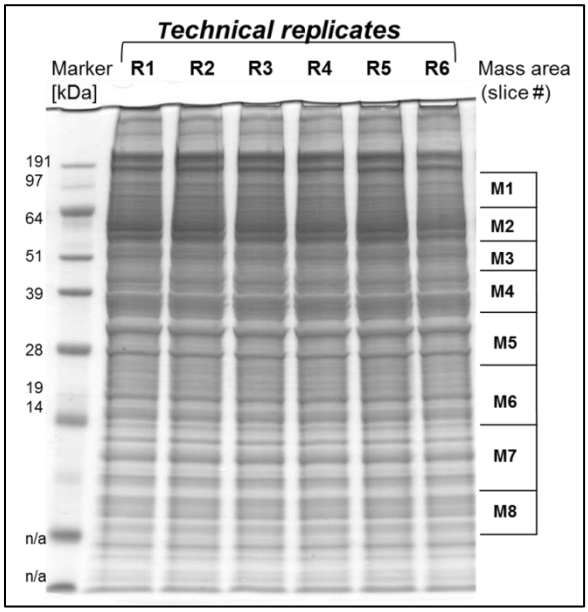


**Fig 43** Training sample replicate gel for reproducibility testing oft he developed LC ESI MS BU approach. Technical replicates for MS analysis were selected from RGC5 replicates (80 µg/lane) focusing on 8 mass regions (M1-M8). Mass area replicates (e.g. M1, R1-R6) were selected, pooled, in-gel digested ZIPTIP® purified and split to identical aliquots for LC ESI MS analysis.

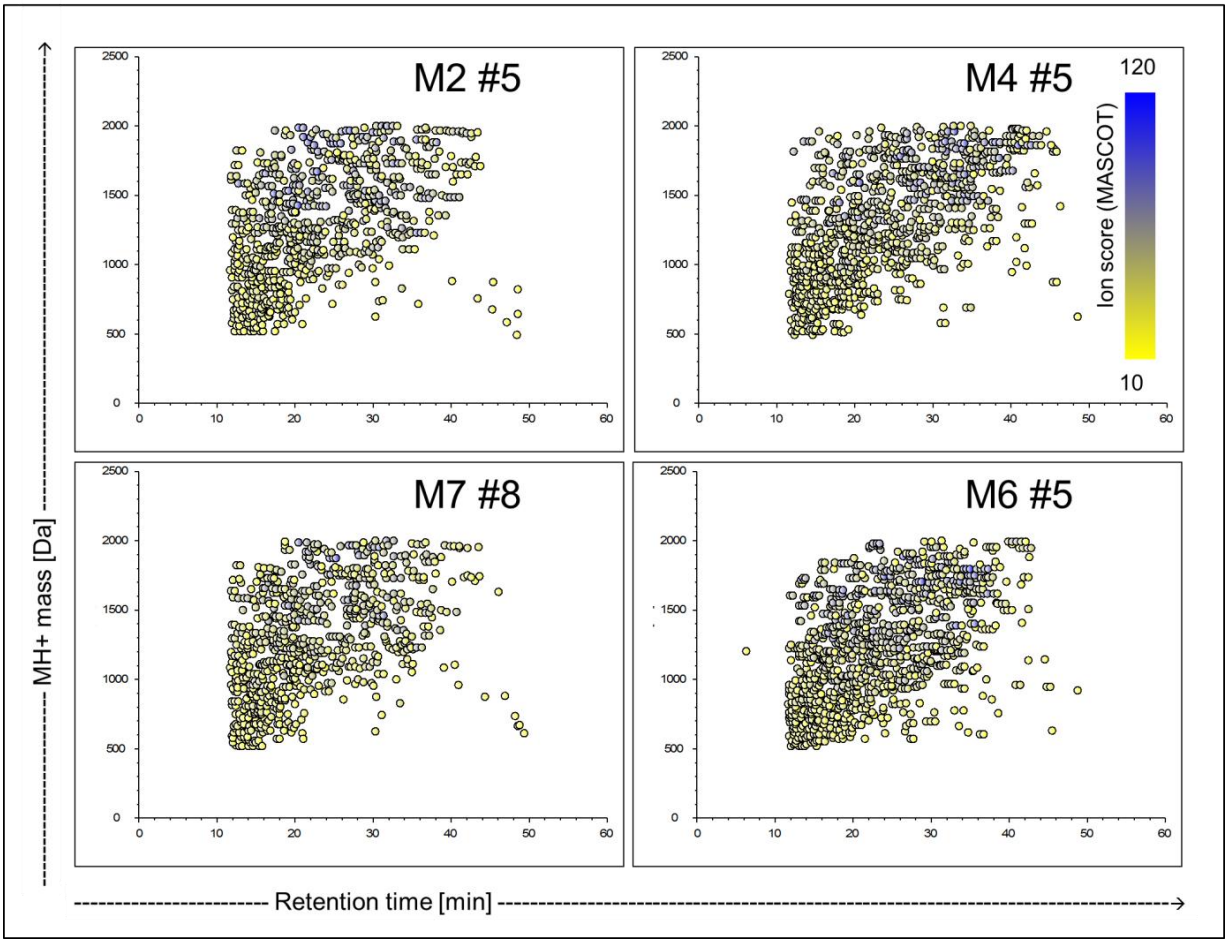


**Fig 44** Exemplary replicate elution profiles of identified peptide masses corresponding to the developed 50 min gradient showing high congruency and optimal fit to the gradient time range.

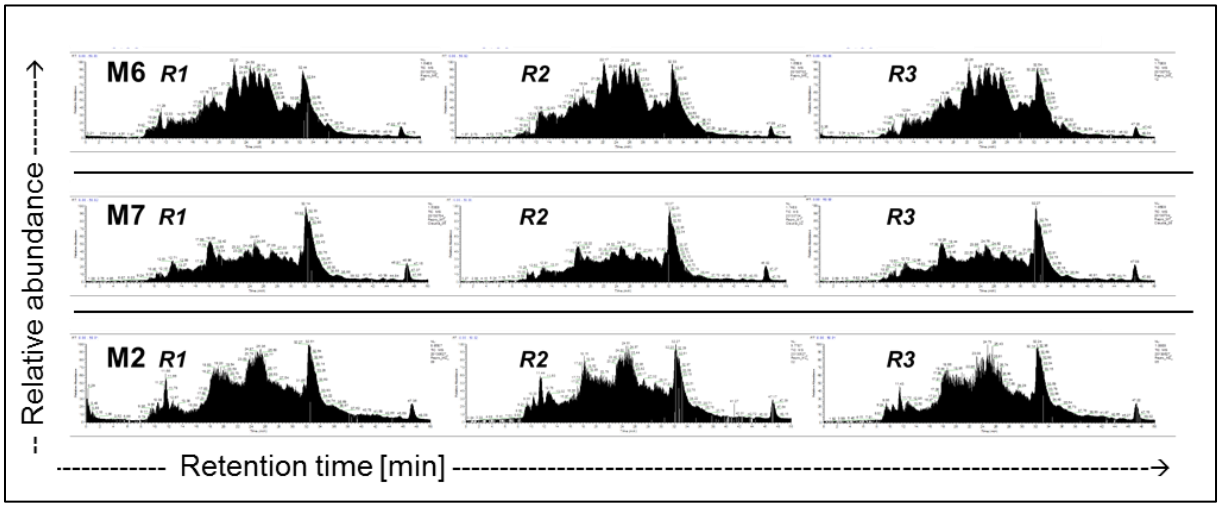


**Fig 45** Exemplary TIC chromatograms corresponding to three exemplary replicate runs for three exemplary mass regions (M6/7/2) showing high elution pattern congruency indicating high technical reproducibility of the HPLC system using the 50 min gradient method.

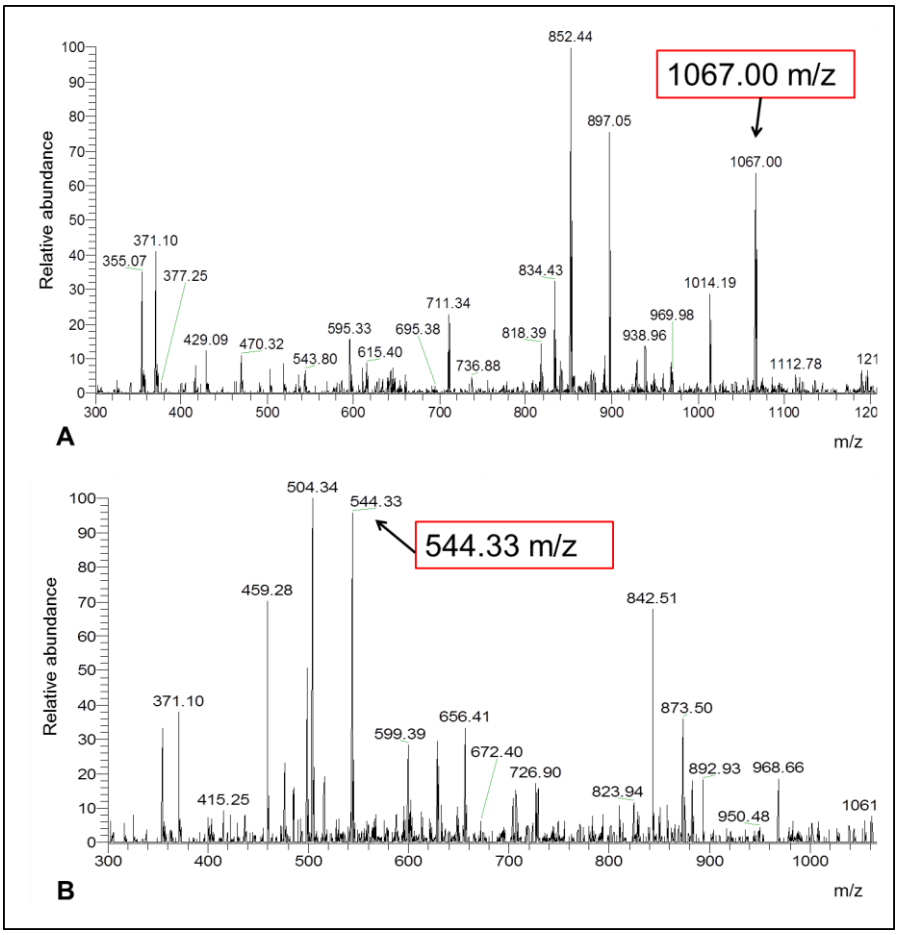


**Fig 46** Two reporter ions representing minimum and maximum RT reproducibility values inferred from RT monitoring of A: 1067.00 *m/z* observed at mean RT 34.02 min in all replicates of M6 and showing a 0.15% *CV*; B: 544.33 *m/z* observed at mean RT 16.65 min in all replicates of M2 showing a 2.37% *CV*.

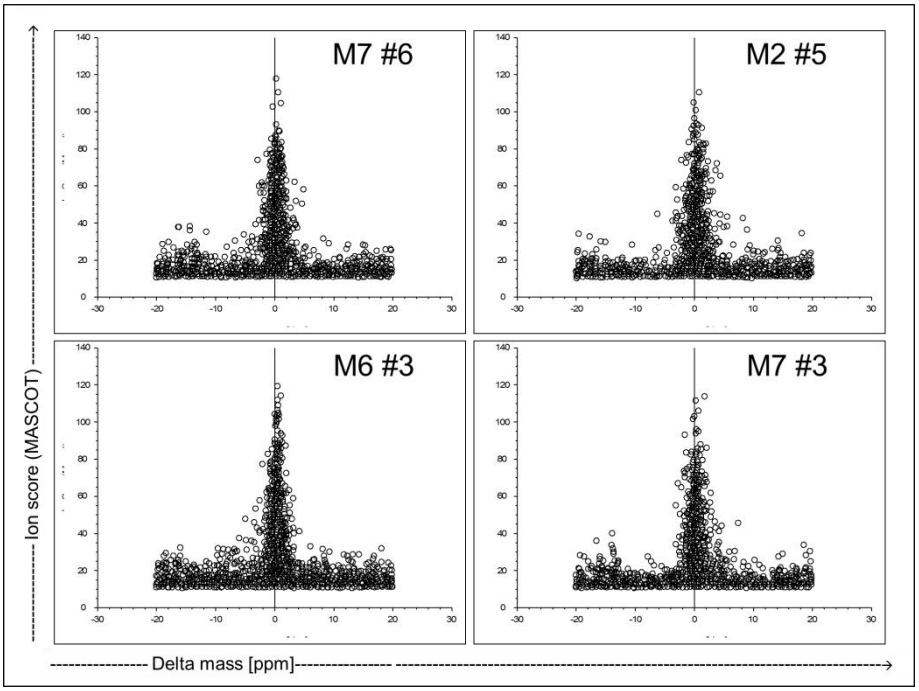


**Fig 47** Mass accuracy achieved during 50 min gradient LC ESI MS analysis exemplary shown for exemplary mass region corresponding technical replicates displaying the majority of high scoring masses detected with 2-4 ppm deviation.

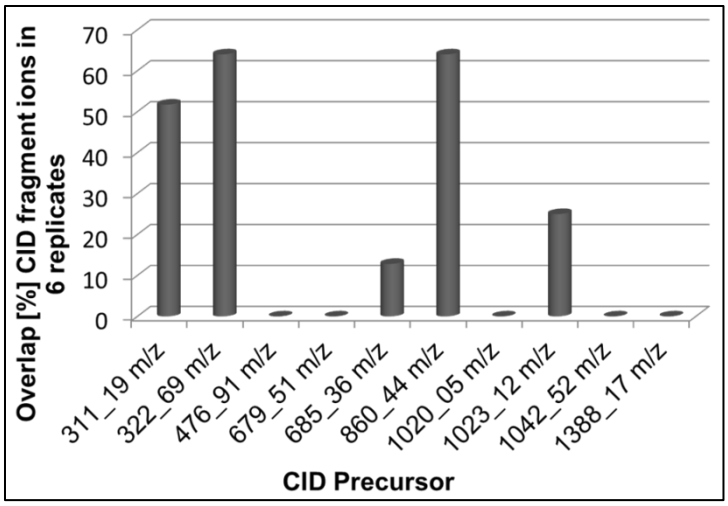


**Fig 48** CID fragmentation observed for reporter precursors (*N*= 10) displaying a highly heterogenic pattern; whereas some reporter ions show high qualitative congruency in obtained CID fragments regarding technical replicates (e.g. 322.69 m/z) several reporter precursors (e.g. 476.91 m/z) should no overlap in fragment contingents.

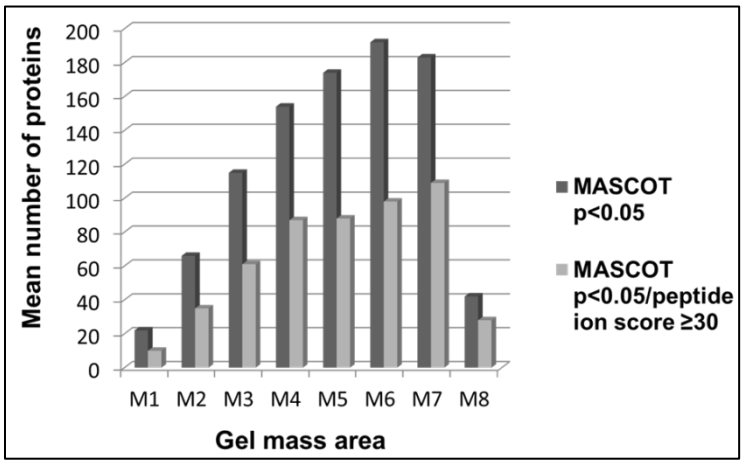


**Fig 49** Mean protein output regarding test mass areas (M1-8) by use of the 50 min gradient LC ESI MS method.

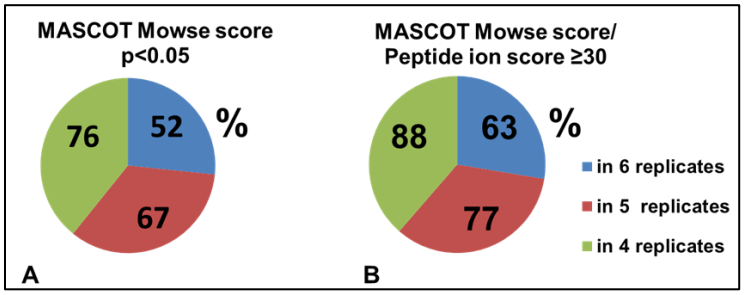


**Fig 50** Qualitative reproducibility of the 50 min gradient LC ESI MS BU approach illustrated by identificated proteins with two scoring strategies; A: relaxed; B: stringent.

## 4.4 Proteomic characterization of ocular surface sample species

### 4.4.1 Capillary tears

Gel images provided a clear pattern of capillary tear proteins with distinct areas of protein migration with respect to protein reducing and protein amount (Fig. 50). The LC MALDI method (15 mass areas/lane) as well as the LC ESI workflow (17 mass areas/lane) (Fig. 51) provided a deep view to the tear proteome in a mass range between 3-188 kDa. Moreover, as already shown for training samples, SDS PAGE showed a high degree of reproducibility inferred from pattern congruency based on pool tears of healthy subjects (*N*= 6) (Fig. 52). In summary, >1000 proteins could be documented with both approaches. Actually, the MALDI approach yielded in 267 proteins from non-reduced capillary tear samples (appendix 1), which was significantly less sensitive despite consumpting a higher number of sample lanes (*N*= 19) in comparison to the LC ESI approach, which provided a significant higher sensitivity resulting from the analysis of only few sample lanes (*N*= 3). Also, the LC ESI approach screening the Swissprot database and implementing an additional Mascot *MOWSE* score threshold value of 35 yielded in the identification of 1427 tear proteins (appendix 2). The output clearly exceeded the results of former “in depth” mapping approaches, identifying 491 (de Souza *et al.*, 2006) and 589 (Zhang *et al.*, 2009) human tear proteins and was comparable to the sensitivity obtained with a high speed Triple TOF workflow leading to the identification of 1543 human tear proteins (Zhou *et al.*, 2012). Regarding the protein ranking in the present work, the 10 top scoring proteins in ESI analyzed capillary tears were lactotransferrin (score 1982), complement C3 precursor (score 1680), basement membrane-specific heparan sulfate proteoglycan core protein (score 1669), serum albumin precursor (score 1448), keratin, type II cytoskeletal 1 (score 1389), titin (score 1300), zinc-α-2-glycoprotein (score 1091), mesothelin (score 845), keratin, type I cytoskeletal 9 (score 742) and polymeric immunoglobulin receptor (score 741). In case of MALDI results the top three prominent tear proteins identified with distinct higher scores than in ESI experiments were lactotransferrin (score 16010), lipocalin-1 (score 15876) and proline-rich 4 protein (score 15116). MALDI identified proteins ranking below these top scoring tear proteins exhibited a rapid score decrease up to 32% like e.g. observed for lysozyme C (score 4800), albumin (score 4415) and polymeric immunoglobuline receptor (score 4283), whereas lipocalin-1 (score 704) was found among the top 20 scoring proteins. In contrast to the MALDI results, proline-rich protein 4 was found as protein number 51 in the scoring rank (score 271) in the ESI analysis. Another example is zinc-α-2 glycoprotein (score 2514), which was found among the top 10 scoring ESI detected proteins, whereas it was found in MALDI experiments at a distinct lower score rank (rank 17). A high portion of proteins was congruently detected using MALDI and ESI ionization techniques, e.g. clusterin, α-2-macroglobin, mammaglobin B, ceruloplasmin, annexin A1, haptoglobin or serotransferrin. Despite several proteins

overlapped with relatively high scores in both, the MALDI and ESI approach, some proteins, e.g. ribosome-binding protein 1 or neutrophil gelatinase-associated lipocalin were found with comparable low scores in result lists of both workflows supporting their existence in tear fluid. Whereas the ESI workflow provided higher sensitivity leading to an increase in protein identifications and identifying hundreds of proteins, that failed to be detected by the MALDI workflow, several proteins like transthyretin (score 241), apoptosis-inducing factor 2 (score 145), fibrinogen (score 37), eukaryotic translation initiation factor 2A (score 152), complement C4 A (score 50) or Nck-associated protein 5 (score 53) could exclusively be detected by LC MALDI. Since both workflows depend on a comparable gel-based fractionation strategy and moreover the MALDI approach depends on a more sophisticated LC technique highlighting a two phase column system, these findings most likely reflect the influence of the used ionization method on the output of the tear fluid analysis. Regarding the 267 capillary tear proteins, which could be identified in the taurine study by MALDI the majority referred to intracellular proteins (Fig. 53A), most likely originated from ocular surface epithelia, whereby most of the detected cellular tear proteins were found to be localized in the cytoplasma, whereas only a minority, were found to be derived from the membrane. Actually, the majority of organelle associated proteins were related to the nucleus. Moreover, a major part of MALDI identified tear proteins was found to be linked to the immune system (Fig. 53B). In accordance, woundhealing related proteins could be documented with high portion (Fig. 53B). Regarding the congruency of the MALDI protein list with the literature an overlap of 23% with the list of de Souza et al. (de Souza *et al.*, 2006), of 50% with the list of Li et al. (Li *et al.*, 2005), of nearly 50% with the lists of Zhou et al (Zhou *et al.*, 2009b, Zhou *et al.*, 2006), of 74% with results of Green-Church et al. (Green-Church *et al.*, 2008) and of 84% with the list of the Cojakaru group (Cojocaru *et al.*, 2011) could be documented. In particular, many of the detected proteins could be annotated to multiple functions, e.g. deleted in malignant brain tumors 1 (score 1305), which had been characterized as a cancer-related multifunctional protein (Mollenhauer *et al.*, 2001) or phospholipase A2 (PLA2), as a membrane traffic involved protein (Brown *et al.*, 2003). Beside PLA2, several other lipid-binding proteins could be detected, e.g. lipocalin-1, apolipoprotein A I (score 425), a reverse cholesterol transport plasma protein (Frank & Marcel 2000) or zinc-α-2-glycoprotein (score 2514) playing a key role in lipid recruitment and immune response (Hassan *et al.*, 2008). Ceruloplasmin (score 39) was reported as a secretory protein from the human lens epithelial cells (Harned *et al.*, 2006), which makes it interesting to be detected in tear fluid, however, it could only be reported with low score. Regarding 1427 capillary tear proteins, identified by LC ESI MS, the list showed a constant high congruency level to the literature. Regarding gene ontology annotation analysis, 73% of all protein hits could be annotated to a cellular component. Of annotated proteins, 88% were intracellular, whereas only 12% were

extracellular originated, which fits well with the results from the MALDI analysis (Fig. 54A) and reflects the proposed involvement of ocular surface epithelia as tear protein source (Gipson, 2007). Like MALDI, also ESI analysis revealed several lipid-binding proteins like apolipoprotein A I (score 398) or phospholipid transfer protein (score 412), which has already been documented for human tear fluid and has been supposed to play a key role in the formation of the tear film with special regards to the lipid layer (Jauhiainen *et al.*, 2005). Transcobalamin-I (score 416), a vitamin B12 binding protein (Hall, 1975), could be detected in tear fluid for the first time by LC ESI MS. Regarding intracellular proteins, two groups could be generated: cytoplasmic and membrane proteins. Thereby, 40% of intracellular proteins were found to be originated from membranes (Fig.54B), which to some degree is contrary to MALDI experiments. According to protein localization, most of the intracellular proteins were found to be associated to the nucleus (44%) (Fig.54C), which is in confidence with MALDI annotation results. Nuclear pore membrane glycoprotein 210-like (score 131), heterogeneous nuclear ribonucleoprotein U (score 48), serine/threonine-protein kinase ICK (score 84) or nuclear receptor-interacting protein 2 (score 75), nucleobindin 2 (score 324) were typically nucleus associated proteins that could be documented in capillary tears by LC ESI MS. Thereby, nesprin 2 (score 250) is a multi-isomeric protein that binds lamin at the nuclear envelope building a subcellular network (Libotte *et al.*, 2005, Padmakumar *et al.*, 2005) and was detected in this work in tears for the first time inferred from literature screening. Prominent intracellular enzymes like glyceraldehyde-3-phosphate dehydrogenase (score 246), α-enolase (score 334) or E3 ubiquitin protein ligase RBBP6 (score 134) could be described for tears and are most likely originated from ocular surface epithelia. Confidently, several epithelia derived protein markers most likely originated from the cornea or conjunctiva could be detected in the tear samples, e.g. periplakin (score 94), desmoplakin (score 263), symplekin (score 94), cadherin 23 (score 83), cadherin EGF LAG seven-pass G-type receptor 1 (score 65), cadherin-like protein 26 (score 62), protocadherin 16 (score 51), protocadherin γ-A11 (score 51), catenin-α1 (score 48), galectin 3 binding protein (score 447), and various cytokeratines by LC ESI MS. The occurrences of these proteins reflect the strong relationship between epithelia and tear film and could be used to estimate the integrity of cornea and conjunctiva. In contrast, the MALDI analysis did not show any of the ESI detected epithelial marker despite a variety of cytokeratines. An antimicrobial membrane corneal epithelial protein marker, mucin 16 (score 245) (Laurie, 2008, Spurr-Michaud *et al.*, 2007) could be detected in capillary tears in this study by the LC ESI workflow. However, by use of both approaches, proteins reported to be associated to ocular surface dryness could be revealed in capillary tear fluid, e.g. lysozyme C, mammaglobin B, protein S100 A 8/A9 and proline-rich protein 4 (Aluru *et al.*, 2012, Boehm *et al.*, 2013). In fact, despite overlapping proteins, a distinct difference between MALDI and ESI maps exists. Nevertheless, a deep

insight view to the capillary tear proteome could be achieved by use of both techniques, while the LC ESI workflow was shown to provide clearly higher sensitivity, analysis speed and lab performance lacking only few proteins, which had been revealed by the MALDI approach. On the other hand the MALDI workflow performed excellently for the detailed analysis of defined abundant tear proteins referring to high scores achieved for tear proteins like lactotransferrin, lipocalin-1 or proline-rich 4 protein. To complete the proteomic view of the fluid component of ocular surface, in the next step, Schirmer collected tears have been examined.

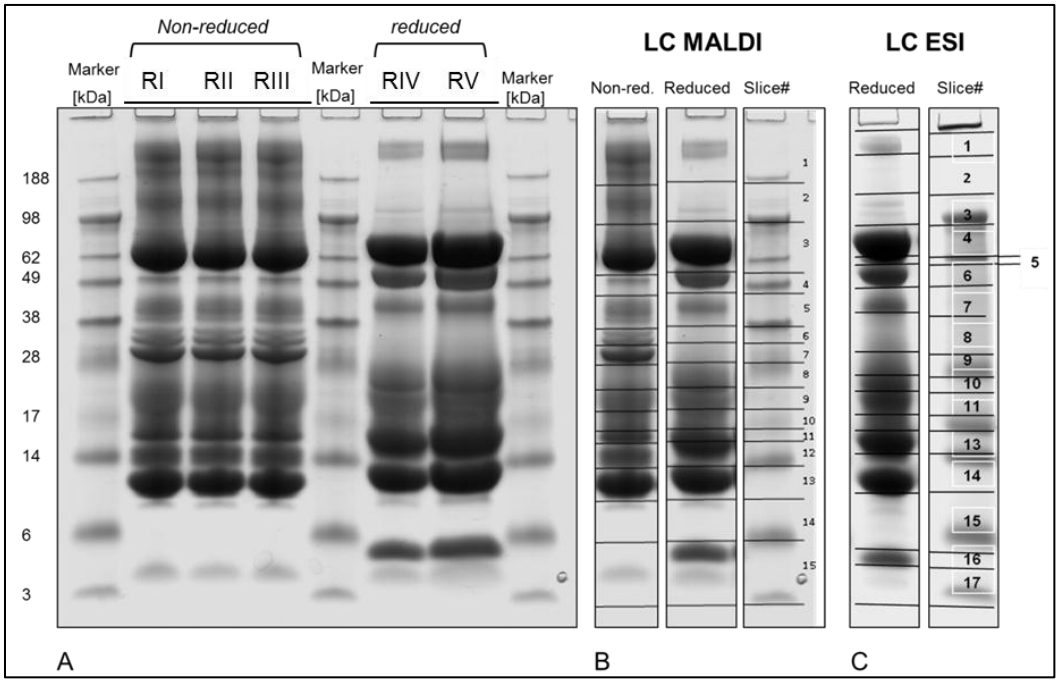


**Fig 51** SDS PAGE migration pattern of microcapillary collected tear proteins and selection for LC MALDI/LC ESI BU analysis; A: Replicates of a representative tear pool (*N*= 6) showing distinct pattern (RI-IV: 50 µg; RV: 80 µg ) and differences due to sample reducing; B: Mass area selection for LC MALDI (15 slics/lane); C: Mass area selection for LC ESI (17 slices/lane).

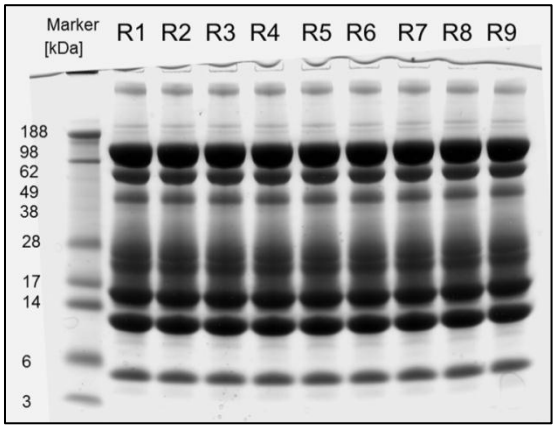


**Fig 52** Tear pool (*N*= 6) replicate (R1-9; 50 µg/lane) runs: The runs show a high degree of pattern congruency indicating high reproducibility of the SDS PAGE system justifying its use as first dimension for MS BU analysis.

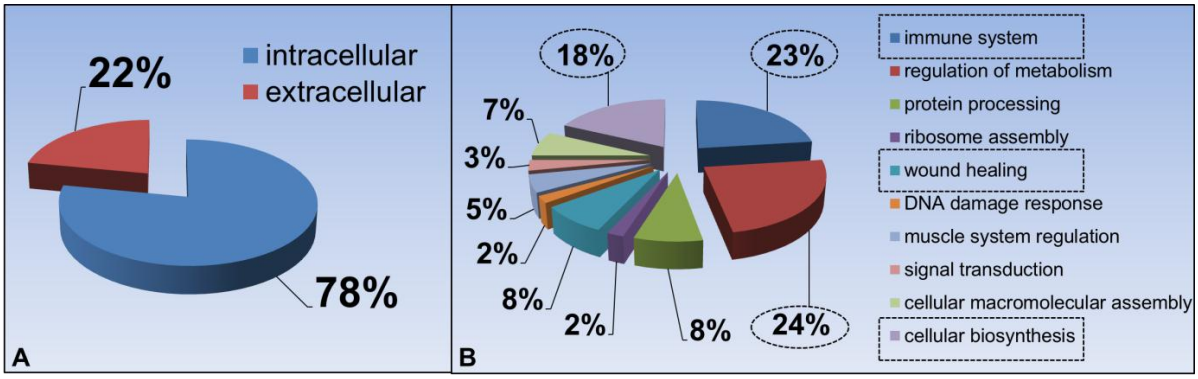


**Fig 53** LC MALDI BU characterization of the capillary tear proteome by Cytoscape GO annotation; A: the majority of capillary tear proteins were found to be intracellular proteins; B: Predominant tear protein contingents refer to immune system, woundhealing and cellular biosynthesis.

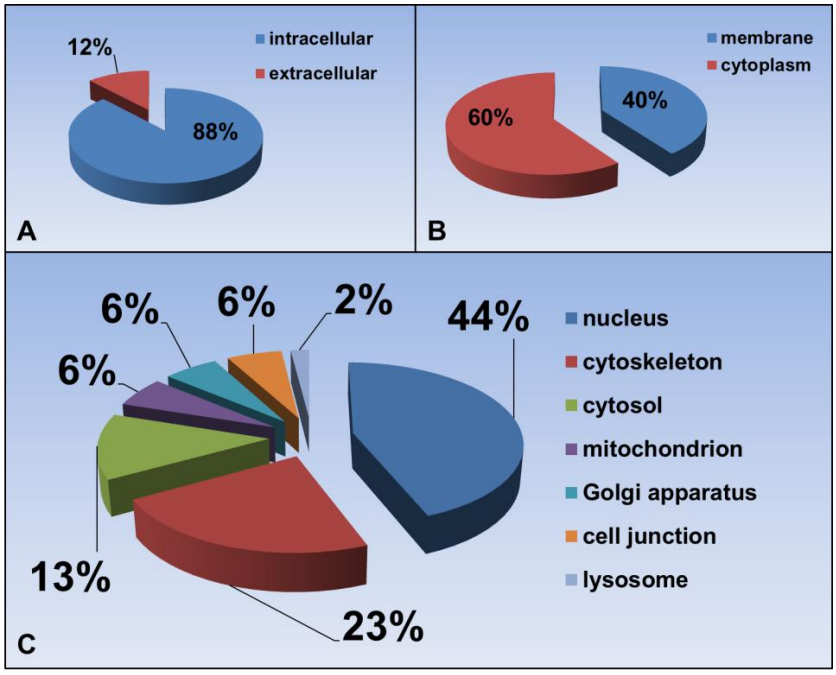


**Fig 54** LC ESI BU characterization of the capillary tear proteome by use of Cytoscape GO annotation; A: Mostly intracellular proteins were detectable; with B: a predominant portion of cytoplasmic proteins; C: Most cytoplasma proteins were originated from organelles with a predominant nucleus protein contingent.

### 4.4.2 Schirmer strip eluted tears

As a first step in Schirmer tear analysis, prior to the Taflotan® sine study various tear protein concentrations had been tested to estimate the optimal sample condition and to ensure representative pooling of individual tear samples taking fluctuations of tear protein amount between patients and time points of sample collection into consideration. Gel pattern showed linearity in a range from 2 to 80 µg total protein referring to CBB abundance. A 9 µg protein

gel load lead to visualization of characteristic tear protein migration areas, whereby nearly all bands could be recognized at 15 µg (Fig. 55). Therefore, 15 µg were found to be suitable to generate a representative tear proteomic snapshot of each patient contributing to the pool sample. Furthermore, there was no difference in the gel pattern comparing 3 kDa MWC filter concentrated Schirmer eluates to crude Schirmer strip eluates which vindicated the use of MWC filters for protein purification and concentration allowing follow-up future studies on the samples, in which salts and small molecular compounds have to be removed, e.g. binding assays. Filtrates of test Schirmer eluates were furthermore inspected by SDS PAGE for the occurrence of proteins <3 kDa probably indicating filter membrane damage or inaccuracies. In fact, no protein gel signals could be detected referring to the filtrates and protein patterns were not found to be affected by the filtering process in the gel-related mass range, resulting in highly dense bands, allowing tear proteome distribution in 17 representative mass areas for LC ESI MS analysis (Fig. 56). Regarding overall protein identification in tear concentrates, after normalization 1039 proteins ($p<0.05$, score≥30) (appendix 3) resulted from combinatory SwissProt database search of all LC ESI measurements and have been focused on for quantification and proteome description, whereby 950 proteins showed scores ≥35. Replicates showed a high consistence emphasized by regression pattern comparison between technical replicate runs referring to qualitative, reproducible analysis. Regarding mapped tear proteins, there was a distinct overlap with tear proteome characterization in the literature so far (de Souza *et al.*, 2006, Karnati *et al.*, 2013, Zhou *et al.*, 2012). A predominant portion of proteins was found to be cellular originated, whereby only a minority of annotated proteins referred to the cytosol (Fig 57A/B), which had also been documented for capillary tears by use of both, MALDI and ESI workflows. Most of the membrane proteins could be associated to organelles (Fig. 57C) with predominant roles in protein binding and enzymatic activities (Fig. 58). Most likely the majority of these proteins were originated from epithelial cells corresponding to the ocular surface. Thereby, ocular surface leakage in the course of POAG therapy and with increasing age could explain the distinct occurrence of intracellular proteins in the tear film (Fukuda *et al.*, 1996, Nielsen *et al.*, 1981, van Haeringen and Glasius, 1976, vanHaeringen, 1997). Nevertheless, also capillary tears including healthy subjects showed high portions of intracellular proteins reveald by LC ESI and MALDI MS. De facto, MS analysis indicated the existence of a large fraction of intracellular proteins in the tear film. In any case, the levels of these proteins are likely to be affected under certain circumstances and need focused investigation. In accordance, some of the top protein hits refer to extracellular tear proteins, but also to cellular proteins. Indicated by protein scores, the most abundant proteins were lactotransferrin (score 2196), serum albumin precursor (score 1721), keratin, type II cytoskeletal 1 (score 1525), keratin, type I cytoskeletal 10 (score 1365), α-enolase (score 1134), zinc-α-2-glycoprotein (score 1075), heparan sulfate

proteoglycan core protein (score 1073) and retinal dehydrogenase 1 (score 1029). Also anti-α-trypsin (score 886) and pyruvate kinase isozymes M1/M2 (score 666) were detected among the top 30 protein hits (Fig. 59), which was comparable to the capillary tear results of prior LC ESI/MALDI experiments. Proline-rich protein 4, which was found among the most prominent proteins, revealed by MALDI MS, was also detected in ESI analysis of capillary tears, only in the medium score rank (score 167, rank 98), probably reflecting its chemical preverence for MALDI ionization. Like in capillary tears several immunoglobuline fractions could be detected with high scores, e.g. Ig α-1 chain C region (score 588), Ig α-2 chain C region (score 525) or Ig κ chain V-III region WOL (score 381). Also, several retina characteristic proteins could be documented with high scores including retinal dehydrogenase 1 (score 1029), peroxiredoxin 1 (score 654) and heat shock protein ß 1 (score 646), which indicates distant ocular regions as additional tear protein source. Actually, scores of detected proteins decline dramatically at a value of 251, whereby after this value also the correlation between score and number of identified peptides for each protein fluctuates to a certain degree. Most peptides were identified for lactotransferrin (7530 peptides), lipocalin-1 (3987 peptides), lysozyme C (3675 peptides) and proline-rich protein 4 (1671 peptides), which were also documented among the predominant MALDI detected proteins. Mammaglobin B (1021 peptides) and secretoglobin family 1D member 1 (550 peptides), both reported as dry eye markers (Boehm *et al.*, 2013, Kramann *et al.*, 2011), could also be characterized with high peptide numbers. Like in capillary tears, also epithelial proteins, most likely derived from conjunctiva or cornea, e.g. desmoplakin (score 273), desmoglein 2 (score 69), desmoglein 4 (score 47), dermatan-sulfate epimerase-like protein (score 47), multiple epidermal growth factor-like domains protein 8 (score 38), protocadherin-9 (score 35) and γ-A12 (score 38), cadherin-5 (score 79), plectin (score 231) as well as various cytokeratine species, also documented for capillary tear fluid, could be identified. In summary, even consumpting a smaller protein amount than in capillary tear analysis the LC ESI MS strategy provided a detailed image of the tear proteome emphasizing the high sensitivity of the developed ESI approach. Moreover, a high degree of congruency between capillary and Schirmer tear proteome could be documented with 95% of Schirmer eluted proteins also detected in capillary tears by the developed LC ESI MS workflow, which most likely shows that different results are unlikely to be a matter of the tear sample species, but are more likely to depend on the sensitivity of the method. In addition, retinal proteins; retinal dehydrogenase 1 (score 1029) and retinal guanylyl cyclase 1 (score 48) could be exclusively detected in the Schirmer eluted tear samples. Also, other highlighting proteins like leukocyte elastastase inhibitor (score 747), aldehyde dehydrogenase (dimeric NADP-preferring) (score 540), *14-3-3* protein Σ (score 373) or alcohol dehydrogenase (score 343) could be exclusively identified with relatively high scores in Schirmer tears. In summary, an in-depth

view to the Schirmer tear proteome could be achieved revealing beside characteristic secretory tear proteins, proteins originated from more distant ocular regions, e.g. retina. Especially, the predominant class of intracellular proteins could be focused on to obtain an impression on the ocular surface status considering epithelia integrity. The high number of identified enzymes and binding proteins furthermore builds a fundament for future activity assays and functional studies.

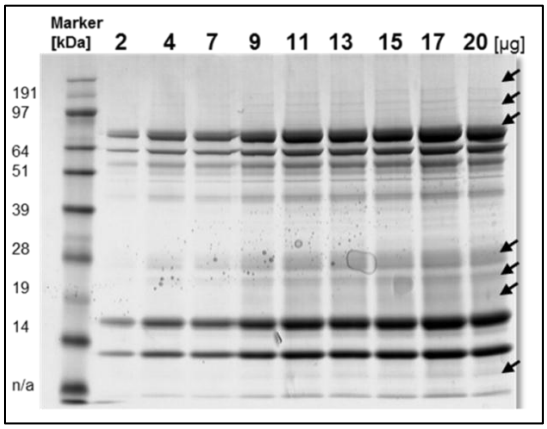


**Fig 55** Dynamic range of the Schirmer tear proteome revealed by 1D SDS PAGE: 9 µg protein tear load generated complete tear proteomic gel pattern (low abundant protein mass areas are indicated by arrow), whereby at nearly 15 µg protein load signal saturation could be observed.

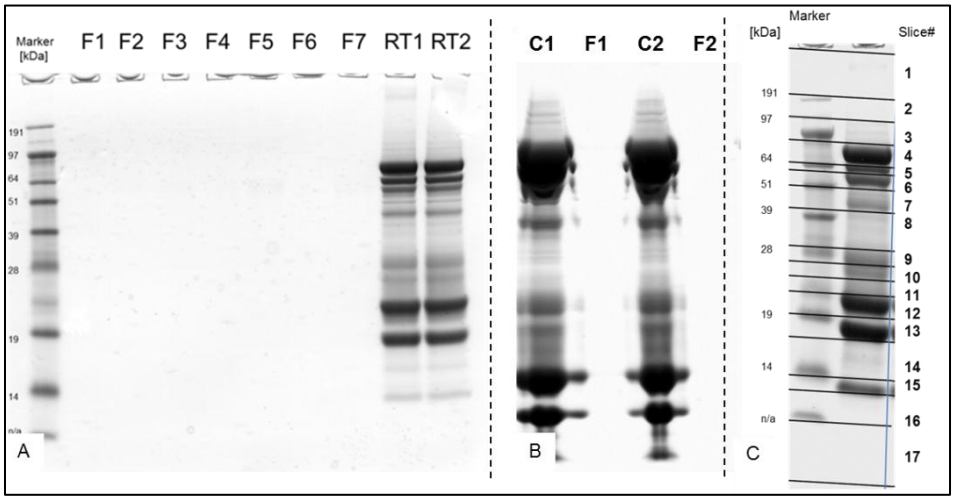


**Fig 56** Performance of 3K MWC spin filters (3 kDa>concentrate) to concentrate Schirmer tear samples prior to LC ESI MS analysis; A: MWC tear filtrates (F1-7) showed no filter leaking proteins >3 kDa indicating high protein recovery (RT1/2= tear control samples); B: Highly concentrated tear samples (C1/2) and corresponding filtrates (F1/2); C: Mass area selection of Schirmer tear tear proteins for LC ESI MS analysis (17 mass area slices/lane).

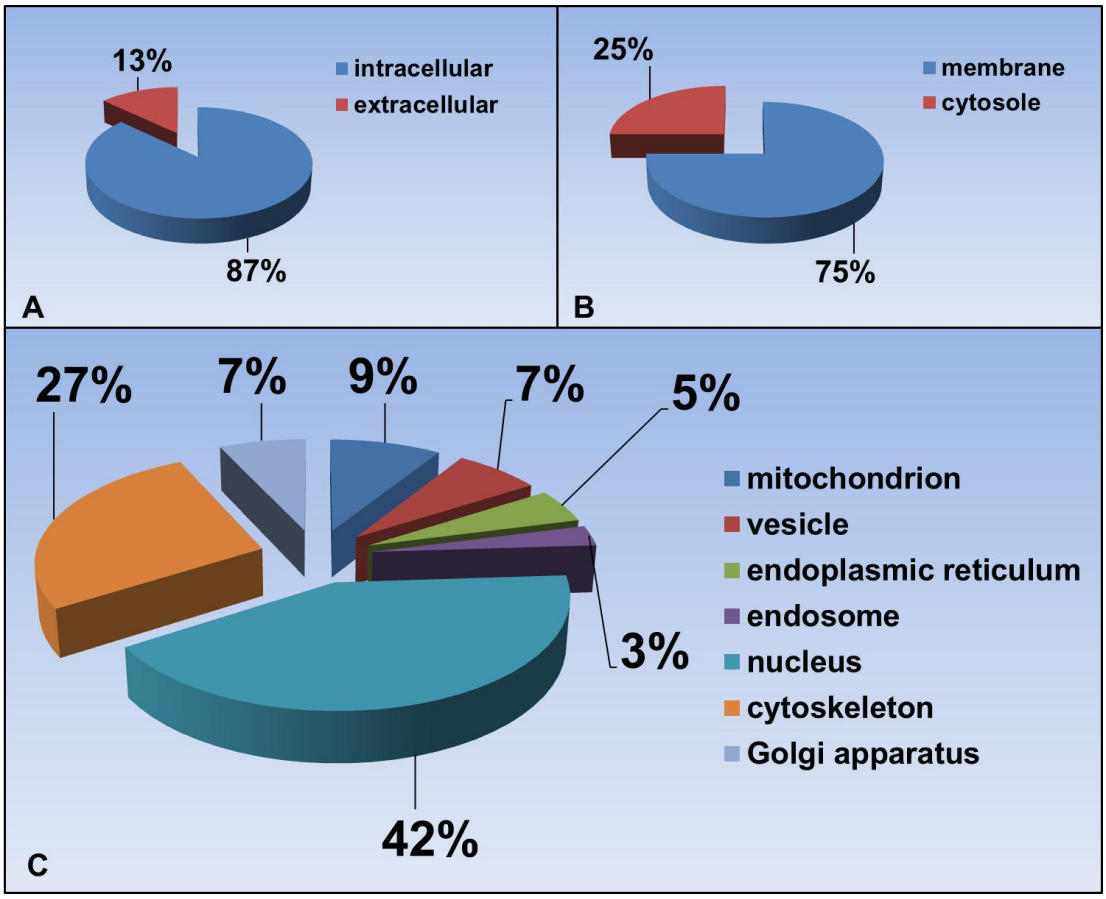


**Fig 57** Functional analysis of the Schirmer tear proteome by Cytoscape GO annotation; A: The majority of LC ESI identified Schirmer tear proteins were associated to cells; B: A predominant portion of cellular proteins were related to membranes; C: The highest protein contingent was associated to the nucleus followed by cytoskeleton.

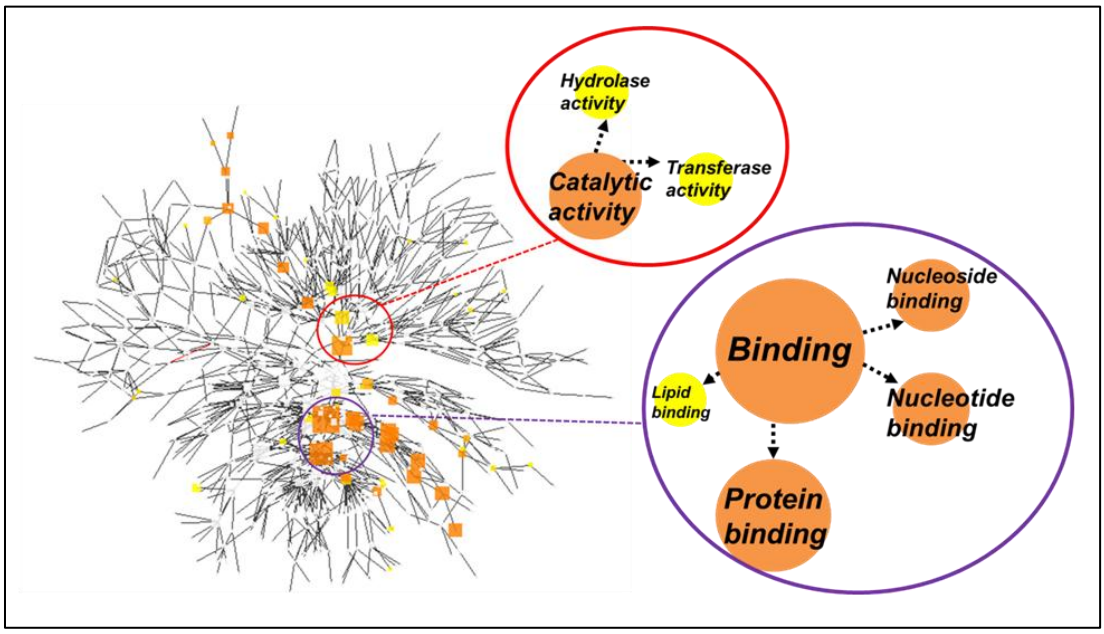


**Fig 58** Molecular function of LC ESI MS identified Schirmer tear proteins by Cytoscape GO annotation indicating predominant tear protein contingents to be involved in molecule binding and enzymatic functioning.

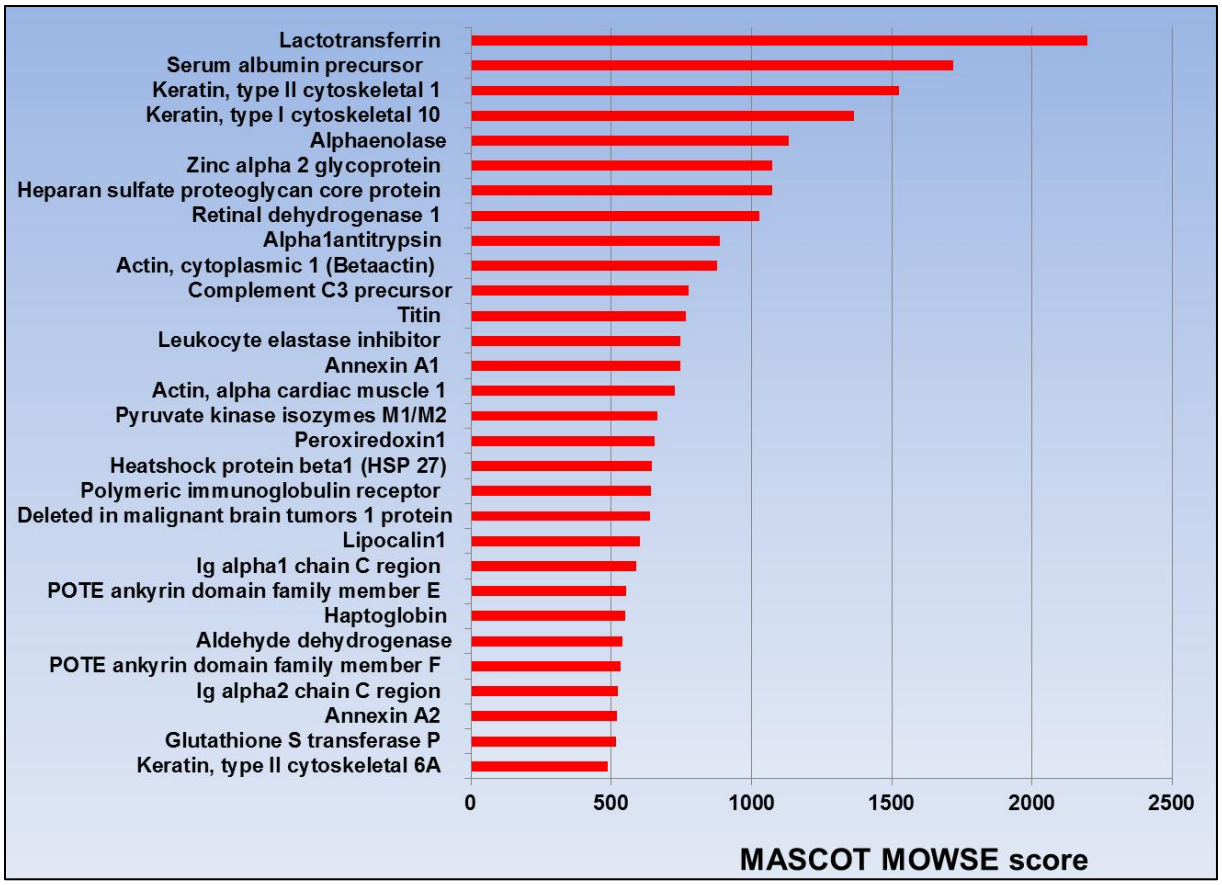


**Fig 59** Top 30 LC ESI MS identified Schirmer tear proteins indicated by the MASCOT *Mowse* Score.

### 4.4.3 General tear results

Taking all LC ESI experiments on capillary and Schirmer tears together, a score independent frequency analysis using Statistica showed that lactotransferrin, lipocalin-1 and secretoglobin family 1D member 1 were the predominant frequent proteins in tear fluid, followed by Ig α-2 chain C region, extracellular glycoprotein lacritin, proline-rich protein 4, uncharacterized protein C1orf127, Ig κ chain C region, zinc-α-2-glycoprotein, polymeric Ig receptor, Ig α-1 chain C region, lysozyme C precursor, prolactin-inducible protein, cystatin S precursor (cystatin 4), mammaglobin B and Ig J chain. Interestingly, beside prominent tear proteins like proline-rich protein 4 and mammaglobin B, a low abundant protein; forkhead-associated domain-containing protein 1 could be detected in all experiments and was not documented for tear fluid before. Also, lymphoid-specific helicase, a nucleus residing DNA-binding protein (Delmas *et al.*, 1993) could be detected in most of the experiments and could be documented for tear fluid for the first time. Centaurin-γ 1 was detected in most of the samples for the first time for tear fluid. Also, cytosolic 5'-nucleotidase III-like protein was documented for tear fluid for the first time detectable with high frequencies. Further prominent proteins detected in the majority of experiments were serum albumin precursor, ß-2-microglobulin, melanotransferrin, putative uncharacterized protein LOC401522, cytoplasmic protein NCK2

and myozenin 2. Transmembrane channel-like protein 8, a multi-pass membrane protein (www.uniprot.org) and myozenin 2 could also be reported for the first time for tear fluid in the majority of experiments. Mesothelin, Ig λ-2 chain C regions, proline-rich protein-1, protein S100-A6, glutathione S-transferase P, α-1-antitrypsin and protein S100-A9 were detectable in 58% of the experiments in confidence with the literature (Karnati *et al.*, 2013, Zhou *et al.*, 2012). Another protein detected in more than 50% of the experiments was MHD domain-containing death-inducing protein, not detected in tear fluid before. Interestingly mucins, especially mucin 5AC or mucin 16, were documented for their presence in tear fluid (Argueso *et al.*, 2003, Jumblatt *et al.*, 1999, Spurr-Michaud *et al.*, 2007, Zhao *et al.*, 2001) and could be identified in few of the experiments. Tear proteins, that were high frequently detected in ESI experiments, even with low scores, have also been detected in most cases in MALDI experiments, e.g lactotransferrin, lipocalin-1, proline.rich protein 4, lysozyme C, mammaglobin B, proline-rich protein 1, cytoplasmic protein NCK2 or protein S100-A9. Also, several of the proteins identified in approximately 50% of the ESI experiments were detectable by MALDI analysis, e.g. neutrophil gelatinase-associated lipocalin or γ-enolase. Indeed, also proteins that were rarely detected in ESI experiments could be documented in MALDI experiments, e.g. ribosome-binding protein-1, POTE ankyrin domain family member I, α-1-acid glycoprotein 1, 2 or centrosomal protein of 164 kDa supporting their existence in tear fluid. A highlighted group of proteins were lipid associated proteins, which could be detected by ESI and/or MALDI analysis. Beside lipocalin-1, apolipoprotein AI and neutrophil gelatinase-associated lipocalin, phospholipase A2 and phospholipid transfer protein numerous other lipid-associated proteins could be frequently observed including liprin α 2/3, lipoxygenase homology domain containing protein 1, patatin-like phospholipase domain containing protein 7, lipid phosphate phosphor hydrolase 3, non-specific lipid transfer protein, StAR related lipid transfer protein 13, phospholipase A2 activating protein, lysophospholipase-like protein 1, putative lipocalin1-like protein 1, apolipoprotein O, Prolow-density lipoprotein receptor-related protein 1, low density lipoprotein receptor-related protein 4, inactive phospholipase C-like protein 2 and arachidonat 5-lipoxygenase. Most likely these proteins are associated to the tear lipid layer and are potential targets for future investigations regarding evaporative dry eye disease. In summary, by use of both, LC ESI and MALDI approaches encircling a huge number of experiments, an in-depth view of the tear proteome could be obtained, whereby the presence of numerous proteins could be supported independently from their scores by their frequencies in ESI experiments as well as by their independently detection by the LC MALDI analysis. In consequence, a sensitive proteomic image of the tear film as the key extracellular ocular surface component could be provided.

### 4.4.4 Conjunctival cells

To achieve a more detailed proteomic image of the ocular surface beyond the fluidic compartment encasing the cellular region, NHC-IOBA conjunctival cells have been examined. By use of the developed LC ESI workflow initially 1412 proteins followed by 1481 proteins in a second experiment could be catalogued (MASCOT ion score $p < 0.05$). Thereby 1044 hits of the first experiment and all proteins of the second experiment were used for quantification assessed by a protein score ≥35. For descriptive proteome characterization a combined list of both experiments was used (for overview protein list see appendix 4; top 30 scoring proteins are illustrated in Fig. 60). Several proteins originated from cytoplasma as well as membrane-associated proteins could be documented. Regarding cytoscape GO annotation analysis 74% of all proteins could be annotated to certain cellular compartments. Actually, 94% of the annotated hits refer to intracellular proteins (Fig. 61A). Several extracellular proteins were detected with high scores and were mainly found to represent secreted proteins. De facto, numerous proteins were intracellular located, but also secreted to the cellular surface like annexin A2 (score 12539), *14-3-3* protein Σ (score 1518), macrophage migration inhibitory factor (score 534), apolipoprotein A-I-binding protein (score 286), peroxiredoxin 4 (score 3295) or calreticulin (score 2542) (www.uniprot.org). Actually, interleukin 17 (score 44)/ 18 (score 280)/ 25 (UPF0556 protein C19orf10) (score 758), serpin B5 (score 1343) spondin-1 (score 89) and mucin-5B (score 242) were confirmed as exclusively secreted proteins (www.uniprot.org). RNA-transcripts for interleukines and other cytokines have been documented in lysates of conjuctival tissue lysates (Pflugfelder *et al.*, 1999) and cytokine induction was indirectly analyzed by ELISA in conjunctival tissue (Solomon *et al.*, 2001) supporting the secretory activity of these cells. The detection of mucin 5B as a characteristic epithelial secreted protein and also the identification of EGF-like module containing mucin-like hormone receptor-like 2 (score 133) is in confidence with the detection of mucin RNA transcripts (MUC2, MUC5AC) (McKenzie *et al.*, 2000) and mucin proteins (MUC16) (Argueso *et al.*, 2003, Gipson and Argueso, 2003) in human conjunctiva and indicates the functional activity of NHC-IOBA cells as an ocular surface model (Tong *et al.*, 2009). Also, numerous cytokeratines, e.g. cytoskeletal keratin type I 13, 15, 17, 19 and 24 (scores 244/333/345/189/96) as well as cuticular keratine Ha1 (score 85) have been reported as characteristic human conjunctiva l proteins (Krenzer and Freddo, 1997) also documented for NHC-IOBA cells (Diebold *et al.*, 2003). Other epithelial marker proteins like desmoglein 1, 2 (score 336/296) (Wan *et al.*, 2003) and epiplakin (score 113) (Spazierer *et al.*, 2006) could be identified in the cell lysates. Furthermore, despite the majority of proteins were found to be cytoplasmic proteins, 30% of all proteins were membrane associated (Fig. 61B). Transmembrane proteins like transmembrane protein 33 (score 566), 109 (score 411), coiled-coil domain containing protein (score 166) or emp24 domain containing protein 10

(score 581) could be recovered by LC ESI. Numerous receptors, e.g. transferrin receptor protein 1 (score 1908), insulin-receptor related protein (score 166) and membrane associated progesterone receptor component 1 (193) could also been revealed. Interestingly, also two neurotransmitter receptors were identified, however, with low scores; dopamine receptor (score 45) and GABA receptor subunit delta (score 39). Also a chemokine receptor, C-C chemokine receptor type 9 has been determined (score 95) fitting well with the interleukine secretion activity of the cells. Identification of vinculin, a high scoring periphere membrane protein (score 1327) associated to cell junctions (www.uniprot.org) supported the functionality of the cell system. GPI transamidase component PIG-T (score 107) residing at the ER membrane (Ohishi et al. 2001) and subunits of the guanine-nuclotide-binding protein, a palmitoylated membrane G protein (www.uniprot.org) are further examples of successful membrane protein recovery. In addition, several membrane-located amino acid transporters have been identified, e.g. sodium-coupled neutral amino acid transporter 2 (score 82), large neutral amino acids transporter small subunit 1 (score 534) or neutral amino acid transporter B(0) (score 504). Furthermore, a cation transporter, probable cation-transporting ATPase 13 A5 (score 131) could be identified. Regarding the annotation of proteins to cellular organelles, 82% of all annotated proteins were found to be associated to organelles. Despite the portion of plasma membrane and cytosolic proteins, predominantly nucleus proteins could be documented in cell lysates followed by mitochondrial and ER proteins (Fig. 61C). Cofilin 1 (score 2800), carboxy-terminal domain RNA polymerase II polypeptide A small phosphatase 2 (score 280), proteasome subunit beta type-5 (score 788), heterogenous nuclear ribonucleoprotein U (score 214) were exemplary detectable nucleus proteins observed in NHC-IOBA lysates. Besides, numerous histone species could be documented. Several proteins like dynamin 1-like protein (score 289) were annotated to ER, Golgi and mitochondria (www.uniprot.org). Furthermore, among nucleus associated proteins oncogene signalling proteins like Ras GTPase-activating-like protein IQGAP1 (score 5207) (Shen *et al.*, 2006) could be detected with high abundance. Up-regulated during skeletal muscle growth protein 5 (score 254), mitochondrial GrpE protein homolog 1 (score 128) and cytochrome b-c1 complex subunit 8 (score 235) represent exemplary catalogued mitochondrial proteins. Most of the found proteins were typical cellular proteins; however, only few of them have been identified for NHC-IOBA cells, so far. Map kinases were reported for NHC-IOBA cells (Liu *et al.*, 2007) and two representatives could also be supported by this work; NHCJNK1/MAPK8-associated membrane protein (score 75) and MAP3K12-binding inhibitory protein 1 (score 64). Despite transglutaminase 2 (protein-glutamine gamma-glutamyltransferase 2) (score 201) could be proven, the prior reported enzyme, conjunctival associated transglutaminase 1 (Nakamura *et al.*, 2001), could not been detected in this work. In fact, there was a certain overlap with the tear proteome indicating the cross-relation

between tear film and ocular surface epithelia, supporting the cellular origin of numerous tear proteins. 12% of all conjunctival cell proteins could be revealed in both types of tear fluid, capillary and Schirmer tears, encircling several intracellular enzyme-linked proteins (scores are indicated for NHC-IOBA), e.g. L-lactate dehydrogenase A chain (score 5121), protein arginine N-methyltransferase 5 (score 131), phosphoglycerate kinase 1 (score 7648), fructose-bisphosphate aldolase A (score 3229), γ-enolase (score 4082), pyruvate kinase isozymes M1/M2 (score 14932) (Fig. 62), glucose-6-phosphate isomerase (score 5578), glutathione S-transferase P (score 5286) and hexokinase 1 (score 73). Characteristical tear film proteins like calreticulin (score 2542), cystatin B (score 1056), POTE ankyrin domain family member F (score 6266) and the proteins S100-A6/A8/A9 (scores 988/69/40) could be documented for NHC-IOBA cells. Additionally, S100-A10 (score 673), A13 (score 396) and A16 (score 236) could be exclusively identified in cell lysates. Moreover, there was overlapping finding in desmoglein, annexin, heat shock protein, myosines and histones in cells and tears. Various members of the *14-3-3* protein family were detected in tears and cells. These findings support the hypothesis, that a majority of tear proteins is originated from ocular surface epithelia. Only a minority of these proteins could be clarified to be actively secreted by the conjunctival cells, e.g. cathepsin D, macrophage migration inhibitory factor, serpin B5, galectin 1, galectin 3 or galectin 3-binding protein (www.uniprot.de). For some of the proteins, it remains unclear, if the protein is secreted or originated from cellular leakage since proteins like annexin A5 are located in the cytoplasma, but are also located at the cell periphery (www.uniprot.org) vulnerable to extracellular release. Several other proteins like galectin 7 or thioredoxin exhibit traffic between nucleus, cytoplasma and extracellular space (www.uniprot.org). Numerous proteins, e.g. *14-3-3* proteins, calreticulin, glucose-6-phosphate isomerase and peroxiredoxin 4 are documented to be as well located in the cytoplasma as to be secreted by the cells (Chang *et al.*, 2006) (www.uniprot.org). Also, inflammation-associated complement decay-accelerating factor (score 192) could be detected in the cells. In summary, by use of the LC ESI MS workflow, a detailed view of the conjunctival cell proteome as a cellular constituent of the ocular surface could be obtained. The proteomic overlap of conjunctival cells with tear fluid as well as the occurrence of characteristic secretory proteins and epithelial marker proteins emphasized the potential of the cell line as a model system for ocular surface research. In summary, a deep proteomic view could be obtained encircling the fluidic and cellular dimension of the ocular surface building a fundament for ocular surface studies regarding Taflotan® sine and taurine.

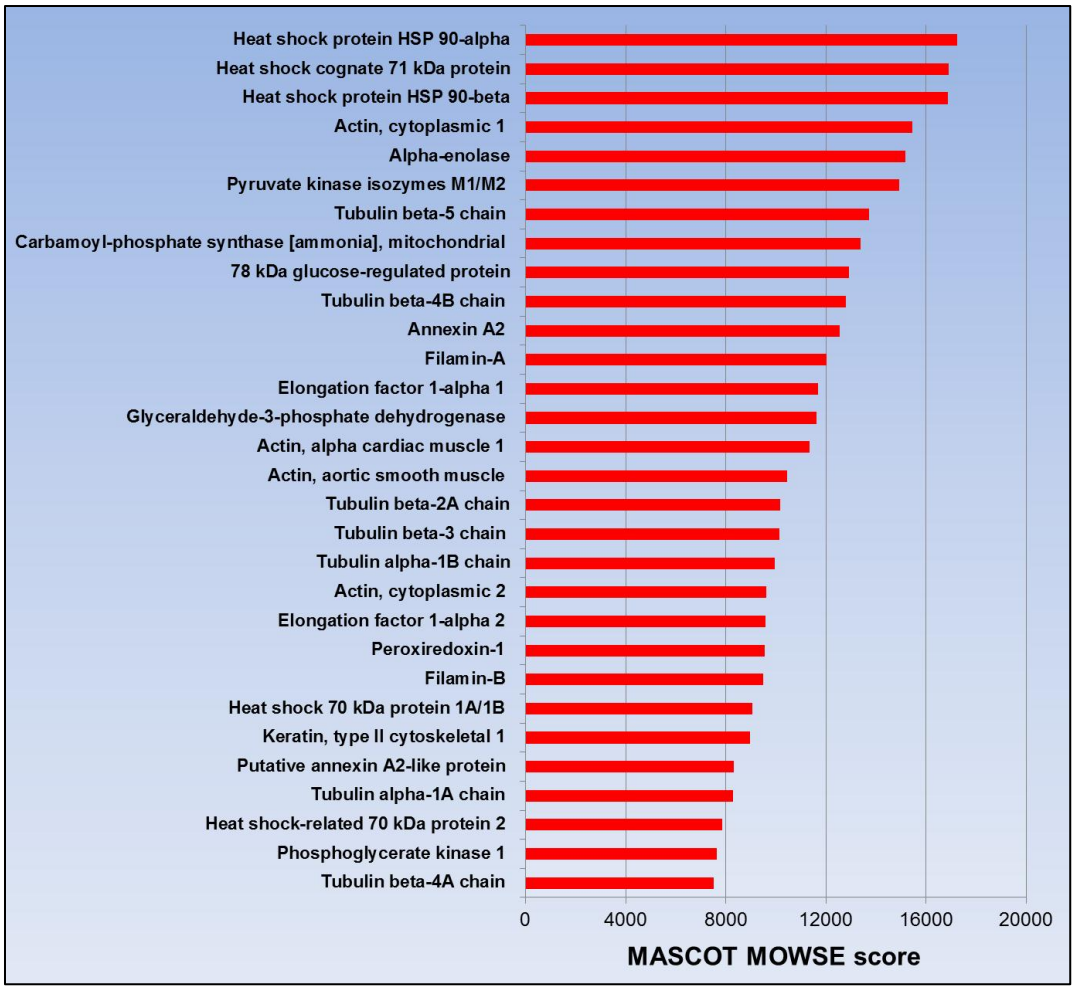


**Fig 60** Top 30 scoring conjunctival cell proteins identified in NHC-IOBA 0.1% DDM lysates by use of the LC ESI MS BU workflow.

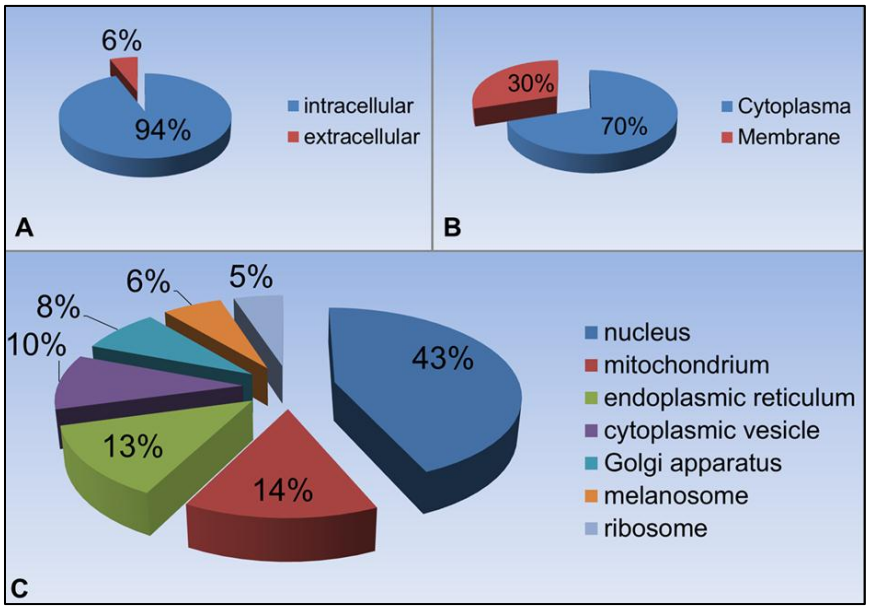


**Fig 61** Functional analysis of the conjunctival cell proteome by Cytoscape GO annotation; A: Most proteins were intracellular protein species with a high contingent of B: Cytoplasma proteins; C: The predominant protein portion was found to be associated to nucleus followed by mitochondrium and ER.

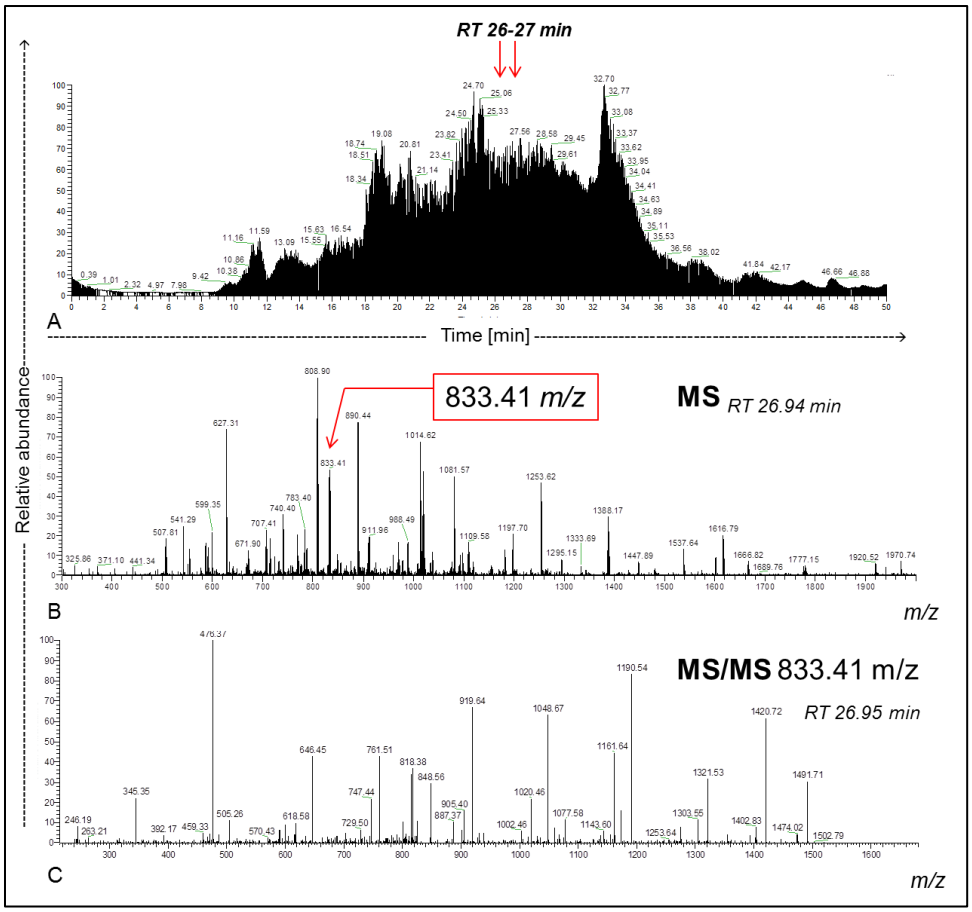


**Fig 62** Exemplary identification of high scoring pyruvate kinase isozymes M1/M2 in conjunctival cells; A: Exemplary TIC chromatogram indicating the elution area for a high scoring PKM precursor between 26/27 min RT; B: PKM precursor 833.41 m/z selected at 26.94 min for fragmentation; C: ITMS fragment spectrum corresponding to precursor 833.41 m/z contributing to PKM identification.

## 4.5 Influence of Taflotan® sine on the ocular surface of POAG patients

Regarding regression analysis of the studied tear proteome, 12% of all identified proteins showed a distinct level change. Thereby, 5% of responding proteins displayed a significant linear level change ($p<0.05$), 3% showed a distinct tendency of linear level regulation ($R^2<0.9$) and 4% significantly corresponded to a polynomial pattern ($p<0.05$) (Fig. 63). Related to linear regression, several dry eye related proteins showed significant level decline. Serotransferrin ($R^2= 0.9384$, $p= 0.0313$, score 444), galectin 7 ($R^2= 0.9298$, $p= 0.0357$, score 64), annexin A11 ($R^2= 0.9085$, $p= 0.0469$, score 51), cadherin 5 ($R^2= 0.9598$, $p= 0.0402$, score 80) and myosin-10 ($R^2= 0.9118$, $p= 0.0451$, score 92) were found to show a significant linear level alleviation (Fig. 64). Interestingly, other myosin family members, myosin 6, 7, 9 and 11 also showed a regulation diminishment, however, with non-significant $R^2$ values. Regarding regression slopes of linear responding proteins the majority of proteins (69%) showed negative values reflecting a longitudinal level decrease, whereby most members (83%) were slightly decreased over time indicated by moderate slope values ($slope<0\leq-50$). Comparable results were obtained from positively responding proteins,

whereby also the majority of proteins (78%) showed slight level increase (slope>0≤50) (Fig. 65). Regarding non-linear time progression, several dry eye related proteins diplayed a significant polynomial decrease over time like e.g. low density lipoprotein receptor-related protein 4 (p= 0.0207, score 59) or manifested a significant increase like ankyrin-3 (p= 0.0432, score 54). Beside polynomial regression fit, the fold change “optimal match” cluster analysis revealed a group of non-linear responding candidate proteins. The analysis calculated four clusters, whereby 56% of all proteins were categorized as non-regulated, showing an “equal”, “equal”, “equal”-level alteration time pattern grouped in cluster #1. Despite proteins that show high fluctuating time pattern in cluster #4 encircling 14% of all proteins, 68% of cluster members showed a distinct fold drop over time (“equal”, “decrease”, “equal”). 45% of the proteins in cluster #3 including 17% of all proteins showed a level increase pattern over time (“equal”, “increase”, “equal”). Moreover, related to all identified proteins the portion of proteins displaying a longitudinal fold decline was 21% higher than the increasing protein contingent. Furthermore, manual screening for longitudinal protein responses focusing on proteins documented as dry eye marker proteins, provided most proteins showing a linear descending tendency ($R^2$≥0.5) like secretoglobin 1 family member D1 ($R^2$= 0.5680, score 245), lactotransferrin ($R^2$= 0.6940, score 2196), heat shock related 70 kDa protein 2 ($R^2$= 0.6415, score 46) or heat shock cognate 71 kDa protein ($R^2$= 0.5842, score 60), whereas some proteins exhibit tendencies of linear ascending like e.g. α-1-anti-trypsin ($R^2$= 0.8007, score 886), interleukine-12-receptor ß-2-chain precursor ($R^2$= 0.7400, score 41) or tumor necrosis factor α induced protein 3 ($R^2$= 0.5951). However, known dry eye marker proteins like S100A4, 6, 8 and 9 failed for response. Also proline-rich protein 4 (score 167) and proline-rich protein 1 (score 261) were found unaffected. Among the proline-rich proteins only the large proline-rich protein BAT2 showed a slight tendency of linear decrease ($R^2$= 0.6256, score 78). Ingenuity® protein allocation analysis classified only 10% of the selected candidate proteins as extracellular proteins, whereas the remaining 90% were depicted to be originated from cellular compartments. Most of these proteins appertain to cytoplasm followed by nucleus related proteins (Fig. 66). The functional process analysis revealed 18 functional process hits above the adjusted protein allocation threshold of 25. Thereby processes like tissue development, cellular development as well as cell survival and cell death including apoptosis were highlighted (Fig. 67). In summary, a high number of cellular proteins could be detected in the tear film of POAG patients most likely reflecting ocular surface epithelial cell leakage events. It could be observed, that in first instance overall cellular processes were influenced by the medical switch since predominantly intracellular proteins most likely originated from ocular surface epithelial cells were found in the tear film and showed a decline over the investigative period after the medical switch. Several marker proteins also showed alterations in their regulation pattern, which indicates a changing health status of the

ocular surface after switching. MA analysis of selected marker candidates emphasized the level decrease of several characteristic proteins highlighted by MS analysis. “A priori” dry eye associated MA tested proteins were: mucin 6, aquaporine 5, proline-rich protein 4, lactotransferrin, lipocalin, hemopexin, mammaglobin B, α-2-macroglobin, cystatin, S100A8, S100A9, lysozyme C, anti-trypsin, complement C3b and cytokines: TGF-ß1, TGF-ß2, TNF-α, IL1a, IL1b, IL2, IL5, IL8, IL9, IL10, IL12, IL13, IL17a, IL23a, mcp1/ccl2, MIP1a/ccl3. For proteomic result validation commercial antibodies against the following marker candidates have been selected: serotransferrin, pyruvate kinase isozymes M1/M2, plectin, annexin A5, annexin A11, myosin 10, galectin 7, tight junction protein ZO1 and cadherin 5. 46% of all tested proteins showed distinct tendencies of linear approximation of the POAG group to the control group in the course of the study (Fig. 68). Thereby, the following “a priori” dry eye associated marker proteins were found to be affected by the Taflotan® sine appliance: aquaporin 5, mammaglobin B, anti-trypsin and complement factor C3/C3b. Interestingly numerous cytokines were found to shift to the control level including the interleukines, IL1a, IL2, IL2b, IL13, IL17, IL23a, and the chemokines MIP1a/ccl3 and TGFB1 (Fig. 69). This finding clearly reflects a diminishment of the inflammatory status of the ocular surface in the course of the study. Focusing on MS derived marker candidates, several proteins showed tendencies of linear level diminution in direction to the healthy control level and furthermore a significant approximation response revealed by t-test (p-values are denoted in brackets; p1= $POAG_{timepoint1}$ compared to $Control_{mean\ level}$, p2= $POAG_{timepoint5}$ compared to $Control_{mean\ level}$). Thereby, pyruvate kinase isozymes M1/M2 (p1= 0.0012, p2= 0.0740), annexin A11 (p1= 0.0009, p2= 0.2026), cadherin 5 (p1= 0.0084, p2= 0.0712), serotransferrin (p1= 0.0013, p2= 0.0700) and kinectin (p1= 0.0007, p2= 0.1320) were found to converge significantly to the healthy control level in the course of Taflotan® sine exertion since at the start of the study protein levels for the highlighted proteins were significantly different between both groups. At the end of the study, no significant level difference could be observed anymore predicting an alignment of protein levels between the POAG and the healthy control group (examples are illustrated in Fig. 70). Beside MS derived candidates, this was also demonstrated for “a priori” MA selected dry eye associated proteins lipocalin (p1= 0.0005, p2= 0.0641) and complement factor c3/c3b (p1= 0.0001, p2= 0.0846). Moreover, the level decline of cytokines IL1b (p1= 0.0009, p2= 0.2794), IL2 (p1= 0.0003, p2= 0.1620) and IL23a (p1= 0.0021, p2= 0.0804) could be evaluated as a significant drawing to the healthy stage. Accordingly, microarray results clearly supported a beneficial effect of Taflotan® sine application reflected by cytokines and MS derived protein candidates. Moreover, objective clinical parameters represented by TBUT and BST strengthen beneficial effects of therapeutic switching since both parameters exhibited significant alterations revealed by t-test “start to endpoint” comparison (Fig. 71). In summary, a strong evidence for ocular surface regeneration in the

course of preservative-free tafluprost appliance in POAG patients could be revealed by use of the developed workflow.

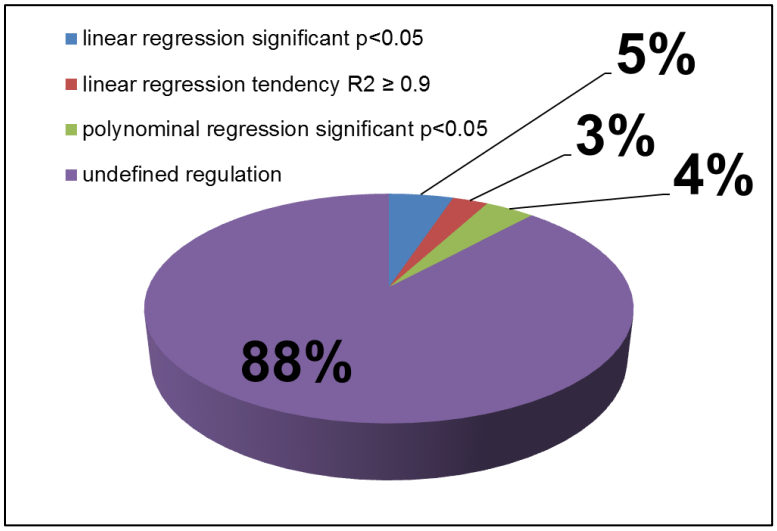


**Fig 63** Distribution of longitudinal tear proteome dynamics observed in POAG patients switching from Xalatan® to preservative-free Taflotan® sine.

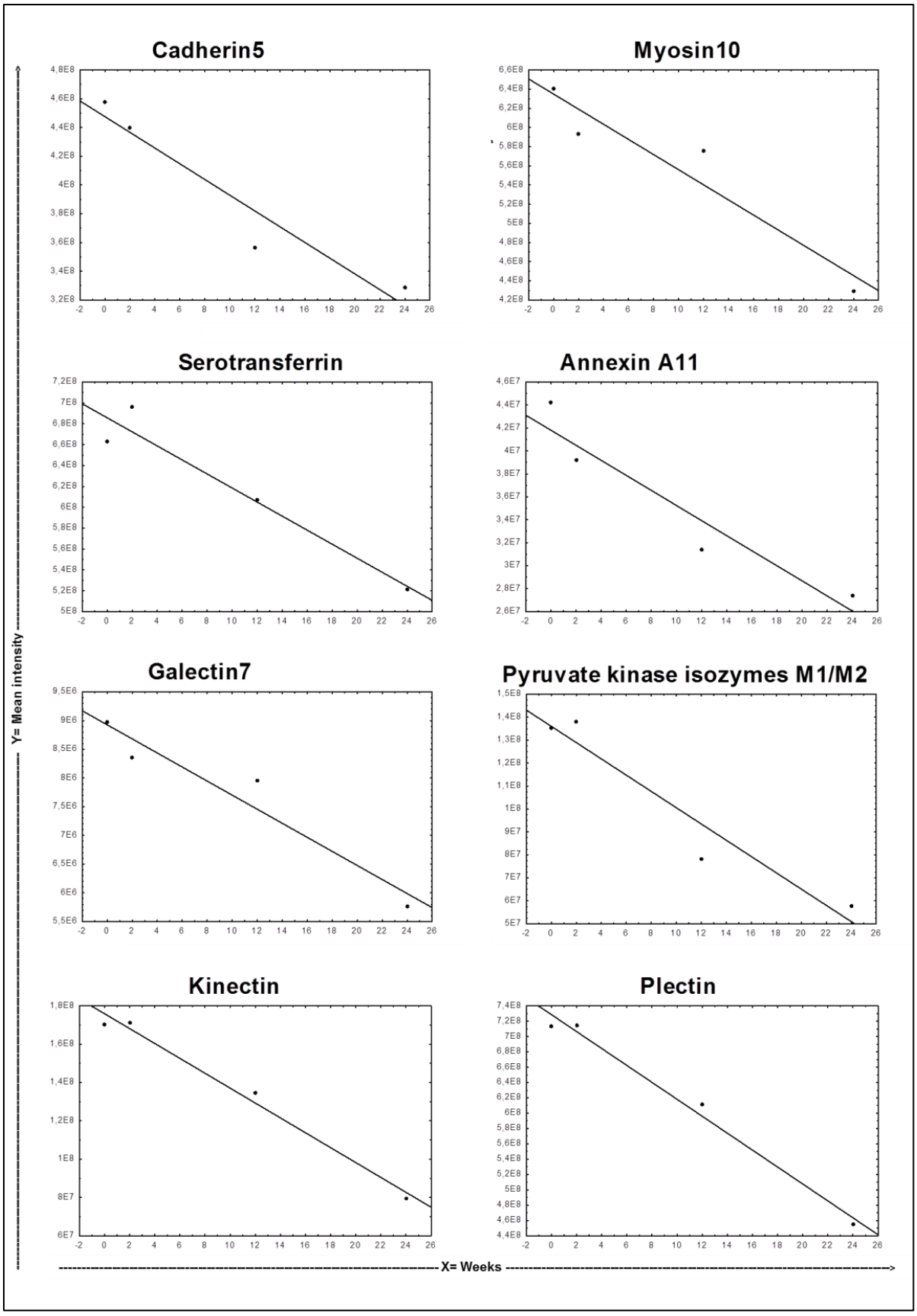


**Fig 64** Longitudinal pattern changes exemplary shown for selected tear proteins displaying a significant linear level decline in POAG patients in the course of Taflotan® sine application after swichting from Xalatan® medication. (Funke *et al.*, 2014)

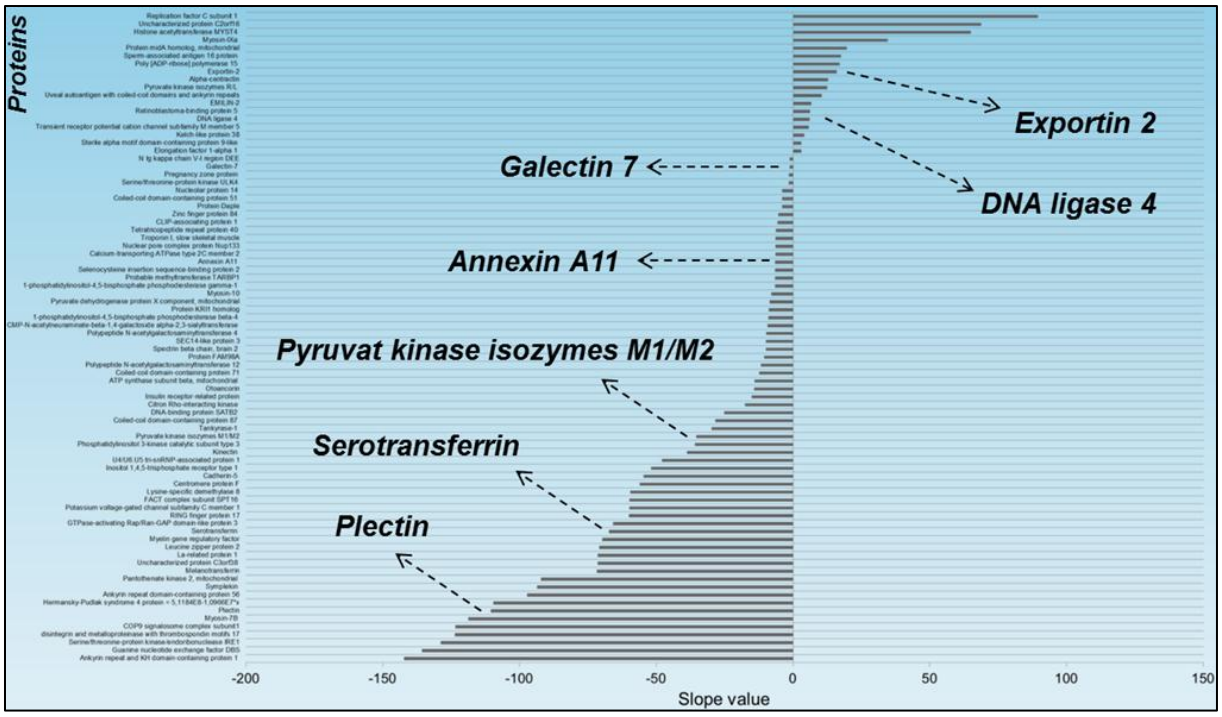


**Fig 65** Slope distribution of linear responding tear proteins in the course of Taflotan® sine medication: The predominant protein contingent showed negative slope values. Modified from (Funke *et al.*, 2014)

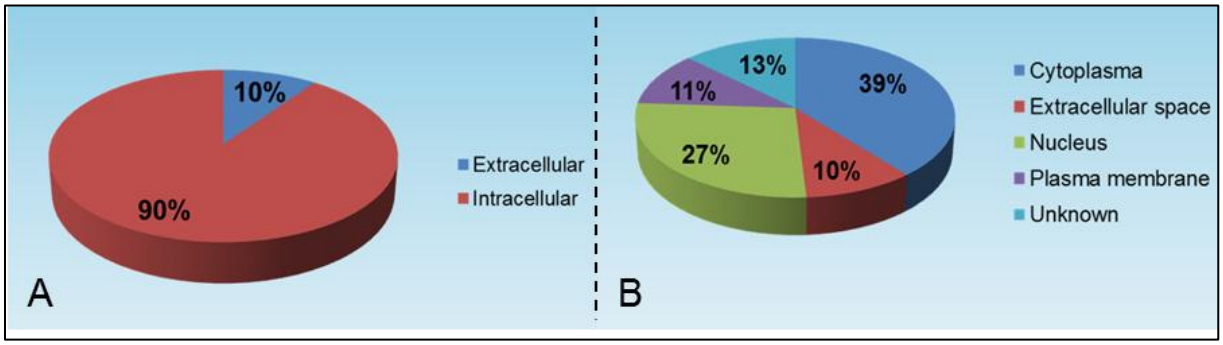


**Fig 66** Ingenuity® functional analysis of regulated candidate tear proteins; A: Most candidate proteins responding in the course of Taflotan® sine application were found to be intracellular proteins; B: The predominant portion of intracellular protein referred to cytoplasma and nucleus. Modified from (Funke *et al.*, 2014)

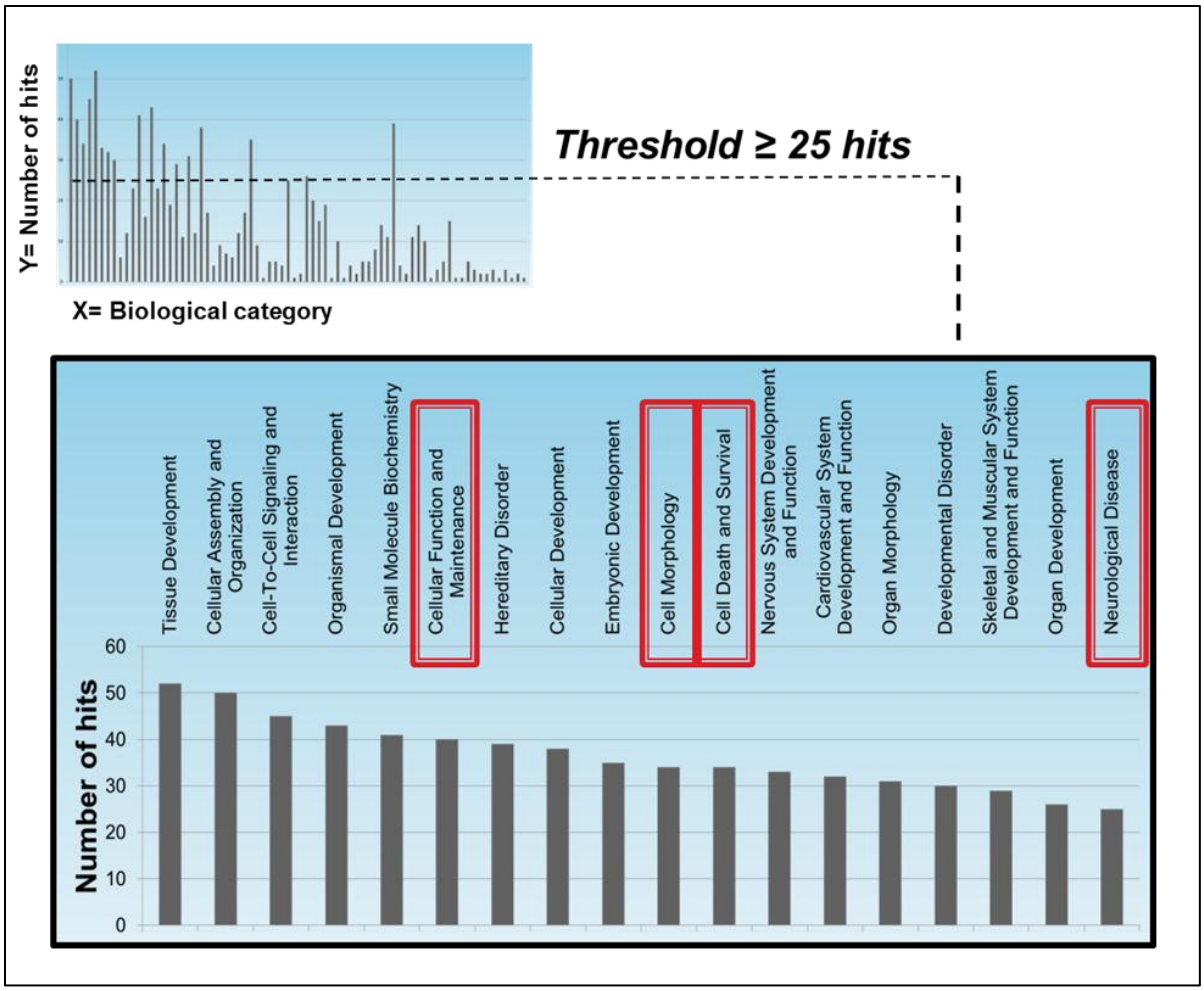


**Fig 67** Ingenuity® functional analysis of candidate tear proteins responding after the medicative switch: Numerous candidates were found to be involved in cell maintenance, survival and death; interestingly also several candidates could be annotated to neurological disease considering glaucoma.

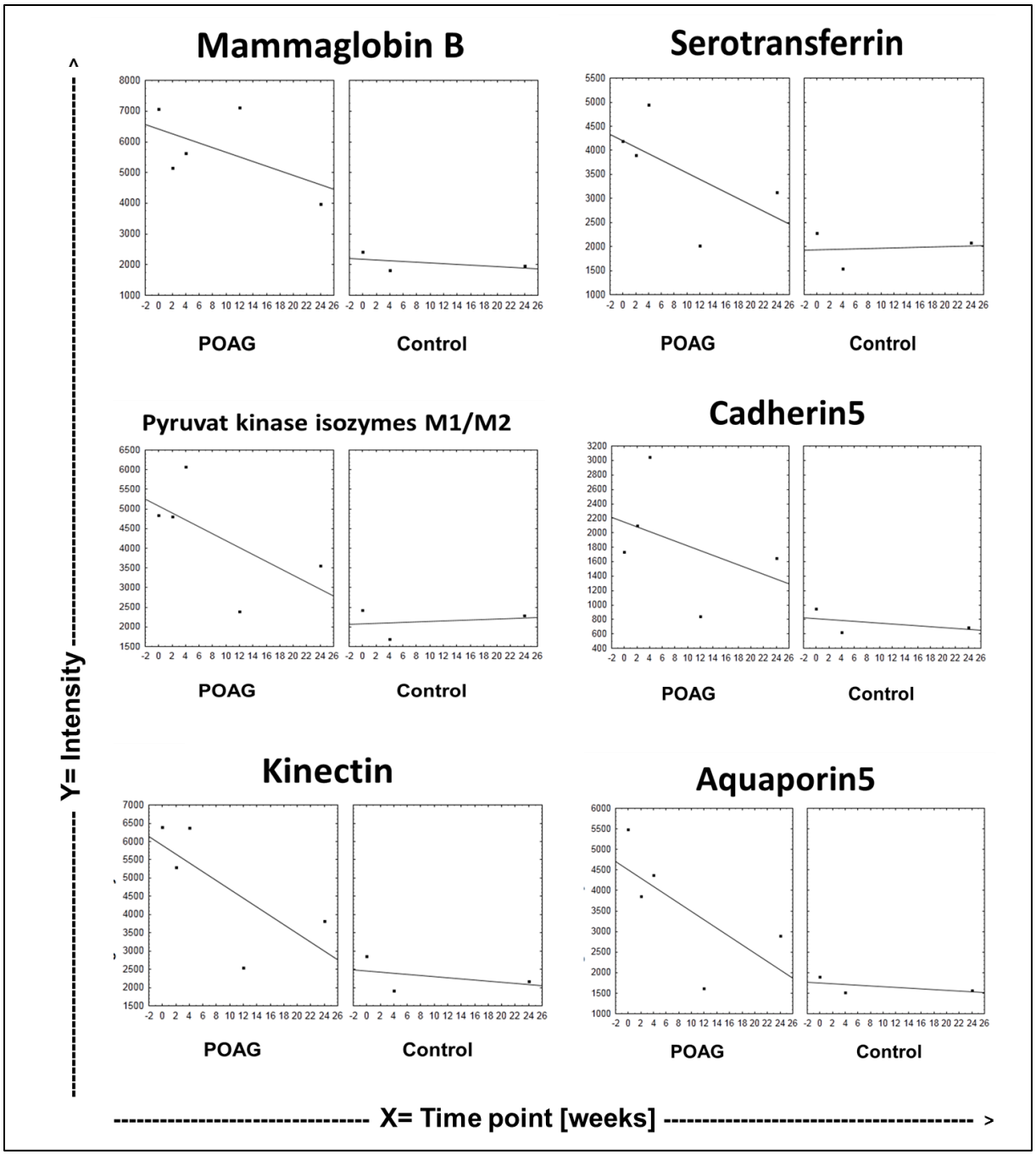


**Fig 68** Microarray (MA) validation of selected MS established candidate tear proteins in a larger subject cohort: The illustrated candidates show a distinct level approximation in the POAG group to the control group in the course of Taflotan® sine appliance indicating a recovery of the ocular surface. (Funke *et al.*, 2014)

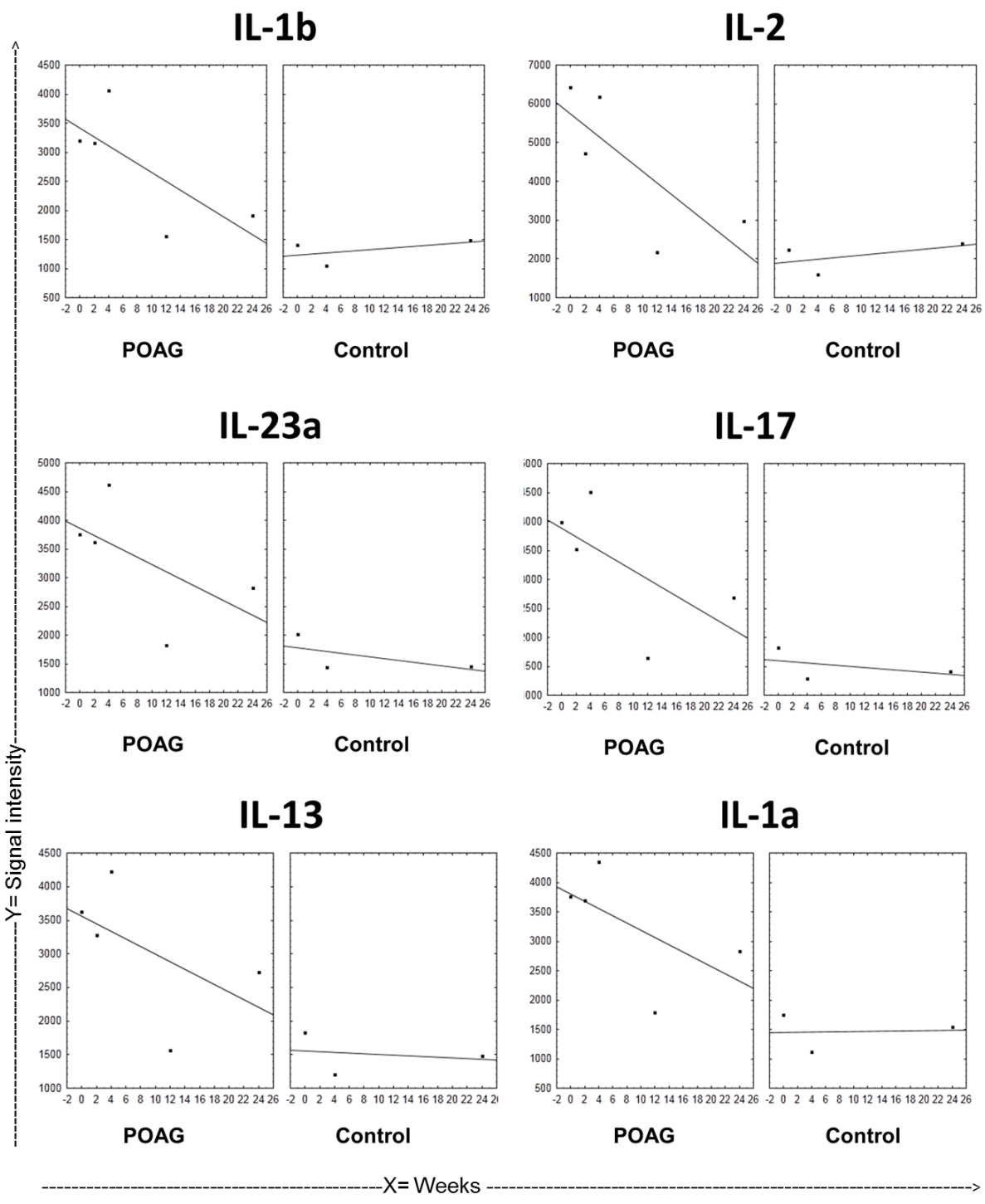


**Fig 69** Microarray (MA) validation tear cytokines: A distinct cytokine level approximation in the POAG group to the control group in the course of Taflotan® sine appliance could be revealed indicating a decline in inflammatory processes on the ocular surface. (Funke *et al.*, 2014)

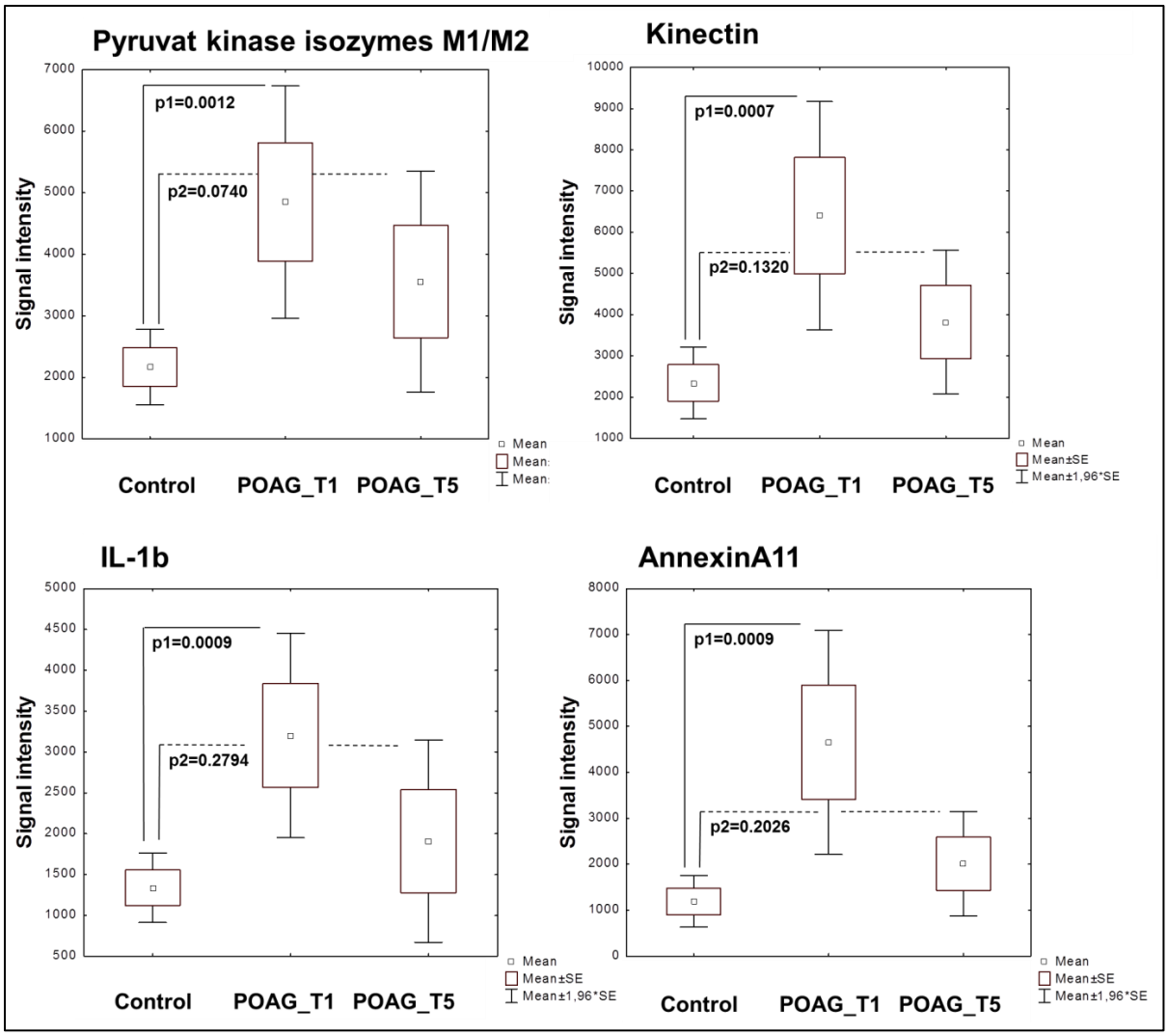


**Fig 70** Statistical estimation of level approximation in the course of Taflotan® sine application comparing control group to POAG group mean levels of exemplary candidate tear proteins (T1= study start, T5= study end): E.g. PKM showed an elevated significant different mean level to control at T1 and approximated to the control level at the end of the study (T5) displaying no significant mean level difference between POAG and control anymore. (Funke *et al.*, 2014)

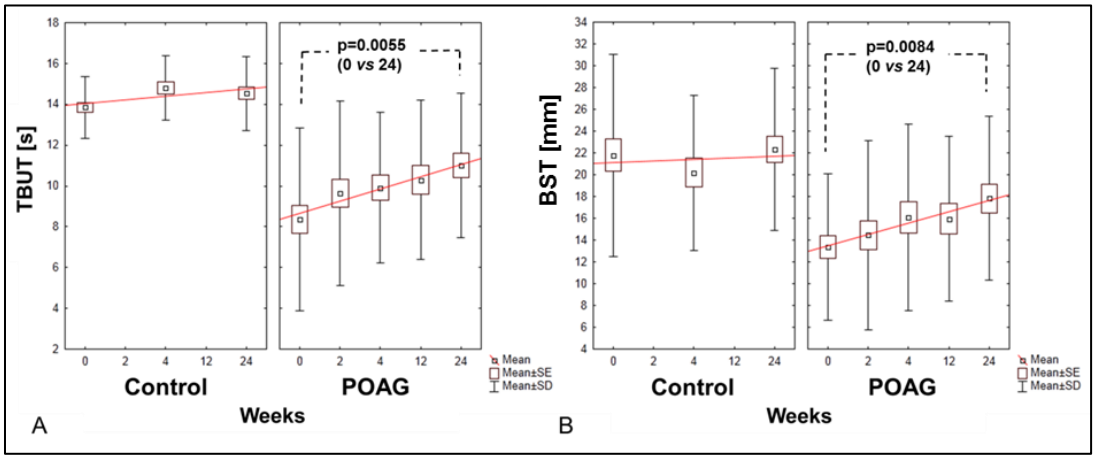


**Fig 71** Significant improvement of clinical parameters, TBUT (A) and BST (B) observed after the therapeutic switch from Xalatan® to Taflotan® sine indicating ocular surface recovery.(Funke *et al.*, 2014)

## 4.6 Influence of taurine on the ocular surface

### 4.6.1 Taurine effects on the tear proteome of contact lens wearers and sicca patients

Regarding 267 LC MALDI identified capillary tear proteins, longitudinal effects of taurine application were found as distinct potential responses concluded from linear regression over the 5 week study period in 9 proteins supported by $R^2$ values ≥0.5 (illustrated for exemplary tear proteins in Fig. 72). All of these corresponding proteins showed negative regression slopes representing a longitudinal protein level decrease as a potential response (Fig. 73). Linear taurine responses were predominantly observed in the contact lens group, whereas in the sicca group no distinct effects could be documented. Interestingly, the main portion of the responding candidate proteins refer to the immune system, e.g. complement C3 (score 383), Ig γ-4 chain C region (score 51), Ig λ-7 chain C region (score 826), secretoglobin 1D1 (score 680), α-2-macroglobulin (score 507) and haptoglobin-related protein (score 125). Thereby α-2-macroglobulin showed the most distinct level decrease towards taurine application reflected by its regression slope value (Fig. 73). Also, secretoglobin 1D1 and Ig λ-7 chain C region showed distinct negative slopes. Revealing non-linear taurine responses the *Kruskal-Wallis* analysis documented additional, prevalent inflammatory proteins like several Ig κ-related subunits. In contrast to linear responding candidates, these proteins showed a connatural bias in both taurine treatment groups; contact lens and sicca. Interestingly, the non-linear responding proteins showed a longitudinal level decline in compliance to the linear trend analysis. Ig κ VIII region HAH (score 107) and Ig κ chain C region (score 4135) (Fig. 74) showed significant effects towards taurine application ($p<0.05$). Post-hoc analysis revealed significant differences between the S_Taurine and CL_NaCl group for these two proteins. Regarding distinct tendencies, protein AMBP (score 39), putative beta-actin-like protein 3 (score 241) and transcription elongation factor B polypeptide 3 (score 129) were found to be downregulated by taurine treatment ($p<0.08$) in the sicca and in the contact lens group. Taurine responding candidate proteins were furthermore verified by comparing initial tear protein levels of contact lens wearers and sicca patients with those of healthy non-contact lens wearers. Distinct changes (≥2fold; ≤-2fold change) in protein levels of both groups; sicca and contact lens compared to those of healthy non-contact lens subjects could be demonstrated (Fig. 75). Focusing on the subset of taurine down-regulated candidates from both, linear and non-linear analysis, levels of all proteins were found to be increased in tears of dry eye and contact lens wearers compared to the healthy non-contact lens wearer tear pool. Ig λ-7 chain C region (score 826) showed a highly consistent strong level increase in both groups, sicca and contact lens compared to the healthy reference, whereas Ig γ-4 chain C was found to be upregulated in the sicca group with a higher level than in the contact

lens group. Most of the other proteins showed moderate differences between contact lens and dry eye, but significant alterations compared to the healthy reference.

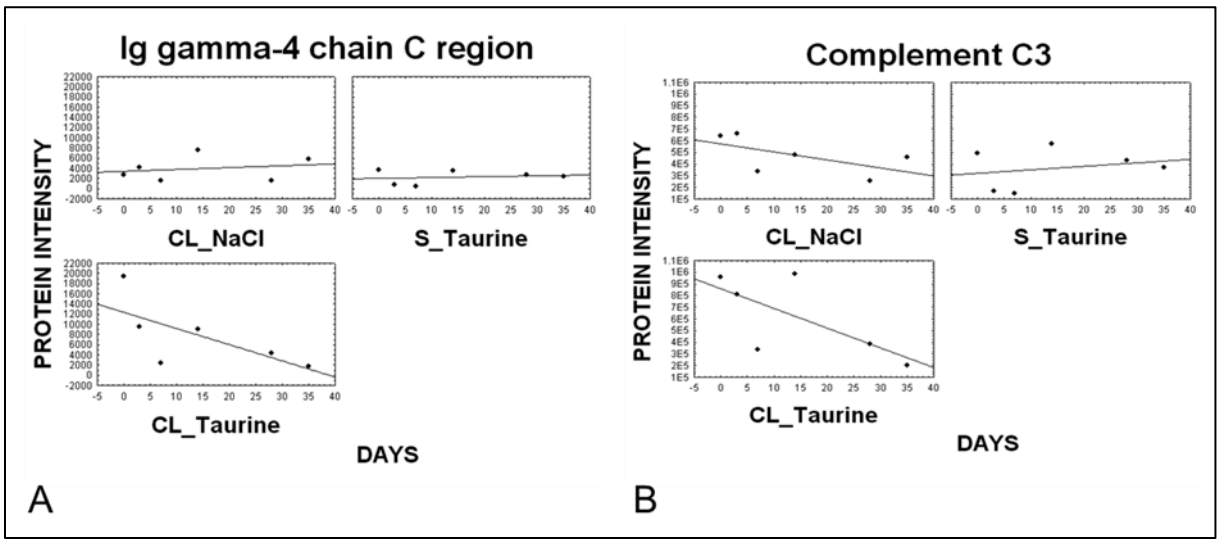


**Fig 72** Exemplary tear proteins responding to taurine application in the course of the study in the contact lens group (CL_Taurine) with linear level decline indicated by $R^2 \geq 0.5$. (Funke *et al.*, 2012)

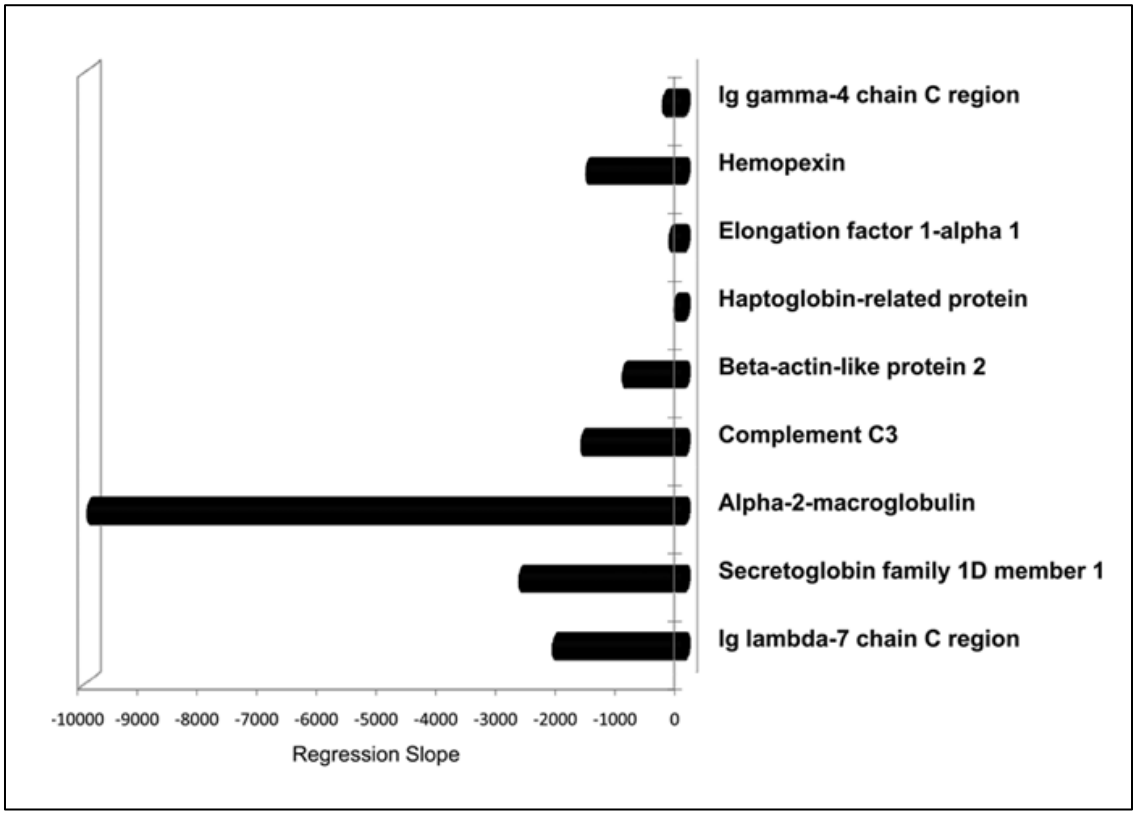


**Fig 73** Slope values illustrated for distinctly linear taurine responding tear proteins: α-2-macroglobulin displayed the highest level decrease towards taurin application. (Funke *et al.*, 2012)

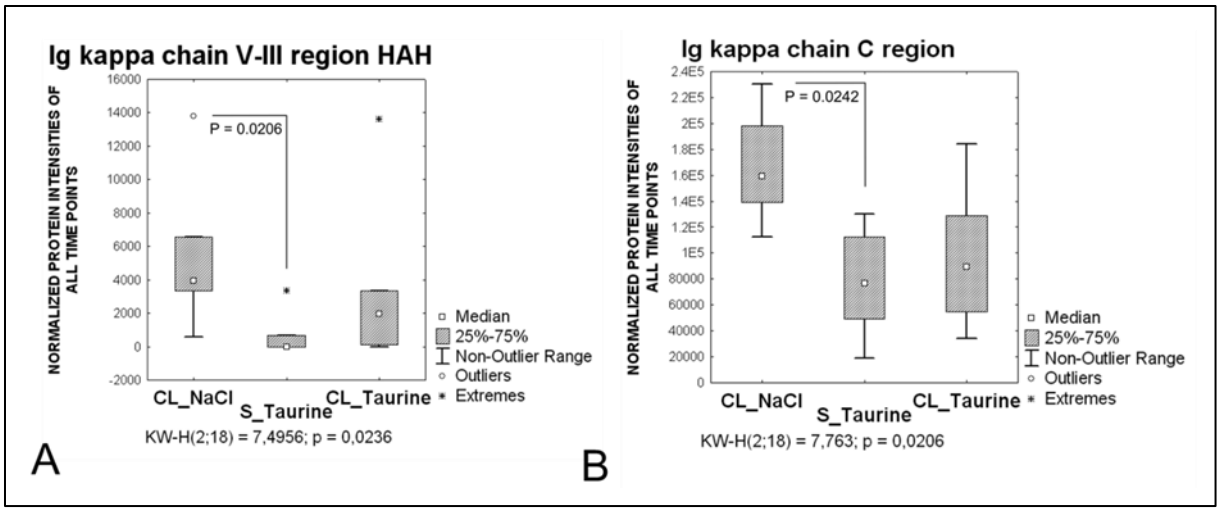


**Fig 74** Non-linear taurine responses revealed by *Kruskal-Wallis* analysis shown for two exemplary tear proteins, whereby both proteins showed significant differences between sicca and control group revealed by post hoc analysis. (Funke *et al.*, 2012)

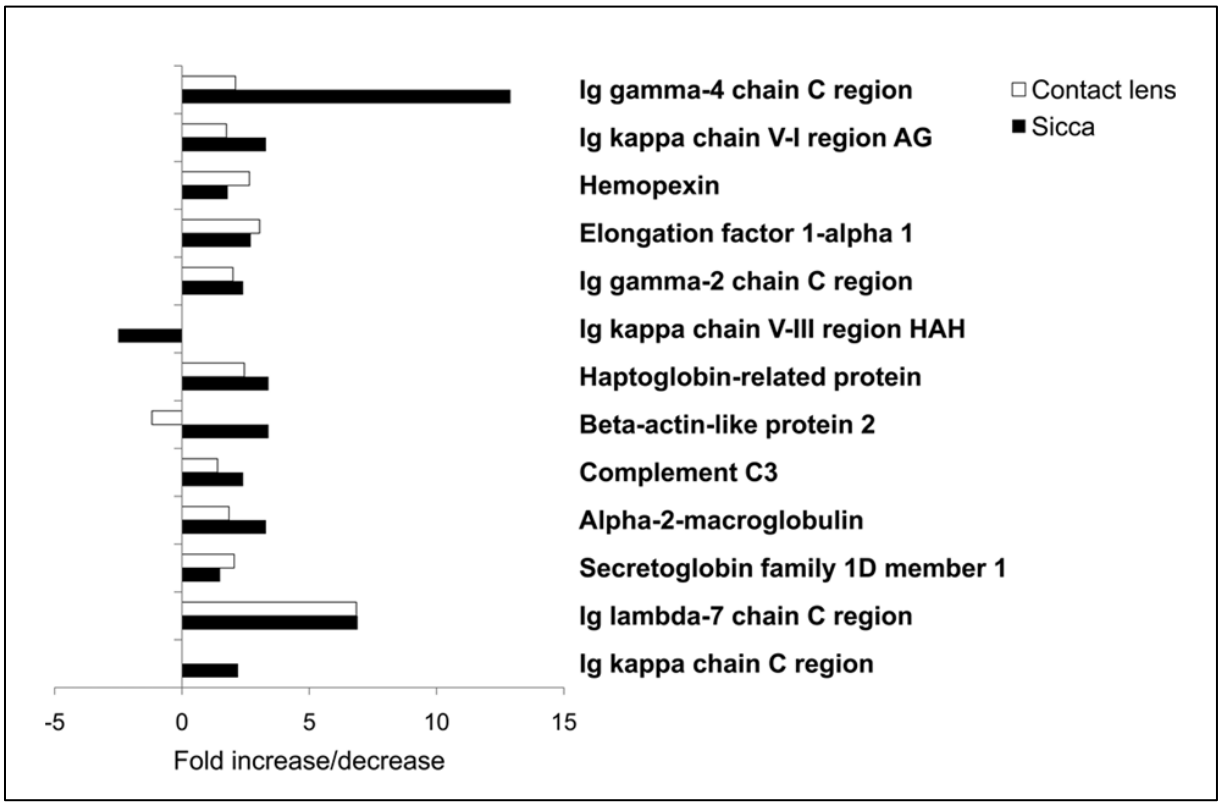


**Fig 75** Level changes between sicca patients and contact lens wearers in reference to a healthy non-contact lens wearer group (*N*= 8) as zero x-axis at study onset. (Funke *et al.*, 2012)

### 4.6.2 Taurine effects on the conjunctival proteome

Regarding the oxidative stress level of $H_2O_2$ stressed NHC-IOBA cells, it could be demonstrated that incubation with tested taurine concentrations (0.05, 0.2, 0.5, 1, 2 mM) lead to a distinct decline in ROS production compared to stressed control cells, which were not taurine treated. Accordingly, application of 0.05 mM taurine lead to a ROS reduction of 26% (p= 0.0356), incubation with 0.2 mM to a decrease of 29% (p= 0.0153) and treatment with 1 mM taurine showed a decline of 32% (p= 0.0016). Also, the other tested concentrations showed distinct ROS decrease responses, however, not significant reactions (Fig. 76A). Despite the obvious effects on ROS production, no significant effects were observed for taurine treatment of $H_2O_2$ stressed cells regarding cell viability. Furthermore, staurosporine stressed cells also failed to show significant viability effects and showed only weak tendencies of increased viability, reflected by a viability increase of 7% in cells incubated with 0.05 mM taurine. In contrast incubation of unstressed cells with taurine lead to a significant increase in viability observed for 0.05 mM (26%, p= 0.0055) and 0.2 mM (19%, p= 0.0181). Whereas also 0.5 mM taurine showed tendency of increased viability (15%, p= 0.0681), concentrations above this value showed no effect or negative responses of cell viability towards taurine treatment (Fig. 76B). Incubation of cells with taurine in a 20-100 mM range concluded in a significant loss of cells up to a percentage of 20% (100 mM, p= 0.0010) (Fig. 77B). Accordingly, in the presence of staurosporine for these critical concentrations additive negative effects could be observed with a maximum of 32% viability decline at 100 mM taurine (p= 0.0001). Moreover, ROS levels were found to be increased significantly from taurine concentrations above 20 mM with a maximum of 102% supplement of ROS production at 100 mM taurine (p= 0.0005). Thereby, incubation of stressed cells with taurine showed no significant counteraction towards ROS production displaying a maximum ROS level of 82% at 100 mM taurine (p= 0.000002). Contrary to ROS results of low taurine concentration, slight ROS elevations could also been observed in the initial concentrations, but were not revealed as significant and clearly differing from higher concentrations above 20 mM (Fig. 77A). In summary, these findings give evidence of taurine dose dependent effects regarding cell viability and ROS production. Whereas taurine incubation performed beneficially on cell viability and ROS generation in a 0.05-0.5 mM range, concentrations >0.5 mM displayed negative effects. For BU proteomic analysis on cellular taurine effects cell lysates obtained from taurine treated unstressed NHC-IOBA cells displayed high qualitative SDS PAGE migration pattern for both study parts corresponding to “elevated” and to “low” taurine concentrations (Fig. 78). Focusing on proteomic results, LC ESI analysis of unstressed conjunctival cells incubated with critical “low” taurine concentrations (4, 20, 50 mM) revealed several taurine target protein candidates. Thereby, taurine affected cellular proteins could be revealed. Interestingly, exclusively significant elevations reflected by a

minimum 2fold level increase in comparison to the control mean level could be observed. 30 proteins showed significantly increased levels in minimum one of the taurine concentration groups (4, 20, 50 mM) and a tendency of increase in the remaining groups (Fig. 79). Among these proteins, phosphoglycerate kinase 2 (score 3317), protein SET (score 2713), ubiquitin 60s ribosomal protein L40 (score 2235), protein S100 P (score 927), enoyl-COA delta isomerase 1 (score 561) were found as the top 5 scoring proteins. Moreover, several of the taurine responding proteins revealed by fold change displayed a significant linear response according to an increasing taurine concentration, which makes them highly suspicious for direct or indirect taurine interaction, e.g. glutamate dehydrogenase 2 ($R^2$= 0.978, p= 0.011) and glutaredoxin 1 ($R^2$= 0.959, p= 0.021). Next to the affected glutaredoxin 1 (score 214), which is indicative for cellular stress (Anathy *et al.*, 2009, Enoksson *et al.*, 2005, Murata *et al.*, 2003, Voehringer, 1999), numerous further altered proteins were found to be involved in cellular stress and apoptotic processes, e.g. cytochrome C oxidase subunit 2 (score 69) (Buron *et al.*, 2006, Green and Reed, 1998, Kadenbach *et al.*, 2004), which showed the highest increase level of all affected proteins (12.4 fold) or septin 2 (score 185) (Garcia-Fernandez *et al.*, 2010, Kinoshita, 2003, Longtine *et al.*, 1996). Also, an interaction with thimet oligopeptidase (score 143), a cytoplasma located metalloprotease (www.uniprot.org) could be proposed since taurine was also demonstrated to interact with matrix metalloproteinase 9 (Park *et al.*, 2000). Also sodium/nucleoside cotransporter 2 (score 37), nevertheless detected with a low score, could be proposed to interact with taurine since taurine was found to be released from cells by treatment with adenosine transport inhibitors (Hada *et al.*, 1996). In summary, the level increases of the mentioned proteins most likely indicate a direct cellular response towards elevated taurine concentrations which fits well with the observed negative taurine effects for these concentrations, demonstrated by ROS and cell viability assays. Additionally, the detected apoptotic and stress response proteins reflect the declined viability of the cells incubated with critical high taurine concentrations. In accordance, these findings support the functionality of the LC ESI MS workflow since apoptitic events on the cellular level could be reflected on a proteomic level. Thus, a huge contingent of responding proteins was not associated to apoptosis, conclusively highly interesting to be modulated by taurine in alternative pathways. Encircling both apoptic associated and non-associated proteins, among the responding proteins several candidates were found to interact in a direct or indirect manner with taurine inferred from the literature, e.g. phosphoglycerate kinase (Midwinter *et al.*, 2004, Nandhini *et al.*, 2005, Peskin and Winterbourn, 2006), cytochrome C oxidase (Millett *et al.*, 1982), protein S100 P (Reymond *et al.*, 1996) and glutamate dehydrogenase 2 (Schaffer *et al.*, 2000). Another interesting protein that was found upregulated by taurine treatment was sepiapterin reductase (score 97), which was suggested to play a crucial role in lipid metabolism (de Roos *et al.*, 2005). Upregulation

of proteolipid protein 2 (score 235), also gave evidence for taurine interaction. Since hydrophobic surfactant proteins had been already detected for tear fluid and/or the lacrimal gland system and had been proposed to play a key role for tear film stability (Brauer *et al.*, 2007a, Brauer *et al.*, 2007b) it is likely to suggest a comparable function for proteolipid 2 and moreover worth to mention, that it responds to taurine treatment. Since the membrane modifying potential of taurine is well documented (Huxtable, 1990, Lleu *et al.*, 1992) proteolipid 2 increase could be a consequence of taurine-membrane interactions. Confidently, transmembrane protein 109 (Mitsugumin 23) (score 411), an ER/nucleus membrane protein (Venturi *et al.*, 2011), detected for the first time for the ocular surface in this study, was found to display a level increase by taurine treatment, which emphasizes the influence of taurine on membrane systems. Regarding response reactions towards taurine treatment, several proteins showed no distinct fold changes, but 87 proteins were found to show a significant linear response correlating with taurine concentration increase, probably indicating a weak taurine response. Among them, the top 5 scoring candidates were heterogeneous carbamoyl-phosphate synthase (score 13385), elongation factor 1-α 2 (score 9574), neuroblast differentiation-associated protein (score 6396), L-lactate dehydrogenase B chain (score 6193) and multifunctional protein ADE2 (score 1718). Candidate related proteins displaying a clear fold change were depicted by the linear analysis. For example, importin-9 (score 131) was found to be significantly elevated, whereas importin-5 (score 815) was found to show a linear increase (slope: 3405, $R^2$= 0.959, p= 0.021) below the fold change threshold. De facto, 47% of potential apoptosis marker proteins, that have been detected in a study of hepatic stellate cells incubated with taurine could also been detected in this study with relatively high scores, e.g. annexin A1 (score 6596), peroxiredoxin 2 (score 4946) or protein DJ-1 (PARK7, Parkinson disease protein 7) (score 633) (Deng *et al.*, 2010). Protein DJ-1 is known to directly interact with EF-hand calcium-binding domain-containg protein 6 (score 150) (www.uniprot.org), a nucleus protein, which was found to be significantly upregulated by taurine treatment in the present study. Since taurine is well documented for its role in calcium translocation and homeostasis (Dolara *et al.*, 1978, Pasantes-Morales, 1982), it is very likely that it interacts with calcium-binding proteins. However, only translationally-controlled tumor protein (score 698), as one of these proteins, showed a significant linear level increase towards taurine treatment in confidence with the results of the hepatic stellate cell study. Interestingly, several proteins associated to oxidative stress response have been also found to respond to taurine treatment in a linear manner, e.g. thioredoxin 1 (score 121) (Holmgren, 2000, Yildirim *et al.*, 2007). In summary, 87 proteins were found to show a linear pattern change with increasing taurine concentration encircling protein up-and downregulations. However, in most cases intensities were below the fold change threshold, but are likely to indicate a regulation prognosis. Regarding

potential taurine protein targets obtained from LC ESI experiments, focusing on cells incubated with 0.05 mM taurine as preselected “beneficial” concentration, numerous responses could be recorded. Accordingly, 41% of the conjunctival cell proteins were found to respond to taurine treatment demonstrated by a minimum 2fold intensity change, whereby a small portion of proteins showed high level alterations towards taurine. Analysis of molecular function showed that the majority of the 2fold regulated proteins are involved in catalytic and molecule binding processes, whereby most of the proteins mediate protein-protein interactions (Fig. 80). In addition, whereas among the group of 2 to 5fold regulated proteins up and downregulation could be documented, the group of “highly regulated” proteins (>10fold) displayed exclusively downregulations, whereby like documented for the “mild regulated” proteins the majority of the “high regulated” proteins were involved in protein and nucleic acid binding (an overview of regulation distribution is given in Fig. 81). Thereby calmodulin, the taurine transporter control major player (Huang *et al.*, 2001, Ramamoorthy *et al.*, 1994), was found to be extremely decreased (24fold). Also, calmodulin-like protein 3 (score 95) was found to be extremely diminished (6fold). Additionally, another calmodulin related protein, calcium/calmodulin-dependent protein kinase type 1 (score 37) showed a slight decrease (2.3fold). ER calcium Atpase 2 (score 64) another calcium depending protein was also found to be weakly downregulated (2fold). These findings support a response of the calcium/calmodulin apparatus towards taurine treatment (Fig. 82). Furthermore a complete class of proteins, the *14-3-3* proteins (α, ß, Σ, γ, η, ε, δ) (scores: 1207-1435) exhibited slight level diminishments (2.2-2.5fold). Beside intracellular proteins, 7% of candidate proteins were found to be associated to the extracellular milieu, whereby the secretory protein galectin-1 (score 203) was slightly decreased (2.5fold) and galectin 3-binding protein (score 94), was found to be highly diminished (14fold). Also, a signalling protein, interleukin enhancer-binding factor 2 showed a distinct decline (10fold). The response of secretory proteins indicates the impact of taurine on cellular interactions with the extracellular environment. Focusing on “highly regulated” candidates, a predominance of downregulated histone species could be observed (Fig. 83). Also, the level of histone binding protein RBBP4 was decreased (10fold). Furthermore, a decline of certain DNA interacting proteins like DNA binding protein A, Y-box protein 2, representative fragments of DNA primase/polymerase/lyase could be documented indicating gene expression changes. Downregulation of F-box only protein 22 is indicative for anti-apoptic processes, due to ubiquitine-dependent proteolysis and apoptosis mediation (Patton *et al.*, 1998, Winston *et al.*, 1999). High abundant stress and apoptose associated proteins, e.g. peroxiredoxin 4 (score 1047), 6 (score 1724), glutamate dehydrogenase 2 (score 73), cytochrome C (score 48), cytochrome C oxidase subunit 2 (score 43), thioredoxin (score 207), glutathione S transferase κ 1 (score 129) showed level declines between 2 and 3fold (Fig. 84). Additionally,

glutathione S-transferase Ω (score 687), superoxide dismutase [Cu-Zn] (score 1419) and microsomal gluthation S-transferase 1 (score 92) exhibited distinct to extreme level diminishments (6fold, 7fold, 12fold). In contrast, several of related oxidative stress proteins, e.g. glutaredoxin 1, thioredoxin 1, glutamate dehydrogenase 2 and peroxiredoxin 2 were found to be upregulated in cells treated with critical taurine concentration >20 mM, which emphasizes the beneficial potential of lower taurine concentrations on cells. In summary, cell viability assays demonstrated a dose-dependent taurine agency on oxidative stress level and viability of NHC-IOBA cells. Distinct proteomic changes could be documented for adverse and beneficial taurine concentrations supporting the impact of taurine on conjunctival cells, thereby revealing numerous potential taurine protein targets.

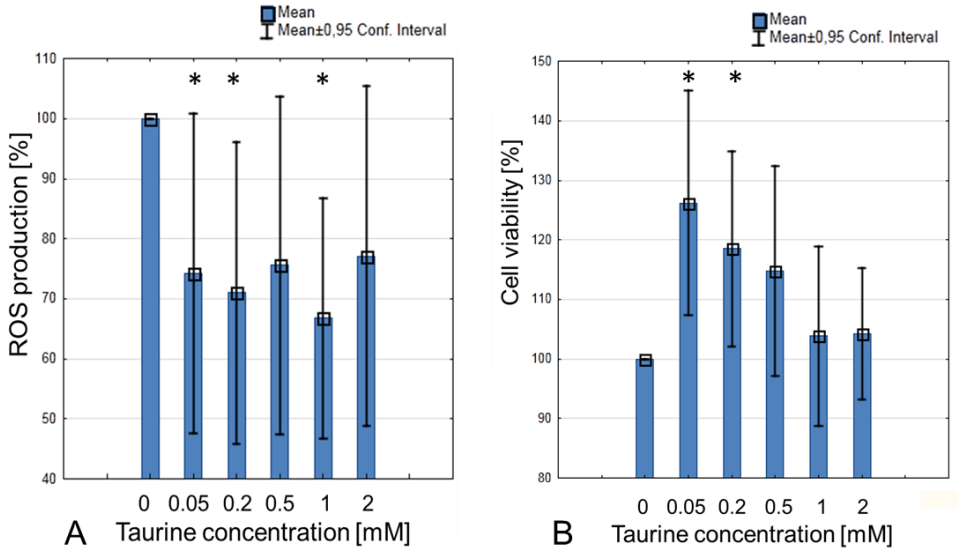


**Fig 76** Influence of different low taurine concentrations on conjunctival cells; A: ROS production is distinctly decreased compared to untreated control cells; B: Viability increased by incubation with 0.05-0.5 mM taurine (significant responses $p<0.05$ are indicated by asterisk).

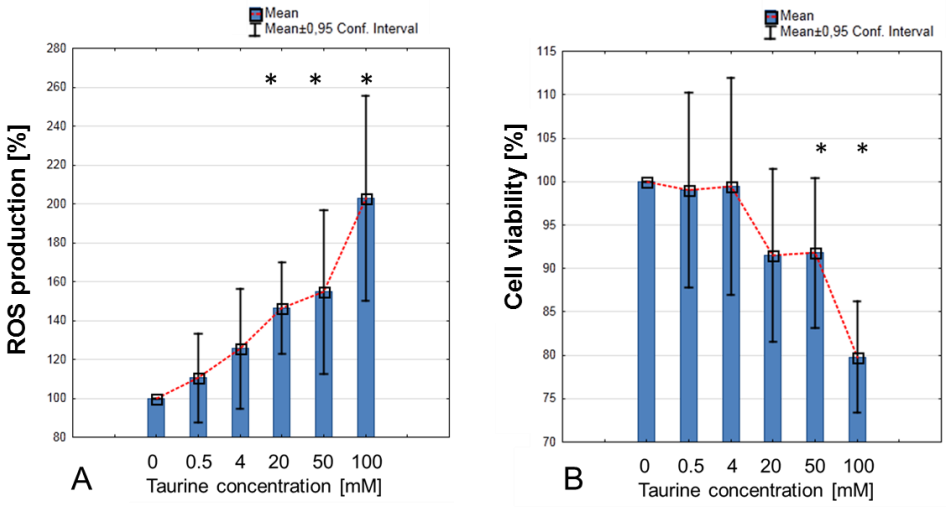


**Fig 77** Influence of different elevated taurine concentrations on conjunctival cells indicating dose-dependent taurine toxicity in elevated levels; A: ROS production levels show an increase towards taurine treatment with significant differences from 20-100 mM taurine; B: Cell viability was found to decline from 20-100 mM. (significant responses $p<0.05$ are highlighted by asterisk)

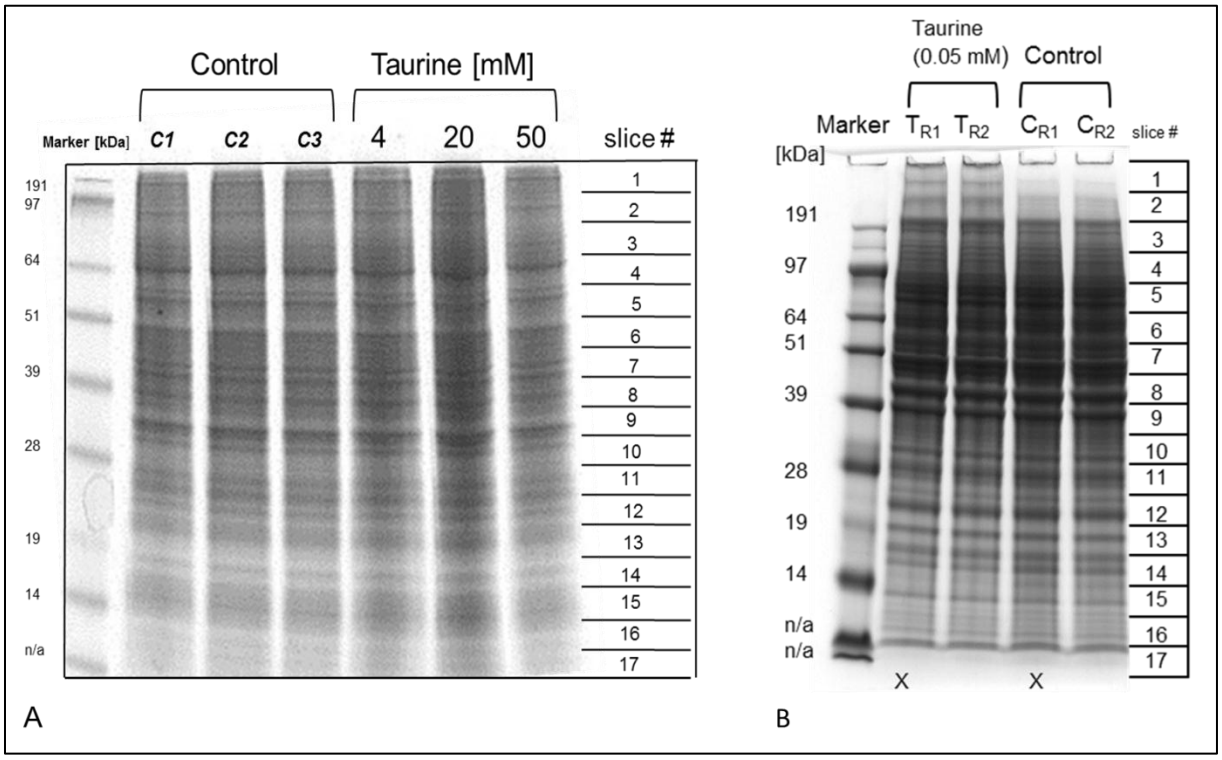


**Fig 78** SDS PAGE migration pattern of lysates corresponding to pooled conjunctival cells treated with different taurine concentrations destinated for LC ESI MS analysis; A: “Elevated” taurine concentration range (C1-C3= untreated control cell lysates, all lanes were selected for MS analysis); B: “Low” taurine concentration range (R1/R2= technical replicates, lanes highlighted by x were selected for MS analysis).

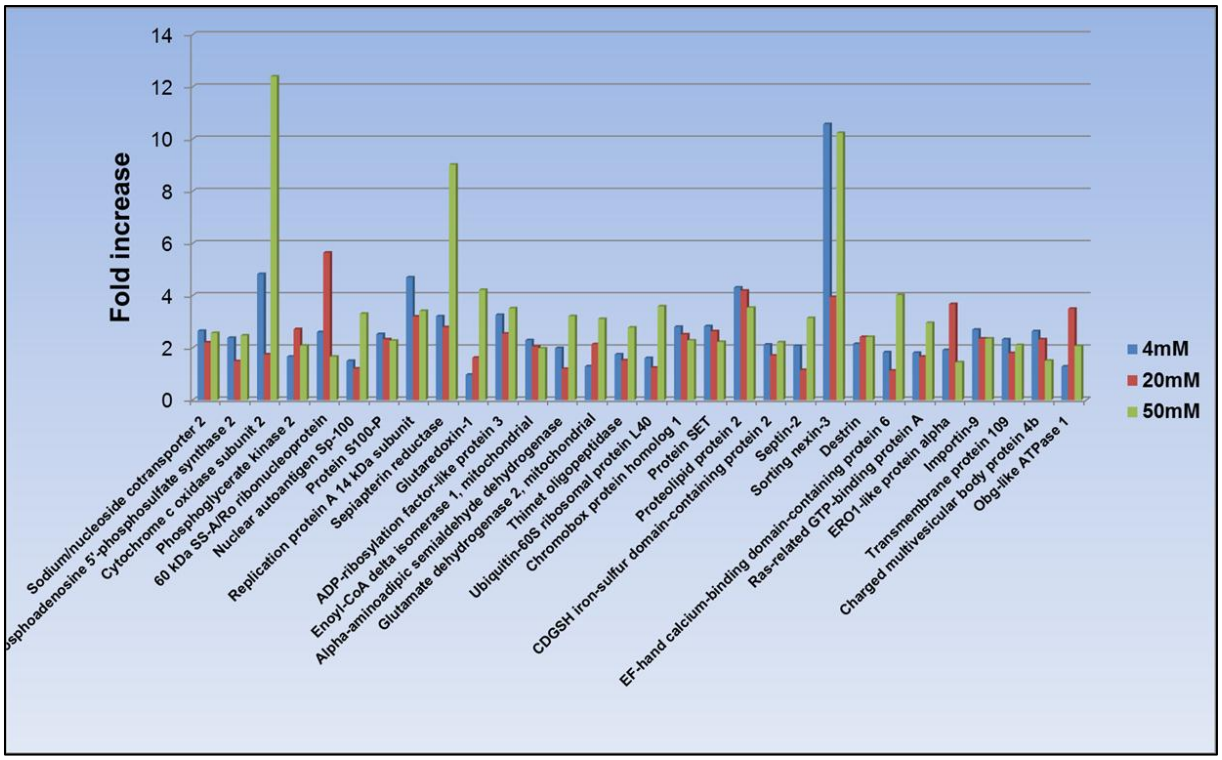


**Fig 79** Conjunctival cell proteins responding to incubation with different “elevated” taurine concentrations inferred from level alteration referring to untreated controls (x-axis: zero-line). High upregulations could be e.g. observed for cytochrome C oxidase subunit 2, sepiapterin reductase, glutaredoxin 1, sortin nexin 3 which are involved in cellular stress.

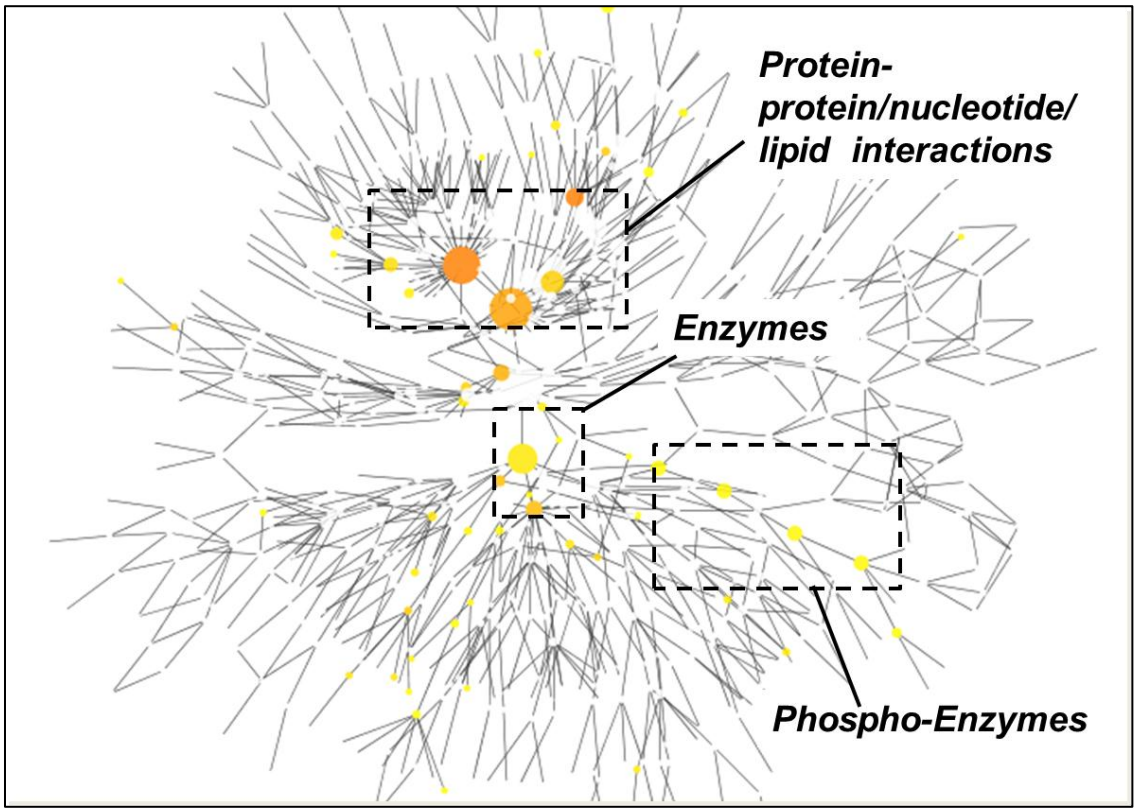


**Fig 80** Cytoscape GO analysis of conjunctival cell proteins responding to incubation with 0.05 mM taurine indicating a predominat contingent of enzymes and binding proteins.

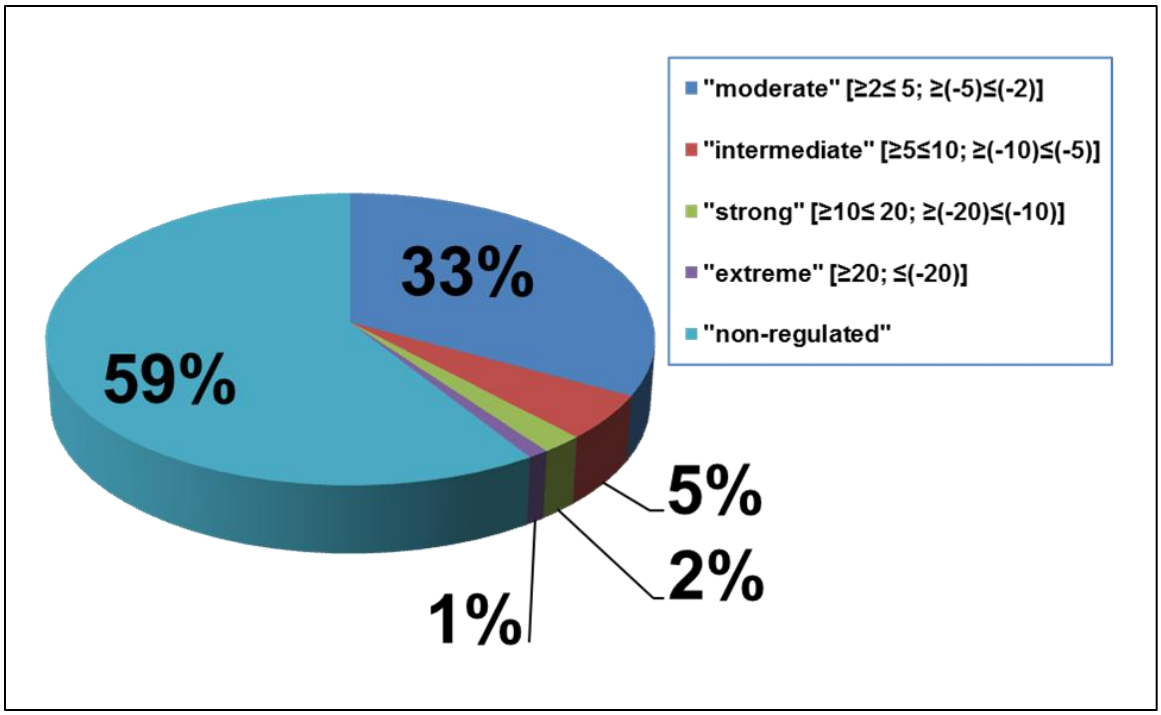


**Fig 81** Classification and distribution of regulation forms towards incubation of conjunctival cells with 0.05 mM taurine.

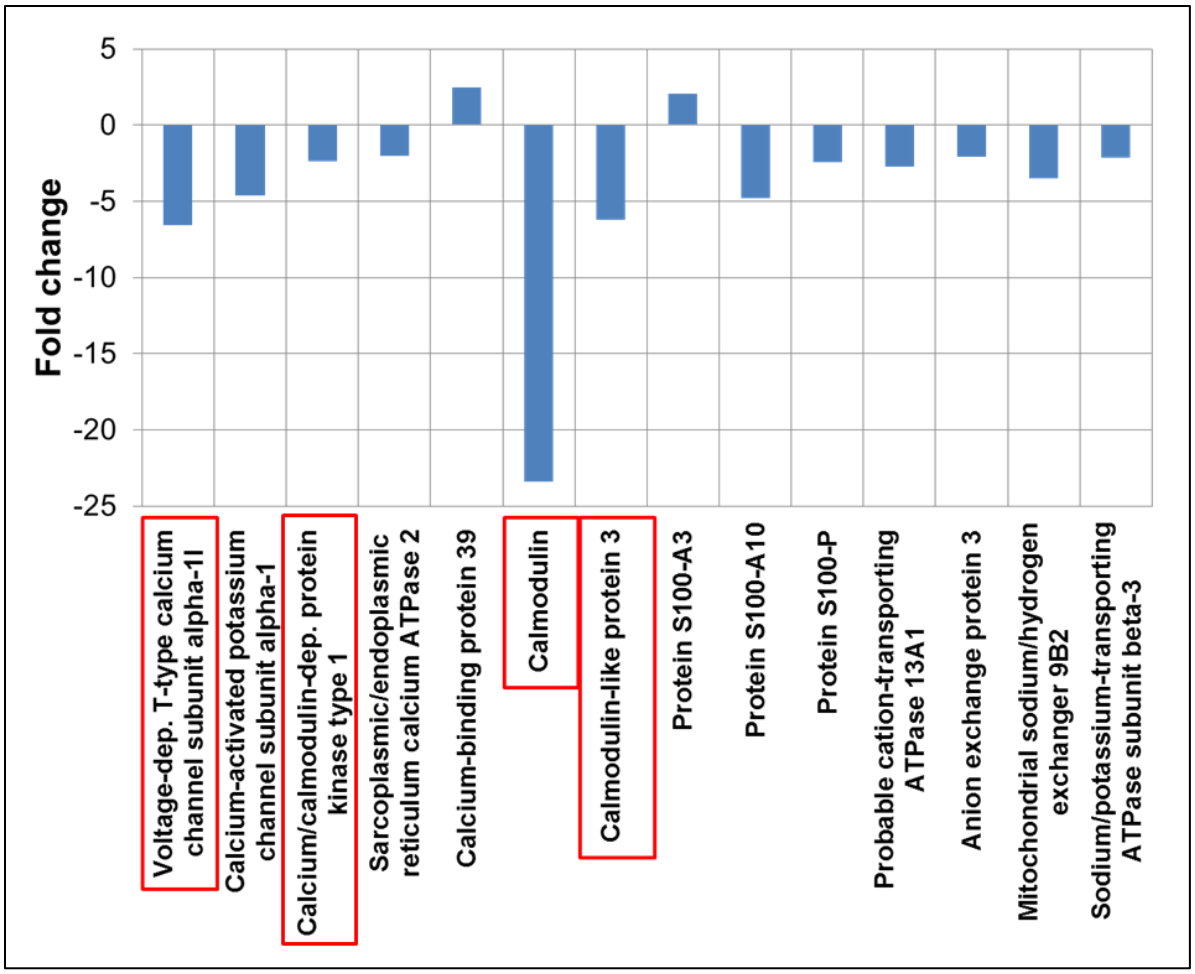


**Fig 82** Exemplary taurine affected proteins revealed by LC ESI MS BU analysis: Members of the calcium/calmodulin system (highlighted in red frames) were distinctly downregulated after incubation with 0.05 mM taurine referring to an untreated control (x-axis, zero line) indicating changes in taurin traffic.

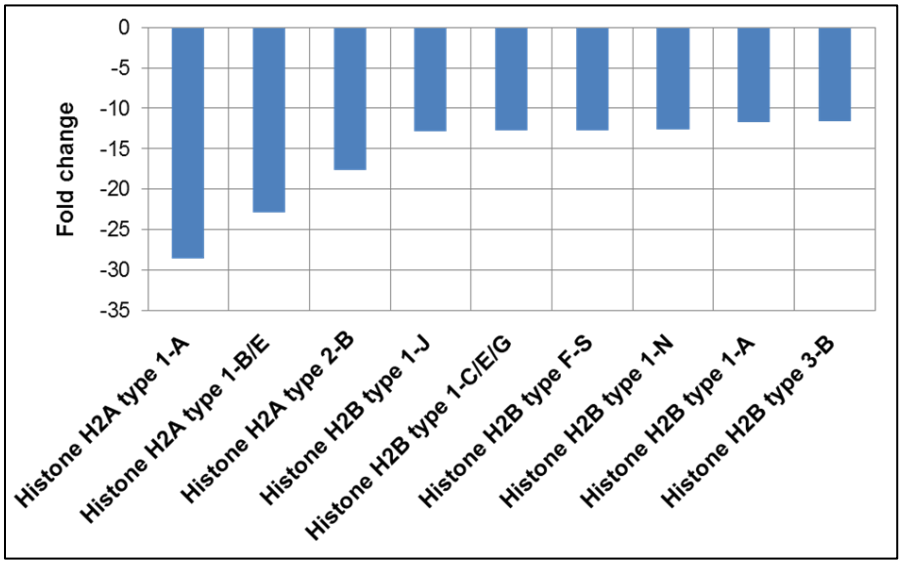


**Fig 83** Distinctly decreased histone species levels revealed by LC ESI MS BU analysis observed in conjunctival cells incubated with 0.05 mM taurine in reference to an untreated control (x-axis, zero line).

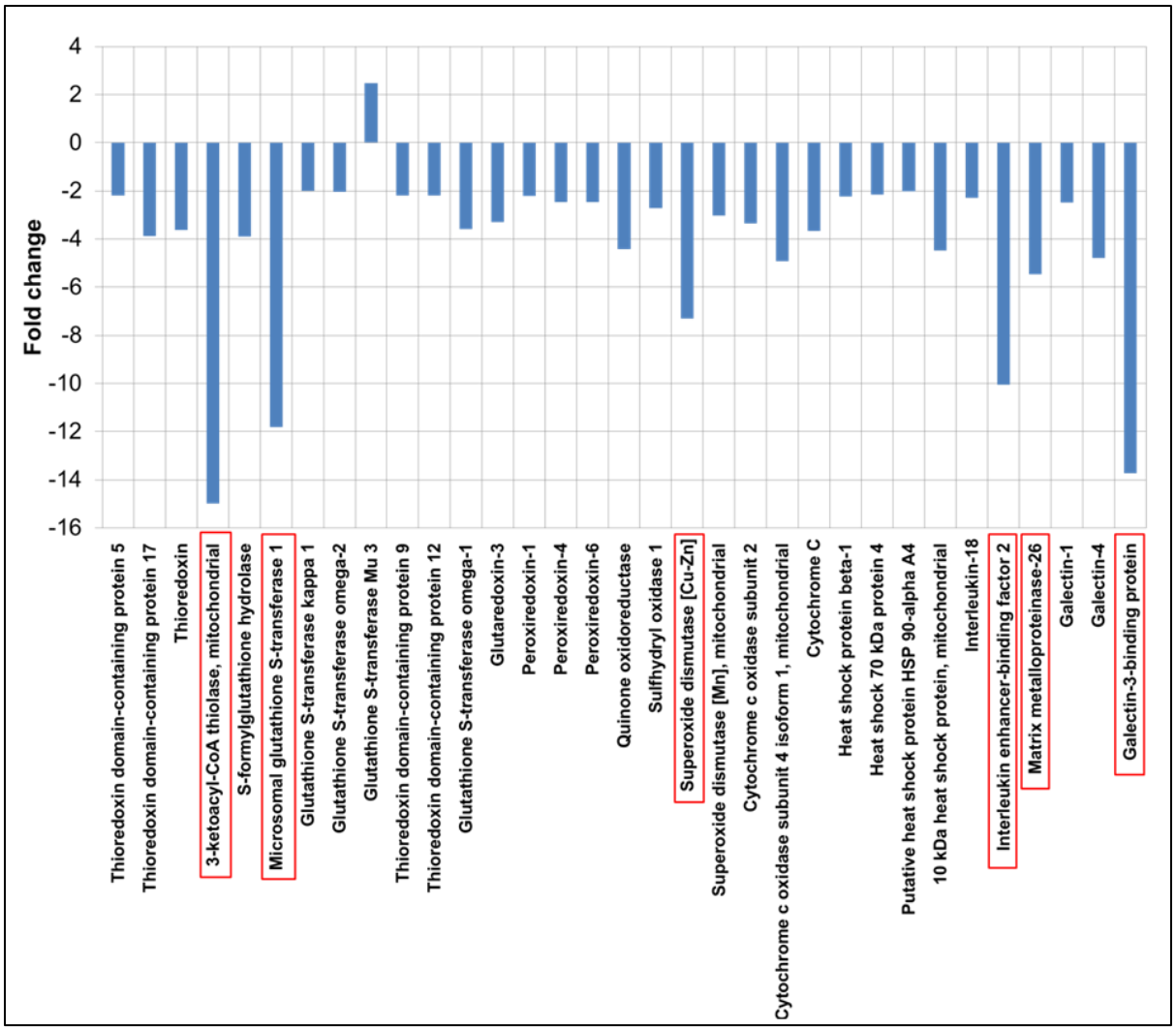


**Fig 84** Cellular stress related proteins affected by 0.05 mM taurine incubation referring to a healthy control (x-axis, zero line) (distinct regulated protein candidates are highlighted in red frames).

# 5 Discussion

## 5.1 Top Down (TD) *vs.* Bottom Up (BU)

Referring to the data, BU analysis showed several advantages over the TD setup. In terms of the advantages of the TD workflow high analysis speed, minimal sample processing, robustness towards crude sample species, suitability for hightroughput studies, sensitivity towards the medium mass range of cellular materials, low costs and easy lab routine integration are highlighted. Besides, the method robustness allowed a highly pure view to the medium mass cell proteome. Like in SELDI, the main drawbacks of the engineered LC MALDI TD approach were attributed in the difficulties to directly identify intact protein (Nilsen *et al.*, 2011). Even by use of more sophisticated instrumentation like quadrupol analyzers, a direct fragmentation >6000 Da is still challenging (Peng *et al.*, 2009). Moreover, the diminished reflector detection sensitivity made it hard to select targets which already displayed low abundance in the linear mode. In fact, proteins of interest have to be enriched and purified for successful identification (Seibert *et al.*, 2004). Accordingly, follow-up strategies for recapturing the component of interest were found time-consuming and difficult, encircling enrichment of the target component by use of SPE, visualization by SDS-PAGE, alignment of the mass area, in-gel digestion and finally alignment to the literature. Time consuming and laborious accumulation of these TD components can also be realized by antibody pull-down experiments with subsequent MS redetection (De Bock *et al.*, 2010) or by use of size-exclusion chromatography combined with SDS-PAGE and reprofiling of the components of interest (Guo *et al.*, 2005). Nilsen and coworkers reported a more promising follow-up strategy for protein reprofiling recommending “on-chip elution” (Nilsen *et al.*, 2011). Nevertheless, in context of protein identification, initial TD benefits were decreased by the drawbacks of the follow-up steps. Furthermore, the low performance of the method to analyze sample species of less protein content, like tears, was found also disadvantageous. However, for fast and reproducible analysis of cellular sample species as demonstrated for RGC5 training samples, the workflow is highly suitable and can also be used for the analysis of ocular surface epithelia lysates to monitor overall proteomic effects that may indicate cellular responses, e.g. in therapeutic studies. Such proteomic patterns have been successfully used in a TD study to monitor the influence of contact lens cleaning solutions on conjunctival cells (Bell *et al.*, 2012a), to evaluate the influence of glaucoma patient serum, antibodies (Bell *et al.*, 2012b) and cyclooxygenase inhibitors (Brust *et al.*, 2006) on retinal cells and to characterize tumor cells (Cazares *et al.*, 2002, Gretzer *et al.*, 2004, Yanagisawa *et al.*, 2003, Zhukov *et al.*, 2003). Another approach could be to address small protein/peptide components (Jimenez *et al.*, 2007a, Kutz *et al.*, 2004, Villanueva *et al.*, 2006) or low molecular components <1000 Da (van Kampen *et al.*, 2011), e.g. ocular surface

degradative fragments (Abalain *et al.*, 2000, Wheater *et al.*, 1999) or profiling of known masses. To overcome the lack of identification, the method can also be suited for the analysis of tryptic digests initially facilitating statistics followed by fragmentation of tryptic peptides of interest (Dekker *et al.*, 2005, Neubert *et al.*, 2008). Nevertheless, in this work for in depth analysis of the ocular surface, encircling conjunctival cells and tear fluid, the BU strategy has turned out the more effective approach characterizing proteins >4000 Da. Also, SDS PAGE as a first fractionation dimension allows visual inspection and densitometric evaluation if needed (Neuhoff *et al.*, 1990). Regarding in-gel digests it is possible to directly monitor protein markers in a wide mass range obtaining knowledge of their identity. In contrast, in TD approaches a high risk remains that significant markers stay unidentified resulting in a costly loss of biological information and making targeted follow-up studies on candidate proteins impossible. In fact, by use of the BU approach “in depth” analysis of human tear fluid and cell samples could be realized providing >1000 proteins per sample type, whereby proteins could be annotated to biological functions and subcellular localizations and could be further reconciled with the literature for disease and clinical acquisition. Nevertheless, also several limitations have to be mentioned. First of all, the approach is more costly, time and lab intensive, since proteins have to be fractionated by SDS-PAGE, in-gel digested and in case of LC ESI purified by SPE prior to analysis. Considering sample preprocessing steps and the more profound analysis protocol the method is less easy to implement to the daily lab routine as the TD approach. Further drawbacks are the use of pool samples to reduce costs and analysis time, especially in labs with a high project contigent. Accordingly, there exists a challenge in statistical evaluation and the need for time consuming and costly validation experiments, which can be realized by antibody-based microarray analysis of MS derived marker candidates. In fact, the use of pool samples is widely practiced in proteomic analysis (Castano *et al.*, 2006, Neubauer *et al.*, 2006, Tonge *et al.*, 2001) addressing costs and limitation of resources, and was found as a valid but considerable strategy in terms of reduction of biological variance and comparison between pool and mean protein expression (Diz *et al.*, 2009). Thus, despite sample pooling has been proposed to “mute unrelated alterations by dilution” (Weinkauf *et al.*, 2006) it seems to exist a sample-dependent ratio between technical and biological variation that has to be considered for the setup of experimental designs (Karp and Lilley, 2009). De facto, an “in depth” analysis of a large number of individual samples is not realistic in case of the developed BU strategy considering costs, effort, analysis time and realization of numerous parallel running projects. However, sensitivity and the possibility to identify large numbers of proteins allowing orthogonal follow up research on identified candidate proteins and the possible establishment of large protein maps with knowledge on protein localization and function achieved by the BU approach surmount the possibilities of the developed TD

approach. However, there is a high potential in combining both developed strategies in the analysis of cellular ocular surface sample species, BU studying proteins >4 kDa and TD monitoring statistical changes in small protein fragments. As an outlook, the fast TD screening for known signal peptides in digests which have already been proven for particular proteins by use of the intensive BU proteomic strategy or orthogonal methods may be a promising future direction to combine benefits of both strategies. For this reason, the protein maps established in this work could be screened for signature peptides that uniquely correspond to a particular protein of interest and their fast reprofiling in large sample cohorts by use of the TD approach, probably allows less costly, lab-intensive and deeper statistical understanding of ocular surface disease processes. However, such signature peptides have to be proven in TD analysis in a first step, which is the challenge in such a combinatory strategy with respect to different ionization mechanism in ESI and MALDI systems.

## 5.2 Bottom-up (BU) analysis: LC-MALDI vs LC-ESI workflow

The obtained results support the high reproducibility for both approaches. However, there are distinct differences between MALDI and ESI workflows regarding the developed BU approaches. The RT reproducibility was excellent in the ESI workflow with low precursor mass shifting additionally supported by *CV* values <1% in confidence with the literature reporting values between 0.1 to 4.5% observed for comparable systems (Duan *et al.*, 2009, Dunn *et al.*, 2008). In comparison, also the MALDI approach showed a high RT reproducibility. An important factor which impacts on LC separation efficiency in LC MALDI experiments is the fraction collection performance and sample space limitation regarding target plates. In contrast, separation efficiency in continuous LC ESI workflows is predominantly limited by the column system and flow rate. However for both approaches there is a need to compromise between efficiency, lab effort, costs and analysis time regarding analysis of multiple sample sets settling pro and contras between both strategies. Focusing on the effort/output ratio for analysis of complex sample types, the LC ESI workflow presented superior over LC MALDI. That is why the sensitivity was found to be clearly higher in the ESI method regarding severe complex sample species like tear fluid to more complex sample species like cell lysates. Without a doubt, this is not explicable by the ionization technique but due to the coupled hybrid MS system providing a higher dynamic range (Makarov *et al.*, 2006b) for higher performance than TOF systems (Zhang *et al.*, 2000). De facto, the main reason for the high accuracy is based on the high resolution achieved by the orbitrap system clearly exceeding TOF systems thereby exceeding a critical value which allows the discrimination between coeluting components (van der Heeft *et al.*, 2009). In comparison with the LC ESI based highly accurate hybrid system, the MALDI platform cannot go strong with its beneficial attributes like high salt and contaminant tolerance, small

sample consumption and sample storage for reanalysis (van Kampen *et al.*, 2011, Zhang *et al.*, 2004a). As a matter of fact, regarding practical aspects of the preionization sample process fraction, deposition complications due to abrasion of the robot tip in the MALDI workflow balanced with spray incursions due to thermal damages of the spray needle in the ESI approach. Nevertheless, whereas the MALDI approach saved time in sample pre-processing due to higher contaminant tolerance it lost speed in fraction deposition and matrix spotting compared to the ESI approach. A further interesting difference was observed by tear film analysis, whereby it was shown that the MALDI approach yielded in extremely high scores for a few prominent tear proteins, whereas the ESI approach identified a higher number of proteins but did not accomplish the absolute score values resulting from the MALDI analysis for selected predominant tear proteins, e.g. proline-rich protein 4 or lysozyme. Most likely this observation reflects adverse of the TOF analyzer resolution performance for complex protein mixtures in comparison to the orbitrap analyzer. Another possibility is the concurrence for ionization and ion suppression effects (Annesley, 2003, Jessome and Volmer, 2006, Muller *et al.*, 2002, Wang *et al.*, 2004), which may lead to a positive discrimination of abundant peptide ionization in the MALDI approach. Preference of high intensive peptides is a well-known phenomenon in MALDI experiments and counteracting strategies like replicate runs considering precursor ion exclusion lists (Chen *et al.*, 2005) have been developed. Furthermore, fragmentation strategies in both instruments are different, whereas the MALDI approach was prepared for PSD, the ESI method was tuned for CID fragmentation leading to different fragment pattern (Hoteling and Owens, 2004, Li *et al.*, 1999). Although, the possibility of reanalysis and optimization of the measuring protocol of identical sample sets is an important advantage of MALDI over ESI technology (Ishihama, 2005), it is hampered by the need for analysis time. Actually, the fragmentation speed of the TOF/TOF systems was found to clearly underlie the speed of the LTQ Orbitrap instrument. A problem observed in both developed BU workflows was the high portion of fragment spectra, which failed to successfully contribute in probability-based protein identification in data bases (Perkins *et al.*, 1999). Accordingly, the generation of large amounts of redundant data, whereby a high percentage of high quality MS/MS spectra fail to contribute to protein identification, is a known phenomenon (Cox *et al.*, 2008, Karty *et al.*, 2002, Nesvizhskii, 2010, Neuhauser *et al.*, 2012, Xu *et al.*, 2005). Consequently, strategies are on the way to exploit biological information out of unassigned spectra, whereby e.g. the use of “de novo sequencing” algorithm was proposed by numerous authors (Ning *et al.*, 2010, Seidler *et al.*, 2010). From a practical point of view the MALDI method is more lab intensive, since fractions have to be deposited and matrix has to be applied by pipetting robotic units, which can be sources of error. On the other hand it is more robust towards contaminants than ESI, which allowed a direct HPLC analysis without SPE purification of gel

digests prior to LC MALDI. However, the more obvious advantage is the decoupling of sample preparation and measuring in the MALDI approach, allowing storage and reanalysis of samples (Kuzyk *et al.*, 2009), whereas in case of system errors samples are lost in the ESI approach. In these studies, during test runs, this happened in case of robot error, column blocking or needle damage. However, in the developed LC ESI workflow each sample provided enough material for one reanalysis. Thereby the storing was a more critical factor since freezing of remaining sample runs in sample buffer or relyophilization of samples was found to impact sample quality. Nevertheless, the complex MALDI software platform was found to be an important source of error in the course of the studies which was not the case in LC ESI. Further differences could be attributed to the complementarity of ionization principles (Bodnar *et al.*, 2003, Stapels and Barofsky, 2004, Stapels *et al.*, 2004, Yang *et al.*, 2007). In up to date literature, it was reported that more hydrophilic peptides had been obtained in MALDI (Yang *et al.*, 2007), whereas ESI favors more hydrophobic species (Cech and Enke, 2000). Moreover, whereas ESI was supported to favor ionization of peptides ending with lysine over those ending with arginine, the opposite was observed for MALDI ionization (Stapels and Barofsky, 2004). The complementary ionization character had been earlier exploited to analyze HDL apolipoproteins (Bondarenko *et al.*, 2002). In confidence, this work showed the differential character of both ionization techniques combined with two different analyzer strategies, which balance advantages and limitations. In conclusion, both approaches have to be used as an amendatory proteomic platform. Whereas the ESI approach exhibited high performance in getting an encompassing view of the ocular surface proteome, the MALDI method achieved high accomplishment in the characterization of particular tear proteins allowing targeted study designs. Both approaches were successfully used in longitudinal study designs, which are of growing interest in proteomics science according to the highly dynamic and complex character of the proteome (Cohen *et al.*, 2008, Corthals *et al.*, 2000, Flood-Nichols *et al.*, 2013, Hawkridge and Muddiman, 2009, Hawkridge *et al.*, 2010, Pratt *et al.*, 2002, Zabel *et al.*, 2012).

## 5.3 Characterization of the ocular surface proteome

By use of the developed workflows an in depth view to tear film and conjuntiva proteome could be obtained. Despite the intensive study of the corneal proteome by Dyrlund and coworkers, who described 3250 proteins associated to different cornea regions encircling epithelium, endothelium and stromal cells proteins by use of a sophisticated TripleTOF 5600 system (Dyrlund *et al.*, 2012), only few explorative investigations had been realized examining conjunctival cells. Actually, Zhou and co-workers identified 600 proteins in NHC-IOBA cells by MS (Zhou *et al.*, 2011). Nevertheless, by use of the developed LC ESI workflow >1000 conjunctival proteins could be catalogued. Furthermore, a rough proteomic

based classification of the IOBA-NHC cells could be achieved in the present work. Conjunctival cells are classified in five groups, whereas only two groups, goblet cells and stratified squamous cells had been successfully biochemical defined so far (Dartt, 2002). Despite the difficulties to characterize conjunctival cell lines, Tong and coworkers found a high degree of congruency between NHC-IOBA cells and primary cultures proposing NHC-IOBA cells as a valid substitute model for the conjunctival epithelium, which had been realized by use of gene expression monitoring (Tong *et al.*, 2009). In confidence with the literature numerous epithelial key proteins encircling cytokeratines, desmogleins, epiplakin (Fukuoka *et al.*, 2012) and others could be identified by use of the developed LC ESI BU workflow, which justified once more the use of NHC-IOBA as an ocular surface epithelia model, e.g. allowing investigation on cellular integrity focusing on cell-cell contact sites. Moreover, several secretory proteins, e.g. interleukines, mucins and other classes of exclusively or secondary secretory proteins have been identified, which additionally emphasizes the active functionality of NHC-IOBA cells shifting them in direction of goblet cells since these cells have been defined for their high mucin secretion activity to the tear film (Dartt, 2002, Dartt *et al.*, 2000, de la Fuente *et al.*, 2010, Watanabe *et al.*, 1995). Commensurate to this Inatomi, Gipson and collegues recorded expression of mucin species, especially mucin 5 in the human conjunctival epithelia, (Gipson *et al.*, 2003, Inatomi *et al.*, 1996), also detected in this work. Mucin 5 was defined as a goblet cell characteristic marker (Gipson and Inatomi, 1997). In fact, altered expression of mucins by goblet cells have been associated to dry eye disease (Danjo, 1998) and mucin and interleukine secretion have been documented for IOBA-NHC cells to be altered under stress condition (Li *et al.*, 2009, Tau, 2012). Moreover, mucin 5AC, expressed in human conjunctiva (McKenzie *et al.*, 2000) and identified in this work, was found as a reduced protein in Sjögren´s dry eye (Gipson *et al.*, 2004) documented together with mucin 16 to be related to atopic keratokonjunctivitis (Dogru *et al.*, 2008) and can therefore be studied in future projects by use of the developed LC ESI monitoring NHC-IOBA cells in different experimental setups. However it could not be identified with high frequency and purification attemps might be needed. Actually, most of the mucin studies focused on RNA or used immune histological approaches for mucin determination, whereby mucins maybe hampered by low ionization frequencies in MS workflows due to oligosaccharide side chains (Thomsson *et al.*, 1999). Besides, secretion of peptides and proteins, e.g. antimicrobial peptides (McDermott, 2009), glycokonjugate secretions encircling non-mucin glycoproteins (Dartt *et al.*, 1996) or mucin associated peptides like TFF-peptides (trefoilfactors) (Langer *et al.*, 1999) have been reported for the human conjunctiva. In accordance, more secretory proteins could be detected, providing a detailed impression on ocular surface epithelia activity in this work. One of these secretory proteins is macrophage migration inhibitory factor, a cytokine, which could be detected with

high score by the LC ESI method and was reported to be upregulated in conjunctival tissues in case of ocular cicraticial pemphigoid (OCP) (Razzaque *et al.*, 2004). Another identified secretory protein was serpin B5, an antimicrobial serine proteinase inhibitor, identified in ocular surface epithelia (Silverman *et al.*, 2001). Actually, serpin B5 could be detected with high score in tear fluid by the developed LC ESI method, which proves the origin of tear serpin B5 from conjunctival cells secreting the protein to the tear film. Moreover, the communicative activity through cytokines could be supported by the identification of a chemokine receptor, C-C chemokine receptor type 9. In accordance Gulati and coworkers proved the expression of chemokine receptor CCR5 on the surface of human conjunctival cells associated to dry eye (Gulati *et al.*, 2006). Interestingly, a GABAnergic and also a dopaminergic neurotransmitter receptor could be revealed, which supports the finding of nerve innervation and nerve secretion control of goblet cells of the human conjunctiva (Diebold *et al.*, 2001). Beside secretory proteins, challenging recovery of membrane proteins has been realized. Thereby, vinculin, a focal adhesion marker (Sosne *et al.*, 2002), proposed to be involved in Sjögren´s pathology (Hjelmervik *et al.*, 2009) could be identified by the developed LC ESI method. Numerous proteins, e.g. the nucleus protein, Ras GTPase-activating-like protein IQGAP1, which most likely plays a key role in corneal development associated to Ras (Burgess *et al.*, 2010) have not been identified for conjunctival cells before. In addition, the identification of oxidative stress proteins in conjunctival cells could clarify the origin of these proteins in tear film, e.g. superoxide dismutase [Mn], [Cu-Zn]; thioredoxin, thioredoxin reductase 1, thioredoxin domain containing protein 6, 17; glutaredoxin 3; glutathione synthetase, glutathione S-transferase P/ Ω-1; lactoglutathion lyase; microsomal glutathione S-transferase 1 and peroxiredoxin 2, 4, 5 and 6. Especially, peroxiredoxin 2 has been associated to ocular surface disorders with overexpression in pterygium conjunctiva tissue (Bautista-de Lucio *et al.*, 2013). Moreover, peroxiredoxin 1, 5 and glutathione S-transferase have been found to be overexpressed in tears of conjunctivochalasis (Acera *et al.*, 2011), which supports the strong pathological relationship between conjunctival cells and tear film. In this work, a deep insight view of the tear proteome could be achieved by MALDI and ESI MS with high literature congruency, while numerous proteins could be catalogued for tear fluid for the first time. For example, centaurin-γ 1 as a autism related brain protein (Wassink *et al.*, 2005), furthermore detected in cephalopod and vertebrate optic lobe neurons of camera eyes (Yoshida and Ogura, 2011). Also, cytosolic 5'-nucleotidase III-like protein, most likely derived from the lens (Cappiello *et al.*, 1992) and transmembrane channel-like protein 8, probably originated from serum (Zhang *et al.*, 2012) and related to Epidermodysplasia verruciformis (Kurima *et al.*, 2003), were documented for the first time in tears. Also forkhead-associated domain-containing protein 1, displaying a neurodegenerative relevant sequence motif (Guzik and Goldstein, 2004), could

be detected in all experiments and was not MS documented for tear fluid before. Interestingly, certain retina proteins, e.g. retinal dehydrogenase 1 or selenium-binding protein 1 could be revealed from tear fluid. In confidence, retinol dehydrogenase has been identified in tear fluid of patients with diabetic retinopathy (Csosz *et al.*, 2012) and traffic between retina and tear film in the course of degenerative processes might be thinkable since intraocular lesions can effect the ocular surface (Lee and Hirst, 1995). Also, identified proteins like myozenin 2, a hypertrophic cardiomyopathy biomarker (Osio *et al.*, 2007) associated to skeletal muscles (Takada *et al.*, 2001) could be suggested to reach the tear film due to internal processes. In contrast, proteins like cadherin, desmoplakin, plektin, desmoglein are clearly derived from cell-cell interactions sites (Buxton and Magee, 1992, Gallicano *et al.*, 1998, Koch *et al.*, 1990, Schmelz and Franke, 1993, Seifert *et al.*, 1992, Wiche *et al.*, 1983). Also, calreticulin identified in tear fluid is associated to cell-cell contact and had been demonstrated to play a key role in integrin control (Coppolino *et al.*, 1997). Without a doubt, these proteins are useful to focus on in studies investigating on epithelia barrier functionality. Most of the tear proteins were found to be intracellular proteins with predominance in cytoplasmic organelle-bound proteins inferred from both workflows. This finding and the predominance in nucleus proteins was also reported by de Souza and collegues using a comparable LC ESI Orbitrap workflow (de Souza *et al.*, 2006). Since a comparable protein distribution could be demonstrated for conjunctival cells, tear fluid provides a reflection of proteomic hierarchy in epithelia. Typical nucleus proteins, e.g. histones have been described for healthy human tear fluid by use of LC ESI (Zhou, 2006) and could confidently been detected in tears in this work. Numerous lipid-associated proteins, e.g. lipocalins, phospholipid transfer protein, apolipoprotein AI or transcobalamin-I could be detected in tears by use of the developed methods. Transcobalamins are lipid and vitamin B12 carriers (Carmel, 1972, Rosenfeld *et al.*, 2003) described for human tears (Csosz *et al.*, 2012). Also, lipocalin a prominent tear protein was intensively studied for its lipid binding features (Delaire *et al.*, 1992, Millar *et al.*, 2009, Redl, 2000). Interestingly, beside its affinity to lipids, it was documented to bind thioredoxin (Redl *et al.*, 1999), which was also detected in tear fluid in this study. Besides, thioredoxin reductase 3, peroxiredoxin (thioredoxin peroxidase 2) could be identified in tears. Most likely these proteins build a functional complex in tears counterstriking oxidative stress (Lechner *et al.*, 2001). Confidently, thioredoxin and associated proteins were detected in conjunctival cells concluding these proteins to be directly or indirectly released by the cells to the tear film. This is supported by a study of Sotozono and coworkers, which could prove thioredoxin in human tear fluid as well as in conjunctival and corneal epithelia proposing a protective role under oxidative stress condition in case of inflammation (Sotozono *et al.*, 2005). Probably, under oxidative stress conditions, the rate of lytic ocular surface epithelial cells increases with a

proportional release rate of thioredoxin and related proteins to the tear film. Since peroxiredoxin has been reported to display elevated levels in diseased conjunctival tissue in pterygium and was proposed to protect cells against oxidative stress (Bautista-de Lucio *et al.*, 2013), it could be released to the tear film after lysis of overexpressing cells, thereby, restoring the oxidative status of the extracellular milieu. It is interesting, that also a complement associated protein; complement decay-accelerating factor, could be detected in the cells. Complement C3 was also detected in tears by use of the developed MALDI and ESI methods. In confidence, Ballow et al. had found evidence for complement factor production in conjunctival tissues (Ballow *et al.*, 1985), which underlines the key role of the conjunctiva for inflammatory processes manifesting in the tear film. In summary, by use of the developed BU workflows a sensitive image of the ocular surface proteome could be obtained showing high confidence with recent studies on the tear proteome. Thereby, numerous new proteins could be mapped for the tear proteome and moreover the origin of several proteins could be allocated to the conjunctiva. The portion of overlapping proteins regarding tear and conjunctival cells most likely suggests a more detailed biological role of the ocular surface epithelium traversing barrier function.

## 5.4 Effects of Taflotan® sine on the ocular surface proteome

At first instance, interestingly, most responding candidate proteins showed longitudinal diminishment. Functional analysis classified the majority of these candidates as cellular proteins deducting evidence for beneficial effects of the therapeutic switch to preservative-free Taflotan® sine appliance. Ocular surface regenerative processes are most likely reflected by the observed longitudinal cellular protein decline in in the POAG patients´ tear film, which can be hypothesized to indicate a decreased leakage rate of epithelium cells. It is proposed, that most of cellular proteins in the tear film are originated from conjunctiva vessel leakage (Fukuda *et al.*, 1996, Janssen and van Bijsterveld, 1983, Tiffany, 2008, Tiffany *et al.*, 1989) and corneal cell leakage events due to cellular breakdown (Choy *et al.*, 2004, de Souza *et al.*, 2006), which can also be associated to atrophy of lacrimal glands (Stern *et al.*, 2004). Accordingly, increased epithelial breakdown in the cornea was reported to be correlated to dry eye (Holly and Lemp, 1977); (Ogawa *et al.*, 2001, Vroman *et al.*, 2005);(Brignole *et al.*, 2000). Also, Chang and collegues clearly demonstrated that BAC included in latanoprost causes corneal cell epithelial membrane leakage (Chang *et al.*, 2000). As a matter of fact, BAC was able to extract intracellular lactat dehydrogenase from rabbit cornea due to its detergent qualities (Grant and Acosta, 1996), which supports the observation of a high number of enzymes and other intracellular proteins with high pre-therapeutic shift abundance in POAG tears in this work. Also, there is clear evidence for cell lytic processes encircling necrotic and apoptotic reactions of ocular surface epithelia in dose-dependant contact with

BAC (Burstein, 1980, De Saint Jean *et al.*, 2000, Tonjum, 1975, Tripathi and Tripathi, 1989). Moreover, BAC was found to alter myosin modification impacting corneal actin cytoskeleton integribility (Guo *et al.*, 2007). Increased disruption of the perjunctional actomyosin ring corresponding to increased cell damage of endothelial corneal cells was reported after treatment of rabbit eyes with BAC eye drops (Chen *et al.*, 2011a). Accordingly, increased levels of myosin fragments most likely reflect tight junction and corneal endothelial barrier defects. Xu and coworkers proved SDS comparable detergent qualities of BAC able to disrupt corneal tight junctions (Nakamura *et al.*, 2010) and increased cornea permeability (Majumdar *et al.*, 2008). Actually, after the medication switch a linear decrease in myosin 10 was detected, most likely indicating corneal regeneration. Cadherin 5, another corneal integrity marker was detected to be linearly decreased after the switch. Cadherins are corneal junction proteins impaired by inflammation (Kimura *et al.*, 2009). This is why a decline in soluble cadherins is indicative for ocular surface restoring. Furthermore, in this study, the association to cellular apoptotic processes of several of the candidates fits well with the observation of an increase in cellular defect indicators. In accordance, Barki & Tahir reported high toxiticity of BAC while observing apoptotic processes in corneal epithelia of guinea pigs treated with BAC eye drops (Barki and Tahir, 2007). De facto, numerous members of the annexin protein family are documented to be strongly correlated to cellular damage, apoptosis and inflammation (Aubry *et al.*, 1999, Gerke *et al.*, 2005, Gerke and Moss, 2002, Perretti and D'Acquisto, 2009, Reutelingsperger and van Heerde, 1997). Annexin A11 detected in tears in this study and significantly exhibiting a linear level decrease also could reflect ocular surface regeneration since overexpression of tear annexin had been associated to dry eye (Soria *et al.*, 2013). Interestingly, annexin 1 was found to be upregulated in tears resulting from parasymphatetic defected lacrimal glands (Nguyen *et al.*, 2004). Besides, level increase of annexin 5 indicated apoptosis (Buehrlen *et al.*, 2007, Koopman *et al.*, 1994, Plasier *et al.*, 1999, van Engeland *et al.*, 1998, Vermes *et al.*, 1995) in cultured conjunctival cells exposed to BAC containing latanoprost, travoprost formulations and BAC alone in comparison to preservative-free travoprost*Z* 0.004% (Baudouin *et al.*, 2007). Since there is a strong relation between annexin family members and their role for physiological stress condition (Gerke and Moss, 2002), time-related decline of annexin 11 is most likely linked to a drop in apoptotic events and reflects ocular surface recovery. Beside its direct relation to annexin 1 as a dry eye marker (Soria *et al.*, 2013), annexin 11 is associated to calcyclin (S100A6) as a further dry eye marker, because of its calcyclin binding motif (Sudo and Hidaka, 1998, Tokumitsu *et al.*, 1993). Serotransferrin detected in tears with high abundance (Li *et al.*, 2005, Srinivasan *et al.*, 2012, Zhou *et al.*, 2009c) was documented to increase during inflammation (Hallquist and Klasing, 1994) and was found to be significantly linear reduced in this study. Interestingly, a conjunctival transferrin receptor had

been identified (Baudouin *et al.*, 1992) and could also be detected in NHC-IOBA cells in this work. Possibly, increased serotransferrin as an acute phase protein (Hallquist and Klasing, 1994) could be sensed by conjunctival cells, leading to proteomic changes. Also, an increased iron supply of ocular surface epithelia under stress condition mediated by elevated tear serotransferrin levels can be assumed (Ismail and Brock, 1993, Kawakami *et al.*, 1990, Oria *et al.*, 1988). Alternatively, elevated serotransferrin levels in tear fluid indicate a counterstrategy to bind iron released from lytic cells (Jurado, 1997) due to preservative-induced damage. Nevertheless, other dry eye associated markers, which showed a clear level shift, are of speculative expressiveness to evaluate the ocular surface condition. For example, galectin 7, which had been documented for numerous ocular tissues including the cornea (Schlotzer-Schrehardt *et al.*, 2012), was found to be clearly receded in the course of time in response to Taflotan® sine usage. In fact, gene expression of galectin 7 has been documented to be elevated in injured corneas and has been supposed to be involved in corneal wound healing (Cao *et al.*, 2002a). This implication fits well with the observed diminishing of the galectin 7 level, most likely reflecting a regenerating ocular surface. Contrary, galectin 7 was found to be decreased in tears of dry eye patients (Soria *et al.*, 2013). However, since galectins, especially galectin 7, are related to apoptosis (Kuwabara *et al.*, 2001, Kuwabara *et al.*, 2002) and wound healing (Cao *et al.*, 2002b), also documented for the cornea (Patron *et al.*, 2004), a time-related decrease of the galectin 7 level most likely corresponds to regenerative processes. Nevertheless it is thinkable that a deficiency of galectin 7 corresponds to the development of dry eye pathology under certain conditions and that preservatives induce a special dry eye phenotype due to multifactorial character of the disease. However, dry eye involvement of galectins (Argueso and Panjwani, 2011, Yabuta *et al.*, 2014), their abundance in epithelial wounds (Pepe *et al.*, 2014) and postulated role in apoptotic/necrotic cell clearance (Beer *et al.*, 2008, Mostowy, 2013, Sarter, 2010) makes the observed galectin 7 highly indicative for ocular surface recovery. The diminishment of leakage of cellular and tight junction proteins in the study course supports this assumption. Most likely, in first instance, ocular surface epithelia are affected by BAC followed by lacrimal and meiobian alterations as a counter reaction to ocular surface damage which is in confidence of the proposed cornea and lacrimal feedback model of Mathers (Mathers, 2000). De facto, MS results were supported by MA findings since longitudinal diminished MS marker candidates encircling e.g. pyruvatekinase isozymes M1/M2, kinectin, annexin A11, serotransferrin or cadherin 5 displayed a significant convergence to the healthy stage in the course of Taflotan® sine appliance. Actually, the release of intracellular proteins has been documented to induce inflammation on target cells (Chase *et al.*, 2007, Harris and Andersson, 2004, Scaffidi *et al.*, 2002) and ocular surface inflammation, which has been indicated by elevated cytokine levels (Boehm *et al.*, 2011, de Paiva *et al.*, 2013, De Paiva *et*

*al.*, 2007, Luo *et al.*, 2004, Pflugfelder *et al.*, 2013). Interestingly, an increase in interleukine mRNA in ocular surface epithelia has been shown in response to topical use of prostaglandine analogues (Lopilly Park *et al.*, 2012), which fits well with MA results of this work. Accordingly, distinct approximation of the majority of analyzed cytokines to the healthy stage in the course of the study indicated a clear reduction of ocular surface inflammation in response to the therapeutic switch. In confidence, Baudouin et al. reported increased expression of inflammatory conjunctival cell membrane markers, e.g. cytokine receptors in glaucoma patients in the course of BAC related topical medication (Baudouin *et al.*, 1994). As already discussed, numerous successfully validated tear proteins are not typical dry eye markers, underlining the suggestion of a superordinate dry eye phenotype according to "medicative induced dry eye" (Fraunfelder *et al.*, 2012). Most likely, the observed proteomic changes indicate reshuffling conditions of the tear film reflected by a diminishment of epithelia cell leaking events and a correlating drop of inflammation represented by declined cytokine levels. Interestingly, Wong and collegues could detect clear proteomic alterations comparing tear fluid of medicated glaucoma patients with healthy and dry eye patients, whereby the *14-3-3* ζ/δ protein, absent in dry eye tears, was found to be increased in medicated groups compared to healthy subjects (Wong *et al.*, 2011). This finding supports a medicative sicca phenotype. Confidently, *14-3-3* isoforms were also identified in POAG tears in this work, but displaying no response towards Taflotan® sine. However, the hypothesis is additionally supported by proteomic illumination of clinical dry eye phenotypes (Boehm *et al.*, 2013). In contrast, prominent enzymes showing an altered status towards preservative-free tafluprost utilization like pyruvate kinase isozymes M1/M2 or mitochondrial pantothenate kinase 2 have not been reported for dry eye. In this work, they certainly refer to cell leakage and have interestingly been documented for tear and lacrimal gland fluid (Vanhaeri.Nj and Glasius, 1974a, b). In general, lysosomal enzymes are derived from the lacrimal gland and levels of cytoplasmic proteins, especially enzymes should be low in tear film "under conditions where the epithelia cells of the conjunctiva remain intact", whereby "the conjunctiva may act as a second source for lysosomal enzymes after mild trauma" (Van Haeringen, 1981). Recently, Nakamori and Koyama used tear film enzyme activity of lactat dehydrogenase to estimate ocular epithelial damage since the enzyme was proposed to reach the tear film through epithelial cell leakage (Koyama *et al.*, 1996, Nakamori *et al.*, 1993b), which was reported in accordance to early studies proposing cellular leakage of intracellular enzyme as direct consequence of cytotoxicity (Nakamura *et al.*, 1985). In confidence, enzymes like pyruvate kinase are known to be highly expressed in cornea keratocytes (Jester *et al.*, 2005) and have been reported to be released by ocular surface epithelia (Sariri and Ghafoori, 2008) to the tear film (Baeyens and Gurny, 1997). Actually, it had been shown that leakage rates correlate with expression levels of intracellular proteins

(Barnes and Pielak, 2011), which is in confidence with the high abundant detection of pyruvate kinase isozymes M1/M2 in tear fluid in this work and its abundant detection in NHC-IOBA cells supporting its epithelial origin. In confidence, Menke and Jokusch used pyruvate kinase release to monitor effects of hyperosmotic shock in myotubes (Menke and Jockusch, 1995), supposing pyruvate kinase as a predominant releasing protein through membrane damage. Nevertheless, it remains unknown if level alterations in these enzymes have a superordinate functions for the ocular surface in case of stress condition. Interestingly pyruvate kinase had been reported to increase post-cautery and declines after 6-7 days during rat cornea angiogenesis (Thompson *et al.*, 2003), proposing a highlighted metabolic function, which fits well with the proposed key role of pyruvate kinase M2 in altered tumor metabolism (Mazurek, 2012). Furthermore, the supposed role of a specific pyruvate isozymes M1/M2 derived peptide as an autoantigen in human polymyositis (Kawachi *et al.*, 2001) may hint to inflammatory functions. Despite the thinkable functions of observed leakage enzymes, a disruption of the cellular barrier as well as cellular lysis is highly likely due to Xalatan® application >6 month considering the destructive BAC potential in extended therapy (Cha *et al.*, 2004), including tear film stability decline (Wilson *et al.*, 1975), tear production (Labbe *et al.*, 2006) and multifactorial ocular surface complication (Xiong *et al.*, 2008). Since BAC is also known to interact with protein membrane receptors, which influence signal transduction (Patarca and Fletcher, 1995), ocular surface processes resulting from long time application are likely to display high complexity. In summary, the study results show that switching to preservative-free formulation leads to ocular surface recovery, also supported by clinical parameters, TBUT and BST. The therapeutic switch provides a patient perspective for life quality enhancement.

## 5.5 Taurine effects on the tear and cell proteome

Regarding taurine eye drop application several tear proteins could be revealed responding with a distinct level decline. Interestingly, these effects were predominantly detected in the contact lens wearer group over the 5 week study period. However, in contrast, using a linear trend model no obvious taurine response reactions in the sicca group could be observed. An explanation could be pathological differences in contact lens ocular surface processes and related effectiveness of taurine as well as the selected application duration. For example, Kokke and collegues studied effects of Ω-6 fatty acid utilization in a 6 month study and could document distinct improvments in the ocular surface health status after 3 month (Kokke *et al.*, 2008). However, since the substance has been applied orally, time dependent effects differ most likely from topical appliance in terms of bioavailability. Additionally, differences in the course of the disease or pathological dispositions may be reflected by the fact, that by use of linear regression analysis, decreased proteins could exclusively been revealed in the

contact lens group. In contrast, the non-linear *Kruskal-Wallis* analysis detected candidate proteins displaying distinct level decreases in both taurine treatment groups (S_Taurine, CL_Taurine). This finding suggests that a strict linear regression model is not applicable to detect all responses in a 5 week study period considering tear protein variation acording to time (Ng *et al.*, 2000a, Ng *et al.*, 2000b, Ng *et al.*, 2001) and hormone system influence (Sullivan *et al.*, 1984, Sullivan and Hann, 1989). For example, glycoproteins show a high degree of diurnal fluctuation (Sack *et al.*, 1997). Regarding the functional context, candidate proteins detected by use of both models, linear and non-linear, were predominantly associated to inflammation. Actually, they could be verified to be upregulated in contact lens and/or dry eye syndrome tears compared to a healthy non contact lens wearer reference. This fits well with the finding of elevated levels of inflammatory proteins in dry eye (Grus *et al.*, 2005b, Lam *et al.*, 2008) and contact lens tears (Grus *et al.*, 2005a). Secretoglobin 1D1, a small anti-inflammatory protein (Mukherjee *et al.*, 2008, Mukherjee *et al.*, 2007), also known as lipophilin A, which was previously found to be a decreased tear biomarker for contact lens wear (Kramann *et al.*, 2011) and dry eye (Nichols and Green-Church, 2009, Versura *et al.*, 2010) was contrary found to be elevated in tears of contact lens and sicca tears in the present study referring to a healthy non-contact lens wearer reference. The protein was reported to build a complex with mammaglobin B (Stoeckelhuber *et al.*, 2006). Interestingly, both proteins; secretoglobin 1D1 and mammaglobin B, were found to be elevated in tears of aqueous-deficient dry eye patients and patients with a combinatory deficit in the lipid and aqueous tear phase (Boehm *et al.*, 2013). In this work, secretoglobin 1D1 was demonstrated to be shifted in direction of the healthy stage in response to taurine utilization. α-2-macroglobin, another taurine responding candidate, was reported to be expressed in the cornea (Laurie, 2008, Twining *et al.*, 1994), but probably could also be originated from micro vascular bleeding (Lembach *et al.*, 2001) since it is a dominant blood protein (McMillan, 1976). It is interesting, that this high molecular weight proteinase can bind a wide range of targeted molecules, e.g.S100A9 (Eue *et al.*, 2002) or ß-2-microglobulin (Gouin-Charnet *et al.*, 2000). Moreover, it is suggested to be involved in dry eye referring to a misbalance between proteinases and inhibitors in the disease pathology (Laurie, 2008), which was also proposed to play a role in contact lens wearing (Cejkova *et al.*, 1992). Also, a decline in complement C3 in response to taurine application was detected. Complement C3 activates the complement cascade and was reported to be the major player in closed eye tear inflammatory processes, that can be compared to inflammation associated to contact lens wearing (Sack *et al.*, 1992). Since hemolytic activity of complement C3 was proofed in tears (Mondino and Zaidman, 1983, Veerhuis and Kijlstra, 1982, Willcox *et al.*, 1997), a potential taurine depending decline could be associated with the observed level decrease of haptoglobin related protein and hemopexin, which are both anti-oxidant protective plasma

proteins occurring in the course of inflammation as acute phase proteins (Ceciliani *et al.*, 2002, Kuhajda *et al.*, 1989). Haptoglobin and haptoglobin related protein can bind hemoglobin during red blood cell lysis (Chen *et al.*, 1998, Dobryszycka, 1997, Karring *et al.*, 2006, Nielsen *et al.*, 2006), whereby haptoglobin has been reported to be increased in tears of climatic droplet keratopathy patients (Zhou *et al.*, 2009d). Hemopexin, which binds free heme during inflammatory hemolysis was first detected by Pong et al. 2010 in tear fluid and moreover, it was demonstrated to be elevated in tears of patients suffering from vernal keratokunjunctivitis increasing with disease stages (Pong *et al.*, 2010, Pong *et al.*, 2011). The protein was also correlated to allergic processes of the ocular surface (Enriquez-de-Salamanca *et al.*, 2012). Hemopexin and α-2-macroglobin are biologically close related and have been reported to display elevated levels in cerebrospinal fluid and serum during inflammation (Saso *et al.*, 1999). Hemopexin was also found to be upregulated in inflammatory nerve injury in the eye (Camborieux *et al.*, 2000). Ig γ, also detected to respond to taurine application, has been proven to be elevated in tears of keratoconus patients (Chandler *et al.*, 1974, Pannebaker *et al.*, 2010) and has been detected in contact lens deposits (Green-Church and Nichols, 2008), probably reflecting its activity in contact lens tear inflammation. Regarding the classes of candidate proteins, it can be suggested, that the taurine impact is predominantely focused on proteins occuring in the course of inflammation and hemolysis, whereby several of these proteins are known to play key roles in dry eye. Actually the response of inflammatory proteins like haptoglobin, α-2-macroglobin, hemopexin together with complement C3 as a prominent type 1 acute phase protein (Baumann and Schendel, 1991, Immenschuh *et al.*, 1995), as well as the response of immunoglobulines, clearly indicates the impact of taurine on the immune response of the ocular surface. It was shown that most of these acute phase proteins are coordinately regulated (Baumann and Mullereberhard, 1987), which fits well with the observation that the proteins responded simultaneously. The differential regulation of tear immunoglobuline components like Ig κ chain C region, Ig α-2 chain C region Ig J chain, Ig α-1 chain C region have been furthermore associated to inflammatory processes in terms of POAG (Pieragostino *et al.*, 2012). Ig κ C level alteration was also documented for keratoconus associated tear fluid (Lema *et al.*, 2010). However, several limitations of the study design have to be solved in future projects. Since tear proteins show a high degree of naturally variability, in future studies the monitoring time has to be extended to detect proteins that correspond later in the time course of taurine application. Additionally, taurine has to be tested in combination with other cleaning solution ingredients expected to have beneficial effects on contact lens-induced dry eye. In fact, only little is known about underlying mechanism how taurine may influence inflammatory response reflected by the observed proteomic changes. Taurine concentration of the supplemented eye drops was approximately 20fold higher than the natural taurine

concentration in tears [195.5 µM] (Nakatsukasa *et al.*, 2011) and therefore it can be suggested, that this taurine overrun lead to a decline in the taurine uptake rate of ocular surface epithelia. Actually, $Na^+$ dependent uptake as well as a high affinity transporter system have been documented for taurine (Karring *et al.*, 2006, Oh *et al.*, 2006, Shioda *et al.*, 2002, Smith *et al.*, 1992). In confidence, by use of the developed LC ESI method numerous transmembrane amino acid transporters could be detected in conjunctival epithelia cells, e.g. large neutral amino acids transporter or sodium coupled neutral amino acid transporter 2, which could be involved in taurine uptake. Interestingly, probable cation-transporting ATPase 13A5 could be identified in the cells, which fits well with the finding of Garrett and collegues, who proposed a carrier-mediated organic cation transport process mediating the apsorption of organic amines, carnitine and drugs supported by the detection of carnitine/organic cation transporters OCTN1, 2 (Garrett *et al.*, 2008). Nevertheless, the question remains, how taurine may induce the observed effects regarding decreased inflammation in contact lens wearers and which cellular targets are affected. In accordance taurine was tested on NHC-IOBA conjunctival cells and a dose-dependent taurine effect could be determined. Whereas elevated concentrations >20 mM lead to stress reactions indicated by reduced viability, increased ROS production and upregulation of stress associated proteins, e.g. elevation of thioredoxin 1, peroxiredoxin 2 and glutaredoxin 1 levels, lower concentrations showed beneficial effects on cells, which is somehow contrary to the relative high effective level of taurine eye drops in the tear study. However, diffusion effects of the tear film are highly likely in comparison to cell culture experiments. Interestingly, taurine was highly effective to reduce ROS production in peroxide stressed cells, however, it was more effective to increase the viability in unstressed than in stressed cells without discrimination between peroxide or staurosporine stress condition. Cellular levels of numerous stress marker proteins (gluthathion S-transferases, peroxiredoxins, thioredoxin, superoxide dismutase and cytochrome C) were clearly found to be decreased. Most of these proteins play a role in counterstriking oxidative stress. Peroxiredoxins had been intensively studied to be increased under oxidative stress condition in various tissues (Ishii and Yanagawa, 2007, Shibata *et al.*, 2003, Sideri *et al.*, 2010) and peroxiredoxin 4 had been demonstrated to succefully remove peroxide (Tavender and Bulleid, 2010). In addition, thioredoxin and glutaredoxin are two enzyme key players in the protection system against oxidative stress in case of inflammation and disease (Arodin *et al.*, 2013, Zhou *et al.*, 2010) and thioredoxin overexpression has been reported to extend life span in mice (Mitsui *et al.*, 2002). In contrast, Chen et al. reported glutathione and thioredoxin to be downregulated with hyperosmolarity in NHC-IOBA cells, but also reported upregulation of certain enzymes like pyrophosphorylase (Chen *et al.*, 2012). Nevertheless, thioredoxin expression has been reported to be increased by oxidative and hypoxic stresses documented for cancers (Karlenius *et al.*, 2012, Karlenius, 2010) and

beneficial effects of overexpression in retinal pigment epithelial cells in response to oxidative stress could been documented (Sugano, 2013). Most likely, antioxidative effects of taurine also influence inflammatory and hemolytic processes caused by e.g. contact lens wear. Interestingly, also increased histone expression has been shown to be associated to life span extension in yeast (Feser *et al.*, 2010). It is thinkable, that a defined surplus in taurine availability relieves this anti-stress system, which is reflected by downregulation of these protein species and by ROS decline and increased cellular viability. Since thioredoxin was found to regenerate oxidative stress in endothelial cells (Fernando *et al.*, 1992), it can be suggested, that taurine acts like a substitute since it was documented to protect proteins from uncontrolled modification, e.g. nitration (Askwith *et al.*, 2012), glycation (Devamanoharan *et al.*, 1997), carbonylation (Son *et al.*, 2007) and denaturation (Arakawa and Timasheff, 1985) under stress condition. Interestingly, Kayuya and co-researchers detected a decline in natural cataract lens taurine levels correlating with glutathione decline (Kasuya *et al.*, 1992), which supports taurine-anti-oxidative enzyme interactions. Regarding the detected histone decline, it had been shown, that downregulation of histone H4 is associated to differentiation processes in single cells (Gerbaulet *et al.*, 1992) and histones have been found to be involved in inflammation (Gilthorpe, 2013, Nicodeme *et al.*, 2010, Xu *et al.*, 2011). Allam et al. intensively studied histones released from dying renal cells and found histones to increase TLR mediated inflammation and kill endothelial and epithelial cells (Allam *et al.*, 2012), which is interesting in case of conjunctival cells and ocular surface inflammation. Moreover, the effectivity of taurine regarding unstressed to peroxide stressed cells may reflect the potential of taurine to improve cell viability in natural to mild stress environment and to fail rescuing cells under harsh stress conditions. This is fitting well with the finding of Nonaka and collegues, who reported taurine to prevent superoxide dismutase expression and secretion in case of homocysteine-induced stress (Nonaka *et al.*, 2001). It is thinkable, that under normal to mild stress condition taurine may exonerate the anti-oxidative enzyme system, but fails to prevent cells under strong stress. Furthermore, stress quality could play a role, since taurine showed good peroxide-counter action but low performance in case of staurosporine induced stress. Taken together, this might contribute to explain the differences in taurine tear proteomic response pattern observed between primary dry eye subjects and contact lens wearers, which might reflect different qualities of stress regarding molecular mechanism. It can be suggested from these findings, that taurine performs differentially depending on dry eye phenotype, stress degree and quality. However, taurine was supported in this work to influence numerous metabolic proteins in conjunctival cells, which emphasizes its modulative potential to improve cell survival under mild condition. De facto, the dramatically downregulation of calmodulin and the associated calmodulin/calcium apparatus in response to 0.05 mM taurine in unstressed cells is highly indicative for a cellular

taurine response and illustrates the direct impact of taurine on epithelia cells of the ocular surface. Because calmodulin is a key mediator of taurine transport, a modified cellular taurine traffic (Falktoft and Lambert, 2004, Law, 1995) and a direct osmolytic effect on conjunctival cells can be assumed. Actually, for corneal cells a 4.5fold intracellular taurine concentration increase within 48 h had been demonstrated to elevate cell viability (Shioda *et al.*, 2002). Confidently, level decrease of galectin-1 and galectin 3-binding protein is interesting since elevated expression of galectin-1 was found to be associated to apoptosis in endothelial cells (Qiu *et al.*, 2008) and galectin 7 decline could also be documented as a potential ocular surface recovery response in the present Taflotan® sine study. Nevertheless, the discrepancy of beneficial effects obtained by topical application of high taurine concentrations in tear fluid and the dose-dependent effects observed in cell culture most likely reflect experimental design differences between in vitro and in vivo studies. The ocular surface as a highly complex functional unit can react to changes in the biochemical environment with a whole organ response, whereas cellular responses have limitations. However, in both study systems, tear flim and conjunctival cells, as representing components of the ocular surface, taurine performed regeneratively. That is why taurine is highly interesting for future studies regarding therapeutic strategies of ocular surface pathologies. Thereby, more detailed studies have to be launched to illuminate the interaction between taurine and different sources of stress. Also, more investigations have to be tasked addressing the direct influence of taurine on tear and ocular surface related proteins, e.g. in terms of post-translational modifications (PTMs) and protein turnover.

## 5.6 Deviated strategies facing dry eye and ocular surface complications

A taurine counteraction on inflammation could be indicated by a decline in inflammatory tear proteins predominantly observed in contact lens tears. However, it can be assumed, that other dry eye forms, also, can be positively affected by taurine appliance, which might be revealed in prolonged studies. Up to date, taurine, beside other osmolytes, could be proposed as an effective agency against hyperosmolar stress and preventing of inflammation and damage of the ocular surface, especially in dry eye therapy (Baudouin *et al.*, 2013), which is in confidence with the beneficial effects of taurine on conjunctival cells in this work. Since taurine was demonstrated to benefit peroxide stressed and untreated NHC-IOBA cells, in this work a loss of mucin-producing goblet cells as well as associated inflammatory cascades in dry eye disease are likely to be prevented by the amino acid. Moreover, since neuronal control of goblet cell mucin secretion had been proposed (Diebold *et al.*, 2001) and taurine was demonstrated for its activity on ionotropic and metabotropic receptors of retina nerves (Rowan *et al.*, 2013), taurine may directly influence mucin secretion and emending tear film properties, which has to be examined intensively in future studies. However, care

has to be taken regarding concentration settings of taurine since a dose dependent cellular agency could be substantiated in the present work. In case of preservative induced ocular surface disorders as shown for BAC containing Xalatan® utilization in terms of glaucoma therapy, taurine could be proposed for its ocular surface damage counteracting potential. De facto, osmolytes like taurine have been intensively studied for their protein stabilization features (Anjum *et al.*, 2000, Arakawa and Timasheff, 1985, Haque *et al.*, 2005, Street *et al.*, 2006) and e.g. trimethylamine *n*-oxide, a naturally occurring osmolyte had been demonstrated to stabilize proteins from urea influence (Zou *et al.*, 2002b). Interestingly, some deep-sea species use taurine derivates as trimethylamine *n*-oxide substitutes, which emphasizes their analog role regarding osmolytic activity (Yin *et al.*, 1999, Yin *et al.*, 2000). The potential of taurine and other osmolytes for protein stabilization and rescuing proteins from misfolding lead to the definition of osmolytes to represent “chemical chaperones” (Rajan *et al.*, 2011, Yancey, 2001). Accordingly, stabilizing and refolding of proteins in a detergent environment could be valuated as a promising key feature of osmolytes, especially a feature of taurine. In ocular surface complications reffering to glaucoma therapy, the use of preservative-free Taflotan® sine can be recommended since a clear ocular surface regeneration could be inferred from the proteomic tear film results. It is thinkable, that a combination of the preservative-free glaucoma therapy with the use of taurine as an formulation “additive” (Hamada *et al.*, 2009) could represent a promising therapeutic strategy for glaucoma medication induced dry eye disease. Moreover, proteins responding to taurine could be studied more intensively for their value as therapeutic targets. For example, thioredoxin, glutathione or peroxiredoxin are trigger points of oxidative stress, which can be addressed for the appliance to counteract inflammatory processes. Actually, research on the therapeutic value of extracellular thioredoxin as an anti-inflammation tool has already been launched (Mahmood *et al.*, 2013, Matsuo and Yodoi, 2013). Also, tear enzymes, especially the pyruvate kinase system has to be studied more intensively, since promising effects have been postulated for pyruvate kinase in terms of cancer therapy (Mazurek, 2012, Tamada *et al.*, 2012). Combinatory effects of potential therapeutic proteins, taurine and osmolytes may show a new direction in dry eye therapy.

# 6 Conclusion

BU clearly exceeded TD performance in this work and a resulting LC MS BU platform encircling MALDI/ESI techniques could be developed, which enabled a deep insight view to the ocular surface containing tear film and conjunctival cells. Moreover, by use of the developed methods the effects of taurine and Taflotan® sine on the ocular surface could be studied intensively, illuminating new molecular proteomic players indicative for dry eye and “medication induced dry eye” providing a deeper view to molecular mechanism. Finally, the proteomic results could give a perspective to develop promising therapeutic strategies regarding dry eye management and encourage future studies.

# 7 Summary

In the present work a top down (TD) MALDI approach and two bottom up (BU) MALDI/ESI mass spectrometric (MS) based methods have been developed integrating HPLC to study the ocular surface encircling tear film and conjunctival cells. A detailed overview of development steps, benefits and limitations was given in the work. Whereas the TD approach was found to be applicable to examine crude cellular specimen, BU approaches resulted in high sensitivity and accuracy regarding the analysis of processed conjunctival cell and also tear film proteins. By use of the LC MALDI BU method more than 200 capillary tear proteins could be detected, LC ESI resulted in more than 1000 capillary tear proteins, which was also achieved for Schirmer strip tears and conjunctival cells. Regarding quality and quantity ESI and MALDI methods showed distinct differences discussed to be useful depending on the proteomic target. Moreover, by use of the developed LC MALDI/ESI BU platform, which clearly performed advantageous over the TD approach, the influence of taurine and Taflotan® sine application on the ocular surface could be studied. Taurine could be demonstrated to lead to anti-inflammatory effects on the ocular surface reflected by dynamic changes in tear film proteins, predominantly documented in contact lens induced dry eye. Beneficial effects could also be supported in conjunctival cell studies, however showing a dose-dependent taurine effect. Regarding the topical application of preservative-free Taflotan® sine, by use of LC ESI BU analysis, an ocular surface recovery could be confirmed in primary open angle glaucoma (POAG) patients with dry eye reflected by dynamic tear film changes after a therapeutic switch from preservative containing Xalatan®. This could also be validated by microarray (MA) experiments. In taurin studies as well as in the Taflotan® sine study, characteristic ocular surface protein candidates could be revealed, which can be used to objectively assess the ocular surface health status. A use of taurine for dry eye therapy and a combinatory strategy of Taflotan® sine and taurine have been proposed for future therapeutic strategies in terms of medication induced dry eye in glaucoma.

# 8 Abbreviations

- 1D/2D=1 Dimensional/2 Dimensional
- ACN= Acetonitrile
- Ambi= Ammoniumbicarbonate
- BAC= Benzalkonium chloride
- BST= Baal Schirmer tear
- BU= Bottom Up
- CBB= Coomassie Brilliant Blue
- CHCA= α-cyano-4-hydroxy.cinnamic acid
- CID= Collision induced decay
- DDM= Dodecyl-ß-D-maltoside
- DMEM= Dulbecco’s modified eagle’s medium
- DPBS= Dulbecco’s phosphate buffered saline
- EDTA= Ethylendiamintetraacetate
- ESI= Electro spray ionization
- FA= Formic acid
- FCS= Fetal calf serum
- GO= Gene ontology
- HPLC= High pressure liquid chromatography
- ID= Inner diameter
- IOP= Intra ocular pressure
- LP= Laser power
- MA= Micro array
- MALDI= Matrix assisted laser desorption ionization
- MeOH= Methanol
- MES=2-(*N*-morpholino)ethanesulfonic acid
- MOPS= 3-(*N*-morpholino)propanesulfonic acid
- MS= Mass spectrometry
- MWC= Molecular weight cut off
- OSDI= Ocular surface disease index
- PKM= Pyruvat kinase isozymes M1/M2
- POAG= Primary open angle glaucoma
- PSD= Post source decay
- RP= Reversed phase
- SDS PAGE= Sodium dodecyl sulfate poly acrylamide gel electrophorese

- SDS= Sodium dodecyl sulfate
- SELDI= Siurface enhanced laser desorption ionization
- SPE= Solid phase extraction
- TBUT= Tear break up time
- TD= Top Down
- TFA= trifluor acetic acid
- TIC= Total ion current
- TLR= Toll like receptor
- TOF= Time of flight

# 9 Instruments/Technical equipment

- 428™ array laser scanner (Affymetrix Inc.)
- A 316 0.5µm online precolumn filter (Upchurch Scientific, Washington, USA)
- Acrodisc 13 mm x 0.45 µm GHP filter (PALL Life Sciences, Ann Arbor, USA)
- BioBasic® C18 analytical column (150 x 0.5mm ID) (Thermo Fisher Scientific, Rockford, USA)
- BioBasic® C18 precolumn (30 x 0.5mm ID) (Thermo Fisher Scientific, Rockford, USA)
- BioBasic® Phenyl analytical column (100 x 0.5mm ID) (Thermo Fisher Scientific, Rockford, USA)
- Cellstar® V-bottom 96 well plates (Greiner Bio-One)
- Concentrator 5301 instrument (Eppendorf, Hamburg, Germany).
- DCP-9042 CDN benchtop scanner (Brother International GMBH)
- Defined capillary tube (20µl) (Eksigent, Dublin, Ireland)
- Heraeus™ Biofuge Primo R centrifuge (Thermo Fisher Scientific, Rockford, USA)
- Jupiter® 4 µ Proteo analytical column (150 x 0.5mm ID) (Phenomenex, Torrence, USA)
- KS250 Basic Intellimixer (Kika Labortechnik, Cologne, Germany)
- Labsonic® M (Sartorius)
- Low Flow Metal Needle for API 2 Probes (Thermo Fisher Scientific, Rockford, USA)
- LTQ Orbitrap XL mass spectrometer (Thermo Fisher Scientific, Rockford, USA)
- MTP 396 Polished/Matt Steel MALDI Target (Bruker Daltonics, Bremen, Germany)
- Multiscan Ascent scanner (Thermo Fisher Scientific, Rockford, USA)
- Nikon Eclipse TS 100 (Nikon)
- Oncyte Avid nitrocellulose slides (Grace Bio-Labs Inc., Oregon, USA)
- Onyx® column couplers (Phenomenex, Torrence, USA)
- P-470/ M-472 graduated micro-split valves (Upchurch Scientific, Washington, USA)
- PAL HTS robot (CTC Analytics, Zwingen, Switzerland)
- PEEK™ tubings/Fingertight fittings/ferrules (Upchurch Scientific, Washington, USA)
- Prosphere P-HR (4µm, 150mm x 1mm ID) (Alltech Associates, Inc., Deerfield, Illinois, USA)
- Rheos Allegro HPLC Pump (Thermo Fisher Scientific, Rockford, USA)
- Ringcaps® Duran® disposable micro pipettes with ring mark (Hirschmann Laborgeräte GmbH & Co.Kg, Eberstadt, Germany).
- sciFLEXARRAYER microarray spotter (Scienion, Dortmund, Germany)
- Security Guard™ cartridge system/RP1 (4x2mmID) filter inlet (Phenomenex, Torrence, USA),
- Stainless steel NanoTight™union (Upchurch Scientific, Washington, USA)

- Sun Collect MALDI spotter (Sunchrom, Friedrichsdorf, Switzerland)
- Tear Test ophthalmic strips (Optitech® Eyecare, Tarun Enterprises, Allahabad, India)
- Teflon-coated needle tip (Tecan, Männedorf, Switzerland)
- Ultraflex II mass spectrometer (Bruker Daltonics, Bremen, Germany)
- Unimax 1010 shaker
- Unimax 1010 shaker (Heidolph Instruments, Schwabach, Germany)
- XCell SureLock™ Mini-Cell Electrophoresis System (Invitrogen, Carlsbad, USA)
- ZIPTIP® C18 pipette tips (EMD Millipore Corporation, Billerica, USA)
- Reaction tubes (0.5/1.5/2 ml) (Eppendorf AG, Hamburg, Germany)
- Pipette tips (Eppendorf AG, Hamburg, Germany)

# 10 Software

- XCalibur® (Thermo Fisher Scientific, Rockford, USA)
- Photoshop C53 (extended version) (Adobe Systems Inc.)
- Ingenuity® IPA® tool system (Ingenuity® Systems)
- P2M (Proteomics Pipeline Mainz)
- Cytoscape (version 2.8.3)
- MarathonControl (version 1.5.7) (Lasertechnik Berlin, Berlin, Germany)
- Warp-LC (version 1.1) (Bruker Daltonics, Bremen, Germany)
- Survey Viewer (version 1.1) (Bruker Daltonics, Bremen, Germany)
- Proteome Discoverer® (version 1.1) (Thermo Fisher Scientific, Rockford, USA)
- Flex Control (version 2.4) (Bruker Daltonics, Bremen, Germany)
- Flex Analysis (version 2.4) (Bruker Daltonics, Bremen, Germany)
- ImaGene® (version 5.5) (BioDiscovery, Hawthorne, USA)
- Statistica (versions 8/10) (StatSoft, Tulsa, USA)
- TramineR
- R-Project (version 2.8)

# 11 Chemicals

- ACN $_{LC-MS}$ (Applichem GmbH, Ilinois Tool Works Inc., Chicago, Ilinoois, USA)
- AMO Complete Moisture Plus® (Abbott Medical Optics Illinois, USA)
- CHCA (Fluka Analytical, Sigma-Aldrich, Co. LLC.)
- Crystall violet assay (Sigma-Aldrich Co. LLC)
- DCFH-DA ROS assays (Sigma-Aldrich Co, St. Louis, USA),
- DDM (Fluka Analytical, Sigma-Aldrich Co, St. Louis, USA)
- DMEM (Ham's F12 1:1) (Biochrome, Merck KGaA, Darmstadt, Germany)
- DPBS (Sigma-Aldrich Co, St. Louis, USA)
- EDTA (Sigma-Aldrich Co, St. Louis, USA)
- FCS (Biochrome, Merck KGaA, Darmstadt, Germany)
- FA $_{LC-MS}$ (Applichem GmbH, Ilinois Tool Works Inc., Chicago, Ilinoois, USA)
- L-alanin/L-glutamine (Biochrome, Merck KGaA, Darmstadt, Germany)
- MeOH $_{LC-MS}$ (Applichem GmbH, Ilinois Tool Works Inc., Chicago, Ilinoois, USA)
- Novex Colloidal Blue staining kit (Invitrogen, Carlsbad, USA)
- NuPage 12% Bis-Tris, 10-well prepared minigels (Invitrogen, Carlsbad, USA)
- NuPAGE LDS sample buffer [4x] (Invitrogen, Carlsbad, USA)
- Penicillin (Sigma-Aldrich Co, St. Louis, USA)
- Sequencing grade modified trypsin (Promega Co, Madison, USA)
- Streptomycin (Sigma-Aldrich Co, St. Louis, USA)
- Insulin (Sigma-Aldrich Co, St. Louis, USA)
- EGF (Invitrogen, Carlsbad, USA)
- Hydrocortison (Sigma-Aldrich Co, St. Louis, USA)
- Peptide Calibration Standard (Bruker Daltonics, Bremen, Germany)
- Peroxide (Carl Roth GMBH & Co.KG, Karlsruhe, Germany)
- Pierce® LTQ ESI positive ion calibration mix (Thermo Fisher Scientific, Rockford, USA)
- Protease inhibitor for use in tissue culture (Sigma-Aldrich Co, St. Louis, USA)
- Protein Calibration Standard I (Bruker Daltonics, Bremen, Germany)
- Reducing agent [10x] (Invitrogen, Carlsbad, USA)
- SeabluePlus 2 prestained protein standard (Invitrogen, Carlsbad, USA)
- Sequencing grade modified trypsin (Promega)
- Staurosporine (Calbiochem, Merck KGaA, Darmstadt, Germany)
- Streptomycin (Sigma-Aldrich Co, St. Louis, USA)
- Taurine (Carl Roth GmbH+Co.KG, Karlsruhe, Germany)
- TFA (Merck KGaA, Darmstadt, Germany)

### Chemicals

- Water $_{LC\text{-}MS}$ (Applichem GmbH, Ilinois Tool Works Inc., Chicago, Ilinoois, USA)

# 12 References

**Abalain, J. H., H. Dossou, J. Colin, and H. H. Floch. 2000.** Levels of collagen degradation products (telopeptides) in the tear film of patients with keratoconus. *Cornea* **19**:474-476.
**Acera, A., T. Suarez, I. Rodriguez-Agirretxe, E. Vecino, and J. A. Duran. 2011.** Changes in tear protein profile in patients with conjunctivochalasis. *Cornea* **30**:42-49.
**Aebersold, R., and M. Mann. 2003.** Mass spectrometry-based proteomics. *Nature* **422**:198-207.
**Aguilar, M. I. 2004.** HPLC of peptides and proteins: basic theory and methodology. *Methods Mol Biol* **251**:3-8.
**Aho, V. V., T. J. Nevalainen, V. Paavilainen, and K. M. Saari. 2002.** Group II phospholipase A2 content of tears in patients with senile cataract and primary open-angle glaucoma. *Eur J Ophthalmol* **12**:40-43.
**Akay, C., H. Yaman, M. Oztosun, E. Cakir, A. O. Yildirim, Y. E. Eyi, M. Agilli, E. O. Akgul, I. Aydin, U. Kaldirim, S. K. Tuncer, A. Eken, E. Oztas, Y. Poyrazoglu, M. Yasar, and Y. Ozkan. 2013.** The protective effects of taurine on experimental acute pancreatitis in a rat model. *Hum Exp Toxicol* **32**:522-529.
**Allam, R., C. R. Scherbaum, M. N. Darisipudi, S. R. Mulay, H. Hagele, J. Lichtnekert, J. H. Hagemann, K. V. Rupanagudi, M. Ryu, C. Schwarzenberger, B. Hohenstein, C. Hugo, B. Uhl, C. A. Reichel, F. Krombach, M. Monestier, H. Liapis, K. Moreth, L. Schaefer, and H. J. Anders. 2012.** Histones from Dying Renal Cells Aggravate Kidney Injury via TLR2 and TLR4. *Journal of the American Society of Nephrology* **23**:1375-1388.
**Aluru, S. V., S. Agarwal, B. Srinivasan, G. K. Iyer, S. M. Rajappa, U. Tatu, P. Padmanabhan, N. Subramanian, and A. Narayanasamy. 2012.** Lacrimal Proline Rich 4 (LPRR4) Protein in the Tear Fluid Is a Potential Biomarker of Dry Eye Syndrome. *PLoS One* **7**.
**Alvarez, J. G., and B. T. Storey. 1983.** Taurine, Hypotaurine, Epinephrine and Albumin Inhibit Lipid-Peroxidation in Rabbit Spermatozoa and Protect against Loss of Motility. *Biol Reprod* **29**:548-555.
**Alves, M., R. N. Angerami, and E. M. Rocha. 2013.** Dry eye disease caused by viral infection: review. *Arq Bras Oftalmol* **76**:129-132.
**Ananthi, S., T. Chitra, R. Bini, N. V. Prajna, P. Lalitha, and K. Dharmalingam. 2008.** Comparative analysis of the tear protein profile in mycotic keratitis patients. *Mol Vis* **14**:500-507.
**Anathy, V., S. W. Aesif, A. S. Guala, M. Havermans, N. L. Reynaert, Y. S. Ho, R. C. Budd, and Y. M. Janssen-Heininger. 2009.** Redox amplification of apoptosis by caspase-dependent cleavage of glutaredoxin 1 and S-glutathionylation of Fas. *J Cell Biol* **184**:241-252.
**Anjum, F., V. Rishi, and F. Ahmad. 2000.** Compatibility of osmolytes with Gibbs energy of stabilization of proteins. *Biochim Biophys Acta* **1476**:75-84.
**Annesley, T. M. 2003.** Ion suppression in mass spectrometry. *Clinical Chemistry* **49**:1041-1044.
**Antoine, M., P. Demirev, H. Le, A. Behrens, and J. Castro. 2010.** Characterizing the Protein Content in Tears for Early Detection of Disease. *J Hopkins Apl Tech D* **28**:228-229.
**Apweiler, R., C. Aslanidis, T. Deufel, and e. al. 2009.** Approaching clinical proteomics: current state and future fields of application in cellular proteomics. *Cytom Part A* **75A**:816-832.
**Aquavella, J. V. 2013.** Dry eyes: are new ideas drying up? *Br J Ophthalmol* **97**:801-802.
**Aragona, P., L. Rania, A. M. Roszkowska, R. Spinella, E. Postorino, D. Puzzolo, and A. Micali. 2013.** Effects of amino acids enriched tears substitutes on the cornea of patients with dysfunctional tear syndrome. *Acta Ophthalmol* **91**:e437-e444.
**Arakawa, T., and S. N. Timasheff. 1985.** The Stabilization of Proteins by Osmolytes. *Biophys J* **47**:411-414.
**Argueso, P., and N. Panjwani. 2011.** Focus on molecules: galectin-3. *Exp Eye Res* **92**:2-3.

**Argueso, P., S. Spurr-Michaud, C. L. Russo, A. Tisdale, and I. K. Gipson. 2003.** MUC16 mucin is expressed by the human ocular surface epithelia and carries the H185 carbohydrate epitope. *Invest Ophth Vis Sci* **44**:2487-2495.

**Arici, M. K., D. S. Arici, A. Topalkara, and C. Guler. 2000.** Adverse effects of topical antiglaucoma drugs on the ocular surface. *Clin Experiment Ophthalmol* **28**:113-117.

**Arnitz, R., B. Sarg, H. W. Ott, A. Neher, H. Lindner, and M. Nagl. 2006.** Protein sites of attack of N-chlorotaurine in Escherichia coli. *Proteomics* **6**:865-869.

**Arodin, L., H. Lamparter, H. Karlsson, I. Nennesmo, M. Bjornstedt, J. Schroder, and A. P. Fernandes. 2013.** Alteration of Thioredoxin and Glutaredoxin in the Progression of Alzheimer's Disease. *J Alzheimers Dis*.

**Askwith, T., W. Zeng, M. C. Eggo, and M. J. Stevens. 2012.** Taurine reduces nitrosative stress and nitric oxide synthase expression in high glucose-exposed human Schwann cells. *Experimental Neurology* **233**:154-162.

**Aubry, J. P., H. Blaecke, S. Lecoanet-Henchoz, P. Jeannin, N. Herbault, G. Caron, V. Moine, and J. Y. Bonnefoy. 1999.** Annexin V used for measuring apoptosis in the early events of cellular cytotoxicity. *Cytometry* **37**:197-204.

**Avni, I., H. J. Garzozi, I. S. Barequet, F. Segev, D. Varssano, G. Sartani, N. Chetrit, E. Bakshi, D. Zadok, O. Tomkins, G. Litvin, K. A. Jacobson, S. Fishman, Z. Harpaz, M. Farbstein, S. B. Yehuda, M. H. Silverman, W. D. Kerns, D. R. Bristol, I. Cohn, and P. Fishman. 2010.** Treatment of dry eye syndrome with orally administered CF101: data from a phase 2 clinical trial. *Ophthalmology* **117**:1287-1293.

**Awapara, J., A. J. Landua, and R. Fuerst. 1950.** Distribution of Free Amino Acids and Related Substances in Organs of the Rat. *Biochimica Et Biophysica Acta* **5**:457-462.

**Azzarolo, A. M., K. Brew, S. Kota, O. Ponomareva, J. Schwartz, and C. Zylberberg. 2004.** Presence of tear lipocalin and other major proteins in lacrimal fluid of rabbits. *Comp Biochem Phys B* **138**:111-117.

**Baessmann, C., D. Suckau, S. Hahner, W. Jabs, M. Lubeck, M. Macht, and C. Becker. 2005.** Coupling LC with on-line ESI and off-line MALDI-MS/MS for maximum information readout from protein samples. *Lc Gc Eur*:22-24.

**Baeyens, V., and R. Gurny. 1997.** Chemical and physical parameters of tears relevant for the design of ocular drug delivery formulations. *Pharm Acta Helv* **72**:191-202.

**Baggerly, K. A., J. S. Morris, and K. R. Coombes. 2004.** Reproducibility of SELDI-TOF protein patterns in serum: comparing datasets from different experiments. *Bioinformatics* **20**:777-U710.

**Bahr, U., A. Deppe, M. Karas, F. Hillenkamp, and U. Giessmann. 1992.** Mass-Spectrometry of Synthetic-Polymers by Uv Matrix-Assisted Laser Desorption Ionization. *Anal Chem* **64**:2866-2869.

**Balkan, J., O. Kanbagli, G. Aykac-Toker, and M. Uysal. 2002.** Taurine treatment reduces hepatic lipids and oxidative stress in chronically ethanol-treated rats. *Biol Pharm Bull* **25**:1231-1233.

**Ballow, M., P. C. Donshik, and L. Mendelson. 1985.** Complement proteins and C3 anaphylatoxin in the tears of patients with conjunctivitis. *J Allergy Clin Immunol* **76**:473-476.

**Barcaroli, M., P. DelBeato, P. Tanzilli, G. DeMattia, and E. M. Vingolo. 1997.** Diabetes mellitus and dry eye syndrome: Tear film glucose level in diabetic patients. *Invest Ophth Vis Sci* **38**:734-734.

**Barka, T., P. A. Asbell, H. Vandernoen, and A. Prasad. 1991.** Cystatins in Human Tear Fluid. *Current Eye Research* **10**:25-34.

**Barki, W. H., and M. Tahir. 2007.** Effects of topical benzalkonium chloride on corneal epithelium. *Biomedica* **23**:65-70.

**Barkman, R., M. Germanis, G. Karpe, and S. Malmborg. 1969.** Preservatives in eye drops. *Acta Ophthalmol (Copenh)* **47**:461-475.

**Barnes, C. O., and G. J. Pielak. 2011.** In-cell protein NMR and protein leakage. *Proteins-Structure Function and Bioinformatics* **79**:347-351.

**Barrera, R., A. Jimenez, R. Lopez, M. C. Mane, J. F. Rodriguez, and J. M. Molleda. 1992.** Evaluation of Total Protein-Content in Tears of Dogs by Polyacrylamide-Gel Disk-Electrophoresis. *Am J Vet Res* **53**:454-456.

**Barroso, B., D. Lubda, and R. Bischoff. 2003.** Applications of monolithic silica capillary columns in proteomics. *J Proteome Res* **2**:633-642.
**Baskin, S. I., E. M. Cohn, and Kocsis. 1977.** The effect of age on taurine levels in eye tissues. *Exp Eye Res* **24**:315-319.
**Baudouin, C. 2001.** The pathology of dry eye. *Survey of Ophthalmology* **45**:S211-S220.
**Baudouin, C., P. Aragona, E. M. Messmer, A. Tomlinson, M. Calonge, K. G. Boboridis, Y. A. Akova, G. Geerling, M. Labetoulle, and M. Rolando. 2013.** Role of hyperosmolarity in the pathogenesis and management of dry eye disease: proceedings of the OCEAN group meeting. *Ocul Surf* **11**:246-258.
**Baudouin, C., F. Brignole, D. Fredj-Reygrobellet, F. Negre, J. Bayle, and P. Gastaud. 1992.** Transferrin receptor expression by retinal pigment epithelial cells in proliferative vitreoretinopathy. *Invest Ophthalmol Vis Sci* **33**:2822-2829.
**Baudouin, C., and C. de Lunardo. 1998.** Short term comparative study of topical 2% carteolol with and without benzalkonium chloride in healthy volunteers. *Brit J Ophthalmol* **82**:39-42.
**Baudouin, C., C. Garcher, N. Haouat, A. Bron, and P. Gastaud. 1994.** Expression of inflammatory membrane markers by conjunctival cells in chronically treated patients with glaucoma. *Ophthalmology* **101**:454-460.
**Baudouin, C., L. Riancho, J. M. Warnet, and F. Brignole. 2007.** In vitro studies of antiglaucomatous prostaglandin analogues: travoprost with and without benzalkonium chloride and preserved latanoprost. *Invest Ophthalmol Vis Sci* **48**:4123-4128.
**Baumann, H., and U. Mullereberhard. 1987.** Synthesis of Hemopexin and Cysteine Protease Inhibitor Is Coordinately Regulated by Hsf-Ii and Interferon-Beta-2 in Rat Hepatoma-Cells. *Biochem Bioph Res Co* **146**:1218-1226.
**Baumann, H., and P. Schendel. 1991.** Interleukin-11 regulates the hepatic expression of the same plasma protein genes as interleukin-6. *J Biol Chem* **266**:20424-20427.
**Baumann, S., U. Ceglarek, G. M. Fiedler, J. Lembcke, A. Leichtle, and J. Thiery. 2005.** Standardized approach to proteome profiling of human serum based on magnetic bead separation and matrix-assisted laser desorption/ionization time-of-flight mass spectrometry. *Clin Chem* **51**:973-980.
**Bautista-de Lucio, V. M., N. L. Lopez-Espinosa, A. Robles-Contreras, H. J. Perez-Cano, H. Mejia-Lopez, G. Mendoza, M. C. Jimenez-Martinez, and Y. Garfias. 2013.** Overexpression of peroxiredoxin 2 in pterygium. A proteomic approach. *Exp Eye Res* **110**:70-75.
**Becquet, F., M. Goldschild, M. S. Moldovan, M. Ettaiche, P. Gastaud, and C. Baudouin. 1998.** Histopathological effects of topical ophthalmic preservatives on rat corneoconjunctival surface. *Curr Eye Res* **17**:419-425.
**Beer, A., S. Andre, H. Kaltner, M. Lensch, S. Franz, K. Sarter, C. Schulze, U. S. Gaipl, P. Kern, M. Herrmann, and H. J. Gabius. 2008.** Human galectins as sensors for apoptosis/necrosis-associated surface changes of granulocytes and lymphocytes. *Cytom Part A* **73A**:139-147.
**Bell, K., E. Buksinska, N. Pfeiffer, and F. H. Grus. 2012a.** Comparison of the effects of different lens-cleaning solutions on the protein profiles of human conjunctival cells. *Graefes Arch Clin Exp Ophthalmol* **250**:1627-1636.
**Bell, K., S. Funke, N. Pfeiffer, and F. H. Grus. 2012b.** Serum and antibodies of glaucoma patients lead to changes in the proteome, especially cell regulatory proteins, in retinal cells. *PLoS One* **7**:e46910.
**Benito, M. J., V. Calder, R. M. Corrales, C. Garcia-Vazquez, S. Narayanan, J. M. Herreras, M. E. Stern, M. Calonge, and A. Enriquez-de-Salamanca. 2013.** Effect of TGF-beta on ocular surface epithelial cells. *Exp Eye Res* **107**:88-100.
**Bennett, K. L., M. Funk, M. Tschernutter, F. P. Breitwieser, M. Planyavsky, C. Ubaida Mohien, A. Muller, Z. Trajanoski, J. Colinge, G. Superti-Furga, and U. Schmidt-Erfurth. 2011.** Proteomic analysis of human cataract aqueous humour: Comparison of one-dimensional gel LCMS with two-dimensional LCMS of unlabelled and iTRAQ(R)-labelled specimens. *J Proteomics* **74**:151-166.

**Berger, S. L., and V. L. King. 1998.** The fluctuation of tear production in the dog. *J Am Anim Hosp Assoc* **34**:79-83.
**Berger, T. A. 1993.** The Effect of Adsorbed Mobile-Phase Components on the Retention Mechanism, Efficiency, and Peak Distortion in Supercritical-Fluid Chromatography. *Chromatographia* **37**:645-652.
**Berkelman, T., S. Petersen, C. J. Sun, and S. Cater. 2010.** Mini-PROTEAN (R) TGX (TM) precast gel for SDS-PAGE with improved stability: comparison with standard Laemmli gels. *Biotechniques* **48**.
**Berven, F. S., A. C. Kroksveen, M. Berle, T. Rajalahti, K. Flikka, R. Arneberg, K. M. Myhr, C. Vedeler, O. M. Kvalheim, and R. J. Ulvik. 2007.** Pre-analytical influence on the low molecular weight cerebrospinal fluid proteome. *Proteom Clin Appl* **1**:699-711.
**Bhattacharya, S. K., J. S. Crabb, V. L. Bonilha, X. Gu, H. Takahara, and J. W. Crabb. 2006.** Proteomics implicates peptidyl arginine deiminase 2 and optic nerve citrullination in glaucoma pathogenesis. *Invest Ophthalmol Vis Sci* **47**:2508-2514.
**Bhown, A. S., J. Wayland, and J. C. Bennett. 1986.** Simple Device for High-Performance Liquid-Chromatographic Separation on Microbore Columns. *J Chromatogr* **370**:508-512.
**BiomarkersDefinitionWorkingGroup. 2001.** Biomarkers and surrogate endpoints: preferred definitions and conceptual framework. *Clin Pharmacol Ther* **69**:89-95.
**Bird, G. H., A. R. Lajmi, and J. A. Shin. 2002.** Manipulation of temperature to improve solubility of hydrophobic proteins and cocrystallization with matrix for analysis by MALDI-TOF mass spectrometry. *Anal Chem* **74**:219-225.
**Birdsall, T. C. 1998.** Therapeutic applications of taurine. *Altern Med Rev* **3**:128-136.
**Bjorhall, K., T. Miliotis, and P. Davidsson. 2005.** Comparison of different depletion strategies for improved resolution in proteomic analysis of human serum samples. *Proteomics* **5**:307-317.
**Blagoev, B., S. E. Ong, I. Kratchmarova, and M. Mann. 2004.** Temporal analysis of phosphotyrosine-dependent signaling networks by quantitative proteomics. *Nature Biotechnology* **22**:1139-1145.
**Blais, F., and M. Rioux. 1986.** Real-Time Numerical Peak Detector. *Signal Process* **11**:145-155.
**Blehm, C., S. Vishnu, A. Khattak, S. Mitra, and R. W. Yee. 2005.** Computer vision syndrome: a review. *Surv Ophthalmol* **50**:253-262.
**Bodnar, W. M., R. K. Blackburn, J. M. Krise, and M. A. Moseley. 2003.** Exploiting the complementary nature of LC/MALDI/MS/MS and LC/ESI/MS/MS for increased proteome coverage. *J Am Soc Mass Spectr* **14**:971-979.
**Boehm, N., S. Funke, M. Wiegand, N. Wehrwein, N. Pfeiffer, and F. H. Grus. 2013.** Alterations in the tear proteome of dry eye patients--a matter of the clinical phenotype. *Invest Ophthalmol Vis Sci* **54**:2385-2392.
**Boehm, N., A. I. Riechardt, M. Wiegand, N. Pfeiffer, and F. H. Grus. 2011.** Proinflammatory Cytokine Profiling of Tears from Dry Eye Patients by Means of Antibody Microarrays. *Invest Ophth Vis Sci* **52**:7725-7730.
**Boernsen, K. O., Floeckher, J. M., Bruin, G., J., M. 2000.** Use of a microplate scintillation counter as a radioactivity detector for miniaturized separation techniques in drug metabolism. *Anal. Chem.* **72**:3956-3959.
**Bondarenko, R., Z. N. Farwig, C. J. McNeal, and R. D. Macfarlane. 2002.** MALDI- and ESI-MS of the HDL apolipoproteins; new isoforms of apoA-I, II. *Int J Mass Spectrom* **219**:671-680.
**Bons, J. A. P., D. de Boer, M. P. van Dieijen-Visser, and W. K. W. H. Wodzig. 2006.** Standardization of calibration and quality control using surface enhanced laser desorption ionization-time of flight-mass spectrometry. *Clinica Chimica Acta* **366**:249-256.
**Bowermaster, J., and H. Mcnair. 1983.** Microbore High-Performance Liquid-Chromatographic Columns - Speed, Efficiency, Sensitivity and Temperature Programming. *J Chromatogr* **279**:431-438.
**Brasnu, E., F. Brignole-Bauclouin, L. Riancho, J. M. Guenoun, J. M. Warnet, and C. Baudouin. 2008.** In vitro effects of preservative-free tafluprost and preserved latanoprost,

travoprost, and bimatoprost in a conjunctival epithelial cell line. *Current Eye Research* **33**:303-312.
**Brauer, L., M. Johl, J. Borgermann, U. Pleyer, M. Tsokos, and F. P. Paulsen. 2007a.** Detection and localization of the hydrophobic surfactant proteins B and C in human tear fluid and the human lacrimal system. *Curr Eye Res* **32**:931-938.
**Brauer, L., C. Kindler, K. Jager, S. Sel, B. Nolle, U. Pleyer, M. Ochs, and F. P. Paulsen. 2007b.** Detection of surfactant proteins A and D in human tear fluid and the human lacrimal system. *Invest Ophthalmol Vis Sci* **48**:3945-3953.
**Brignole, F., P. J. Pisella, M. Goldschild, M. De saint Jean, A. Goguel, and C. Baudouin. 2000.** Flow cytometric analysis of inflammatory markers in conjunctival epithelial cells of patients with dry eyes. *Invest Ophth Vis Sci* **41**:1356-1363.
**Brivio, M., R. H. Fokkens, W. Verboom, D. N. Reinhoudt, N. R. Tas, M. Goedbloed, and A. van den Berg. 2002.** Integrated microfluidic system enabling (bio)chemical reactions with on-line MALDI-TOF mass spectrometry. *Anal Chem* **74**:3972-3976.
**Broekhuyse, R. M. 1974.** Tear lactoferrin: a bacteriostatic and complexing protein. *Invest Ophthalmol* **13**:550-554.
**Bron, A. J., J. M. Tiffany, S. M. Gouveia, N. Yokoi, and L. W. Voon. 2004.** Functional aspects of the tear film lipid layer. *Exp Eye Res* **78**:347-360.
**Brosnan, J. T., and M. E. Brosnan. 2006.** The sulfur-containing amino acids: an overview. *J Nutr* **136**:1636S-1640S.
**Brown, W. J., K. Chambers, and A. Doody. 2003.** Phospholipase A2 (PLA2) enzymes in membrane trafficking: mediators of membrane shape and function. *Traffic* **4**:214-221.
**Bruand, J., T. Alexandrov, S. Sistla, M. Wisztorski, C. Meriaux, M. Becker, M. Salzet, I. Fournier, E. Macagno, and V. Bafna. 2011.** AMASS: algorithm for MSI analysis by semi-supervised segmentation. *J Proteome Res* **10**:4734-4743.
**Brust, A. K., H. K. Ulbrich, G. M. Seigel, N. Pfeiffer, and F. H. Grus. 2008.** Effects of Cyclooxygenase Inhibitors on Apoptotic Neuroretinal Cells. *Biomark Insights* **3**:387-402.
**Brust, K., H. Ulbrich, G. Seigel, N. Pfeiffer, and F. H. Grus. 2006.** Neuroprotective Effects Of Cyclooxygenase Inhibitors On Apoptotic Retinal Ganglion Cells *Invest Ophthalmol Vis Sci* **47: E-Abstract 404**.
**Bruzdziak, P., A. Panuszko, and J. Stangret. 2013.** Influence of Osmolytes on Protein and Water Structure: A Step To Understanding the Mechanism of Protein Stabilization. *J Phys Chem B*.
**Buehrlen, M., U. A. Harreus, F. Gamarra, R. Hagen, and N. H. Kleinsasser. 2007.** Cumulative genotoxic and apoptotic effects of xenobiotics in a mini organ culture model of human nasal mucosa as detected by the alkaline single cell microgel electrophoresis assay and the annexin V-affinity assay. *Toxicol Lett* **169**:152-161.
**Bureau, M. H., and R. W. Olsen. 1991.** Taurine Acts on a Subclass of Gaba-a Receptors in Mammalian Brain Invitro. *Eur J Pharm-Molec Ph* **207**:9-16.
**Burgess, D., Y. Zhang, E. Siefker, R. Vaca, M. R. Kuracha, L. Reneker, P. A. Overbeek, and V. Govindarajan. 2010.** Activated Ras alters lens and corneal development through induction of distinct downstream targets. *Bmc Dev Biol* **10**.
**Buron, N., O. Micheau, S. Cathelin, P. O. Lafontaine, C. Creuzot-Garcher, and E. Solary. 2006.** Differential mechanisms of conjunctival cell death induction by ultraviolet irradiation and benzalkonium chloride. *Invest Ophthalmol Vis Sci* **47**:4221-4230.
**Burstein, N. L. 1980.** Preservative cytotoxic threshold for benzalkonium chloride and chlorhexidine digluconate in cat and rabbit corneas. *Invest Ophthalmol Vis Sci* **19**:308-313.
**Burton, L., G. Ivosev, G. Tate, G. Impey, J. Wingate, and R. Bonner. 2008.** Instrumental and experimental effects in LC-MS-based metabolomics. *J Chromatogr B* **871**:227-235.
**Buxton, R. S., and A. I. Magee. 1992.** Structure and interactions of desmosomal and other cadherins. *Semin Cell Biol* **3**:157-167.
**Caffery, B., E. Joyce, A. Boone, A. Slomovic, T. Simpson, L. Jones, and M. Senchyna. 2008.** Tear lipocalin and lysozyme in Sjogren and non-Sjogren dry eye. *Optom Vis Sci* **85**:661-667.

**Caillier, L., E. T. de Givenchy, R. Levy, Y. Vandenberghe, S. Geribaldi, and F. Guittard. 2009.** Synthesis and antimicrobial properties of polymerizable quaternary ammoniums. *Eur J Med Chem* **44**:3201-3208.
**Callesen, A. K., O. Mogensen, A. K. Jensen, T. A. Kruse, T. Martinussen, O. N. Jensen, and J. S. Madsen. 2012.** Reproducibility of mass spectrometry based protein profiles for diagnosis of ovarian cancer across clinical studies: A systematic review. *Journal of Proteomics* **75**:2758-2772.
**Callesen, A. K., W. Vach, P. E. Jorgensen, S. Cold, O. Mogensen, T. A. Kruse, O. N. Jensen, and J. S. Madsen. 2008.** Reproducibility of mass spectrometry based protein profiles for diagnosis of breast cancer across clinical studies: A systematic review. *J Proteome Res* **7**:1395-1402.
**Calonge, M. 2001.** The treatment of dry eye. *Survey of Ophthalmology* **45**:S227-S239.
**Camborieux, L., V. Julia, B. Pipy, and J. P. Swerts. 2000.** Respective roles of inflammation and axonal breakdown in the regulation of peripheral nerve hemopexin: an analysis in rats and in C57BL/Wlds mice. *J Neuroimmunol* **107**:29-41.
**Canas, B., C. Pineiro, E. Calvo, D. Lopez-Ferrer, and J. M. Gallardo. 2007.** Trends in sample preparation for classical and second generation proteomics. *J Chromatogr A* **1153**:235-258.
**Cao, Z., H. K. Wu, A. Bruce, K. Wollenberg, and N. Panjwani. 2002a.** Detection of differentially expressed genes in healing mouse corneas, using cDNA microarrays. *Invest Ophthalmol Vis Sci* **43**:2897-2904.
**Cao, Z. Y., N. Said, S. Amin, H. K. Wu, A. Bruce, M. Garate, D. K. Hsu, I. Kuwabara, F. T. Liu, and N. Panjwani. 2002b.** Galectins-3 and-7, but not galectin-1, play a role in re-epithelialization of wounds. *Journal of Biological Chemistry* **277**:42299-42305.
**Cappiello, M., D. Barsacchi, A. Delcorso, M. G. Tozzi, M. Camici, U. Mura, and P. L. Ipata. 1992.** Purine Salvage as a Metabolite and Energy Saving Mechanism in the Ocular Lens. *Current Eye Research* **11**:435-444.
**Capriotti, A. L., C. Cavaliere, P. Foglia, R. Samperi, and A. Lagana. 2011.** Intact protein separation by chromatographic and/or electrophoretic techniques for top-down proteomics. *J Chromatogr A* **1218**:8760-8776.
**Carmel, R. 1972.** The vitamin B 12 -binding proteins of saliva and tears and their relationship to other vitamin B 12 binders. *Biochim Biophys Acta* **263**:747-752.
**Castano, E. M., A. E. Roher, C. L. Esh, T. A. Kokjohn, and T. Beach. 2006.** Comparative proteomics of cerebrospinal fluid in neuropathologically-confirmed Alzheimer's disease and non-demented elderly subjects. *Neurol Res* **28**:155-163.
**Castells, C. B., and R. C. Castells. 1998.** Peak distortion in reversed-phase liquid chromatography as a consequence of viscosity differences between sample solvent and mobile phase. *Journal of Chromatography A* **805**:55-61.
**Cazares, L. H., B. L. Adam, M. D. Ward, S. Nasim, P. F. Schellhammer, O. J. Semmes, and G. L. Wright. 2002.** Normal, benign, preneoplastic, and malignant prostate cells have distinct protein expression profiles resolved by surface enhanced laser desorption/ionization mass spectrometry. *Clin Cancer Res* **8**:2541-2552.
**Cech, N. B., and C. G. Enke. 2000.** Relating electrospray ionization response to nonpolar character of small peptides. *Anal Chem* **72**:2717-2723.
**Ceciliani, F., A. Giordano, and V. Spagnolo. 2002.** The systemic reaction during inflammation: the acute-phase proteins. *Protein Pept Lett* **9**:211-223.
**Cejkova, J., Z. Lojda, J. Vacik, G. A. Digenis, and S. Dropcova. 1992.** Histochemical-Changes in the Rabbit Cornea and Plasmin Activity in the Tear Fluid during Contact-Lens Wear - Favorable Influence of Protease Inhibitors (Aprotinin, Pc5, Elastatinal). *Histochemistry* **97**:69-76.
**Cha, S. H., J. S. Lee, B. S. Oum, and C. D. Kim. 2004.** Corneal epithelial cellular dysfunction from benzalkonium chloride (BAC) in vitro. *Clin Exp Ophthalmol* **32**:180-184.
**Chalmers, R. L., and C. G. Begley. 2006.** Dryness symptoms among an unselected clinical population with and without contact lens wear. *Cont Lens Anterior Eye* **29**:25-30.

**Chandler, J. W., R. Leder, H. E. Kaufman, and J. R. Caldwell. 1974.** Quantitative determinations of complement components and immunoglobulins in tears and aqueous humor. *Invest Ophthalmol* **13**:151-153.
**Chang, J. W., S. H. Lee, Y. Lu, and Y. J. Yoo. 2006.** Transforming growth factor-beta1 induces the non-classical secretion of peroxiredoxin-I in A549 cells. *Biochem Biophys Res Commun* **345**:118-123.
**Chang, L., J. Zhao, J. Xu, W. Jiang, C. S. Tang, and Y. F. Qi. 2004.** Effects of taurine and homocysteine on calcium homeostasis and hydrogen peroxide and superoxide anions in rat myocardial mitochondria. *Clin Exp Pharmacol Physiol* **31**:237-243.
**Chang, S. W., R. F. Chi, C. C. Wu, and M. J. Su. 2000.** Benzalkonium chloride and gentamicin cause a leak in corneal epithelial cell membrane. *Exp Eye Res* **71**:3-10.
**Chase, M. A., D. S. Wheeler, K. M. Lierl, V. S. Hughes, H. R. Wong, and K. Page. 2007.** Hsp72 induces inflammation and regulates cytokine production in airway epithelium through a TLR4- and NF-kappa B-Dependent mechanism. *J Immunol* **179**:6318-6324.
**Chen, E. I., J. Hewel, B. Felding-Habermann, and J. R. Yates. 2006.** Large scale protein profiling by combination of protein fractionation and multidimensional protein identification technology (MudPIT). *Mol Cell Proteomics* **5**:53-56.
**Chen, G., C. Nan, J. Tian, P. Jean-Charles, Y. Li, H. Weissbach, and X. P. Huang. 2012.** Protective effects of taurine against oxidative stress in the heart of MsrA knockout mice. *J Cell Biochem* **113**:3559-3566.
**Chen, H. B., S. Yamabayashi, B. Ou, Y. Tanaka, S. Ohno, and S. Tsukahara. 1997.** Structure and composition of rat precorneal tear film. A study by an in vivo cryofixation. *Invest Ophthalmol Vis Sci* **38**:381-387.
**Chen, H. S., T. Rejtar, V. Andreev, E. Moskovets, and B. L. Karger. 2005.** Enhanced characterization of complex proteomic samples using LC-MALDI MS/MS: Exclusion of redundant peptides from MS/MS analysis in replicate runs. *Anal Chem* **77**:7816-7825.
**Chen, W., Z. Li, J. Hu, Z. Zhang, L. Chen, Y. Chen, and Z. Liu. 2011a.** Corneal alterations induced by topical application of benzalkonium chloride in rabbit. *PLoS One* **6**.
**Chen, W. H., H. S. Lu, K. Dutt, A. Smith, D. M. Hunt, and R. C. Hunt. 1998.** Expression of the protective proteins hemopexin and haptoglobin by cells of the neural retina. *Experimental Eye Research* **67**:83-93.
**Chen, Z. Y., F. A. Shamsi, K. J. Li, Q. A. Huang, A. A. Al-Rajhi, I. A. Chaudhry, and K. L. Wu. 2011b.** Comparison of camel tear proteins between summer and winter. *Molecular Vision* **17**:323-331.
**Chertov, O., A. Biragyn, L. W. Kwak, J. T. Simpson, T. Boronina, V. M. Hoang, D. A. Prieto, T. P. Conrads, T. D. Veenstra, and R. J. Fisher. 2004.** Organic solvent extraction of proteins and peptides from serum as an effective sample preparation for detection and identification of biomarkers by mass spectrometry. *Proteomics* **4**:1195-1203.
**Chertov, O., J. T. Simpson, A. Biragyn, T. P. Conrads, T. D. Veenstra, and R. J. Fisher. 2005.** Enrichment of low-molecular-weight proteins from biofluids for biomarker discovery. *Expert Rev Proteomic* **2**:139-145.
**Chervet, J. P., M. Ursem, and J. B. Salzmann. 1996.** Instrumental requirements for nanoscale liquid chromatography. *Anal Chem* **68**:1507-1512.
**Chesney, R. W. 1985.** Taurine: its biological role and clinical implications. *Adv Pediatr* **32**:1-42.
**Chiba, Y., K. Ando, and T. Fujita. 2002.** The protective effects of taurine against renal damage by salt loading in Dahl salt-sensitive rats. *J Hypertens* **20**:2269-2274.
**Cho, H. K., M. H. Park, and J. I. Moon. 2011.** Effects of antiglaucoma drugs on the ocular surface in rabbits: a fixed-combination drug versus two concomitant drugs. *Jpn J Ophthalmol* **55**:670-675.
**Choe, L. H., K. Aggarwal, Z. Franck, and K. H. Lee. 2005.** A comparison of the consistency of proteome quantitation using two-dimensional electrophoresis and shotgun isobaric tagging in Escherichia coli cells. *Electrophoresis* **26**:2437-2449.
**Chowdhury, U. R., B. J. Madden, M. C. Charlesworth, and M. P. Fautsch. 2010.** Proteome Analysis of Human Aqueous Humor. *Invest Ophth Vis Sci* **51**:4921-4931.

**Choy, C. K. M., P. Cho, I. F. F. Benzie, and V. Ng. 2004.** Effect of one overnight wear of orthokeratology lenses on tear composition. *Optometry Vision Sci* **81**:414-420.
**Chromy, B. A., A. D. Gonzales, J. Perkins, M. W. Choi, M. H. Corzett, B. C. Chang, C. H. Corzett, and S. L. McCutchen-Maloney. 2004.** Proteomic analysis of human serum by two-dimensional differential gel electrophoresis after depletion of high-abundant proteins. *J Proteome Res* **3**:1120-1127.
**Claeys, E., L. Uytterhaegen, B. Buts, and D. Demeyer. 1995.** Quantification of Beef Myofibrillar Proteins by Sds-Page. *Meat Sci* **39**:177-193.
**Cohen, A. A., N. Geva-Zatorsky, E. Eden, M. Frenkel-Morgenstern, I. Issaeva, A. Sigal, R. Milo, C. Cohen-Saidon, Y. Liron, Z. Kam, L. Cohen, T. Danon, N. Perzov, and U. Alon. 2008.** Dynamic Proteomics of Individual Cancer Cells in Response to a Drug. *Science* **322**:1511-1516.
**Cojocaru, V. M., C. Ciurtin, E. Uyy, and F. A. Antohe. 2011.** Nano-LC mass spectrometry proteomic tear secretion analysis in patients with secondary Sjögrens syndrome. *Digest J Nanomaterials and Biostructures* **6**:507-514.
**Conder, J. R. 1982.** Peak Distortion in Chromatography .2. Kinetically Controlled Factors. *J High Res Chromatog* **5**:397-403.
**Coppolino, M. G., M. J. Woodside, N. Demaurex, S. Grinstein, R. StArnaud, and S. Dedhar. 1997.** Calreticulin is essential for integrin-mediated calcium signalling and cell adhesion. *Nature* **386**:843-847.
**Corrales, R. M., S. Narayanan, I. Fernandez, A. Mayo, D. J. Galarreta, G. Fuentes-Paez, F. J. Chaves, J. M. Herreras, and M. Calonge. 2011.** Ocular mucin gene expression levels as biomarkers for the diagnosis of dry eye syndrome. *Invest Ophthalmol Vis Sci* **52**:8363-8369.
**Corthals, G. L., V. C. Wasinger, D. F. Hochstrasser, and J. C. Sanchez. 2000.** The dynamic range of protein expression: A challenge for proteomic research. *Electrophoresis* **21**:1104-1115.
**Costagliola, C., A. Del Prete, C. Incorvaia, R. Fusco, F. Parmeggiani, and A. Di Giovanni. 2001.** Ocular surface changes induced by topical application of latanoprost and timolol: a short-term study in glaucomatous patients with and without allergic conjunctivitis. *Graef Arch Clin Exp* **239**:809-814.
**Cox, B., and A. Emili. 2006.** Tissue subcellular fractionation and protein extraction for use in mass-spectrometry-based proteomics. *Nat Protoc* **1**:1872-1878.
**Cox, J., N. C. Hubner, and M. Mann. 2008.** How Much Peptide Sequence Information Is Contained in Ion Trap Tandem Mass Spectra? *J Am Soc Mass Spectr* **19**:1813-1820.
**Cozzi, R., R. Ricordy, F. Bartolini, L. Ramadori, P. Perticone, and R. De Salvia. 1995.** Taurine and ellagic acid: two differently-acting natural antioxidants. *Environ Mol Mutagen* **26**:248-254.
**Crabb , J. W. personal communication 2013.** Quantitative Proteomics. *271 Tips and techniques for using proteomics and metabolomics in your clinical and translational research-SIG. Seattle, USA. ARVO Life-changing Research World Conference 2013*

**Crabb, J. W., X. Yuan, G. Dvoriantchikova, D. Ivanov, J. S. Crabb, and V. I. Shestopalov. 2010.** Preliminary quantitative proteomic characterization of glaucomatous rat retinal ganglion cells. *Exp Eye Res* **91**:107-110.
**Craig, J. P., and A. Tomlinson. 1997.** Importance of the lipid layer in human tear film stability and evaporation. *Optom Vis Sci* **74**:8-13.
**Csosz, E., P. Boross, A. Csutak, A. Berta, F. Toth, S. Poliska, Z. Torok, and J. Tozser. 2012.** Quantitative analysis of proteins in the tear fluid of patients with diabetic retinopathy. *J Proteomics* **75**:2196-2204.
**Cuatrecasas, P. 1970a.** Agarose derivatives for purification of protein by affinity chromatography. *Nature* **228**:1327-1328.
**Cuatrecasas, P. 1970b.** Protein purification by affinity chromatography. Derivatizations of agarose and polyacrylamide beads. *J Biol Chem* **245**:3059-3065.
**Cvenkel, B., and A. Ihan. 2002.** Ocular surface changes induced by topical antiglaucoma monotherapy. *Ophthalmologica* **216**:175-179.

**Daniel, J. M., S. D. Friess, S. Rajagopalan, S. Wendt, and R. Zenobi. 2002.** Quantitative determination of noncovalent binding interactions using soft ionization mass spectrometry. *Int J of Mass Spec* **216**:1-27.
**Danjo, Y. W., H.; Tisdale, A. S.; George, M.; Tsumura, T.; Abelson, M. B.; Gipson, I. K. 1998.** Alteration of mucin in human conjunctival epithelia in dry eye. *Invest Ophthalmol Vis Sci* **39**:2602-2609.
**Dartt, D. A. 2002.** Regulation of mucin and fluid secretion by conjunctival epithelial cells. *Prog Retin Eye Res* **21**:555-576.
**Dartt, D. A., T. L. Kessler, E. H. Chung, and J. D. Zieske. 1996.** Vasoactive intestinal peptide-stimulated glycoconjugate secretion from conjunctival goblet cells. *Exp Eye Res* **63**:27-34.
**Dartt, D. A., J. D. Rios, H. Kanno, I. M. Rawe, J. D. Zieske, N. Ralda, R. R. Hodges, and D. Zoukhri. 2000.** Regulation of conjunctival goblet cell secretion by Ca(2+)and protein kinase C. *Exp Eye Res* **71**:619-628.
**Das, J., J. Ghosh, P. Manna, and P. C. Sil. 2011.** Taurine suppresses doxorubicin-triggered oxidative stress and cardiac apoptosis in rat via up-regulation of PI3-K/Akt and inhibition of p53, p38-JNK. *Biochem Pharmacol* **81**:891-909.
**Davidson, H. J., and V. J. Kuonen. 2004.** The tear film and ocular mucins. *Vet Ophthalmol* **7**:71-77.
**Dawson, R., Jr., M. Biasetti, S. Messina, and J. Dominy. 2002.** The cytoprotective role of taurine in exercise-induced muscle injury. *Amino Acids* **22**:309-324.
**De Bock, M., D. de Seny, M. A. Meuwis, J. P. Chapelle, E. Louis, M. Malaise, M. P. Merville, and M. Fillet. 2010.** Challenges for Biomarker Discovery in Body Fluids Using SELDI-TOF-MS. *Journal of Biomedicine and Biotechnology*.
**de Freitas Campos, C., N. Cole, D. Van Dyk, B. J. Walsh, P. Diakos, D. Almeida, A. Torrecilhas, J. L. Laus, and M. D. Willcox. 2008.** Proteomic analysis of dog tears for potential cancer markers. *Res Vet Sci* **85**:349-352.
**de la Fuente, M., M. Ravina, P. Paolicelli, A. Sanchez, B. Seijo, and M. J. Alonso. 2010.** Chitosan-based nanostructures: A delivery platform for ocular therapeutics. *Adv Drug Deliver Rev* **62**:100-117.
**de Noo, M. E., A. Deelder, M. van der Werff, A. Ozalp, B. Mertens, and R. Tollenaar. 2006.** MALDI-TOF serum protein profiling for the detection of breast cancer. *Onkologie* **29**:501-506.
**de Paiva, C. S., R. M. Corrales, and S. C. Pflugfelder. 2013.** Biomarkers in dry eye disease. *J Mol Biomark Diagn* **4**.
**De Paiva, C. S., R. M. Corrales, A. L. Villarreal, W. J. Farley, D. Q. Li, M. E. Stern, and S. C. Pfiugfelder. 2006.** Corticosteroid and doxycycline suppress MMP-9 and inflammatory cytokine expression, MAPK activation in the corneal epithelium in experimental dry eye. *Experimental Eye Research* **83**:526-535.
**De Paiva, C. S., A. L. Villarreal, R. M. Corrales, H. T. Rahman, V. Y. Chang, W. J. Farley, M. E. Stern, J. Y. Niederkorn, D. Q. Li, and S. C. Pflugfelder. 2007.** Dry eye-induced conjunctival epithelial squamous metaplasia is modulated by interferon-gamma. *Invest Ophthalmol Vis Sci* **48**:2553-2560.
**de Roos, B., I. Duivenvoorden, G. Rucklidge, M. Reid, K. Ross, R. J. Lamers, P. J. Voshol, L. M. Havekes, and B. Teusink. 2005.** Response of apolipoprotein E*3-Leiden transgenic mice to dietary fatty acids: combining liver proteomics with physiological data. *FASEB J* **19**:813-815.
**De Saint Jean, M., C. Debbasch, F. Brignole, P. Rat, J. M. Warnet, and C. Baudouin. 2000.** Toxicity of preserved and unpreserved antiglaucoma topical drugs in an in vitro model of conjunctival cells. *Current Eye Research* **20**:85-94.
**de Souza, G. A., L. M. Godoy, and M. Mann. 2006.** Identification of 491 proteins in the tear fluid proteome reveals a large number of proteases and protease inhibitors. *Genome Biol* **7**:R72.
**Debbasch, C., F. Brignole, P. J. Pisella, J. M. Warnet, P. Rat, and C. Baudouin. 2001.** Quaternary ammoniums and other preservatives' contribution in oxidative stress and apoptosis on Chang conjunctival cells. *Invest Ophthalmol Vis Sci* **42**:642-652.

**Deeg, C. A., B. Amann, S. M. Hauck, and B. Kaspers. 2006.** Defining cytochemical markers for different cell types in the equine retina. *Anat Histol Embryol* **35**:412-415.
**Degim, Z., N. Celebi, H. Sayan, A. Babul, D. Erdogan, and G. Take. 2002.** An investigation on skin wound healing in mice with a taurine-chitosan gel formulation. *Amino Acids* **22**:187-198.
**Dejong, C., T. Stolwijk, E. Kuppens, R. Dekeizer, and J. Vanbest. 1994.** Topical Timolol with and without Benzalkonium Chloride - Epithelial Permeability and Autofluorescence of the Cornea in Glaucoma. *Graef Arch Clin Exp* **232**:221-224.
**Dekker, L. J., W. Boogerd, G. Stockhammer, J. C. Dalebout, I. Siccama, P. Zheng, J. M. Bonfrer, J. J. Verschuuren, G. Jenster, M. M. Verbeek, T. M. Luider, and P. A. Smitt. 2005.** MALDI-TOF mass spectrometry analysis of cerebrospinal fluid tryptic peptide profiles to diagnose leptomeningeal metastases in patients with breast cancer. *Mol Cell Proteomics* **4**:1341-1349.
**Delaire, A., H. Lassagne, and A. M. Gachon. 1992.** New members of the lipocalin family in human tear fluid. *Exp Eye Res* **55**:645-647.
**Delmas, V., D. G. Stokes, and R. P. Perry. 1993.** A Mammalian DNA-Binding Protein That Contains a Chromodomain and an Snf2 Swi2-Like Helicase Domain. *P Natl Acad Sci USA* **90**:2414-2418.
**Deng, X., J. Liang, Z. X. Lin, F. S. Wu, Y. P. Zhang, and Z. W. Zhang. 2010.** Natural taurine promotes apoptosis of human hepatic stellate cells in proteomic analysis. *World J Gastroenterol* **16**:1916-1923.
**Deschamps, N., and C. Baudouin. 2013.** Dry Eye and Biomarkers: Present and Future. *Curr Ophthalmol Rep* **1**:65-74.
**Deschamps, N., X. Ricaud, G. Rabut, A. Labbe, C. Baudouin, and A. Denoyer. 2013.** The Impact of Dry Eye Disease on Visual Performance While Driving. *Am J Ophthalmol* **156**:184-189.
**Devamanoharan, P. S., A. H. Ali, and S. D. Varma. 1997.** Prevention of lens protein glycation by taurine. *Mol Cell Biochem* **177**:245-250.
**Di Wu, Q., J. H. Wang, F. Fennessy, H. P. Redmond, and D. Bouchier-Hayes. 1999.** Taurine prevents high-glucose-induced human vascular endothelial cell apoptosis. *Am J Physiol-Cell Ph* **277**:C1229-C1238.
**Diebold, Y., M. Calonge, A. E. de Salamanca, S. Callejo, R. M. Corrales, V. Saez, K. F. Siemasko, and M. E. Stern. 2003.** Characterization of a spontaneously immortalized cell line (IOBA-NHC) from normal human conjunctiva. *Invest Ophth Vis Sci* **44**:4263-4274.
**Diebold, Y., J. D. Rios, R. R. Hodges, I. Rawe, and D. A. Dartt. 2001.** Presence of nerves and their receptors in mouse and human conjunctival goblet cells. *Invest Ophth Vis Sci* **42**:2270-2282.
**Dincer, S., A. Babul, D. Erdogan, C. Ozogul, and S. L. Dincer. 1996.** Effect of taurine on wound healing. *Amino Acids* **10**:59-71.
**Diz, A. P., M. Truebano, and D. O. F. Skibinski. 2009.** The consequences of sample pooling in proteomics: An empirical study. *Electrophoresis* **30**:2967-2975.
**Dobryszycka, W. 1997.** Biological functions of haptoglobin - New pieces to an old puzzle. *Eur J Clin Chem Clin* **35**:647-654.
**Dogru, M., Y. Matsumoto, N. Okada, A. Igarashi, K. Fukagawa, J. Shimazaki, K. Tsubota, and H. Fujishima. 2008.** Alterations of the ocular surface epithelial MUC16 and goblet cell MUC5AC in patients with atopic keratoconjunctivitis. *Allergy* **63**:1324-1334.
**Dogru, M., M. Nakamura, J. Shimazaki, and K. Tsubota. 2013.** Changing trends in the treatment of dry-eye disease. *Expert Opin Investig Drugs*.
**Dolara, P., F. Franconi, A. Giotti, R. Basosi, and G. Valensin. 1978.** Taurine-calcium interaction measured by means of 13C nuclear magnetic resonance. *Biochem Pharmacol* **27**:803-804.
**Domon, B., and R. Aebersold. 2006.** Review - Mass spectrometry and protein analysis. *Science* **312**:212-217.
**Donnenfeld, E. D., K. Solomon, H. D. Perry, S. J. Doshi, M. Ehrenhaus, R. Solomon, and S. Biser. 2003.** The effect of hinge position on corneal sensation and dry eye after LASIK. *Ophthalmology* **110**:1023-1029; discussion 1029-1030.

**Du, Z., Y. L. Yu, and J. H. Wang. 2007.** Extraction of proteins from biological fluids by use of an ionic liquid/aqueous two-phase system. *Chem-Eur J* **13**:2130-2137.
**Dua, H. S., L. A. Faraj, D. G. Said, T. Gray, and J. Lowe. 2013.** Human corneal anatomy redefined: a novel pre-Descemet's layer (Dua's layer). *Ophthalmology* **120**:1778-1785.
**Duan, X. M., Q. J. Lu, P. Xue, H. J. Zhang, Z. Dong, F. Q. Yang, and N. L. Wang. 2008.** Proteomic analysis of aqueous humor from patients with myopia. *Molecular Vision* **14**:370-377.
**Duan, X. T., R. Young, R. M. Straubinger, B. Page, J. Cao, H. Wang, H. Y. Yu, J. M. Canty, and J. Qu. 2009.** A Straightforward and Highly Efficient Precipitation/On-Pellet Digestion Procedure Coupled with a Long Gradient Nano-LC Separation and Orbitrap Mass Spectrometry for Label-Free Expression Profiling of the Swine Heart Mitochondrial Proteome. *J Proteome Res* **8**:2838-2850.
**Duncan, M. W., R. Aebersold, and R. M. Caprioli. 2010.** The pros and cons of peptide-centric proteomics. *Nat Biotechnol* **28**:659-664.
**Dunn, W. B., D. Broadhurst, M. Brown, P. N. Baker, C. W. G. Redman, L. C. Kenny, and D. B. Kell. 2008.** Metabolic profiling of serum using Ultra Performance Liquid Chromatography and the LTQ-Orbitrap mass spectrometry system. *J Chromatogr B* **871**:288-298.
**Dunson, W. A. 1970.** Some Aspects of Electrolyte and Water Balance in 3 Estuarine Reptiles, Diamondback Terrapin, American and Salt-Water Crocodiles. *Comp Biochem Physiol* **32**:161-&.
**Dyrlund, T. F., E. T. Poulsen, C. Scavenius, C. L. Nikolajsen, I. B. Thogersen, H. Vorum, and J. J. Enghild. 2012.** Human cornea proteome: identification and quantitation of the proteins of the three main layers including epithelium, stroma, and endothelium. *J Proteome Res* **11**:4231-4239.
**Ebeling, D. D., M. S. Westphall, M. Scalf, and L. M. Smith. 2000.** Corona discharge in charge reduction electrospray mass spectrometry. *Anal Chem* **72**:5158-5161.
**Ebert, M. P., D. Niemeyer, S. O. Deininger, T. Wex, C. Knippig, J. Hoffmann, J. Sauer, W. Albrecht, P. Malfertheiner, and C. Rocken. 2006.** Identification and confirmation of increased fibrinopeptide a serum protein levels in gastric cancer sera by magnet bead assisted MALDI-TOF mass spectrometry. *J Proteome Res* **5**:2152-2158.
**El Ayed, M., D. Bonnel, R. Longuespee, C. Castellier, J. Franck, D. Vergara, A. Desmons, A. Tasiemski, A. Kenani, D. Vinatier, R. Day, I. Fournier, and M. Salzet. 2010.** MALDI imaging mass spectrometry in ovarian cancer for tracking, identifying, and validating biomarkers. *Med Sci Monitor* **16**:Br233-Br245.
**Endo, Y., K. Hanada, M. Miyake, K. Ogawara, K. Higaki, and T. Kimura. 2002.** Mechanisms of cytoprotective effect of amino acids on local toxicity caused by sodium laurate, a drug absorption enhancer, in intestinal epithelium. *Journal of Pharmaceutical Sciences* **91**:730-743.
**Enoksson, M., A. P. Fernandes, S. Prast, C. H. Lillig, A. Hohngren, and S. Orrenius. 2005.** Overexpression of glutaredoxin 2 attenuates apoptosis by preventing cytochrome c release. *Biochem Bioph Res Co* **327**:774-779.
**Enriquez-de-Salamanca, A., S. Bonini, and M. Calonge. 2012.** Molecular and cellular biomarkers in dry eye disease and ocular allergy. *Curr Opin Allergy Clin Immunol* **12**:523-533.
**Erb, C., U. Gast, and D. Schremmer. 2008.** German register for glaucoma patients with dry eye. I. Basic outcome with respect to dry eye. *Graef Arch Clin Exp* **246**:1593-1601.
**Erb, C., I. Lanzl, S. F. Seidova, and F. Kimmich. 2011.** Preservative-free tafluprost 0.0015% in the treatment of patients with glaucoma and ocular hypertension. *Adv Ther* **28**:575-585.
**Erra-Balsells, R., and H. Nonami. 2003.** UV-matrix-assisted laser desorption/ionization time-of-flight mass spectrometry analysis of synthetic polymers by using nor-harmane as matrix. *Arkivoc*:517-537.
**Etzioni, R., N. Urban, S. Ramsey, M. McIntosh, S. Schwartz, B. Reid, J. Radich, G. Anderson, and L. Hartwell. 2003.** The case for early detection. *Nat Rev Cancer* **3**:243-252.

**Eue, I., S. Konig, J. Pior, and C. Sorg. 2002.** S100A8, S100A9 and the S100A8/A9 heterodimer complex specifically bind to human endothelial cells: identification and characterization of ligands for the myeloid-related proteins S100A9 and S100A8/A9 on human dermal microvascular endothelial cell line-1 cells. *Int Immunol* **14**:287-297.
**Evans, J. E., K. M. Green, R. M. Sullivan, D. A. Schaumberg, M. R. Dana, and D. A. Sullivan. 2003.** Proteomic analysis of human meibomian gland secretions. *Invest Ophth Vis Sci* **44**:U432-U432.
**Evans, V., C. Vockler, M. Friedlander, B. Walsh, and M. D. Willcox. 2001.** Lacryglobin in human tears, a potential marker for cancer. *Clin Experiment Ophthalmol* **29**:161-163.
**Falktoft, B., and I. H. Lambert. 2004.** Ca2+-mediated potentiation of the swelling-induced taurine efflux from HeLa cells: On the role of calmodulin and novel protein kinase C isoforms. *J Membrane Biol* **201**:59-75.
**Fenn, J. B., M. Mann, C. K. Meng, S. F. Wong, and C. M. Whitehouse. 1989.** Electrospray Ionization for Mass-Spectrometry of Large Biomolecules. *Science* **246**:64-71.
**Fenn, J. B., M. Mann, C. K. Meng, S. F. Wong, and C. M. Whitehouse. 1990.** Electrospray Ionization-Principles and Practice. *Mass Spectrometry Reviews* **9**:37-70.
**Fernando, M. R., H. Nanri, S. Yoshitake, K. Nagata-Kuno, and S. Minakami. 1992.** Thioredoxin regenerates proteins inactivated by oxidative stress in endothelial cells. *Eur J Biochem* **209**:917-922.
**Ferro, M., D. Seigneurin-Berny, N. Rolland, A. Chapel, D. Salvi, J. Garin, and J. Joyard. 2000.** Organic solvent extraction as a versatile procedure to identify hydrophobic chloroplast membrane proteins. *Electrophoresis* **21**:3517-3526.
**Feser, J., D. Truong, C. Das, J. J. Carson, J. Kieft, T. Harkness, and J. K. Tyler. 2010.** Elevated Histone Expression Promotes Life Span Extension. *Mol Cell* **39**:724-735.
**Feuerstein, I., M. Rainer, K. Bernardo, G. Stecher, C. W. Huck, K. Kofler, A. Pelzer, W. Horninger, H. Klocker, G. Bartsch, and G. K. Bonn. 2005.** Derivatized cellulose combined with MALDI-TOF MS: A new tool for serum protein profiling. *J Proteome Res* **4**:2320-2326.
**Fiedler, G. M., S. Baumann, A. Leichtle, A. Oltmann, J. Kase, J. Thiery, and U. Ceglarek. 2007.** Standardized peptidome profiling of human urine by magnetic bead separation and matrix-assisted laser desorption/ionization time-of-flight mass spectrometry. *Clin Chem* **53**:421-428.
**Flanagan, J. L., and M. D. P. Willcox. 2009.** Role of lactoferrin in the tear film. *Biochimie* **91**:35-43.
**FlexAnalysis2.4OperatorManual. 2005.** Bruker Daltonik GmbH, Bremen, Germany. **1st Edition**.
**Flood-Nichols, S. K., D. Tinnemore, M. A. Wingerd, A. I. Abu-Alya, P. G. Napolitano, J. D. Stallings, and D. L. Ippolito. 2013.** Longitudinal analysis of maternal plasma apolipoproteins in pregnancy: a targeted proteomics approach. *Mol Cell Proteomics* **12**:55-64.
**Flower, D. R. 1996.** The lipocalin protein family: structure and function. *Biochem J* **318 ( Pt 1)**:1-14.
**Fluckinger, M., H. Haas, P. Merschak, B. J. Glasgow, and B. Redl. 2004.** Human tear lipocalin exhibits antimicrobial activity by scavenging microbial siderophores. *Antimicrob Agents Chemother* **48**:3367-3372.
**Fonn, D., N. Pritchard, D. Brazeau, and L. Michaud. 1995.** Discontinuation of Contact-Lens Wear - the Numbers, Reasons and Patient Profiles. *Invest Ophth Vis Sci* **36**:S312-S312.
**Foong, A. W., S. M. Saw, J. L. Loo, S. Shen, S. C. Loon, M. Rosman, T. Aung, D. T. Tan, E. S. Tai, and T. Y. Wong. 2007.** Rationale and methodology for a population-based study of eye diseases in Malay people: The Singapore Malay eye study (SiMES). *Ophthalmic Epidemiol* **14**:25-35.
**Fountoulakis, M., and H. Langen. 1997.** Identification of proteins by matrix-assisted laser desorption ionization-mass spectrometry following in-gel digestion in low-salt, nonvolatile buffer and simplified peptide recovery. *Anal Biochem* **250**:153-156.

**Fraga, C. G., B. J. Prazen, and R. E. Synovec. 2001.** Objective data alignment and chemometric analysis of comprehensive two-dimensional separations with run-to-run peak shifting on both dimensions. *Anal Chem* **73**:5833-5840.
**Franconi, F., I. Stendardi, P. Failli, R. Matucci, C. Baccaro, L. Montorsi, R. Bandinelli, and A. Giotti. 1985.** The protective effects of taurine on hypoxia (performed in the absence of glucose) and on reoxygenation (in the presence of glucose) in guinea-pig heart. *Biochem Pharmacol* **34**:2611-2615.
**Fratantoni, S. A., S. R. Piersma, and C. R. Jimenez. 2010.** Comparison of the performance of two affinity depletion spin filters for quantitative proteomics of CSF: Evaluation of sensitivity and reproducibility of CSF analysis using GeLC-MS/MS and spectral counting. *Proteomics Clin Appl* **4**:613-617.
**Fraunfelder, F. T., J. J. Sciubba, and W. D. Mathers. 2012.** The role of medications in causing dry eye. *J Ophthalmol* **2012**:285851.
**Freed, G. L., L. H. Cazares, C. E. Fichandler, T. W. Fuller, C. A. Sawyer, B. C. Stack, S. Schraff, O. J. Semmes, J. T. Wadsworth, and R. R. Drake. 2008.** Differential Capture of Serum Proteins for Expression Profiling and Biomarker Discovery in Pre- and Posttreatment Head and Neck Cancer Samples. *Laryngoscope* **118**:61-68.
**Friedman, D. B., S. Hill, J. W. Keller, N. B. Merchant, S. E. Levy, R. J. Coffey, and R. M. Caprioli. 2004.** Proteome analysis of human colon cancer by two-dimensional difference gel electrophoresis and mass spectrometry. *Proteomics* **4**:793-811.
**Froger, N., L. Cadetti, H. Lorach, J. Martins, A. P. Bemelmans, E. Dubus, J. Degardin, D. Pain, V. Forster, L. Chicaud, I. Ivkovic, M. Simonutti, S. Fouquet, F. Jammoul, T. Leveillard, R. Benosman, J. A. Sahel, and S. Picaud. 2012.** Taurine provides neuroprotection against retinal ganglion cell degeneration. *PLoS One* **7**:e42017.
**Frohlich, T., and G. J. Arnold. 2006.** Proteome research based on modern liquid chromatography - tandem mass spectrometry: separation, identification and quantification. *J Neural Transm* **113**:973-994.
**Frost, M. R., and T. T. Norton. 2007.** Differential protein expression in tree shrew sclera during development of lens-induced myopia and recovery. *Molecular Vision* **13**:1580-1588.
**Frost, M. R., and T. T. Norton. 2012.** Alterations in Protein Expression in Tree Shrew Sclera during Development of Lens-Induced Myopia and Recovery. *Invest Ophth Vis Sci* **53**:322-336.
**Fu, Q., C. P. Garnham, S. T. Elliott, D. E. Bovenkamp, and J. E. Van Eyk. 2005.** A robust, streamlined, and reproducible method for proteomic analysis of serum by delipidation, albumin and IgG depletion, and two-dimensional gel electrophoresis. *Proteomics* **5**:2656-2664.
**Fukuda, M., R. J. Fullard, M. D. Willcox, C. Baleriola-Lucas, F. Bestawros, D. Sweeney, and B. A. Holden. 1996.** Fibronectin in the tear film. *Invest Ophthalmol Vis Sci* **37**:459-467.
**Fukuoka, H., S. Kawasaki, N. Yokoi, and S. Kinoshita. 2012.** Three-dimensional Culture Of N-cadherin-expressing Conjunctival Epithelial Cells. *ARVO 2012 Annual Meeting, Fort Lauderdale, USA*
**Program Number: 3977**.
**Funding, M., H. Vorum, B. Honore, E. Nexo, and N. Ehlers. 2005.** Proteomic analysis of aqueous humour from patients with acute corneal rejection. *Acta Ophthalmol Scan* **83**:31-39.
**Fung, E. T., and C. Enderwick. 2002.** ProteinChip clinical proteomics: computational challenges and solutions. *Biotechniques* **Suppl**:34-38, 40-31.
**Fung, K. Y., C. Morris, S. Sathe, R. Sack, and M. W. Duncan. 2004.** Characterization of the in vivo forms of lacrimal-specific proline-rich proteins in human tear fluid. *Proteomics* **4**:3953-3959.
**Funke, S., D. Azimi, D. Wolters, F. H. Grus, and N. Pfeiffer. 2012.** Longitudinal analysis of taurine induced effects on the tear proteome of contact lens wearers and dry eye patients using a RP-RP-Capillary-HPLC-MALDI TOF/TOF MS approach. *J Proteomics* **75**:3177-3190.
**Funke, S., S. Beck, K. Lorenz, M. Kotterer, D. Wolters, N. Pfeiffer, and F. H. Grus. 2014.** Analysis of the Effects of Preservative-free Tafluprost on the Tear Proteome *Ophthalmology* **submitted**.

**Furrer, P., J. M. Mayer, and R. Gurny. 2002.** Ocular tolerance of preservatives and alternatives. *Eur J Pharm Biopharm* **53**:263-280.
**Gabadinho, A., G. Ritschard, N. S. Muller, and M. Studer. 2011.** Analyzing and Visualizing State Sequences in R with TraMineR. *J Stat Softw* **40**:1-37.
**Gadaria-Rathod, N., K. I. Lee, and P. A. Asbell. 2013.** Emerging drugs for the treatment of dry eye disease. *Expert Opin Emerg Drugs* **18**:121-136.
**Galiacy, S. D., C. Froment, E. Mouton-Barbosa, A. Erraud, K. Chaoui, L. Desjardins, B. Monsarrat, F. Malecaze, and O. Burlet-Schiltz. 2011.** Deeper in the human cornea proteome using nanoLC-Orbitrap MS/MS: An improvement for future studies on cornea homeostasis and pathophysiology. *Journal of Proteomics* **75**:81-92.
**Galletti, J. G., M. L. Gabelloni, P. E. Morande, F. Sabbione, M. E. Vermeulen, A. S. Trevani, and M. N. Giordano. 2013.** Benzalkonium chloride breaks down conjunctival immunological tolerance in a murine model. *Mucosal Immunol* **6**:24-34.
**Gallicano, G. I., P. Kouklis, C. Bauer, M. Yin, V. Vasioukhin, L. Degenstein, and E. Fuchs. 1998.** Desmoplakin is required early in development for assembly of desmosomes and cytoskeletal linkage. *Journal of Cell Biology* **143**:2009-2022.
**Gamez-Pozo, A., I. Sanchez-Navarro, M. Nistal, E. Calvo, R. Madero, E. Diaz, E. Camafeita, J. de Castro, J. A. Lopez, M. Gonzalez-Baron, E. Espinosa, and J. A. F. Vara. 2009.** MALDI Profiling of Human Lung Cancer Subtypes. *PLoS One* **4**.
**Gao, B. B., X. H. Chen, N. Timothy, L. P. Aiello, and E. P. Feener. 2008.** Characterization of the vitreous proteome in diabetes without diabetic retinopathy and diabetes with proliferative diabetic retinopathy. *J Proteome Res* **7**:2516-2525.
**Garcia-Fernandez, M., H. Kissel, S. Brown, T. Gorenc, A. J. Schile, S. Rafii, S. Larisch, and H. Steller. 2010.** Sept4/ARTS is required for stem cell apoptosis and tumor suppression. *Gene Dev* **24**:2282-2293.
**Garcia, J. F., and D. Barcelo. 1993.** An Overview of Lc-Ms Interfacing Systems with Selected Applications. *Hrc-J High Res Chrom* **16**:633-641.
**Garrett, Q., S. Xu, P. A. Simmons, J. Vehige, J. L. Flanagan, and M. D. Willcox. 2008.** Expression and localization of carnitine/organic cation transporter OCTN1 and OCTN2 in ocular epithelium. *Invest Ophthalmol Vis Sci* **49**:4844-4849.
**Gasset, A. R., Y. Ishii, H. E. Kaufman, and T. Miller. 1974.** Cytotoxicity of ophthalmic preservatives. *Am J Ophthalmol* **78**:98-105.
**Gast, M. C. W., C. H. van Gils, L. F. A. Wessels, N. Harris, J. M. G. Bonfrer, E. J. T. Rutgers, J. H. M. Schellens, and J. H. Beijnen. 2009.** Influence of sample storage duration on serum protein profiles assessed by surface-enhanced laser desorption/ionisation time-of-flight mass spectrometry (SELDI-TOF MS). *Clinical Chemistry and Laboratory Medicine* **47**:694-705.
**Gaucher, D., E. Arnault, Z. Husson, N. Froger, E. Dubus, P. Gondouin, D. Dherbecourt, J. Degardin, M. Simonutti, S. Fouquet, M. A. Benahmed, K. Elbayed, I. J. Namer, P. Massin, J. A. Sahel, and S. Picaud. 2012.** Taurine deficiency damages retinal neurones: cone photoreceptors and retinal ganglion cells. *Amino Acids* **43**:1979-1993.
**Gayton, J. L. 2009.** Etiology, prevalence, and treatment of dry eye disease. *Clin Ophthalmol* **3**:405-412.
**Georgiev, G. A. Y., N.; Koev, K.; Kutsarova, E.; Ivanova, S.; Kyumurkov, A.; Jordanova, A.; Krastev, R.; Lalchev, Z. 2011.** Surface chemistry study of the interactions of benzalkonium chloride with films of meibom, corneal cells lipids, and whole tears. *Invest Ophthalmol Vis Sci* **52**:4645-4654.
**Gerbaulet, S. P., A. J. van Wijnen, N. Aronin, M. S. Tassinari, J. B. Lian, J. L. Stein, and G. S. Stein. 1992.** Downregulation of histone H4 gene transcription during postnatal development in transgenic mice and at the onset of differentiation in transgenically derived calvarial osteoblast cultures. *J Cell Biochem* **49**:137-147.
**Gerke, V., C. E. Creutz, and S. E. Moss. 2005.** Annexins: Linking Ca2+ signalling to membrane dynamics. *Nat Rev Mol Cell Bio* **6**:449-461.
**Gerke, V., and S. E. Moss. 2002.** Annexins: From structure to function. *Physiol Rev* **82**:331-371.

**Ghiso, J., N. Cowan, and B. Frangione. 1988.** Isolation of a sequence encoding human cystatin C. Conservation of exon-intron structure between members of the cysteine proteinase inhibitors superfamily. *Biol Chem Hoppe Seyler* **369 Suppl**:205-208.
**Gilar, M., P. Olivova, A. E. Daly, and J. C. Gebler. 2005.** Two-dimensional separation of peptides using RP-RP-HPLC system with different pH in first and second separation dimensions. *Journal of Separation Science* **28**:1694-1703.
**Gilthorpe, J. D. O., F.; Nash, J.; Calvo, M.; Bennett, D. L. H.; Lumsden, A.; Pini, A. 2013.** Extracellular histone H1 is neurotoxic and drives a pro-inflammatory response in microglia. *F1000Research 2013, 2:148* **2**:1-13.
**Gipson, I. K. 1994.** Evidence That the Entire Ocular Surface Epithelium Produces Mucins for the Tear Film. *Invest Ophth Vis Sci* **35**:1811-1811.
**Gipson, I. K. 2007.** The ocular surface: The challenge to enable and protect vision: The Friedenwald lecture. *Invest Ophth Vis Sci* **48**:4391-4398.
**Gipson, I. K., and P. Argueso. 2003.** Role of mucins in the function of the corneal and conjunctival epithelia. *Int Rev Cytol* **231**:1-49.
**Gipson, I. K., Y. Hori, and P. Argueso. 2004.** Character of ocular surface mucins and their alteration in dry eye disease. *Ocul Surf* **2**:131-148.
**Gipson, I. K., and T. Inatomi. 1997.** Mucin genes expressed by the ocular surface epithelium. *Prog Retin Eye Res* **16**:81-98.
**Gipson, I. K., and T. Inatomi. 1998.** Cellular origin of mucins of the ocular surface tear film. *Lacrimal Gland, Tear Film, and Dry Eye Syndromes 2* **438**:221-227.
**Gipson, I. K., S. Spurr-Michaud, P. Argueso, A. Tisdale, T. F. Ng, and C. L. Russo. 2003.** Mucin gene expression in immortalized human corneal-limbal and conjunctival epithelial cell lines. *Invest Ophthalmol Vis Sci* **44**:2496-2506.
**Glanzer, J. G., Y. Enose, T. Wang, I. Kadiu, N. Gong, W. Rozek, J. N. Liu, J. D. Schlautman, P. S. Ciborowski, M. P. Thomas, and H. E. Gendelman. 2007.** Genomic and proteomic microglial profiling: pathways for neuroprotective inflammatory responses following nerve fragment clearance and activation. *J Neurochem* **102**:627-645.
**Glasgow, B. J., A. R. Abduragimov, Z. T. Farahbakhsh, K. F. Faull, and W. L. Hubbell. 1995.** Tear lipocalins bind a broad array of lipid ligands. *Curr Eye Res* **14**:363-372.
**Glasson, M. J., F. Stapleton, L. Keay, and M. D. Willcox. 2006.** The effect of short term contact lens wear on the tear film and ocular surface characteristics of tolerant and intolerant wearers. *Cont Lens Anterior Eye* **29**:41-47; quiz 49.
**Goklen, K. E., and T. A. Hatton. 1987.** Liquid-Liquid-Extraction of Low-Molecular-Weight Proteins by Selective Solubilization in Reversed Micelles. *Separ Sci Technol* **22**:831-841.
**Goodman, E. C., and L. L. Iversen. 1986.** Calcitonin Gene-Related Peptide - Novel Neuropeptide. *Life Sci* **38**:2169-2178.
**Gordon, R. E., A. A. Shaked, and D. F. Solano. 1986.** Taurine Protects Hamster Bronchioles from Acute No2-Induced Alterations - a Histologic, Ultrastructural, and Freeze-Fracture Study. *Am J Pathol* **125**:585-600.
**Gorry, P. A. 1990.** General Least-Squares Smoothing and Differentiation by the Convolution (Savitzky-Golay) Method. *Anal Chem* **62**:570-573.
**Goto, E., Y. Yagi, Y. Matsumoto, and K. Tsubota. 2002.** Impaired functional visual acuity of dry eye patients. *Am J Ophthalmol* **133**:181-186.
**Gouin-Charnet, A., D. Laune, C. Granier, J. C. Mani, B. Pau, G. Mourad, and A. Argiles. 2000.** alpha2-Macroglobulin, the main serum antiprotease, binds beta2-microglobulin, the light chain of the class I major histocompatibility complex, which is involved in human disease. *Clin Sci (Lond)* **98**:427-433.
**Gouveia, S. M., and J. M. Tiffany. 2005.** Human tear viscosity: an interactive role for proteins and lipids. *Biochim Biophys Acta* **1753**:155-163.
**Govek, S. P., G. Oshiro, J. V. Anzola, C. Beauregard, J. Chen, A. R. Coyle, D. A. Gamache, M. R. Hellberg, J. N. Hsien, J. M. Lerch, J. C. Liao, J. W. Malecha, L. M. Staszewski, D. J. Thomas, J. M. Yanni, S. A. Noble, and A. K. Shiau. 2010.** Water-soluble PDE4 inhibitors for the treatment of dry eye. *Bioorg Med Chem Lett* **20**:2928-2932.

**Granger, J., J. Siddiqui, S. Copeland, and D. Remick. 2005.** Albumin depletion of human plasma also removes low abundance proteins including the cytokines. *Proteomics* **5**:4713-4718.
**Grant, R. L., and D. Acosta. 1996.** Prolonged adverse effects of benzalkonium chloride and sodium dodecyl sulfate in a primary culture system of rabbit corneal epithelial cells. *Fundam Appl Toxicol* **33**:71-82.
**Green-Church, K. B., and J. J. Nichols. 2008.** Mass spectrometry-based proteomic analyses of contact lens deposition. *Mol Vis* **14**:291-297.
**Green-Church, K. B., K. K. Nichols, N. M. Kleinholz, L. W. Zhang, and J. J. Nichols. 2008.** Investigation of the human tear film proteome using multiple proteomic approaches. *Molecular Vision* **14**:456-470.
**Green, D. R., and J. C. Reed. 1998.** Mitochondria and apoptosis. *Science* **281**:1309-1312.
**Gretzer, M. B., D. W. Chan, C. L. van Rootselaar, J. M. Rosenzweig, S. Dalrymple, L. A. Mangold, A. W. Partin, and R. W. Veltri. 2004.** Proteomic analysis of dunning prostate cancer cell lines with variable metastatic potential using SELDI-TOF. *Prostate* **60**:325-331.
**Grey, A. C., and K. L. Schey. 2009.** Age-related changes in the spatial distribution of human lens alpha-crystallin products by MALDI imaging mass spectrometry. *Invest Ophthalmol Vis Sci* **50**:4319-4329.
**Groseclose, M. R., P. R. Massion, P. Chaurand, and R. M. Caprioli. 2008.** High-throughput proteomic analysis of formalin-fixed paraffin-embedded tissue microarrays using MALDI imaging mass spectrometry. *Proteomics* **8**:3715-3724.
**Grus, F. H., and A. J. Augustin. 1999.** Analysis of tear protein patterns by a neural network as a diagnostical tool for the detection of dry eyes. *Electrophoresis* **20**:875-880.
**Grus, F. H., S. C. Joachim, S. Sandmann, U. Thiel, K. Bruns, K. J. Lackner, and N. Pfeiffer. 2008.** Transthyretin and complex protein pattern in aqueous humor of patients with primary open-angle glaucoma. *Molecular Vision* **14**:1437-1445.
**Grus, F. H., C. Kramann, N. Bozkurt, N. Wiegel, K. Bruns, N. Lackner, and N. Pfeiffer. 2005a.** Effects of multipurpose contact lens solutions on the protein composition of the tear film. *Cont Lens Anterior Eye* **28**:103-112.
**Grus, F. H., V. N. Podust, K. Bruns, K. Lackner, S. Fu, E. A. Dalmasso, A. Wirthlin, and N. Pfeiffer. 2005b.** SELDI-TOF-MS ProteinChip array profiling of tears from patients with dry eye. *Invest Ophthalmol Vis Sci* **46**:863-876.
**Guerrera, I. C., and O. Kleiner. 2005.** Application of mass spectrometry in proteomics. *Biosci Rep* **25**:71-93.
**Gulati, A., M. Sacchetti, S. Bonini, and R. Dana. 2006.** Chemokine receptor CCR5 expression in conjunctival epithelium of patients with dry eye syndrome. *Arch Ophthalmol* **124**:710-716.
**Gumerov, D. R., A. Dobo, and I. A. Kaltashov. 2002.** Protein-ion charge-state distributions in electrospray ionization mass spectrometry: distinguishing conformational contributions from masking effects. *Eur J Mass Spectrom* **8**:123-129.
**Guo, B., P. Lu, X. Chen, W. Zhang, and R. Chen. 2010.** Prevalence of dry eye disease in Mongolians at high altitude in China: the Henan eye study. *Ophthalmic Epidemiol* **17**:234-241.
**Guo, J., E. C. Yang, L. Desouza, G. Diehl, M. J. Rodrigues, A. D. Romaschin, T. J. Colgan, and K. W. Siu. 2005.** A strategy for high-resolution protein identification in surface-enhanced laser desorption/ionization mass spectrometry: calgranulin A and chaperonin 10 as protein markers for endometrial carcinoma. *Proteomics* **5**:1953-1966.
**Guo, Y., M. Satpathy, G. Wilson, and S. P. Srinivas. 2007.** Benzalkonium chloride induces dephosphorylation of myosin light chain in cultured corneal epithelial cells. *Invest Ophthalmol Vis Sci* **48**:2001-2008.
**Gupta, K., and R. L. Mathur. 1983.** Distribution of taurine in the crystalline lens of vertebrate species and in cataractogenesis. *Exp Eye Res* **37**:379-384.
**Gustavsson, S. A., J. Samskog, K. E. Markides, and B. Langstrom. 2001.** Studies of signal suppression in liquid chromatography-electrospray ionization mass spectrometry using volatile ion-pairing reagents. *Journal of Chromatography A* **937**:41-47.

**Guzik, B. W., and L. S. Goldstein. 2004.** Microtubule-dependent transport in neurons: steps towards an understanding of regulation, function and dysfunction. *Curr Opin Cell Biol* **16**:443-450.
**Hada, J., T. Kaku, K. Morimoto, Y. Hayashi, and K. Nagai. 1996.** Adenosine transport inhibitors enhance high K(+)-evoked taurine release from rat hippocampus. *Eur J Pharmacol* **305**:101-107.
**Hager, J. W. 2004.** Recent trends in mass spectrometer development. *Anal Bioanal Chem* **378**:845-850.
**Hakansson, L. 2007.** Development of Biomarkers: What Are the Scientific Hurdles? *Ejc Suppl* **5**:10-11.
**Hall, C. A. 1975.** Transcobalamin I and II as natural transport proteins of vitamin B12. *J Clin Invest* **56**:1125-1131.
**Hallquist, N. A., and K. C. Klasing. 1994.** Serotransferrin, ovotransferrin and metallothionein levels during an immune response in chickens. *Comp Biochem Physiol Biochem Mol Biol* **108**:375-384.
**Halquist, M. S., and H. T. Karnes. 2011.** Quantification of Alefacept, an immunosuppressive fusion protein in human plasma using a protein analogue internal standard, trypsin cleaved signature peptides and liquid chromatography tandem mass spectrometry. *J Chromatogr B* **879**:789-798.
**Hamacher, T., J. Airaksinen, V. Saarela, M. J. Liinamaa, U. Richter, and A. Ropo. 2008.** Efficacy and safety levels of preserved and preservative-free tafluprost are equivalent in patients with glaucoma or ocular hypertension: results from a pharmacodynamics analysis. *Acta Ophthalmol Suppl (Oxf )* **242**:14-19.
**Hamada, H., T. Arakawa, and K. Shiraki. 2009.** Effect of Additives on Protein Aggregation. *Curr Pharm Biotechno* **10**:400-407.
**Hanrieder, J. W., G.; Bergquist, J.; Andersson, M.; Fex-Svenningsen, A. 2011.** MALDI mass spectrometry based molecular phenotyping of CNS glial cells for prediction in mammalian brain tissue. *Anal Bioanal Chem* **401**:135-147.
**Hansen, S. H., M. L. Andersen, C. Cornett, R. Gradinaru, and N. Grunnet. 2010.** A role for taurine in mitochondrial function. *Journal of Biomedical Science* **17**.
**Haque, I., R. Singh, F. Ahmad, and A. A. Moosavi-Movahedi. 2005.** Testing polyols' compatibility with Gibbs energy of stabilization of proteins under conditions in which they behave as compatible osmolytes. *FEBS Lett* **579**:3891-3898.
**Hardenborg, E., A. Botling-Taube, J. Hanrieder, M. Andersson, A. Alm, and J. Bergquist. 2009.** Protein content in aqueous humor from patients with pseudoexfoliation (PEX) investigated by capillary LC MALDI-TOF/TOF MS. *Proteom Clin Appl* **3**:299-306.
**Hardman, M., and A. A. Makarov. 2003.** Interfacing the orbitrap mass analyzer to an electrospray ion source. *Anal Chem* **75**:1699-1705.
**Harned, J., L. N. Fleisher, and M. C. McGahan. 2006.** Lens epithelial cells synthesize and secrete ceruloplasmin: effects of ceruloplasmin and transferrin on iron efflux and intracellular iron dynamics. *Exp Eye Res* **83**:721-727.
**Harris, H. E., and U. Andersson. 2004.** The nuclear protein HMGB1 as a proinflammatory mediator. *European Journal of Immunology* **34**:1503-1512.
**Hassan, M. I., A. Waheed, S. Yadav, T. P. Singh, and F. Ahmad. 2008.** Zinc alpha 2-glycoprotein: a multidisciplinary protein. *Mol Cancer Res* **6**:892-906.
**Hawkridge, A. M., and D. C. Muddiman. 2009.** Mass spectrometry-based biomarker discovery: toward a global proteome index of individuality. *Annu Rev Anal Chem (Palo Alto Calif)* **2**:265-277.
**Hawkridge, A. M., R. B. Wysocky, J. N. Petitte, K. E. Anderson, P. E. Mozdziak, O. J. Fletcher, J. M. Horowitz, and D. C. Muddiman. 2010.** Measuring the intra-individual variability of the plasma proteome in the chicken model of spontaneous ovarian adenocarcinoma. *Anal Bioanal Chem* **398**:737-749.
**Haynes, R. J., P. J. Tighe, and H. S. Dua. 1999.** Antimicrobial defensin peptides of the human ocular surface. *Br J Ophthalmol* **83**:737-741.

**He, X. G. 2000.** On-line identification of phytochemical constituents in botanical extracts by combined high-performance liquid chromatographic-diode array detection-mass spectrometric techniques. *Journal of Chromatography A* **880**:203-232.
**Heinamaki, A. A., A. S. Muhonen, and R. S. Piha. 1986.** Taurine and other free amino acids in the retina, vitreous, lens, iris-ciliary body, and cornea of the rat eye. *Neurochem Res* **11**:535-542.
**Herber, S., F. H. Grus, P. Sabuncuo, and A. J. Augustin. 2001.** Two-dimensional analysis of tear protein patterns of diabetic patients. *Electrophoresis* **22**:1838-1844.
**Herbert, B. R., J. L. Harry, N. H. Packer, A. A. Gooley, S. K. Pedersen, and K. L. Williams. 2001.** What place for polyacrylamide in proteomics? *Trends in Biotechnology* **19**:S3-S9.
**Herrero Vanrell, R. 2007.** Preservatives in ophthalmic formulations: an overview. *Arch Soc Esp Oftalmol* **82**:531-532.
**Hikichi, T., A. Yoshida, Y. Fukui, T. Hamano, M. Ri, K. Araki, K. Horimoto, E. Takamura, K. Kitagawa, M. Oyama, Y. Danjo, S. Kondo, H. Fujishima, I. Toda, and K. Tsubota. 1995.** Prevalence of Dry Eye in Japanese Eye Centers. *Graef Arch Clin Exp* **233**:555-558.
**Hirabayashi, A., M. Ishimaru, N. Manri, T. Yokosuka, and H. Hanzawa. 2007.** Detection of potential ion suppression for peptide analysis in nanoflow liquid chromatography/mass spectrometry. *Rapid Commun Mass Sp* **21**:2860-2866.
**Hjelmervik, T. O., R. Jonsson, and A. I. Bolstad. 2009.** The minor salivary gland proteome in Sjogren's syndrome. *Oral Dis* **15**:342-353.
**Hoehenwarter, W., N. M. Kumar, M. Wacker, U. Zimny-Arndt, J. Klose, and P. R. Jungblut. 2005.** Eye lens proteomics: from global approach to detailed information about phakinin and gamma E and F crystallin genes. *Proteomics* **5**:245-257.
**Holly, F. J., and M. A. Lemp. 1977.** Tear Physiology and Dry Eyes. *Survey of Ophthalmology* **22**:69-87.
**Holmgren, A. 2000.** Antioxidant function of thioredoxin and glutaredoxin systems. *Antioxid Redox Signal* **2**:811-820.
**Holmquist, L., and K. Carlson. 1977.** Selective Extraction of Human-Serum Very Low-Density Apolipoproteins with Organic-Solvents. *Biochimica Et Biophysica Acta* **493**:400-409.
**Hommer, A., O. Mohammed Ramez, M. Burchert, and F. Kimmich. 2010.** IOP-lowering efficacy and tolerability of preservative-free tafluprost 0.0015% among patients with ocular hypertension or glaucoma. *Curr Med Res Opin* **26**:1905-1913.
**Horsley, M. B., and M. Y. Kahook. 2009.** Effects of prostaglandin analog therapy on the ocular surface of glaucoma patients. *Clin Ophthalmol* **3**:291-295.
**Hortin, G. L. 2006.** The MALDI-TOF mass spectrometric view of the plasma proteome and peptidome. *Clin Chem* **52**:1223-1237.
**Hos, D., K. R. Koch, F. Bock, R. S. Grajewski, T. S. Dietlein, C. Cursiefen, and L. M. Heindl. 2013.** Short- and long-term corneal vascular effects of tafluprost eye drops. *Graefes Arch Clin Exp Ophthalmol* **251**:1919-1927.
**Hoteling, A. J., K. Kawaoka, M. C. Goodberlet, W. M. Yu, and K. G. Owens. 2003.** Optimization of matrix-assisted laser desorption/ionization time-of-flight collision-induced dissociation using poly(ethylene glycol). *Rapid Commun Mass Sp* **17**:1671-1676.
**Hoteling, A. J., and K. G. Owens. 2004.** Improved PSD and CID on a MALDI TOFMS. *J Am Soc Mass Spectr* **15**:523-535.
**Hsu, Y. W., S. M. Yeh, Y. Y. Chen, Y. C. Chen, S. L. Lin, and J. K. Tseng. 2012.** Protective effects of taurine against alloxan-induced diabetic cataracts and refraction changes in New Zealand White rabbits. *Exp Eye Res* **103**:71-77.
**Hu, Q. Z., R. J. Noll, H. Y. Li, A. Makarov, M. Hardman, and R. G. Cooks. 2005.** The Orbitrap: a new mass spectrometer. *Journal of Mass Spectrometry* **40**:430-443.
**Hu, S., T. Yu, Y. Xie, Y. Yang, Y. Li, X. Zhou, S. Tsung, R. R. Loo, J. R. Loo, and D. T. Wong. 2007.** Discovery of oral fluid biomarkers for human oral cancer by mass spectrometry. *Cancer Genomics Proteomics* **4**:55-64.
**Huang, C. C., C. B. Chang, J. Y. Liu, S. Basavappa, and P. H. Lim. 2001.** Effects of calcium, calmodulin, protein kinase C and protein tyrosine kinases on volume-activated taurine efflux in human erythroleukemia cells. *Journal of Cellular Physiology* **189**:316-322.

**Huang, H. L., T. Stasyk, S. Morandell, H. Dieplinger, G. Falkensammer, A. Griesmacher, M. Mogg, M. Schreiber, I. Feuerstein, C. W. Huck, G. Stecher, G. K. Bonn, and L. A. Huber. 2006.** Biomarker discovery in breast cancer serum using 2-D differential gel electrophoresis/MALDI-TOF/TOF and data validation by routine clinical assays. *Electrophoresis* **27**:1641-1650.
**Huang, J. C., C. C. Sun, C. K. Chang, D. H. Ma, and Y. F. Lin. 2012.** Effect of hinge position on corneal sensation and dry eye parameters after femtosecond laser-assisted LASIK. *J Refract Surg* **28**:625-631.
**Huber, L. A., K. Pfaller, and I. Vietor. 2003.** Organelle proteomics - Implications for subcellular fractionation in proteomics. *Circulation Research* **92**:962-968.
**Hutchens, T. W., and T. T. Yip. 1993.** New Desorption Strategies for the Mass-Spectrometric Analysis of Macromolecules. *Rapid Commun Mass Sp* **7**:576-580.
**Huxtable, R. J. 1990.** The Interaction between Taurine, Calcium and Phospholipids - Further Investigations of a Trinitarian Hypothesis. *Prog Clin Biol Res* **351**:185-196.
**Huxtable, R. J. 1992.** Physiological Actions of Taurine. *Physiol Rev* **72**:101-163.
**Ilina, E. N., A. D. Borovskaya, M. V. Serebryakova, V. V. Chelysheva, K. T. Momynaliev, T. Maier, M. Kostrzewa, and V. M. Govorun. 2010.** Application of matrix-assisted laser desorption/ionization time-of-flight mass spectrometry for the study of Helicobacter pylori. *Rapid Commun Mass Spectrom* **24**:328-334.
**Immenschuh, S., D. X. Song, H. Satoh, and U. Mullereberhard. 1995.** The Type-Ii Hemopexin Interleukin-6 Response Element Predominates the Transcriptional Regulation of the Hemopexin Acute-Phase Responsiveness. *Biochem Bioph Res Co* **207**:202-208.
**Inatomi, T., S. Spurr-Michaud, A. S. Tisdale, Q. Zhan, S. T. Feldman, and I. K. Gipson. 1996.** Expression of secretory mucin genes by human conjunctival epithelia. *Invest Ophthalmol Vis Sci* **37**:1684-1692.
**Ireland, D. C., M. L. Colgrave, and D. J. Craik. 2006.** A novel suite of cyclotides from Viola odorata: sequence variation and the implications for structure, function and stability. *Biochem J* **400**:1-12.
**Ishihama, Y. 2005.** Proteomic LC-MS systems using nanoscale liquid chromatography with tandem mass spectrometry. *Journal of Chromatography A* **1067**:73-83.
**Ishii, T., and T. Yanagawa. 2007.** Stress-induced peroxiredoxins. *Subcell Biochem* **44**:375-384.
**Ismail, M., and J. H. Brock. 1993.** Binding of lactoferrin and transferrin to the human promonocytic cell line U937. Effect on iron uptake and release. *J Biol Chem* **268**:21618-21625.
**Issaq, H. J. 2001.** The role of separation science in proteomics research. *Electrophoresis* **22**:3629-3638.
**Issaq, H. J., K. C. Chan, G. M. Janini, T. P. Conrads, and T. D. Veenstra. 2005.** Multidimensional separation of peptides for effective proteomic analysis. *J Chromatogr B Analyt Technol Biomed Life Sci* **817**:35-47.
**Issaq, H. J., T. P. Conrads, D. A. Prieto, R. Tirumalai, and T. D. Veenstra. 2003.** SELDI-TOF MS for diagnostic proteomics. *Anal Chem* **75**:148a-155a.
**Issaq, H. J., T. D. Veenstra, T. P. Conrads, and D. Felschow. 2002.** The SELDI-TOF MS approach to proteomics: protein profiling and biomarker identification. *Biochem Biophys Res Commun* **292**:587-592.
**Iwata, S. 1973.** Chemical composition of the aqueous phase. *Int Ophthalmol Clin* **13**:29-46.
**Jacobsen, J. G., and L. H. Smith. 1968.** Biochemistry and physiology of taurine and taurine derivatives. *Physiol Rev* **48**:424-511.
**Jandrokovic, S., S. P. Suic, R. Kordic, T. Kuzman, and I. Petricek. 2013.** Tear film status in glaucoma patients. *Coll Antropol* **37 Suppl 1**:137-140.
**Janssen, P. T., and O. P. van Bijsterveld. 1983.** Origin and biosynthesis of human tear fluid proteins. *Invest Ophthalmol Vis Sci* **24**:623-630.
**Januleviciene, I., I. Derkac, L. Grybauskiene, R. Paulauskaite, R. Gromnickaite, and L. Kuzmiene. 2012.** Effects of preservative-free tafluprost on tear film osmolarity, tolerability, and intraocular pressure in previously treated patients with open-angle glaucoma. *Clin Ophthalmol* **6**:103-109.

**Jauhiainen, M., N. L. Setala, C. Ehnholm, J. Metso, T. M. T. Tervo, O. Erikkson, and J. M. Holopainen. 2005.** Phospholipid transfer protein is present in human tear fluid. *Biochemistry* **44**:8111-8116.
**Jensen, O. L., and B. S. Gluud. 1985.** Bacterial-Growth in the Conjunctival Sac and the Local Defense of the Outer Eye. *Acta Ophthalmol* **63**:80-82.
**Jessome, L. L., and D. A. Volmer. 2006.** Ion suppression: A major concern in mass spectrometry. *Lc Gc N Am* **24**:498-+.
**Jester, J. V., A. Budge, S. Fisher, and J. Huang. 2005.** Corneal keratocytes: phenotypic and species differences in abundant protein expression and in vitro light-scattering. *Invest Ophthalmol Vis Sci* **46**:2369-2378.
**Jiang, X. S., H. Zhou, L. Zhang, Q. H. Sheng, S. J. Li, L. Li, P. Hao, Y. X. Li, Q. C. Xia, J. R. Wu, and R. Zeng. 2004.** A high-throughput approach for subcellular proteome: identification of rat liver proteins using subcellular fractionation coupled with two-dimensional liquid chromatography tandem mass spectrometry and bioinformatic analysis. *Mol Cell Proteomics* **3**:441-455.
**Jie, Y., L. Xu, Y. Y. Wu, and J. B. Jonas. 2009.** Prevalence of dry eye among adult chinese in the Beijing eye study. *Eye* **23**:688-693.
**Jimenez, C. R., Z. El Filali, J. C. Knol, K. Hoekman, F. A. Kruyt, G. Giaccone, A. B. Smit, and K. W. Li. 2007a.** Automated serum peptide profiling using novel magnetic C18 beads off-line coupled to MALDI-TOF-MS. *Proteomics Clin Appl* **1**:598-604.
**Jimenez, C. R., M. Koel-Simmelink, T. V. Pham, L. van der Voort, and C. E. Teunissen. 2007b.** Endogeneous peptide profiling of cerebrospinal fluid by MALDI-TOF mass spectrometry: Optimization of magnetic bead-based peptide capture and analysis of preanalytical variables. *Proteomics Clin Appl* **1**:1385-1392.
**Joachim, S. C., K. Bruns, K. J. Lackner, N. Pfeiffer, and F. H. Grus. 2007a.** Analysis of IgG antibody patterns against retinal antigens and antibodies to alpha-crystallin, GFAP, and alpha-enolase in sera of patients with "wet" age-related macular degeneration. *Graefes Arch Clin Exp Ophthalmol* **245**:619-626.
**Joachim, S. C., K. Bruns, K. J. Lackner, N. Pfeiffer, and F. H. Grus. 2007b.** Antibodies to alpha B-crystallin, vimentin, and heat shock protein 70 in aqueous humor of patients with normal tension glaucoma and IgG antibody patterns against retinal antigen in aqueous humor. *Curr Eye Res* **32**:501-509.
**Joachim, S. C., F. H. Grus, D. Kraft, K. White-Farrar, G. Barnes, M. Barbeck, S. Ghanaati, S. Cao, B. Li, and M. B. Wax. 2009.** Complex antibody profile changes in an experimental autoimmune glaucoma animal model. *Invest Ophthalmol Vis Sci* **50**:4734-4742.
**Joachim, S. C., J. Reichelt, S. Berneiser, N. Pfeiffer, and F. H. Grus. 2008.** Sera of glaucoma patients show autoantibodies against myelin basic protein and complex autoantibody profiles against human optic nerve antigens. *Graef Arch Clin Exp* **246**:573-580.
**Joachim, S. C., M. B. Wax, P. Seidel, N. Pfeiffer, and F. H. Grus. 2010.** Enhanced characterization of serum autoantibody reactivity following HSP 60 immunization in a rat model of experimental autoimmune glaucoma. *Curr Eye Res* **35**:900-908.
**Johnson, M. E., and P. J. Murphy. 2004.** Changes in the tear film and ocular surface from dry eye syndrome. *Prog Retin Eye Res* **23**:449-474.
**Jong, C. J., J. Azuma, and S. Schaffer. 2012.** Mechanism underlying the antioxidant activity of taurine: prevention of mitochondrial oxidant production. *Amino Acids* **42**:2223-2232.
**Jonhagen, S., P. Ackermann, T. Saartok, and P. A. Renstrom. 2006.** Calcitonin gene related peptide and neuropeptide Y in skeletal muscle after eccentric exercise: a microdialysis study. *Brit J Sport Med* **40**:264-267.
**Jr, G. W., L. H. Cazares, S. M. Leung, S. Nasim, B. L. Adam, T. T. Yip, P. F. Schellhammer, L. Gong, and A. Vlahou. 1999.** Proteinchip(R) surface enhanced laser desorption/ionization (SELDI) mass spectrometry: a novel protein biochip technology for detection of prostate cancer biomarkers in complex protein mixtures. *Prostate Cancer Prostatic Dis* **2**:264-276.
**Jumblatt, M. M., R. W. McKenzie, and J. E. Jumblatt. 1999.** MUC5AC mucin is a component of the human precorneal tear film. *Invest Ophth Vis Sci* **40**:43-49.

**Jurado, R. L. 1997.** Iron, infections, and anemia of inflammation. *Clin Infect Dis* **25**:888-895.
**Kadenbach, B., S. Arnold, I. Lee, and M. Huttemann. 2004.** The possible role of cytochrome c oxidase in stress-induced apoptosis and degenerative diseases. *Bba-Bioenergetics* **1655**:400-408.
**Kaiserman, I., N. Kaiserman, S. Nakar, and S. Vinker. 2005.** Dry eye in diabetic patients. *Am J Ophthalmol* **139**:498-503.
**Kamoi, K., and M. Mochizuki. 2012.** HTLV infection and the eye. *Curr Opin Ophthalmol* **23**:557-561.
**Kampik, A., Grehn, F. et al. . 2002.** Augenärztliche Therapie. *Georg Thieme Verlag KG, Stuttgart, Germany*.
**Kanamoto, T., T. Ue, T. Yokoyama, N. Souchelnytskyi, and Y. Kiuchi. 2009.** Proteomic study of DBA/2J mice retina: Down-regulation of Integrin beta 7 correlated with retinal ganglion cell death. *Proteomics* **9**:4962-4969.
**Kapp, E., F. Schutz, and R. Simpson. 2005.** An evaluation, comparison, and accurate benchmarking of several publicly available MS/MS search algorithms; Sensitivity and specificity analysis. *Mol Cell Proteomics* **4**:S24-S24.
**Karas, M., U. Bahr, and T. Dulcks. 2000a.** Nano-electrospray ionization mass spectrometry: addressing analytical problems beyond routine. *Fresen J Anal Chem* **366**:669-676.
**Karas, M., M. Gluckmann, and J. Schafer. 2000b.** Ionization in matrix-assisted laser desorption/ionization: singly charged molecular ions are the lucky survivors. *Journal of Mass Spectrometry* **35**:1-12.
**Karas, M., and F. Hillenkamp. 1988.** Laser Desorption Ionization of Proteins with Molecular Masses Exceeding 10000 Daltons. *Anal Chem* **60**:2299-2301.
**Karlenius, T. C., F. Shah, G. Di Trapani, F. M. Clarke, and K. F. Tonissen. 2012.** Cycling hypoxia up-regulates thioredoxin levels in human MDA-MB-231 breast cancer cells. *Biochem Bioph Res Co* **419**:350-355.
**Karlenius, T. C. T., K. F. . 2010.** Thioredoxin and Cancer: A Role for Thioredoxin in all States of Tumor Oxygenation. *Cancers 2010, 2, 209-232;* **2**:209-232;.
**Karnati, R., D. E. Laurie, and G. W. Laurie. 2013.** Lacritin and the tear proteome as natural replacement therapy for dry eye. *Exp Eye Res*.
**Karp, N. A., and K. S. Lilley. 2009.** Investigating sample pooling strategies for DIGE experiments to address biological variability. *Proteomics* **9**:388-397.
**Karring, H., I. Thogersen, G. Klintworth, T. Moller-Pedersen, and J. Enghild. 2006.** The human cornea proteome: Bioinformatic analyses indicate import of plasma proteins into the cornea. *Molecular Vision* **12**:451-460.
**Karring, H., I. B. Thogersen, G. K. Klintworth, T. Moller-Pedersen, and J. J. Enghild. 2005.** A dataset of human cornea proteins identified by peptide mass fingerprinting and tandem mass spectrometry. *Mol Cell Proteomics* **4**:1406-1408.
**Karty, J. A., M. M. E. Ireland, Y. V. Brun, and J. P. Reilly. 2002.** Artifacts and unassigned masses encountered in peptide mass mapping. *J Chromatogr B* **782**:363-383.
**Kasuya, M., M. Itoi, S. Kobayashi, H. Sunaga, and K. T. Suzuki. 1992.** Changes of glutathione and taurine concentrations in lenses of rat eyes induced by galactose-cataract formation or ageing. *Exp Eye Res* **54**:49-53.
**Katz, A., P. Waridel, A. Shevchenko, and U. Pick. 2007.** Salt-induced changes in the plasma membrane proteome of the halotolerant alga Dunaliella salina as revealed by blue native gel electrophoresis and nano-LC-MS/MS analysis. *Mol Cell Proteomics* **6**:1459-1472.
**Kawachi, I., K. Tanaka, M. Tanaka, and S. Tsuji. 2001.** Dendritic cells presenting pyruvate kinase M1/M2 isozyme peptide can induce experimental allergic myositis in BALB/c mice. *Journal of Neuroimmunology* **117**:108-115.
**Kawakami, H., S. Dosako, and B. Lonnerdal. 1990.** Iron uptake from transferrin and lactoferrin by rat intestinal brush-border membrane vesicles. *Am J Physiol* **258**:G535-541.
**Kedik, S. A., S. M. Levachev, A. V. Panov, I. V. Sakaeva, A. E. Kharlov, O. A. Grigor'eva, E. S. Zhavoronok, Y. V. Cherta, M. A. Zaitsev, and H. K. An. 2011.** Formation of Ultrathin Protective Films for Ophthalmological Use from Aqueous Solutions of Polymers and Taurine. *Pharm Chem J+* **45**:245-247.

**Kelleher, N. L., H. Y. Lin, G. A. Valaskovic, D. J. Aaserud, E. K. Fridriksson, and F. W. McLafferty. 1999.** Top down versus bottom up protein characterization by tandem high-resolution mass spectrometry. *J Am Chem Soc* **121**:806-812.
**Kendler, B. S. 1989.** Taurine: an overview of its role in preventive medicine. *Prev Med* **18**:79-100.
**Kerai, M. D., C. J. Waterfield, S. H. Kenyon, D. S. Asker, and J. A. Timbrell. 1998.** Taurine: protective properties against ethanol-induced hepatic steatosis and lipid peroxidation during chronic ethanol consumption in rats. *Amino Acids* **15**:53-76.
**Ketterlinus, R., S. Y. Hsieh, S. H. Teng, H. Lee, and W. Pusch. 2005.** Fishing for biomarkers: analyzing mass spectrometry data with the new ClinProTools software. *Biotechniques* **Suppl**:37-40.
**Kettman, J. R., J. R. Frey, and I. Lefkovits. 2001.** Proteome, transcriptome and genome: top down or bottom up analysis? *Biomol Eng* **18**:207-212.
**Keys, S. A., and W. F. Zimmerman. 1999.** Antioxidant activity of retinol, glutathione, and taurine in bovine photoreceptor cell membranes. *Exp Eye Res* **68**:693-702.
**Kilic, F., R. Bhardwaj, J. Caulfeild, and J. R. Trevithick. 1999.** Modelling cortical cataractogenesis 22: Is in vitro reduction of damage in model diabetic rat cataract by taurine due to its antioxidant activity? *Experimental Eye Research* **69**:291-300.
**Kim, C. 2006.** Accumulation of taurine in tumor and inflammatory lesions. *Taurine 6* **583**:213-217.
**Kim, C., S. H. Lee, G. J. Seong, Y. H. Kim, and M. Y. Lee. 2006.** Nuclear translocation and overexpression of GAPDH by the hyper-pressure in retinal ganglion cell. *Biochem Bioph Res Co* **341**:1237-1243.
**Kim, E. C., J. S. Choi, and C. K. Joo. 2009a.** A comparison of vitamin a and cyclosporine a 0.05% eye drops for treatment of dry eye syndrome. *Am J Ophthalmol* **147**:206-213 e203.
**Kim, J. J., Y. H. Kim, and M. Y. Lee. 2009b.** Proteomic characterization of differentially expressed proteins associated with no stress in retinal ganglion cells. *Bmb Rep* **42**:456-461.
**Kim, K. W., S. B. Han, E. R. Han, S. J. Woo, J. J. Lee, J. C. Yoon, and J. Y. Hyon. 2011.** Association between depression and dry eye disease in an elderly population. *Invest Ophthalmol Vis Sci* **52**:7954-7958.
**Kim, S. J., C. Ramesh, H. Gupta, and W. Lee. 2007a.** Taurine-diabetes interaction: from involvement to protection. *J Biol Reg Homeos Ag* **21**:63-77.
**Kim, T., S. J. Kim, K. Kim, U. B. Kang, C. Lee, K. S. Park, H. G. Yu, and Y. Kim. 2007b.** Profiling of vitreous proteomes from proliferative diabetic retinopathy and nondiabetic patients. *Proteomics* **7**:4203-4215.
**Kim, Y., V. Ignatchenko, C. Q. Yao, I. Kalatskaya, J. O. Nyalwidhe, R. S. Lance, A. O. Gramolini, D. A. Troyer, L. D. Stein, P. C. Boutros, J. A. Medin, O. J. Semmes, R. R. Drake, and T. Kislinger. 2012.** Identification of differentially expressed proteins in direct expressed prostatic secretions of men with organ-confined versus extracapsular prostate cancer. *Mol Cell Proteomics*.
**Kimura, K., S. Teranishi, and T. Nishida. 2009.** Interleukin-1ß-induced disruption of barrier function in cultured human corneal epithelial cells. *Invest Ophthalmol Vis Sci* **50**:597-603.
**Kinoshita, M. 2003.** The septins. *Genome Biol* **4**:236.
**Kirkland, J. J. 2000.** Ultrafast reversed-phase high-performance liquid chromatographic separations: an overview. *J Chromatogr Sci* **38**:535-544.
**Kislinger, T., A. O. Gramolini, D. H. MacLennan, and A. Emili. 2005.** Multidimensional protein identification technology (MudPIT): Technical overview of a profiling method optimized for the comprehensive proteomic investigation of normal and diseased heart tissue. *J Am Soc Mass Spectr* **16**:1207-1220.
**Kjellstrom, S., and O. N. Jensen. 2003.** In situ liquid - Liquid extraction as a sample preparation method for matrix-assisted laser desorption/ionization MS analysis of polypeptide mixtures. *Anal Chem* **75**:2362-2369.
**Kobayashi, T. K., K. Tsubota, E. Takamura, M. Sawa, Y. Ohashi, and M. Usui. 1997.** Effect of retinol palmitate as a treatment for dry eye: A cytological evaluation. *Ophthalmologica* **211**:358-361.

**Koch, P. J., M. J. Walsh, M. Schmelz, M. D. Goldschmidt, R. Zimbelmann, and W. W. Franke. 1990.** Identification of Desmoglein, a Constitutive Desmosomal Glycoprotein, as a Member of the Cadherin Family of Cell-Adhesion Molecules. *Eur J Cell Biol* **53**:1-12.
**Koh, S., C. Ikeda, Y. Takai, H. Watanabe, N. Maeda, and K. Nishida. 2013.** Long-term results of treatment with diquafosol ophthalmic solution for aqueous-deficient dry eye. *Jpn J Ophthalmol*.
**Kojima, K., S. Asmellash, C. A. Klug, W. E. Grizzle, J. A. Mobley, and J. D. Christein. 2008.** Applying proteomic-based biomarker tools for the accurate diagnosis of pancreatic cancer. *J Gastrointest Surg* **12**:1683-1690.
**Kokke, K. H., J. A. Morris, and J. G. Lawrenson. 2008.** Oral omega-6 essential fatty acid treatment in contact lens associated dry eye. *Cont Lens Anterior Eye* **31**:141-146; quiz 170.
**Koomen, J. M., D. H. Li, L. C. Xiao, T. C. Liu, K. R. Coombes, J. Abbruzzese, and R. Kobayashi. 2005.** Direct tandem mass spectrometry reveals limitations in protein profiling experiments for plasma biomarker discovery. *J Proteome Res* **4**:972-981.
**Koopman, G., C. P. Reutelingsperger, G. A. Kuijten, R. M. Keehnen, S. T. Pals, and M. H. van Oers. 1994.** Annexin V for flow cytometric detection of phosphatidylserine expression on B cells undergoing apoptosis. *Blood* **84**:1415-1420.
**Kosanam, H., S. Makawita, B. Judd, A. Newman, and E. P. Diamandis. 2011.** Mining the malignant ascites proteome for pancreatic cancer biomarkers. *Proteomics* **11**:4551-4558.
**Koubenakis, A., V. Frankevich, J. Zhang, and R. Zenobi. 2004.** Time-resolved surface temperature measurement of MALDI matrices under pulsed UV laser irradiation. *J Phys Chem A* **108**:2405-2410.
**Koyama, I., K. Nakamori, T. Nagahama, M. Ogasawara, and M. Nemoto. 1996.** The reactivity of taurine with hypochlorous acid and its application for eye drops. *Adv Exp Med Biol* **403**:9-18.
**Kozerski, G. E., R. H. Gallavan, and M. J. Ziemelis. 2003.** Investigation of trialkoxysilane hydrolysis kinetics using liquid chromatography with inductively coupled plasma atomic emission spectrometric detection and non-linear regression modeling. *Analytica Chimica Acta* **489**:103-114.
**Kraj, A., and J. Silberring. 2008.** Proteomics: Introduction to methods and applications. *Wiley: John Wiley & Sons, Inc., New Jersey, USA*.
**Kramann, C., N. Boehm, K. Lorenz, N. Wehrwein, B. M. Stoffelns, N. Pfeiffer, and F. H. Grus. 2011.** Effect of contact lenses on the protein composition in tear film: a ProteinChip study. *Graefes Arch Clin Exp Ophthalmol* **249**:233-243.
**Kramann, C. A., N. Pfeiffer, and F. Grus. 2005.** SELDI-TOF-MS ProteinChip array profiling of tears from dry-eye patients: Diagnostic applications of new protein biomarkers. *Invest Ophth Vis Sci* **46**.
**Krenzer, K. L., and T. F. Freddo. 1997.** Cytokeratin expression in normal human bulbar conjunctiva obtained by impression cytology. *Invest Ophth Vis Sci* **38**:142-152.
**Kuhajda, F. P., S. Piantadosi, and G. R. Pasternack. 1989.** Haptoglobin-Related Protein (Hpr) Epitopes in Breast-Cancer as a Predictor of Recurrence of the Disease. *New Engl J Med* **321**:636-641.
**Kuppens, E. V. M. J., C. A. Dejong, T. R. Stolwijk, R. J. W. Dekeizer, and J. A. Vanbest. 1995.** Effect of Timolol with and without Preservative on the Basal Tear Turnover in Glaucoma. *Brit J Ophthalmol* **79**:339-342.
**Kurima, K., Y. Yang, K. Sorber, and A. J. Griffith. 2003.** Characterization of the transmembrane channel-like (TMC) gene family: functional clues from hearing loss and epidermodysplasia verruciformis. *Genomics* **82**:300-308.
**Kushnirov, V. V. 2000.** Rapid and reliable protein extraction from yeast. *Yeast* **16**:857-860.
**Kutz, K. K., J. J. Schmidt, and L. Li. 2004.** In situ tissue analysis of neuropeptides by MALDI FTMS in-cell accumulation. *Anal Chem* **76**:5630-5640.
**Kuwabara, I., Y. Kuwabara, R. Y. Yang, D. Hsu, and F. T. Liu. 2001.** Galectin-7 (PIG1 : p53-induced gene 1) exhibits pro-apoptotic function through mitochondrial cytochrome C release and JNK activation. *J Invest Dermatol* **117**:404-404.

**Kuwabara, I., Y. Kuwabara, R. Y. Yang, M. Schuler, D. R. Green, B. L. Zuraw, D. K. Hsu, and F. T. Liu. 2002.** Galectin-7 (PIG1) exhibits pro-apoptotic function through JNK activation and mitochondrial cytochrome c release. *Journal of Biological Chemistry* **277**:3487-3497.
**Kuwayama, Y., and R. A. Stone. 1987.** Distinct Substance-P and Calcitonin Gene-Related Peptide Immunoreactive Nerves in the Guinea-Pig Eye. *Invest Ophth Vis Sci* **28**:1947-1954.
**Kuzyk, M. A., L. B. Ohlund, M. H. Elliott, D. Smith, H. Qian, A. Delaney, C. L. Hunter, and C. H. Borchers. 2009.** A comparison of MS/MS-based, stable-isotope-labeled, quantitation performance on ESI-quadrupole TOF and MALDI-TOF/TOF mass spectrometers. *Proteomics* **9**:3328-3340.
**Labbe, A., A. Pauly, H. Liang, F. Brignole-Baudouin, C. Martin, J. M. Warnet, and C. Baudouin. 2006.** Comparison of toxicological profiles of benzalkonium chloride and polyquaternium-1: an experimental study. *J Ocul Pharmacol Ther* **22**:267-278.
**Laemmli, U. K. 1970.** Cleavage of structural proteins during the assembly of the head of bacteriophage T4. *Nature* **227**:680-685.
**Lake, N., and C. Verdonesmith. 1989.** Immunocytochemical Localization of Taurine in the Mammalian Retina. *Current Eye Research* **8**:163-173.
**Lam, T. C., R. K. Chun, K. K. Li, and C. H. To. 2008.** Application of proteomic technology in eye research: a mini review. *Clin Exp Optom* **91**:23-33.
**Lang, G., K., Gareis, O., Lang, G., E., Recker, D., Spraul, C., W., Wagner, P. 2008.** Augenheilkunde. *Georg Thieme Verlag KG, Stuttgart, Germany* **4th Edition**.
**Lange, R. 1963.** The Osmotic Function of Amino Acids and Taurine in the Mussel, Mytilus Edulis. *Comp Biochem Physiol* **10**:173-179.
**Langer, G., W. Jagla, W. Behrens-Baumann, S. Walter, and W. Hoffmann. 1999.** Secretory peptides TFF1 and TFF3 synthesized in human conjunctival goblet cells. *Invest Ophthalmol Vis Sci* **40**:2220-2224.
**Lapiere, C. L., and L. Thunus. 1967.** Quaternary ammoniums. *Farmaco Prat* **22**:359-402.
**Laurie, G. A. W. K. O., L. A.; Conway, B. P.; McKown, R. L.; Kitagawa, K.; Nichols, J. J. 2008.** Dry eye and designer ophthalmic. *Optom Vis Sci* **85**:1–18.
**Lavanya, R., V. S. Jeganathan, Y. Zheng, P. Raju, N. Cheung, E. S. Tai, J. J. Wang, E. Lamoureux, P. Mitchell, T. L. Young, H. Cajucom-Uy, P. J. Foster, T. Aung, S. M. Saw, and T. Y. Wong. 2009.** Methodology of the Singapore Indian Chinese Cohort (SICC) eye study: quantifying ethnic variations in the epidemiology of eye diseases in Asians. *Ophthalmic Epidemiol* **16**:325-336.
**Law, R. O. 1995.** Taurine efflux and cell volume regulation in cerebral cortical slices during chronic hypernatraemia. *Neurosci Lett* **185**:56-59.
**Leal, M. F., J. Chung, D. Q. Calcagno, P. P. Assumpcao, S. Demachki, I. D. da Silva, R. Chammas, R. R. Burbano, and M. de Arruda Cardoso Smith. 2012.** Differential proteomic analysis of noncardia gastric cancer from individuals of northern Brazil. *PLoS One* **7**:e42255.
**LeBlanc, A. 1995.** Increased production of a 4kDa amyloid ß peptide in serum deprived human primary neuron cultures: possible involvment of apoptosis. *J Neurosci* **15**:7837-7846.
**Lebrecht, A., D. Boehm, M. Schmidt, H. Koelbl, and F. H. Grus. 2009.** Surface-enhanced Laser Desorption/Ionisation Time-of-flight Mass Spectrometry to Detect Breast Cancer Markers in Tears and Serum. *Cancer Genomics Proteomics* **6**:75-83.
**Lechner, M., P. Wojnar, and B. Redl. 2001.** Human tear lipocalin acts as an oxidative-stress-induced scavenger of potentially harmful lipid peroxidation products in a cell culture system. *Biochem J* **356**:129-135.
**Lee, A. J., J. Lee, S. M. Saw, G. Gazzard, D. Koh, D. Widjaja, and D. T. Tan. 2002.** Prevalence and risk factors associated with dry eye symptoms: a population based study in Indonesia. *Br J Ophthalmol* **86**:1347-1351.
**Lee, G. A., and L. W. Hirst. 1995.** Ocular surface squamous neoplasia. *Survey of Ophthalmology* **39**:429-450.
**Lee, K. A., C. Farnsworth, W. Yu, and L. E. Bonilla. 2011.** 24-Hour Lock Mass Protection. *J Proteome Res* **10**:880-885.
**Lema, I., D. Brea, R. Rodriguez-Gonzalez, E. Diez-Feijoo, and T. Sobrino. 2010.** Proteomic analysis of the tear film in patients with keratoconus. *Mol Vis* **16**:2055-2061.

**Lemaire, R., S. A. Menguellet, J. Stauber, V. Marchaudon, J. P. Lucot, P. Collinet, M. O. Farine, D. Vinatier, R. Day, P. Ducoroy, M. Salzet, and I. Fournier. 2007.** Specific MALDI imaging and profiling for biomarker hunting and validation: fragment of the 11S proteasome activator complex, Reg alpha fragment, is a new potential ovary cancer biomarker. *J Proteome Res* **6**:4127-4134.
**Lembach, M., C. Linenberg, S. Sathe, A. Beaton, O. Ucakhan, P. Asbell, and R. Sack. 2001.** Effect of external ocular surgery and mode of post-operative care on plasminogen, plasmin, angiostatins and alpha(2)-macroglobulin in tears. *Curr Eye Res* **22**:286-294.
**Lemp, M. A. 1973.** Surfacing the precorneal tear film. *Ann Ophthalmol* **5**:819-826.
**Lemp, M. A. 1995.** Report of the National Eye Institute/Industry workshop on Clinical Trials in Dry Eyes. *CLAO J* **21**:221-232.
**Lemp, M. A. 2008.** Advances in understanding and managing dry eye disease. *Am J Ophthalmol* **146**:350-356.
**Lemp, M. A., and Foulks, G. N. 2008.** The Definition & Classification of Dry
Eye Disease-Guidelines from the 2007 International Dry Eye
Workshop. *http://www.tearfilm.org*.
**Lerdweeraphon, W., J. M. Wyss, T. Boonmars, and S. Roysommuti. 2013.** Perinatal taurine exposure affects adult oxidative stress. *Am J Physiol Regul Integr Comp Physiol* **305**:R95-97.
**Lescuyer, P., D. Hochstrasser, and T. Rabilloud. 2007.** How shall we use the proteomics toolbox for biomarker discovery? *J Proteome Res* **6**:3371-3376.
**Lestari, Y. D., R. Sitompul, L. Edwar, and Z. Djoerban. 2013.** Ocular diseases among HIV/AIDS patients in Jakarta, Indonesia. *Southeast Asian J Trop Med Public Health* **44**:62-71.
**Li, J., H. Y. Zhu, and R. W. Beuerman. 2009.** Stimulation of specific cytokines in human conjunctival epithelial cells by defensins HNP1, HBD2, and HBD3. *Invest Ophthalmol Vis Sci* **50**:644-653.
**Li, L. J., R. W. Garden, E. V. Romanova, and J. V. Sweedler. 1999.** In situ sequencing of peptides from biological tissues and single cells using MALDI-PSD/CID analysis. *Anal Chem* **71**:5451-5458.
**Li, M., L. Gong, W. J. Chapin, and M. Zhu. 2012.** Assessment of vision-related quality of life in dry eye patients. *Invest Ophthalmol Vis Sci* **53**:5722-5727.
**Li, N., N. Wang, J. Zheng, X. M. Liu, O. W. Lever, P. M. Erickson, and L. Li. 2005.** Characterization of human tear proteome using multiple proteomic analysis techniques. *J Proteome Res* **4**:2052-2061.
**Li, Z., J. M. Woo, S. W. Chung, M. Y. Kwon, J. S. Choi, H. J. Oh, and K. C. Yoon. 2013.** Therapeutic effect of topical adiponectin in a mouse model of desiccating stress-induced dry eye. *Invest Ophthalmol Vis Sci* **54**:155-162.
**Liang, H., C. Baudouin, A. Pauly, and F. Brignole-Baudouin. 2008.** Conjunctival and corneal reactions in rabbits following short- and repeated exposure to preservative-free tafluprost, commercially available latanoprost and 0.02% benzalkonium chloride. *Brit J Ophthalmol* **92**:1275-1282.
**Libotte, T., H. Zaim, S. Abraham, and e. al. 2005.** Lamin A/C-dependent localization of nesprin-2, a giant scaffolder at the nuclear envelope. *Mol Biol Cell* **16**:3411-3424.
**Lichtenthaler, R., R. B. Rodrigues, J. G. S. Maia, M. Papagiannopoulos, H. Fabricius, and F. Marx. 2005.** Total oxidant scavenging capacities of Euterpe oleracea Mart. (Acai) fruits. *Int J Food Sci Nutr* **56**:53-64.
**Lima, L., P. Matus, and B. Drujan. 1993.** Taurine-Induced Regeneration of Goldfish Retina in Culture May Involve a Calcium-Mediated Mechanism. *J Neurochem* **60**:2153-2158.
**Link, A. J. 2002.** Multidimensional peptide separations in proteomics. *Trends Biotechnol* **20**:S8-13.
**Lippa, C. F. H., J. E.; Smith, T. W.; Pulaski-Salo, D.; Drachman, D. A.; . 1993.** Vascular amyloid deposition in Alzheimer's disease-Neither necessary nor sufficient for the local formation of plaques or tangles. *Arch Neurol* **50**:1088-1092.

**Liu, S. H., J. Li, D. T. H. Tan, and R. W. Beuerman. 2007.** Expression and function of muscarinic receptor subtypes on human cornea and conjunctiva. *Invest Ophth Vis Sci* **48**:2987-2996.
**Liu, Y., and W. Mao. 2013.** Tafluprost once daily for treatment of elevated intraocular pressure in patients with open-angle glaucoma. *Clin Ophthalmol* **7**:7-14.
**Lleu, P. L., S. Croswell, and R. J. Huxtable. 1992.** Phospholipids, Phospholipid Methylation and Taurine Content in Synaptosomes of Developing Rat-Brain. *Taurine* **315**:221-228.
**Löffler, G. 2003.** Basiswissen Biochemie mit Pathobiochemie. *Springer-Verlag Berlin/Heidelberg, Germany* **5th Edition**.
**Lombardini, J. B. 1985.** Effects of taurine on calcium ion uptake and protein phosphorylation in rat retinal membrane preparations. *J Neurochem* **45**:268-275.
**Lombardini, J. B., R. S. L. Young, and C. L. Props. 1996.** Taurine depletion increases phosphorylation of a specific protein in the rat retina. *Amino Acids* **10**:153-165.
**Longtine, M. S., D. J. DeMarini, M. L. Valencik, O. S. AlAwar, H. Fares, C. DeVirgilio, and J. R. Pringle. 1996.** The septins: Roles in cytokinesis and other processes. *Curr Opin Cell Biol* **8**:106-119.
**Lopez-Colome, A. M., and H. Pasantes-Morales. 1981.** Taurine binding to membranes from rat brain regions. *J Neurosci Res* **6**:475-485.
**Lopilly Park, H. Y., J. H. Kim, K. M. Lee, and C. K. Park. 2012.** Effect of prostaglandin analogues on tear proteomics and expression of cytokines and matrix metalloproteinases in the conjunctiva and cornea. *Exp Eye Res* **94**:13-21.
**Louzada, P. R., A. C. P. Lima, D. L. Mendonca-Silva, F. Noel, F. G. De Mello, and S. T. Ferreira. 2004.** Taurine prevents the neurotoxicity of beta-amyloid and glutamate receptor agonists: activation of GABA receptors and possible implications for Alzheimer's disease and other neurological disorders. *Faseb Journal* **18**:511-518.
**Lu, A., A. Zougman, M. Pudelko, M. Bebenek, P. Ziolkowski, M. Mann, and J. R. Wisniewski. 2009.** Mapping of lysine monomethylation of linker histones in human breast and its cancer. *J Proteome Res* **8**:4207-4215.
**Lu, X., and H. Zhu. 2005.** Tube-gel digestion: a novel proteomic approach for high throughput analysis of membrane proteins. *Mol Cell Proteomics* **4**:1948-1958.
**Luo, L., D. Q. Li, A. Doshi, W. Farley, R. M. Corrales, and S. C. Pflugfelder. 2004.** Experimental dry eye stimulates production of inflammatory cytokines and MMP-9 and activates MAPK signaling pathways on the ocular surface. *Invest Ophthalmol Vis Sci* **45**:4293-4301.
**Mackie, I. A. 1985.** Contact lenses in dry eyes. *Trans Ophthalmol Soc U K* **104 ( Pt 4)**:477-483.
**Macri, A., and S. Pflugfelder. 2000.** Correlation of the Schirmer 1 and fluorescein clearance tests with the severity of corneal epithelial and eyelid disease. *Arch Ophthalmol* **118**:1632-1638.
**Magagnotti, C., I. Fermo, R. M. Carletti, M. Ferrari, and A. Bachi. 2010.** Comparison of different depletion strategies for improving resolution of the human urine proteome. *Clin Chem Lab Med* **48**:531-535.
**Mahalakshmi, K., G. Pushpakiran, and C. V. Anuradha. 2003.** Taurine prevents acrylonitrile-induced oxidative stress in rat brain. *Pol J Pharmacol* **55**:1037-1043.
**Mahmood, D. F. D., A. Abderrazak, K. El Hadri, T. Simmet, and M. Rouis. 2013.** The Thioredoxin System as a Therapeutic Target in Human Health and Disease. *Antioxid Redox Sign* **19**:1266-1303.
**Majumdar, S., K. Hippalgaonkar, and M. A. Repka. 2008.** Effect of chitosan, benzalkonium chloride and ethylenediaminetetraacetic acid on permeation of acyclovir across isolated rabbit cornea. *Int J Pharm* **348**:175-178.
**Makarov, A. 2000.** Electrostatic axially harmonic orbital trapping: A high-performance technique of mass analysis. *Anal Chem* **72**:1156-1162.
**Makarov, A., E. Denisov, A. Kholomeev, W. Balschun, O. Lange, K. Strupat, and S. Horning. 2006a.** Performance evaluation of a hybrid linear ion trap/orbitrap mass spectrometer. *Anal Chem* **78**:2113-2120.

**Makarov, A., E. Denisov, O. Lange, and S. Horning. 2006b.** Dynamic range of mass accuracy in LTQ Orbitrap hybrid mass spectrometer. *J Am Soc Mass Spectr* **17**:977-982.
**Malone, J. I., S. A. Benford, and J. Malone, Jr. 1993.** Taurine prevents galactose-induced cataracts. *J Diabetes Complications* **7**:44-48.
**Malone, J. I., S. Lowitt, and W. R. Cook. 1990.** Nonosmotic Diabetic Cataracts. *Pediatr Res* **27**:293-296.
**Malvitte, L., T. Montange, A. Vejux, C. Baudouin, A. M. Bron, C. Creuzot-Garcher, and G. Lizard. 2007.** Measurement of inflammatory cytokines by multicytokine assay in tears of patients with glaucoma topically treated with chronic drugs. *Br J Ophthalmol* **91**:29-32.
**Manaviat, M. R., M. Rashidi, M. Afkhami-Ardekani, and M. R. Shoja. 2008.** Prevalence of dry eye syndrome and diabetic retinopathy in type 2 diabetic patients. *Bmc Ophthalmol* **8**.
**Mann, M., R. C. Hendrickson, and A. Pandey. 2001a.** Analysis of proteins and proteomes by mass spectrometry. *Annual Review of Biochemistry* **70**:437-473.
**Mann, M., R. C. Hendrickson, and A. Pandey. 2001b.** Analysis of proteins and proteomes by mass spectrometry. *Annu Rev Biochem* **70**:437-473.
**Mann, M., and N. L. Kelleher. 2008.** Precision proteomics: The case for high resolution and high mass accuracy. *P Natl Acad Sci USA* **105**:18132-18138.
**Marcinkiewicz, J. 2009.** Taurine bromamine: a new therapeutic option in inflammatory skin diseases. *Pol Arch Med Wewn* **119**:673-675.
**Marcinkiewicz, J. 2010.** Taurine bromamine (TauBr) - its role in immunity and new perspectives for clinical use. *Journal of Biomedical Science* **17**.
**Marcinkiewicz, J., A. Grabowska, J. Bereta, and T. Stelmaszynska. 1995.** Taurine chloramine, a product of activated neutrophils, inhibits in vitro the generation of nitric oxide and other macrophage inflammatory mediators. *J Leukocyte Biol* **58**:667-674.
**Marcinkiewicz, J., and E. Kontny. 2012.** Taurine and inflammatory diseases. *Amino Acids*.
**Marshall, A. G., and C. L. Hendrickson. 2008.** High-resolution mass spectrometers. *Annu Rev Anal Chem (Palo Alto Calif)* **1**:579-599.
**Martin, E., J. M. Molleda, P. J. Ginel, M. Novales, R. Lucena, and R. Lopez. 1997.** Total protein and immunoglobulin concentrations in equine tears. *J Vet Med A* **44**:461-465.
**Maruska, A., A. Rocco, O. Kornysova, and S. Fanali. 2007.** Synthesis and evaluation of polymeric continuous bed (monolithic) reversed-phase gradient stationary phases for capillary liquid chromatography and capillary electrochromatography. *J Biochem Biophys Methods* **70**:47-55.
**Mathers, W. D. 2000.** Why the eye becomes dry: a cornea and lacrimal gland feedback model. *CLAO J* **26**:159-165.
**Matsuo, Y., and J. Yodoi. 2013.** Extracellular thioredoxin: a therapeutic tool to combat inflammation. *Cytokine Growth Factor Rev* **24**:345-353.
**Maturo, J., and E. C. Kulakowski. 1988.** Taurine Binding to the Purified Insulin-Receptor. *Biochem Pharmacol* **37**:3755-3760.
**Mazurek, S. 2012.** Pyruvate kinase M2: A key enzyme of the tumor metabolome and its medical relevance. *Biomed Res-India* **23**:133-141.
**McCabe, E., and S. Narayanan. 2009.** Advancements in anti-inflammatory therapy for dry eye syndrome. *Optometry* **80**:555-566.
**McCarty, C. A., A. K. Bansal, P. M. Livingston, Y. L. Stanislavsky, and H. R. Taylor. 1998.** The epidemiology of dry eye in Melbourne, Australia. *Ophthalmology* **105**:1114-1119.
**McCulley, J. P., and W. Shine. 1997.** A compositional based model for the tear film lipid layer. *Trans Am Ophthalmol Soc* **95**:79-88; discussion 88-93.
**McDermott, A. M. 2009.** The Role of Antimicrobial Peptides at the Ocular Surface. *Ophthal Res* **41**:60-75.
**McDonald, W. H., R. Ohi, D. T. Miyamoto, T. J. Mitchison, and J. R. Yates. 2002.** Comparison of three directly coupled HPLC MS/MS strategies for identification of proteins from complex mixtures: single-dimension LC-MS/MS, 2-phase MudPIT, and 3-phase MudPIT. *Int J Mass Spectrom* **219**:245-251.
**McGowan, R. P., F.; Kim, J. et al. 2005.** Aß42 is essential for parenchymal and vascular amyloid deposition in mice. *Neuron* **47**:191-199.

**McKenzie, R. W., J. E. Jumblatt, and M. M. Jumblatt. 2000.** Quantification of MUC2 and MUC5AC transcripts in human conjunctiva. *Invest Ophth Vis Sci* **41**:703-708.
**McMillan, D. E. 1976.** Plasma protein changes, blood viscosity, and diabetic microangiopathy. *Diabetes* **25**:858-864.
**McQueen, P., and O. Krokhin. 2012.** Optimal selection of 2D reversed-phase-reversed-phase HPLC separation techniques in bottom-up proteomics. *Expert Rev Proteomics* **9**:125-128.
**Medzihradszky, K. F., J. M. Campbell, M. A. Baldwin, A. M. Falick, P. Juhasz, M. L. Vestal, and A. L. Burlingame. 2000.** The characteristics of peptide collision-induced dissociation using a high-performance MALDI-TOF/TOF tandem mass spectrometer. *Anal Chem* **72**:552-558.
**Menke, A., and H. Jockusch. 1995.** Extent of Shock-Induced Membrane Leakage in Human and Mouse Myotubes Depends on Dystrophin. *J Cell Sci* **108**:727-733.
**Messmer, E. M. 2012.** Preservatives in ophthalmology. *Ophthalmologe* **109**:1064-1070.
**Mezhoud, K., A. L. Bauchet, S. Chateau-Joubert, D. Praseuth, A. Marie, J. C. Francois, J. J. Fontaine, J. P. Jaeg, J. P. Cravedi, S. Puiseux-Dao, and M. Edery. 2008.** Proteomic and phosphoproteomic analysis of cellular responses in medaka fish (Oryzias latipes) following oral gavage with microcystin-LR. *Toxicon* **51**:1431-1439.
**Midwinter, R. G., A. V. Peskin, M. C. Vissers, and C. C. Winterbourn. 2004.** Extracellular oxidation by taurine chloramine activates ERK via the epidermal growth factor receptor. *J Biol Chem* **279**:32205-32211.
**Mikesh, L. M., B. Ueberheide, A. Chi, J. J. Coon, J. E. P. Syka, J. Shabanowitz, and D. F. Hunt. 2006.** The utility of ETD mass spectrometry in proteomic analysis. *Bba-Proteins Proteom* **1764**:1811-1822.
**Militante, J., and J. B. Lombardini. 2004.** Age-related retinal degeneration in animal models of aging: Possible involvement of taurine deficiency and oxidative stress. *Neurochem Res* **29**:151-160.
**Miljanovic, B., R. Dana, D. A. Sullivan, and D. A. Schaumberg. 2007.** Impact of dry eye syndrome on vision-related quality of life. *Am J Ophthalmol* **143**:409-415.
**Miljanovic, B., K. A. Trivedi, M. R. Dana, J. P. Gilbard, J. E. Buring, and D. A. Schaumberg. 2005.** Relation between dietary n-3 and n-6 fatty acids and clinically diagnosed dry eye syndrome in women. *American Journal of Clinical Nutrition* **82**:887-893.
**Miljanovic, B. M., R. Dana, D. A. Sullivan, and D. A. Schaumberg. 2004.** Impact of dry eye syndrome on vision-related quality of life among women. *Invest Ophth Vis Sci* **45**:U204-U204.
**Millar, T. J., P. Mudgil, I. A. Butovich, and C. K. Palaniappan. 2009.** Adsorption of human tear lipocalin to human meibomian lipid films. *Invest Ophthalmol Vis Sci* **50**:140-151.
**Millett, F., V. Darleyusmar, and R. A. Capaldi. 1982.** Cytochrome-C Is Cross-Linked to Subunit-Ii of Cytochrome-C Oxidase by a Water-Soluble Carbodiimide. *Biochemistry* **21**:3857-3862.
**Mitsui, A., J. Hamuro, H. Nakamura, N. Kondo, Y. Hirabayashi, S. Ishizaki-Koizumi, T. Hirakawa, T. Inoue, and J. Yodoi. 2002.** Overexpression of human thioredoxin in transgenic mice controls oxidative stress and life span. *Antioxid Redox Signal* **4**:693-696.
**Mitton, K. P., H. A. Linklater, T. Dzialoszynski, S. E. Sanford, K. Starkey, and J. R. Trevithick. 1999.** Modelling cortical cataractogenesis 21: In diabetic rat lenses taurine supplementation partially reduces damage resulting from osmotic compensation leading to osmolyte loss and antioxidant depletion. *Experimental Eye Research* **69**:279-289.
**Mitulovic, G., and K. Mechtler. 2006.** HPLC techniques for proteomics analysis--a short overview of latest developments. *Brief Funct Genomic Proteomic* **5**:249-260.
**Mo, W., and B. L. Karger. 2002.** Analytical aspects of mass spectrometry and proteomics. *Curr Opin Chem Biol* **6**:666-675.
**Mollenhauer, J., S. Herbertz, B. Helmke, G. Kollender, I. Krebs, J. Madsen, U. Holmskov, K. Sorger, L. Schmitt, S. Wiemann, H. F. Otto, H. J. Grone, and A. Poustka. 2001.** Deleted in Malignant Brain Tumors 1 is a versatile mucin-like molecule likely to play a differential role in digestive tract cancer. *Cancer Research* **61**:8880-8886.

**Mollerup, J., and I. H. Lambert. 1996.** Phosphorylation is involved in the regulation of the taurine influx via the beta-system in Ehrlich ascites tumor cells. *J Membrane Biol* **150**:73-82.
**Molloy, M. P., S. Bolis, B. R. Herbert, K. Ou, M. I. Tyler, D. D. van Dyk, M. D. Willcox, A. A. Gooley, K. L. Williams, C. A. Morris, and B. J. Walsh. 1997.** Establishment of the human reflex tear two-dimensional polyacrylamide gel electrophoresis reference map: new proteins of potential diagnostic value. *Electrophoresis* **18**:2811-2815.
**Molloy, M. P., E. E. Brzezinski, J. Hang, M. T. McDowell, and R. A. VanBogelen. 2003.** Overcoming technical variation and biological variation in quantitative proteomics. *Proteomics* **3**:1912-1919.
**Molloy, M. P., B. R. Herbert, K. L. Williams, and A. A. Gooley. 1999.** Extraction of Escherichia coli proteins with organic solvents prior to two-dimensional electrophoresis. *Electrophoresis* **20**:701-704.
**Mondino, B. J., and G. W. Zaidman. 1983.** Hemolytic complement in tears. *Ophthalmic Res* **15**:208-211.
**Moritz, R. L. 2007.** Configuration, column construction, and column packing for a capillary liquid chromatography system. *CSH Protoc* **2007**:pdb prot4578.
**Moss, S. E., R. Klein, and B. E. Klein. 2000.** Prevalence of and risk factors for dry eye syndrome. *Arch Ophthalmol* **118**:1264-1268.
**Mostowy, S. 2013.** Autophagy and bacterial clearance: a not so clear picture. *Cell Microbiol* **15**:395-402.
**Mrukwa-Kominek, E., A. Rogowska-Godela, and S. Gierek-Ciaciura. 2007.** [Effect of anti-inflammatory therapy on the treatment of dry eye syndrome]. *Klin Oczna* **109**:79-84.
**Muhling, J., M. Fuchs, C. Fleck, A. Sablotzki, M. Krull, M. G. Dehne, J. Gonter, S. Weiss, J. Engel, and G. Hempelmann. 2002.** Effects of arginine, L-alanyl-L-glutamine or taurine on neutrophil (PMN) free amino acid profiles and immune functions in vitro. *Amino Acids* **22**:39-53.
**Mukherjee, A. B., Z. Zhang, and B. S. Chilton. 2008.** Uteroglobin: A steroid-inducible immunomodulatory protein that founded the secretoglobin superfamily (vol 28, pg 707, 2007). *Endocr Rev* **29**:131-131.
**Mukherjee, A. B., Z. J. Zhang, and B. S. Chilton. 2007.** Uteroglobin: a steroid-inducible immunomodulatory protein that founded the Secretoglobin superfamily. *Endocr Rev* **28**:707-725.
**Mukhopadhyay, R. 2005.** The automated union of LC and MALDI MS. *Anal Chem* **77**:150a-152a.
**Muller, C., P. Schafer, M. Stortzel, S. Vogt, and W. Weinmann. 2002.** Ion suppression effects in liquid chromatography-electrospray-ionisation transport-region collision induced dissociation mass spectrometry with different serum extraction methods for systematic toxicological analysis with mass spectra libraries. *J Chromatogr B Analyt Technol Biomed Life Sci* **773**:47-52.
**Mulvenna, I., F. Stapleton, P. G. Hains, A. Cengiz, M. Tan, B. Walsh, and B. Holden. 2000.** Low molecular weight analysis of tears using matrix assisted laser desorption ionization-time of flight mass spectrometry. *Clin Exp Ophthalmol* **28**:205-207.
**Murata, H., Y. Ihara, H. Nakamura, J. Yodoi, K. Sumikawa, and T. Kondo. 2003.** Glutaredoxin exerts an antiapoptotic effect by regulating the redox state of Akt. *J Biol Chem* **278**:50226-50233.
**Murray, K. K. 1997.** Coupling matrix-assisted laser desorption/ionization to liquid separations. *Mass Spectrometry Reviews* **16**:283-299.
**Mustafa, D. A. N., P. C. Burgers, L. J. Dekker, H. Charif, M. K. Titulaer, P. A. E. Sillevis Smitt, T. M. Luider, and J. M. Kros. 2007.** Identification of glioma neovascularization-related proteins by using MALDI-FTMS and Nano-LC fractionation to microdissected tumor vessels. *Mol Cell Proteomics* **6**:1147-1157.
**Musyimi, H. K., J. Guy, D. A. Narcisse, S. A. Soper, and K. K. Murray. 2005.** Direct coupling of polymer-based microchip electrophoresis to online MALDI-MS using a rotating ball inlet. *Electrophoresis* **26**:4703-4710.
**Musyimi, H. K., D. A. Narcisse, X. Zhang, W. Stryjewski, S. A. Soper, and K. K. Murray. 2004.** Online CE-MALDI-TOF MS using a rotating ball interface. *Anal Chem* **76**:5968-5973.

**Nagl, M., B. Teuchner, E. Pottinger, H. Ulmer, and W. Gottardi. 2000.** Tolerance of N-chlorotaurine, a new antimicrobial agent, in infectious conjunctivitis - A phase II pilot study. *Ophthalmologica* **214**:111-114.
**Najafi, L., M. Malek, A. E. Valojerdi, R. Aghili, M. E. Khamseh, A. E. Fallah, M. R. Tokhmehchi, and M. J. Behrouz. 2013.** Dry eye and its correlation to diabetes microvascular complications in people with type 2 diabetes mellitus. *J Diabetes Complications*.
**Nakamori, K., I. Koyama, T. Nakamura, M. Nemoto, T. Yoshida, M. Umeda, and K. Inoue. 1993a.** Quantitative-Evaluation of the Effectiveness of Taurine in Protecting the Ocular Surface against Oxidant. *Chem Pharm Bull* **41**:335-338.
**Nakamori, K., I. Koyama, T. Nakamura, M. Nemoto, T. Yoshida, M. Umeda, and K. Inoue. 1993b.** Quantitative evaluation of the effectiveness of taurine in protecting the ocular surface against oxidant. *Chem Pharm Bull (Tokyo)* **41**:335-338.
**Nakamura, M., T. Imanaka, and A. Sakamoto. 2012.** Diquafosol ophthalmic solution for dry eye treatment. *Adv Ther* **29**:579-589.
**Nakamura, T., T. Fujii, and A. Ichihara. 1985.** Enzyme Leakage Due to Change of Membrane-Permeability of Primary Cultured Rat Hepatocytes Treated with Various Hepatotoxins and Its Prevention by Glycyrrhizin. *Cell Biol Toxicol* **1**:285-295.
**Nakamura, T., K. Nishida, A. Dota, M. Matsuki, K. Yamanishi, and S. Kinoshita. 2001.** Elevated expression of transglutaminase 1 and keratinization-related proteins in conjunctiva in severe ocular surface disease. *Invest Ophth Vis Sci* **42**:549-556.
**Nakamura, T., M. Teshima, T. Kitahara, H. Sasaki, M. Uematsu, T. Kitaoka, M. Nakashima, K. Nishida, J. Nakamura, and S. Higuchi. 2010.** Sensitive and real-time method for evaluating corneal barrier considering tear flow. *Biol Pharm Bull* **33**:107-110.
**Nakatsukasa, M., C. Sotozono, K. Shimbo, N. Ono, H. Miyano, A. Okano, J. Hamuro, and S. Kinoshita. 2011.** Amino Acid Profiles in Human Tear Fluids Analyzed by High-Performance Liquid Chromatography and Electrospray Ionization Tandem Mass Spectrometry. *Am J Ophthalmol* **151**:799-808.
**Nandhini, A. T. A., V. Thirunavukkarasu, and C. V. Anuradha. 2005.** Taurine modifies insulin signaling enzymes in the fructose-fed insulin resistant-rats. *Diabetes Metab* **31**:337-344.
**Nandhini, T. A., and C. V. Anuradha. 2003.** Inhibition of lipid peroxidation, protein glycation and elevation of membrane ion pump activity by taurine in RBC exposed to high glucose. *Clinica Chimica Acta* **336**:129-135.
**Naoe, K., M. Nishino, T. Ohsa, M. Kawagoe, and M. Imai. 1999.** Protein extraction using sugar ester reverse micelles. *J Chem Technol Biot* **74**:221-226.
**Naoe, K., O. Ura, M. Hattori, M. Kawagoe, and M. Imai. 1998.** Protein extraction using non-ionic reverse micelles of Span 60. *Biochem Eng J* **2**:113-119.
**Nelson, J. D., H. Helms, R. Fiscella, Y. Southwell, and J. D. Hirsch. 2000.** A new look at dry eye disease and its treatment. *Adv Ther* **17**:84-93.
**Nesvizhskii, A. I. 2010.** A survey of computational methods and error rate estimation procedures for peptide and protein identification in shotgun proteomics. *Journal of Proteomics* **73**:2092-2123.
**Neubauer, H., S. E. Clare, R. Kurek, T. Fehm, D. Wallwiener, K. Sotlar, A. Nordheim, W. Wozny, G. P. Schwall, S. Poznanovic, C. Sastri, C. Hunzinger, W. Stegmann, A. Schrattenholz, and M. A. Cahill. 2006.** Breast cancer proteomics by laser capture microdissection, sample pooling, 54-cm IPG IEF, and differential iodine radioisotope detection. *Electrophoresis* **27**:1840-1852.
**Neubert, H., T. P. Bonnert, K. Rumpel, B. T. Hunt, E. S. Henle, and I. T. James. 2008.** Label-free detection of differential protein expression by LC/MALDI mass spectrometry. *J Proteome Res* **7**:2270-2279.
**Neuhauser, N., A. Michalski, J. Cox, and M. Mann. 2012.** Expert System for Computer-assisted Annotation of MS/MS Spectra. *Mol Cell Proteomics* **11**:1500-1509.
**Neuhoff, N. V., T. Kaiser, S. Wittke, R. Krebs, A. Pitt, A. Burchard, A. Sundmacher, B. Schlegelberger, W. Kolch, and H. Mischak. 2004.** Mass spectrometry for the detection of differentially expressed proteins: a comparison of surface-enhanced laser

desorption/ionization and capillary electrophoresis/mass spectrometry. *Rapid Commun Mass Sp* **18**:149-156.
**Neuhoff, V., R. Stamm, I. Pardowitz, N. Arold, W. Ehrhardt, and D. Taube. 1990.** Essential Problems in Quantification of Proteins Following Colloidal Staining with Coomassie Brilliant Blue Dyes in Polyacrylamide Gels, and Their Solution. *Electrophoresis* **11**:101-117.
**Ng, V., P. Cho, S. Mak, and A. Lee. 2000a.** Variability of tear protein levels in normal young adults: between-day variation. *Graef Arch Clin Exp* **238**:892-899.
**Ng, V., P. Cho, and C. H. To. 2000b.** Tear proteins of normal young Hong Kong Chinese. *Graef Arch Clin Exp* **238**:738-745.
**Ng, V., P. Cho, F. Wong, and Y. Chan. 2001.** Variability of tear protein levels in normal young adults: diurnal (daytime) variation. *Graef Arch Clin Exp* **239**:257-263.
**Nguyen, D. H., H. Toshida, J. Schurr, and R. W. Beuerman. 2004.** Microarray analysis of the rat lacrimal gland following the loss of parasympathetic control of secretion. *Physiol Genomics* **18**:108-118.
**Nichols, J. J., and K. B. Green-Church. 2009.** Mass Spectrometry-Based Proteomic Analyses in Contact Lens-Related Dry Eye. *Cornea* **28**:1109-1117.
**Nichols, J. J., and L. T. Sinnott. 2006.** Tear film, contact lens, and patient-related factors associated with contact lens-related dry eye. *Invest Ophth Vis Sci* **47**:1319-1328.
**Nichols, K. K., B. Yerxa, and D. J. Kellerman. 2004.** Diquafosol tetrasodium: a novel dry eye therapy. *Expert Opin Inv Drug* **13**:47-54.
**Nicodeme, E., K. L. Jeffrey, U. Schaefer, S. Beinke, S. Dewell, C. W. Chung, R. Chandwani, I. Marazzi, P. Wilson, H. Coste, J. White, J. Kirilovsky, C. M. Rice, J. M. Lora, R. K. Prinjha, K. Lee, and A. Tarakhovsky. 2010.** Suppression of inflammation by a synthetic histone mimic. *Nature* **468**:1119-1123.
**Nielsen, M. J., S. V. Petersen, C. Jacobsen, C. Oxvig, D. Rees, H. J. Moller, and S. K. Moestrup. 2006.** Haptoglobin-related protein is a high-affinity hemoglobin-binding plasma protein. *Blood* **108**:2846-2849.
**Nielsen, N. V., J. U. Prause, and J. S. Eriksen. 1981.** Lysozyme, Alpha-1-Antitrypsin and Serum-Albumin in Tear Fluid of Timolol Treated Glaucoma Patients with and without Symptoms of Dry Eyes. *Acta Ophthalmol* **59**:503-509.
**Nilsen, M. M., E. A. M. Janssen, J. P. A. Baak, O. K. Andersen, and A. Hjelle. 2011.** From SELDI-TOF MS to protein identification by on-chip elution. *J Proteomics* **74**:2995-2998.
**Ning, K., D. Fermin, and A. I. Nesvizhskii. 2010.** Computational analysis of unassigned high-quality MS/MS spectra in proteomic data sets. *Proteomics* **10**:2712-2718.
**Nishikawa, A. H., and P. Bailon. 1975.** Affinity purification methods. Nonspecific adsorption of proteins due to ionic groups in cyanogen bromide treated agarose. *Arch Biochem Biophys* **168**:576-584.
**Niu, S., W. Zhang, and B. T. Chait. 1998.** Direct comparison of infrared and ultraviolet wavelength matrix-assisted laser desorption/ionization mass spectrometry of proteins. *J Am Soc Mass Spectrom* **9**:1-7.
**Noecker, R. 2001.** Effects of common ophthalmic preservatives on ocular health. *Adv Ther* **18**:205-215.
**Noga, M., F. Sucharski, P. Suder, and J. Silberring. 2007.** A practical guide to nano-LC troubleshooting. *Journal of Separation Science* **30**:2179-2189.
**Nonaka, H., T. Tsujino, Y. Watari, N. Emoto, and M. Yokoyama. 2001.** Taurine prevents the decrease in expression and secretion of extracellular superoxide dismutase induced by homocysteine - Amelioration of homocysteine-induced endoplasmic reticulum stress by taurine. *Circulation* **104**:1165-1170.
**Nordmann, J. P., N. Auzanneau, S. Ricard, and G. Berdeaux. 2003.** Vision related quality of life and topical glaucoma treatment side effects. *Health Qual Life Outcomes* **1**:75.
**Nowack, C., and A. Wohrmann-Repenning. 2010.** The nasolacrimal duct of anuran amphibians: suggestions on its functional role in vomeronasal perception. *J Anat* **216**:510-517.
**Obrosova, I. G., and M. J. Stevens. 1999.** Effect of dietary taurine supplementation on GSH and NAD(P)-redox status, lipid peroxidation, and energy metabolism in diabetic precataractous lens. *Invest Ophthalmol Vis Sci* **40**:680-688.

**Ogawa, Y., K. Yamazaki, M. Kuwana, Y. Mashima, Y. Nakamura, S. Ishida, I. Toda, Y. Oguchi, K. Tsubota, S. Okamoto, and Y. Kawakami. 2001.** A significant role of stromal fibroblasts in rapidly progressive dry eye in patients with chronic GVHD. *Invest Ophth Vis Sci* **42**:111-119.
**Oh, C., Y. J. Choi, H. G. Kim, and D. H. Lee. 2006.** Osmosensitive gene expression of taurine transporter and cyclin C in embryonic fibroblast cells. *Adv Exp Med Biol* **583**:49-57.
**Ohlmeier, S., A. J. Kastaniotis, J. K. Hiltunen, and U. Bergmann. 2004.** The yeast mitochondrial proteome, a study of fermentative and respiratory growth. *J Biol Chem* **279**:3956-3979.
**Old, W. M., K. Meyer-Arendt, L. Aveline-Wolf, K. G. Pierce, A. Mendoza, J. R. Sevinsky, K. A. Resing, and N. G. Ahn. 2005.** Comparison of label-free methods for quantifying human proteins by shotgun proteomics. *Mol Cell Proteomics* **4**:1487-1502.
**Olsen, J. V., L. M. F. de Godoy, G. Q. Li, B. Macek, P. Mortensen, R. Pesch, A. Makarov, O. Lange, S. Horning, and M. Mann. 2005.** Parts per million mass accuracy on an orbitrap mass spectrometer via lock mass injection into a C-trap. *Mol Cell Proteomics* **4**:2010-2021.
**Olsen, J. V., B. Macek, O. Lange, A. Makarov, S. Horning, and M. Mann. 2007.** Higher-energy C-trap dissociation for peptide modification analysis. *Nat Methods* **4**:709-712.
**Olson, R. J., and G. L. White, Jr. 1990.** Preservatives in ophthalmic topical medications: a significant cause of disease. *Cornea* **9**:363-364.
**Oppenheimer, S. R., D. Mi, M. E. Sanders, and R. M. Caprioli. 2010.** Molecular analysis of tumor margins by MALDI mass spectrometry in renal carcinoma. *J Proteome Res* **9**:2182-2190.
**Oria, R., X. Alvarez-Hernandez, J. Liceaga, and J. H. Brock. 1988.** Uptake and handling of iron from transferrin, lactoferrin and immune complexes by a macrophage cell line. *Biochem J* **252**:221-225.
**Orr, H. T., A. I. Cohen, and O. H. Lowry. 1976.** The distribution of taurine in the vertebrate retina. *J Neurochem* **26**:609-611.
**Osio, A., L. Tan, S. N. Chen, R. Lombardi, S. F. Nagueh, S. Shete, R. Roberts, J. T. Willerson, and A. J. Marian. 2007.** Myozenin 2 is a novel gene for human hypertrophic cardiomyopathy. *Circulation Research* **100**:766-768.
**Ouchi, M., K. West, J. W. Crabb, S. Kinoshita, and M. Kamei. 2005.** Proteomic analysis of vitreous from diabetic macular edema. *Experimental Eye Research* **81**:176-182.
**Padmakumar, V. C., T. Libotte, W. Lu, H. Zaim, S. Abraham, A. A. Noegel, J. Gotzmann, R. Foisner, and I. karakesisoglou. 2005.** The inner nuclear membrane protein Sun1 mediates the anchorage of nesprin-2 to the nuclear envelope. *J Cell Science* **118**:3419-3430.
**Pan, C. L., G. S. Giraldo, H. Prentice, and J. Y. Wu. 2010.** Taurine protection of PC12 cells against endoplasmic reticulum stress induced by oxidative stress. *Journal of Biomedical Science* **17**.
**Pan, C. L., H. Prentice, A. L. Price, and J. Y. Wu. 2012.** Beneficial effect of taurine on hypoxia- and glutamate-induced endoplasmic reticulum stress pathways in primary neuronal culture. *Amino Acids* **43**:845-855.
**Pannebaker, C., H. L. Chandler, and J. J. Nichols. 2010.** Tear proteomics in keratoconus. *Molecular Vision* **16**:1949-1957.
**Papayannopoulos, I. A. 1995.** The Interpretation of Collision-Induced Dissociation Tandem Mass-Spectra of Peptides. *Mass Spectrometry Reviews* **14**:49-73.
**Pappin, D. J., P. Hojrup, and A. J. Bleasby. 1993.** Rapid identification of proteins by peptide-mass fingerprinting. *Curr Biol* **3**:327-332.
**Park, E., M. R. Quinn, and G. Schuller-Levis. 2000.** Taurine chloramine attenuates the hydrolytic activity of matrix metalloproteinase-9 in LPS-activated murine peritoneal macrophages. *Adv Exp Med Biol* **483**:389-398.
**Parma, A. E., A. S. Fernandez, C. G. Santisteban, R. A. Bowden, and S. I. Cerone. 1987.** Tears and Aqueous-Humor from Horses Inoculated with Leptospira Contain Antibodies Which Bind to Cornea. *Vet Immunol Immunop* **14**:181-185.
**Pasantes-Morales, H. 1982.** Taurine-calcium interactions in frog rod outer segments: taurine effects on an ATP-dependent calcium translocation process. *Vision Res* **22**:1487-1493.

**Pasantes-Morales, H., and C. Cruz. 1984.** Protective effect of taurine and zinc on peroxidation-induced damage in photoreceptor outer segments. *J Neurosci Res* **11**:303-311.
**Pasantes-Morales, H., and C. Cruz. 1985.** Taurine and hypotaurine inhibit light-induced lipid peroxidation and protect rod outer segment structure. *Brain Res* **330**:154-157.
**Pasantesmorales, H., C. E. Wright, and G. E. Gaull. 1984.** Protective Effect of Taurine, Zinc and Tocopherol on Retinol-Induced Damage in Human-Lymphoblastoid Cells. *J Nutr* **114**:2256-2261.
**Patarca, R., and M. A. Fletcher. 1995.** Effects of benzalkonium salts on eukaryotic and microbial G-protein-mediated processes and surface membranes. *Crit Rev Oncog* **6**:327-356.
**Patron, M. E., Z. Cao, L. Urim, F. T. Liu, M. H. Goldstein, and N. Panjwani. 2004.** Immunohistochemical localization of counterreceptors for galectins-3 and-7 in normal and healing corneas. *Invest Ophth Vis Sci* **45**:U556-U556.
**Patton, E. E., A. R. Willems, and M. Tyers. 1998.** Combinatorial control in ubiquitin-dependent proteolysis: don't Skp the F-box hypothesis. *Trends Genet* **14**:236-243.
**Paweletz, C. P., B. Trock, M. Pennanen, T. Tsangaris, C. Magnant, L. A. Liotta, and E. F. Petricoin. 2001.** Proteomic patterns of nipple aspirate fluids obtained by SELDI-TOF: Potential for new biomarkers to aid in the diagnosis of breast cancer. *Dis Markers* **17**:301-307.
**Peng, C. C., C. Cerretani, R. J. Braun, and C. J. Radke. 2013.** Evaporation-driven instability of the precorneal tear film. *Adv Colloid Interface Sci*.
**Peng, J., A. J. Stanley, D. Cairns, P. J. Selby, and R. E. Banks. 2009.** Using the protein chip interface with quadrupole time-of-flight mass spectrometry to directly identify peaks in SELDI profiles - initial evaluation using low molecular weight serum peaks. *Proteomics* **9**:492-498.
**Pepe, D., C. G. Elliott, T. Forbes, and D. W. Hamilton. 2014.** Detection of galectin-3 and localization of advanced glycation end products (AGE) in human chronic skin wounds. *Histol Histopathol* **29**:251-258.
**Peral, A., C. O. Dominguez-Godinez, G. Carracedo, and J. Pintor. 2008.** Therapeutic targets in dry eye syndrome. *Drug News Perspect* **21**:166-176.
**Perkins, D. N., D. J. C. Pappin, D. M. Creasy, and J. S. Cottrell. 1999.** Probability-based protein identification by searching sequence databases using mass spectrometry data. *Electrophoresis* **20**:3551-3567.
**Perretti, M., and F. D'Acquisto. 2009.** Annexin A1 and glucocorticoids as effectors of the resolution of inflammation. *Nat Rev Immunol* **9**:62-70.
**Perry, H. D., R. Solomon, E. D. Donnenfeld, A. R. Perry, J. R. Wittpenn, H. E. Greenman, and H. E. Savage. 2008.** Evaluation of topical cyclosporine for the treatment of dry eye disease. *Arch Ophthalmol* **126**:1046-1050.
**Pescosolido, N., B. Imperatrice, A. Koverech, and M. Messano. 2009.** L-carnitine and short chain ester in tears from patients with dry eye. *Optom Vis Sci* **86**:E132-138.
**Peskin, A. V., and C. C. Winterbourn. 2006.** Taurine chloramine is more selective than hypochlorous acid at targeting critical cysteines and inactivating creatine kinase and glyceraldehyde-3-phosphate dehydrogenase. *Free Radical Bio Med* **40**:45-53.
**Petricoin, E., J. Wulfkuhle, V. Espina, and L. A. Liotta. 2004.** Clinical proteomics: revolutionizing disease detection and patient tailoring therapy. *J Proteome Res* **3**:209-217.
**Petrosian, A. M., and J. E. Haroutounian. 2000.** Taurine as a universal carrier of lipid soluble vitamins: a hypothesis. *Amino Acids* **19**:409-421.
**Petznick, A., M. D. M. Evans, M. C. Madigan, Q. Garrett, and D. F. Sweeney. 2012.** A preliminary study of changes in tear film proteins in the feline eye following nictitating membrane removal. *Vet Ophthalmol* **15**:164-171.
**Petznick, A., M. D. M. Evans, M. C. Madigan, M. Markoulli, Q. Garrett, and D. F. Sweeney. 2011.** A comparison of basal and eye-flush tears for the analysis of cat tear proteins. *Acta Ophthalmol* **89**:E75-E81.
**Pfister, R. R., and N. Burstein. 1976.** The effects of ophthalmic drugs, vehicles, and preservatives on corneal epithelium: a scanning electron microscope study. *Invest Ophthalmol* **15**:246-259.

**Pflugfelder, S. C. 2003.** Anti-inflammatory therapy of dry eye. *Ocul Surf* **1**:31-36.
**Pflugfelder, S. C. 2004.** Antiinflammatory therapy for dry eye. *Am J Ophthalmol* **137**:337-342.
**Pflugfelder, S. C., R. M. Corrales, and C. S. de Paiva. 2013.** T helper cytokines in dry eye disease. *Exp Eye Res*.
**Pflugfelder, S. C., D. Jones, Z. H. Ji, A. Afonso, and D. Monroy. 1999.** Altered cytokine balance in the tear fluid and conjunctiva of patients with Sjogren's syndrome keratoconjunctivitis sicca. *Current Eye Research* **19**:201-211.
**Pieragostino, D., L. Agnifili, V. Fasanella, S. D'Aguanno, R. Mastropasqua, C. Di Ilio, P. Sacchetta, A. Urbani, and P. Del Boccio. 2013.** Shotgun proteomics reveals specific modulated protein patterns in tears of patients with primary open angle glaucoma naive to therapy. *Molecular Biosystems* **9**:1108-1116.
**Pieragostino, D., S. Bucci, L. Agnifili, V. Fasanella, S. D'Aguanno, A. Mastropasqua, M. Ciancaglini, L. Mastropasqua, C. Di Ilio, P. Sacchetta, A. Urbani, and P. Del Boccio. 2012.** Differential protein expression in tears of patients with primary open angle and pseudoexfoliative glaucoma. *Mol Biosyst* **8**:1017-1028.
**Pierson, J., J. L. Norris, H. R. Aerni, P. Svenningsson, R. M. Caprioli, and P. E. Andren. 2004.** Molecular profiling of experimental Parkinson's disease: direct analysis of peptides and proteins on brain tissue sections by MALDI mass spectrometry. *J Proteome Res* **3**:289-295.
**Pisella, P. J., F. Brignole, C. Debbasch, P. A. Lozato, C. Creuzot-Garcher, J. Bara, P. Saiag, J. M. Warnet, and C. Baudouin. 2000.** Flow cytometric analysis of conjunctival epithelium in ocular rosacea and keratoconjunctivitis sicca. *Ophthalmology* **107**:1841-1849.
**Piwowar, A. M., N. P. Lockyer, and J. C. Vickerman. 2009.** Salt Effects on Ion Formation in Desorption Mass Spectrometry: An Investigation into the Role of Alkali Chlorides on Peak Suppression in Time-of-Flight-Secondary Ion Mass Spectrometry. *Anal Chem* **81**:1040-1048.
**Plasier, B., D. R. Lloyd, G. C. Paul, C. R. Thomas, and M. Al-Rubeai. 1999.** Automatic image analysis for quantification of apoptosis in animal cell culture by annexin-V affinity assay. *J Immunol Methods* **229**:81-95.
**Pong, J. C., C. Y. Chu, K. O. Chu, T. C. Poon, S. M. Ngai, C. P. Pang, and C. C. Wang. 2010.** Identification of hemopexin in tear film. *Anal Biochem* **404**:82-85.
**Pong, J. C., C. Y. Chu, W. Y. Li, L. Y. Tang, L. Li, W. T. Lui, T. C. Poon, S. K. Rao, D. S. Lam, C. C. Wang, and C. P. Pang. 2011.** Association of hemopexin in tear film and conjunctival macrophages with vernal keratoconjunctivitis. *Arch Ophthalmol* **129**:453-461.
**Pow, D. V., R. Sullivan, P. Reye, and S. Hermanussen. 2002.** Localization of taurine transporters, taurine, and (3)H taurine accumulation in the rat retina, pituitary, and brain. *Glia* **37**:153-168.
**Pratt, J. M., J. Petty, I. Riba-Garcia, D. H. L. Robertson, S. J. Gaskell, S. G. Oliver, and R. J. Beynon. 2002.** Dynamics of protein turnover, a missing dimension in proteomics. *Mol Cell Proteomics* **1**:579-591.
**Preisler, J., F. Foret, and B. L. Karger. 1998.** On-line MALDI-TOF MS using a continuous vacuum deposition interface. *Anal Chem* **70**:5278-5287.
**Profrock, D. 2010.** Hyphenation of capillary-LC with ICP-MS and parallel on-line micro fraction collection for MALDI-TOF-TOF analysis-complementary tools for protein phosphorylation analysis. *J Anal Atom Spectrom* **25**:334-344.
**Qiu, J., H. Q. Gao, B. Y. Li, and L. Shen. 2008.** Proteomics investigation of protein expression changes in ouabain induced apoptosis in human umbilical vein endothelial cells. *J Cell Biochem* **104**:1054-1064.
**Qu, X. D., and R. I. Lehrer. 1998.** Secretory phospholipase A(2) is the principal bactericide for staphylococci and other gram-positive bacteria in human tears. *Infection and Immunity* **66**:2791-2797.
**Rajan, R. S., K. Tsumoto, M. Tokunaga, H. Tokunaga, Y. Kita, and T. Arakawa. 2011.** Chemical and pharmacological chaperones: application for recombinant protein production and protein folding diseases. *Curr Med Chem* **18**:1-15.
**Ramamoorthy, S., M. A. Delmonte, F. H. Leibach, and V. Ganapathy. 1994.** Molecular Identity and Calmodulin-Mediated Regulation of the Taurine Transporter in a Human Retinal-Pigment Epithelial-Cell Line. *Current Eye Research* **13**:523-529.

**Ramselaar, J. A., J. P. Boot, N. J. van Haeringen, J. A. van Best, and J. A. Oosterhuis. 1988.** Corneal epithelial permeability after instillation of ophthalmic solutions containing local anaesthetics and preservatives. *Curr Eye Res* **7**:947-950.
**Rashid, S., Y. Jin, T. Ecoiffier, S. Barabino, D. A. Schaumberg, and M. R. Dana. 2008.** Topical omega-3 and omega-6 fatty acids for treatment of dry eye. *Arch Ophthalmol* **126**:219-225.
**Rassin, D. K., J. A. Sturman, K. C. Hayes, and G. E. Gaull. 1978.** Taurine deficiency in the kitten subcellular distribution of taurine and [35S]taurine in brain. *Neurochem Res* **3**:401-410.
**Rattan, S. I. S. 1996.** Synthesis, modifications, and turnover of proteins during aging. *Exp Gerontol* **31**:33-47.
**Razzaque, M. S., C. S. Foster, and A. R. Ahmed. 2004.** Role of macrophage migration inhibitory factor in conjunctival pathology in ocular cicatricial pemphigoid. *Invest Ophthalmol Vis Sci* **45**:1174-1181.
**Reddy, D. V. 1967.** Distribution of free amino acids and related compounds in ocular fluids, lens, and plasma of various mammalian species. *Invest Ophthalmol* **6**:478-483.
**Reddy, V. N. 1970.** Studies on Intraocular Transport of Taurine .2. Accumulation in Rabbit Lens. *Invest Ophth Visual* **9**:206-&.
**Redl, B. 2000.** Human tear lipocalin. *Biochim Biophys Acta* **1482**:241-248.
**Redl, B., P. Merschak, B. Abt, and P. Wojnar. 1999.** Phage display reveals a novel interaction of human tear lipocalin and thioredoxin which is relevant for ligand binding. *FEBS Lett* **460**:182-186.
**Redmond, H. P., P. P. Stapleton, P. Neary, and D. Bouchier-Hayes. 1998.** Immunonutrition: the role of taurine. *Nutrition* **14**:599-604.
**Rehm, H. 2006.** Der Experimentator: Proteinbiochemie/Proteomics. *Elsevier GmbH, Spektrum Akademischer Verlag, München, Germany* **5th Edition**.
**Rehorek, S. J., E. J. Legenzoff, K. Carmody, T. D. Smith, and J. C. Sedlmayr. 2005.** Alligator tears: A reevaluation of the lacrimal apparatus of the crocodilians. *J Morphol* **266**:298-308.
**Reid, G. E., and S. A. McLuckey. 2002.** 'Top down' protein characterization via tandem mass spectrometry. *J Mass Spectrom* **37**:663-675.
**Rejtar, T., P. Hu, P. Juhasz, J. M. Campbell, M. L. Vestal, J. Preisler, and B. L. Karger. 2002.** Off-line coupling of high-resolution capillary electrophoresis to MALDI-TOF and TOF/TOF MS. *J Proteome Res* **1**:171-179.
**Remane, D., M. R. Meyer, D. K. Wissenbach, and H. H. Maurer. 2010a.** Ion suppression and enhancement effects of co-eluting analytes in multi-analyte approaches: systematic investigation using ultra-high-performance liquid chromatography/mass spectrometry with atmospheric-pressure chemical ionization or electrospray ionization. *Rapid Commun Mass Spectrom* **24**:3103-3108.
**Remane, D., M. R. Meyer, D. K. Wissenbach, and H. H. Maurer. 2010b.** Ion suppression and enhancement effects of co-eluting analytes in multi-analyte approaches: systematic investigation using ultra-high-performance liquid chromatography/mass spectrometry with atmosphericpressure chemical ionization or electrospray ionization. *Rapid Commun Mass Sp* **24**:3103-3108.
**Reutelingsperger, C. P., and W. L. van Heerde. 1997.** Annexin V, the regulator of phosphatidylserine-catalyzed inflammation and coagulation during apoptosis. *Cell Mol Life Sci* **53**:527-532.
**Reymond, I., K. Almarghini, and M. Tappaz. 1996.** Immunocytochemical localization of cysteine sulfinate decarboxylase in astrocytes in the cerebellum and hippocampus: A quantitative double immunofluorescence study with glial fibrillary acidic protein and S-100 protein. *Neuroscience* **75**:619-633.
**Rifai, N., M. A. Gillette, and S. A. Carr. 2006.** Protein biomarker discovery and validation: the long and uncertain path to clinical utility. *Nature Biotechnology* **24**:971-983.
**Ripps, H., and W. Shen. 2012.** Review: Taurine: A "very essential" amino acid. *Molecular Vision* **18**:2673-2686.
**Rocha, E. M., F. Mantelli, L. F. Nominato, and S. Bonini. 2013.** Hormones and dry eye syndrome: an update on what we do and don't know. *Curr Opin Ophthalmol* **24**:348-355.

**Rodriguez-Martinez, E., C. Rugerio-Vargas, A. I. Rodriguez, G. Borgonio-Perez, and S. Rivas-Arancibia. 2004.** Antioxidant effects of taurine, vitamin C, and vitamin E on oxidative damage in hippocampus caused by the administration of 3-nitropropionic acid in rats. *Int J Neurosci* **114**:1133-1145.
**Roedl, J. B., S. Bleich, U. Reulbach, R. Rejdak, J. Kornhuber, F. E. Kruse, U. Schlotzer-Schrehardt, and A. G. Junemann. 2007.** Homocysteine in tear fluid of patients with pseudoexfoliation glaucoma. *J Glaucoma* **16**:234-239.
**Roedl, J. B., S. Bleich, U. Schlotzer-Schrehardt, N. von Ahsen, J. Kornhuber, G. O. H. Naumann, F. E. Kruse, and A. G. M. Junemann. 2008.** Increased homocysteine levels in tear fluid of patients with primary open-angle glaucoma. *Ophthal Res* **40**:249-256.
**Rogatsky, E., G. Cruikshank, and D. T. Stein. 2009.** Reduction in delay time of high-dwell volume pumps in LC-MS applications using short-term low-ratio split flow. *J Sep Sci* **32**:321-327.
**Rogers, R., M. Dharsee, S. Ackloo, and J. G. Flanagan. 2012.** Proteomics analyses of activated human optic nerve head lamina cribrosa cells following biomechanical strain. *Invest Ophthalmol Vis Sci* **53**:3806-3816.
**Rohner, T. C. S., D.; Stockli, M. 2005.** MALDI mass spectrometric imaging of biological tissue sections. *Mech Ageing Dev* **126**:177-185.
**Rolando, M., and M. Zierhut. 2001.** The ocular surface and tear film and their dysfunction in dry eye disease. *Survey of Ophthalmology* **45**:S203-S210.
**Rosenfeld, J., J. Capdevielle, J. C. Guillemot, and P. Ferrara. 1992.** In-gel digestion of proteins for internal sequence analysis after one- or two-dimensional gel electrophoresis. *Anal Biochem* **203**:173-179.
**Rosenfeld, J. M., R. Vargas, W. Xie, and R. M. Evans. 2003.** Genetic profiling defines the xenobiotic gene network controlled by the nuclear receptor pregnane X receptor. *Mol Endocrinol* **17**:1268-1282.
**Rowan, M. J., S. Bulley, L. A. Purpura, H. Ripps, and W. Shen. 2013.** Taurine regulation of voltage-gated channels in retinal neurons. *Adv Exp Med Biol* **775**:85-99.
**Rozing, G. 2003.** Trends in HPLC column formats - Microbore, nanobore and smaller. *Lc Gc Eur* **16**:14-19.
**Rozing, G., E. Nagele, P. Horth, M. Vollmer, R. Moritz, B. Glatz, and A. Gratzfeld-Husgen. 2004.** Instrumentation for advanced microseparations in pharmaceutical analysis and proteomics. *J Biochem Biophys Methods* **60**:233-263.
**Saad, S. Y., and A. C. Al-Rikabi. 2002.** Protection effects of Taurine supplementation against cisplatin-induced nephrotoxicity in rats. *Chemotherapy* **48**:42-48.
**Sack, R. A., B. I. Bogart, A. Beaton, S. Sathe, and G. Lew. 1997.** Diurnal variations in tear glycoproteins: evidence for an epithelial origin for the major non-reducible > or = 450 kDa sialoglycoprotein(s). *Curr Eye Res* **16**:577-588.
**Sack, R. A., I. Nunes, A. Beaton, and C. Morris. 2001.** Host-defense mechanism of the ocular surfaces. *Bioscience Rep* **21**:463-480.
**Sack, R. A., K. O. Tan, and A. Tan. 1992.** Diurnal tear cycle: evidence for a nocturnal inflammatory constitutive tear fluid. *Invest Ophthalmol Vis Sci* **33**:626-640.
**Sanders, M. E., E. C. Dias, B. J. Xu, J. A. Mobley, D. Billheimer, H. Roder, J. Grigorieva, M. Dowsett, C. L. Arteaga, and R. M. Caprioli. 2008.** Differentiating proteomic biomarkers in breast cancer by laser capture microdissection and MALDI MS. *J Proteome Res* **7**:1500-1507.
**Saratsis, A. M., S. Yadavilli, S. Magge, B. R. Rood, J. Perez, D. A. Hill, E. Hwang, L. Kilburn, R. J. Packer, and J. Nazarian. 2012.** Insights into pediatric diffuse intrinsic pontine glioma through proteomic analysis of cerebrospinal fluid. *Neuro Oncol* **14**:547-560.
**Sariri, R., and H. Ghafoori. 2008.** Tear proteins in health, disease, and contact lens wear. *Biochemistry-Moscow+* **73**:381-392.
**Sarter, K. 2010.** The Role of Galectins in Clearance and Immunogenicity of Apoptotic and Secondary Necrotic Cells. *Dissertation: Friedrich-Alexander-Universität Erlangen-Nürnberg*.
**Saso, L., M. G. Leone, M. Y. Mo, E. Grippa, C. Y. Cheng, and B. Silvestrini. 1999.** Differential changes in alpha2-macroglobulin and hemopexin in brain and liver in response to acute inflammation. *Biochemistry (Mosc)* **64**:839-844.

**Savitzky, A., and M. J. E. Golay. 1964.** Smoothing + Differentiation of Data by Simplified Least Squares Procedures. *Anal Chem* **36**:1627-&.
**Scaffidi, P., T. Misteli, and M. E. Bianchi. 2002.** Release of chromatin protein HMGB1 by necrotic cells triggers inflammation. *Nature* **418**:191-195.
**Scalf, M., M. S. Westphall, and L. M. Smith. 2000.** Charge reduction electrospray mass spectrometry. *Anal Chem* **72**:52-60.
**Schaffer, S., K. Takahashi, and J. Azuma. 2000.** Role of osmoregulation in the actions of taurine. *Amino Acids* **19**:527-546.
**Schagger, H., and G. von Jagow. 1987.** Tricine-sodium dodecyl sulfate-polyacrylamide gel electrophoresis for the separation of proteins in the range from 1 to 100 kDa. *Anal Biochem* **166**:368-379.
**Schaumberg, D. A., D. A. Sullivan, J. E. Buring, and M. R. Dana. 2003.** Prevalence of dry eye syndrome among US women. *Am J Ophthalmol* **136**:318-326.
**Scheltema, R. A., A. Kamleh, D. Wildridge, C. Ebikeme, D. G. Watson, M. R. Barrett, R. C. Jansen, and R. Breitling. 2008.** Increasing the mass accuracy of high-resolution LC-MS data using background ions - a case study on the LTQ-Orbitrap. *Proteomics* **8**:4647-4656.
**Schiffman, R. M. 2001.** Reliability and validity of a proposed dry eye evaluation scheme - Reply. *Arch Ophthalmol-Chic* **119**:456-456.
**Schiller, J., R. Suss, B. Fuchs, M. Muller, O. Zschornig, and K. Arnold. 2007.** MALDI-TOF MS in lipidomics. *Front Biosci* **12**:2568-2579.
**Schlosser, A., and W. D. Lehmann. 2000.** Special feature: Commentary - Five-membered ring formation in unimolecular reactions of peptides: a key structural element controlling low-energy collision-induced dissociation of peptides. *Journal of Mass Spectrometry* **35**:1382-1390.
**Schlote, T., G. Kadner, and N. Freudenthaler. 2004.** Marked reduction and distinct patterns of eye blinking in patients with moderately dry eyes during video display terminal use. *Graef Arch Clin Exp* **242**:306-312.
**Schlotzer-Schrehardt, U., S. Andre, C. Janko, H. Kaltner, J. Kopitz, H. J. Gabius, and M. Herrmann. 2012.** Adhesion/growth-regulatory galectins in the human eye: localization profiles and tissue reactivities as a standard to detect disease-associated alterations. *Graef Arch Clin Exp* **250**:1169-1180.
**Schmelz, M., and W. W. Franke. 1993.** Complexus Adhaerentes, a New Group of Desmoplakin-Containing Junctions in Endothelial-Cells - the Syndesmos Connecting Retothelial Cells of Lymph-Nodes. *Eur J Cell Biol* **61**:274-289.
**Schmidtnielsen, K., and R. Fange. 1958.** Salt Glands in Marine Reptiles. *Nature* **182**:783-785.
**Schoenwald, R. D., S. Vidvauns, D. E. Wurster, and C. F. Barfknecht. 1997.** Tear film stability of protein extracts from dry eye patients administered a sigma agonist. *J Ocul Pharmacol Ther* **13**:151-161.
**Schuller-Levis, G. B., and E. Park. 2003.** Taurine: new implications for an old amino acid. *Fems Microbiol Lett* **226**:195-202.
**Schuller-Levis, G. B., and E. Park. 2004.** Taurine and its chloramine: Modulators of immunity. *Neurochem Res* **29**:117-126.
**Scigelova, M., and A. Makarov. 2006.** Orbitrap mass analyzer--overview and applications in proteomics. *Proteomics* **6 Suppl 2**:16-21.
**Sebring, L. A., and R. J. Huxtable. 1986.** Low Affinity Binding of Taurine to Phospholiposomes and Cardiac Sarcolemma. *Biochimica Et Biophysica Acta* **884**:559-566.
**Seibert, V., A. Wiesner, T. Buschmann, and J. Meuer. 2004.** Surface-enhanced laser desorption ionization time-of-flight mass spectrometry (SELDI TOF-MS) and ProteinChip technology in proteomics research. *Pathol Res Pract* **200**:83-94.
**Seibold, L. K., D. A. Ammar, and M. Y. Kahook. 2013.** Acute effects of glaucoma medications and benzalkonium chloride on pre-adipocyte proliferation and adipocyte cytotoxicity in vitro. *Curr Eye Res* **38**:70-74.
**Seidler, J., N. Zinn, M. E. Boehm, and W. D. Lehmann. 2010.** De novo sequencing of peptides by MS/MS. *Proteomics* **10**:634-649.

**Seifart, U., and I. Strempel. 1994.** [The dry eye and diabetes mellitus]. *Ophthalmologe* **91**:235-239.
**Seifert, G. J., D. Lawson, and G. Wiche. 1992.** Immunolocalization of the Intermediate Filament-Associated Protein Plectin at Focal Contacts and Actin Stress Fibers. *Eur J Cell Biol* **59**:138-147.
**Sekiyama, E., Y. Matsuyama, D. Higo, T. Nirasawa, M. Ikegawa, S. Kinoshita, and K. Tashiro. 2008.** Applying magnetic bead separation/MALDI-TOF mass spectrometry to human tear fluid proteome analysis. *J Proteom Bioinform* **1**:368-373.
**Selber, K., F. Tjerneld, A. Collen, T. Hyytia, T. Nakari-Setala, M. Bailey, R. Fagerstrom, J. Kan, J. van der Laan, M. Penttila, and M. R. Kula. 2004.** Large-scale separation and production of engineered proteins, designed for facilitated recovery in detergent-based aqueous two-phase extraction systems. *Process Biochem* **39**:889-896.
**Selinger, D. S., R. C. Selinger, and W. P. Reed. 1979.** Resistance to Infection of the External Eye - Role of Tears. *Survey of Ophthalmology* **24**:33-38.
**Sener, G., A. O. Sehirli, Y. Ipci, S. Cetinel, E. Cikler, N. Gedik, and I. Alican. 2005.** Taurine treatment protects against chronic nicotine-induced oxidative changes. *Fund Clin Pharmacol* **19**:155-164.
**Shamsi, F. A., Z. Chen, J. Liang, K. Li, A. A. Al-Rajhi, I. A. Chaudhry, M. Li, and K. Wu. 2011.** Analysis and comparison of proteomic profiles of tear fluid from human, cow, sheep, and camel eyes. *Invest Ophthalmol Vis Sci* **52**:9156-9165.
**Shearer, D., W. Ens, K. Standing, and G. Valdimarsson. 2008.** Posttranslational modifications in lens fiber connexins identified by off-line-HPLC MALDI-quadrupole time-of-flight mass spectrometry. *Invest Ophthalmol Vis Sci* **49**:1553-1562.
**Shen, H. L., G. Cheng, H. Z. Fan, J. Zhang, X. M. Zhang, H. J. Lu, C. L. Liu, F. X. Sun, H. Jin, X. J. Xu, G. B. Xu, S. Wang, C. Y. Fang, H. M. Bao, Y. Wang, J. Wang, H. Zhong, Z. I. Yu, Y. K. Liu, Z. Y. Tang, and P. Y. Yang. 2006.** Expressed proteome analysis of human hepatocellular carcinoma in nude mice (LCI-D20) with high metastasis potential. *Proteomics* **6**:528-537.
**Shevchenko, A., H. Tomas, J. Havlis, J. V. Olsen, and M. Mann. 2006.** In-gel digestion for mass spectrometric characterization of proteins and proteomes. *Nat Protoc* **1**:2856-2860.
**Shibata, E., H. Nanri, K. Ejima, M. Araki, J. Fukuda, K. Yoshimura, N. Toki, M. Ikeda, and M. Kashimura. 2003.** Enhancement of mitochondrial oxidative stress and up-regulation of antioxidant protein peroxiredoxin III/SP-22 in the mitochondria of human pre-eclamptic placentae. *Placenta* **24**:698-705.
**Shine, W. E., and J. P. McCulley. 2003.** Polar lipids in human meibomian gland secretions. *Curr Eye Res* **26**:89-94.
**Shioda, R., P. S. Reinach, T. Hisatsune, and Y. Miyamoto. 2002.** Osmosensitive taurine transporter expression and activity in human corneal epithelial cells. *Invest Ophthalmol Vis Sci* **43**:2916-2922.
**Sideri, T. C., K. Stojanovski, M. F. Tuite, and C. M. Grant. 2010.** Ribosome-associated peroxiredoxins suppress oxidative stress-induced de novo formation of the [PSI+] prion in yeast. *Proc Natl Acad Sci U S A* **107**:6394-6399.
**Silverman, G. A., P. I. Bird, R. W. Carrell, F. C. Church, P. B. Coughlin, P. G. Gettins, J. A. Irving, D. A. Lomas, C. J. Luke, R. W. Moyer, P. A. Pemberton, E. Remold-O'Donnell, G. S. Salvesen, J. Travis, and J. C. Whisstock. 2001.** The serpins are an expanding superfamily of structurally similar but functionally diverse proteins. Evolution, mechanism of inhibition, novel functions, and a revised nomenclature. *J Biol Chem* **276**:33293-33296.
**Silverman, J. D., and L. Kruger. 1989.** Calcitonin-Gene-Related-Peptide-Immunoreactive Innervation of the Rat Head with Emphasis on Specialized Sensory Structures. *J Comp Neurol* **280**:303-330.
**Simon, S. A., L. J. Liu, and R. P. Erickson. 2003.** Neuropeptides modulate rat chorda tympani responses. *Am J Physiol-Reg I* **284**:R1494-R1505.
**Sindt, C. W., and G. N. Foulks. 2013.** Efficacy of an artificial tear emulsion in patients with dry eye associated with meibomian gland dysfunction. *Clin Ophthalmol* **7**:1713-1722.

**Sjodahl, J., M. Kempka, K. Hermansson, A. Thorsen, and J. Roeraade. 2005.** Chip with twin anchors for reduced ion suppression and improved mass accuracy in MALDI-TOF mass spectrometry. *Anal Chem* **77**:827-832.
**Skalicky, S. E., C. Petsoglou, A. Gurbaxani, C. L. Fraser, and P. McCluskey. 2013.** New agents for treating dry eye syndrome. *Curr Allergy Asthma Rep* **13**:322-328.
**Skofitsch, G., and D. M. Jacobowitz. 1985.** Quantitative distribution of calcitonin gene-related peptide in the rat central nervous system. *Peptides* **6**:1069-1073.
**Smith, K. E., L. A. Borden, C. H. Wang, P. R. Hartig, T. A. Branchek, and R. L. Weinshank. 1992.** Cloning and expression of a high affinity taurine transporter from rat brain. *Mol Pharmacol* **42**:563-569.
**Solomon, A., D. Dursun, Z. G. Liu, Y. H. Xie, A. Macri, and S. C. Pflugfelder. 2001.** Pro- and anti-inflammatory forms of interleukin-1 in the tear fluid and conjunctiva of patients with dry-eye disease. *Invest Ophth Vis Sci* **42**:2283-2292.
**Son, H. Y., H. Kim, and H. K. Y. 2007.** Taurine prevents oxidative damage of high glucose-induced cataractogenesis in isolated rat lenses. *J Nutr Sci Vitaminol (Tokyo)* **53**:324-330.
**Soria, J., J. A. Duran, J. Etxebarria, J. Merayo, N. Gonzalez, R. Reigada, I. Garcia, A. Acera, and T. Suarez. 2013.** Tear proteome and protein network analyses reveal a novel pentamarker panel for tear film characterization in dry eye and meibomian gland dysfunction. *J Proteomics* **78**:94-112.
**Soskic, V., K. Groebe, and A. Schrattenholz. 2008.** Nonenzymatic posttranslational protein modifications in ageing. *Exp Gerontol* **43**:247-257.
**Sosne, G., S. Hafeez, A. L. Greenberry, 2nd, and M. Kurpakus-Wheater. 2002.** Thymosin beta4 promotes human conjunctival epithelial cell migration. *Curr Eye Res* **24**:268-273.
**Sosne, G., P. Qiu, G. W. Ousler, S. P. Dunn, and D. Crockford. 2012.** Thymosin beta 4: a potential novel dry eye therapy. *Thymosins in Health and Disease Ii* **1270**:45-50.
**Sotozono, C., S. Ermis, K. Yamasaki, H. Nakamura, J. Yodoi, and S. Kinoshita. 2005.** Thioredoxin in human tears. *Invest Ophth Vis Sci* **46**.
**Spazierer, D., P. Fuchs, S. Reipert, I. Fischer, M. Schmuth, H. Lassmann, and G. Wiche. 2006.** Epiplakin is dispensable for skin barrier function and for integrity of keratin network cytoarchitecture in simple and stratified epithelia. *Mol Cell Biol* **26**:559-568.
**Spurr-Michaud, S., P. Argueso, and I. Gipson. 2007.** Assay of mucins in human tear fluid. *Experimental Eye Research* **84**:939-950.
**Srinivasan, S., M. Thangavelu, L. Zhang, K. B. Green, and K. K. Nichols. 2012.** iTRAQ Quantitative Proteomics in the Analysis of Tears in Dry Eye Patients. *Invest Ophthalmol Vis Sci* **53**:5052-5059.
**Stapels, M. D., and D. F. Barofsky. 2004.** Complementary use of MALDI and ESI for the HPLC-MS/MS analysis of DNA-binding proteins. *Anal Chem* **76**:5423-5430.
**Stapels, M. D., J. C. Cho, S. J. Giovannoni, and D. F. Barofsky. 2004.** Proteomic analysis of novel marine bacteria using MALDI and ESI mass spectrometry. *J Biomol Tech* **15**:191-198.
**Stasyk, T., and L. A. Huber. 2004.** Zooming in: fractionation strategies in proteomics. *Proteomics* **4**:3704-3716.
**Stern, M. E., R. W. Beuerman, R. I. Fox, J. P. Gao, A. K. Mircheff, and S. C. Pflugfelder. 1998.** The pathology of dry eye: The interaction between the ocular surface and lacrimal glands. *Cornea* **17**:584-589.
**Stern, M. E., J. Gao, K. F. Siemasko, R. W. Beuerman, and S. C. Pflugfelder. 2004.** The role of the lacrimal functional unit in the pathophysiology of dry eye. *Exp Eye Res* **78**:409-416.
**Steven, P., and C. Cursiefen. 2013.** Glaucoma and dry eye : Current concepts and future perspectives. *Ophthalmologe*.
**Stevenson, T. I., and J. A. Loo. 1998.** A simple off-line sample spotter for coupling HPLC with MALDI MS. *Lc Gc-Mag Sep Sci* **16**:54-+.
**Stewart, W. C., J. A. Stewart, and L. A. Nelson. 2011.** Ocular surface disease in patients with ocular hypertension and glaucoma. *Curr Eye Res* **36**:391-398.

**Stoeckelhuber, M., E. M. Messmer, C. Schmidt, F. Xiao, C. Schubert, and J. Klug. 2006.** Immunohistochemical analysis of secretoglobin SCGB 2A1 expression in human ocular glands and tissues. *Histochem Cell Biol* **126**:103-109.
**Stoka, V., M. Nycander, B. Lenarcic, C. Labriola, J. J. Cazzulo, I. Bjork, and V. Turk. 1995.** Inhibition of cruzipain, the major cysteine proteinase of the protozoan parasite, Trypanosoma cruzi, by proteinase inhibitors of the cystatin superfamily. *FEBS Lett* **370**:101-104.
**Streckfus, C. F., L. R. Bigler, and M. Zwick. 2006.** The use of surface-enhanced laser desorption/ionization time-of-flight mass spectrometry to detect putative breast cancer markers in saliva: a feasibility study. *J Oral Pathol Med* **35**:292-300.
**Street, T. O., D. W. Bolen, and G. D. Rose. 2006.** A molecular mechanism for osmolyte-induced protein stability (vol 103, pg 13997, 2006). *P Natl Acad Sci USA* **103**:17064-17064.
**Strimbu, K., and J. A. Tavel. 2010.** What are biomarkers? *Curr Opin Hiv Aids* **5**:463-466.
**Sturman, J. A., D. K. Rassin, K. C. Hayes, and G. E. Gaull. 1978.** Taurine deficiency in the kitten: exchange and turnover of [35S] taurine in brain, retina, and other tissues. *J Nutr* **108**:1462-1476.
**Suckau, D., A. Resemann, M. Schuerenberg, P. Hufnagel, J. Franzen, and A. Holle. 2003.** A novel MALDI LIFT-TOF/TOF mass spectrometer for proteomics. *Anal Bioanal Chem* **376**:952-965.
**Sudo, T., and H. Hidaka. 1998.** Regulation of calcyclin (S100A6) binding by alternative splicing in the N-terminal regulatory domain of annexin XI isoforms. *Journal of Biological Chemistry* **273**:6351-6357.
**Sugano, E. M., N.; Takahashi, M.; Tabata, K.; Tamai, M.; Tomita; H. 2013.** Essential Role of Thioredoxin 2 in Mitigating Oxidative Stress in Retinal Epithelial Cells. *Journal of Ophthalmology* **2013**:1-7.
**Sullivan, D. A. 2004.** Tearful relationships? Sex, hormones, the lacrimal gland, and aqueous-deficient dry eye. *Ocul Surf* **2**:92-123.
**Sullivan, D. A., K. J. Bloch, and M. R. Allansmith. 1984.** Hormonal influence on the secretory immune system of the eye: androgen control of secretory component production by the rat exorbital gland. *Immunology* **52**:239-246.
**Sullivan, D. A., and L. E. Hann. 1989.** Hormonal influence on the secretory immune system of the eye: endocrine impact on the lacrimal gland accumulation and secretion of IgA and IgG. *J Steroid Biochem* **34**:253-262.
**Sullivan, D. A., B. D. Sullivan, J. E. Evans, F. Schirra, H. Yamagami, M. Liu, S. M. Richards, T. Suzuki, D. A. Schaumberg, R. M. Sullivan, and M. R. Dana. 2002.** Androgen deficiency, meibomian gland dysfunction, and evaporative dry eye. *Neuroendocrine Immune Basis of the Rheumatic Diseases Ii, Proceedings* **966**:211-222.
**Sun, M., and C. Xu. 2008.** Neuroprotective mechanism of taurine due to up-regulating calpastatin and down-regulating calpain and caspase-3 during focal cerebral ischemia. *Cellular and Molecular Neurobiology* **28**:593-611.
**Sun, M., Y. Zhao, Y. Gu, and Y. Zhang. 2013.** Protective effects of taurine against closed head injury in rats. *J Neurotrauma*.
**Sweeney, D. F., T. J. Millar, and S. R. Raju. 2013.** Tear film stability: A review. *Exp Eye Res*.
**Syka, J. E. P., J. J. Coon, M. J. Schroeder, J. Shabanowitz, and D. F. Hunt. 2004.** Peptide and protein sequence analysis by electron transfer dissociation mass spectrometry. *P Natl Acad Sci USA* **101**:9528-9533.
**Szwergold, B. S. 2005.** Intrinsic toxicity of glucose, due to non-enzymatic glycation, is controlled in-vivo by deglycation systems including: FN3K-mediated deglycation of fructosamines and transglycation of aldosamines. *Med Hypotheses* **65**:337-348.
**Szwergold, B. S. 2006.** alpha-Thiolamines such as cysteine and cysteamine act as effective transglycating agents due to formation of irreversible thiazolidine derivatives. *Med Hypotheses* **66**:698-707.
**Tabb, D. L., L. Vega-Montoto, P. A. Rudnick, A. M. Variyath, A. J. Ham, D. M. Bunk, L. E. Kilpatrick, D. D. Billheimer, R. K. Blackman, H. L. Cardasis, S. A. Carr, K. R. Clauser, J. D. Jaffe, K. A. Kowalski, T. A. Neubert, F. E. Regnier, B. Schilling, T. J. Tegeler, M.**

**Wang, P. Wang, J. R. Whiteaker, L. J. Zimmerman, S. J. Fisher, B. W. Gibson, C. R. Kinsinger, M. Mesri, H. Rodriguez, S. E. Stein, P. Tempst, A. G. Paulovich, D. C. Liebler, and C. Spiegelman. 2010.** Repeatability and reproducibility in proteomic identifications by liquid chromatography-tandem mass spectrometry. *J Proteome Res* **9**:761-776.

**Takada, F., D. L. Vander Woude, H. Q. Tong, T. G. Thompson, S. C. Watkins, L. M. Kunkel, and A. H. Beggs. 2001.** Myozenin: an alpha-actinin- and gamma-filamin-binding protein of skeletal muscle Z lines. *Proc Natl Acad Sci U S A* **98**:1595-1600.

**Takagi, Y., T. Nakajima, A. Shimazaki, M. Kageyama, T. Matsugi, Y. Matsumura, B. T. Gabelt, P. L. Kaufman, and H. Hara. 2004.** Pharmacological characteristics of AFP-168 (tafluprost), a new prostanoid FP receptor agonist, as an ocular hypotensive drug. *Exp Eye Res* **78**:767-776.

**Takatani, T., K. Takahashi, Y. Uozumi, E. Shikata, Y. Yamamoto, T. Ito, T. Matsuda, S. W. Schaffer, Y. Fujio, and J. Azuma. 2004.** Taurine inhibits apoptosis by preventing formation of the Apaf-1/caspase-9 apoptosome. *Am J Physiol-Cell Ph* **287**:C949-C953.

**Tamada, M., M. Suematsu, and H. Saya. 2012.** Pyruvate Kinase M2: Multiple Faces for Conferring Benefits on Cancer Cells. *Clin Cancer Res* **18**:5554-5561.

**Tanaka, K., H. Waki, y. Ido, S. Akita, Y. Yoshida, and T. Yoshida. 1988.** Protein and polymer analyses up to m/z 100000 by laser ionization time-of-flight mass spectrometry. *Rapid Commun Mass Spectrom* **2**:151-153.

**Tang, N., P. Tornatore, and S. R. Weinberger. 2004.** Current developments in SELDI affinity technology. *Mass Spectrometry Reviews* **23**:34-44.

**Tarpley, R. J., and S. H. Ridgway. 1991.** Orbital Gland Structure and Secretions in the Atlantic Bottle-Nosed-Dolphin (Tursiops-Truncatus). *J Morphol* **207**:173-184.

**Tau, J., Novaes, P.; Matsuda, M.; Saldiva, P. H. N.; Berra, A. 2012.** Diesel Exhaust Particles selectively induce both proinflamatories cytokines and mucins production in Cornea and Conjunctiva Human Cell Lines. *Fort Lauderdale, USA: ARVO Translational Research Annual Meeting 2012* **Program # 2319 Poster # A336**.

**Tavender, T. J., and N. J. Bulleid. 2010.** Peroxiredoxin IV protects cells from oxidative stress by removing H2O2 produced during disulphide formation. *J Cell Sci* **123**:2672-2679.

**Tesseraud, S., S. Metayer-Coustard, A. Collin, and I. Seiliez. 2009.** Role of sulfur amino acids in controlling nutrient metabolism and cell functions: implications for nutrition. *Brit J Nutr* **101**:1132-1139.

**Teuchner, B., M. Nagl, A. Schidlbauer, H. Ishiko, E. Dragosits, H. Ulmer, K. Aoki, S. Ohno, N. Mizuki, V. Gottardi, and C. Larcher. 2005.** Tolerability and efficacy of N-chlorotaurine in epidemic keratoconjunctivitis - a double-blind, randomized, phase-2 clinical trial. *J Ocul Pharmacol Th* **21**:157-165.

**Tezel, G., X. Yang, and J. Cai. 2005.** Proteomic identification of oxidatively modified retinal proteins in a chronic pressure-induced rat model of glaucoma. *Invest Ophth Vis Sci* **46**.

**Thomas, J., G. P. Jacob, L. Abraham, and B. Noushad. 2012.** The effect of smoking on the ocular surface and the precorneal tear film. *Australas Med J* **5**:221-226.

**Thompson, L. J., F. Wang, A. D. Proia, K. G. Peters, B. Jarrold, and K. D. Greis. 2003.** Proteome analysis of the rat cornea during angiogenesis. *Proteomics* **3**:2258-2266.

**Thomsson, K. A., N. G. Karlsson, and G. C. Hansson. 1999.** Liquid chromatography-electrospray mass spectrometry as a tool for the analysis of sulfated oligosaccharides from mucin glycoproteins. *Journal of Chromatography A* **854**:131-139.

**Thurston, J. H., R. E. Hauhart, and J. A. Dirgo. 1980.** Taurine - a Role in Osmotic Regulation of Mammalian Brain and Possible Clinical-Significance. *Life Sci* **26**:1561-1568.

**Tiffany, J. M. 2008.** The normal tear film. *Dev Ophthalmol* **41**:1-20.

**Tiffany, J. M., N. Winter, and G. Bliss. 1989.** Tear film stability and tear surface tension. *Curr Eye Res* **8**:507-515.

**Timbrell, J. A., V. Seabra, and C. J. Waterfield. 1995.** The in-Vivo and in-Vitro Protective Properties of Taurine. *Gen Pharmacol-Vasc S* **26**:453-462.

**Toda, I. 2007.** LASIK and dry eye. *Compr Ophthalmol Update* **8**:79-85; discussion 87-79.

**Toda, I., N. Asano-Kato, Y. Komai-Hori, and K. Tsubota. 2001.** Dry eye after laser in situ keratomileusis. *Am J Ophthalmol* **132**:1-7.

**Toda, I., H. Fujishima, and K. Tsubota. 1993.** Ocular Fatigue Is the Major Symptom of Dry Eye. *Acta Ophthalmol* **71**:347-352.
**Tokumitsu, H., A. Mizutani, and H. Hidaka. 1993.** Calcyclin-Binding Site Located on the Nh2-Terminal Domain of Rabbit Cap-50 (Annexin-Xi) - Functional Expression of Cap-50 in Escherichia-Coli. *Archives of Biochemistry and Biophysics* **303**:302-306.
**Tomlinson, A., S. Khanal, K. Ramaesh, C. Diaper, and A. McFadyen. 2006.** Tear film osmolarity: Determination of a referent for dry eye diagnosis. *Invest Ophth Vis Sci* **47**:4309-4315.
**Tomlinson, A., L. C. McCann, and E. I. Pearce. 2010.** Comparison of Human Tear Film Osmolarity Measured by Electrical Impedance and Freezing Point Depression Techniques. *Cornea* **29**:1036-1041.
**Tomosugi, N., K. Kitagawa, N. Takahashi, S. Sugai, and I. Ishikawa. 2005a.** Diagnostic potential of tear proteomic patterns in Sjdgren's syndrome. *J Proteome Res* **4**:820-825.
**Tomosugi, N., K. Kitagawa, N. Takahashi, S. Sugai, and I. Ishikawa. 2005b.** Diagnostic potential of tear proteomic patterns in Sjogren's syndrome. *J Proteome Res* **4**:820-825.
**Tong, L., Y. Diebold, M. Calonge, J. P. Gao, M. E. Stern, and R. W. Beuerman. 2009.** Comparison of Gene Expression Profiles of Conjunctival Cell Lines With Primary Cultured Conjunctival Epithelial Cells and Human Conjunctival Tissue. *Gene Expression* **14**:265-278.
**Tong, L., L. Zhou, R. W. Beuerman, S. Z. Zhao, and X. R. Li. 2011.** Association of tear proteins with Meibomian gland disease and dry eye symptoms. *Brit J Ophthalmol* **95**:848-852.
**Tonge, R., J. Shaw, B. Middleton, R. Rowlinson, S. Rayner, J. Young, F. Pognan, E. Hawkins, I. Currie, and M. Davison. 2001.** Validation and development of fluorescence two-dimensional differential gel electrophoresis proteomics technology. *Proteomics* **1**:377-396.
**Tonjum, A. M. 1975.** Effects of benzalkonium chloride upon the corneal epithelium studied with scanning electron microscopy. *Acta Ophthalmol (Copenh)* **53**:358-366.
**Trachtman, H., S. Futterweit, and R. S. Bienkowski. 1993.** Taurine prevents glucose-induced lipid peroxidation and increased collagen production in cultured rat mesangial cells. *Biochem Biophys Res Commun* **191**:759-765.
**Tran, N., A. D. Graham, and M. C. Lin. 2013.** Ethnic differences in dry eye symptoms: Effects of corneal staining and length of contact lens wear. *Cont Lens Anterior Eye*.
**Tripathi, B. J., and R. C. Tripathi. 1989.** Cytotoxic effects of benzalkonium chloride and chlorobutanol on human corneal epithelial cells in vitro. *Lens Eye Toxic Res* **6**:395-403.
**Tripathi, B. J., R. C. Tripathi, and S. P. Kolli. 1992.** Cytotoxicity of ophthalmic preservatives on human corneal epithelium. *Lens Eye Toxic Res* **9**:361-375.
**Tsai, P. S., J. E. Evans, K. M. Green, R. M. Sullivan, D. A. Schaumberg, S. M. Richards, M. R. Dana, and D. A. Sullivan. 2006.** Proteomic analysis of human meibomian gland secretions. *Br J Ophthalmol* **90**:372-377.
**Tschoerner, F. B., N.; Kroll, P.; Blindert, M.; Pfeiffer, N.; Grus, F., H. 2008.** Proteomics Pipeline Mainz (P2M) and profiling of mass spectrometric data. *Amsterdam, Netherlands: HUPO Annual World Congress*.
**Tsubota, K., and K. Nakamori. 1993.** Dry Eyes and Video Display Terminals. *New Engl J Med* **328**:584-584.
**Tsuji, F. K., K. 2012.** Biomarker identification of tear fluid. *Metabolomics: Open Access* **2**:1-7.
**Tu, E. Y., M. E. Shoff, W. Gao, and C. E. Joslin. 2013.** Effect of low concentrations of benzalkonium chloride on acanthamoebal survival and its potential impact on empirical therapy of infectious keratitis. *JAMA Ophthalmol* **131**:595-600.
**Tutt, R., A. Bradley, C. Begley, and L. N. Thibos. 2000.** Optical and visual impact of tear break-up in human eyes. *Invest Ophthalmol Vis Sci* **41**:4117-4123.
**Twining, S. S., T. Fukuchi, B. Y. J. T. Yue, P. M. Wilson, X. Y. Zhou, and G. Loushin. 1994.** Alpha-2-Macroglobulin Is Present in and Synthesized by the Cornea. *Invest Ophth Vis Sci* **35**:3226-3233.
**Uchida, S., T. Nakanishi, H. M. Kwon, A. S. Preston, and J. S. Handler. 1991.** Taurine Behaves as an Osmolyte in Madin-Darby Canine Kidney-Cells - Protection by Polarized, Regulated Transport of Taurine. *J Clin Invest* **88**:656-662.

**Uchino, M., N. Yokoi, Y. Uchino, M. Dogru, M. Kawashima, A. Komuro, Y. Sonomura, H. Kato, S. Kinoshita, D. A. Schaumberg, and K. Tsubota. 2013.** Prevalence of dry eye disease and its risk factors in visual display terminal users: the osaka study. *Am J Ophthalmol* **156**:759-766 e751.
**Ueda, Y., M. K. Duncan, and L. L. David. 2002.** Lens proteomics: the accumulation of crystallin modifications in the mouse lens with age. *Invest Ophthalmol Vis Sci* **43**:205-215.
**UltraflexTOF/TOFOperatorManual. 2001.** *Bruker Daltonik GmbH, Bremen, Germany* **1st Edition**.
**UserGuideforRPZipTipPipetteTipsforSamplePreparation. 2007.** EMD Millipore Corporation, Billerica, USA. **PR02358, Rev. A, 02/07**.
**Uusitalo, H., E. P. Chen, N. Pfeiffer, F. Brignole-Baudouin, K. Kaarniranta, M. Leino, P. Puska, E. Palmgren, T. Hamacher, G. Hofmann, G. Petzold, U. Richter, T. Riedel, M. Winter, and A. Ropo. 2010.** Switching from a preserved to a preservative-free prostaglandin preparation in topical glaucoma medication. *Acta Ophthalmol* **88**:329-336.
**Van Bergen, N. J., J. P. Wood, G. Chidlow, I. A. Trounce, R. J. Casson, W. K. Ju, R. N. Weinreb, and J. G. Crowston. 2009.** Recharacterization of the RGC-5 retinal ganglion cell line. *Invest Ophthalmol Vis Sci* **50**:4267-4272.
**van der Heeft, E., Y. J. C. Bolck, B. Beumer, A. W. J. M. Nijrolder, A. A. M. Stolker, and M. W. F. Nielen. 2009.** Full-Scan Accurate Mass Selectivity of Ultra-Performance Liquid Chromatography Combined with Time-of-Flight and Orbitrap Mass Spectrometry in Hormone and Veterinary Drug Residue Analysis. *J Am Soc Mass Spectr* **20**:451-463.
**van Engeland, M., L. J. Nieland, F. C. Ramaekers, B. Schutte, and C. P. Reutelingsperger. 1998.** Annexin V-affinity assay: a review on an apoptosis detection system based on phosphatidylserine exposure. *Cytometry* **31**:1-9.
**Van Haeringen, N. J. 1981.** Clinical biochemistry of tears. *Surv Ophthalmol* **26**:84-96.
**van Haeringen, N. J., and E. Glasius. 1976.** The origin of some enzymes in tear fluid, determined by comparative investigation with two collection methods. *Exp Eye Res* **22**:267-272.
**van Hagen, J. 2008.** Proteomics sample preparation. *WILEY-VCH Verlag GmbH & Co. KGaA, Weinheim, Germany*.
**van Kampen, J. J. A., P. C. Burgers, R. de Groot, R. A. Gruters, and T. M. Luider. 2011.** Biomedical Application of Maldi Mass Spectrometry for Small-Molecule Analysis. *Mass Spectrometry Reviews* **30**:101-120.
**van Landingham, S. W., S. K. West, E. K. Akpek, B. Munoz, and P. Y. Ramulu. 2013.** Impact of dry eye on reading in a population based sample of the elderly: the Salisbury Eye Evaluation. *Br J Ophthalmol*.
**Vanhaeri.Nj, and E. Glasius. 1974a.** Enzymatic Studies in Lacrimal Secretion. *Experimental Eye Research* **19**:135-139.
**Vanhaeri.Nj, and E. Glasius. 1974b.** Enzymes of Energy-Producing Metabolism in Human Tear Fluid. *Experimental Eye Research* **18**:407-409.
**vanHaeringen, N. J. 1997.** Aging and the lacrimal system. *Brit J Ophthalmol* **81**:824-826.
**Veenstra, T. D., T. P. Conrads, B. L. Hood, A. M. Avellino, R. G. Ellenbogen, and R. S. Morrison. 2005.** Biomarkers: mining the biofluid proteome. *Mol Cell Proteomics* **4**:409-418.
**Veerhuis, R., and A. Kijlstra. 1982.** Inhibition of hemolytic complement activity by lactoferrin in tears. *Exp Eye Res* **34**:257-265.
**Venkatesan, N., P. Venkatesan, J. Karthikeyan, and V. Arumugam. 1997.** Protection by taurine against adriamycin-induced proteinuria and hyperlipidemia in rats. *Proc Soc Exp Biol Med* **215**:158-164.
**Venturi, E., K. Mio, M. Nishi, T. Ogura, T. Moriya, S. J. Pitt, K. Okuda, S. Kakizawa, R. Sitsapesan, C. Sato, and H. Takeshima. 2011.** Mitsugumin 23 Forms a Massive Bowl-Shaped Assembly and Cation-Conducting Channel. *Biochemistry* **50**:2623-2632.
**Verdrengh, M., and A. Tarkowski. 2005.** Inhibition of septic arthritis by local administration of taurine chloramine, a product of activated neutrophils. *J Rheumatol* **32**:1513-1517.
**Vermes, I., C. Haanen, H. Steffens-Nakken, and C. Reutelingsperger. 1995.** A novel assay for apoptosis. Flow cytometric detection of phosphatidylserine expression on early apoptotic cells using fluorescein labelled Annexin V. *J Immunol Methods* **184**:39-51.

**Versura, P., P. Nanni, A. Bavelloni, W. L. Blalock, M. Piazzi, A. Roda, and E. C. Campos. 2010.** Tear proteomics in evaporative dry eye disease. *Eye (Lond)* **24**:1396-1402.
**Verzola, D., M. B. Bertolotto, B. Villaggio, L. Ottonello, F. Dallegri, G. Frumento, V. Berruti, M. T. Gandolfo, G. Garibotto, and G. Deferrari. 2002.** Taurine prevents apoptosis induced by high ambient glucose in human tubule renal cells. *J Invest Med* **50**:443-451.
**Vijmasi, T., F. L. Y. T. Chen, Y. T. Chen, M. Gallup, and N. McNamara. 2013.** Topical administration of interleukin-1 receptor antagonist as a therapy for aqueous-deficient dry eye in autoimmune disease. *Molecular Vision* **19**:1957-1965.
**Villanueva, J., K. Lawlor, R. Toledo-Crow, and P. Tempst. 2006.** Automated serum peptide profiling. *Nat Protoc* **1**:880-891.
**Villanueva, J., J. Philip, D. Entenberg, C. A. Chaparro, M. K. Tanwar, E. C. Holland, and P. Tempst. 2004.** Serum peptide profiling by magnetic particle-assisted, automated sample processing and MALDI-TOF mass spectrometry. *Anal Chem* **76**:1560-1570.
**Viso, E., M. T. Rodriguez-Ares, and F. Gude. 2009.** Prevalence of and associated factors for dry eye in a spanish adult population (the Salnes eye study). *Ophthalmic Epidemiol* **16**:15-21.
**Voaden, M. J., N. Lake, J. Marshall, and B. Morjaria. 1977.** Studies on the distribution of taurine and other neuroactive amino acids in the retina. *Exp Eye Res* **25**:249-257.
**Voehringer, D. W. 1999.** BCL-2 and glutathione: alterations in cellular redox state that regulate apoptosis sensitivity. *Free Radic Biol Med* **27**:945-950.
**Von Stroh, R. 1993.** Computer vision syndrome. *Occup Health Saf* **62**:62-66.
**von Thun Und Hohenstein-Blaul, N., S. Funke, and F. H. Grus. 2013.** Tears as a source of biomarkers for ocular and systemic diseases. *Exp Eye Res*.
**Vroman, D. T., H. P. Sandoval, L. E. F. de Castro, T. J. Kasper, M. P. Holzer, and K. D. Solomon. 2005.** Effect of hinge location on corneal sensation and dry eye after laser in situ keratomileusis for myopia. *J Cataract Refr Surg* **31**:1881-1887.
**Vu, D. H., R. A. Koster, A. M. A. Wessels, B. Greijdanus, J. W. C. Alffenaar, and D. R. A. Uges. 2013.** Troubleshooting carry-over of LC-MS/MS method for rifampicin, clarithromycin and metabolites in human plasma. *J Chromatogr B* **917-918**:1-4.
**Wall, D. B., D. M. Lubman, and S. J. Flynn. 1999.** Rapid profiling of induced proteins in bacteria using MALDI-TOF mass spectrometric detection of nonporous RP HPLC-separated whole cell lysates. *Anal Chem* **71**:3894-3900.
**Wan, H., M. G. Stone, C. Simpson, L. E. Reynolds, J. F. Marshall, I. R. Hart, K. M. Hodivala-Dilke, and R. A. J. Eady. 2003.** Desmosomal proteins, including desmoglein 3, serve as novel negative markers for epidermal stem cell-containing population of keratinocytes. *J Cell Sci* **116**:4239-4248.
**Wang, J., Y. W. Wang, and J. K. Gu. 2004.** Ion suppression in proteomics analysis with ESI and MALDI/Mass Spectrometry. *Mol Cell Proteomics* **3**:S142-S142.
**Wang, J. L., Y. J. Zhang, H. Jiang, Y. Cai, and X. H. Qian. 2006.** Phosphopeptide detection using automated online IMAC-capillary LC-ESI-MS/MS. *Proteomics* **6**:404-411.
**Wang, L., L. Zhang, Y. Yu, Y. Wang, and N. Niu. 2008.** The protective effects of taurine against early renal injury in STZ-induced diabetic rats, correlated with inhibition of renal LOX-1-mediated ICAM-1 expression. *Ren Fail* **30**:763-771.
**Wang, Y. Y., P. Cheng, and D. W. Chan. 2003.** A simple affinity spin tube filter method for removing high-abundant common proteins or enriching low-abundant biomarkers for serum proteomic analysis. *Proteomics* **3**:243-248.
**WARP-LC1.1UserManual. 2006.** Bruker Daltonik GmbH, Bremen, Germany.
**Wasinger, V. C., S. J. Cordwell, A. Cerpa-Poljak, J. X. Yan, A. A. Gooley, M. R. Wilkins, M. W. Duncan, R. Harris, K. L. Williams, and I. Humphery-Smith. 1995.** Progress with gene-product mapping of the mollicutes: Mycoplasma genitalium. *Electrophoresis* **16**:1090-1094.
**Wassink, T. H., J. Piven, V. J. Vieland, L. Jenkins, R. Frantz, C. W. Bartlett, R. Goedken, D. Childress, M. A. Spence, M. Smith, and V. C. Sheffield. 2005.** Evaluation of the chromosome 2q37.3 gene CENTG2 as an autism susceptibility gene. *Am J Med Genet B* **136B**:36-44.

**Watanabe, A., B. Araki, K. Noso, H. Kakizaki, and S. Kinoshita. 2006.** Histopathology of blepharoptosis induced by prolonged hard contact lens wear. *Am J Ophthalmol* **141**:1092-1096.
**Watanabe, H., M. Fabricant, A. S. Tisdale, S. J. Spurr-Michaud, K. Lindberg, and I. K. Gipson. 1995.** Human corneal and conjunctival epithelia produce a mucin-like glycoprotein for the apical surface. *Invest Ophthalmol Vis Sci* **36**:337-344.
**Waterfield, C. J., M. Mesquita, P. Parnham, and J. A. Timbrell. 1994.** Cytoprotective effects of taurine in isolated rat hepatocytes. *Toxicol In Vitro* **8**:573-575.
**Weinkauf, M., W. Hiddemann, and M. Dreyling. 2006.** Sample pooling in 2-D gel electrophoresis: A new approach to reduce nonspecific expression background. *Electrophoresis* **27**:4555-4558.
**Weiss, S. J., R. Klein, A. Slivka, and M. Wei. 1982.** Chlorination of taurine by human neutrophils. Evidence for hypochlorous acid generation. *J Clin Invest* **70**:598-607.
**Weston, A., and E. S. Assem. 1994.** Possible link between anaphylactoid reactions to anaesthetics and chemicals in cosmetics and biocides. *Agents Actions* **41 Spec No**:C138-139.
**Wettstein, M., and D. Haussinger. 1997.** Cytoprotection by the osmolytes betaine and taurine in ischemia-reoxygenation injury in the perfused rat liver. *Hepatology* **26**:1560-1566.
**Wheater, M. K., K. A. Kernacki, and L. D. Hazlett. 1999.** Corneal cell proteins and ocular surface pathology. *Biotech Histochem* **74**:146-159.
**Whelan, S. A., M. Lu, J. He, W. Yan, R. E. Saxton, K. F. Faull, J. P. Whitelegge, and H. R. Chang. 2009.** Mass spectrometry (LC-MS/MS) site-mapping of N-glycosylated membrane proteins for breast cancer biomarkers. *J Proteome Res* **8**:4151-4160.
**Whitcher, J. P. 1987.** Clinical diagnosis of the dry eye. *Int Ophthalmol Clin* **27**:7-24.
**Whitehouse, C. M., R. N. Dreyer, M. Yamashita, and J. B. Fenn. 1985.** Electrospray Interface for Liquid Chromatographs and Mass Spectrometers. *Anal Chem* **57**:675-679.
**Whitson, J. T., H. D. Cavanagh, N. Lakshman, and W. M. Petroll. 2006.** Assessment of corneal epithelial integrity after acute exposure to ocular hypotensive agents preserved with and without benzalkonium chloride. *Adv Ther* **23**:663-671.
**Wiche, G., R. Krepler, U. Artlieb, R. Pytela, and H. Denk. 1983.** Occurrence and Immunolocalization of Plectin in Tissues. *Journal of Cell Biology* **97**:887-901.
**Wilkins, M. R., C. Pasquali, R. D. Appel, K. Ou, O. Golaz, J. C. Sanchez, J. X. Yan, A. A. Gooley, G. A. Hughes, I. Humphery-Smith, K. L. Williams, and D. F. Hochstrasser. 1996a.** From proteins to proteomes: large scale protein identification by two-dimensional electrophoresis and amino acid analysis. *Biotechnology (NY)* **14**:61-65.
**Wilkins, M. R., J. C. Sanchez, A. A. Gooley, R. D. Appel, I. Humphery-Smith, D. F. Hochstrasser, and K. L. Williams. 1996b.** Progress with proteome projects: why all proteins expressed by a genome should be identified and how to do it. *Biotechnology and Genetic Engineering Reviews* **13**:19-50.
**Wilkins, M. R. e. a. 2006.** Guidelines for the next 10 years of proteomics. *Proteomics* **6**:4-8.
**Willcox, M. P. P., C. A. Morris, A. Thakur, R. A. Sack, J. Wickson, and W. Boey. 1997.** Complement and complement regulatory proteins in human tears. *Invest Ophthalmol Vis Sci* **38**:1-8.
**Wilmarth, P. A., M. A. Riviere, and L. L. David. 2009.** Techniques for accurate protein identification in shotgun proteomic studies of human, mouse, bovine, and chicken lenses. *J Ocul Biol Dis Infor* **2**:223-234.
**Wilson, W. S., A. J. Duncan, and J. L. Jay. 1975.** Effect of benzalkonium chloride on the stability of the precorneal tear film in rabbit and man. *Br J Ophthalmol* **59**:667-669.
**Winston, J. T., D. M. Koepp, C. H. Zhu, S. J. Elledge, and J. W. Harper. 1999.** A family of mammalian F-box proteins. *Current Biology* **9**:1180-1182.
**Wojcik, O. P., K. L. Koenig, A. Zeleniuch-Jacquotte, M. Costa, and Y. Chen. 2010.** The potential protective effects of taurine on coronary heart disease. *Atherosclerosis* **208**:19-25.
**Wolff, E. 1946.** The muco-cutaneous junction of the lid margin and the distribution of the tear fluid. *Trans. Ophthalmol. Soc. UK* **66**:291–308.
**Wolff, E. 1954.** The Anatomy of the Eye and Orbit, fourth ed. *H.K. Lewis and Co, London*.

**Wolters, D. B., N.; Pfeiffer, N.; Grus, F. H. 2011.** A new software pipeline for the analysis and quantification of mass specctrometry based proteomics data. *Obergurgl, Austria: ARVO Optic Nerve Degeneration, Protection and Autoimmunity conference 2011*.
**Wolters, D. F., S.; Grus, F. H.; Pfeiffer, N. . 2012.** Post transcriptional modifications in mass spectrometry based proteomics data. *Obergurgl, Austria: ARVO Optic Nerve Degeneration and Ageing Conference 2012*.
**Wong, T. T., L. Zhou, J. Li, L. Tong, S. Z. Zhao, X. R. Li, S. J. Yu, S. K. Koh, and R. W. Beuerman. 2011.** Proteomic profiling of inflammatory signaling molecules in the tears of patients on chronic glaucoma medication. *Invest Ophthalmol Vis Sci* **52**:7385-7391.
**Wood, J. P., G. Chidlow, T. Tran, J. G. Crowston, and R. J. Casson. 2010.** A comparison of differentiation protocols for RGC-5 cells. *Invest Ophthalmol Vis Sci* **51**:3774-3783.
**Woodward, G., P. Kroon, A. Cassidy, and C. Kay. 2009.** Anthocyanin Stability and Recovery: Implications for the Analysis of Clinical and Experimental Samples. *J Agr Food Chem* **57**:5271-5278.
**Wright, C. E., H. H. Tallan, Y. Y. Lin, and G. E. Gaull. 1986.** Taurine - Biological Update. *Annual Review of Biochemistry* **55**:427-453.
**Wright, J. C., and G. E. Meger. 1962.** A review of the Schirmer test for tear production. *Arch Ophthalmol* **67**:564-565.
**Wu, G. Y. 2009.** Amino acids: metabolism, functions, and nutrition. *Amino Acids* **37**:1-17.
**Wu, J. Y., H. Wu, Y. Jin, J. N. Wei, D. Sha, H. Prentice, H. H. Lee, C. H. Lin, Y. H. Lee, and L. L. Yang. 2009a.** Mechanism of Neuroprotective Function of Taurine. *Taurine 7* **643**:169-179.
**Wu, Q. D., J. H. Wang, F. Fennessy, H. P. Redmond, and D. Bouchier-Hayes. 1999.** Taurine prevents high-glucose-induced human vascular endothelial cell apoptosis. *Am J Physiol* **277**:C1229-1238.
**Wu, Z. Z., J. G. Wang, and X. L. Zhang. 2009b.** Diagnostic model of saliva protein finger print analysis of patients with gastric cancer. *World J Gastroenterol* **15**:865-870.
**Xiang, F., Y. H. Lin, J. Wen, D. W. Matson, and R. D. Smith. 1999.** An integrated microfabricated device for dual microdialysis and on-line ESI ion trap mass spectrometry for analysis of complex biological samples. *Anal Chem* **71**:1485-1490.
**Xiong, C., D. Chen, J. Liu, B. Liu, N. Li, Y. Zhou, X. Liang, P. Ma, C. Ye, J. Ge, and Z. Wang. 2008.** A rabbit dry eye model induced by topical medication of a preservative benzalkonium chloride. *Invest Ophthalmol Vis Sci* **49**:1850-1856.
**Xu, J., X. M. Zhang, M. Monestier, N. L. Esmon, and C. T. Esmon. 2011.** Extracellular Histones Are Mediators of Death through TLR2 and TLR4 in Mouse Fatal Liver Injury. *J Immunol* **187**:2626-2631.
**Xu, M., L. Y. Geer, S. H. Bryant, J. S. Roth, J. A. Kowalak, D. M. Maynard, and S. P. Markey. 2005.** Assessing data quality of peptide mass spectra obtained by quadrupole ion trap mass spectrometry. *J Proteome Res* **4**:300-305.
**Yabuta, C., F. Yano, A. Fujii, T. R. Shearer, and M. Azuma. 2014.** Galectin-3 enhances epithelial cell adhesion and wound healing in rat cornea. *Ophthalmic Res* **51**:96-103.
**Yalvac, I. S., G. Gedikoglu, Y. Karagoz, U. Akgun, A. Nurozler, F. Koc, R. Kasim, and S. Duman. 1995.** Effects of antiglaucoma drugs on ocular surface. *Acta Ophthalmol Scand* **73**:246-248.
**Yamauchitakihara, K., J. Azuma, and S. Kishimoto. 1986.** Taurine Protection against Experimental Arterial Calcinosis in Mice. *Biochem Bioph Res Co* **140**:679-683.
**Yanagisawa, K., Y. Shyr, B. J. Xu, P. P. Massion, P. H. Larsen, B. C. White, J. R. Roberts, M. Edgerton, A. Gonzalez, S. Nadaf, J. H. Moore, R. M. Caprioli, and D. P. Carbone. 2003.** Proteomic patterns of tumour subsets in non-small-cell lung cancer. *Lancet* **362**:433-439.
**Yancey, P. H. 2001.** Water stress, osmolytes and proteins. *Am Zool* **41**:699-709.
**Yang, C., Z. He, and W. Yu. 2009.** Comparison of public peak detection algorithms for MALDI mass spectrometry data analysis. *BMC Bioinformatics* **10**:4.
**Yang, C. Q., W. Sun, and Y. S. Gu. 2006.** A clinical study of the efficacy of topical corticosteroids on dry eye. *J Zhejiang Univ Sci B* **7**:675-678.

**Yang, M., S. Fazio, D. Munch, and P. Drumm. 2005.** Impact of methanol and acetonitrile on separations based on pi-pi interactions with a reversed-phase phenyl column. *Journal of Chromatography A* **1097**:124-129.
**Yang, X. J., and G. Tezel. 2005.** Proteomic analysis of retinal ganglion cells: Toward retinal ganglion cell protein mapping. *Invest Ophth Vis Sci* **46**.
**Yang, Y., S. Zhang, K. Howe, D. B. Wilson, F. Moser, D. Irwin, and T. W. Thannhauser. 2007.** A comparison of nLC-ESI-MS/MS and nLC-MALDI-MS/MS for GeLC-based protein identification and iTRAQ-based shotgun quantitative proteomics. *J Biomol Tech* **18**:226-237.
**Yates, J. R. 2000.** Mass spectrometry - from genomics to proteomics. *Trends Genet* **16**:5-8.
**Yates, J. R., C. I. Ruse, and A. Nakorchevsky. 2009.** Proteomics by mass spectrometry: approaches, advances, and applications. *Annu Rev Biomed Eng* **11**:49-79.
**Ye, H. B., H. B. Shi, and S. K. Yin. 2013.** Mechanisms underlying taurine protection against glutamate-induced neurotoxicity. *Can J Neurol Sci* **40**:628-634.
**Yee, R. W., E. G. Norcom, and X. P. C. Zhao. 2006.** Comparison of the relative toxicity of travoprost 0.004% without benzalkonium chloride and latanoprost 0.005% in an immortalized human cornea epithelial cell culture system. *Adv Ther* **23**:511-518.
**Yi, E. C., H. Lee, R. Aebersold, and D. R. Goodlett. 2003.** A microcapillary trap cartridge-microcapillary high-performance liquid chromatography electrospray ionization emitter device capable of peptide tandem mass spectrometry at the attomole level on an ion trap mass spectrometer with automated routine operation. *Rapid Commun Mass Sp* **17**:2093-2098.
**Yildirim, Z. L., N. Kilic, C. Ozer, A. Babul, G. Take, and D. Erdogan. 2007.** Effects of taurine in cellular responses to oxidative stress in young and middle-aged rat liver. *Biogerontology: Mechanisms and Interventions* **1100**:553-561.
**Yin, M., H. R. Palmer, J. J. Bedford, A. Fyfe-Johnson, F. Santoso, J. Suko, and P. H. Yancey. 1999.** Unusual osmolytes in deep-sea vestimentiferans, gastropods, and echinoderms. *Am Zool* **39**:65a-65a.
**Yin, M., H. R. Palmer, A. L. Fyfe-Johnson, J. J. Bedford, R. A. J. Smith, and P. H. Yancey. 2000.** Hypotaurine, N-methyltaurine, taurine, and glycine betaine as dominant osmolytes of vestimentiferan tubeworms from hydrothermal vents and cold seeps. *Physiol Biochem Zool* **73**:629-637.
**Yocum, A. K., K. Yu, T. Oe, and I. A. Blair. 2005.** Effect of immunoaffinity depletion of human serum during proteomic investigations. *J Proteome Res* **4**:1722-1731.
**Yoshida, M. A., and A. Ogura. 2011.** Genetic mechanisms involved in the evolution of the cephalopod camera eye revealed by transcriptomic and developmental studies. *Bmc Evol Biol* **11**.
**Young, G., R. L. Chalmers, L. Napier, C. Hunt, and J. Kern. 2011.** Characterizing contact lens-related dryness symptoms in a cross-section of UK soft lens wearers. *Cont Lens Anterior Eye* **34**:64-70.
**Young, N. M., and W. W. Dawson. 1992.** The Ocular Secretions of the Bottle-Nosed-Dolphin Tursiops-Truncatus. *Mar Mammal Sci* **8**:57-68.
**Yu, J., F. Liu, S. J. Cui, Y. Liu, Z. Y. Song, H. Cao, F. E. Chen, W. J. Wang, T. Sun, and F. Wang. 2008.** Vitreous proteomic analysis of proliferative vitreoretinopathy. *Proteomics* **8**:3667-3678.
**Zabel, M., M. Schrag, C. Mueller, W. D. Zhou, A. Crofton, F. Petersen, A. Dickson, and W. M. Kirsch. 2012.** Assessing Candidate Serum Biomarkers for Alzheimer's Disease: A Longitudinal Study. *Journal of Alzheimers Disease* **30**:311-321.
**Zeng, K., H. Xu, M. Mi, K. Chen, J. Zhu, L. Yi, T. Zhang, Q. Zhang, and X. Yu. 2010.** Effects of taurine on glial cells apoptosis and taurine transporter expression in retina under diabetic conditions. *Neurochem Res* **35**:1566-1574.
**Zeng, Z., M. Hincapie, S. J. Pitteri, S. Hanash, J. Schalkwijk, J. M. Hogan, H. Wang, and W. S. Hancock. 2011.** A proteomics platform combining depletion, multi-lectin affinity chromatography (M-LAC), and isoelectric focusing to study the breast cancer proteome. *Anal Chem* **83**:4845-4854.
**Zhang, J., D. R. Goodlett, J. F. Quinn, E. Peskind, J. A. Kaye, Y. Zhou, C. Pan, E. Yi, J. Eng, Q. Wang, R. H. Aebersold, and T. J. Montine. 2005.** Quantitative proteomics of

cerebrospinal fluid from patients with Alzheimer disease. *J Alzheimers Dis* **7**:125-133; discussion 173-180.
**Zhang, K., Y. Liu, Y. Shang, H. Zheng, J. Guo, H. Tian, Y. Jin, J. He, and X. Liu. 2012.** Analysis of pig serum proteins based on shotgun liquid chromatography-tandem mass spectrometry. *African J Biotech* **11**:12118-12127.
**Zhang, N., N. Li, and L. Li. 2004a.** Liquid chromatography MALDI MS/MS for membrane proteome analysis. *J Proteome Res* **3**:719-727.
**Zhang, N., A. R. Shaw, N. Li, R. Chen, A. Mak, X. Hu, N. Young, D. Wishart, and L. Li. 2008.** Liquid chromatography electrospray ionization and matrix-assisted laser desorption ionization tandem mass spectrometry for the analysis of lipid raft proteome of monocytes. *Anal Chim Acta* **627**:82-90.
**Zhang, N. Y., S. T. Fountain, H. G. Bi, and D. T. Rossi. 2000.** Quantification and rapid metabolite identification in drug discovery using API time-of-flight LC/MS. *Anal Chem* **72**:800-806.
**Zhang, X., S. M. Leung, C. R. Morris, and M. K. Shigenaga. 2004b.** Evaluation of a novel, integrated approach using functionalized magnetic beads, bench-top MALDI-TOF-MS with prestructured sample supports, and pattern recognition software for profiling potential biomarkers in human plasma. *J Biomol Tech* **15**:167-175.
**Zhang, X. R., M. H. Xiang, Q. Q. Wu, Q. S. Li, Y. Xu, and A. G. Sun. 2009.** The tear proteomics analysis of conjunctivochalasis. *Zhonghua Yan Ke Za Zhi* **45**:135-140.
**Zhao, H., J. E. Jumblatt, T. O. Wood, and M. M. Jumblatt. 2001.** Quantification of MUC5AC protein in human tears. *Cornea* **20**:873-877.
**Zhao, Z., N. A. Carnt, Y. Aliwarga, X. Wei, T. Naduvilath, Q. Garrett, J. Korth, and M. D. Willcox. 2009.** Care regimen and lens material influence on silicone hydrogel contact lens deposition. *Optom Vis Sci* **86**:251-259.
**Zhou, L., R. W. Beuerman, L. P. K. Ang, C. M. Chan, S. F. Y. Li, F. T. Chew, and D. T. H. Tan. 2009a.** Elevation of Human alpha-Defensins and S100 Calcium-Binding Proteins A8 and A9 in Tear Fluid of Patients with Pterygium. *Invest Ophth Vis Sci* **50**:2077-2086.
**Zhou, L., R. W. Beuerman, C. M. Chan, S. Z. Zhao, X. R. Li, H. Yang, L. Tong, S. Liu, M. E. Stern, and D. Tan. 2009b.** Identification of tear fluid biomarkers in dry eye syndrome using iTRAQ quantitative proteomics. *J Proteome Res* **8**:4889-4905.
**Zhou, L., R. W. Beuerman, C. M. Chan, S. Z. Zhao, X. R. Li, H. Yang, L. Tong, S. P. Liu, M. E. Stern, and D. Tan. 2009c.** Identification of Tear Fluid Biomarkers in Dry Eye Syndrome Using iTRAQ Quantitative Proteomics. *J Proteome Res* **8**:4889-4905.
**Zhou, L., R. W. Beuerman, A. P. Chew, S. K. Koh, T. A. Cafaro, E. A. Urrets-Zavalia, J. A. Urrets-Zavalia, S. F. Y. Li, and H. M. Serra. 2009d.** Quantitative Analysis of N-Linked Glycoproteins in Tear Fluid of Climatic Droplet Keratopathy by Glycopeptide Capture and iTRAQ. *J Proteome Res* **8**:1992-2003.
**Zhou, L., R. W. Beuerman, Y. Foo, S. Liu, L. P. K. Ang, and D. T. H. Tan. 2006.** Characterisation of human tear proteins using high-resolution mass spectrometry. *Ann Acad Med Singap* **35**:400-407.
**Zhou, L., R. W. Beuerman, L. Huang, A. Barathi, Y. H. Foo, S. F. Li, F. T. Chew, and D. Tan. 2007.** Proteomic analysis of rabbit tear fluid: Defensin levels after an experimental corneal wound are correlated to wound closure. *Proteomics* **7**:3194-3206.
**Zhou, L., J. Li, S. K. Koh, M. Setiawan, H. L. Kiu, and R. W. Beuerman. 2011.** Quantitative proteomic analysis of cellular response to hyperosmolarity in human conjunctival epithelial cells. *ARVO 2011 Annual Meeting, Fort Lauderdale, USA* **Program Number: 3809**.
**Zhou, L., S. Z. Zhao, S. K. Koh, L. Chen, C. Vaz, V. Tanavde, X. R. Li, and R. W. Beuerman. 2012.** In-depth analysis of the human tear proteome. *J Proteomics* **75**:3877-3885.
**Zhou, L. B., R. W.; Foo, Y.; Liu, S.; Ang, L. P. K.; Tan, D. T. H. 2006.** Characterisation of human tear proteins using high-resolution mass spectrometry. *Ann Acad Med Singapore* **35**:400-407.
**Zhou, R., A. Tardivel, B. Thorens, I. Choi, and J. Tschopp. 2010.** Thioredoxin-interacting protein links oxidative stress to inflammasome activation. *Nat Immunol* **11**:136-140.

**Zhukov, T. A., R. A. Johanson, A. B. Cantor, R. A. Clark, and M. S. Tockman. 2003.** Discovery of distinct protein profiles specific for lung tumors and pre-malignant lung lesions by SELDI mass spectrometry. *Lung Cancer* **40**:267-279.

**Zou, H., X. Huang, M. Ye, and Q. Luo. 2002a.** Monolithic stationary phases for liquid chromatography and capillary electrochromatography. *J Chromatogr A* **954**:5-32.

**Zou, Q., B. J. Bennion, V. Daggett, and K. P. Murphy. 2002b.** The molecular mechanism of stabilization of proteins by TMAO and its ability to counteract the effects of urea. *J Am Chem Soc* **124**:1192-1202.

# 13 Appendices

**Appendix 1** LC MALDI MS identified capillary tear proteins (Funke *et al.*, 2012)

| | |
|---|---|
| **1.** | TRFL_HUMAN Mass: 78132 Score: 16010 Queries matched: 614 emPAI: 15.25 |
| | Lactotransferrin OS=Homo sapiens GN=LTF PE=1 SV=6 |
| **2.** | LCN1_HUMAN Mass: 19238 Score: 15876 Queries matched: 489 emPAI: 4.60 |
| | Lipocalin-1 OS=Homo sapiens GN=LCN1 PE=1 SV=1 |
| **3.** | PROL4_HUMAN Mass: 15116 Score: 14746 Queries matched: 371 emPAI: 3.28 |
| | Proline-rich protein 4 OS=Homo sapiens GN=PRR4 PE=1 SV=2 |
| **4.** | LYSC_HUMAN Mass: 16526 Score: 4800 Queries matched: 208 emPAI: 6.34 |
| | Lysozyme C OS=Homo sapiens GN=LYZ PE=1 SV=1 |
| **5.** | ALBU_HUMAN Mass: 69321 Score: 4415 Queries matched: 230 emPAI: 5.90 |
| | Serum albumin OS=Homo sapiens GN=ALB PE=1 SV=2 |
| **6.** | PIGR_HUMAN Mass: 83232 Score: 4283 Queries matched: 211 emPAI: 1.09 |
| | Polymeric immunoglobulin receptor OS=Homo sapiens GN=PIGR PE=1 SV=4 |
| **7.** | IGKC_HUMAN Mass: 11602 Score: 4135 Queries matched: 113 emPAI: 9.36 |
| | Ig kappa chain C region OS=Homo sapiens GN=IGKC PE=1 SV=1 |
| **8.** | IGHA1_HUMAN Mass: 37631 Score: 4096 Queries matched: 126 emPAI: 1.43 |
| | Ig alpha-1 chain C region OS=Homo sapiens GN=IGHA1 PE=1 SV=2 |
| **9.** | LC1L1_HUMAN Mass: 17907 Score: 3707 Queries matched: 156 emPAI: 0.36 |
| | Putative lipocalin 1-like protein 1 OS=Homo sapiens GN=LCN1L1 PE=5 SV=1 |
| **10.** | IGHA2_HUMAN Mass: 36503 Score: 3488 Queries matched: 98 emPAI: 1.14 |
| | Ig alpha-2 chain C region OS=Homo sapiens GN=IGHA2 PE=1 SV=3 |
| **11.** | CYTS_HUMAN Mass: 16204 Score: 3473 Queries matched: 116 emPAI: 4.45 |
| | Cystatin-S OS=Homo sapiens GN=CST4 PE=1 SV=3 |
| **12.** | LACRT_HUMAN Mass: 14237 Score: 3135 Queries matched: 112 emPAI: 2.18 |
| | Extracellular glycoprotein lacritin OS=Homo sapiens GN=LACRT PE=1 SV=1 |
| **13.** | PIP_HUMAN Mass: 16562 Score: 2998 Queries matched: 210 emPAI: 6.34 |
| | Prolactin-inducible protein OS=Homo sapiens GN=PIP PE=1 SV=1 |
| **14.** | TRY1_HUMAN Mass: 26541 Score: 2917 Queries matched: 226 emPAI: 0.23 |
| | Trypsin-1 OS=Homo sapiens GN=PRSS1 PE=1 SV=1 |
| **15.** | TRY2_HUMAN Mass: 26471 Score: 2917 Queries matched: 224 emPAI: 0.23 |
| | Trypsin-2 OS=Homo sapiens GN=PRSS2 PE=1 SV=1 |
| **16.** | TRY6_HUMAN Mass: 26522 Score: 2917 Queries matched: 223 emPAI: 0.23 |
| | Putative trypsin-6 OS=Homo sapiens GN=TRY6 PE=5 SV=1 |
| **17.** | ZA2G_HUMAN Mass: 34237 Score: 2514 Queries matched: 107 emPAI: 6.03 |
| | Zinc-alpha-2-glycoprotein OS=Homo sapiens GN=AZGP1 PE=1 SV=2 |
| **18.** | SG2A1_HUMAN Mass: 10876 Score: 2373 Queries matched: 89 emPAI: 11.18 |
| | Mammaglobin-B OS=Homo sapiens GN=SCGB2A1 PE=1 SV=1 |
| **19.** | CYTN_HUMAN Mass: 16351 Score: 1949 Queries matched: 75 emPAI: 2.85 |
| | Cystatin-SN OS=Homo sapiens GN=CST1 PE=1 SV=2 |
| **20.** | DMBT1_HUMAN Mass: 260569 Score: 1305 Queries matched: 59 emPAI: 0.09 |
| | Deleted in malignant brain tumors 1 protein OS=Homo sapiens GN=DMBT1 PE=1 SV=2 |
| **21.** | PROL1_HUMAN Mass: 27199 Score: 1081 Queries matched: 59 emPAI: 1.77 |
| | Proline-rich protein 1 OS=Homo sapiens GN=PROL1 PE=1 SV=2 |
| **22.** | LAC2_HUMAN Mass: 11287 Score: 829 Queries matched: 46 emPAI: 3.23 |
| | Ig lambda-2 chain C regions OS=Homo sapiens GN=IGLC2 PE=1 SV=1 |
| **23.** | LAC3_HUMAN Mass: 11231 Score: 829 Queries matched: 46 emPAI: 3.29 |
| | Ig lambda-3 chain C regions OS=Homo sapiens GN=IGLC3 PE=1 SV=1 |
| **24.** | LAC7_HUMAN Mass: 11296 Score: 826 Queries matched: 41 emPAI: 1.62 |
| | Ig lambda-7 chain C region OS=Homo sapiens GN=IGLC7 PE=1 SV=2 |
| **25.** | ZG16B_HUMAN Mass: 22725 Score: 806 Queries matched: 63 emPAI: 1.07 |
| | Zymogen granule protein 16 homolog B OS=Homo sapiens GN=ZG16B PE=1 SV=3 |
| **26.** | HV305_HUMAN Mass: 13218 Score: 750 Queries matched: 32 emPAI: 0.51 |
| | Ig heavy chain V-III region BRO OS=Homo sapiens PE=1 SV=1 |
| **27.** | HV316_HUMAN Mass: 12794 Score: 750 Queries matched: 32 emPAI: 0.53 |
| | Ig heavy chain V-III region TEI OS=Homo sapiens PE=1 SV=1 |
| **28.** | SG1D1_HUMAN Mass: 9891 Score: 680 Queries matched: 50 emPAI: 2.00 |
| | Secretoglobin family 1D member 1 OS=Homo sapiens GN=SCGB1D1 PE=1 SV=1 |
| **29.** | IGJ_HUMAN Mass: 18087 Score: 677 Queries matched: 43 emPAI: 0.84 |
| | Immunoglobulin J chain OS=Homo sapiens GN=IGJ PE=1 SV=4 |
| **30.** | CLUS_HUMAN Mass: 52461 Score: 527 Queries matched: 34 emPAI: 0.53 |
| | Clusterin OS=Homo sapiens GN=CLU PE=1 SV=1 |

| | |
|---|---|
| **31.** | A2MG_HUMAN Mass: 163189 Score: 507 Queries matched: 45 emPAI: 0.46 |
| | Alpha-2-macroglobulin OS=Homo sapiens GN=A2M PE=1 SV=2 |
| **32.** | IGHG1_HUMAN Mass: 36083 Score: 481 Queries matched: 23 emPAI: 1.94 |
| | Ig gamma-1 chain C region OS=Homo sapiens GN=IGHG1 PE=1 SV=1 |
| **33.** | APOA1_HUMAN Mass: 30759 Score: 425 Queries matched: 43 emPAI: 1.95 |
| | Apolipoprotein A-I OS=Homo sapiens GN=APOA1 PE=1 SV=1 |
| **34.** | CO3_HUMAN Mass: 187030 Score: 383 Queries matched: 74 emPAI: 0.39 |
| | Complement C3 OS=Homo sapiens GN=C3 PE=1 SV=2 |
| **35.** | A1AT_HUMAN Mass: 46707 Score: 340 Queries matched: 24 emPAI: 1.59 |
| | Alpha-1-antitrypsin OS=Homo sapiens GN=SERPINA1 PE=1 SV=3 |
| **36.** | ACTB_HUMAN Mass: 41710 Score: 331 Queries matched: 43 emPAI: 0.70 |
| | Actin, cytoplasmic 1 OS=Homo sapiens GN=ACTB PE=1 SV=1 |
| **37.** | KV302_HUMAN Mass: 11768 Score: 331 Queries matched: 51 emPAI: 1.53 |
| | Ig kappa chain V-III region SIE OS=Homo sapiens PE=1 SV=1 |
| **38.** | K2C1_HUMAN Mass: 65999 Score: 255 Queries matched: 81 emPAI: 0.81 |
| | Keratin, type II cytoskeletal 1 OS=Homo sapiens GN=KRT1 PE=1 SV=6 |
| **39.** | TRFE_HUMAN Mass: 77000 Score: 249 Queries matched: 36 emPAI: 0.24 |
| | Serotransferrin OS=Homo sapiens GN=TF PE=1 SV=2 |
| **40.** | KV301_HUMAN Mass: 11628 Score: 249 Queries matched: 33 emPAI: 0.60 |
| | Ig kappa chain V-III region B6 OS=Homo sapiens PE=1 SV=1 |
| **41.** | POTEF_HUMAN Mass: 121367 Score: 242 Queries matched: 37 emPAI: 0.15 |
| | POTE ankyrin domain family member F OS=Homo sapiens GN=POTEF PE=1 SV=2 |
| **42.** | POTEE_HUMAN Mass: 121286 Score: 242 Queries matched: 36 emPAI: 0.15 |
| | POTE ankyrin domain family member E OS=Homo sapiens GN=POTEE PE=1 SV=3 |
| **43.** | ACTBM_HUMAN Mass: 41989 Score: 241 Queries matched: 25 emPAI: 0.30 |
| | Putative beta-actin-like protein 3 OS=Homo sapiens GN=POTEKP PE=5 SV=1 |
| **44.** | TTHY_HUMAN Mass: 15877 Score: 241 Queries matched: 20 emPAI: 1.82 |
| | Transthyretin OS=Homo sapiens GN=TTR PE=1 SV=1 |
| **45.** | HV318_HUMAN Mass: 12423 Score: 241 Queries matched: 19 emPAI: 0.55 |
| | Ig heavy chain V-III region TUR OS=Homo sapiens PE=1 SV=1 |
| **46.** | HV315_HUMAN Mass: 13082 Score: 241 Queries matched: 19 emPAI: 0.52 |
| | Ig heavy chain V-III region WAS OS=Homo sapiens PE=1 SV=1 |
| **47.** | HV304_HUMAN Mass: 12348 Score: 241 Queries matched: 19 emPAI: 0.56 |
| | Ig heavy chain V-III region TIL OS=Homo sapiens PE=1 SV=1 |
| **48.** | HV313_HUMAN Mass: 12945 Score: 241 Queries matched: 19 emPAI: 0.52 |
| | Ig heavy chain V-III region POM OS=Homo sapiens PE=1 SV=1 |
| **49.** | ACTBL_HUMAN Mass: 41976 Score: 200 Queries matched: 27 emPAI: 0.14 |
| | Beta-actin-like protein 2 OS=Homo sapiens GN=ACTBL2 PE=1 SV=2 |
| **50.** | ZAGL1_HUMAN Mass: 22965 Score: 178 Queries matched: 20 emPAI: 0.62 |
| | Putative zinc-alpha-2-glycoprotein-like 1 OS=Homo sapiens PE=5 SV=2 |
| **51.** | S10A8_HUMAN Mass: 10828 Score: 169 Queries matched: 13 emPAI: 1.72 |
| | Protein S100-A8 OS=Homo sapiens GN=S100A8 PE=1 SV=1 |
| **52.** | EIF2A_HUMAN Mass: 64949 Score: 152 Queries matched: 126 emPAI: 0.09 |
| | Eukaryotic translation initiation factor 2A OS=Homo sapiens GN=EIF2A PE=1 SV=3 |
| **53.** | AIFM2_HUMAN Mass: 40501 Score: 145 Queries matched: 15 emPAI: 0.15 |
| | Apoptosis-inducing factor 2 OS=Homo sapiens GN=AIFM2 PE=2 SV=1 |
| **54.** | IGHM_HUMAN Mass: 49276 Score: 138 Queries matched: 22 emPAI: 0.12 |
| | Ig mu chain C region OS=Homo sapiens GN=IGHM PE=1 SV=3 |
| **55.** | MUCB_HUMAN Mass: 43030 Score: 138 Queries matched: 21 emPAI: 0.14 |
| | Ig mu heavy chain disease protein OS=Homo sapiens PE=1 SV=1 |
| **56.** | ELOA1_HUMAN Mass: 89853 Score: 129 Queries matched: 136 emPAI: 0.06 |
| | Transcription elongation factor B polypeptide 3 OS=Homo sapiens GN=TCEB3 PE=1 SV=2 |
| **57.** | HPT_HUMAN Mass: 45177 Score: 125 Queries matched: 20 emPAI: 0.45 |
| | Haptoglobin OS=Homo sapiens GN=HP PE=1 SV=1 |
| **58.** | HPTR_HUMAN Mass: 39005 Score: 125 Queries matched: 13 emPAI: 0.53 |
| | Haptoglobin-related protein OS=Homo sapiens GN=HPR PE=2 SV=2 |
| **59.** | LAC1_HUMAN Mass: 11341 Score: 122 Queries matched: 19 emPAI: 3.23 |
| | Ig lambda-1 chain C regions OS=Homo sapiens GN=IGLC1 PE=1 SV=1 |
| **60.** | IGHG3_HUMAN Mass: 41260 Score: 108 Queries matched: 16 emPAI: 0.31 |
| | Ig gamma-3 chain C region OS=Homo sapiens GN=IGHG3 PE=1 SV=2 |

| | |
|---|---|
| **61.** | KV312_HUMAN Mass: 14064 Score: 107 Queries matched: 26 emPAI: 0.47 |
| | Ig kappa chain V-III region HAH OS=Homo sapiens PE=2 SV=1 |
| **62.** | IGHG2_HUMAN Mass: 35878 Score: 101 Queries matched: 10 emPAI: 0.17 |
| | Ig gamma-2 chain C region OS=Homo sapiens GN=IGHG2 PE=1 SV=2 |
| **63.** | ABCA3_HUMAN Score: 97 Queries matched: 28 |
| | ATP-binding cassette sub-family A member 3 OS=Homo sapiens GN=ABCA3 PE=1 SV=2 |
| **64.** | K22E_HUMAN Mass: 65393 Score: 94 Queries matched: 51 emPAI: 0.09 |
| | Keratin, type II cytoskeletal 2 epidermal OS=Homo sapiens GN=KRT2 PE=1 SV=2 |
| **65.** | S10A9_HUMAN Mass: 13234 Score: 90 Queries matched: 8 emPAI: 0.51 |
| | Protein S100-A9 OS=Homo sapiens GN=S100A9 PE=1 SV=1 |
| **66.** | HS90B_HUMAN Mass: 83212 Score: 84 Queries matched: 24 emPAI: 0.40 |
| | Heat shock protein HSP 90-beta OS=Homo sapiens GN=HSP90AB1 PE=1 SV=4 |
| **67.** | HBA_HUMAN Mass: 15248 Score: 83 Queries matched: 8 emPAI: 1.06 |
| | Hemoglobin subunit alpha OS=Homo sapiens GN=HBA1 PE=1 SV=2 |
| **68.** | K1C10_HUMAN Mass: 58792 Score: 79 Queries matched: 64 emPAI: 0.33 |
| | Keratin, type I cytoskeletal 10 OS=Homo sapiens GN=KRT10 PE=1 SV=6 |
| **69.** | EF1A2_HUMAN Mass: 50438 Score: 70 Queries matched: 7 emPAI: 0.25 |
| | Elongation factor 1-alpha 2 OS=Homo sapiens GN=EEF1A2 PE=1 SV=1 |
| **70.** | EF1A1_HUMAN Mass: 50109 Score: 70 Queries matched: 8 emPAI: 0.25 |
| | Elongation factor 1-alpha 1 OS=Homo sapiens GN=EEF1A1 PE=1 SV=1 |
| **71.** | HEMO_HUMAN Mass: 51643 Score: 68 Queries matched: 10 emPAI: 0.11 |
| | Hemopexin OS=Homo sapiens GN=HPX PE=1 SV=2 |
| **72.** | K1C9_HUMAN Mass: 62027 Score: 68 Queries matched: 23 emPAI: 0.20 |
| | Keratin, type I cytoskeletal 9 OS=Homo sapiens GN=KRT9 PE=1 SV=3 |
| **73.** | KV105_HUMAN Mass: 11654 Score: 66 Queries matched: 2 emPAI: 0.60 |
| | Ig kappa chain V-I region DEE OS=Homo sapiens PE=1 SV=1 |
| **74.** | H90B2_HUMAN Score: 66 Queries matched: 3 |
| | Putative heat shock protein HSP 90-beta 2 OS=Homo sapiens GN=HSP90AB2P PE=1 SV=2 |
| **75.** | POTEI_HUMAN Mass: 121205 Score: 65 Queries matched: 21 emPAI: 0.10 |
| | POTE ankyrin domain family member I OS=Homo sapiens GN=POTEI PE=3 SV=1 |
| **76.** | ENOG_HUMAN Mass: 47239 Score: 64 Queries matched: 16 emPAI: 0.13 |
| | Gamma-enolase OS=Homo sapiens GN=ENO2 PE=1 SV=3 |
| **77.** | ENOA_HUMAN Mass: 47139 Score: 64 Queries matched: 13 emPAI: 0.13 |
| | Alpha-enolase OS=Homo sapiens GN=ENO1 PE=1 SV=2 |
| **78.** | ENOB_HUMAN Mass: 46902 Score: 64 Queries matched: 9 emPAI: 0.13 |
| | Beta-enolase OS=Homo sapiens GN=ENO3 PE=1 SV=4 |
| **79.** | POTEJ_HUMAN Mass: 117315 Score: 63 Queries matched: 23 emPAI: 0.05 |
| | POTE ankyrin domain family member J OS=Homo sapiens GN=POTEJ PE=3 SV=1 |
| **80.** | NGAL_HUMAN Mass: 22574 Score: 62 Queries matched: 12 emPAI: 0.63 |
| | Neutrophil gelatinase-associated lipocalin OS=Homo sapiens GN=LCN2 PE=1 SV=2 |
| **81.** | SMCA4_HUMAN Mass: 184530 Score: 59 Queries matched: 74 emPAI: 0.03 |
| | Transcription activator BRG1 OS=Homo sapiens GN=SMARCA4 PE=1 SV=2 |
| **82.** | RRBP1_HUMAN Mass: 152381 Score: 59 Queries matched: 139 emPAI: 0.04 |
| | Ribosome-binding protein 1 OS=Homo sapiens GN=RRBP1 PE=1 SV=4 |
| **83.** | HV310_HUMAN Mass: 13557 Score: 57 Queries matched: 11 emPAI: 0.50 |
| | Ig heavy chain V-III region HIL OS=Homo sapiens PE=1 SV=1 |
| **84.** | A1AG1_HUMAN Mass: 23497 Score: 56 Queries matched: 3 emPAI: 0.26 |
| | Alpha-1-acid glycoprotein 1 OS=Homo sapiens GN=ORM1 PE=1 SV=1 |
| **85.** | KV101_HUMAN Mass: 11985 Score: 54 Queries matched: 4 emPAI: 0.58 |
| | Ig kappa chain V-I region AG OS=Homo sapiens PE=1 SV=1 |
| **86.** | KV118_HUMAN Mass: 11833 Score: 54 Queries matched: 3 emPAI: 0.58 |
| | Ig kappa chain V-I region WEA OS=Homo sapiens PE=1 SV=1 |
| **87.** | NCKP5_HUMAN Mass: 208409 Score: 53 Queries matched: 27 emPAI: 0.03 |
| | Nck-associated protein 5 OS=Homo sapiens GN=NCKAP5 PE=1 SV=2 |
| **88.** | LV403_HUMAN Mass: 11510 Score: 53 Queries matched: 4 emPAI: 0.60 |
| | Ig lambda chain V-IV region Hil OS=Homo sapiens PE=1 SV=1 |
| **89.** | MECP2_HUMAN Score: 53 Queries matched: 24 |
| | Methyl-CpG-binding protein 2 OS=Homo sapiens GN=MECP2 PE=1 SV=1 |
| **90.** | GSTCD_HUMAN Mass: 71033 Score: 52 Queries matched: 20 emPAI: 0.08 |
| | Glutathione S-transferase C-terminal domain-containing protein OS=Homo sapiens GN=GSTCD PE=1 SV= |

| | |
|---|---|
| **91.** | IGHG4_HUMAN Mass: 35918 Score: 51 Queries matched: 9 emPAI: 0.36 |
| | Ig gamma-4 chain C region OS=Homo sapiens GN=IGHG4 PE=1 SV=1 |
| **92.** | CO4A_HUMAN Mass: 192650 Score: 50 Queries matched: 20 emPAI: 0.03 |
| | Complement C4-A OS=Homo sapiens GN=C4A PE=1 SV=1 |
| **93.** | K2C5_HUMAN Mass: 62340 Score: 50 Queries matched: 15 emPAI: 0.09 |
| | Keratin, type II cytoskeletal 5 OS=Homo sapiens GN=KRT5 PE=1 SV=3 |
| **94.** | PATZ1_HUMAN Mass: 74013 Score: 49 Queries matched: 35 emPAI: 0.08 |
| | POZ-, AT hook-, and zinc finger-containing protein 1 OS=Homo sapiens GN=PATZ1 PE=1 SV=1 |
| **95.** | CE164_HUMAN Mass: 164214 Score: 48 Queries matched: 26 emPAI: 0.07 |
| | Centrosomal protein of 164 kDa OS=Homo sapiens GN=CEP164 PE=1 SV=3 |
| **96.** | PA2GA_HUMAN Mass: 16072 Score: 47 Queries matched: 10 emPAI: 0.41 |
| | Phospholipase A2, membrane associated OS=Homo sapiens GN=PLA2G2A PE=1 SV=2 |
| **97.** | NOTC4_HUMAN Mass: 209480 Score: 46 Queries matched: 31 emPAI: 0.03 |
| | Neurogenic locus notch homolog protein 4 OS=Homo sapiens GN=NOTCH4 PE=1 SV=2 |
| **98.** | KCNU1_HUMAN Score: 45 Queries matched: 27 |
| | Potassium channel subfamily U member 1 OS=Homo sapiens GN=KCNU1 PE=2 SV=2 |
| **99.** | RXFP2_HUMAN Mass: 86396 Score: 43 Queries matched: 4 emPAI: 0.07 |
| | Relaxin receptor 2 OS=Homo sapiens GN=RXFP2 PE=1 SV=1 |
| **100.** | A1AG2_HUMAN Mass: 23588 Score: 43 Queries matched: 4 emPAI: 0.26 |
| | Alpha-1-acid glycoprotein 2 OS=Homo sapiens GN=ORM2 PE=1 SV=2 |
| **101.** | SSH2_HUMAN Mass: 158116 Score: 43 Queries matched: 20 emPAI: 0.04 |
| | Protein phosphatase Slingshot homolog 2 OS=Homo sapiens GN=SSH2 PE=1 SV=1 |
| **102.** | CT194_HUMAN Mass: 132202 Score: 43 Queries matched: 30 emPAI: 0.04 |
| | Uncharacterized protein C20orf194 OS=Homo sapiens GN=C20orf194 PE=2 SV=1 |
| **103.** | HV319_HUMAN Mass: 12555 Score: 43 Queries matched: 6 emPAI: 0.55 |
| | Ig heavy chain V-III region JON OS=Homo sapiens PE=1 SV=1 |
| **104.** | SPIR2_HUMAN Mass: 79620 Score: 42 Queries matched: 25 emPAI: 0.07 |
| | Protein spire homolog 2 OS=Homo sapiens GN=SPIRE2 PE=1 SV=3 |
| **105.** | LRC4C_HUMAN Score: 41 Queries matched: 13 |
| | Leucine-rich repeat-containing protein 4C OS=Homo sapiens GN=LRRC4C PE=1 SV=1 |
| **106.** | COBA2_HUMAN Mass: 171670 Score: 40 Queries matched: 44 emPAI: 0.03 |
| | Collagen alpha-2(XI) chain OS=Homo sapiens GN=COL11A2 PE=1 SV=4 |
| **107.** | POP1_HUMAN Mass: 114636 Score: 40 Queries matched: 36 emPAI: 0.05 |
| | Ribonucleases P/MRP protein subunit POP1 OS=Homo sapiens GN=POP1 PE=1 SV=2 |
| **108.** | DPOLN_HUMAN Mass: 100244 Score: 39 Queries matched: 20 emPAI: 0.06 |
| | DNA polymerase nu OS=Homo sapiens GN=POLN PE=1 SV=2 |
| **109.** | AMBP_HUMAN Score: 39 Queries matched: 61 |
| | Protein AMBP OS=Homo sapiens GN=AMBP PE=1 SV=1 |
| **110.** | CERU_HUMAN Mass: 122128 Score: 39 Queries matched: 23 emPAI: 0.10 |
| | Ceruloplasmin OS=Homo sapiens GN=CP PE=1 SV=1 |
| **111.** | HV307_HUMAN Mass: 13659 Score: 38 Queries matched: 26 emPAI: 1.23 |
| | Ig heavy chain V-III region CAM OS=Homo sapiens PE=1 SV=1 |
| **112.** | K2C4_HUMAN Mass: 57250 Score: 37 Queries matched: 26 emPAI: 0.22 |
| | Keratin, type II cytoskeletal 4 OS=Homo sapiens GN=KRT4 PE=1 SV=4 |
| **113.** | FIBB_HUMAN Mass: 55892 Score: 37 Queries matched: 7 emPAI: 0.10 |
| | Fibrinogen beta chain OS=Homo sapiens GN=FGB PE=1 SV=2 |
| **114.** | ANXA1_HUMAN Mass: 38690 Score: 37 Queries matched: 4 emPAI: 0.15 |
| | Annexin A1 OS=Homo sapiens GN=ANXA1 PE=1 SV=2 |
| **115.** | TTL11_HUMAN Score: 37 Queries matched: 71 |
| | Tubulin polyglutamylase TTLL11 OS=Homo sapiens GN=TTLL11 PE=2 SV=1 |
| **116.** | CENPE_HUMAN Mass: 316219 Score: 37 Queries matched: 73 emPAI: 0.02 |
| | Centromere-associated protein E OS=Homo sapiens GN=CENPE PE=1 SV=2 |
| **117.** | RGPA2_HUMAN Mass: 210636 Score: 37 Queries matched: 120 emPAI: 0.03 |
| | Ral GTPase-activating protein subunit alpha-2 OS=Homo sapiens GN=RALGAPA2 PE=1 SV=2 |
| **118.** | E41LA_HUMAN Mass: 79010 Score: 36 Queries matched: 27 emPAI: 0.07 |
| | Band 4.1-like protein 4A OS=Homo sapiens GN=EPB41L4A PE=1 SV=2 |
| **119.** | FGD6_HUMAN Mass: 160715 Score: 36 Queries matched: 39 emPAI: 0.04 |
| | FYVE, RhoGEF and PH domain-containing protein 6 OS=Homo sapiens GN=FGD6 PE=1 SV=2 |
| **120.** | KLH34_HUMAN Mass: 70568 Score: 36 Queries matched: 32 emPAI: 0.08 |
| | Kelch-like protein 34 OS=Homo sapiens GN=KLHL34 PE=2 SV=1 |

| | |
|---|---|
| **121.** | SPYA_HUMAN Mass: 42982 Score: 36 Queries matched: 46 emPAI: 0.14 |
| | Serine--pyruvate aminotransferase OS=Homo sapiens GN=AGXT PE=1 SV=1 |
| **122.** | TBA1A_HUMAN Mass: 50104 Score: 36 Queries matched: 14 emPAI: 0.25 |
| | Tubulin alpha-1A chain OS=Homo sapiens GN=TUBA1A PE=1 SV=1 |
| **123.** | HMGN2_HUMAN Mass: 9387 Score: 36 Queries matched: 1 emPAI: 0.77 |
| | Non-histone chromosomal protein HMG-17 OS=Homo sapiens GN=HMGN2 PE=1 SV=3 |
| **124.** | ZFAN1_HUMAN Score: 35 Queries matched: 17 |
| | AN1-type zinc finger protein 1 OS=Homo sapiens GN=ZFAND1 PE=1 SV=1 |
| **125.** | BEST1_HUMAN Mass: 67640 Score: 35 Queries matched: 9 emPAI: 0.09 |
| | Bestrophin-1 OS=Homo sapiens GN=BEST1 PE=1 SV=1 |
| **126.** | TLR4_HUMAN Mass: 95619 Score: 35 Queries matched: 23 emPAI: 0.06 |
| | Toll-like receptor 4 OS=Homo sapiens GN=TLR4 PE=1 SV=2 |
| **127.** | NAV2_HUMAN Mass: 267969 Score: 35 Queries matched: 60 emPAI: 0.02 |
| | Neuron navigator 2 OS=Homo sapiens GN=NAV2 PE=1 SV=2 |
| **128.** | SIRT6_HUMAN Mass: 39094 Score: 34 Queries matched: 39 emPAI: 0.15 |
| | NAD-dependent deacetylase sirtuin-6 OS=Homo sapiens GN=SIRT6 PE=1 SV=2 |
| **129.** | MDGA1_HUMAN Mass: 105724 Score: 34 Queries matched: 37 emPAI: 0.05 |
| | MAM domain-containing glycosylphosphatidylinositol anchor protein 1 OS=Homo sapiens GN=MDGA1 PE=1 |
| **130.** | TUB_HUMAN Mass: 55617 Score: 34 Queries matched: 17 emPAI: 0.11 |
| | Tubby protein homolog OS=Homo sapiens GN=TUB PE=1 SV=1 |
| **131.** | K2C73_HUMAN Mass: 58887 Score: 34 Queries matched: 11 emPAI: 0.10 |
| | Keratin, type II cytoskeletal 73 OS=Homo sapiens GN=KRT73 PE=1 SV=1 |
| **132.** | H15_HUMAN Mass: 22566 Score: 34 Queries matched: 3 emPAI: 0.28 |
| | Histone H1.5 OS=Homo sapiens GN=HIST1H1B PE=1 SV=3 |
| **133.** | DEF6_HUMAN Mass: 10968 Score: 34 Queries matched: 6 emPAI: 0.64 |
| | Defensin-6 OS=Homo sapiens GN=DEFA6 PE=1 SV=1 |
| **134.** | URB2_HUMAN Mass: 170435 Score: 34 Queries matched: 49 emPAI: 0.03 |
| | Unhealthy ribosome biogenesis protein 2 homolog OS=Homo sapiens GN=URB2 PE=1 SV=2 |
| **135.** | CP059_HUMAN Mass: 46373 Score: 34 Queries matched: 12 emPAI: 0.13 |
| | Uncharacterized protein C16orf59 OS=Homo sapiens GN=C16orf59 PE=2 SV=1 |
| **136.** | SPA9_HUMAN Mass: 46527 Score: 34 Queries matched: 20 emPAI: 0.13 |
| | Serpin A9 OS=Homo sapiens GN=SERPINA9 PE=1 SV=3 |
| **137.** | FIBG_HUMAN Mass: 51479 Score: 34 Queries matched: 9 emPAI: 0.24 |
| | Fibrinogen gamma chain OS=Homo sapiens GN=FGG PE=1 SV=3 |
| **138.** | CIC_HUMAN Mass: 163719 Score: 34 Queries matched: 15 emPAI: 0.03 |
| | Protein capicua homolog OS=Homo sapiens GN=CIC PE=1 SV=2 |
| **139.** | CAPON_HUMAN Mass: 56115 Score: 34 Queries matched: 12 emPAI: 0.10 |
| | Carboxyl-terminal PDZ ligand of neuronal nitric oxide synthase protein OS=Homo sapiens GN=NOS1AP PE |
| **140.** | CLCA_HUMAN Mass: 27060 Score: 33 Queries matched: 27 emPAI: 0.23 |
| | Clathrin light chain A OS=Homo sapiens GN=CLTA PE=1 SV=1 |
| **141.** | MCCB_HUMAN Mass: 61294 Score: 33 Queries matched: 57 emPAI: 0.10 |
| | Methylcrotonoyl-CoA carboxylase beta chain, mitochondrial OS=Homo sapiens GN=MCCC2 PE=1 SV=1 |
| **142.** | PDE12_HUMAN Score: 33 Queries matched: 14 |
| | 2',5'-phosphodiesterase 12 OS=Homo sapiens GN=PDE12 PE=1 SV=2 |
| **143.** | HSPB1_HUMAN Mass: 22768 Score: 33 Queries matched: 8 emPAI: 0.63 |
| | Heat shock protein beta-1 OS=Homo sapiens GN=HSPB1 PE=1 SV=2 |
| **144.** | KI26A_HUMAN Mass: 194468 Score: 33 Queries matched: 93 emPAI: 0.03 |
| | Kinesin-like protein KIF26A OS=Homo sapiens GN=KIF26A PE=1 SV=3 |
| **145.** | CH60_HUMAN Mass: 61016 Score: 33 Queries matched: 15 emPAI: 0.10 |
| | 60 kDa heat shock protein, mitochondrial OS=Homo sapiens GN=HSPD1 PE=1 SV=2 |
| **146.** | PSME4_HUMAN Mass: 211199 Score: 33 Queries matched: 17 emPAI: 0.03 |
| | Proteasome activator complex subunit 4 OS=Homo sapiens GN=PSME4 PE=1 SV=2 |
| **147.** | KIF17_HUMAN Mass: 115043 Score: 33 Queries matched: 19 emPAI: 0.05 |
| | Kinesin-like protein KIF17 OS=Homo sapiens GN=KIF17 PE=1 SV=2 |
| **148.** | USP9Y_HUMAN Mass: 290891 Score: 33 Queries matched: 49 emPAI: 0.02 |
| | Probable ubiquitin carboxyl-terminal hydrolase FAF-Y OS=Homo sapiens GN=USP9Y PE=1 SV=2 |
| **149.** | GPTC4_HUMAN Mass: 50351 Score: 33 Queries matched: 18 emPAI: 0.12 |
| | G patch domain-containing protein 4 OS=Homo sapiens GN=GPATCH4 PE=1 SV=2 |
| **150.** | RSF1_HUMAN Mass: 163720 Score: 33 Queries matched: 33 emPAI: 0.03 |
| | Remodeling and spacing factor 1 OS=Homo sapiens GN=RSF1 PE=1 SV=2 |

| | |
|---|---|
| **151.** | USP9X_HUMAN Mass: 289356 Score: 33 Queries matched: 52 emPAI: 0.04 |
| | Probable ubiquitin carboxyl-terminal hydrolase FAF-X OS=Homo sapiens GN=USP9X PE=1 SV=2 |
| **152.** | LPHN3_HUMAN Mass: 161710 Score: 32 Queries matched: 32 emPAI: 0.04 |
| | Latrophilin-3 OS=Homo sapiens GN=LPHN3 PE=1 SV=2 |
| **153.** | HSP7C_HUMAN Mass: 70854 Score: 32 Queries matched: 14 emPAI: 0.08 |
| | Heat shock cognate 71 kDa protein OS=Homo sapiens GN=HSPA8 PE=1 SV=1 |
| **154.** | HSP72_HUMAN Mass: 69978 Score: 32 Queries matched: 8 emPAI: 0.08 |
| | Heat shock-related 70 kDa protein 2 OS=Homo sapiens GN=HSPA2 PE=1 SV=1 |
| **155.** | SNED1_HUMAN Mass: 152104 Score: 32 Queries matched: 36 emPAI: 0.04 |
| | Sushi, nidogen and EGF-like domain-containing protein 1 OS=Homo sapiens GN=SNED1 PE=1 SV=2 |
| **156.** | DPYL1_HUMAN Score: 32 Queries matched: 5 |
| | Dihydropyrimidinase-related protein 1 OS=Homo sapiens GN=CRMP1 PE=1 SV=1 |
| **157.** | TIFA_HUMAN Mass: 21431 Score: 32 Queries matched: 1 emPAI: 0.29 |
| | TRAF-interacting protein with FHA domain-containing protein A OS=Homo sapiens GN=TIFA PE=1 SV=1 |
| **158.** | SCLT1_HUMAN Mass: 80861 Score: 32 Queries matched: 17 emPAI: 0.07 |
| | Sodium channel and clathrin linker 1 OS=Homo sapiens GN=SCLT1 PE=1 SV=2 |
| **159.** | RRP5_HUMAN Mass: 208570 Score: 32 Queries matched: 46 emPAI: 0.06 |
| | Protein RRP5 homolog OS=Homo sapiens GN=PDCD11 PE=1 SV=3 |
| **160.** | PGBM_HUMAN Mass: 468501 Score: 32 Queries matched: 58 emPAI: 0.05 |
| | Basement membrane-specific heparan sulfate proteoglycan core protein OS=Homo sapiens GN=HSPG2 P |
| **161.** | WDFY3_HUMAN Mass: 395006 Score: 32 Queries matched: 65 emPAI: 0.03 |
| | WD repeat and FYVE domain-containing protein 3 OS=Homo sapiens GN=WDFY3 PE=1 SV=2 |
| **162.** | CSPP1_HUMAN Mass: 141736 Score: 31 Queries matched: 19 emPAI: 0.04 |
| | Centrosome and spindle pole-associated protein 1 OS=Homo sapiens GN=CSPP1 PE=1 SV=3 |
| **163.** | RL31_HUMAN Mass: 14454 Score: 31 Queries matched: 31 emPAI: 0.46 |
| | 60S ribosomal protein L31 OS=Homo sapiens GN=RPL31 PE=1 SV=1 |
| **164.** | MCR_HUMAN Mass: 106999 Score: 31 Queries matched: 15 emPAI: 0.05 |
| | Mineralocorticoid receptor OS=Homo sapiens GN=NR3C2 PE=1 SV=1 |
| **165.** | K1C28_HUMAN Mass: 50536 Score: 31 Queries matched: 24 emPAI: 0.12 |
| | Keratin, type I cytoskeletal 28 OS=Homo sapiens GN=KRT28 PE=1 SV=2 |
| **166.** | FSIP2_HUMAN Mass: 780119 Score: 31 Queries matched: 134 emPAI: 0.01 |
| | Fibrous sheath-interacting protein 2 OS=Homo sapiens GN=FSIP2 PE=1 SV=4 |
| **167.** | HS90A_HUMAN Mass: 84607 Score: 31 Queries matched: 14 emPAI: 0.14 |
| | Heat shock protein HSP 90-alpha OS=Homo sapiens GN=HSP90AA1 PE=1 SV=5 |
| **168.** | UACA_HUMAN Mass: 162404 Score: 31 Queries matched: 44 emPAI: 0.04 |
| | Uveal autoantigen with coiled-coil domains and ankyrin repeats OS=Homo sapiens GN=UACA PE=1 SV=2 |
| **169.** | GLDN_HUMAN Mass: 58920 Score: 31 Queries matched: 20 emPAI: 0.10 |
| | Gliomedin OS=Homo sapiens GN=GLDN PE=2 SV=1 |
| **170.** | PRAML_HUMAN Mass: 58127 Score: 31 Queries matched: 6 emPAI: 0.10 |
| | Leucine-rich repeat-containing protein PRAME-like OS=Homo sapiens GN=PRAMEL PE=2 SV=2 |
| **171.** | DGKK_HUMAN Mass: 141739 Score: 31 Queries matched: 47 emPAI: 0.04 |
| | Diacylglycerol kinase kappa OS=Homo sapiens GN=DGKK PE=1 SV=1 |
| **172.** | CP057_HUMAN Score: 31 Queries matched: 5 |
| | UPF0406 protein C16orf57 OS=Homo sapiens GN=C16orf57 PE=1 SV=1 |
| **173.** | WNK2_HUMAN Mass: 242525 Score: 31 Queries matched: 25 emPAI: 0.02 |
| | Serine/threonine-protein kinase WNK2 OS=Homo sapiens GN=WNK2 PE=1 SV=4 |
| **174.** | K2C7_HUMAN Mass: 51373 Score: 31 Queries matched: 39 emPAI: 0.11 |
| | Keratin, type II cytoskeletal 7 OS=Homo sapiens GN=KRT7 PE=1 SV=4 |
| **175.** | K2C8_HUMAN Mass: 53671 Score: 31 Queries matched: 17 emPAI: 0.11 |
| | Keratin, type II cytoskeletal 8 OS=Homo sapiens GN=KRT8 PE=1 SV=7 |
| **176.** | GFAP_HUMAN Mass: 49850 Score: 31 Queries matched: 42 emPAI: 0.12 |
| | Glial fibrillary acidic protein OS=Homo sapiens GN=GFAP PE=1 SV=1 |
| **177.** | K2C80_HUMAN Mass: 50494 Score: 31 Queries matched: 9 emPAI: 0.12 |
| | Keratin, type II cytoskeletal 80 OS=Homo sapiens GN=KRT80 PE=1 SV=2 |
| **178.** | CI14B_HUMAN Mass: 148003 Score: 31 Queries matched: 27 emPAI: 0.04 |
| | Transmembrane protein C9orf144B OS=Homo sapiens GN=C9orf144B PE=2 SV=4 |
| **179.** | TRAK2_HUMAN Mass: 101356 Score: 30 Queries matched: 14 emPAI: 0.06 |
| | Trafficking kinesin-binding protein 2 OS=Homo sapiens GN=TRAK2 PE=1 SV=2 |
| **180.** | COE4_HUMAN Mass: 64433 Score: 30 Queries matched: 5 emPAI: 0.09 |
| | Transcription factor COE4 OS=Homo sapiens GN=EBF4 PE=2 SV=2 |

| | |
|---|---|
| **181.** | SPTA2_HUMAN Mass: 284364 Score: 30 Queries matched: 36 emPAI: 0.02 |
| | Spectrin alpha chain, brain OS=Homo sapiens GN=SPTAN1 PE=1 SV=3 |
| **182.** | GA2L2_HUMAN Mass: 96460 Score: 30 Queries matched: 48 emPAI: 0.06 |
| | GAS2-like protein 2 OS=Homo sapiens GN=GAS2L2 PE=2 SV=1 |
| **183.** | FBX37_HUMAN Mass: 32977 Score: 30 Queries matched: 25 emPAI: 0.18 |
| | F-box only protein 37 OS=Homo sapiens GN=FBXL15 PE=2 SV=2 |
| **184.** | CP4Z1_HUMAN Mass: 59048 Score: 30 Queries matched: 7 emPAI: 0.10 |
| | Cytochrome P450 4Z1 OS=Homo sapiens GN=CYP4Z1 PE=2 SV=1 |
| **185.** | TR112_HUMAN Mass: 14190 Score: 30 Queries matched: 12 emPAI: 0.47 |
| | tRNA methyltransferase 112 homolog OS=Homo sapiens GN=TRMT112 PE=1 SV=1 |
| **186.** | LAMA3_HUMAN Mass: 366414 Score: 30 Queries matched: 48 emPAI: 0.03 |
| | Laminin subunit alpha-3 OS=Homo sapiens GN=LAMA3 PE=1 SV=2 |
| **187.** | DMXL2_HUMAN Score: 30 Queries matched: 40 |
| | DmX-like protein 2 OS=Homo sapiens GN=DMXL2 PE=1 SV=2 |
| **188.** | PHS2_HUMAN Mass: 14356 Score: 30 Queries matched: 5 emPAI: 0.47 |
| | Pterin-4-alpha-carbinolamine dehydratase 2 OS=Homo sapiens GN=PCBD2 PE=1 SV=4 |
| **189.** | ZN536_HUMAN Mass: 141328 Score: 30 Queries matched: 7 emPAI: 0.04 |
| | Zinc finger protein 536 OS=Homo sapiens GN=ZNF536 PE=1 SV=3 |
| **190.** | ASPM_HUMAN Mass: 409540 Score: 30 Queries matched: 70 emPAI: 0.01 |
| | Abnormal spindle-like microcephaly-associated protein OS=Homo sapiens GN=ASPM PE=1 SV=2 |
| **191.** | ZBTB6_HUMAN Score: 30 Queries matched: 10 |
| | Zinc finger and BTB domain-containing protein 6 OS=Homo sapiens GN=ZBTB6 PE=2 SV=1 |
| **192.** | SEM3F_HUMAN Mass: 88325 Score: 30 Queries matched: 29 emPAI: 0.07 |
| | Semaphorin-3F OS=Homo sapiens GN=SEMA3F PE=2 SV=2 |
| **193.** | IDH3A_HUMAN Mass: 39566 Score: 30 Queries matched: 9 emPAI: 0.15 |
| | Isocitrate dehydrogenase [NAD] subunit alpha, mitochondrial OS=Homo sapiens GN=IDH3A PE=1 SV=1 |
| **194.** | LRC49_HUMAN Mass: 78845 Score: 30 Queries matched: 62 emPAI: 0.07 |
| | Leucine-rich repeat-containing protein 49 OS=Homo sapiens GN=LRRC49 PE=2 SV=2 |
| **195.** | M4K4_HUMAN Mass: 142013 Score: 30 Queries matched: 21 emPAI: 0.04 |
| | Mitogen-activated protein kinase kinase kinase kinase 4 OS=Homo sapiens GN=MAP4K4 PE=1 SV=2 |
| **196.** | KI67_HUMAN Mass: 358474 Score: 30 Queries matched: 78 emPAI: 0.02 |
| | Antigen KI-67 OS=Homo sapiens GN=MKI67 PE=1 SV=2 |
| **197.** | YM012_HUMAN Mass: 59375 Score: 30 Queries matched: 55 emPAI: 0.10 |
| | Uncharacterized protein DKFZp434B061 OS=Homo sapiens PE=2 SV=2 |
| **198.** | YV021_HUMAN Mass: 30934 Score: 30 Queries matched: 48 emPAI: 0.20 |
| | Uncharacterized protein LOC284861 OS=Homo sapiens PE=2 SV=1 |
| **199.** | MRGRD_HUMAN Mass: 36094 Score: 30 Queries matched: 47 emPAI: 0.17 |
| | Mas-related G-protein coupled receptor member D OS=Homo sapiens GN=MRGPRD PE=2 SV=1 |
| **200.** | HV320_HUMAN Mass: 12722 Score: 30 Queries matched: 5 emPAI: 0.53 |
| | Ig heavy chain V-III region GAL OS=Homo sapiens PE=1 SV=1 |
| **201.** | KIF7_HUMAN Mass: 150495 Score: 30 Queries matched: 47 emPAI: 0.04 |
| | Kinesin-like protein KIF7 OS=Homo sapiens GN=KIF7 PE=1 SV=2 |
| **202.** | MDN1_HUMAN Mass: 632420 Score: 30 Queries matched: 90 emPAI: 0.01 |
| | Midasin OS=Homo sapiens GN=MDN1 PE=1 SV=2 |
| **203.** | RN150_HUMAN Mass: 48041 Score: 29 Queries matched: 5 emPAI: 0.12 |
| | RING finger protein 150 OS=Homo sapiens GN=RNF150 PE=2 SV=2 |
| **204.** | CA195_HUMAN Score: 29 Queries matched: 22 |
| | Putative uncharacterized protein C1orf195 OS=Homo sapiens GN=C1orf195 PE=2 SV=1 |
| **205.** | CCKN_HUMAN Mass: 12661 Score: 29 Queries matched: 3 emPAI: 0.54 |
| | Cholecystokinin OS=Homo sapiens GN=CCK PE=1 SV=1 |
| **206.** | IRS1_HUMAN Mass: 131509 Score: 29 Queries matched: 28 emPAI: 0.04 |
| | Insulin receptor substrate 1 OS=Homo sapiens GN=IRS1 PE=1 SV=1 |
| **207.** | CHD7_HUMAN Mass: 335717 Score: 29 Queries matched: 47 emPAI: 0.02 |
| | Chromodomain-helicase-DNA-binding protein 7 OS=Homo sapiens GN=CHD7 PE=1 SV=3 |
| **208.** | SUCR1_HUMAN Mass: 38672 Score: 29 Queries matched: 27 emPAI: 0.15 |
| | Succinate receptor 1 OS=Homo sapiens GN=SUCNR1 PE=1 SV=2 |
| **209.** | FLRT1_HUMAN Mass: 71313 Score: 29 Queries matched: 11 emPAI: 0.08 |
| | Leucine-rich repeat transmembrane protein FLRT1 OS=Homo sapiens GN=FLRT1 PE=1 SV=3 |
| **210.** | PTC1_HUMAN Mass: 160442 Score: 29 Queries matched: 14 emPAI: 0.04 |
| | Protein patched homolog 1 OS=Homo sapiens GN=PTCH1 PE=1 SV=2 |

| | |
|---|---|
| **211.** | FBXW8_HUMAN Mass: 67352 Score: 29 Queries matched: 32 emPAI: 0.09 |
| | F-box/WD repeat-containing protein 8 OS=Homo sapiens GN=FBXW8 PE=1 SV=2 |
| **212.** | AINX_HUMAN Score: 29 Queries matched: 7 |
| | Alpha-internexin OS=Homo sapiens GN=INA PE=1 SV=2 |
| **213.** | TRIB1_HUMAN Mass: 40983 Score: 29 Queries matched: 24 emPAI: 0.15 |
| | Tribbles homolog 1 OS=Homo sapiens GN=TRIB1 PE=1 SV=2 |
| **214.** | DIP2C_HUMAN Mass: 170658 Score: 29 Queries matched: 19 emPAI: 0.03 |
| | Disco-interacting protein 2 homolog C OS=Homo sapiens GN=DIP2C PE=2 SV=2 |
| **215.** | WRIP1_HUMAN Mass: 72088 Score: 29 Queries matched: 13 emPAI: 0.08 |
| | ATPase WRNIP1 OS=Homo sapiens GN=WRNIP1 PE=1 SV=2 |
| **216.** | GELS_HUMAN Mass: 85644 Score: 29 Queries matched: 13 emPAI: 0.07 |
| | Gelsolin OS=Homo sapiens GN=GSN PE=1 SV=1 |
| **217.** | AL8A1_HUMAN Mass: 53367 Score: 29 Queries matched: 9 emPAI: 0.11 |
| | Aldehyde dehydrogenase family 8 member A1 OS=Homo sapiens GN=ALDH8A1 PE=1 SV=1 |
| **218.** | SYCP3_HUMAN Mass: 27711 Score: 29 Queries matched: 9 emPAI: 0.22 |
| | Synaptonemal complex protein 3 OS=Homo sapiens GN=SYCP3 PE=2 SV=1 |
| **219.** | ZC11A_HUMAN Mass: 89076 Score: 29 Queries matched: 17 emPAI: 0.06 |
| | Zinc finger CCCH domain-containing protein 11A OS=Homo sapiens GN=ZC3H11A PE=1 SV=3 |
| **220.** | CT096_HUMAN Mass: 42832 Score: 29 Queries matched: 10 emPAI: 0.14 |
| | Uncharacterized protein C20orf96 OS=Homo sapiens GN=C20orf96 PE=2 SV=2 |
| **221.** | ZF161_HUMAN Mass: 50924 Score: 28 Queries matched: 5 emPAI: 0.12 |
| | Zinc finger protein 161 homolog OS=Homo sapiens GN=ZFP161 PE=2 SV=2 |
| **222.** | NPA1P_HUMAN Mass: 254227 Score: 28 Queries matched: 19 emPAI: 0.02 |
| | Nucleolar pre-ribosomal-associated protein 1 OS=Homo sapiens GN=URB1 PE=1 SV=4 |
| **223.** | WBS22_HUMAN Score: 28 Queries matched: 8 |
| | Uncharacterized methyltransferase WBSCR22 OS=Homo sapiens GN=WBSCR22 PE=1 SV=2 |
| **224.** | CHST3_HUMAN Mass: 54671 Score: 28 Queries matched: 15 emPAI: 0.11 |
| | Carbohydrate sulfotransferase 3 OS=Homo sapiens GN=CHST3 PE=1 SV=3 |
| **225.** | K1C23_HUMAN Mass: 48101 Score: 28 Queries matched: 21 emPAI: 0.12 |
| | Keratin, type I cytoskeletal 23 OS=Homo sapiens GN=KRT23 PE=1 SV=2 |
| **226.** | PF21B_HUMAN Mass: 57419 Score: 28 Queries matched: 8 emPAI: 0.10 |
| | PHD finger protein 21B OS=Homo sapiens GN=PHF21B PE=2 SV=1 |
| **227.** | NCK2_HUMAN Mass: 42889 Score: 28 Queries matched: 29 emPAI: 0.14 |
| | Cytoplasmic protein NCK2 OS=Homo sapiens GN=NCK2 PE=1 SV=2 |
| **228.** | FZD8_HUMAN Mass: 73252 Score: 28 Queries matched: 10 emPAI: 0.08 |
| | Frizzled-8 OS=Homo sapiens GN=FZD8 PE=1 SV=1 |
| **229.** | FANCJ_HUMAN Mass: 140789 Score: 28 Queries matched: 62 emPAI: 0.04 |
| | Fanconi anemia group J protein OS=Homo sapiens GN=BRIP1 PE=1 SV=1 |
| **230.** | ANT3_HUMAN Mass: 52569 Score: 28 Queries matched: 6 emPAI: 0.11 |
| | Antithrombin-III OS=Homo sapiens GN=SERPINC1 PE=1 SV=1 |
| **231.** | VIP2_HUMAN Mass: 140318 Score: 28 Queries matched: 23 emPAI: 0.04 |
| | Inositol hexakisphosphate and diphosphoinositol-pentakisphosphate kinase 2 OS=Homo sapiens GN=PPIP5 |
| **232.** | SMC3_HUMAN Mass: 141454 Score: 28 Queries matched: 21 emPAI: 0.04 |
| | Structural maintenance of chromosomes protein 3 OS=Homo sapiens GN=SMC3 PE=1 SV=2 |
| **233.** | CF132_HUMAN Mass: 124016 Score: 28 Queries matched: 119 emPAI: 0.05 |
| | Uncharacterized protein C6orf132 OS=Homo sapiens GN=C6orf132 PE=1 SV=3 |
| **234.** | COOA1_HUMAN Mass: 175388 Score: 28 Queries matched: 54 emPAI: 0.03 |
| | Collagen alpha-1(XXIV) chain OS=Homo sapiens GN=COL24A1 PE=2 SV=2 |
| **235.** | CF168_HUMAN Mass: 46813 Score: 28 Queries matched: 6 emPAI: 0.13 |
| | Uncharacterized protein C6orf168 OS=Homo sapiens GN=C6orf168 PE=2 SV=2 |
| **236.** | DTL_HUMAN Mass: 79417 Score: 28 Queries matched: 25 emPAI: 0.07 |
| | Denticleless protein homolog OS=Homo sapiens GN=DTL PE=1 SV=3 |
| **237.** | P4R3A_HUMAN Mass: 95308 Score: 28 Queries matched: 19 emPAI: 0.06 |
| | Serine/threonine-protein phosphatase 4 regulatory subunit 3A OS=Homo sapiens GN=SMEK1 PE=1 SV=1 |
| **238.** | STOX1_HUMAN Mass: 110893 Score: 28 Queries matched: 29 emPAI: 0.05 |
| | Storkhead-box protein 1 OS=Homo sapiens GN=STOX1 PE=1 SV=2 |
| **239.** | MSLN_HUMAN Mass: 68942 Score: 28 Queries matched: 19 emPAI: 0.08 |
| | Mesothelin OS=Homo sapiens GN=MSLN PE=1 SV=2 |
| **240.** | CABP1_HUMAN Mass: 39841 Score: 28 Queries matched: 14 emPAI: 0.15 |
| | Calcium-binding protein 1 OS=Homo sapiens GN=CABP1 PE=1 SV=4 |

| | |
|---|---|
| **241.** | APC_HUMAN Mass: 311455 Score: 27 Queries matched: 35 emPAI: 0.02 |
| | Adenomatous polyposis coli protein OS=Homo sapiens GN=APC PE=1 SV=2 |
| **242.** | BAALC_HUMAN Mass: 19212 Score: 27 Queries matched: 30 emPAI: 0.33 |
| | Brain and acute leukemia cytoplasmic protein OS=Homo sapiens GN=BAALC PE=2 SV=3 |
| **243.** | CSN6_HUMAN Score: 27 Queries matched: 4 |
| | COP9 signalosome complex subunit 6 OS=Homo sapiens GN=COPS6 PE=1 SV=1 |
| **244.** | LUZP4_HUMAN Mass: 35916 Score: 27 Queries matched: 11 emPAI: 0.17 |
| | Leucine zipper protein 4 OS=Homo sapiens GN=LUZP4 PE=2 SV=1 |
| **245.** | ANXA2_HUMAN Mass: 38580 Score: 27 Queries matched: 7 emPAI: 0.15 |
| | Annexin A2 OS=Homo sapiens GN=ANXA2 PE=1 SV=2 |
| **246.** | HSP76_HUMAN Mass: 70984 Score: 27 Queries matched: 8 emPAI: 0.08 |
| | Heat shock 70 kDa protein 6 OS=Homo sapiens GN=HSPA6 PE=1 SV=2 |
| **247.** | HS71L_HUMAN Mass: 70331 Score: 27 Queries matched: 7 emPAI: 0.08 |
| | Heat shock 70 kDa protein 1-like OS=Homo sapiens GN=HSPA1L PE=1 SV=2 |
| **248.** | HSP71_HUMAN Mass: 70009 Score: 27 Queries matched: 6 emPAI: 0.08 |
| | Heat shock 70 kDa protein 1A/1B OS=Homo sapiens GN=HSPA1A PE=1 SV=5 |
| **249.** | TARA_HUMAN Mass: 261217 Score: 27 Queries matched: 99 emPAI: 0.02 |
| | TRIO and F-actin-binding protein OS=Homo sapiens GN=TRIOBP PE=1 SV=3 |
| **250.** | ZN831_HUMAN Mass: 177839 Score: 27 Queries matched: 43 emPAI: 0.03 |
| | Zinc finger protein 831 OS=Homo sapiens GN=ZNF831 PE=2 SV=4 |
| **251.** | RIMKB_HUMAN Mass: 42436 Score: 27 Queries matched: 17 emPAI: 0.14 |
| | Ribosomal protein S6 modification-like protein B OS=Homo sapiens GN=RIMKLB PE=2 SV=2 |
| **252.** | PAPOG_HUMAN Mass: 82751 Score: 27 Queries matched: 16 emPAI: 0.07 |
| | Poly(A) polymerase gamma OS=Homo sapiens GN=PAPOLG PE=1 SV=2 |
| **253.** | HMGX3_HUMAN Mass: 168228 Score: 27 Queries matched: 30 emPAI: 0.03 |
| | HMG domain-containing protein 3 OS=Homo sapiens GN=HMGXB3 PE=2 SV=2 |
| **254.** | ANKL2_HUMAN Mass: 104050 Score: 27 Queries matched: 54 emPAI: 0.06 |
| | Ankyrin repeat and LEM domain-containing protein 2 OS=Homo sapiens GN=ANKLE2 PE=1 SV=4 |
| **255.** | SG269_HUMAN Mass: 192986 Score: 27 Queries matched: 49 emPAI: 0.03 |
| | Tyrosine-protein kinase SgK269 OS=Homo sapiens GN=SGK269 PE=1 SV=4 |
| **256.** | LIME1_HUMAN Mass: 31268 Score: 27 Queries matched: 11 emPAI: 0.19 |
| | Lck-interacting transmembrane adapter 1 OS=Homo sapiens GN=LIME1 PE=1 SV=1 |
| **257.** | TYW1B_HUMAN Mass: 76897 Score: 27 Queries matched: 37 emPAI: 0.08 |
| | tRNA wybutosine-synthesizing protein 1 homolog B OS=Homo sapiens GN=TYW1B PE=2 SV=2 |
| **258.** | TYW1_HUMAN Mass: 83649 Score: 27 Queries matched: 33 emPAI: 0.07 |
| | tRNA wybutosine-synthesizing protein 1 homolog OS=Homo sapiens GN=TYW1 PE=1 SV=2 |
| **259.** | PHLB2_HUMAN Mass: 142070 Score: 27 Queries matched: 12 emPAI: 0.04 |
| | Pleckstrin homology-like domain family B member 2 OS=Homo sapiens GN=PHLDB2 PE=1 SV=2 |
| **260.** | HV306_HUMAN Mass: 12371 Score: 27 Queries matched: 5 emPAI: 1.43 |
| | Ig heavy chain V-III region BUT OS=Homo sapiens PE=1 SV=1 |
| **261.** | AHNK_HUMAN Mass: 628699 Score: 27 Queries matched: 72 emPAI: 0.01 |
| | Neuroblast differentiation-associated protein AHNAK OS=Homo sapiens GN=AHNAK PE=1 SV=2 |
| **262.** | RL7_HUMAN Mass: 29207 Score: 27 Queries matched: 10 emPAI: 0.21 |
| | 60S ribosomal protein L7 OS=Homo sapiens GN=RPL7 PE=1 SV=1 |
| **263.** | ZN284_HUMAN Mass: 68974 Score: 27 Queries matched: 6 emPAI: 0.08 |
| | Zinc finger protein 284 OS=Homo sapiens GN=ZNF284 PE=2 SV=1 |
| **264.** | NU188_HUMAN Mass: 195917 Score: 26 Queries matched: 23 emPAI: 0.03 |
| | Nucleoporin NUP188 homolog OS=Homo sapiens GN=NUP188 PE=1 SV=1 |
| **265.** | CCD38_HUMAN Mass: 65274 Score: 26 Queries matched: 31 emPAI: 0.09 |
| | Coiled-coil domain-containing protein 38 OS=Homo sapiens GN=CCDC38 PE=2 SV=1 |
| **266.** | AXN2_HUMAN Mass: 93499 Score: 26 Queries matched: 35 emPAI: 0.06 |
| | Axin-2 OS=Homo sapiens GN=AXIN2 PE=1 SV=1 |
| **267.** | CECR9_HUMAN Mass: 23587 Score: 26 Queries matched: 19 emPAI: 0.26 |
| | Putative cat eye syndrome critical region protein 9 OS=Homo sapiens GN=CECR9 PE=5 SV=1 |

## **Appendix 2**: LC ESI MS identified capillary tear proteins

| Accession | # Peptides | # AAs | MW [kDa] | calc. pI | Score | Description |
|---|---|---|---|---|---|---|
| P02788 | 1821 | 710 | 78,1 | 8,12 | 1981 | Lactotransferrin OS=Homo sapiens GN=LTF PE=1 SV=6 - [TRFL_HUMAN] |
| P01024 | 179 | 1663 | 187,0 | 6,4 | 1680 | Complement C3 precursor [Contains: Complement C3 beta chain; Complement C |
| P98160 | 177 | 4391 | 468,5 | 6,51 | 1669 | Basement membrane-specific heparan sulfate proteoglycan core protein OS=Hor |
| P02768 | 306 | 609 | 69,3 | 6,28 | 1448 | Serum albumin precursor - Homo sapiens (Human) - [ALBU_HUMAN] |
| P04264 | 199 | 644 | 66,0 | 8,12 | 1389 | Keratin, type II cytoskeletal 1 OS=Homo sapiens GN=KRT1 PE=1 SV=6 - [K2C1_HUM |
| Q8WZ42 | 271 | 34350 | 3813,8 | 6,34 | 1300 | Titin OS=Homo sapiens GN=TTN PE=1 SV=2 - [TITIN_HUMAN] |
| P25311 | 540 | 298 | 34,2 | 6,05 | 1090 | Zinc-alpha-2-glycoprotein OS=Homo sapiens GN=AZGP1 PE=1 SV=2 - [ZA2G_HUM/ |
| Q13421 | 102 | 630 | 68,9 | 6,38 | 845 | Mesothelin OS=Homo sapiens GN=MSLN PE=1 SV=2 - [MSLN_HUMAN] |
| P35527 | 83 | 623 | 62,0 | 5,24 | 742 | Keratin, type I cytoskeletal 9 OS=Homo sapiens GN=KRT9 PE=1 SV=3 - [K1C9_HUM |
| P01833 | 286 | 764 | 83,2 | 5,74 | 741 | Polymeric immunoglobulin receptor OS=Homo sapiens GN=PIGR PE=1 SV=4 - [PIG |
| Q9UGM3 | 229 | 2413 | 260,6 | 5,44 | 718 | Deleted in malignant brain tumors 1 protein OS=Homo sapiens GN=DMBT1 PE=1 S |
| P31025 | 706 | 176 | 19,2 | 5,58 | 704 | Lipocalin-1 OS=Homo sapiens GN=LCN1 PE=1 SV=1 - [LCN1_HUMAN] |
| P00450 | 82 | 1065 | 122,1 | 5,72 | 697 | Ceruloplasmin OS=Homo sapiens GN=CP PE=1 SV=1 - [CERU_HUMAN] |
| P10909 | 145 | 449 | 52,5 | 6,27 | 679 | Clusterin OS=Homo sapiens GN=CLU PE=1 SV=1 - [CLUS_HUMAN] |
| P01876 | 710 | 353 | 37,6 | 6,51 | 615 | Ig alpha-1 chain C region OS=Homo sapiens GN=IGHA1 PE=1 SV=2 - [IGHA1_HUMA |
| P60709 | 97 | 375 | 41,7 | 5,48 | 609 | Actin, cytoplasmic 1 (Beta-actin) - Homo sapiens (Human) - [ACTB_HUMAN] |
| P01871 | 83 | 452 | 49,3 | 6,77 | 563 | Ig mu chain C region OS=Homo sapiens GN=IGHM PE=1 SV=3 - [IGHM_HUMAN] |
| P00738 | 97 | 406 | 45,2 | 6,58 | 550 | Haptoglobin OS=Homo sapiens GN=HP PE=1 SV=1 - [HPT_HUMAN] |
| P01877 | 580 | 340 | 36,5 | 6,1 | 550 | Ig alpha-2 chain C region OS=Homo sapiens GN=IGHA2 PE=1 SV=3 - [IGHA2_HUMA |
| P62737 | 79 | 377 | 42,0 | 5,39 | 514 | Actin, aortic smooth muscle (Alpha-actin-2) - Mus musculus (Mouse) - [ACTA_MC |
| Q96DA0 | 213 | 208 | 22,7 | 7,39 | 474 | Zymogen granule protein 16 homolog B OS=Homo sapiens GN=ZG16B PE=1 SV=3 - |
| P01009 | 23 | 418 | 46,7 | 5,59 | 460 | Alpha-1-antitrypsin OS=Homo sapiens GN=SERPINA1 PE=1 SV=3 - [A1AT_HUMAN] |
| P61626 | 959 | 148 | 16,5 | 9,16 | 460 | Lysozyme C precursor (EC 3.2.1.17) (1,4-beta-N-acetylmuramidase C) - Homo sapi |
| Q08380 | 54 | 585 | 65,3 | 5,27 | 447 | Galectin-3-binding protein OS=Homo sapiens GN=LGALS3BP PE=1 SV=1 - [LG3BP_ |
| P13645 | 68 | 584 | 58,8 | 5,21 | 443 | Keratin, type I cytoskeletal 10 OS=Homo sapiens GN=KRT10 PE=1 SV=6 - [K1C10_H |
| P04083 | 25 | 346 | 38,7 | 7,02 | 428 | Annexin A1 OS=Homo sapiens GN=ANXA1 PE=1 SV=2 - [ANXA1_HUMAN] |
| P12273 | 288 | 146 | 16,6 | 8,05 | 422 | Prolactin-inducible protein OS=Homo sapiens GN=PIP PE=1 SV=1 - [PIP_HUMAN] |
| P20061 | 83 | 433 | 48,2 | 5,03 | 416 | Transcobalamin-1 OS=Homo sapiens GN=TCN1 PE=1 SV=2 - [TCO1_HUMAN] |
| Q9GZZ8 | 498 | 138 | 14,2 | 5,5 | 415 | Extracellular glycoprotein lacritin OS=Homo sapiens GN=LACRT PE=1 SV=1 - [LACR |
| P55058 | 37 | 493 | 54,7 | 7,01 | 412 | Phospholipid transfer protein OS=Homo sapiens GN=PLTP PE=1 SV=1 - [PLTP_HUM |
| P35908 | 49 | 639 | 65,4 | 8 | 408 | Keratin, type II cytoskeletal 2 epidermal OS=Homo sapiens GN=KRT2 PE=1 SV=2 - |
| P02647 | 36 | 267 | 30,8 | 5,76 | 398 | Apolipoprotein A-I precursor (Apo-AI) (ApoA-I) [Contains: Apolipoprotein A-I(1-2 |
| P01623 | 96 | 109 | 11,7 | 8,91 | 376 | Ig kappa chain V-III region WOL OS=Homo sapiens PE=1 SV=1 - [KV305_HUMAN] |
| Q8NF91 | 53 | 8797 | 1010,4 | 5,53 | 363 | Nesprin-1 OS=Homo sapiens GN=SYNE1 PE=1 SV=3 - [SYNE1_HUMAN] |
| P01036 | 189 | 141 | 16,2 | 5,02 | 354 | Cystatin-S precursor (Cystatin-4) (Salivary acidic protein 1) (Cystatin-SA-III) - Hom |
| Q8IZT6 | 111 | 3477 | 409,5 | 10,45 | 344 | Abnormal spindle-like microcephaly-associated protein OS=Homo sapiens GN=A |
| Q03001 | 43 | 7570 | 860,1 | 5,25 | 337 | Dystonin OS=Homo sapiens GN=DST PE=1 SV=4 - [DYST_HUMAN] |
| P80188 | 62 | 198 | 22,6 | 8,91 | 334 | Neutrophil gelatinase-associated lipocalin OS=Homo sapiens GN=LCN2 PE=1 SV=2 |
| P06733 | 42 | 434 | 47,1 | 7,39 | 334 | Alpha-enolase (EC 4.2.1.11) (2-phospho-D-glycerate hydro-lyase) (Non-neural en |
| P80303 | 29 | 420 | 50,2 | 5,12 | 324 | Nucleobindin-2 OS=Homo sapiens GN=NUCB2 PE=1 SV=2 - [NUCB2_HUMAN] |
| P0CG05 | 192 | 106 | 11,3 | 7,24 | 317 | Ig lambda-2 chain C regions OS=Homo sapiens GN=IGLC2 PE=1 SV=1 - [LAC2_HUM/ |
| O75556 | 326 | 95 | 10,9 | 5,78 | 306 | Mammaglobin-B OS=Homo sapiens GN=SCGB2A1 PE=1 SV=1 - [SG2A1_HUMAN] |
| Q6S8J3 | 37 | 1075 | 121,3 | 6,2 | 304 | POTE ankyrin domain family member E OS=Homo sapiens GN=POTEE PE=1 SV=3 - |
| P04259 | 25 | 564 | 60,0 | 8 | 302 | Keratin, type II cytoskeletal 6B OS=Homo sapiens GN=KRT6B PE=1 SV=5 - [K2C6B_ |
| A5A3E0 | 33 | 1075 | 121,4 | 6,2 | 301 | POTE ankyrin domain family member F OS=Homo sapiens GN=POTEF PE=1 SV=2 - |
| Q15149 | 66 | 4684 | 531,5 | 5,96 | 293 | Plectin OS=Homo sapiens GN=PLEC PE=1 SV=3 - [PLEC_HUMAN] |
| O15078 | 92 | 2479 | 290,2 | 5,95 | 289 | Centrosomal protein of 290 kDa OS=Homo sapiens GN=CEP290 PE=1 SV=2 - [CE290 |
| P01011 | 27 | 423 | 47,6 | 5,52 | 283 | Alpha-1-antichymotrypsin OS=Homo sapiens GN=SERPINA3 PE=1 SV=2 - [AACT_H |
| P20929 | 52 | 6669 | 772,4 | 9,07 | 278 | Nebulin OS=Homo sapiens GN=NEB PE=1 SV=4 - [NEBU_HUMAN] |
| Q99935 | 149 | 248 | 27,2 | 10,42 | 274 | Proline-rich protein 1 OS=Homo sapiens GN=PROL1 PE=1 SV=2 - [PROL1_HUMAN] |
| Q16378 | 472 | 134 | 15,1 | 7,06 | 272 | Proline-rich protein 4 OS=Homo sapiens GN=PRR4 PE=1 SV=3 - [PROL4_HUMAN] |
| Q9UQ35 | 36 | 2752 | 299,4 | 12,06 | 272 | Serine/arginine repetitive matrix protein 2 OS=Homo sapiens GN=SRRM2 PE=1 SV |
| Q8IVF4 | 76 | 4471 | 514,5 | 5,88 | 266 | Dynein heavy chain 10, axonemal OS=Homo sapiens GN=DNAH10 PE=1 SV=4 - [DY |
| Q06830 | 14 | 199 | 22,1 | 8,13 | 264 | Peroxiredoxin-1 (EC 1.11.1.15) (Thioredoxin peroxidase 2) (Thioredoxin-depende |
| P15924 | 53 | 2871 | 331,6 | 6,81 | 263 | Desmoplakin OS=Homo sapiens GN=DSP PE=1 SV=3 - [DESP_HUMAN] |
| Q562R1 | 55 | 376 | 42,0 | 5,59 | 257 | Beta-actin-like protein 2 OS=Homo sapiens GN=ACTBL2 PE=1 SV=2 - [ACTBL_HUM |
| P0CG38 | 56 | 1075 | 121,2 | 6,21 | 256 | POTE ankyrin domain family member I OS=Homo sapiens GN=POTEI PE=3 SV=1 - [ |
| Q5VSP4 | 218 | 162 | 17,9 | 5 | 251 | Putative lipocalin 1-like protein 1 OS=Homo sapiens GN=LCN1L1 PE=5 SV=1 - [LC1 |
| Q8WXH0 | 32 | 6885 | 795,9 | 5,36 | 250 | Nesprin-2 OS=Homo sapiens GN=SYNE2 PE=1 SV=3 - [SYNE2_HUMAN] |
| P49792 | 67 | 3224 | 358,0 | 6,2 | 246 | E3 SUMO-protein ligase RanBP2 OS=Homo sapiens GN=RANBP2 PE=1 SV=2 - [RBP2 |
| P04406 | 21 | 335 | 36,0 | 8,46 | 245 | Glyceraldehyde-3-phosphate dehydrogenase OS=Homo sapiens GN=GAPDH PE=1 |
| Q8WXI7 | 48 | 22152 | 2351,2 | 6 | 245 | Mucin-16 OS=Homo sapiens GN=MUC16 PE=1 SV=2 - [MUC16_HUMAN] |
| P01619 | 78 | 108 | 11,6 | 9,25 | 239 | Ig kappa chain V-III region B6 OS=Homo sapiens PE=1 SV=1 - [KV301_HUMAN] |
| A0M8Q6 | 104 | 106 | 11,3 | 8,28 | 236 | Ig lambda-7 chain C region OS=Homo sapiens GN=IGLC7 PE=1 SV=2 - [LAC7_HUMA |

| | | | | | | |
|---|---|---|---|---|---|---|
| Q12955 | 64 | 4377 | 480,1 | 6,49 | 234 | Ankyrin-3 OS=Homo sapiens GN=ANK3 PE=1 SV=3 - [ANK3_HUMAN] |
| P01625 | 40 | 114 | 12,6 | 7,93 | 225 | Ig kappa chain V-IV region Len OS=Homo sapiens PE=1 SV=2 - [KV402_HUMAN] |
| P13647 | 15 | 590 | 62,3 | 7,74 | 225 | Keratin, type II cytoskeletal 5 OS=Homo sapiens GN=KRT5 PE=1 SV=3 - [K2C5_HUM |
| Q8NCM8 | 160 | 4307 | 492,3 | 6,54 | 223 | Cytoplasmic dynein 2 heavy chain 1 OS=Homo sapiens GN=DYNC2H1 PE=1 SV=4 - [ |
| P25054 | 112 | 2843 | 311,5 | 7,8 | 221 | Adenomatous polyposis coli protein OS=Homo sapiens GN=APC PE=1 SV=2 - [APC |
| Q9Y4A5 | 32 | 3859 | 437,3 | 8,19 | 220 | Transformation/transcription domain-associated protein (350/400 kDa PCAF-assc |
| Q02224 | 22 | 2701 | 316,2 | 5,64 | 218 | Centromere-associated protein E OS=Homo sapiens GN=CENPE PE=1 SV=2 - [CENI |
| P26447 | 31 | 101 | 11,7 | 6,11 | 214 | Protein S100-A4 OS=Homo sapiens GN=S100A4 PE=1 SV=1 - [S10A4_HUMAN] |
| O95968 | 171 | 90 | 9,9 | 9,25 | 214 | Secretoglobin family 1D member 1 OS=Homo sapiens GN=SCGB1D1 PE=1 SV=1 - [S |
| P46100 | 28 | 2492 | 282,4 | 6,58 | 212 | Transcriptional regulator ATRX OS=Homo sapiens GN=ATRX PE=1 SV=5 - [ATRX_HU |
| P06702 | 39 | 114 | 13,2 | 6,13 | 211 | Protein S100-A9 OS=Homo sapiens GN=S100A9 PE=1 SV=1 - [S10A9_HUMAN] |
| O75592 | 21 | 4640 | 509,8 | 7,03 | 209 | Probable E3 ubiquitin-protein ligase MYCBP2 OS=Homo sapiens GN=MYCBP2 PE= |
| Q9P225 | 107 | 4427 | 507,4 | 6,37 | 209 | Dynein heavy chain 2, axonemal OS=Homo sapiens GN=DNAH2 PE=1 SV=3 - [DYH2 |
| P01834 | 224 | 106 | 11,6 | 5,87 | 207 | Ig kappa chain C region - Homo sapiens (Human) - [KAC_HUMAN] |
| Q9Y6V0 | 44 | 5183 | 566,3 | 6,54 | 202 | Protein piccolo OS=Homo sapiens GN=PCLO PE=1 SV=3 - [PCLO_HUMAN] |
| P01598 | 25 | 108 | 11,8 | 8,44 | 199 | Ig kappa chain V-I region EU OS=Homo sapiens PE=1 SV=1 - [KV106_HUMAN] |
| Q01484 | 45 | 3924 | 430,0 | 5,12 | 199 | Ankyrin-2 OS=Homo sapiens GN=ANK2 PE=1 SV=3 - [ANK2_HUMAN] |
| P0CG04 | 76 | 106 | 11,3 | 7,87 | 197 | Ig lambda-1 chain C regions OS=Homo sapiens GN=IGLC1 PE=1 SV=1 - [LAC1_HUM |
| P0C6X7 | 57 | 7073 | 789,7 | 6,62 | 195 | Replicase polyprotein 1ab OS=Human SARS coronavirus GN=rep PE=1 SV=1 - [R1A |
| O95613 | 20 | 3336 | 377,8 | 5,55 | 194 | Pericentrin OS=Homo sapiens GN=PCNT PE=1 SV=4 - [PCNT_HUMAN] |
| P01781 | 55 | 116 | 12,7 | 8,48 | 191 | Ig heavy chain V-III region GAL OS=Homo sapiens PE=1 SV=1 - [HV320_HUMAN] |
| P21817 | 49 | 5038 | 564,8 | 5,3 | 191 | Ryanodine receptor 1 OS=Homo sapiens GN=RYR1 PE=1 SV=3 - [RYR1_HUMAN] |
| P01593 | 48 | 108 | 12,0 | 5,99 | 189 | Ig kappa chain V-I region AG - Homo sapiens (Human) - [KV101_HUMAN] |
| P01591 | 87 | 159 | 18,1 | 5,24 | 188 | Immunoglobulin J chain OS=Homo sapiens GN=IGJ PE=1 SV=4 - [IGJ_HUMAN] |
| Q5TZA2 | 25 | 2017 | 228,4 | 5,5 | 187 | Rootletin OS=Homo sapiens GN=CROCC PE=1 SV=1 - [CROCC_HUMAN] |
| Q92736 | 47 | 4967 | 564,2 | 6,07 | 184 | Ryanodine receptor 2 OS=Homo sapiens GN=RYR2 PE=1 SV=3 - [RYR2_HUMAN] |
| Q12789 | 22 | 2109 | 238,7 | 7,3 | 184 | General transcription factor 3C polypeptide 1 OS=Homo sapiens GN=GTF3C1 PE=1 |
| Q2LD37 | 25 | 5005 | 555,1 | 6,58 | 183 | Uncharacterized protein KIAA1109 OS=Homo sapiens GN=KIAA1109 PE=1 SV=2 - [I |
| P09211 | 11 | 210 | 23,3 | 5,64 | 182 | Glutathione S-transferase P OS=Homo sapiens GN=GSTP1 PE=1 SV=2 - [GSTP1_HU |
| P01857 | 16 | 330 | 36,1 | 8,19 | 182 | Ig gamma-1 chain C region - Homo sapiens (Human) - [IGHG1_HUMAN] |
| A6NKT7 | 58 | 1766 | 198,3 | 6,39 | 181 | RanBP2-like and GRIP domain-containing protein 3 OS=Homo sapiens GN=RGPD3 |
| P08758 | 11 | 320 | 35,9 | 5,05 | 181 | Annexin A5 OS=Homo sapiens GN=ANXA5 PE=1 SV=2 - [ANXA5_HUMAN] |
| Q5VST9 | 42 | 7968 | 867,9 | 5,99 | 181 | Obscurin OS=Homo sapiens GN=OBSCN PE=1 SV=3 - [OBSCN_HUMAN] |
| P06313 | 35 | 133 | 14,6 | 6,58 | 181 | Ig kappa chain V-IV region JI OS=Homo sapiens PE=4 SV=1 - [KV403_HUMAN] |
| Q09666 | 35 | 5890 | 628,7 | 6,15 | 180 | Neuroblast differentiation-associated protein AHNAK OS=Homo sapiens GN=AHI |
| Q9BYX7 | 25 | 375 | 42,0 | 6,33 | 177 | Putative beta-actin-like protein 3 OS=Homo sapiens GN=POTEKP PE=5 SV=1 - [AC |
| P06703 | 43 | 90 | 10,2 | 5,48 | 177 | Protein S100-A6 OS=Homo sapiens GN=S100A6 PE=1 SV=1 - [S10A6_HUMAN] |
| P00338 | 11 | 332 | 36,7 | 8,27 | 177 | L-lactate dehydrogenase A chain OS=Homo sapiens GN=LDHA PE=1 SV=2 - [LDHA_ |
| P63104 | 18 | 245 | 27,7 | 4,79 | 174 | 14-3-3 protein zeta/delta OS=Homo sapiens GN=YWHAZ PE=1 SV=1 - [1433Z_HUM |
| Q8TCU4 | 23 | 4167 | 460,7 | 6,28 | 172 | Alstrom syndrome protein 1 OS=Homo sapiens GN=ALMS1 PE=1 SV=3 - [ALMS1_H |
| O95678 | 9 | 551 | 59,5 | 7,74 | 170 | Keratin, type II cytoskeletal 75 OS=Homo sapiens GN=KRT75 PE=1 SV=2 - [K2C75_H |
| P80748 | 30 | 111 | 11,9 | 5,08 | 169 | Ig lambda chain V-III region LOI OS=Homo sapiens PE=1 SV=1 - [LV302_HUMAN] |
| Q96HP0 | 26 | 2047 | 229,4 | 6,74 | 169 | Dedicator of cytokinesis protein 6 OS=Homo sapiens GN=DOCK6 PE=1 SV=3 - [DOC |
| P02533 | 21 | 472 | 51,5 | 5,16 | 168 | Keratin, type I cytoskeletal 14 OS=Homo sapiens GN=KRT14 PE=1 SV=4 - [K1C14_H |
| Q5XKE5 | 27 | 535 | 57,8 | 7,2 | 168 | Keratin, type II cytoskeletal 79 OS=Homo sapiens GN=KRT79 PE=1 SV=2 - [K2C79_H |
| P05109 | 40 | 93 | 10,8 | 7,03 | 167 | Protein S100-A8 OS=Homo sapiens GN=S100A8 PE=1 SV=1 - [S10A8_HUMAN] |
| Q8IVL1 | 29 | 2488 | 268,0 | 9,03 | 166 | Neuron navigator 2 OS=Homo sapiens GN=NAV2 PE=1 SV=3 - [NAV2_HUMAN] |
| Q4G0P3 | 67 | 5120 | 575,5 | 6,07 | 165 | Hydrocephalus-inducing protein homolog OS=Homo sapiens GN=HYDIN PE=1 SV= |
| Q9UFH2 | 76 | 4485 | 511,5 | 5,77 | 165 | Dynein heavy chain 17, axonemal OS=Homo sapiens GN=DNAH17 PE=2 SV=2 - [DY |
| Q14515 | 12 | 664 | 75,2 | 4,81 | 164 | SPARC-like protein 1 OS=Homo sapiens GN=SPARCL1 PE=1 SV=2 - [SPRL1_HUMAN |
| Q5CZC0 | 34 | 6907 | 780,1 | 6,71 | 163 | Fibrous sheath-interacting protein 2 OS=Homo sapiens GN=FSIP2 PE=1 SV=4 - [FSI |
| Q15782 | 17 | 390 | 43,5 | 7,53 | 162 | Chitinase-3-like protein 2 OS=Homo sapiens GN=CHI3L2 PE=1 SV=1 - [CH3L2_HUM |
| O75122 | 74 | 1294 | 141,0 | 8,47 | 161 | CLIP-associating protein 2 OS=Homo sapiens GN=CLASP2 PE=1 SV=2 - [CLAP2_HUM |
| Q5T4S7 | 28 | 5183 | 573,5 | 6,04 | 160 | E3 ubiquitin-protein ligase UBR4 OS=Homo sapiens GN=UBR4 PE=1 SV=1 - [UBR4_ |
| Q14643 | 26 | 2758 | 313,7 | 6,04 | 159 | Inositol 1,4,5-trisphosphate receptor type 1 OS=Homo sapiens GN=ITPR1 PE=1 SV |
| Q96T23 | 21 | 1441 | 163,7 | 5,01 | 159 | Remodeling and spacing factor 1 OS=Homo sapiens GN=RSF1 PE=1 SV=2 - [RSF1_H |
| A6NE01 | 34 | 2351 | 262,6 | 8,6 | 159 | Protein FAM186A OS=Homo sapiens GN=FAM186A PE=2 SV=3 - [F186A_HUMAN] |
| P07339 | 35 | 412 | 44,5 | 6,54 | 158 | Cathepsin D OS=Homo sapiens GN=CTSD PE=1 SV=1 - [CATD_HUMAN] |
| Q8N3K9 | 25 | 4069 | 448,9 | 4,78 | 157 | Cardiomyopathy-associated protein 5 OS=Homo sapiens GN=CMYA5 PE=1 SV=3 - [ |
| P01766 | 68 | 120 | 13,2 | 6,57 | 157 | Ig heavy chain V-III region BRO OS=Homo sapiens PE=1 SV=1 - [HV305_HUMAN] |
| P61769 | 64 | 119 | 13,7 | 6,52 | 156 | Beta-2-microglobulin OS=Homo sapiens GN=B2M PE=1 SV=1 - [B2MG_HUMAN] |
| Q5T200 | 21 | 1668 | 196,5 | 9,42 | 155 | Zinc finger CCCH domain-containing protein 13 OS=Homo sapiens GN=ZC3H13 PE= |
| P49454 | 13 | 3210 | 367,5 | 5,07 | 155 | Centromere protein F OS=Homo sapiens GN=CENPF PE=1 SV=2 - [CENPF_HUMAN |
| Q9UMN6 | 34 | 2715 | 293,3 | 8,22 | 154 | Histone-lysine N-methyltransferase MLL4 OS=Homo sapiens GN=WBP7 PE=1 SV= |
| B1AJZ9 | 324 | 1412 | 161,8 | 6,95 | 154 | Forkhead-associated domain-containing protein 1 OS=Homo sapiens GN=FHAD1 |

| | | | | | | |
|---|---|---|---|---|---|---|
| P35580 | 17 | 1976 | 228,9 | 5,54 | 153 | Myosin-10 OS=Homo sapiens GN=MYH10 PE=1 SV=3 - [MYH10_HUMAN] |
| O14578 | 59 | 2027 | 231,3 | 6,57 | 153 | Citron Rho-interacting kinase OS=Homo sapiens GN=CIT PE=1 SV=2 - [CTRO_HUM |
| Q9UIF8 | 52 | 2168 | 240,3 | 6,54 | 153 | Bromodomain adjacent to zinc finger domain protein 2B OS=Homo sapiens GN=B |
| O95153 | 32 | 1857 | 199,9 | 5,11 | 151 | Peripheral-type benzodiazepine receptor-associated protein 1 OS=Homo sapien |
| Q9BXX2 | 18 | 1477 | 167,6 | 6,16 | 151 | Ankyrin repeat domain-containing protein 30B OS=Homo sapiens GN=ANKRD30B |
| Q07864 | 36 | 2286 | 261,4 | 6,39 | 150 | DNA polymerase epsilon catalytic subunit A OS=Homo sapiens GN=POLE PE=1 SV |
| Q92614 | 66 | 2054 | 233,0 | 6,3 | 149 | Myosin-XVIIIa OS=Homo sapiens GN=MYO18A PE=1 SV=3 - [MY18A_HUMAN] |
| P01594 | 33 | 108 | 11,9 | 5,33 | 149 | Ig kappa chain V-I region AU OS=Homo sapiens PE=1 SV=1 - [KV102_HUMAN] |
| Q13029 | 23 | 1718 | 188,8 | 7,31 | 149 | PR domain zinc finger protein 2 OS=Homo sapiens GN=PRDM2 PE=1 SV=3 - [PRDM |
| Q14152 | 44 | 1382 | 166,5 | 6,79 | 149 | Eukaryotic translation initiation factor 3 subunit A OS=Homo sapiens GN=EIF3A PI |
| P01606 | 51 | 108 | 11,8 | 9,91 | 148 | Ig kappa chain V-I region OU OS=Homo sapiens PE=1 SV=1 - [KV114_HUMAN] |
| Q14669 | 20 | 1992 | 220,3 | 8,48 | 147 | Probable E3 ubiquitin-protein ligase TRIP12 OS=Homo sapiens GN=TRIP12 PE=1 S |
| Q86VF7 | 30 | 1730 | 197,0 | 9,2 | 147 | Nebulin-related-anchoring protein OS=Homo sapiens GN=NRAP PE=2 SV=2 - [NRA |
| P01596 | 24 | 107 | 11,7 | 9,41 | 147 | Ig kappa chain V-I region CAR OS=Homo sapiens PE=1 SV=1 - [KV104_HUMAN] |
| Q13428 | 51 | 1488 | 152,0 | 9,04 | 145 | Treacle protein OS=Homo sapiens GN=TCOF1 PE=1 SV=3 - [TCOF_HUMAN] |
| Q92817 | 26 | 2033 | 231,5 | 6,96 | 144 | Envoplakin OS=Homo sapiens GN=EVPL PE=1 SV=3 - [EVPL_HUMAN] |
| Q9UIG0 | 60 | 1483 | 170,8 | 8,48 | 142 | Tyrosine-protein kinase BAZ1B OS=Homo sapiens GN=BAZ1B PE=1 SV=2 - [BAZ1B_ |
| Q8TE73 | 23 | 4624 | 528,7 | 6,1 | 142 | Dynein heavy chain 5, axonemal OS=Homo sapiens GN=DNAH5 PE=1 SV=3 - [DYH5 |
| P22079 | 11 | 712 | 80,2 | 8,62 | 140 | Lactoperoxidase OS=Homo sapiens GN=LPO PE=1 SV=2 - [PERL_HUMAN] |
| P01768 | 60 | 122 | 13,7 | 9,63 | 140 | Ig heavy chain V-III region CAM OS=Homo sapiens PE=1 SV=1 - [HV307_HUMAN] |
| A7E2Y1 | 21 | 1941 | 221,3 | 6,01 | 140 | Myosin-7B OS=Homo sapiens GN=MYH7B PE=2 SV=3 - [MYH7B_HUMAN] |
| P80362 | 25 | 108 | 11,7 | 5,31 | 139 | Ig kappa chain V-I region WAT OS=Homo sapiens PE=1 SV=1 - [KV125_HUMAN] |
| P24043 | 17 | 3122 | 343,7 | 6,4 | 138 | Laminin subunit alpha-2 OS=Homo sapiens GN=LAMA2 PE=1 SV=4 - [LAMA2_HUM |
| O60673 | 17 | 3130 | 352,6 | 8,47 | 138 | DNA polymerase zeta catalytic subunit OS=Homo sapiens GN=REV3L PE=1 SV=2 - |
| P07858 | 10 | 339 | 37,8 | 6,3 | 137 | Cathepsin B OS=Homo sapiens GN=CTSB PE=1 SV=3 - [CATB_HUMAN] |
| A2RUB6 | 47 | 948 | 109,3 | 8,25 | 137 | Coiled-coil domain-containing protein 66 OS=Homo sapiens GN=CCDC66 PE=1 SV |
| Q96Q89 | 20 | 1820 | 210,5 | 5,67 | 137 | Kinesin-like protein KIF20B OS=Homo sapiens GN=KIF20B PE=1 SV=3 - [KI20B_HU |
| Q8WXG9 | 20 | 6307 | 692,2 | 4,64 | 137 | G-protein coupled receptor 98 OS=Homo sapiens GN=GPR98 PE=1 SV=1 - [GPR98_ |
| Q68DN6 | 48 | 1748 | 196,5 | 6,1 | 137 | RANBP2-like and GRIP domain-containing protein 1/2 OS=Homo sapiens GN=RGP |
| Q7Z5J4 | 46 | 1906 | 203,2 | 8,79 | 137 | Retinoic acid-induced protein 1 OS=Homo sapiens GN=RAI1 PE=1 SV=2 - [RAI1_HU |
| Q5VT06 | 16 | 3117 | 350,7 | 6,33 | 136 | Centrosome-associated protein 350 OS=Homo sapiens GN=CEP350 PE=1 SV=1 - [C |
| Q12923 | 18 | 2485 | 276,7 | 6,42 | 135 | Tyrosine-protein phosphatase non-receptor type 13 OS=Homo sapiens GN=PTPN |
| P01607 | 26 | 108 | 11,9 | 6,51 | 135 | Ig kappa chain V-I region Rei OS=Homo sapiens PE=1 SV=1 - [KV115_HUMAN] |
| Q8TD26 | 14 | 2715 | 305,2 | 6,27 | 135 | Chromodomain-helicase-DNA-binding protein 6 OS=Homo sapiens GN=CHD6 PE= |
| Q14980 | 22 | 2115 | 238,1 | 5,78 | 135 | Nuclear mitotic apparatus protein 1 OS=Homo sapiens GN=NUMA1 PE=1 SV=2 - [N |
| P01765 | 49 | 115 | 12,3 | 9,13 | 134 | Ig heavy chain V-III region TIL - Homo sapiens (Human) - [HV304_HUMAN] |
| Q8IZD9 | 14 | 2030 | 233,0 | 6,98 | 134 | Dedicator of cytokinesis protein 3 OS=Homo sapiens GN=DOCK3 PE=1 SV=1 - [DO |
| Q04695 | 12 | 432 | 48,1 | 5,02 | 134 | Keratin, type I cytoskeletal 17 OS=Homo sapiens GN=KRT17 PE=1 SV=2 - [K1C17_H |
| O60293 | 33 | 1989 | 226,2 | 8,13 | 134 | Zinc finger C3H1 domain-containing protein OS=Homo sapiens GN=ZFC3H1 PE=1 S |
| Q96SN8 | 74 | 1893 | 214,9 | 5,58 | 134 | CDK5 regulatory subunit-associated protein 2 OS=Homo sapiens GN=CDK5RAP2 P |
| Q96PE2 | 28 | 2063 | 221,5 | 6,29 | 134 | Rho guanine nucleotide exchange factor 17 OS=Homo sapiens GN=ARHGEF17 PE= |
| Q7Z6E9 | 17 | 1792 | 201,4 | 9,64 | 133 | E3 ubiquitin-protein ligase RBBP6 OS=Homo sapiens GN=RBBP6 PE=1 SV=1 - [RBB |
| Q9Y4F4 | 167 | 1720 | 189,2 | 8,5 | 132 | Protein FAM179B OS=Homo sapiens GN=FAM179B PE=1 SV=4 - [F179B_HUMAN] |
| Q9Y4D8 | 64 | 3996 | 439,1 | 6,19 | 132 | Probable E3 ubiquitin-protein ligase C12orf51 OS=Homo sapiens GN=C12orf51 PE |
| P07711 | 11 | 333 | 37,5 | 5,45 | 132 | Cathepsin L1 OS=Homo sapiens GN=CTSL1 PE=1 SV=2 - [CATL1_HUMAN] |
| Q9BV73 | 31 | 2442 | 281,0 | 5,02 | 131 | Centrosome-associated protein CEP250 OS=Homo sapiens GN=CEP250 PE=1 SV=2 |
| P01624 | 32 | 109 | 11,9 | 8,94 | 131 | Ig kappa chain V-III region POM OS=Homo sapiens PE=1 SV=1 - [KV306_HUMAN] |
| Q8N474 | 15 | 314 | 35,4 | 8,85 | 131 | Secreted frizzled-related protein 1 OS=Homo sapiens GN=SFRP1 PE=1 SV=1 - [SFR |
| Q5VU65 | 13 | 1888 | 210,5 | 7,5 | 131 | Nuclear pore membrane glycoprotein 210-like OS=Homo sapiens GN=NUP210L PE |
| P07602 | 11 | 524 | 58,1 | 5,17 | 130 | Proactivator polypeptide OS=Homo sapiens GN=PSAP PE=1 SV=2 - [SAP_HUMAN] |
| Q7Z460 | 28 | 1538 | 169,3 | 9,03 | 130 | CLIP-associating protein 1 OS=Homo sapiens GN=CLASP1 PE=1 SV=1 - [CLAP1_HU |
| P07355 | 12 | 339 | 38,6 | 7,75 | 129 | Annexin A2 OS=Homo sapiens GN=ANXA2 PE=1 SV=2 - [ANXA2_HUMAN] |
| Q7Z406 | 11 | 1995 | 227,9 | 5,92 | 129 | Myosin-14 OS=Homo sapiens GN=MYH14 PE=1 SV=1 - [MYH14_HUMAN] |
| Q8WZ64 | 25 | 1704 | 193,3 | 7,39 | 129 | Arf-GAP with Rho-GAP domain, ANK repeat and PH domain-containing protein 2 |
| P30414 | 76 | 1462 | 165,6 | 9,99 | 129 | NK-tumor recognition protein OS=Homo sapiens GN=NKTR PE=1 SV=2 - [NKTR_HU |
| Q9H2D6 | 23 | 2365 | 261,2 | 8,48 | 128 | TRIO and F-actin-binding protein OS=Homo sapiens GN=TRIOBP PE=1 SV=3 - [TAR |
| Q7Z7A1 | 19 | 2325 | 268,7 | 5,55 | 128 | Centriolin OS=Homo sapiens GN=CEP110 PE=1 SV=2 - [CE110_HUMAN] |
| Q14966 | 47 | 1978 | 220,5 | 6,38 | 128 | Zinc finger protein 638 OS=Homo sapiens GN=ZNF638 PE=1 SV=2 - [ZN638_HUMAN |
| P11717 | 24 | 2491 | 274,2 | 5,94 | 127 | Cation-independent mannose-6-phosphate receptor OS=Homo sapiens GN=IGF2 |
| Q2KHM9 | 16 | 967 | 109,3 | 7,68 | 127 | Uncharacterized protein KIAA0753 OS=Homo sapiens GN=KIAA0753 PE=2 SV=3 - [ |
| Q86TE4 | 81 | 346 | 38,9 | 8,73 | 127 | Leucine zipper protein 2 OS=Homo sapiens GN=LUZP2 PE=2 SV=2 - [LUZP2_HUMAN |
| Q14004 | 18 | 1512 | 164,8 | 9,69 | 127 | Cyclin-dependent kinase 13 OS=Homo sapiens GN=CDK13 PE=1 SV=2 - [CDK13_HU |
| Q63HN8 | 15 | 3280 | 373,7 | 6,92 | 126 | RING finger protein 213 OS=Homo sapiens GN=RNF213 PE=1 SV=2 - [RN213_HUMA |
| Q9Y2K3 | 11 | 1946 | 224,5 | 5,85 | 126 | Myosin-15 OS=Homo sapiens GN=MYH15 PE=1 SV=5 - [MYH15_HUMAN] |
| Q9NR99 | 50 | 2828 | 312,0 | 8,32 | 126 | Matrix-remodeling-associated protein 5 OS=Homo sapiens GN=MXRA5 PE=2 SV=3 |

| | | | | | | |
|---|---|---|---|---|---|---|
| Q14571 | 29 | 2701 | 307,9 | 6,43 | 125 | Inositol 1,4,5-trisphosphate receptor type 2 OS=Homo sapiens GN=ITPR2 PE=1 SV |
| Q7Z794 | 31 | 578 | 61,9 | 5,99 | 125 | Keratin, type II cytoskeletal 1b OS=Homo sapiens GN=KRT77 PE=1 SV=3 - [K2C1B_ |
| P01597 | 54 | 108 | 11,7 | 9,36 | 125 | Ig kappa chain V-I region DEE OS=Homo sapiens PE=1 SV=1 - [KV105_HUMAN] |
| Q6ZQQ6 | 12 | 2873 | 333,0 | 7,28 | 124 | WD repeat-containing protein 87 OS=Homo sapiens GN=WDR87 PE=2 SV=3 - [WDF |
| Q86UR5 | 22 | 1692 | 189,0 | 9,66 | 124 | Regulating synaptic membrane exocytosis protein 1 OS=Homo sapiens GN=RIMS1 |
| P12270 | 23 | 2363 | 267,1 | 5,02 | 124 | Nucleoprotein TPR OS=Homo sapiens GN=TPR PE=1 SV=3 - [TPR_HUMAN] |
| Q9NS87 | 19 | 1388 | 160,1 | 6 | 122 | Kinesin-like protein KIF15 OS=Homo sapiens GN=KIF15 PE=1 SV=1 - [KIF15_HUMA |
| Q96AY4 | 12 | 2481 | 270,7 | 6,89 | 122 | Tetratricopeptide repeat protein 28 OS=Homo sapiens GN=TTC28 PE=1 SV=4 - [TT |
| P01767 | 48 | 115 | 12,4 | 9,25 | 122 | Ig heavy chain V-III region BUT OS=Homo sapiens PE=1 SV=1 - [HV306_HUMAN] |
| O00192 | 35 | 962 | 104,6 | 6,81 | 122 | Armadillo repeat protein deleted in velo-cardio-facial syndrome OS=Homo sapie |
| P06309 | 25 | 117 | 12,7 | 7,12 | 122 | Ig kappa chain V-II region GM607 (Fragment) OS=Homo sapiens PE=4 SV=1 - [KV2( |
| Q9Y2F5 | 30 | 2266 | 247,7 | 5,48 | 121 | Uncharacterized protein KIAA0947 OS=Homo sapiens GN=KIAA0947 PE=1 SV=5 - [ |
| P20930 | 20 | 4061 | 434,9 | 9,25 | 121 | Filaggrin OS=Homo sapiens GN=FLG PE=1 SV=3 - [FILA_HUMAN] |
| O00584 | 9 | 256 | 29,5 | 7,08 | 121 | Ribonuclease T2 OS=Homo sapiens GN=RNASET2 PE=1 SV=2 - [RNT2_HUMAN] |
| Q13402 | 23 | 2215 | 254,2 | 8,56 | 120 | Myosin-VIIa OS=Homo sapiens GN=MYO7A PE=1 SV=1 - [MYO7A_HUMAN] |
| P01617 | 25 | 113 | 12,3 | 6 | 120 | Ig kappa chain V-II region TEW OS=Homo sapiens PE=1 SV=1 - [KV204_HUMAN] |
| Q9UKJ3 | 26 | 1502 | 164,1 | 8,66 | 120 | G patch domain-containing protein 8 OS=Homo sapiens GN=GPATCH8 PE=1 SV=2 - |
| Q13129 | 72 | 1914 | 217,8 | 6,77 | 120 | Zinc finger protein Rlf OS=Homo sapiens GN=RLF PE=1 SV=2 - [RLF_HUMAN] |
| Q9H583 | 11 | 2144 | 242,2 | 6,54 | 119 | HEAT repeat-containing protein 1 OS=Homo sapiens GN=HEATR1 PE=1 SV=3 - [HEA |
| Q9P2P6 | 31 | 4614 | 506,4 | 6,46 | 118 | StAR-related lipid transfer protein 9 OS=Homo sapiens GN=STARD9 PE=2 SV=2 - [S |
| P35498 | 35 | 2009 | 228,8 | 5,81 | 118 | Sodium channel protein type 1 subunit alpha OS=Homo sapiens GN=SCN1A PE=1 |
| Q96JB1 | 22 | 4490 | 514,3 | 6,32 | 118 | Dynein heavy chain 8, axonemal OS=Homo sapiens GN=DNAH8 PE=1 SV=2 - [DYH8 |
| Q8WXG6 | 123 | 1647 | 183,2 | 6,04 | 118 | MAP kinase-activating death domain protein OS=Homo sapiens GN=MADD PE=1 S |
| O60244 | 24 | 1454 | 160,5 | 8,73 | 117 | Mediator of RNA polymerase II transcription subunit 14 OS=Homo sapiens GN=M |
| Q5THJ4 | 40 | 4387 | 491,5 | 6,58 | 117 | Vacuolar protein sorting-associated protein 13D OS=Homo sapiens GN=VPS13D P |
| Q8TF72 | 21 | 1996 | 216,7 | 7,8 | 116 | Protein Shroom3 OS=Homo sapiens GN=SHROOM3 PE=1 SV=2 - [SHRM3_HUMAN] |
| O95359 | 37 | 2948 | 309,2 | 4,79 | 116 | Transforming acidic coiled-coil-containing protein 2 OS=Homo sapiens GN=TACC2 |
| Q9UQE7 | 11 | 1217 | 141,5 | 7,18 | 116 | Structural maintenance of chromosomes protein 3 OS=Homo sapiens GN=SMC3 P |
| O14490 | 56 | 977 | 108,8 | 7,08 | 116 | Disks large-associated protein 1 OS=Homo sapiens GN=DLGAP1 PE=1 SV=1 - [DLGF |
| Q9P2D3 | 19 | 2071 | 224,2 | 7,17 | 116 | HEAT repeat-containing protein 5B OS=Homo sapiens GN=HEATR5B PE=1 SV=2 - [H |
| P33992 | 15 | 734 | 82,2 | 8,37 | 115 | DNA replication licensing factor MCM5 OS=Homo sapiens GN=MCM5 PE=1 SV=5 - |
| Q9HAU5 | 11 | 1272 | 147,7 | 5,69 | 115 | Regulator of nonsense transcripts 2 OS=Homo sapiens GN=UPF2 PE=1 SV=1 - [REN |
| P16591 | 29 | 822 | 94,6 | 7,14 | 113 | Proto-oncogene tyrosine-protein kinase FER (EC 2.7.10.2) (p94-FER) (c-FER) (Tyro |
| Q13796 | 16 | 1616 | 176,3 | 7,09 | 113 | Protein Shroom2 OS=Homo sapiens GN=SHROOM2 PE=1 SV=1 - [SHRM2_HUMAN] |
| O15417 | 13 | 2968 | 314,3 | 8,7 | 112 | Trinucleotide repeat-containing gene 18 protein OS=Homo sapiens GN=TNRC18 P |
| Q8NCU4 | 10 | 936 | 110,5 | 9,6 | 112 | Coiled-coil domain-containing protein KIAA1407 OS=Homo sapiens GN=KIAA1407 |
| Q9Y496 | 19 | 699 | 80,0 | 6,54 | 111 | Kinesin-like protein KIF3A OS=Homo sapiens GN=KIF3A PE=1 SV=4 - [KIF3A_HUMA |
| Q6WRI0 | 22 | 2623 | 290,7 | 9,13 | 111 | Immunoglobulin superfamily member 10 OS=Homo sapiens GN=IGSF10 PE=1 SV= |
| Q96L93 | 36 | 1317 | 151,9 | 6,16 | 111 | Kinesin-like protein KIF16B OS=Homo sapiens GN=KIF16B PE=1 SV=2 - [KI16B_HUM |
| P12036 | 53 | 1026 | 112,4 | 6,18 | 111 | Neurofilament heavy polypeptide OS=Homo sapiens GN=NEFH PE=1 SV=4 - [NFH_ |
| Q8NB90 | 24 | 893 | 97,8 | 5,66 | 110 | Spermatogenesis-associated protein 5 OS=Homo sapiens GN=SPATA5 PE=1 SV=3 - |
| O75747 | 116 | 1445 | 165,6 | 6,93 | 110 | Phosphatidylinositol-4-phosphate 3-kinase C2 domain-containing subunit gamm |
| Q9Y2W1 | 20 | 955 | 108,6 | 10,15 | 109 | Thyroid hormone receptor-associated protein 3 OS=Homo sapiens GN=THRAP3 P |
| Q9H254 | 20 | 2564 | 288,8 | 6,01 | 109 | Spectrin beta chain, brain 3 OS=Homo sapiens GN=SPTBN4 PE=1 SV=2 - [SPTN4_H |
| Q8IWJ2 | 12 | 1684 | 195,8 | 5,14 | 109 | GRIP and coiled-coil domain-containing protein 2 OS=Homo sapiens GN=GCC2 PE |
| Q13576 | 30 | 1575 | 180,5 | 5,64 | 108 | Ras GTPase-activating-like protein IQGAP2 OS=Homo sapiens GN=IQGAP2 PE=1 SV |
| P01859 | 9 | 326 | 35,9 | 7,59 | 108 | Ig gamma-2 chain C region OS=Homo sapiens GN=IGHG2 PE=1 SV=2 - [IGHG2_HUM |
| Q15772 | 21 | 3267 | 354,1 | 8,51 | 108 | Striated muscle preferentially expressed protein kinase OS=Homo sapiens GN=S |
| Q7Z6G8 | 24 | 1249 | 138,1 | 6,37 | 108 | Ankyrin repeat and sterile alpha motif domain-containing protein 1B OS=Homo s |
| Q6AWC2 | 18 | 1192 | 133,8 | 5,53 | 108 | Protein WWC2 OS=Homo sapiens GN=WWC2 PE=1 SV=2 - [WWC2_HUMAN] |
| Q07954 | 15 | 4544 | 504,3 | 5,39 | 107 | Prolow-density lipoprotein receptor-related protein 1 OS=Homo sapiens GN=LRP |
| Q7Z736 | 28 | 793 | 85,3 | 7,83 | 107 | Pleckstrin homology domain-containing family H member 3 OS=Homo sapiens GI |
| Q92616 | 18 | 2671 | 292,6 | 7,47 | 106 | Translational activator GCN1 OS=Homo sapiens GN=GCN1L1 PE=1 SV=6 - [GCN1L_ |
| O60281 | 22 | 2723 | 304,6 | 7,39 | 106 | Zinc finger protein 292 OS=Homo sapiens GN=ZNF292 PE=1 SV=3 - [ZN292_HUMAN |
| Q8NFU7 | 26 | 2136 | 235,2 | 8,24 | 106 | Methylcytosine dioxygenase TET1 OS=Homo sapiens GN=TET1 PE=1 SV=2 - [TET1_ |
| Q02779 | 57 | 954 | 103,6 | 7,01 | 106 | Mitogen-activated protein kinase kinase kinase 10 OS=Homo sapiens GN=MAP3K |
| Q5VYK3 | 116 | 1845 | 204,2 | 7,12 | 106 | Proteasome-associated protein ECM29 homolog OS=Homo sapiens GN=ECM29 PE |
| Q6TFL3 | 23 | 1326 | 152,7 | 6,81 | 106 | Uncharacterized protein C9orf93 OS=Homo sapiens GN=C9orf93 PE=2 SV=1 - [CI09 |
| Q9C0D4 | 23 | 1074 | 119,5 | 9,45 | 105 | Zinc finger protein 518B OS=Homo sapiens GN=ZNF518B PE=2 SV=2 - [Z518B_HUM |
| P42695 | 17 | 1498 | 168,8 | 7,5 | 105 | Condensin-2 complex subunit D3 OS=Homo sapiens GN=NCAPD3 PE=1 SV=2 - [CN |
| Q92878 | 18 | 1312 | 153,8 | 6,89 | 104 | DNA repair protein RAD50 OS=Homo sapiens GN=RAD50 PE=1 SV=1 - [RAD50_HUM |
| P01764 | 46 | 117 | 12,6 | 8,28 | 104 | Ig heavy chain V-III region VH26 OS=Homo sapiens PE=1 SV=1 - [HV303_HUMAN] |
| Q15147 | 57 | 1175 | 134,4 | 6,9 | 104 | 1-phosphatidylinositol-4,5-bisphosphate phosphodiesterase beta-4 OS=Homo sa |
| Q7Z7B0 | 24 | 1213 | 138,0 | 8,32 | 104 | Filamin-A-interacting protein 1 OS=Homo sapiens GN=FILIP1 PE=1 SV=1 - [FLIP1_H |
| Q8N8E3 | 32 | 955 | 112,7 | 6,68 | 103 | Coiled-coil domain-containing protein 46 OS=Homo sapiens GN=CCDC46 PE=2 SV= |

| | | | | | | |
|---|---|---|---|---|---|---|
| Q494V2 | 18 | 611 | 71,1 | 7,11 | 103 | Coiled-coil domain-containing protein 37 OS=Homo sapiens GN=CCDC37 PE=1 SV= |
| Q16651 | 8 | 343 | 36,4 | 5,85 | 103 | Prostasin OS=Homo sapiens GN=PRSS8 PE=1 SV=1 - [PRSS8_HUMAN] |
| P31949 | 20 | 105 | 11,7 | 7,12 | 103 | Protein S100-A11 (S100 calcium-binding protein A11) (Protein S100C) (Calgizzarin |
| Q8N9B5 | 19 | 988 | 111,4 | 6,18 | 103 | Junction-mediating and -regulatory protein OS=Homo sapiens GN=JMY PE=1 SV= |
| Q96JM4 | 18 | 1722 | 199,2 | 6,19 | 103 | Leucine-rich repeat and IQ domain-containing protein 1 OS=Homo sapiens GN=LR |
| Q9NPG3 | 20 | 1134 | 121,4 | 9,33 | 102 | Ubinuclein-1 OS=Homo sapiens GN=UBN1 PE=1 SV=2 - [UBN1_HUMAN] |
| O75165 | 27 | 2243 | 254,3 | 6,74 | 102 | DnaJ homolog subfamily C member 13 OS=Homo sapiens GN=DNAJC13 PE=1 SV= |
| Q9NSD9 | 11 | 589 | 66,1 | 6,84 | 102 | Phenylalanyl-tRNA synthetase beta chain OS=Homo sapiens GN=FARSB PE=1 SV= |
| Q9H6R4 | 24 | 1146 | 127,5 | 7,64 | 102 | Nucleolar protein 6 OS=Homo sapiens GN=NOL6 PE=1 SV=2 - [NOL6_HUMAN] |
| P04792 | 10 | 205 | 22,8 | 6,4 | 102 | Heat-shock protein beta-1 (HspB1) (Heat shock 27 kDa protein) (HSP 27) (Stress-r |
| Q8IY37 | 14 | 1157 | 129,5 | 8,1 | 102 | Probable ATP-dependent RNA helicase DHX37 OS=Homo sapiens GN=DHX37 PE= |
| P12035 | 23 | 628 | 64,4 | 6,48 | 102 | Keratin, type II cytoskeletal 3 OS=Homo sapiens GN=KRT3 PE=1 SV=3 - [K2C3_HUM |
| O14727 | 46 | 1248 | 141,7 | 6,4 | 102 | Apoptotic protease-activating factor 1 OS=Homo sapiens GN=APAF1 PE=1 SV=2 - [ |
| Q14687 | 16 | 1217 | 136,1 | 7,74 | 101 | Genetic suppressor element 1 OS=Homo sapiens GN=GSE1 PE=1 SV=3 - [GSE1_HU |
| Q29RF7 | 14 | 1337 | 150,7 | 7,91 | 101 | Sister chromatid cohesion protein PDS5 homolog A OS=Homo sapiens GN=PDS5A |
| Q9NPF5 | 29 | 467 | 53,0 | 9,5 | 101 | DNA methyltransferase 1-associated protein 1 OS=Homo sapiens GN=DMAP1 PE= |
| Q4L180 | 10 | 1135 | 130,3 | 6,57 | 101 | Filamin A-interacting protein 1-like OS=Homo sapiens GN=FILIP1L PE=1 SV=2 - [FI |
| Q5T2S8 | 32 | 1044 | 115,6 | 7,77 | 101 | Armadillo repeat-containing protein 4 OS=Homo sapiens GN=ARMC4 PE=2 SV=1 - |
| Q8ND23 | 70 | 1372 | 150,1 | 7,44 | 101 | Leucine-rich repeat-containing protein 16B OS=Homo sapiens GN=LRRC16B PE=2 |
| Q5TCY1 | 84 | 1321 | 142,6 | 5,6 | 100 | Tau-tubulin kinase 1 OS=Homo sapiens GN=TTBK1 PE=1 SV=2 - [TTBK1_HUMAN] |
| O95477 | 9 | 2261 | 254,1 | 6,86 | 100 | ATP-binding cassette sub-family A member 1 OS=Homo sapiens GN=ABCA1 PE=1 |
| Q96JP5 | 35 | 570 | 63,4 | 7,36 | 100 | E3 ubiquitin-protein ligase ZFP91 OS=Homo sapiens GN=ZFP91 PE=1 SV=1 - [ZFP9 |
| Q96DT5 | 34 | 4523 | 520,7 | 6,44 | 100 | Dynein heavy chain 11, axonemal OS=Homo sapiens GN=DNAH11 PE=1 SV=3 - [DY |
| P35579 | 17 | 1960 | 226,4 | 5,6 | 100 | Myosin-9 OS=Homo sapiens GN=MYH9 PE=1 SV=4 - [MYH9_HUMAN] |
| Q14566 | 156 | 821 | 92,8 | 5,41 | 100 | DNA replication licensing factor MCM6 OS=Homo sapiens GN=MCM6 PE=1 SV=1 - |
| Q8IWK6 | 43 | 1321 | 146,1 | 8,48 | 99 | Probable G-protein coupled receptor 125 OS=Homo sapiens GN=GPR125 PE=1 SV= |
| P05787 | 40 | 483 | 53,7 | 5,59 | 98 | Keratin, type II cytoskeletal 8 OS=Homo sapiens GN=KRT8 PE=1 SV=7 - [K2C8_HUM |
| Q9NZM1 | 21 | 2061 | 234,6 | 6,18 | 98 | Myoferlin OS=Homo sapiens GN=MYOF PE=1 SV=1 - [MYOF_HUMAN] |
| P78344 | 24 | 907 | 102,3 | 7,14 | 98 | Eukaryotic translation initiation factor 4 gamma 2 OS=Homo sapiens GN=EIF4G2 P |
| P01616 | 16 | 112 | 12,0 | 9,29 | 98 | Ig kappa chain V-II region MIL OS=Homo sapiens PE=1 SV=1 - [KV203_HUMAN] |
| Q9BRK5 | 9 | 362 | 41,8 | 4,86 | 98 | 45 kDa calcium-binding protein OS=Homo sapiens GN=SDF4 PE=1 SV=1 - [CAB45_H |
| Q8WWN8 | 30 | 1544 | 169,7 | 7,08 | 97 | Arf-GAP with Rho-GAP domain, ANK repeat and PH domain-containing protein 3 |
| Q01546 | 9 | 638 | 65,8 | 8,12 | 97 | Keratin, type II cytoskeletal 2 oral OS=Homo sapiens GN=KRT76 PE=1 SV=2 - [K22C |
| Q9Y4D1 | 10 | 1078 | 123,4 | 7,23 | 97 | Disheveled-associated activator of morphogenesis 1 OS=Homo sapiens GN=DAAI |
| Q7L7X3 | 11 | 1001 | 116,0 | 7,65 | 97 | Serine/threonine-protein kinase TAO1 OS=Homo sapiens GN=TAOK1 PE=1 SV=1 - |
| Q8TBY8 | 15 | 1022 | 119,0 | 6,29 | 97 | Polyamine-modulated factor 1-binding protein 1 OS=Homo sapiens GN=PMFBP1 |
| P01621 | 49 | 100 | 10,7 | 6,52 | 97 | Ig kappa chain V-III region NG9 (Fragment) OS=Homo sapiens PE=1 SV=1 - [KV303 |
| P01037 | 62 | 141 | 16,4 | 7,21 | 97 | Cystatin-SN OS=Homo sapiens GN=CST1 PE=1 SV=3 - [CYTN_HUMAN] |
| O75151 | 17 | 1096 | 120,7 | 9,17 | 97 | PHD finger protein 2 OS=Homo sapiens GN=PHF2 PE=1 SV=4 - [PHF2_HUMAN] |
| Q6VAB6 | 42 | 950 | 107,6 | 8,69 | 96 | Kinase suppressor of Ras 2 OS=Homo sapiens GN=KSR2 PE=1 SV=2 - [KSR2_HUMAI |
| Q8N9T8 | 36 | 709 | 83,2 | 5,17 | 96 | Protein KRI1 homolog OS=Homo sapiens GN=KRI1 PE=1 SV=2 - [KRI1_HUMAN] |
| Q9NTI5 | 12 | 1447 | 164,6 | 8,47 | 96 | Sister chromatid cohesion protein PDS5 homolog B OS=Homo sapiens GN=PDS5B |
| Q8WWZ7 | 26 | 1642 | 186,4 | 6,95 | 96 | ATP-binding cassette sub-family A member 5 OS=Homo sapiens GN=ABCA5 PE=2 |
| Q96RV3 | 7 | 2341 | 258,5 | 7,21 | 96 | Pecanex-like protein 1 OS=Homo sapiens GN=PCNX PE=2 SV=2 - [PCX1_HUMAN] |
| Q9UHB6 | 17 | 759 | 85,2 | 6,84 | 96 | LIM domain and actin-binding protein 1 OS=Homo sapiens GN=LIMA1 PE=1 SV=1 - |
| Q92797 | 80 | 1274 | 141,1 | 6,13 | 95 | Symplekin OS=Homo sapiens GN=SYMPK PE=1 SV=2 - [SYMPK_HUMAN] |
| Q8IYB3 | 25 | 904 | 102,3 | 11,84 | 95 | Serine/arginine repetitive matrix protein 1 OS=Homo sapiens GN=SRRM1 PE=1 SV |
| Q14997 | 13 | 1843 | 211,2 | 6,9 | 95 | Proteasome activator complex subunit 4 OS=Homo sapiens GN=PSME4 PE=1 SV=2 |
| Q96SB8 | 10 | 1091 | 126,2 | 6,99 | 95 | Structural maintenance of chromosomes protein 6 OS=Homo sapiens GN=SMC6 P |
| Q7Z3E2 | 14 | 898 | 103,6 | 6,27 | 95 | Uncharacterized protein C10orf118 OS=Homo sapiens GN=C10orf118 PE=2 SV=2 - |
| P09104 | 5 | 434 | 47,2 | 5,03 | 95 | Gamma-enolase (EC 4.2.1.11) (2-phospho-D-glycerate hydro-lyase) (Neural enola |
| P23468 | 21 | 1912 | 214,6 | 6,57 | 95 | Receptor-type tyrosine-protein phosphatase delta OS=Homo sapiens GN=PTPRD |
| Q6ZV29 | 11 | 1317 | 145,6 | 7,74 | 95 | Patatin-like phospholipase domain-containing protein 7 OS=Homo sapiens GN=P |
| Q5TH69 | 37 | 2177 | 240,5 | 5,82 | 94 | Brefeldin A-inhibited guanine nucleotide-exchange protein 3 OS=Homo sapiens |
| Q9UPU5 | 26 | 2620 | 294,2 | 6,14 | 94 | Ubiquitin carboxyl-terminal hydrolase 24 OS=Homo sapiens GN=USP24 PE=1 SV= |
| Q9BYW2 | 31 | 2564 | 287,4 | 6,14 | 94 | Histone-lysine N-methyltransferase SETD2 OS=Homo sapiens GN=SETD2 PE=1 SV= |
| Q9HBT8 | 12 | 521 | 60,1 | 8,32 | 94 | Zinc finger protein 286A OS=Homo sapiens GN=ZNF286A PE=2 SV=1 - [Z286A_HUM |
| O60437 | 23 | 1756 | 204,6 | 5,6 | 94 | Periplakin OS=Homo sapiens GN=PPL PE=1 SV=4 - [PEPL_HUMAN] |
| Q8IWZ3 | 30 | 2542 | 269,3 | 5,73 | 94 | Ankyrin repeat and KH domain-containing protein 1 OS=Homo sapiens GN=ANKH |
| P14555 | 49 | 144 | 16,1 | 9,23 | 94 | Phospholipase A2, membrane associated OS=Homo sapiens GN=PLA2G2A PE=1 SV |
| P06396 | 6 | 782 | 85,6 | 6,28 | 94 | Gelsolin OS=Homo sapiens GN=GSN PE=1 SV=1 - [GELS_HUMAN] |
| Q9BQS8 | 10 | 1478 | 166,9 | 4,92 | 94 | FYVE and coiled-coil domain-containing protein 1 OS=Homo sapiens GN=FYCO1 P |
| P31946 | 12 | 246 | 28,1 | 4,83 | 94 | 14-3-3 protein beta/alpha OS=Homo sapiens GN=YWHAB PE=1 SV=3 - [1433B_HUM |
| Q5RHP9 | 16 | 1530 | 168,4 | 4,88 | 93 | Uncharacterized protein C1orf173 OS=Homo sapiens GN=C1orf173 PE=2 SV=1 - [C |
| O14802 | 14 | 1390 | 155,5 | 8,48 | 93 | DNA-directed RNA polymerase III subunit RPC1 OS=Homo sapiens GN=POLR3A PE |

| | | | | | | |
|---|---|---|---|---|---|---|
| Q8NA31 | 30 | 727 | 83,0 | 7,46 | 93 | Coiled-coil domain-containing protein 79 OS=Homo sapiens GN=CCDC79 PE=2 SV |
| Q9HCE1 | 12 | 1003 | 113,6 | 8,82 | 93 | Putative helicase MOV-10 OS=Homo sapiens GN=MOV10 PE=1 SV=2 - [MOV10_HU |
| Q9Y5S2 | 46 | 1711 | 194,2 | 6,37 | 93 | Serine/threonine-protein kinase MRCK beta OS=Homo sapiens GN=CDC42BPB PE |
| O75923 | 12 | 2080 | 237,1 | 5,64 | 92 | Dysferlin OS=Homo sapiens GN=DYSF PE=1 SV=1 - [DYSF_HUMAN] |
| O75417 | 36 | 1762 | 197,5 | 7,01 | 92 | DNA polymerase theta OS=Homo sapiens GN=POLQ PE=1 SV=1 - [DPOLQ_HUMAN |
| Q6N069 | 73 | 864 | 101,4 | 7,87 | 92 | N-alpha-acetyltransferase 16, NatA auxiliary subunit OS=Homo sapiens GN=NAA |
| P53367 | 23 | 373 | 41,7 | 6,7 | 92 | Arfaptin-1 OS=Homo sapiens GN=ARFIP1 PE=1 SV=2 - [ARFP1_HUMAN] |
| Q99490 | 59 | 1192 | 124,6 | 9,89 | 92 | Centaurin-gamma 1 (ARF-GAP with GTP-binding protein-like, ankyrin repeat and |
| P02787 | 73 | 698 | 77,0 | 7,12 | 92 | Serotransferrin OS=Homo sapiens GN=TF PE=1 SV=3 - [TRFE_HUMAN] |
| Q5VT97 | 11 | 1116 | 124,9 | 8,15 | 92 | Rho GTPase-activating protein SYDE2 OS=Homo sapiens GN=SYDE2 PE=1 SV=1 - [S |
| O75691 | 11 | 2785 | 318,2 | 7,39 | 92 | Small subunit processome component 20 homolog OS=Homo sapiens GN=UTP20 |
| Q8TDY2 | 15 | 1594 | 183,0 | 5,41 | 92 | RB1-inducible coiled-coil protein 1 OS=Homo sapiens GN=RB1CC1 PE=1 SV=3 - [RE |
| Q9NRA8 | 15 | 985 | 108,1 | 8,32 | 92 | Eukaryotic translation initiation factor 4E transporter OS=Homo sapiens GN=EIF4E |
| Q13393 | 12 | 1074 | 124,1 | 8,78 | 92 | Phospholipase D1 OS=Homo sapiens GN=PLD1 PE=1 SV=1 - [PLD1_HUMAN] |
| O43166 | 10 | 1804 | 199,9 | 8,19 | 92 | Signal-induced proliferation-associated 1-like protein 1 OS=Homo sapiens GN=SI |
| Q8IYE0 | 13 | 955 | 112,7 | 8,48 | 91 | Coiled-coil domain-containing protein 146 OS=Homo sapiens GN=CCDC146 PE=2 S |
| P11137 | 34 | 1827 | 199,4 | 4,91 | 91 | Microtubule-associated protein 2 OS=Homo sapiens GN=MAP2 PE=1 SV=4 - [MAP |
| Q2M296 | 20 | 383 | 42,1 | 8,73 | 91 | Methenyltetrahydrofolate synthase domain-containing protein OS=Homo sapien |
| Q2TAC6 | 10 | 998 | 111,3 | 8,69 | 91 | Kinesin-like protein KIF19 OS=Homo sapiens GN=KIF19 PE=2 SV=2 - [KIF19_HUMA |
| Q9NYF0 | 45 | 836 | 90,1 | 8,69 | 91 | Dapper homolog 1 OS=Homo sapiens GN=DACT1 PE=2 SV=2 - [DACT1_HUMAN] |
| Q5VSL9 | 20 | 837 | 95,5 | 6,29 | 90 | Protein FAM40A OS=Homo sapiens GN=FAM40A PE=1 SV=1 - [FA40A_HUMAN] |
| Q86WJ1 | 39 | 897 | 100,9 | 6,9 | 90 | Chromodomain-helicase-DNA-binding protein 1-like OS=Homo sapiens GN=CHD |
| Q9Y4I1 | 79 | 1855 | 215,3 | 8,48 | 90 | Myosin-Va OS=Homo sapiens GN=MYO5A PE=1 SV=2 - [MYO5A_HUMAN] |
| P68104 | 7 | 462 | 50,1 | 9,01 | 89 | Elongation factor 1-alpha 1 OS=Homo sapiens GN=EEF1A1 PE=1 SV=1 - [EF1A1_HU |
| P08069 | 25 | 1367 | 154,7 | 5,8 | 89 | Insulin-like growth factor 1 receptor OS=Homo sapiens GN=IGF1R PE=1 SV=1 - [IG |
| Q9Y2K7 | 11 | 1162 | 132,7 | 7,58 | 89 | Lysine-specific demethylase 2A OS=Homo sapiens GN=KDM2A PE=1 SV=3 - [KDM2 |
| P31146 | 25 | 461 | 51,0 | 6,68 | 89 | Coronin-1A OS=Homo sapiens GN=CORO1A PE=1 SV=4 - [COR1A_HUMAN] |
| O60229 | 28 | 2985 | 340,0 | 6,07 | 88 | Kalirin OS=Homo sapiens GN=KALRN PE=1 SV=2 - [KALRN_HUMAN] |
| Q96JG9 | 12 | 3925 | 409,9 | 7,72 | 88 | Zinc finger protein 469 OS=Homo sapiens GN=ZNF469 PE=1 SV=3 - [ZN469_HUMAN |
| Q5VUA4 | 13 | 2279 | 251,0 | 7,2 | 88 | Zinc finger protein 318 OS=Homo sapiens GN=ZNF318 PE=1 SV=2 - [ZN318_HUMAN |
| P13533 | 12 | 1939 | 223,6 | 5,73 | 87 | Myosin-6 OS=Homo sapiens GN=MYH6 PE=1 SV=5 - [MYH6_HUMAN] |
| P08727 | 12 | 400 | 44,1 | 5,14 | 87 | Keratin, type I cytoskeletal 19 OS=Homo sapiens GN=KRT19 PE=1 SV=4 - [K1C19_H |
| Q9Y2G9 | 50 | 1366 | 150,2 | 6,52 | 87 | Protein strawberry notch homolog 2 OS=Homo sapiens GN=SBNO2 PE=2 SV=3 - [S |
| Q96MR6 | 10 | 1250 | 144,9 | 5,8 | 87 | WD repeat-containing protein 65 OS=Homo sapiens GN=WDR65 PE=2 SV=3 - [WDF |
| Q6KC79 | 34 | 2804 | 315,9 | 7,91 | 87 | Nipped-B-like protein OS=Homo sapiens GN=NIPBL PE=1 SV=2 - [NIPBL_HUMAN] |
| Q13618 | 20 | 768 | 88,9 | 8,48 | 87 | Cullin-3 OS=Homo sapiens GN=CUL3 PE=1 SV=2 - [CUL3_HUMAN] |
| Q96QB1 | 46 | 1528 | 170,5 | 6,4 | 86 | Rho GTPase-activating protein 7 OS=Homo sapiens GN=DLC1 PE=1 SV=4 - [RHG07_ |
| Q13233 | 10 | 1512 | 164,4 | 7,74 | 86 | Mitogen-activated protein kinase kinase kinase 1 OS=Homo sapiens GN=MAP3K1 |
| Q8TDN4 | 26 | 633 | 67,6 | 9,17 | 85 | CDK5 and ABL1 enzyme substrate 1 OS=Homo sapiens GN=CABLES1 PE=1 SV=2 - [C |
| Q9Y3M8 | 17 | 1113 | 124,9 | 7,02 | 85 | StAR-related lipid transfer protein 13 OS=Homo sapiens GN=STARD13 PE=1 SV=2 - |
| Q9NXH9 | 11 | 659 | 72,2 | 7,64 | 85 | N(2),N(2)-dimethylguanosine tRNA methyltransferase OS=Homo sapiens GN=TRI |
| Q8NG31 | 8 | 2342 | 265,2 | 5,47 | 85 | Protein CASC5 OS=Homo sapiens GN=CASC5 PE=1 SV=3 - [CASC5_HUMAN] |
| Q9ULV0 | 79 | 1848 | 213,5 | 7,2 | 85 | Myosin-Vb OS=Homo sapiens GN=MYO5B PE=1 SV=3 - [MYO5B_HUMAN] |
| Q9ULJ8 | 12 | 1098 | 123,3 | 5,1 | 85 | Neurabin-1 OS=Homo sapiens GN=PPP1R9A PE=1 SV=2 - [NEB1_HUMAN] |
| Q9H582 | 98 | 1327 | 149,5 | 8,16 | 85 | Zinc finger protein 644 OS=Homo sapiens GN=ZNF644 PE=1 SV=2 - [ZN644_HUMAN |
| Q68D51 | 11 | 928 | 106,8 | 8,48 | 85 | DENN domain-containing protein 2C OS=Homo sapiens GN=DENND2C PE=2 SV=2 - |
| Q7Z2Y8 | 20 | 2422 | 278,9 | 6,55 | 85 | Interferon-induced very large GTPase 1 OS=Homo sapiens GN=GVIN1 PE=2 SV=2 - |
| Q149N8 | 11 | 1683 | 193,0 | 7,47 | 85 | E3 ubiquitin-protein ligase SHPRH OS=Homo sapiens GN=SHPRH PE=1 SV=2 - [SHP |
| O14777 | 7 | 642 | 73,9 | 5,6 | 85 | Kinetochore protein NDC80 homolog OS=Homo sapiens GN=NDC80 PE=1 SV=1 - [N |
| Q9UPZ9 | 100 | 632 | 71,4 | 9,77 | 84 | Serine/threonine-protein kinase ICK OS=Homo sapiens GN=ICK PE=1 SV=1 - [ICK_ |
| Q9NYC9 | 45 | 4486 | 511,6 | 5,91 | 84 | Dynein heavy chain 9, axonemal OS=Homo sapiens GN=DNAH9 PE=1 SV=3 - [DYH9 |
| Q9P2L0 | 34 | 1181 | 133,5 | 6,38 | 84 | WD repeat-containing protein 35 OS=Homo sapiens GN=WDR35 PE=2 SV=3 - [WDF |
| O15021 | 79 | 2626 | 284,2 | 8,62 | 84 | Microtubule-associated serine/threonine-protein kinase 4 OS=Homo sapiens GN |
| Q7Z3Y7 | 9 | 464 | 50,5 | 5,47 | 84 | Keratin, type I cytoskeletal 28 OS=Homo sapiens GN=KRT28 PE=1 SV=2 - [K1C28_H |
| P12883 | 10 | 1935 | 223,0 | 5,8 | 84 | Myosin-7 OS=Homo sapiens GN=MYH7 PE=1 SV=5 - [MYH7_HUMAN] |
| Q9ULD4 | 12 | 1205 | 135,7 | 6,58 | 84 | Bromodomain and PHD finger-containing protein 3 OS=Homo sapiens GN=BRPF3 |
| P01700 | 21 | 112 | 11,9 | 8,91 | 84 | Ig lambda chain V-I region HA OS=Homo sapiens PE=1 SV=1 - [LV102_HUMAN] |
| A6NKB5 | 52 | 2137 | 237,1 | 6,76 | 84 | Pecanex-like protein 2 OS=Homo sapiens GN=PCNXL2 PE=1 SV=3 - [PCX2_HUMAN |
| P08582 | 72 | 738 | 80,2 | 6,01 | 84 | Melanotransferrin OS=Homo sapiens GN=MFI2 PE=1 SV=1 - [TRFM_HUMAN] |
| P01611 | 8 | 108 | 11,6 | 7,28 | 84 | Ig kappa chain V-I region Wes OS=Homo sapiens PE=1 SV=1 - [KV119_HUMAN] |
| Q9P212 | 20 | 2302 | 258,6 | 6,48 | 83 | 1-phosphatidylinositol-4,5-bisphosphate phosphodiesterase epsilon-1 OS=Homo |
| Q14722 | 14 | 419 | 46,5 | 8,94 | 83 | Voltage-gated potassium channel subunit beta-1 OS=Homo sapiens GN=KCNAB1 |
| A6NCI4 | 13 | 1184 | 133,9 | 8,46 | 83 | von Willebrand factor A domain-containing protein 3A OS=Homo sapiens GN=VW |
| Q7Z4L5 | 8 | 1316 | 150,8 | 6,96 | 83 | Tetratricopeptide repeat protein 21B OS=Homo sapiens GN=TTC21B PE=2 SV=2 - [ |
| Q9H251 | 28 | 3354 | 369,3 | 4,67 | 83 | Cadherin-23 OS=Homo sapiens GN=CDH23 PE=1 SV=1 - [CAD23_HUMAN] |

| | | | | | | |
|---|---|---|---|---|---|---|
| Q9C0H6 | 9 | 718 | 80,2 | 6,86 | 83 | Kelch-like protein 4 OS=Homo sapiens GN=KLHL4 PE=2 SV=2 - [KLHL4_HUMAN] |
| Q9NRZ9 | 78 | 838 | 97,0 | 7,93 | 83 | Lymphoid-specific helicase OS=Homo sapiens GN=HELLS PE=1 SV=1 - [HELLS_HUM |
| Q9NQ76 | 44 | 525 | 58,4 | 8,57 | 83 | Matrix extracellular phosphoglycoprotein OS=Homo sapiens GN=MEPE PE=1 SV=1 |
| Q6PCB5 | 16 | 846 | 94,8 | 8,78 | 83 | Round spermatid basic protein 1-like protein OS=Homo sapiens GN=RSBN1L PE=1 |
| Q9H611 | 17 | 641 | 69,8 | 9,72 | 83 | ATP-dependent DNA helicase PIF1 OS=Homo sapiens GN=PIF1 PE=1 SV=2 - [PIF1_ |
| P52209 | 5 | 483 | 53,1 | 7,23 | 83 | 6-phosphogluconate dehydrogenase, decarboxylating OS=Homo sapiens GN=PGD |
| Q9NQX4 | 10 | 1742 | 202,7 | 7,71 | 82 | Myosin-Vc OS=Homo sapiens GN=MYO5C PE=1 SV=2 - [MYO5C_HUMAN] |
| Q8NEC7 | 43 | 633 | 71,0 | 7,78 | 82 | Glutathione S-transferase C-terminal domain-containing protein OS=Homo sapie |
| Q03111 | 19 | 559 | 62,0 | 8,59 | 82 | Protein ENL OS=Homo sapiens GN=MLLT1 PE=1 SV=2 - [ENL_HUMAN] |
| Q9Y6A5 | 34 | 838 | 90,3 | 5,05 | 82 | Transforming acidic coiled-coil-containing protein 3 OS=Homo sapiens GN=TACC3 |
| Q9Y566 | 16 | 2161 | 224,8 | 8,15 | 82 | SH3 and multiple ankyrin repeat domains protein 1 OS=Homo sapiens GN=SHANK |
| Q8N3T6 | 16 | 1108 | 121,7 | 6,35 | 82 | Transmembrane protein 132C OS=Homo sapiens GN=TMEM132C PE=2 SV=3 - [T13 |
| Q9C0F0 | 49 | 2248 | 241,8 | 6,14 | 82 | Putative Polycomb group protein ASXL3 OS=Homo sapiens GN=ASXL3 PE=2 SV=3 - |
| Q8WV44 | 10 | 630 | 71,6 | 5,06 | 82 | E3 ubiquitin-protein ligase TRIM41 OS=Homo sapiens GN=TRIM41 PE=1 SV=3 - [TR |
| Q09161 | 10 | 790 | 91,8 | 6,43 | 82 | Nuclear cap-binding protein subunit 1 OS=Homo sapiens GN=NCBP1 PE=1 SV=1 - |
| P49815 | 17 | 1807 | 200,5 | 7,31 | 82 | Tuberin OS=Homo sapiens GN=TSC2 PE=1 SV=2 - [TSC2_HUMAN] |
| Q9NW08 | 19 | 1133 | 127,7 | 8,5 | 82 | DNA-directed RNA polymerase III subunit RPC2 OS=Homo sapiens GN=POLR3B PE |
| Q66K14 | 16 | 1250 | 140,4 | 5,25 | 82 | TBC1 domain family member 9B OS=Homo sapiens GN=TBC1D9B PE=1 SV=3 - [TBC |
| Q9BXX3 | 15 | 1397 | 158,7 | 6,48 | 82 | Ankyrin repeat domain-containing protein 30A OS=Homo sapiens GN=ANKRD30A |
| Q9H5P4 | 6 | 517 | 55,6 | 8,92 | 81 | PDZ domain-containing protein 7 OS=Homo sapiens GN=PDZD7 PE=1 SV=1 - [PDZD |
| P14136 | 14 | 432 | 49,8 | 5,52 | 81 | Glial fibrillary acidic protein OS=Homo sapiens GN=GFAP PE=1 SV=1 - [GFAP_HUM |
| Q14684 | 12 | 758 | 84,4 | 9,76 | 81 | Ribosomal RNA processing protein 1 homolog B OS=Homo sapiens GN=RRP1B PE= |
| Q9Y4C0 | 24 | 1643 | 180,5 | 5,54 | 81 | Neurexin-3-alpha OS=Homo sapiens GN=NRXN3 PE=2 SV=4 - [NRX3A_HUMAN] |
| Q9BWS9 | 16 | 393 | 44,9 | 8,63 | 81 | Chitinase domain-containing protein 1 OS=Homo sapiens GN=CHID1 PE=1 SV=1 - |
| Q05D60 | 49 | 604 | 70,9 | 6,21 | 81 | Coiled-coil domain-containing protein 67 OS=Homo sapiens GN=CCDC67 PE=2 SV |
| Q9HAU0 | 18 | 1116 | 127,4 | 7,53 | 81 | Pleckstrin homology domain-containing family A member 5 OS=Homo sapiens GN |
| P20807 | 21 | 821 | 94,2 | 6,18 | 81 | Calpain-3 OS=Homo sapiens GN=CAPN3 PE=1 SV=2 - [CAN3_HUMAN] |
| Q9C093 | 32 | 1822 | 209,7 | 5,54 | 81 | Sperm flagellar protein 2 OS=Homo sapiens GN=SPEF2 PE=1 SV=2 - [SPEF2_HUMA |
| Q6ZU35 | 14 | 1233 | 136,7 | 5,6 | 80 | Uncharacterized protein KIAA1211 OS=Homo sapiens GN=KIAA1211 PE=1 SV=3 - [K |
| Q9P227 | 25 | 1491 | 162,1 | 9,19 | 80 | Rho GTPase-activating protein 23 OS=Homo sapiens GN=ARHGAP23 PE=1 SV=2 - [R |
| Q9HCM1 | 15 | 1747 | 194,7 | 8,78 | 80 | Uncharacterized protein C12orf35 OS=Homo sapiens GN=C12orf35 PE=1 SV=3 - [CL |
| O75037 | 25 | 1637 | 182,5 | 7,08 | 80 | Kinesin-like protein KIF21B OS=Homo sapiens GN=KIF21B PE=1 SV=2 - [KI21B_HUM |
| Q8NEG5 | 13 | 633 | 72,7 | 8,62 | 80 | E3 ubiquitin-protein ligase ZSWIM2 OS=Homo sapiens GN=ZSWIM2 PE=1 SV=2 - [Z |
| Q9ULI0 | 12 | 1458 | 164,8 | 6,8 | 80 | ATPase family AAA domain-containing protein 2B OS=Homo sapiens GN=ATAD2B |
| P14618 | 3 | 531 | 57,9 | 7,84 | 80 | Pyruvate kinase isozymes M1/M2 (EC 2.7.1.40) (Pyruvate kinase muscle isozyme) |
| Q9BY89 | 12 | 1806 | 196,6 | 8,47 | 80 | Uncharacterized protein KIAA1671 OS=Homo sapiens GN=KIAA1671 PE=1 SV=2 - [K |
| P42345 | 8 | 2549 | 288,7 | 7,17 | 80 | Serine/threonine-protein kinase mTOR OS=Homo sapiens GN=MTOR PE=1 SV=1 - |
| Q70CQ2 | 25 | 3546 | 404,0 | 5,82 | 80 | Ubiquitin carboxyl-terminal hydrolase 34 OS=Homo sapiens GN=USP34 PE=1 SV=2 |
| Q14667 | 20 | 2235 | 253,5 | 7,14 | 80 | UPF0378 protein KIAA0100 OS=Homo sapiens GN=KIAA0100 PE=1 SV=3 - [K0100_H |
| Q5VZK9 | 28 | 1371 | 151,5 | 7,85 | 80 | Leucine-rich repeat-containing protein 16A OS=Homo sapiens GN=LRRC16A PE=1 |
| Q9NQ38 | 30 | 1064 | 120,6 | 8,06 | 80 | Serine protease inhibitor Kazal-type 5 OS=Homo sapiens GN=SPINK5 PE=1 SV=2 - |
| P01702 | 22 | 111 | 11,4 | 4,89 | 80 | Ig lambda chain V-I region NIG-64 OS=Homo sapiens PE=1 SV=1 - [LV104_HUMAN] |
| P29728 | 13 | 719 | 82,4 | 8,25 | 79 | 2'-5'-oligoadenylate synthase 2 OS=Homo sapiens GN=OAS2 PE=1 SV=3 - [OAS2_H |
| P02549 | 7 | 2419 | 279,8 | 5,05 | 79 | Spectrin alpha chain, erythrocyte OS=Homo sapiens GN=SPTA1 PE=1 SV=5 - [SPTA |
| O96028 | 7 | 1365 | 152,2 | 8,69 | 79 | Probable histone-lysine N-methyltransferase NSD2 OS=Homo sapiens GN=WHSC |
| P04433 | 14 | 115 | 12,6 | 4,96 | 79 | Ig kappa chain V-III region VG (Fragment) OS=Homo sapiens PE=1 SV=1 - [KV309_H |
| Q9NSB2 | 75 | 600 | 64,8 | 7,56 | 79 | Keratin, type II cuticular Hb4 OS=Homo sapiens GN=KRT84 PE=1 SV=2 - [KRT84_HU |
| Q2M2Z5 | 11 | 673 | 75,1 | 5,62 | 79 | Centrosomal protein kizuna OS=Homo sapiens GN=PLK1S1 PE=1 SV=2 - [KIZ_HUM |
| Q15678 | 11 | 1187 | 135,2 | 8,31 | 79 | Tyrosine-protein phosphatase non-receptor type 14 OS=Homo sapiens GN=PTPN |
| Q9H1D0 | 11 | 725 | 83,2 | 7,62 | 79 | Transient receptor potential cation channel subfamily V member 6 (TrpV6) (Epith |
| Q9BZJ0 | 18 | 848 | 100,4 | 8 | 79 | Crooked neck-like protein 1 OS=Homo sapiens GN=CRNKL1 PE=1 SV=4 - [CRNL1_H |
| Q8TCU6 | 11 | 1659 | 186,1 | 6,44 | 79 | Phosphatidylinositol 3,4,5-trisphosphate-dependent Rac exchanger 1 protein OS |
| P19013 | 7 | 534 | 57,2 | 6,61 | 78 | Keratin, type II cytoskeletal 4 OS=Homo sapiens GN=KRT4 PE=1 SV=4 - [K2C4_HUM |
| P78539 | 14 | 464 | 51,5 | 8,66 | 78 | Sushi repeat-containing protein SRPX OS=Homo sapiens GN=SRPX PE=2 SV=1 - [SR |
| Q12774 | 8 | 1597 | 176,7 | 5,53 | 78 | Rho guanine nucleotide exchange factor 5 OS=Homo sapiens GN=ARHGEF5 PE=1 S |
| Q8NFT6 | 24 | 615 | 67,2 | 8,34 | 78 | Protein DBF4 homolog B OS=Homo sapiens GN=DBF4B PE=1 SV=1 - [DBF4B_HUMA |
| Q6YHU6 | 8 | 1953 | 219,5 | 6,06 | 78 | Thyroid adenoma-associated protein OS=Homo sapiens GN=THADA PE=1 SV=1 - [T |
| Q05519 | 24 | 484 | 53,5 | 10,52 | 78 | Serine/arginine-rich splicing factor 11 OS=Homo sapiens GN=SRSF11 PE=1 SV=1 - |
| Q5TCS8 | 15 | 1911 | 221,3 | 5,01 | 78 | Adenylate kinase domain-containing protein 1 OS=Homo sapiens GN=AKD1 PE=1 |
| P16157 | 11 | 1881 | 206,1 | 6,01 | 77 | Ankyrin-1 OS=Homo sapiens GN=ANK1 PE=1 SV=3 - [ANK1_HUMAN] |
| Q9Y666 | 22 | 1083 | 119,0 | 6,71 | 77 | Solute carrier family 12 member 7 OS=Homo sapiens GN=SLC12A7 PE=1 SV=3 - [S1 |
| P01034 | 3 | 146 | 15,8 | 8,75 | 77 | Cystatin-C OS=Homo sapiens GN=CST3 PE=1 SV=1 - [CYTC_HUMAN] |
| Q9UC06 | 28 | 446 | 50,8 | 8,31 | 77 | Zinc finger protein 70 OS=Homo sapiens GN=ZNF70 PE=2 SV=2 - [ZNF70_HUMAN] |
| P25705 | 14 | 553 | 59,7 | 9,13 | 77 | ATP synthase subunit alpha, mitochondrial OS=Homo sapiens GN=ATP5A1 PE=1 S |
| Q8IZJ3 | 17 | 1885 | 206,6 | 6,42 | 77 | C3 and PZP-like alpha-2-macroglobulin domain-containing protein 8 OS=Homo sa |

| | | | | | | |
|---|---|---|---|---|---|---|
| Q8WXR4 | 6 | 1341 | 151,7 | 8,15 | 77 | Myosin-IIIb OS=Homo sapiens GN=MYO3B PE=2 SV=4 - [MYO3B_HUMAN] |
| P12107 | 9 | 1806 | 181,0 | 5,17 | 77 | Collagen alpha-1(XI) chain OS=Homo sapiens GN=COL11A1 PE=1 SV=4 - [COBA1_H |
| P13929 | 16 | 434 | 46,9 | 7,71 | 77 | Beta-enolase OS=Homo sapiens GN=ENO3 PE=1 SV=4 - [ENOB_HUMAN] |
| O95803 | 17 | 873 | 100,8 | 8,06 | 77 | Bifunctional heparan sulfate N-deacetylase/N-sulfotransferase 3 OS=Homo sapie |
| P23634 | 11 | 1241 | 137,8 | 6,6 | 77 | Plasma membrane calcium-transporting ATPase 4 OS=Homo sapiens GN=ATP2B4 |
| Q5CZ79 | 12 | 823 | 93,9 | 8,32 | 77 | Ankyrin repeat domain-containing protein 20B OS=Homo sapiens GN=ANKRD20B |
| Q8NAP3 | 7 | 1195 | 134,2 | 8,03 | 77 | Zinc finger and BTB domain-containing protein 38 OS=Homo sapiens GN=ZBTB38 I |
| Q9Y6D9 | 8 | 718 | 83,0 | 5,92 | 77 | Mitotic spindle assembly checkpoint protein MAD1 OS=Homo sapiens GN=MAD1 |
| Q8N157 | 20 | 1196 | 137,0 | 7,12 | 77 | Jouberin OS=Homo sapiens GN=AHI1 PE=1 SV=1 - [AHI1_HUMAN] |
| Q86V15 | 103 | 1759 | 189,9 | 7,03 | 77 | Zinc finger protein castor homolog 1 OS=Homo sapiens GN=CASZ1 PE=2 SV=4 - [CA |
| Q8TBF8 | 21 | 365 | 42,0 | 9,04 | 76 | Protein FAM81A OS=Homo sapiens GN=FAM81A PE=2 SV=1 - [FA81A_HUMAN] |
| Q6ZRQ5 | 21 | 1243 | 142,2 | 7,12 | 76 | Protein MMS22-like OS=Homo sapiens GN=MMS22L PE=1 SV=3 - [MMS22_HUMAN |
| Q13395 | 49 | 1621 | 181,6 | 7,05 | 76 | Probable methyltransferase TARBP1 OS=Homo sapiens GN=TARBP1 PE=1 SV=1 - [ |
| Q8NCA5 | 48 | 519 | 55,4 | 9,03 | 76 | Protein FAM98A OS=Homo sapiens GN=FAM98A PE=1 SV=1 - [FA98A_HUMAN] |
| Q9HC62 | 25 | 589 | 67,8 | 9,48 | 76 | Sentrin-specific protease 2 OS=Homo sapiens GN=SENP2 PE=1 SV=3 - [SENP2_HUI |
| Q86SQ7 | 24 | 713 | 82,6 | 5,81 | 75 | Serologically defined colon cancer antigen 8 OS=Homo sapiens GN=SDCCAG8 PE= |
| O95185 | 22 | 931 | 103,1 | 6,1 | 75 | Netrin receptor UNC5C OS=Homo sapiens GN=UNC5C PE=1 SV=2 - [UNC5C_HUMA |
| Q86VH2 | 10 | 1401 | 160,2 | 7,28 | 75 | Kinesin-like protein KIF27 OS=Homo sapiens GN=KIF27 PE=2 SV=1 - [KIF27_HUMA |
| Q8WWI1 | 7 | 1683 | 192,6 | 8,09 | 75 | LIM domain only protein 7 OS=Homo sapiens GN=LMO7 PE=1 SV=3 - [LMO7_HUM |
| Q9BQI9 | 89 | 281 | 31,3 | 8,4 | 75 | Nuclear receptor-interacting protein 2 OS=Homo sapiens GN=NRIP2 PE=2 SV=3 - [ |
| O00257 | 52 | 560 | 61,3 | 9,36 | 75 | E3 SUMO-protein ligase CBX4 OS=Homo sapiens GN=CBX4 PE=1 SV=3 - [CBX4_HUI |
| Q9Y6X9 | 44 | 1032 | 117,7 | 8,38 | 75 | MORC family CW-type zinc finger protein 2 OS=Homo sapiens GN=MORC2 PE=1 SV |
| Q5JU85 | 6 | 1478 | 161,6 | 8,56 | 75 | IQ motif and SEC7 domain-containing protein 2 OS=Homo sapiens GN=IQSEC2 PE= |
| O43548 | 10 | 720 | 80,7 | 6,44 | 75 | Protein-glutamine gamma-glutamyltransferase 5 OS=Homo sapiens GN=TGM5 PE |
| Q9UPP5 | 21 | 1409 | 155,6 | 6,19 | 75 | Uncharacterized protein KIAA1107 OS=Homo sapiens GN=KIAA1107 PE=1 SV=2 - [I |
| Q86VQ6 | 116 | 682 | 74,8 | 8,22 | 75 | Thioredoxin reductase 3 (Fragment) OS=Homo sapiens GN=TXNRD3 PE=1 SV=3 - [ |
| O43272 | 9 | 516 | 59,2 | 6,89 | 75 | Proline dehydrogenase, mitochondrial OS=Homo sapiens GN=PRODH PE=1 SV=2 - |
| Q0P6D6 | 15 | 951 | 110,4 | 6,47 | 75 | Coiled-coil domain-containing protein 15 OS=Homo sapiens GN=CCDC15 PE=2 SV= |
| P07197 | 5 | 916 | 102,4 | 4,91 | 74 | Neurofilament medium polypeptide OS=Homo sapiens GN=NEFM PE=1 SV=3 - [N |
| Q5KSL6 | 107 | 1271 | 141,7 | 5,53 | 74 | Diacylglycerol kinase kappa OS=Homo sapiens GN=DGKK PE=1 SV=1 - [DGKK_HUM |
| Q9H4I2 | 11 | 956 | 104,6 | 6,07 | 74 | Zinc fingers and homeoboxes protein 3 OS=Homo sapiens GN=ZHX3 PE=1 SV=3 - [ |
| O75164 | 12 | 1064 | 120,6 | 5,85 | 74 | Lysine-specific demethylase 4A OS=Homo sapiens GN=KDM4A PE=1 SV=2 - [KDM4 |
| Q96RS0 | 10 | 853 | 96,6 | 4,94 | 74 | Trimethylguanosine synthase OS=Homo sapiens GN=TGS1 PE=1 SV=3 - [TGS1_HUI |
| P17040 | 11 | 1043 | 117,5 | 6,43 | 74 | Zinc finger and SCAN domain-containing protein 20 OS=Homo sapiens GN=ZSCAN |
| Q86Y22 | 6 | 540 | 51,9 | 7,25 | 74 | Collagen alpha-1(XXIII) chain OS=Homo sapiens GN=COL23A1 PE=1 SV=1 - [CONA1 |
| Q9H0R1 | 17 | 490 | 54,7 | 6,61 | 74 | MHD domain-containing death-inducing protein OS=Homo sapiens GN=MUDENG |
| Q1MSJ5 | 11 | 1256 | 145,4 | 6,8 | 74 | Centrosome and spindle pole-associated protein 1 OS=Homo sapiens GN=CSPP1 |
| Q14678 | 9 | 1352 | 147,2 | 5,3 | 73 | KN motif and ankyrin repeat domain-containing protein 1 OS=Homo sapiens GN= |
| Q92901 | 17 | 407 | 46,3 | 10,45 | 73 | 60S ribosomal protein L3-like OS=Homo sapiens GN=RPL3L PE=1 SV=3 - [RL3L_HUI |
| Q7L2E3 | 14 | 1194 | 133,9 | 8,78 | 73 | Putative ATP-dependent RNA helicase DHX30 OS=Homo sapiens GN=DHX30 PE=1 |
| Q17R98 | 29 | 1081 | 119,1 | 6,89 | 73 | Zinc finger protein 827 OS=Homo sapiens GN=ZNF827 PE=2 SV=1 - [ZN827_HUMAN |
| Q05397 | 35 | 1052 | 119,2 | 6,62 | 73 | Focal adhesion kinase 1 OS=Homo sapiens GN=PTK2 PE=1 SV=2 - [FAK1_HUMAN] |
| Q9H3R0 | 11 | 1056 | 119,9 | 6,46 | 73 | Lysine-specific demethylase 4C OS=Homo sapiens GN=KDM4C PE=1 SV=2 - [KDM4 |
| O95453 | 6 | 639 | 73,4 | 6,2 | 73 | Poly(A)-specific ribonuclease PARN OS=Homo sapiens GN=PARN PE=1 SV=1 - [PA |
| Q6UWX4 | 29 | 724 | 80,7 | 9,01 | 73 | HHIP-like protein 2 OS=Homo sapiens GN=HHIPL2 PE=2 SV=1 - [HIPL2_HUMAN] |
| O95071 | 33 | 2799 | 309,2 | 5,85 | 73 | E3 ubiquitin-protein ligase UBR5 OS=Homo sapiens GN=UBR5 PE=1 SV=2 - [UBR5_ |
| Q9Y285 | 9 | 508 | 57,5 | 7,8 | 73 | Phenylalanyl-tRNA synthetase alpha chain OS=Homo sapiens GN=FARSA PE=1 SV |
| Q9Y6K9 | 93 | 419 | 48,2 | 5,71 | 73 | NF-kappa-B essential modulator (NEMO) (NF-kappa-B essential modifier) (Inhibi |
| Q9HAV4 | 11 | 1204 | 136,2 | 5,8 | 73 | Exportin-5 OS=Homo sapiens GN=XPO5 PE=1 SV=1 - [XPO5_HUMAN] |
| Q96T17 | 24 | 732 | 81,9 | 8,84 | 73 | MAP7 domain-containing protein 2 OS=Homo sapiens GN=MAP7D2 PE=1 SV=2 - [M |
| Q86Z14 | 12 | 1044 | 119,7 | 9,22 | 73 | Beta-klotho OS=Homo sapiens GN=KLB PE=1 SV=1 - [KLOTB_HUMAN] |
| Q96A65 | 39 | 974 | 110,4 | 6,49 | 73 | Exocyst complex component 4 OS=Homo sapiens GN=EXOC4 PE=1 SV=1 - [EXOC4_ |
| Q7Z478 | 24 | 1369 | 155,1 | 8,09 | 72 | ATP-dependent RNA helicase DHX29 OS=Homo sapiens GN=DHX29 PE=1 SV=2 - [D |
| Q5VV67 | 18 | 1664 | 177,4 | 6,51 | 72 | Peroxisome proliferator-activated receptor gamma coactivator-related protein 1 |
| Q502W7 | 33 | 563 | 65,3 | 8,75 | 72 | Coiled-coil domain-containing protein 38 OS=Homo sapiens GN=CCDC38 PE=2 SV= |
| Q8NB25 | 15 | 1140 | 132,9 | 5,83 | 72 | Protein FAM184A OS=Homo sapiens GN=FAM184A PE=2 SV=3 - [F184A_HUMAN] |
| Q9BXL6 | 20 | 1004 | 113,2 | 5,92 | 72 | Caspase recruitment domain-containing protein 14 OS=Homo sapiens GN=CARD1 |
| Q9P2K1 | 11 | 1620 | 186,1 | 6,74 | 72 | Coiled-coil and C2 domain-containing protein 2A OS=Homo sapiens GN=CC2D2A I |
| Q9BPU6 | 15 | 564 | 61,4 | 7,2 | 72 | Dihydropyrimidinase-related protein 5 OS=Homo sapiens GN=DPYSL5 PE=1 SV=1 |
| P23458 | 49 | 1154 | 133,2 | 7,55 | 72 | Tyrosine-protein kinase JAK1 OS=Homo sapiens GN=JAK1 PE=1 SV=2 - [JAK1_HUM |
| P08922 | 15 | 2347 | 263,7 | 6,11 | 72 | Proto-oncogene tyrosine-protein kinase ROS OS=Homo sapiens GN=ROS1 PE=2 SV |
| A4D1F6 | 29 | 860 | 98,0 | 7,46 | 72 | Leucine-rich repeat and death domain-containing protein LOC401387 OS=Homo s |
| Q7Z7G8 | 16 | 4022 | 448,4 | 6,46 | 72 | Vacuolar protein sorting-associated protein 13B OS=Homo sapiens GN=VPS13B PI |
| Q9P2E9 | 13 | 1410 | 152,4 | 8,6 | 72 | Ribosome-binding protein 1 OS=Homo sapiens GN=RRBP1 PE=1 SV=4 - [RRBP1_HU |
| Q9P2E3 | 17 | 1918 | 220,1 | 7,3 | 72 | NFX1-type zinc finger-containing protein 1 OS=Homo sapiens GN=ZNFX1 PE=1 SV= |

| | | | | | | |
|---|---|---|---|---|---|---|
| O95425 | 11 | 2214 | 247,6 | 6,98 | 72 | Supervillin OS=Homo sapiens GN=SVIL PE=1 SV=2 - [SVIL_HUMAN] |
| Q07283 | 4 | 1943 | 253,8 | 5,78 | 71 | Trichohyalin OS=Homo sapiens GN=TCHH PE=1 SV=2 - [TRHY_HUMAN] |
| P51825 | 12 | 1210 | 131,3 | 9,2 | 71 | AF4/FMR2 family member 1 OS=Homo sapiens GN=AFF1 PE=1 SV=1 - [AFF1_HUMA |
| Q4W5G0 | 93 | 525 | 59,6 | 9 | 71 | Tigger transposable element-derived protein 2 OS=Homo sapiens GN=TIGD2 PE= |
| Q9HCK8 | 16 | 2581 | 290,3 | 6,47 | 71 | Chromodomain-helicase-DNA-binding protein 8 OS=Homo sapiens GN=CHD8 PE= |
| Q9C0D6 | 10 | 1143 | 124,7 | 9,03 | 71 | FH2 domain-containing protein 1 OS=Homo sapiens GN=FHDC1 PE=2 SV=2 - [FHDC |
| Q86UK5 | 15 | 1308 | 147,9 | 6,96 | 71 | Limbin OS=Homo sapiens GN=EVC2 PE=1 SV=1 - [LBN_HUMAN] |
| Q9NYB0 | 15 | 399 | 44,2 | 4,73 | 71 | Telomeric repeat-binding factor 2-interacting protein 1 OS=Homo sapiens GN=TE |
| Q86WI1 | 16 | 4243 | 465,4 | 6,11 | 71 | Fibrocystin-L OS=Homo sapiens GN=PKHD1L1 PE=2 SV=2 - [PKHL1_HUMAN] |
| A4FU69 | 7 | 1503 | 173,3 | 5,85 | 71 | EF-hand calcium-binding domain-containing protein 5 OS=Homo sapiens GN=EFC |
| Q7Z5Q5 | 21 | 900 | 100,2 | 8,29 | 71 | DNA polymerase nu OS=Homo sapiens GN=POLN PE=1 SV=2 - [DPOLN_HUMAN] |
| Q5VVJ2 | 110 | 828 | 95,0 | 5,53 | 71 | Histone H2A deubiquitinase MYSM1 OS=Homo sapiens GN=MYSM1 PE=1 SV=1 - [M |
| Q08AN1 | 17 | 781 | 90,2 | 9,57 | 71 | Zinc finger protein 616 OS=Homo sapiens GN=ZNF616 PE=2 SV=2 - [ZN616_HUMAN |
| Q8IWN7 | 15 | 2480 | 261,0 | 4,41 | 71 | Retinitis pigmentosa 1-like 1 protein OS=Homo sapiens GN=RP1L1 PE=1 SV=4 - [RI |
| Q53ET0 | 25 | 693 | 73,3 | 7,11 | 71 | CREB-regulated transcription coactivator 2 OS=Homo sapiens GN=CRTC2 PE=1 SV= |
| P17480 | 6 | 764 | 89,4 | 5,81 | 71 | Nucleolar transcription factor 1 OS=Homo sapiens GN=UBTF PE=1 SV=1 - [UBF1_HU |
| Q9UPX8 | 14 | 1470 | 158,7 | 6,9 | 70 | SH3 and multiple ankyrin repeat domains protein 2 OS=Homo sapiens GN=SHANK |
| Q9NRC6 | 9 | 3674 | 416,6 | 6,67 | 70 | Spectrin beta chain, brain 4 OS=Homo sapiens GN=SPTBN5 PE=1 SV=1 - [SPTN5_HU |
| Q58F21 | 13 | 947 | 107,9 | 8,95 | 70 | Bromodomain testis-specific protein OS=Homo sapiens GN=BRDT PE=1 SV=4 - [BR |
| O43306 | 6 | 1168 | 130,5 | 8,22 | 70 | Adenylate cyclase type 6 OS=Homo sapiens GN=ADCY6 PE=1 SV=2 - [ADCY6_HUMA |
| Q96JG6 | 12 | 964 | 111,1 | 6,2 | 70 | Coiled-coil domain-containing protein 132 OS=Homo sapiens GN=CCDC132 PE=1 S |
| O15234 | 11 | 703 | 76,2 | 6,48 | 70 | Protein CASC3 OS=Homo sapiens GN=CASC3 PE=1 SV=2 - [CASC3_HUMAN] |
| Q96CP6 | 68 | 724 | 80,6 | 6,74 | 70 | GRAM domain-containing protein 1A OS=Homo sapiens GN=GRAMD1A PE=1 SV=2 |
| Q8NFA0 | 7 | 1604 | 181,5 | 6,44 | 70 | Ubiquitin carboxyl-terminal hydrolase 32 OS=Homo sapiens GN=USP32 PE=1 SV=1 |
| Q9BZF1 | 70 | 889 | 101,1 | 6,96 | 70 | Oxysterol-binding protein-related protein 8 OS=Homo sapiens GN=OSBPL8 PE=1 |
| Q96JI7 | 15 | 2443 | 278,7 | 5,97 | 70 | Spatacsin OS=Homo sapiens GN=SPG11 PE=1 SV=3 - [SPTCS_HUMAN] |
| Q502W6 | 22 | 1294 | 145,7 | 7,33 | 70 | von Willebrand factor A domain-containing protein 3B OS=Homo sapiens GN=VW |
| Q13217 | 4 | 504 | 57,5 | 6,15 | 70 | DnaJ homolog subfamily C member 3 OS=Homo sapiens GN=DNAJC3 PE=1 SV=1 - |
| Q7Z3Z0 | 8 | 450 | 49,3 | 5,08 | 70 | Keratin, type I cytoskeletal 25 OS=Homo sapiens GN=KRT25 PE=1 SV=1 - [K1C25_H |
| Q13535 | 41 | 2644 | 301,2 | 7,43 | 69 | Serine/threonine-protein kinase ATR OS=Homo sapiens GN=ATR PE=1 SV=3 - [ATR |
| P01763 | 39 | 114 | 12,2 | 8,5 | 69 | Ig heavy chain V-III region WEA OS=Homo sapiens PE=1 SV=1 - [HV302_HUMAN] |
| Q96BP3 | 8 | 646 | 73,5 | 7,15 | 69 | Peptidylprolyl isomerase domain and WD repeat-containing protein 1 (EC 5.2.1.8 |
| Q9H9Y6 | 80 | 1135 | 128,1 | 7,83 | 69 | DNA-directed RNA polymerase I subunit RPA2 OS=Homo sapiens GN=POLR1B PE= |
| P01033 | 4 | 207 | 23,2 | 8,1 | 69 | Metalloproteinase inhibitor 1 OS=Homo sapiens GN=TIMP1 PE=1 SV=1 - [TIMP1_H |
| Q8IWC1 | 12 | 876 | 98,4 | 9,32 | 69 | MAP7 domain-containing protein 3 OS=Homo sapiens GN=MAP7D3 PE=1 SV=2 - [M |
| O94762 | 12 | 991 | 108,8 | 8,56 | 69 | ATP-dependent DNA helicase Q5 OS=Homo sapiens GN=RECQL5 PE=1 SV=2 - [REC |
| Q9ULH0 | 51 | 1771 | 196,4 | 6,62 | 69 | Kinase D-interacting substrate of 220 kDa OS=Homo sapiens GN=KIDINS220 PE=1 S |
| Q96M83 | 10 | 486 | 55,7 | 7,78 | 69 | Coiled-coil domain-containing protein 7 OS=Homo sapiens GN=CCDC7 PE=2 SV=2 |
| P01613 | 19 | 112 | 12,2 | 5,36 | 69 | Ig kappa chain V-I region Ni - Homo sapiens (Human) - [KV121_HUMAN] |
| Q9H9B1 | 12 | 1267 | 138,2 | 5,94 | 69 | Histone-lysine N-methyltransferase, H3 lysine-9 specific 5 OS=Homo sapiens GN= |
| P20591 | 9 | 662 | 75,5 | 5,83 | 69 | Interferon-induced GTP-binding protein Mx1 OS=Homo sapiens GN=MX1 PE=1 SV |
| Q5SRE5 | 13 | 1749 | 195,9 | 6,73 | 69 | Nucleoporin NUP188 homolog OS=Homo sapiens GN=NUP188 PE=1 SV=1 - [NU188 |
| Q6DJT9 | 10 | 500 | 55,9 | 8,56 | 69 | Zinc finger protein PLAG1 OS=Homo sapiens GN=PLAG1 PE=1 SV=1 - [PLAG1_HUM |
| Q14C86 | 19 | 1478 | 164,9 | 5,22 | 68 | GTPase-activating protein and VPS9 domain-containing protein 1 OS=Homo sapie |
| Q3ZCX4 | 50 | 644 | 74,3 | 8,22 | 68 | Zinc finger protein 568 OS=Homo sapiens GN=ZNF568 PE=2 SV=2 - [ZN568_HUMAN |
| Q7Z3V4 | 10 | 1068 | 123,0 | 8,19 | 68 | Ubiquitin-protein ligase E3B OS=Homo sapiens GN=UBE3B PE=1 SV=3 - [UBE3B_HU |
| Q9UPW8 | 11 | 1703 | 192,9 | 5,35 | 68 | Protein unc-13 homolog A OS=Homo sapiens GN=UNC13A PE=2 SV=3 - [UN13A_HU |
| P13639 | 13 | 858 | 95,3 | 6,83 | 68 | Elongation factor 2 OS=Homo sapiens GN=EEF2 PE=1 SV=4 - [EF2_HUMAN] |
| P14616 | 7 | 1297 | 143,6 | 6,47 | 68 | Insulin receptor-related protein OS=Homo sapiens GN=INSRR PE=2 SV=2 - [INSRR |
| Q14444 | 130 | 709 | 78,3 | 5,25 | 68 | Caprin-1 OS=Homo sapiens GN=CAPRIN1 PE=1 SV=2 - [CAPR1_HUMAN] |
| Q8NA03 | 15 | 581 | 66,1 | 5,16 | 68 | Fibrous sheath-interacting protein 1 OS=Homo sapiens GN=FSIP1 PE=2 SV=1 - [FSI |
| A8MUU9 | 7 | 505 | 55,3 | 13,3 | 68 | Putative uncharacterized protein ENSP00000383309 OS=Homo sapiens PE=5 SV=3 |
| Q06210 | 36 | 699 | 78,8 | 7,11 | 68 | Glucosamine--fructose-6-phosphate aminotransferase [isomerizing] 1 OS=Homo |
| Q9Y696 | 58 | 253 | 28,8 | 5,59 | 68 | Chloride intracellular channel protein 4 OS=Homo sapiens GN=CLIC4 PE=1 SV=4 - |
| O00571 | 9 | 662 | 73,2 | 7,18 | 67 | ATP-dependent RNA helicase DDX3X OS=Homo sapiens GN=DDX3X PE=1 SV=3 - [D |
| A7MCY6 | 12 | 615 | 67,7 | 5,86 | 67 | TANK-binding kinase 1-binding protein 1 OS=Homo sapiens GN=TBKBP1 PE=1 SV= |
| Q14416 | 8 | 872 | 95,5 | 8,12 | 67 | Metabotropic glutamate receptor 2 OS=Homo sapiens GN=GRM2 PE=2 SV=2 - [GRI |
| Q9UFD9 | 12 | 1545 | 169,7 | 6,54 | 67 | RIMS-binding protein 3A OS=Homo sapiens GN=RIMBP3 PE=1 SV=3 - [RIM3A_HUM |
| Q9P2M7 | 6 | 1197 | 136,3 | 5,54 | 67 | Cingulin OS=Homo sapiens GN=CGN PE=1 SV=2 - [CING_HUMAN] |
| O94906 | 19 | 941 | 106,9 | 8,25 | 67 | Pre-mRNA-processing factor 6 OS=Homo sapiens GN=PRPF6 PE=1 SV=1 - [PRP6_H |
| Q9NRW7 | 9 | 570 | 65,0 | 8,24 | 67 | Vacuolar protein sorting-associated protein 45 OS=Homo sapiens GN=VPS45 PE=1 |
| Q92750 | 117 | 862 | 91,0 | 9,54 | 67 | Transcription initiation factor TFIID subunit 4B OS=Homo sapiens GN=TAF4B PE=1 |
| P42694 | 11 | 1942 | 218,8 | 7,42 | 67 | Probable helicase with zinc finger domain OS=Homo sapiens GN=HELZ PE=1 SV=2 |
| P09884 | 12 | 1462 | 165,8 | 5,85 | 67 | DNA polymerase alpha catalytic subunit OS=Homo sapiens GN=POLA1 PE=1 SV=2 |
| P52333 | 9 | 1124 | 125,0 | 7,18 | 67 | Tyrosine-protein kinase JAK3 OS=Homo sapiens GN=JAK3 PE=1 SV=2 - [JAK3_HUM |

| | | | | | | |
|---|---|---|---|---|---|---|
| P04208 | 23 | 109 | 11,7 | 6,54 | 67 | Ig lambda chain V-I region WAH OS=Homo sapiens PE=1 SV=1 - [LV106_HUMAN] |
| Q8N283 | 11 | 1001 | 109,9 | 6,02 | 67 | Ankyrin repeat domain-containing protein 35 OS=Homo sapiens GN=ANKRD35 PE |
| Q13206 | 28 | 875 | 100,8 | 8,63 | 67 | Probable ATP-dependent RNA helicase DDX10 OS=Homo sapiens GN=DDX10 PE= |
| Q6P2H3 | 9 | 762 | 85,6 | 6 | 66 | Coiled-coil domain-containing protein 21 OS=Homo sapiens GN=CCDC21 PE=1 SV |
| Q9NS91 | 26 | 495 | 56,2 | 7,58 | 66 | E3 ubiquitin-protein ligase RAD18 OS=Homo sapiens GN=RAD18 PE=1 SV=2 - [RAD |
| Q08378 | 32 | 1498 | 167,3 | 5,44 | 66 | Golgin subfamily A member 3 OS=Homo sapiens GN=GOLGA3 PE=1 SV=2 - [GOGA |
| Q14118 | 8 | 895 | 97,4 | 8,56 | 66 | Dystroglycan OS=Homo sapiens GN=DAG1 PE=1 SV=2 - [DAG1_HUMAN] |
| P31040 | 9 | 664 | 72,6 | 7,39 | 66 | Succinate dehydrogenase [ubiquinone] flavoprotein subunit, mitochondrial OS= |
| O94822 | 6 | 1766 | 200,4 | 6,25 | 66 | E3 ubiquitin-protein ligase listerin OS=Homo sapiens GN=LTN1 PE=1 SV=6 - [LTN1 |
| O60504 | 19 | 671 | 75,3 | 9,45 | 66 | Vinexin OS=Homo sapiens GN=SORBS3 PE=1 SV=2 - [VINEX_HUMAN] |
| Q5VYS8 | 13 | 1495 | 171,1 | 6,83 | 66 | Terminal uridylyltransferase 7 OS=Homo sapiens GN=ZCCHC6 PE=1 SV=1 - [TUT7_ |
| Q9H8K7 | 23 | 445 | 49,2 | 6,25 | 66 | Uncharacterized protein C10orf88 OS=Homo sapiens GN=C10orf88 PE=2 SV=2 - [CJ |
| P48553 | 53 | 1259 | 142,1 | 6,04 | 66 | Trafficking protein particle complex subunit 10 OS=Homo sapiens GN=TRAPPC10 |
| Q8IXR9 | 14 | 625 | 71,3 | 9,16 | 66 | Uncharacterized protein C12orf56 OS=Homo sapiens GN=C12orf56 PE=2 SV=2 - [CI |
| Q92608 | 94 | 1830 | 211,8 | 6,87 | 66 | Dedicator of cytokinesis protein 2 OS=Homo sapiens GN=DOCK2 PE=1 SV=2 - [DO |
| O15068 | 22 | 1137 | 128,0 | 6,43 | 66 | Guanine nucleotide exchange factor DBS OS=Homo sapiens GN=MCF2L PE=1 SV=2 |
| Q7Z7J5 | 17 | 298 | 33,8 | 9,2 | 66 | Developmental pluripotency-associated protein 2 (Pluripotent embryonic stem c |
| Q9Y388 | 10 | 322 | 37,3 | 9,83 | 66 | RNA-binding motif protein, X-linked 2 OS=Homo sapiens GN=RBMX2 PE=1 SV=2 - |
| Q5TAX3 | 16 | 1644 | 185,0 | 7,97 | 66 | Terminal uridylyltransferase 4 OS=Homo sapiens GN=ZCCHC11 PE=1 SV=3 - [TUT4_ |
| Q9BQI3 | 46 | 630 | 71,1 | 5,99 | 66 | Eukaryotic translation initiation factor 2-alpha kinase 1 OS=Homo sapiens GN=EIF |
| P35749 | 11 | 1972 | 227,2 | 5,5 | 65 | Myosin-11 OS=Homo sapiens GN=MYH11 PE=1 SV=3 - [MYH11_HUMAN] |
| Q96T21 | 48 | 854 | 95,4 | 8,12 | 65 | Selenocysteine insertion sequence-binding protein 2 OS=Homo sapiens GN=SECI |
| Q5SR76 | 14 | 1530 | 173,4 | 8,06 | 65 | TPR repeat-containing protein C10orf93 OS=Homo sapiens GN=C10orf93 PE=2 SV= |
| Q68CP9 | 11 | 1835 | 197,3 | 7,42 | 65 | AT-rich interactive domain-containing protein 2 OS=Homo sapiens GN=ARID2 PE= |
| P98179 | 3 | 157 | 17,2 | 8,91 | 65 | Putative RNA-binding protein 3 OS=Homo sapiens GN=RBM3 PE=1 SV=1 - [RBM3_ |
| Q14674 | 6 | 2120 | 233,0 | 7,55 | 65 | Separin OS=Homo sapiens GN=ESPL1 PE=1 SV=3 - [ESPL1_HUMAN] |
| O75410 | 36 | 805 | 87,7 | 4,88 | 65 | Transforming acidic coiled-coil-containing protein 1 OS=Homo sapiens GN=TACC1 |
| Q8TDD5 | 14 | 553 | 64,2 | 6,18 | 65 | Mucolipin-3 OS=Homo sapiens GN=MCOLN3 PE=2 SV=1 - [MCLN3_HUMAN] |
| A6PVC2 | 12 | 814 | 90,7 | 8,13 | 65 | Protein monoglycylase TTLL8 OS=Homo sapiens GN=TTLL8 PE=1 SV=3 - [TTLL8_HUI |
| Q8IU68 | 40 | 726 | 81,6 | 9,36 | 65 | Transmembrane channel-like protein 8 OS=Homo sapiens GN=TMC8 PE=1 SV=1 - |
| P57768 | 17 | 344 | 39,1 | 4,65 | 65 | Sorting nexin-16 OS=Homo sapiens GN=SNX16 PE=1 SV=2 - [SNX16_HUMAN] |
| Q9GZR2 | 22 | 422 | 46,6 | 9,77 | 65 | RNA exonuclease 4 OS=Homo sapiens GN=REXO4 PE=1 SV=2 - [REXO4_HUMAN] |
| Q9Y3Z3 | 7 | 626 | 72,2 | 7,14 | 65 | SAM domain and HD domain-containing protein 1 OS=Homo sapiens GN=SAMHD1 |
| Q9H3S7 | 5 | 1636 | 178,9 | 6,92 | 65 | Tyrosine-protein phosphatase non-receptor type 23 OS=Homo sapiens GN=PTPN |
| O15550 | 8 | 1401 | 154,1 | 7,44 | 65 | Lysine-specific demethylase 6A OS=Homo sapiens GN=KDM6A PE=1 SV=2 - [KDM6 |
| Q9P2D1 | 18 | 2997 | 335,7 | 6,34 | 65 | Chromodomain-helicase-DNA-binding protein 7 OS=Homo sapiens GN=CHD7 PE= |
| Q9Y239 | 25 | 953 | 107,6 | 7,11 | 65 | Nucleotide-binding oligomerization domain-containing protein 1 OS=Homo sapi |
| Q9NYQ6 | 7 | 3014 | 329,3 | 5,92 | 65 | Cadherin EGF LAG seven-pass G-type receptor 1 OS=Homo sapiens GN=CELSR1 PE |
| Q13523 | 6 | 1007 | 116,9 | 10,26 | 65 | Serine/threonine-protein kinase PRP4 homolog OS=Homo sapiens GN=PRPF4B P |
| Q9HDC5 | 9 | 661 | 71,6 | 9,32 | 65 | Junctophilin-1 OS=Homo sapiens GN=JPH1 PE=1 SV=2 - [JPH1_HUMAN] |
| Q6ZR08 | 11 | 3092 | 356,7 | 6,19 | 65 | Dynein heavy chain 12, axonemal OS=Homo sapiens GN=DNAH12 PE=1 SV=2 - [DY |
| Q0ZGT2 | 5 | 675 | 80,6 | 5,33 | 65 | Nexilin OS=Homo sapiens GN=NEXN PE=1 SV=1 - [NEXN_HUMAN] |
| Q8TEW0 | 9 | 1356 | 151,3 | 7,68 | 64 | Partitioning defective 3 homolog OS=Homo sapiens GN=PARD3 PE=1 SV=2 - [PARI |
| Q8NDI1 | 11 | 1231 | 139,9 | 5,35 | 64 | EH domain-binding protein 1 OS=Homo sapiens GN=EHBP1 PE=1 SV=3 - [EHBP1_H |
| Q9UDT6 | 9 | 1046 | 115,8 | 6,73 | 64 | CAP-Gly domain-containing linker protein 2 OS=Homo sapiens GN=CLIP2 PE=1 SV |
| Q14241 | 15 | 798 | 89,9 | 9,57 | 64 | Transcription elongation factor B polypeptide 3 OS=Homo sapiens GN=TCEB3 PE= |
| Q8IW93 | 13 | 802 | 89,1 | 7,53 | 64 | Rho guanine nucleotide exchange factor 19 OS=Homo sapiens GN=ARHGEF19 PE= |
| O94911 | 6 | 1581 | 179,1 | 7,18 | 64 | ATP-binding cassette sub-family A member 8 OS=Homo sapiens GN=ABCA8 PE=1 |
| O75145 | 25 | 1194 | 133,4 | 5,68 | 64 | Liprin-alpha-3 OS=Homo sapiens GN=PPFIA3 PE=1 SV=3 - [LIPA3_HUMAN] |
| Q9H4L7 | 40 | 1026 | 117,3 | 5,55 | 64 | SWI/SNF-related matrix-associated actin-dependent regulator of chromatin subf |
| Q13098 | 86 | 491 | 55,5 | 6,74 | 64 | COP9 signalosome complex subunit 1 OS=Homo sapiens GN=GPS1 PE=1 SV=4 - [CS |
| P32780 | 40 | 548 | 62,0 | 8,66 | 64 | General transcription factor IIH subunit 1 OS=Homo sapiens GN=GTF2H1 PE=1 SV= |
| Q9UQ03 | 33 | 480 | 54,9 | 8,27 | 64 | Coronin-2B OS=Homo sapiens GN=CORO2B PE=2 SV=4 - [COR2B_HUMAN] |
| Q93100 | 11 | 1093 | 124,8 | 6,95 | 64 | Phosphorylase b kinase regulatory subunit beta OS=Homo sapiens GN=PHKB PE= |
| B1AK53 | 32 | 854 | 91,7 | 6,93 | 64 | Espin OS=Homo sapiens GN=ESPN PE=1 SV=1 - [ESPN_HUMAN] |
| Q9HCL2 | 6 | 828 | 93,7 | 7,74 | 64 | Glycerol-3-phosphate acyltransferase 1, mitochondrial OS=Homo sapiens GN=GP |
| Q5SQS7 | 43 | 431 | 51,2 | 6,23 | 64 | SH2 domain-containing protein 4B OS=Homo sapiens GN=SH2D4B PE=2 SV=1 - [SH |
| Q6UXY8 | 7 | 1006 | 114,7 | 8,21 | 63 | Transmembrane channel-like protein 5 OS=Homo sapiens GN=TMC5 PE=2 SV=3 - |
| P17987 | 9 | 556 | 60,3 | 6,11 | 63 | T-complex protein 1 subunit alpha OS=Homo sapiens GN=TCP1 PE=1 SV=1 - [TCPA |
| P58107 | 18 | 5090 | 555,3 | 5,6 | 63 | Epiplakin OS=Homo sapiens GN=EPPK1 PE=1 SV=2 - [EPIPL_HUMAN] |
| Q8WVM7 | 6 | 1258 | 144,3 | 5,59 | 63 | Cohesin subunit SA-1 OS=Homo sapiens GN=STAG1 PE=1 SV=3 - [STAG1_HUMAN] |
| Q9BTW9 | 8 | 1192 | 132,5 | 6,19 | 63 | Tubulin-specific chaperone D OS=Homo sapiens GN=TBCD PE=1 SV=2 - [TBCD_HUI |
| O75460 | 15 | 977 | 109,7 | 6,42 | 63 | Serine/threonine-protein kinase/endoribonuclease IRE1 OS=Homo sapiens GN=E |
| Q96RL7 | 9 | 3174 | 360,0 | 6,33 | 63 | Vacuolar protein sorting-associated protein 13A OS=Homo sapiens GN=VPS13A P |
| Q6DN14 | 17 | 999 | 111,6 | 8,15 | 63 | Multiple C2 and transmembrane domain-containing protein 1 OS=Homo sapiens |

| | | | | | | |
|---|---|---|---|---|---|---|
| Q460N3 | 38 | 656 | 72,5 | 8,82 | 63 | Poly [ADP-ribose] polymerase 15 OS=Homo sapiens GN=PARP15 PE=1 SV=1 - [PAF |
| O94885 | 10 | 1247 | 136,6 | 6,09 | 63 | SAM and SH3 domain-containing protein 1 OS=Homo sapiens GN=SASH1 PE=1 SV= |
| Q7Z6J4 | 94 | 655 | 74,8 | 6,93 | 63 | FYVE, RhoGEF and PH domain-containing protein 2 OS=Homo sapiens GN=FGD2 P |
| Q9UK32 | 22 | 745 | 83,8 | 6,34 | 63 | Ribosomal protein S6 kinase alpha-6 OS=Homo sapiens GN=RPS6KA6 PE=1 SV=1 - |
| Q6PRD1 | 6 | 2367 | 257,2 | 5,71 | 63 | Probable G-protein coupled receptor 179 OS=Homo sapiens GN=GPR179 PE=2 SV= |
| P58317 | 31 | 390 | 44,7 | 8,05 | 63 | Zinc finger protein 121 OS=Homo sapiens GN=ZNF121 PE=2 SV=2 - [ZN121_HUMAN |
| Q6ZMW3 | 49 | 1958 | 217,8 | 7,44 | 63 | Echinoderm microtubule-associated protein-like 6 OS=Homo sapiens GN=EML6 P |
| P51523 | 33 | 738 | 85,4 | 8,78 | 63 | Zinc finger protein 84 (Zinc finger protein HPF2) - Homo sapiens (Human) - [ZNF8 |
| Q96RU3 | 7 | 617 | 71,3 | 5,72 | 63 | Formin-binding protein 1 OS=Homo sapiens GN=FNBP1 PE=1 SV=2 - [FNBP1_HUM |
| Q9H078 | 10 | 707 | 78,7 | 9,01 | 63 | Caseinolytic peptidase B protein homolog OS=Homo sapiens GN=CLPB PE=1 SV=1 |
| Q99743 | 9 | 824 | 91,7 | 6,81 | 63 | Neuronal PAS domain-containing protein 2 OS=Homo sapiens GN=NPAS2 PE=2 SV |
| P56715 | 5 | 2156 | 240,5 | 5,8 | 63 | Oxygen-regulated protein 1 OS=Homo sapiens GN=RP1 PE=1 SV=1 - [RP1_HUMAN |
| Q8IZY2 | 7 | 2146 | 234,2 | 7,24 | 63 | ATP-binding cassette sub-family A member 7 OS=Homo sapiens GN=ABCA7 PE=1 |
| Q96BY6 | 7 | 2183 | 249,2 | 6,93 | 62 | Dedicator of cytokinesis protein 10 OS=Homo sapiens GN=DOCK10 PE=1 SV=2 - [D |
| Q16363 | 20 | 1823 | 202,4 | 6,28 | 62 | Laminin subunit alpha-4 OS=Homo sapiens GN=LAMA4 PE=1 SV=4 - [LAMA4_HUM |
| Q9Y6J0 | 6 | 2220 | 246,2 | 6,02 | 62 | Calcineurin-binding protein cabin-1 OS=Homo sapiens GN=CABIN1 PE=1 SV=1 - [C |
| Q9H1Z4 | 12 | 485 | 53,7 | 9,14 | 62 | WD repeat-containing protein 13 OS=Homo sapiens GN=WDR13 PE=1 SV=2 - [WDF |
| P33261 | 30 | 490 | 55,9 | 7,39 | 62 | Cytochrome P450 2C19 OS=Homo sapiens GN=CYP2C19 PE=1 SV=3 - [CP2CJ_HUMA |
| Q9BYB0 | 15 | 1741 | 186,2 | 9,03 | 62 | SH3 and multiple ankyrin repeat domains protein 3 OS=Homo sapiens GN=SHANK |
| Q8IXH8 | 15 | 852 | 95,2 | 5,94 | 62 | Cadherin-like protein 26 OS=Homo sapiens GN=CDH26 PE=2 SV=3 - [CAD26_HUMA |
| A4D1E1 | 84 | 1349 | 152,5 | 8,54 | 62 | Zinc finger protein 804B OS=Homo sapiens GN=ZNF804B PE=1 SV=2 - [Z804B_HUM |
| O43830 | 15 | 326 | 38,2 | 9,17 | 62 | Zinc finger protein 73 OS=Homo sapiens GN=ZNF73 PE=3 SV=1 - [ZNF73_HUMAN] |
| Q9Y2W6 | 13 | 606 | 67,0 | 5,08 | 62 | Tudor and KH domain-containing protein OS=Homo sapiens GN=TDRKH PE=1 SV= |
| O75096 | 17 | 1905 | 211,9 | 5,27 | 62 | Low-density lipoprotein receptor-related protein 4 OS=Homo sapiens GN=LRP4 P |
| Q13813 | 5 | 2472 | 284,4 | 5,35 | 62 | Spectrin alpha chain, brain OS=Homo sapiens GN=SPTAN1 PE=1 SV=3 - [SPTA2_HU |
| Q96A00 | 10 | 147 | 16,7 | 9,38 | 62 | Protein phosphatase 1 regulatory subunit 14A OS=Homo sapiens GN=PPP1R14A P |
| Q6B0I6 | 7 | 523 | 58,6 | 9,16 | 62 | Lysine-specific demethylase 4D OS=Homo sapiens GN=KDM4D PE=1 SV=3 - [KDM4 |
| Q6ZN79 | 7 | 300 | 34,7 | 9,2 | 62 | Zinc finger protein 705A OS=Homo sapiens GN=ZNF705A PE=2 SV=1 - [Z705A_HUM |
| P10632 | 37 | 490 | 55,8 | 8,5 | 62 | Cytochrome P450 2C8 OS=Homo sapiens GN=CYP2C8 PE=1 SV=2 - [CP2C8_HUMAN |
| O43852 | 8 | 315 | 37,1 | 4,64 | 62 | Calumenin OS=Homo sapiens GN=CALU PE=1 SV=2 - [CALU_HUMAN] |
| Q9HCC0 | 50 | 563 | 61,3 | 7,68 | 62 | Methylcrotonoyl-CoA carboxylase beta chain, mitochondrial OS=Homo sapiens G |
| Q9UKK3 | 34 | 1724 | 192,5 | 5,66 | 62 | Poly [ADP-ribose] polymerase 4 OS=Homo sapiens GN=PARP4 PE=1 SV=3 - [PARP4 |
| Q96RR4 | 5 | 588 | 64,7 | 6,68 | 62 | Calcium/calmodulin-dependent protein kinase kinase 2 OS=Homo sapiens GN=C |
| O94953 | 12 | 1096 | 121,8 | 7,09 | 61 | Lysine-specific demethylase 4B OS=Homo sapiens GN=KDM4B PE=1 SV=4 - [KDM4 |
| Q8NAN2 | 23 | 632 | 71,0 | 5,63 | 61 | Protein FAM73A OS=Homo sapiens GN=FAM73A PE=2 SV=1 - [FA73A_HUMAN] |
| P13942 | 8 | 1736 | 171,7 | 6,21 | 61 | Collagen alpha-2(XI) chain OS=Homo sapiens GN=COL11A2 PE=1 SV=4 - [COBA2_H |
| Q6F5E8 | 27 | 1435 | 154,6 | 6,76 | 61 | Leucine-rich repeat-containing protein 16C OS=Homo sapiens GN=RLTPR PE=1 SV |
| O75179 | 7 | 2603 | 274,1 | 6,52 | 61 | Ankyrin repeat domain-containing protein 17 OS=Homo sapiens GN=ANKRD17 PE |
| Q9NP60 | 4 | 686 | 78,6 | 6,46 | 61 | X-linked interleukin-1 receptor accessory protein-like 2 OS=Homo sapiens GN=IL |
| Q96L91 | 26 | 3159 | 343,3 | 9,19 | 61 | E1A-binding protein p400 OS=Homo sapiens GN=EP400 PE=1 SV=4 - [EP400_HUMA |
| O60290 | 9 | 1169 | 131,6 | 7,23 | 61 | Zinc finger protein 862 OS=Homo sapiens GN=ZNF862 PE=2 SV=2 - [ZN862_HUMAN |
| Q9UKV0 | 4 | 1011 | 111,2 | 6,89 | 61 | Histone deacetylase 9 OS=Homo sapiens GN=HDAC9 PE=1 SV=2 - [HDAC9_HUMAN |
| Q9Y2R2 | 8 | 807 | 91,6 | 7,59 | 61 | Tyrosine-protein phosphatase non-receptor type 22 OS=Homo sapiens GN=PTPN |
| Q8WVB6 | 14 | 975 | 107,3 | 7,21 | 61 | Chromosome transmission fidelity protein 18 homolog OS=Homo sapiens GN=CH |
| P51654 | 6 | 580 | 65,5 | 6,37 | 61 | Glypican-3 OS=Homo sapiens GN=GPC3 PE=1 SV=1 - [GPC3_HUMAN] |
| Q8NEE6 | 8 | 735 | 83,9 | 8,72 | 61 | F-box/LRR-repeat protein 13 OS=Homo sapiens GN=FBXL13 PE=2 SV=3 - [FXL13_H |
| P04745 | 6 | 511 | 57,7 | 6,93 | 61 | Alpha-amylase 1 OS=Homo sapiens GN=AMY1A PE=1 SV=2 - [AMY1_HUMAN] |
| P55040 | 12 | 296 | 33,9 | 8,51 | 61 | GTP-binding protein GEM OS=Homo sapiens GN=GEM PE=1 SV=1 - [GEM_HUMAN] |
| P06753 | 19 | 284 | 32,8 | 4,72 | 61 | Tropomyosin alpha-3 chain (Tropomyosin-3) (Tropomyosin gamma) (hTM5) - Hon |
| P10155 | 8 | 538 | 60,6 | 8,03 | 61 | 60 kDa SS-A/Ro ribonucleoprotein OS=Homo sapiens GN=TROVE2 PE=1 SV=2 - [RO |
| Q15596 | 33 | 1464 | 159,1 | 6,64 | 61 | Nuclear receptor coactivator 2 OS=Homo sapiens GN=NCOA2 PE=1 SV=2 - [NCOA2 |
| Q8NAV1 | 21 | 312 | 37,5 | 9,96 | 61 | Pre-mRNA-splicing factor 38A OS=Homo sapiens GN=PRPF38A PE=1 SV=1 - [PR38A |
| Q9NZ08 | 4 | 941 | 107,2 | 6,46 | 61 | Endoplasmic reticulum aminopeptidase 1 OS=Homo sapiens GN=ERAP1 PE=1 SV= |
| Q9Y232 | 39 | 598 | 66,4 | 9,45 | 61 | Chromodomain Y-like protein OS=Homo sapiens GN=CDYL PE=1 SV=2 - [CDYL1_HU |
| Q96SB3 | 20 | 815 | 89,1 | 4,97 | 60 | Neurabin-2 OS=Homo sapiens GN=PPP1R9B PE=1 SV=2 - [NEB2_HUMAN] |
| Q8TC71 | 29 | 538 | 61,1 | 8,63 | 60 | Spermatogenesis-associated protein 18 OS=Homo sapiens GN=SPATA18 PE=1 SV= |
| Q8N9H9 | 23 | 656 | 69,7 | 5,43 | 60 | Uncharacterized protein C1orf127 OS=Homo sapiens GN=C1orf127 PE=2 SV=2 - [C |
| Q8N9M1 | 11 | 422 | 44,7 | 10,11 | 60 | Uncharacterized protein C19orf47 OS=Homo sapiens GN=C19orf47 PE=1 SV=1 - [C |
| O75376 | 13 | 2440 | 270,0 | 7,11 | 60 | Nuclear receptor corepressor 1 OS=Homo sapiens GN=NCOR1 PE=1 SV=2 - [NCOR |
| Q9UL54 | 7 | 1235 | 138,2 | 7,27 | 60 | Serine/threonine-protein kinase TAO2 (EC 2.7.11.1) (Thousand and one amino ac |
| Q7Z591 | 6 | 1439 | 155,0 | 6,32 | 60 | AT-hook-containing transcription factor OS=Homo sapiens GN=AKNA PE=1 SV=2 - |
| Q2M2I5 | 8 | 525 | 55,1 | 4,96 | 60 | Keratin, type I cytoskeletal 24 OS=Homo sapiens GN=KRT24 PE=1 SV=1 - [K1C24_H |
| Q8N961 | 17 | 839 | 93,2 | 5,9 | 60 | Ankyrin repeat and BTB/POZ domain-containing protein 2 OS=Homo sapiens GN= |
| O15360 | 5 | 1455 | 162,7 | 6,6 | 60 | Fanconi anemia group A protein OS=Homo sapiens GN=FANCA PE=1 SV=2 - [FANC |
| Q8N239 | 101 | 644 | 70,6 | 5,6 | 60 | Kelch-like protein 34 OS=Homo sapiens GN=KLHL34 PE=2 SV=1 - [KLH34_HUMAN] |

| | | | | | | |
|---|---|---|---|---|---|---|
| Q9Y4E6 | 32 | 1490 | 163,7 | 6,92 | 60 | WD repeat-containing protein 7 OS=Homo sapiens GN=WDR7 PE=2 SV=2 - [WDR7 |
| Q5T4T6 | 12 | 812 | 93,5 | 5,8 | 60 | Synaptonemal complex protein 2-like OS=Homo sapiens GN=SYCP2L PE=1 SV=2 - |
| Q13424 | 8 | 505 | 53,9 | 6,8 | 60 | Alpha-1-syntrophin OS=Homo sapiens GN=SNTA1 PE=1 SV=1 - [SNTA1_HUMAN] |
| P21580 | 24 | 790 | 89,6 | 8,22 | 60 | Tumor necrosis factor alpha-induced protein 3 OS=Homo sapiens GN=TNFAIP3 PE |
| Q8N1T3 | 19 | 1032 | 119,0 | 9,09 | 60 | Myosin-Ih OS=Homo sapiens GN=MYO1H PE=2 SV=2 - [MYO1H_HUMAN] |
| Q92973 | 41 | 898 | 102,3 | 4,98 | 60 | Transportin-1 OS=Homo sapiens GN=TNPO1 PE=1 SV=2 - [TNPO1_HUMAN] |
| Q96N67 | 37 | 2140 | 242,4 | 6,8 | 60 | Dedicator of cytokinesis protein 7 OS=Homo sapiens GN=DOCK7 PE=1 SV=4 - [DOC |
| Q08462 | 16 | 1091 | 123,5 | 8,09 | 60 | Adenylate cyclase type 2 OS=Homo sapiens GN=ADCY2 PE=1 SV=5 - [ADCY2_HUM |
| O15523 | 7 | 660 | 73,1 | 7,55 | 60 | ATP-dependent RNA helicase DDX3Y OS=Homo sapiens GN=DDX3Y PE=1 SV=2 - [D |
| Q8NEM0 | 27 | 835 | 92,8 | 8,25 | 60 | Microcephalin OS=Homo sapiens GN=MCPH1 PE=1 SV=3 - [MCPH1_HUMAN] |
| Q13075 | 6 | 1403 | 159,5 | 5,99 | 60 | Baculoviral IAP repeat-containing protein 1 OS=Homo sapiens GN=NAIP PE=1 SV= |
| Q6PKG0 | 72 | 1096 | 123,4 | 8,82 | 60 | La-related protein 1 OS=Homo sapiens GN=LARP1 PE=1 SV=2 - [LARP1_HUMAN] |
| Q8IZQ1 | 7 | 3526 | 395,0 | 6,76 | 60 | WD repeat and FYVE domain-containing protein 3 OS=Homo sapiens GN=WDFY3 |
| Q15413 | 22 | 4870 | 551,6 | 5,66 | 60 | Ryanodine receptor 3 OS=Homo sapiens GN=RYR3 PE=1 SV=2 - [RYR3_HUMAN] |
| Q5TID7 | 10 | 509 | 60,1 | 5,91 | 59 | Uncharacterized protein C1orf114 OS=Homo sapiens GN=C1orf114 PE=2 SV=1 - [C |
| Q96S53 | 92 | 571 | 63,6 | 7,06 | 59 | Dual specificity testis-specific protein kinase 2 OS=Homo sapiens GN=TESK2 PE=2 |
| O94779 | 25 | 1100 | 120,6 | 6,34 | 59 | Contactin-5 OS=Homo sapiens GN=CNTN5 PE=1 SV=2 - [CNTN5_HUMAN] |
| A3KN83 | 5 | 1393 | 154,2 | 7,88 | 59 | Protein strawberry notch homolog 1 OS=Homo sapiens GN=SBNO1 PE=1 SV=1 - [S |
| P49788 | 5 | 294 | 33,3 | 8,51 | 59 | Retinoic acid receptor responder protein 1 OS=Homo sapiens GN=RARRES1 PE=2 S |
| Q9NQW6 | 26 | 1124 | 124,1 | 8,07 | 59 | Actin-binding protein anillin OS=Homo sapiens GN=ANLN PE=1 SV=2 - [ANLN_HU |
| Q53F19 | 12 | 620 | 70,5 | 5,73 | 59 | Uncharacterized protein C17orf85 OS=Homo sapiens GN=C17orf85 PE=1 SV=2 - [C |
| Q4G0X9 | 5 | 1142 | 130,0 | 5,29 | 59 | Coiled-coil domain-containing protein 40 OS=Homo sapiens GN=CCDC40 PE=2 SV |
| Q9Y6N6 | 13 | 1575 | 171,1 | 6,58 | 59 | Laminin subunit gamma-3 OS=Homo sapiens GN=LAMC3 PE=2 SV=3 - [LAMC3_HU |
| O95197 | 12 | 1032 | 112,5 | 4,96 | 59 | Reticulon-3 OS=Homo sapiens GN=RTN3 PE=1 SV=2 - [RTN3_HUMAN] |
| Q9NX58 | 4 | 379 | 43,6 | 9,54 | 59 | Cell growth-regulating nucleolar protein OS=Homo sapiens GN=LYAR PE=1 SV=2 - |
| A0AVI2 | 8 | 2093 | 241,8 | 7,96 | 59 | Fer-1-like protein 5 OS=Homo sapiens GN=FER1L5 PE=2 SV=2 - [FR1L5_HUMAN] |
| Q9NXD2 | 12 | 777 | 88,2 | 8,53 | 59 | Myotubularin-related protein 10 OS=Homo sapiens GN=MTMR10 PE=1 SV=3 - [MT |
| Q13057 | 11 | 564 | 62,3 | 6,99 | 59 | Bifunctional coenzyme A synthase OS=Homo sapiens GN=COASY PE=1 SV=4 - [CO |
| Q8NEP3 | 12 | 725 | 80,0 | 4,67 | 59 | Leucine-rich repeat-containing protein 50 OS=Homo sapiens GN=LRRC50 PE=1 SV |
| Q9NQ87 | 96 | 328 | 35,1 | 10,68 | 59 | Hairy/enhancer-of-split related with YRPW motif-like protein OS=Homo sapiens |
| Q05BV3 | 8 | 1969 | 219,3 | 7,74 | 59 | Echinoderm microtubule-associated protein-like 5 OS=Homo sapiens GN=EML5 P |
| O94913 | 5 | 1555 | 172,9 | 8,48 | 59 | Pre-mRNA cleavage complex 2 protein Pcf11 OS=Homo sapiens GN=PCF11 PE=1 S |
| Q52LW3 | 5 | 1261 | 142,0 | 6,74 | 59 | Rho GTPase-activating protein 29 OS=Homo sapiens GN=ARHGAP29 PE=1 SV=2 - [ |
| Q9Y485 | 6 | 3027 | 337,6 | 6,34 | 59 | DmX-like protein 1 OS=Homo sapiens GN=DMXL1 PE=1 SV=3 - [DMXL1_HUMAN] |
| Q9BRD0 | 4 | 619 | 70,5 | 9,86 | 59 | BUD13 homolog OS=Homo sapiens GN=BUD13 PE=1 SV=1 - [BUD13_HUMAN] |
| P26599 | 9 | 531 | 57,2 | 9,17 | 58 | Polypyrimidine tract-binding protein 1 OS=Homo sapiens GN=PTBP1 PE=1 SV=1 - |
| Q4FZB7 | 11 | 885 | 99,1 | 8,78 | 58 | Histone-lysine N-methyltransferase SUV420H1 OS=Homo sapiens GN=SUV420H1 |
| O95263 | 22 | 885 | 98,9 | 6,83 | 58 | High affinity cAMP-specific and IBMX-insensitive 3',5'-cyclic phosphodiesterase 8 |
| Q6ZRV2 | 9 | 1179 | 127,0 | 6,98 | 58 | Protein FAM83H OS=Homo sapiens GN=FAM83H PE=1 SV=3 - [FA83H_HUMAN] |
| O60524 | 4 | 1076 | 122,9 | 6,35 | 58 | Serologically defined colon cancer antigen 1 OS=Homo sapiens GN=SDCCAG1 PE= |
| Q9UDY4 | 20 | 337 | 37,8 | 8,5 | 58 | DnaJ homolog subfamily B member 4 OS=Homo sapiens GN=DNAJB4 PE=1 SV=1 - |
| Q9UN79 | 16 | 622 | 69,2 | 6,71 | 58 | Transcription factor SOX-13 OS=Homo sapiens GN=SOX13 PE=1 SV=3 - [SOX13_HU |
| Q5T6S3 | 11 | 580 | 65,5 | 8,84 | 58 | PHD finger protein 19 OS=Homo sapiens GN=PHF19 PE=1 SV=1 - [PHF19_HUMAN] |
| Q9HCS4 | 16 | 588 | 62,6 | 8,94 | 58 | Transcription factor 7-like 1 OS=Homo sapiens GN=TCF7L1 PE=2 SV=1 - [TF7L1_HU |
| Q96NH3 | 21 | 1257 | 144,7 | 6,74 | 58 | Protein broad-minded OS=Homo sapiens GN=BROMI PE=2 SV=4 - [BROMI_HUMAN |
| Q6NV74 | 5 | 962 | 102,1 | 7,96 | 58 | Uncharacterized protein C2orf55 OS=Homo sapiens GN=C2orf55 PE=1 SV=3 - [CB05 |
| Q2VWP7 | 31 | 1150 | 127,0 | 7,59 | 58 | Protogenin OS=Homo sapiens GN=PRTG PE=2 SV=1 - [PRTG_HUMAN] |
| Q9BZ67 | 11 | 464 | 51,2 | 6,23 | 58 | FERM domain-containing protein 8 OS=Homo sapiens GN=FRMD8 PE=1 SV=1 - [FR |
| Q9HCE3 | 7 | 1301 | 141,6 | 8,65 | 58 | Zinc finger protein 532 OS=Homo sapiens GN=ZNF532 PE=1 SV=2 - [ZN532_HUMAN |
| Q8NFP4 | 50 | 955 | 105,7 | 8,34 | 58 | MAM domain-containing glycosylphosphatidylinositol anchor protein 1 OS=Hom |
| Q8NB66 | 7 | 2214 | 250,8 | 5,92 | 58 | Protein unc-13 homolog C OS=Homo sapiens GN=UNC13C PE=1 SV=3 - [UN13C_HU |
| Q9UPW6 | 30 | 733 | 82,5 | 6,9 | 58 | DNA-binding protein SATB2 OS=Homo sapiens GN=SATB2 PE=1 SV=2 - [SATB2_HU |
| Q9BZV3 | 6 | 1241 | 138,5 | 4,61 | 58 | Interphotoreceptor matrix proteoglycan 2 OS=Homo sapiens GN=IMPG2 PE=1 SV= |
| O43424 | 23 | 1007 | 113,3 | 6,07 | 58 | Glutamate receptor delta-2 subunit OS=Homo sapiens GN=GRID2 PE=2 SV=2 - [GR |
| Q9NNX1 | 9 | 390 | 44,2 | 6 | 58 | Tuftelin OS=Homo sapiens GN=TUFT1 PE=2 SV=1 - [TUFT1_HUMAN] |
| P05177 | 4 | 515 | 58,3 | 9,06 | 58 | Cytochrome P450 1A2 OS=Homo sapiens GN=CYP1A2 PE=1 SV=3 - [CP1A2_HUMAN |
| Q9NQ90 | 18 | 1003 | 113,9 | 6,55 | 58 | Anoctamin-2 OS=Homo sapiens GN=ANO2 PE=1 SV=2 - [ANO2_HUMAN] |
| O14964 | 11 | 777 | 86,1 | 6,16 | 57 | Hepatocyte growth factor-regulated tyrosine kinase substrate OS=Homo sapiens |
| Q16352 | 3 | 499 | 55,4 | 5,4 | 57 | Alpha-internexin OS=Homo sapiens GN=INA PE=1 SV=2 - [AINX_HUMAN] |
| Q9Y597 | 15 | 815 | 88,9 | 7,03 | 57 | BTB/POZ domain-containing protein KCTD3 OS=Homo sapiens GN=KCTD3 PE=1 SV |
| Q92613 | 6 | 823 | 93,7 | 7,18 | 57 | Protein Jade-3 OS=Homo sapiens GN=PHF16 PE=1 SV=1 - [JADE3_HUMAN] |
| Q5T481 | 5 | 1227 | 134,3 | 5,69 | 57 | Probable RNA-binding protein 20 OS=Homo sapiens GN=RBM20 PE=1 SV=3 - [RBM |
| Q9BY77 | 71 | 421 | 46,1 | 9,99 | 57 | Polymerase delta-interacting protein 3 (46 kDa DNA polymerase delta interactior |
| Q8TDG4 | 12 | 1101 | 124,1 | 6,58 | 57 | Helicase POLQ-like OS=Homo sapiens GN=HELQ PE=1 SV=2 - [HELQ_HUMAN] |
| Q9NS56 | 10 | 1045 | 119,1 | 9,51 | 57 | E3 ubiquitin-protein ligase Topors OS=Homo sapiens GN=TOPORS PE=1 SV=1 - [TO |

| | | | | | | |
|---|---|---|---|---|---|---|
| O60522 | 14 | 2096 | 236,4 | 5,25 | 57 | Tudor domain-containing protein 6 OS=Homo sapiens GN=TDRD6 PE=2 SV=2 - [TD |
| P52848 | 5 | 882 | 100,8 | 7,97 | 57 | Bifunctional heparan sulfate N-deacetylase/N-sulfotransferase 1 OS=Homo sapie |
| Q6NSJ5 | 9 | 796 | 90,2 | 6,96 | 57 | Leucine-rich repeat-containing protein 8E OS=Homo sapiens GN=LRRC8E PE=2 SV |
| P04430 | 2 | 108 | 11,8 | 8,44 | 57 | Ig kappa chain V-I region BAN OS=Homo sapiens PE=1 SV=1 - [KV122_HUMAN] |
| P35711 | 21 | 763 | 84,0 | 6,6 | 57 | Transcription factor SOX-5 OS=Homo sapiens GN=SOX5 PE=2 SV=3 - [SOX5_HUMA |
| P17213 | 27 | 487 | 53,9 | 9,38 | 57 | Bactericidal permeability-increasing protein OS=Homo sapiens GN=BPI PE=1 SV= |
| Q9BQA5 | 28 | 517 | 59,6 | 6,19 | 57 | Histone H4 transcription factor OS=Homo sapiens GN=HINFP PE=1 SV=2 - [HINFP_ |
| P17252 | 17 | 672 | 76,7 | 7,05 | 57 | Protein kinase C alpha type OS=Homo sapiens GN=PRKCA PE=1 SV=4 - [KPCA_HU |
| Q9NYU2 | 4 | 1555 | 177,1 | 5,63 | 57 | UDP-glucose:glycoprotein glucosyltransferase 1 OS=Homo sapiens GN=UGGT1 PE |
| Q6ZNA1 | 49 | 936 | 107,6 | 9,22 | 57 | Zinc finger protein 836 OS=Homo sapiens GN=ZNF836 PE=2 SV=2 - [ZN836_HUMA |
| P15822 | 26 | 2718 | 296,7 | 7,84 | 56 | Zinc finger protein 40 OS=Homo sapiens GN=HIVEP1 PE=1 SV=3 - [ZEP1_HUMAN] |
| A5D8W1 | 15 | 941 | 105,8 | 7,17 | 56 | Uncharacterized protein C7orf63 OS=Homo sapiens GN=C7orf63 PE=2 SV=3 - [CG0 |
| Q9NXF1 | 16 | 929 | 105,6 | 9,36 | 56 | Testis-expressed sequence 10 protein OS=Homo sapiens GN=TEX10 PE=1 SV=2 - [ |
| Q8IY92 | 10 | 1834 | 199,9 | 6,06 | 56 | Structure-specific endonuclease subunit SLX4 OS=Homo sapiens GN=SLX4 PE=1 S |
| Q9NRX1 | 8 | 252 | 27,9 | 9,73 | 56 | RNA-binding protein PNO1 OS=Homo sapiens GN=PNO1 PE=1 SV=1 - [PNO1_HUM |
| O75676 | 15 | 772 | 85,6 | 8,28 | 56 | Ribosomal protein S6 kinase alpha-4 OS=Homo sapiens GN=RPS6KA4 PE=1 SV=1 - |
| Q9ULR0 | 6 | 285 | 33,0 | 5,17 | 56 | Pre-mRNA-splicing factor ISY1 homolog OS=Homo sapiens GN=ISY1 PE=1 SV=3 - [I |
| P98196 | 5 | 1134 | 129,7 | 6,6 | 56 | Probable phospholipid-transporting ATPase IH OS=Homo sapiens GN=ATP11A PE |
| Q9NQ75 | 9 | 786 | 87,1 | 7,08 | 56 | Cas scaffolding protein family member 4 OS=Homo sapiens GN=CASS4 PE=1 SV=2 |
| Q00341 | 3 | 1268 | 141,4 | 6,87 | 56 | Vigilin OS=Homo sapiens GN=HDLBP PE=1 SV=2 - [VIGLN_HUMAN] |
| Q9BWW8 | 13 | 343 | 38,1 | 8,35 | 56 | Apolipoprotein L6 OS=Homo sapiens GN=APOL6 PE=2 SV=1 - [APOL6_HUMAN] |
| Q9UPT5 | 9 | 735 | 83,3 | 6,79 | 56 | Exocyst complex component 7 OS=Homo sapiens GN=EXOC7 PE=1 SV=3 - [EXOC7_ |
| Q5T447 | 4 | 861 | 97,1 | 5,64 | 56 | E3 ubiquitin-protein ligase HECTD3 OS=Homo sapiens GN=HECTD3 PE=1 SV=1 - [H |
| P35251 | 9 | 1148 | 128,2 | 9,36 | 56 | Replication factor C subunit 1 OS=Homo sapiens GN=RFC1 PE=1 SV=4 - [RFC1_HU |
| Q96BN8 | 32 | 352 | 40,2 | 5,47 | 56 | Protein FAM105B OS=Homo sapiens GN=FAM105B PE=1 SV=3 - [F105B_HUMAN] |
| Q9UQL6 | 5 | 1122 | 121,9 | 6,24 | 56 | Histone deacetylase 5 OS=Homo sapiens GN=HDAC5 PE=1 SV=2 - [HDAC5_HUMA |
| O94808 | 35 | 682 | 76,9 | 7,37 | 56 | Glucosamine--fructose-6-phosphate aminotransferase [isomerizing] 2 OS=Homo |
| Q5JTW2 | 5 | 689 | 76,3 | 8,18 | 56 | Centrosomal protein of 78 kDa OS=Homo sapiens GN=CEP78 PE=1 SV=1 - [CEP78_ |
| Q6ZV70 | 23 | 420 | 46,3 | 7,09 | 56 | LanC-like protein 3 OS=Homo sapiens GN=LANCL3 PE=2 SV=2 - [LANC3_HUMAN] |
| Q8TB72 | 9 | 1066 | 114,1 | 7,08 | 56 | Pumilio homolog 2 OS=Homo sapiens GN=PUM2 PE=1 SV=2 - [PUM2_HUMAN] |
| Q96C24 | 46 | 671 | 76,0 | 8,98 | 56 | Synaptotagmin-like protein 4 OS=Homo sapiens GN=SYTL4 PE=1 SV=2 - [SYTL4_HU |
| Q6P9B6 | 7 | 456 | 51,0 | 6,24 | 55 | TLD domain-containing protein KIAA1609 OS=Homo sapiens GN=KIAA1609 PE=1 S |
| P05165 | 66 | 728 | 80,0 | 7,52 | 55 | Propionyl-CoA carboxylase alpha chain, mitochondrial OS=Homo sapiens GN=PC |
| Q14D04 | 21 | 833 | 94,7 | 6,71 | 55 | Ventricular zone-expressed PH domain-containing protein homolog 1 OS=Homo |
| Q5JPE7 | 12 | 1267 | 139,4 | 5,76 | 55 | Nodal modulator 2 OS=Homo sapiens GN=NOMO2 PE=1 SV=1 - [NOMO2_HUMAN] |
| P01714 | 2 | 108 | 11,4 | 6,52 | 55 | Ig lambda chain V-III region SH OS=Homo sapiens PE=1 SV=1 - [LV301_HUMAN] |
| Q9C0B2 | 3 | 762 | 86,9 | 5,52 | 55 | Uncharacterized protein KIAA1751 OS=Homo sapiens GN=KIAA1751 PE=2 SV=2 - [ |
| Q9UKG1 | 6 | 709 | 79,6 | 5,41 | 55 | DCC-interacting protein 13-alpha OS=Homo sapiens GN=APPL1 PE=1 SV=1 - [DP13 |
| Q9HCE0 | 8 | 2579 | 292,3 | 6,43 | 55 | UPF0493 protein KIAA1632 OS=Homo sapiens GN=KIAA1632 PE=2 SV=2 - [K1632_H |
| Q86XH1 | 12 | 822 | 95,3 | 9,47 | 55 | IQ and AAA domain-containing protein 1 OS=Homo sapiens GN=IQCA1 PE=2 SV=1 |
| Q8TDI7 | 6 | 906 | 102,5 | 9,47 | 55 | Transmembrane channel-like protein 2 OS=Homo sapiens GN=TMC2 PE=2 SV=3 - |
| P29597 | 10 | 1187 | 133,6 | 7,15 | 55 | Non-receptor tyrosine-protein kinase TYK2 OS=Homo sapiens GN=TYK2 PE=1 SV= |
| Q99250 | 11 | 2005 | 227,8 | 5,73 | 55 | Sodium channel protein type 2 subunit alpha OS=Homo sapiens GN=SCN2A PE=1 |
| Q7Z403 | 15 | 805 | 90,0 | 8,66 | 55 | Transmembrane channel-like protein 6 OS=Homo sapiens GN=TMC6 PE=1 SV=2 - |
| Q96CW5 | 8 | 907 | 103,5 | 8,12 | 55 | Gamma-tubulin complex component 3 OS=Homo sapiens GN=TUBGCP3 PE=1 SV= |
| A1L390 | 16 | 1219 | 134,3 | 6,55 | 55 | Pleckstrin homology domain-containing family G member 3 OS=Homo sapiens GI |
| P01780 | 37 | 115 | 12,6 | 9,29 | 55 | Ig heavy chain V-III region JON - Homo sapiens (Human) - [HV319_HUMAN] |
| O75381 | 10 | 377 | 41,2 | 4,94 | 55 | Peroxisomal membrane protein PEX14 OS=Homo sapiens GN=PEX14 PE=1 SV=1 - |
| Q59EK9 | 22 | 446 | 49,7 | 5,27 | 55 | RUN domain-containing protein 3A OS=Homo sapiens GN=RUNDC3A PE=2 SV=2 - |
| Q5T1M5 | 8 | 1219 | 133,5 | 5,2 | 55 | FK506-binding protein 15 OS=Homo sapiens GN=FKBP15 PE=1 SV=2 - [FKB15_HUM |
| Q9ULM3 | 15 | 1422 | 150,7 | 8,98 | 55 | YEATS domain-containing protein 2 OS=Homo sapiens GN=YEATS2 PE=1 SV=2 - [YE |
| Q96H22 | 54 | 339 | 39,5 | 9,13 | 55 | Centromere protein N OS=Homo sapiens GN=CENPN PE=1 SV=2 - [CENPN_HUMA |
| Q5U651 | 3 | 963 | 103,4 | 7,96 | 55 | Ras-interacting protein 1 OS=Homo sapiens GN=RASIP1 PE=1 SV=1 - [RAIN_HUMA |
| P19174 | 47 | 1290 | 148,4 | 6,05 | 55 | 1-phosphatidylinositol-4,5-bisphosphate phosphodiesterase gamma-1 OS=Homo |
| Q8N884 | 101 | 522 | 58,8 | 9,48 | 55 | Uncharacterized protein C6orf150 OS=Homo sapiens GN=C6orf150 PE=1 SV=2 - [C |
| Q8IXA5 | 19 | 215 | 23,4 | 7,94 | 54 | Sperm acrosome membrane-associated protein 3 OS=Homo sapiens GN=SPACA3 |
| Q9UP95 | 14 | 1085 | 120,6 | 6,44 | 54 | Solute carrier family 12 member 4 OS=Homo sapiens GN=SLC12A4 PE=1 SV=2 - [S1 |
| Q8N6Q8 | 6 | 603 | 68,2 | 7,08 | 54 | Uncharacterized protein C12orf26 OS=Homo sapiens GN=C12orf26 PE=2 SV=2 - [C |
| Q96FB5 | 21 | 475 | 52,9 | 7,97 | 54 | UPF0431 protein C1orf66 OS=Homo sapiens GN=C1orf66 PE=2 SV=2 - [CA066_HUM |
| Q969T7 | 11 | 292 | 33,5 | 6,68 | 54 | Cytosolic 5'-nucleotidase III-like protein OS=Homo sapiens GN=NT5C3L PE=1 SV= |
| Q68D86 | 11 | 513 | 60,4 | 5,95 | 54 | Coiled-coil domain-containing protein 102B OS=Homo sapiens GN=CCDC102B PE= |
| Q63HK5 | 13 | 1081 | 118,5 | 7,25 | 54 | Teashirt homolog 3 OS=Homo sapiens GN=TSHZ3 PE=1 SV=2 - [TSH3_HUMAN] |
| P27815 | 6 | 886 | 98,1 | 5,21 | 54 | cAMP-specific 3',5'-cyclic phosphodiesterase 4A OS=Homo sapiens GN=PDE4A PE |
| Q6ZUT9 | 60 | 1274 | 144,9 | 6,73 | 54 | DENN domain-containing protein 5B OS=Homo sapiens GN=DENND5B PE=1 SV=2 |
| Q8NCM2 | 14 | 988 | 111,8 | 7,58 | 54 | Potassium voltage-gated channel subfamily H member 5 OS=Homo sapiens GN=K |

| | | | | | | |
|---|---|---|---|---|---|---|
| P48995 | 19 | 793 | 91,2 | 8,05 | 54 | Short transient receptor potential channel 1 OS=Homo sapiens GN=TRPC1 PE=1 S |
| Q6EMK4 | 18 | 673 | 71,7 | 7,39 | 54 | Vasorin OS=Homo sapiens GN=VASN PE=1 SV=1 - [VASN_HUMAN] |
| Q9UHL9 | 69 | 959 | 106,0 | 6,87 | 54 | General transcription factor II-I repeat domain-containing protein 1 OS=Homo sa |
| Q3SY89 | 5 | 546 | 59,7 | 9,85 | 54 | RNA polymerase II transcription factor SIII subunit A3-like-1 OS=Homo sapiens GI |
| Q9H3U1 | 18 | 944 | 103,0 | 6,07 | 54 | Protein unc-45 homolog A OS=Homo sapiens GN=UNC45A PE=1 SV=1 - [UN45A_HU |
| O75152 | 22 | 810 | 89,1 | 8,37 | 54 | Zinc finger CCCH domain-containing protein 11A OS=Homo sapiens GN=ZC3H11A |
| Q7Z3T8 | 13 | 1539 | 168,8 | 4,82 | 54 | Zinc finger FYVE domain-containing protein 16 OS=Homo sapiens GN=ZFYVE16 PE |
| P19971 | 2 | 482 | 49,9 | 5,53 | 54 | Thymidine phosphorylase OS=Homo sapiens GN=TYMP PE=1 SV=2 - [TYPH_HUMA |
| O43150 | 7 | 1006 | 111,6 | 6,68 | 54 | Arf-GAP with SH3 domain, ANK repeat and PH domain-containing protein 2 OS=H |
| Q96G42 | 19 | 594 | 63,3 | 9 | 54 | Kelch domain-containing protein 7B OS=Homo sapiens GN=KLHDC7B PE=2 SV=2 - |
| Q86XE3 | 4 | 530 | 60,7 | 8,21 | 53 | EF-hand domain-containing family member A2 OS=Homo sapiens GN=EFHA2 PE= |
| Q92771 | 3 | 950 | 105,9 | 8,24 | 53 | Probable ATP-dependent RNA helicase DDX12 OS=Homo sapiens GN=DDX12 PE=2 |
| Q8TED9 | 6 | 768 | 86,4 | 6,8 | 53 | Actin filament-associated protein 1-like 1 OS=Homo sapiens GN=AFAP1L1 PE=1 S |
| A8MXY4 | 46 | 1036 | 120,0 | 9,31 | 53 | Zinc finger protein 99 OS=Homo sapiens GN=ZNF99 PE=2 SV=2 - [ZNF99_HUMAN] |
| Q9BVG8 | 32 | 833 | 92,7 | 7,69 | 53 | Kinesin-like protein KIFC3 OS=Homo sapiens GN=KIFC3 PE=1 SV=3 - [KIFC3_HUMA |
| Q8NEN9 | 42 | 1154 | 128,5 | 6,09 | 53 | PDZ domain-containing protein 8 OS=Homo sapiens GN=PDZD8 PE=1 SV=1 - [PDZD |
| Q9H1J1 | 36 | 476 | 54,7 | 9,03 | 53 | Regulator of nonsense transcripts 3A OS=Homo sapiens GN=UPF3A PE=1 SV=1 - [R |
| Q8NC67 | 8 | 525 | 59,4 | 6,81 | 53 | Neuropilin and tolloid-like protein 2 precursor (Brain-specific transmembrane pr |
| Q5VU57 | 15 | 503 | 58,2 | 8,41 | 53 | Cytosolic carboxypeptidase 6 OS=Homo sapiens GN=AGBL4 PE=2 SV=3 - [CBPC6_H |
| A6NI56 | 6 | 674 | 76,0 | 8,38 | 53 | Coiled-coil domain-containing protein 154 OS=Homo sapiens GN=CCDC154 PE=2 S |
| Q6P179 | 4 | 960 | 110,4 | 6,71 | 53 | Endoplasmic reticulum aminopeptidase 2 OS=Homo sapiens GN=ERAP2 PE=1 SV= |
| Q9BTV7 | 8 | 478 | 52,2 | 9,82 | 53 | CDK5 and ABL1 enzyme substrate 2 OS=Homo sapiens GN=CABLES2 PE=1 SV=3 - [C |
| Q15005 | 19 | 226 | 25,0 | 8,47 | 53 | Signal peptidase complex subunit 2 OS=Homo sapiens GN=SPCS2 PE=1 SV=3 - [SP |
| P02763 | 4 | 201 | 23,5 | 5,02 | 53 | Alpha-1-acid glycoprotein 1 precursor (AGP 1) (Orosomucoid-1) (OMD 1) - Homo s |
| Q6ZNG1 | 10 | 722 | 83,1 | 9,25 | 53 | Zinc finger protein 600 OS=Homo sapiens GN=ZNF600 PE=1 SV=2 - [ZN600_HUMAN |
| Q96A61 | 16 | 297 | 34,6 | 4,25 | 53 | Tripartite motif-containing protein 52 OS=Homo sapiens GN=TRIM52 PE=2 SV=1 - |
| Q8WY91 | 13 | 577 | 62,9 | 9,28 | 53 | THAP domain-containing protein 4 OS=Homo sapiens GN=THAP4 PE=1 SV=2 - [THA |
| Q587J8 | 8 | 217 | 24,3 | 9,48 | 53 | ES cell-associated transcript 1 protein OS=Homo sapiens GN=ECAT1 PE=2 SV=1 - [E |
| Q9ULQ0 | 16 | 834 | 95,3 | 5,91 | 53 | Protein FAM40B OS=Homo sapiens GN=FAM40B PE=2 SV=2 - [FA40B_HUMAN] |
| Q6NUK1 | 27 | 477 | 53,3 | 6,33 | 53 | Calcium-binding mitochondrial carrier protein SCaMC-1 OS=Homo sapiens GN=SL |
| P01703 | 16 | 103 | 10,9 | 9,29 | 53 | Ig lambda chain V-I region NEWM OS=Homo sapiens PE=1 SV=1 - [LV105_HUMAN] |
| Q01844 | 9 | 656 | 68,4 | 9,33 | 53 | RNA-binding protein EWS OS=Homo sapiens GN=EWSR1 PE=1 SV=1 - [EWS_HUMA |
| Q9Y679 | 15 | 476 | 53,0 | 8,09 | 53 | Ancient ubiquitous protein 1 OS=Homo sapiens GN=AUP1 PE=1 SV=1 - [AUP1_HUM |
| Q8N3Y1 | 4 | 598 | 67,4 | 5,67 | 53 | F-box/WD repeat-containing protein 8 OS=Homo sapiens GN=FBXW8 PE=1 SV=2 - |
| Q9UBT7 | 102 | 734 | 81,8 | 6,64 | 53 | Alpha-catulin OS=Homo sapiens GN=CTNNAL1 PE=1 SV=2 - [CTNL1_HUMAN] |
| P08237 | 16 | 780 | 85,1 | 7,99 | 53 | 6-phosphofructokinase, muscle type OS=Homo sapiens GN=PFKM PE=1 SV=2 - [K |
| O76074 | 14 | 875 | 99,9 | 6,09 | 53 | cGMP-specific 3',5'-cyclic phosphodiesterase OS=Homo sapiens GN=PDE5A PE=1 S |
| Q8NEH6 | 5 | 495 | 60,5 | 7,12 | 52 | Meiosis-specific nuclear structural protein 1 OS=Homo sapiens GN=MNS1 PE=2 SV |
| Q9Y263 | 12 | 795 | 87,1 | 6,37 | 52 | Phospholipase A-2-activating protein OS=Homo sapiens GN=PLAA PE=1 SV=2 - [PL |
| Q8N8U2 | 34 | 506 | 56,5 | 8,79 | 52 | Chromodomain Y-like protein 2 OS=Homo sapiens GN=CDYL2 PE=2 SV=2 - [CDYL2_ |
| Q15057 | 7 | 778 | 88,0 | 6,8 | 52 | Arf-GAP with coiled-coil, ANK repeat and PH domain-containing protein 2 OS=Ho |
| Q9UPS6 | 7 | 1923 | 208,6 | 4,96 | 52 | Histone-lysine N-methyltransferase SETD1B OS=Homo sapiens GN=SETD1B PE=1 S |
| Q8IXK2 | 35 | 581 | 66,9 | 6,8 | 52 | Polypeptide N-acetylgalactosaminyltransferase 12 OS=Homo sapiens GN=GALNT |
| Q9ULJ1 | 7 | 636 | 73,7 | 6,48 | 52 | Outer dense fiber protein 2-like OS=Homo sapiens GN=ODF2L PE=2 SV=2 - [ODF2L |
| Q07343 | 6 | 736 | 83,3 | 5,25 | 52 | cAMP-specific 3',5'-cyclic phosphodiesterase 4B OS=Homo sapiens GN=PDE4B PE= |
| Q13619 | 10 | 759 | 87,6 | 8,13 | 52 | Cullin-4A OS=Homo sapiens GN=CUL4A PE=1 SV=3 - [CUL4A_HUMAN] |
| Q8WZ75 | 4 | 1007 | 107,4 | 6,64 | 52 | Roundabout homolog 4 precursor (Magic roundabout) - Homo sapiens (Human) - |
| Q16236 | 19 | 605 | 67,8 | 4,78 | 52 | Nuclear factor erythroid 2-related factor 2 OS=Homo sapiens GN=NFE2L2 PE=1 SV |
| Q13332 | 17 | 1948 | 216,9 | 6,46 | 52 | Receptor-type tyrosine-protein phosphatase S OS=Homo sapiens GN=PTPRS PE=2 |
| Q8N4A0 | 35 | 578 | 66,6 | 7,75 | 52 | Polypeptide N-acetylgalactosaminyltransferase 4 OS=Homo sapiens GN=GALNT4 |
| Q96AD5 | 19 | 504 | 55,3 | 7,08 | 52 | Patatin-like phospholipase domain-containing protein 2 OS=Homo sapiens GN=P |
| P61247 | 6 | 264 | 29,9 | 9,73 | 52 | 40S ribosomal protein S3a OS=Homo sapiens GN=RPS3A PE=1 SV=2 - [RS3A_HUMA |
| Q8IUF8 | 8 | 465 | 52,8 | 6,7 | 52 | MYC-induced nuclear antigen OS=Homo sapiens GN=MINA PE=1 SV=1 - [MINA_HU |
| O75558 | 4 | 287 | 33,2 | 6,55 | 52 | Syntaxin-11 OS=Homo sapiens GN=STX11 PE=1 SV=1 - [STX11_HUMAN] |
| Q9NVE4 | 134 | 849 | 96,3 | 8,59 | 52 | Coiled-coil domain-containing protein 87 OS=Homo sapiens GN=CCDC87 PE=2 SV |
| Q14679 | 34 | 1199 | 133,3 | 8,85 | 52 | Tubulin polyglutamylase TTLL4 OS=Homo sapiens GN=TTLL4 PE=1 SV=2 - [TTLL4_H |
| P50995 | 44 | 505 | 54,4 | 7,65 | 52 | Annexin A11 OS=Homo sapiens GN=ANXA11 PE=1 SV=1 - [ANX11_HUMAN] |
| O75093 | 45 | 1534 | 167,8 | 6,57 | 52 | Slit homolog 1 protein OS=Homo sapiens GN=SLIT1 PE=2 SV=4 - [SLIT1_HUMAN] |
| Q96JF6 | 8 | 807 | 93,8 | 8,7 | 52 | Zinc finger protein 594 OS=Homo sapiens GN=ZNF594 PE=2 SV=3 - [ZN594_HUMAN |
| Q15468 | 10 | 1287 | 142,9 | 6,46 | 52 | SCL-interrupting locus protein OS=Homo sapiens GN=STIL PE=1 SV=2 - [STIL_HUM |
| Q9ULT8 | 5 | 2610 | 289,2 | 5,35 | 52 | E3 ubiquitin-protein ligase HECTD1 OS=Homo sapiens GN=HECTD1 PE=1 SV=3 - [H |
| O60870 | 11 | 393 | 45,3 | 8,95 | 52 | DNA/RNA-binding protein KIN17 OS=Homo sapiens GN=KIN PE=1 SV=2 - [KIN17_H |
| Q96MX3 | 10 | 618 | 67,8 | 9,36 | 52 | Zinc finger protein 48 OS=Homo sapiens GN=ZNF48 PE=2 SV=2 - [ZNF48_HUMAN] |
| Q9Y267 | 9 | 594 | 66,6 | 8,38 | 51 | Solute carrier family 22 member 14 OS=Homo sapiens GN=SLC22A14 PE=2 SV=4 - [ |
| Q99728 | 12 | 777 | 86,6 | 8,72 | 51 | BRCA1-associated RING domain protein 1 OS=Homo sapiens GN=BARD1 PE=1 SV= |

| | | | | | | |
|---|---|---|---|---|---|---|
| Q5T601 | 39 | 910 | 101,3 | 8,62 | 51 | Probable G-protein coupled receptor 110 OS=Homo sapiens GN=GPR110 PE=2 SV= |
| P17302 | 15 | 382 | 43,0 | 8,76 | 51 | Gap junction alpha-1 protein OS=Homo sapiens GN=GJA1 PE=1 SV=2 - [CXA1_HUM |
| P41219 | 9 | 470 | 53,6 | 5,47 | 51 | Peripherin OS=Homo sapiens GN=PRPH PE=1 SV=2 - [PERI_HUMAN] |
| P06133 | 7 | 528 | 60,5 | 8,51 | 51 | UDP-glucuronosyltransferase 2B4 OS=Homo sapiens GN=UGT2B4 PE=1 SV=2 - [UD |
| Q92888 | 5 | 912 | 102,4 | 5,66 | 51 | Rho guanine nucleotide exchange factor 1 (p115-RhoGEF) (p115RhoGEF) (115 kDa |
| Q68CJ6 | 31 | 796 | 91,1 | 8,63 | 51 | GTPase SLIP-GC OS=Homo sapiens GN=C8orf80 PE=1 SV=3 - [SLIP_HUMAN] |
| Q8NET8 | 5 | 790 | 90,6 | 6,6 | 51 | Transient receptor potential cation channel subfamily V member 3 OS=Homo sap |
| O14531 | 9 | 572 | 61,8 | 7,09 | 51 | Dihydropyrimidinase-related protein 4 OS=Homo sapiens GN=DPYSL4 PE=1 SV=2 |
| Q9BT78 | 52 | 406 | 46,2 | 5,83 | 51 | COP9 signalosome complex subunit 4 OS=Homo sapiens GN=COPS4 PE=1 SV=1 - [ |
| Q9HCZ1 | 11 | 680 | 79,6 | 9,16 | 51 | Zinc finger protein 334 - Homo sapiens (Human) - [ZN334_HUMAN] |
| Q96IL0 | 15 | 193 | 22,9 | 9,91 | 51 | UPF0671 protein C14orf153 OS=Homo sapiens GN=C14orf153 PE=1 SV=2 - [CN153_ |
| O60568 | 6 | 738 | 84,7 | 6,05 | 51 | Procollagen-lysine,2-oxoglutarate 5-dioxygenase 3 OS=Homo sapiens GN=PLOD3 |
| A4D1S0 | 12 | 409 | 42,8 | 5,87 | 51 | Killer cell lectin-like receptor subfamily G member 2 OS=Homo sapiens GN=KLRG |
| O75808 | 19 | 1086 | 117,2 | 6,71 | 51 | Calpain-15 OS=Homo sapiens GN=SOLH PE=1 SV=1 - [CAN15_HUMAN] |
| Q9NRD9 | 16 | 1551 | 177,1 | 7,9 | 51 | Dual oxidase 1 OS=Homo sapiens GN=DUOX1 PE=1 SV=1 - [DUOX1_HUMAN] |
| P13716 | 20 | 330 | 36,3 | 6,79 | 51 | Delta-aminolevulinic acid dehydratase OS=Homo sapiens GN=ALAD PE=1 SV=1 - [ |
| O00555 | 3 | 2505 | 282,2 | 8,84 | 51 | Voltage-dependent P/Q-type calcium channel subunit alpha-1A OS=Homo sapier |
| Q9Y2I1 | 11 | 1504 | 166,5 | 5,14 | 51 | Nischarin OS=Homo sapiens GN=NISCH PE=1 SV=3 - [NISCH_HUMAN] |
| Q8TAA5 | 20 | 225 | 25,4 | 7,72 | 51 | GrpE protein homolog 2, mitochondrial precursor (Mt-GrpE#2) - Homo sapiens (H |
| Q3B820 | 31 | 660 | 76,7 | 8,03 | 51 | Protein FAM161A OS=Homo sapiens GN=FAM161A PE=2 SV=2 - [F161A_HUMAN] |
| Q5W5X9 | 6 | 447 | 50,0 | 8,38 | 51 | Tetratricopeptide repeat protein 23 OS=Homo sapiens GN=TTC23 PE=2 SV=1 - [TT |
| Q96JM3 | 7 | 812 | 89,0 | 8,44 | 51 | Zinc finger protein 828 OS=Homo sapiens GN=ZNF828 PE=1 SV=2 - [ZN828_HUMAN |
| P09758 | 14 | 323 | 35,7 | 8,87 | 51 | Tumor-associated calcium signal transducer 2 OS=Homo sapiens GN=TACSTD2 PE= |
| Q9H1X1 | 23 | 276 | 31,3 | 5,43 | 51 | Radial spoke head protein 9 homolog OS=Homo sapiens GN=RSPH9 PE=1 SV=1 - [ |
| Q96JQ0 | 4 | 3298 | 346,0 | 4,94 | 50 | Protocadherin-16 OS=Homo sapiens GN=DCHS1 PE=2 SV=1 - [PCD16_HUMAN] |
| Q7Z494 | 23 | 1330 | 150,8 | 6,76 | 50 | Nephrocystin-3 OS=Homo sapiens GN=NPHP3 PE=1 SV=1 - [NPHP3_HUMAN] |
| Q49MI3 | 68 | 558 | 62,6 | 8,27 | 50 | Ceramide kinase-like protein OS=Homo sapiens GN=CERKL PE=1 SV=1 - [CERKL_H |
| P16150 | 7 | 400 | 40,3 | 5,1 | 50 | Leukosialin OS=Homo sapiens GN=SPN PE=1 SV=1 - [LEUK_HUMAN] |
| Q9Y5H2 | 11 | 935 | 101,5 | 4,96 | 50 | Protocadherin gamma-A11 OS=Homo sapiens GN=PCDHGA11 PE=1 SV=1 - [PCDGB |
| Q9P2B2 | 15 | 879 | 98,5 | 6,61 | 50 | Prostaglandin F2 receptor negative regulator OS=Homo sapiens GN=PTGFRN PE= |
| Q9UPN9 | 11 | 1127 | 122,5 | 6,67 | 50 | E3 ubiquitin-protein ligase TRIM33 OS=Homo sapiens GN=TRIM33 PE=1 SV=3 - [TR |
| P52895 | 11 | 323 | 36,7 | 7,49 | 50 | Aldo-keto reductase family 1 member C2 OS=Homo sapiens GN=AKR1C2 PE=1 SV= |
| Q86YH6 | 29 | 399 | 44,1 | 8,24 | 50 | Decaprenyl-diphosphate synthase subunit 2 OS=Homo sapiens GN=PDSS2 PE=1 S |
| P00558 | 4 | 417 | 44,6 | 8,1 | 50 | Phosphoglycerate kinase 1 (EC 2.7.2.3) (Primer recognition protein 2) (PRP 2) - Ho |
| Q96L96 | 6 | 1907 | 201,1 | 7,58 | 50 | Alpha-protein kinase 3 OS=Homo sapiens GN=ALPK3 PE=2 SV=2 - [ALPK3_HUMAN |
| Q9H6Q4 | 5 | 476 | 53,0 | 7,23 | 50 | Cytosolic Fe-S cluster assembly factor NARFL OS=Homo sapiens GN=NARFL PE=1 S |
| Q12767 | 6 | 1356 | 151,1 | 6,44 | 50 | Uncharacterized protein KIAA0195 OS=Homo sapiens GN=KIAA0195 PE=1 SV=1 - [ |
| Q7Z401 | 5 | 1863 | 209,1 | 7,31 | 50 | C-myc promoter-binding protein OS=Homo sapiens GN=DENND4A PE=1 SV=2 - [M |
| P35240 | 8 | 595 | 69,6 | 6,47 | 50 | Merlin OS=Homo sapiens GN=NF2 PE=1 SV=1 - [MERL_HUMAN] |
| Q4G0T1 | 4 | 1027 | 108,5 | 6,15 | 50 | Putative scavenger receptor cysteine-rich domain-containing protein LOC619207 |
| Q8NDM7 | 4 | 1665 | 191,9 | 5,99 | 50 | WD repeat-containing protein C10orf79 OS=Homo sapiens GN=C10orf79 PE=2 SV= |
| Q9BQK8 | 4 | 851 | 93,6 | 5,52 | 50 | Phosphatidate phosphatase LPIN3 OS=Homo sapiens GN=LPIN3 PE=1 SV=3 - [LPIN |
| Q9H825 | 16 | 291 | 33,4 | 6,95 | 50 | Methyltransferase-like protein 8 OS=Homo sapiens GN=METTL8 PE=2 SV=2 - [MET |
| Q9H992 | 6 | 704 | 78,0 | 6,77 | 50 | E3 ubiquitin-protein ligase MARCH7 OS=Homo sapiens GN=MARCH7 PE=1 SV=1 - [ |
| P52746 | 14 | 1687 | 187,8 | 7,91 | 50 | Zinc finger protein 142 OS=Homo sapiens GN=ZNF142 PE=1 SV=4 - [ZN142_HUMAN |
| Q8TDZ2 | 6 | 1067 | 117,8 | 6,4 | 50 | NEDD9-interacting protein with calponin homology and LIM domains OS=Homo s |
| Q9NP72 | 6 | 206 | 23,0 | 5,24 | 50 | Ras-related protein Rab-18 OS=Homo sapiens GN=RAB18 PE=1 SV=1 - [RAB18_HU |
| Q6ZSB9 | 4 | 765 | 85,0 | 6,98 | 50 | Zinc finger and BTB domain-containing protein 49 OS=Homo sapiens GN=ZBTB49 |
| Q9UHK0 | 5 | 495 | 56,3 | 9,13 | 50 | Nuclear fragile X mental retardation-interacting protein 1 OS=Homo sapiens GN= |
| Q6PJ61 | 6 | 646 | 69,0 | 7,99 | 50 | F-box only protein 46 OS=Homo sapiens GN=FBXO46 PE=1 SV=2 - [FBX46_HUMAN |
| Q6QEF8 | 18 | 472 | 52,7 | 5,96 | 50 | Coronin-6 OS=Homo sapiens GN=CORO6 PE=1 SV=2 - [CORO6_HUMAN] |
| Q8IY17 | 7 | 1366 | 149,9 | 7,81 | 50 | Neuropathy target esterase OS=Homo sapiens GN=PNPLA6 PE=1 SV=2 - [PLPL6_H |
| Q9BWV1 | 16 | 1114 | 121,0 | 7,01 | 49 | Brother of CDO OS=Homo sapiens GN=BOC PE=1 SV=1 - [BOC_HUMAN] |
| Q9UBL3 | 13 | 628 | 68,7 | 5,69 | 49 | Set1/Ash2 histone methyltransferase complex subunit ASH2 (ASH2-like protein) |
| Q14289 | 7 | 1009 | 115,8 | 6,25 | 49 | Protein-tyrosine kinase 2-beta OS=Homo sapiens GN=PTK2B PE=1 SV=2 - [FAK2_H |
| Q9UIK4 | 6 | 370 | 42,9 | 6,92 | 49 | Death-associated protein kinase 2 OS=Homo sapiens GN=DAPK2 PE=1 SV=1 - [DAI |
| O95684 | 48 | 399 | 43,0 | 4,81 | 49 | FGFR1 oncogene partner OS=Homo sapiens GN=FGFR1OP PE=1 SV=1 - [FR1OP_HU |
| Q5SYE7 | 14 | 1610 | 170,6 | 6,96 | 49 | NHS-like protein 1 OS=Homo sapiens GN=NHSL1 PE=1 SV=2 - [NHSL1_HUMAN] |
| Q8N0X2 | 10 | 631 | 70,8 | 6,33 | 49 | Sperm-associated antigen 16 protein OS=Homo sapiens GN=SPAG16 PE=2 SV=2 - [ |
| Q8TDR2 | 11 | 534 | 58,0 | 9,74 | 49 | Serine/threonine-protein kinase 35 OS=Homo sapiens GN=STK35 PE=1 SV=2 - [STI |
| Q5TEA3 | 12 | 1177 | 132,2 | 6,57 | 49 | Uncharacterized protein C20orf194 OS=Homo sapiens GN=C20orf194 PE=2 SV=1 - |
| Q8NBI6 | 168 | 393 | 43,8 | 8,13 | 49 | Uncharacterized protein C3orf21 OS=Homo sapiens GN=C3orf21 PE=2 SV=1 - [CC0 |
| Q6P3X8 | 14 | 592 | 68,0 | 8,54 | 49 | PiggyBac transposable element-derived protein 2 OS=Homo sapiens GN=PGBD2 |
| Q70UQ0 | 15 | 350 | 39,3 | 9,17 | 49 | Inhibitor of nuclear factor kappa-B kinase-interacting protein OS=Homo sapiens |
| P42680 | 8 | 631 | 73,5 | 8,44 | 49 | Tyrosine-protein kinase Tec OS=Homo sapiens GN=TEC PE=1 SV=2 - [TEC_HUMAN |

| | | | | | | |
|---|---|---|---|---|---|---|
| Q92621 | 9 | 2012 | 227,8 | 6,19 | 49 | Nuclear pore complex protein Nup205 OS=Homo sapiens GN=NUP205 PE=1 SV=3 |
| Q9UBJ2 | 11 | 740 | 83,2 | 8,92 | 49 | ATP-binding cassette sub-family D member 2 OS=Homo sapiens GN=ABCD2 PE=1 |
| P61164 | 10 | 376 | 42,6 | 6,64 | 49 | Alpha-centractin OS=Mus musculus GN=Actr1a PE=2 SV=1 - [ACTZ_MOUSE] |
| Q9NRJ5 | 15 | 636 | 71,6 | 6,44 | 49 | Poly(A) polymerase beta OS=Homo sapiens GN=PAPOLB PE=2 SV=1 - [PAPOB_HU |
| Q86UX7 | 11 | 667 | 75,9 | 6,98 | 49 | Fermitin family homolog 3 OS=Homo sapiens GN=FERMT3 PE=1 SV=1 - [URP2_HUI |
| P55011 | 6 | 1212 | 131,4 | 6,4 | 49 | Solute carrier family 12 member 2 OS=Homo sapiens GN=SLC12A2 PE=1 SV=1 - [S1 |
| Q9HC36 | 31 | 420 | 47,0 | 8,73 | 49 | RNA methyltransferase-like protein 1 OS=Homo sapiens GN=RNMTL1 PE=1 SV=2 - |
| Q96PQ7 | 6 | 755 | 84,4 | 6,64 | 49 | Kelch-like protein 5 OS=Homo sapiens GN=KLHL5 PE=2 SV=3 - [KLHL5_HUMAN] |
| Q15326 | 5 | 562 | 66,2 | 8,22 | 49 | Zinc finger MYND domain-containing protein 11 OS=Homo sapiens GN=ZMYND11 |
| C9J069 | 27 | 976 | 106,6 | 9,03 | 49 | Uncharacterized protein C9orf172 OS=Homo sapiens GN=C9orf172 PE=3 SV=1 - [CI |
| Q15424 | 8 | 915 | 102,6 | 5,47 | 49 | Scaffold attachment factor B1 OS=Homo sapiens GN=SAFB PE=1 SV=4 - [SAFB1_HU |
| O60812 | 13 | 293 | 32,1 | 5,06 | 49 | Heterogeneous nuclear ribonucleoprotein C-like 1 OS=Homo sapiens GN=HNRNP |
| Q494X1 | 5 | 144 | 16,6 | 8,88 | 49 | Protein FAM153C OS=Homo sapiens GN=FAM153C PE=2 SV=1 - [F153C_HUMAN] |
| Q15561 | 10 | 434 | 48,3 | 7,33 | 49 | Transcriptional enhancer factor TEF-3 OS=Homo sapiens GN=TEAD4 PE=1 SV=3 - [T |
| O43566 | 144 | 566 | 61,4 | 8,19 | 48 | Regulator of G-protein signaling 14 OS=Homo sapiens GN=RGS14 PE=1 SV=4 - [RG |
| P51795 | 16 | 746 | 83,1 | 6,81 | 48 | H(+)/Cl(-) exchange transporter 5 OS=Homo sapiens GN=CLCN5 PE=1 SV=1 - [CLCN |
| O15335 | 36 | 359 | 40,5 | 9,39 | 48 | Chondroadherin OS=Homo sapiens GN=CHAD PE=2 SV=2 - [CHAD_HUMAN] |
| Q8IXQ6 | 27 | 854 | 96,3 | 7,91 | 48 | Poly [ADP-ribose] polymerase 9 OS=Homo sapiens GN=PARP9 PE=1 SV=2 - [PARP |
| Q96ST8 | 4 | 783 | 89,5 | 6,8 | 48 | Coiled-coil domain-containing protein 123, mitochondrial OS=Homo sapiens GN= |
| Q9UMS0 | 6 | 254 | 28,4 | 5,07 | 48 | NFU1 iron-sulfur cluster scaffold homolog, mitochondrial OS=Homo sapiens GN= |
| Q15025 | 19 | 636 | 71,8 | 6,62 | 48 | TNFAIP3-interacting protein 1 OS=Homo sapiens GN=TNIP1 PE=1 SV=2 - [TNIP1_H |
| P11498 | 6 | 1178 | 129,6 | 6,84 | 48 | Pyruvate carboxylase, mitochondrial OS=Homo sapiens GN=PC PE=1 SV=2 - [PYC_ |
| Q8IUC6 | 16 | 712 | 76,4 | 5,41 | 48 | TIR domain-containing adapter molecule 1 OS=Homo sapiens GN=TICAM1 PE=1 S |
| Q8NDL9 | 3 | 886 | 97,5 | 9,17 | 48 | Cytosolic carboxypeptidase-like protein 5 OS=Homo sapiens GN=AGBL5 PE=2 SV= |
| Q16589 | 24 | 344 | 38,8 | 5,48 | 48 | Cyclin-G2 OS=Homo sapiens GN=CCNG2 PE=1 SV=1 - [CCNG2_HUMAN] |
| Q02446 | 5 | 784 | 81,9 | 7,05 | 48 | Transcription factor Sp4 OS=Homo sapiens GN=SP4 PE=1 SV=2 - [SP4_HUMAN] |
| Q96JN2 | 5 | 1154 | 134,0 | 4,65 | 48 | Coiled-coil domain-containing protein 136 OS=Homo sapiens GN=CCDC136 PE=1 S |
| P35221 | 4 | 906 | 100,0 | 6,29 | 48 | Catenin alpha-1 (Cadherin-associated protein) (Alpha E-catenin) (NY-REN-13 anti |
| Q9H0M0 | 6 | 922 | 105,1 | 5,9 | 48 | NEDD4-like E3 ubiquitin-protein ligase WWP1 OS=Homo sapiens GN=WWP1 PE=1 |
| Q96JX3 | 9 | 654 | 74,1 | 7,68 | 48 | Protein SERAC1 OS=Homo sapiens GN=SERAC1 PE=2 SV=1 - [SRAC1_HUMAN] |
| Q4G148 | 14 | 440 | 50,5 | 8,65 | 48 | Glucoside xylosyltransferase 1 OS=Homo sapiens GN=GXYLT1 PE=1 SV=2 - [GXLT1_ |
| Q9H2S9 | 3 | 585 | 64,1 | 6,86 | 48 | Zinc finger protein Eos OS=Homo sapiens GN=IKZF4 PE=1 SV=2 - [IKZF4_HUMAN] |
| Q8N1V2 | 10 | 620 | 68,3 | 6,95 | 48 | WD repeat-containing protein 16 OS=Homo sapiens GN=WDR16 PE=1 SV=3 - [WDI |
| Q9NP99 | 7 | 234 | 26,4 | 8,84 | 48 | Triggering receptor expressed on myeloid cells 1 OS=Homo sapiens GN=TREM1 P |
| P31939 | 10 | 592 | 64,6 | 6,71 | 48 | Bifunctional purine biosynthesis protein PURH OS=Homo sapiens GN=ATIC PE=1 S |
| Q00839 | 8 | 825 | 90,5 | 6 | 48 | Heterogeneous nuclear ribonucleoprotein U OS=Homo sapiens GN=HNRNPU PE= |
| Q96MT3 | 17 | 831 | 94,2 | 6,24 | 48 | Prickle-like protein 1 OS=Homo sapiens GN=PRICKLE1 PE=1 SV=2 - [PRIC1_HUMAN |
| Q0VDD8 | 54 | 3507 | 399,6 | 6,93 | 48 | Dynein heavy chain 14, axonemal OS=Homo sapiens GN=DNAH14 PE=2 SV=3 - [DY |
| P17024 | 11 | 532 | 61,5 | 8,62 | 48 | Zinc finger protein 20 OS=Homo sapiens GN=ZNF20 PE=2 SV=2 - [ZNF20_HUMAN] |
| Q9BSK4 | 21 | 669 | 73,6 | 6,07 | 48 | Protein fem-1 homolog A OS=Homo sapiens GN=FEM1A PE=1 SV=1 - [FEM1A_HUM |
| Q9NVH2 | 7 | 962 | 106,8 | 8,02 | 48 | Integrator complex subunit 7 OS=Homo sapiens GN=INTS7 PE=1 SV=1 - [INT7_HUM |
| O14793 | 3 | 375 | 42,7 | 6,76 | 48 | Growth/differentiation factor 8 OS=Homo sapiens GN=MSTN PE=1 SV=1 - [GDF8_H |
| O60733 | 17 | 806 | 89,8 | 7,27 | 48 | 85 kDa calcium-independent phospholipase A2 OS=Homo sapiens GN=PLA2G6 PE |
| Q9Y651 | 16 | 276 | 28,6 | 9,73 | 47 | Transcription factor SOX-21 OS=Homo sapiens GN=SOX21 PE=2 SV=1 - [SOX21_HU |
| Q9BWF2 | 10 | 469 | 53,3 | 8,48 | 47 | TRAF-interacting protein OS=Homo sapiens GN=TRAIP PE=1 SV=1 - [TRAIP_HUMA |
| Q9Y6R7 | 6 | 5405 | 571,6 | 5,34 | 47 | IgGFc-binding protein OS=Homo sapiens GN=FCGBP PE=1 SV=3 - [FCGBP_HUMAN |
| O35593 | 11 | 310 | 34,6 | 6,52 | 47 | 26S proteasome non-ATPase regulatory subunit 14 OS=Mus musculus GN=Psmd14 |
| Q9NZ56 | 17 | 1722 | 180,0 | 5,47 | 47 | Formin-2 OS=Homo sapiens GN=FMN2 PE=1 SV=4 - [FMN2_HUMAN] |
| Q2M329 | 40 | 555 | 62,7 | 4,94 | 47 | Coiled-coil domain-containing protein 96 OS=Homo sapiens GN=CCDC96 PE=2 SV= |
| Q96RK0 | 10 | 1608 | 163,7 | 8,56 | 47 | Protein capicua homolog OS=Homo sapiens GN=CIC PE=1 SV=2 - [CIC_HUMAN] |
| Q9P2E2 | 6 | 1029 | 115,0 | 5,5 | 47 | Kinesin-like protein KIF17 OS=Homo sapiens GN=KIF17 PE=1 SV=3 - [KIF17_HUMA |
| Q9Y620 | 13 | 910 | 102,9 | 8,12 | 47 | DNA repair and recombination protein RAD54B OS=Homo sapiens GN=RAD54B PE |
| O60307 | 12 | 1309 | 143,0 | 8,06 | 47 | Microtubule-associated serine/threonine-protein kinase 3 OS=Homo sapiens GN |
| P14625 | 11 | 803 | 92,4 | 4,84 | 47 | Endoplasmin OS=Homo sapiens GN=HSP90B1 PE=1 SV=1 - [ENPL_HUMAN] |
| Q9GZU2 | 12 | 1588 | 180,7 | 5,48 | 47 | Paternally-expressed gene 3 protein OS=Homo sapiens GN=PEG3 PE=2 SV=1 - [PE |
| Q86V48 | 5 | 1076 | 120,2 | 8,5 | 47 | Leucine zipper protein 1 OS=Homo sapiens GN=LUZP1 PE=1 SV=2 - [LUZP1_HUMAI |
| Q658Y4 | 27 | 838 | 93,8 | 6,39 | 47 | Protein FAM91A1 OS=Homo sapiens GN=FAM91A1 PE=1 SV=3 - [F91A1_HUMAN] |
| Q9BTE3 | 20 | 642 | 72,9 | 5,87 | 47 | UPF0557 protein C10orf119 OS=Homo sapiens GN=C10orf119 PE=1 SV=2 - [CJ119_H |
| Q8NEF3 | 12 | 446 | 53,5 | 9,48 | 47 | Coiled-coil domain-containing protein 112 OS=Homo sapiens GN=CCDC112 PE=2 S |
| Q5QJE6 | 90 | 756 | 84,4 | 6,16 | 47 | Deoxynucleotidyltransferase terminal-interacting protein 2 OS=Homo sapiens GI |
| Q8TBP0 | 55 | 767 | 86,3 | 5,82 | 47 | TBC1 domain family member 16 OS=Homo sapiens GN=TBC1D16 PE=1 SV=1 - [TBC |
| Q9H6Y5 | 151 | 334 | 35,2 | 10,81 | 47 | PDZ domain-containing protein MAGIX OS=Homo sapiens GN=MAGIX PE=1 SV=3 - |
| P23141 | 9 | 567 | 62,5 | 6,6 | 47 | Liver carboxylesterase 1 OS=Homo sapiens GN=CES1 PE=1 SV=2 - [EST1_HUMAN] |
| A6NNM8 | 7 | 815 | 93,6 | 8,91 | 47 | Tubulin polyglutamylase TTLL13 OS=Homo sapiens GN=TTLL13 PE=1 SV=2 - [TTL13_ |
| Q9NQX6 | 16 | 463 | 53,7 | 8,91 | 47 | Zinc finger protein 331 (Zinc finger protein 463) (C2H2-like zinc finger protein rea |

| | | | | | | |
|---|---|---|---|---|---|---|
| P23470 | 19 | 1445 | 161,9 | 6,42 | 47 | Receptor-type tyrosine-protein phosphatase gamma OS=Homo sapiens GN=PTPR |
| Q03252 | 4 | 600 | 67,6 | 5,35 | 47 | Lamin-B2 OS=Homo sapiens GN=LMNB2 PE=1 SV=3 - [LMNB2_HUMAN] |
| P32927 | 9 | 897 | 97,3 | 5,52 | 47 | Cytokine receptor common subunit beta OS=Homo sapiens GN=CSF2RB PE=1 SV= |
| P00480 | 50 | 354 | 39,9 | 8,63 | 47 | Ornithine carbamoyltransferase, mitochondrial precursor (EC 2.1.3.3) (OTCase) ( |
| Q9H0I9 | 19 | 626 | 67,8 | 6,33 | 47 | Transketolase-like protein 2 OS=Homo sapiens GN=TKTL2 PE=1 SV=1 - [TKTL2_HUI |
| Q6ZWJ8 | 10 | 1503 | 159,8 | 5,74 | 47 | Kielin/chordin-like protein OS=Homo sapiens GN=KCP PE=2 SV=2 - [KCP_HUMAN |
| Q8TBC3 | 16 | 707 | 76,3 | 8,28 | 47 | SH3KBP1-binding protein 1 OS=Homo sapiens GN=SHKBP1 PE=1 SV=2 - [SHKB1_HU |
| Q13825 | 10 | 339 | 35,6 | 9,48 | 46 | Methylglutaconyl-CoA hydratase, mitochondrial OS=Homo sapiens GN=AUH PE=1 |
| P09327 | 6 | 827 | 92,6 | 6,39 | 46 | Villin-1 OS=Homo sapiens GN=VIL1 PE=1 SV=4 - [VILI_HUMAN] |
| O15075 | 13 | 740 | 82,2 | 8,66 | 46 | Serine/threonine-protein kinase DCLK1 OS=Homo sapiens GN=DCLK1 PE=1 SV=2 - |
| Q8WUM0 | 31 | 1156 | 128,9 | 5,1 | 46 | Nuclear pore complex protein Nup133 OS=Homo sapiens GN=NUP133 PE=1 SV=2 |
| Q15825 | 24 | 494 | 56,9 | 6,62 | 46 | Neuronal acetylcholine receptor subunit alpha-6 OS=Homo sapiens GN=CHRNA6 |
| Q9NY12 | 6 | 217 | 22,3 | 10,92 | 46 | H/ACA ribonucleoprotein complex subunit 1 OS=Homo sapiens GN=GAR1 PE=1 SV |
| P19634 | 3 | 815 | 90,7 | 7,21 | 46 | Sodium/hydrogen exchanger 1 OS=Homo sapiens GN=SLC9A1 PE=1 SV=2 - [SL9A1_ |
| O75683 | 10 | 361 | 41,4 | 10,64 | 46 | Surfeit locus protein 6 OS=Homo sapiens GN=SURF6 PE=1 SV=3 - [SURF6_HUMAN] |
| P15311 | 96 | 586 | 69,4 | 6,27 | 46 | Ezrin OS=Homo sapiens GN=EZR PE=1 SV=4 - [EZRI_HUMAN] |
| Q76M96 | 9 | 950 | 108,1 | 9,72 | 46 | Coiled-coil domain-containing protein 80 OS=Homo sapiens GN=CCDC80 PE=1 SV |
| Q5T0Z8 | 15 | 1188 | 124,0 | 9,42 | 46 | Uncharacterized protein C6orf132 OS=Homo sapiens GN=C6orf132 PE=1 SV=3 - [C |
| Q9C0B5 | 26 | 715 | 77,5 | 9,01 | 46 | Probable palmitoyltransferase ZDHHC5 OS=Homo sapiens GN=ZDHHC5 PE=1 SV=2 |
| P56730 | 15 | 875 | 97,0 | 8,03 | 46 | Neurotrypsin OS=Homo sapiens GN=PRSS12 PE=2 SV=2 - [NETR_HUMAN] |
| Q15746 | 11 | 1914 | 210,6 | 6,15 | 46 | Myosin light chain kinase, smooth muscle OS=Homo sapiens GN=MYLK PE=1 SV=4 |
| Q5M8T2 | 14 | 416 | 44,2 | 7,27 | 46 | Solute carrier family 35 member D3 OS=Homo sapiens GN=SLC35D3 PE=2 SV=1 - [S |
| Q96C03 | 4 | 454 | 49,2 | 5,12 | 46 | Smith-Magenis syndrome chromosomal region candidate gene 7 protein OS=Hon |
| P05181 | 3 | 493 | 56,8 | 8,1 | 46 | Cytochrome P450 2E1 OS=Homo sapiens GN=CYP2E1 PE=1 SV=1 - [CP2E1_HUMAN] |
| Q9UI12 | 4 | 483 | 55,8 | 6,48 | 46 | Vacuolar ATP synthase subunit H (EC 3.6.3.14) (V-ATPase H subunit) (Vacuolar pro |
| Q86TC9 | 6 | 1320 | 145,2 | 6,77 | 46 | Myopalladin OS=Homo sapiens GN=MYPN PE=1 SV=2 - [MYPN_HUMAN] |
| Q9UJV3 | 5 | 735 | 83,2 | 7,39 | 46 | Probable E3 ubiquitin-protein ligase MID2 OS=Homo sapiens GN=MID2 PE=1 SV=3 |
| Q16222 | 13 | 522 | 58,7 | 6,33 | 46 | UDP-N-acetylhexosamine pyrophosphorylase OS=Homo sapiens GN=UAP1 PE=1 S |
| Q9BSV6 | 58 | 310 | 33,6 | 8,43 | 46 | tRNA-splicing endonuclease subunit Sen34 OS=Homo sapiens GN=TSEN34 PE=1 S |
| Q5VTE6 | 3 | 544 | 62,3 | 7,81 | 46 | Protein angel homolog 2 OS=Homo sapiens GN=ANGEL2 PE=2 SV=1 - [ANGE2_HUM |
| Q12912 | 109 | 555 | 62,1 | 5,85 | 46 | Lymphoid-restricted membrane protein OS=Homo sapiens GN=LRMP PE=1 SV=3 - |
| Q9NZN5 | 16 | 1544 | 173,1 | 5,74 | 46 | Rho guanine nucleotide exchange factor 12 OS=Homo sapiens GN=ARHGEF12 PE= |
| Q01581 | 50 | 520 | 57,3 | 5,41 | 46 | Hydroxymethylglutaryl-CoA synthase, cytoplasmic (EC 2.3.3.10) (HMG-CoA synth |
| Q3MIX3 | 4 | 580 | 65,9 | 8,97 | 45 | Uncharacterized aarF domain-containing protein kinase 5 OS=Homo sapiens GN= |
| O14744 | 6 | 637 | 72,6 | 6,29 | 45 | Protein arginine N-methyltransferase 5 OS=Homo sapiens GN=PRMT5 PE=1 SV=4 |
| P10074 | 5 | 688 | 77,0 | 8,18 | 45 | Zinc finger and BTB domain-containing protein 48 OS=Homo sapiens GN=ZBTB48 |
| P81408 | 14 | 668 | 71,3 | 8,46 | 45 | Protein FAM189B OS=Homo sapiens GN=FAM189B PE=1 SV=2 - [F189B_HUMAN] |
| Q9HD64 | 8 | 160 | 17,7 | 9,67 | 45 | G antigen family D member 2 OS=Homo sapiens GN=XAGE1A PE=2 SV=2 - [GAGD2 |
| P06331 | 11 | 146 | 16,2 | 8,28 | 45 | Ig heavy chain V-II region ARH-77 OS=Homo sapiens PE=4 SV=1 - [HV209_HUMAN] |
| P19525 | 3 | 551 | 62,1 | 8,4 | 45 | Interferon-induced, double-stranded RNA-activated protein kinase OS=Homo sa |
| Q7Z6M2 | 10 | 555 | 62,6 | 7,36 | 45 | F-box only protein 33 OS=Homo sapiens GN=FBXO33 PE=2 SV=1 - [FBX33_HUMAN |
| Q9NP61 | 9 | 516 | 56,9 | 7,36 | 45 | ADP-ribosylation factor GTPase-activating protein 3 OS=Homo sapiens GN=ARFGA |
| P17676 | 6 | 345 | 36,1 | 8,31 | 45 | CCAAT/enhancer-binding protein beta OS=Homo sapiens GN=CEBPB PE=1 SV=2 - |
| O95759 | 25 | 1140 | 130,8 | 5,52 | 45 | TBC1 domain family member 8 OS=Homo sapiens GN=TBC1D8 PE=1 SV=3 - [TBCD8 |
| Q0IIM8 | 34 | 1120 | 128,6 | 5,95 | 45 | TBC1 domain family member 8B OS=Homo sapiens GN=TBC1D8B PE=2 SV=2 - [TBC |
| Q99575 | 9 | 1024 | 114,6 | 9,22 | 45 | Ribonucleases P/MRP protein subunit POP1 OS=Homo sapiens GN=POP1 PE=1 SV |
| O15446 | 8 | 510 | 55,0 | 8,51 | 45 | DNA-directed RNA polymerase I subunit RPA34 OS=Homo sapiens GN=CD3EAP PE |
| P01612 | 7 | 109 | 11,9 | 6,57 | 45 | Ig kappa chain V-I region Mev - Homo sapiens (Human) - [KV120_HUMAN] |
| Q86UE8 | 44 | 772 | 87,6 | 8,41 | 45 | Serine/threonine-protein kinase tousled-like 2 OS=Homo sapiens GN=TLK2 PE=1 |
| O95948 | 21 | 504 | 54,3 | 9,61 | 45 | One cut domain family member 2 OS=Homo sapiens GN=ONECUT2 PE=2 SV=2 - [C |
| Q96SI1 | 9 | 283 | 31,9 | 7,44 | 45 | BTB/POZ domain-containing protein KCTD15 OS=Homo sapiens GN=KCTD15 PE=1 |
| O60662 | 4 | 606 | 68,0 | 5,29 | 45 | Kelch repeat and BTB domain-containing protein 10 OS=Homo sapiens GN=KBTBD |
| Q6NT55 | 4 | 531 | 61,9 | 8,73 | 45 | Cytochrome P450 4F22 OS=Homo sapiens GN=CYP4F22 PE=2 SV=1 - [CP4FN_HUMA |
| Q8WXK1 | 15 | 588 | 65,8 | 5,83 | 45 | Ankyrin repeat and SOCS box protein 15 OS=Homo sapiens GN=ASB15 PE=2 SV=3 |
| O94827 | 5 | 1062 | 117,4 | 6,3 | 45 | Pleckstrin homology domain-containing family G member 5 OS=Homo sapiens GI |
| Q7KYR7 | 6 | 527 | 59,6 | 6,48 | 45 | Butyrophilin subfamily 2 member A1 OS=Homo sapiens GN=BTN2A1 PE=1 SV=3 - |
| P06401 | 4 | 933 | 98,9 | 6,49 | 45 | Progesterone receptor OS=Homo sapiens GN=PGR PE=1 SV=4 - [PRGR_HUMAN] |
| Q86XX4 | 8 | 4007 | 442,6 | 5,59 | 45 | Extracellular matrix protein FRAS1 OS=Homo sapiens GN=FRAS1 PE=2 SV=1 - [FRA |
| O75818 | 8 | 363 | 41,8 | 6,67 | 45 | Ribonuclease P protein subunit p40 OS=Homo sapiens GN=RPP40 PE=1 SV=3 - [RP |
| P78318 | 22 | 339 | 39,2 | 5,38 | 45 | Immunoglobulin-binding protein 1 OS=Homo sapiens GN=IGBP1 PE=1 SV=1 - [IGB |
| Q6P1J9 | 2 | 531 | 60,5 | 9,61 | 45 | Parafibromin OS=Homo sapiens GN=CDC73 PE=1 SV=1 - [CDC73_HUMAN] |
| P51451 | 31 | 505 | 57,7 | 7,87 | 45 | Tyrosine-protein kinase Blk OS=Homo sapiens GN=BLK PE=1 SV=3 - [BLK_HUMAN] |
| Q96CX6 | 7 | 371 | 40,6 | 6,84 | 45 | Leucine-rich repeat-containing protein 58 OS=Homo sapiens GN=LRRC58 PE=1 SV |
| Q8N1G4 | 24 | 583 | 63,4 | 8,28 | 45 | Leucine-rich repeat-containing protein 47 OS=Homo sapiens GN=LRRC47 PE=1 SV |
| Q9UKD2 | 33 | 239 | 27,5 | 8,29 | 44 | mRNA turnover protein 4 homolog OS=Homo sapiens GN=MRTO4 PE=1 SV=2 - [MI |

| | | | | | | |
|---|---|---|---|---|---|---|
| Q9BXW9 | 7 | 1471 | 166,4 | 6,24 | 44 | Fanconi anemia group D2 protein OS=Homo sapiens GN=FANCD2 PE=1 SV=1 - [FA |
| P08174 | 10 | 381 | 41,4 | 7,59 | 44 | Complement decay-accelerating factor OS=Homo sapiens GN=CD55 PE=1 SV=4 - [ |
| Q8WZ94 | 3 | 311 | 34,3 | 8,31 | 44 | Olfactory receptor 5P3 OS=Homo sapiens GN=OR5P3 PE=2 SV=1 - [OR5P3_HUMAN |
| P49754 | 12 | 854 | 98,5 | 5,85 | 44 | Vacuolar protein sorting-associated protein 41 homolog OS=Homo sapiens GN=V |
| O43639 | 11 | 380 | 42,9 | 6,95 | 44 | Cytoplasmic protein NCK2 OS=Homo sapiens GN=NCK2 PE=1 SV=2 - [NCK2_HUMA |
| Q6ZUL3 | 4 | 223 | 24,7 | 9,45 | 44 | Uncharacterized protein C8orf86 OS=Homo sapiens GN=C8orf86 PE=2 SV=1 - [CH0 |
| O75762 | 14 | 1119 | 127,4 | 7,12 | 44 | Transient receptor potential cation channel subfamily A member 1 OS=Homo sap |
| Q16854 | 14 | 277 | 32,0 | 8,66 | 44 | Deoxyguanosine kinase, mitochondrial OS=Homo sapiens GN=DGUOK PE=1 SV=2 |
| P78333 | 17 | 572 | 63,7 | 6,81 | 44 | Glypican-5 OS=Homo sapiens GN=GPC5 PE=1 SV=1 - [GPC5_HUMAN] |
| P36955 | 2 | 418 | 46,3 | 6,38 | 44 | Pigment epithelium-derived factor OS=Homo sapiens GN=SERPINF1 PE=1 SV=4 - [ |
| Q9BXX0 | 6 | 1053 | 115,6 | 6,46 | 44 | EMILIN-2 OS=Homo sapiens GN=EMILIN2 PE=1 SV=3 - [EMIL2_HUMAN] |
| Q6PIW4 | 11 | 674 | 74,0 | 7,85 | 44 | Fidgetin-like protein 1 OS=Homo sapiens GN=FIGNL1 PE=1 SV=2 - [FIGL1_HUMAN |
| Q9BXT2 | 16 | 260 | 28,1 | 9,17 | 44 | Voltage-dependent calcium channel gamma-6 subunit OS=Homo sapiens GN=CA |
| P30740 | 7 | 379 | 42,7 | 6,28 | 44 | Leukocyte elastase inhibitor OS=Homo sapiens GN=SERPINB1 PE=1 SV=1 - [ILEU_H |
| Q8TDY3 | 12 | 377 | 41,7 | 5,47 | 44 | Actin-related protein T2 OS=Homo sapiens GN=ACTRT2 PE=2 SV=2 - [ACTT2_HUM |
| P37802 | 2 | 199 | 22,4 | 8,25 | 44 | Transgelin-2 (SM22-alpha homolog) - Homo sapiens (Human) - [TAGL2_HUMAN] |
| B4DS77 | 80 | 424 | 46,9 | 8,66 | 44 | Protein shisa-9 OS=Homo sapiens GN=SHISA9 PE=2 SV=3 - [SHSA9_HUMAN] |
| Q9NX95 | 3 | 663 | 72,3 | 6,25 | 44 | Syntabulin OS=Homo sapiens GN=SYBU PE=1 SV=2 - [SYBU_HUMAN] |
| Q15633 | 10 | 366 | 39,0 | 6,54 | 44 | RISC-loading complex subunit TARBP2 OS=Homo sapiens GN=TARBP2 PE=1 SV=3 - |
| O60258 | 32 | 216 | 24,9 | 10,42 | 44 | Fibroblast growth factor 17 OS=Homo sapiens GN=FGF17 PE=2 SV=1 - [FGF17_HUM |
| A6NES4 | 18 | 1706 | 193,1 | 6,68 | 44 | HEAT repeat-containing protein 7B1 OS=Homo sapiens GN=HEATR7B1 PE=4 SV=3 - |
| Q96PH1 | 12 | 765 | 86,4 | 8,59 | 44 | NADPH oxidase 5 OS=Homo sapiens GN=NOX5 PE=1 SV=1 - [NOX5_HUMAN] |
| Q9NVP4 | 3 | 579 | 62,9 | 7,59 | 44 | Ankyrin repeat-containing protein C20orf12 OS=Homo sapiens GN=C20orf12 PE=2 |
| P01920 | 14 | 261 | 30,0 | 7,25 | 44 | HLA class II histocompatibility antigen, DQ beta 1 chain OS=Homo sapiens GN=HL |
| Q9P2D8 | 9 | 2635 | 295,1 | 6,32 | 43 | Protein unc-79 homolog OS=Homo sapiens GN=KIAA1409 PE=2 SV=3 - [UNC79_HU |
| Q7L622 | 15 | 706 | 80,5 | 7,65 | 43 | G2/M phase-specific E3 ubiquitin-protein ligase OS=Homo sapiens GN=G2E3 PE=1 |
| Q5T7W7 | 12 | 516 | 58,2 | 7,2 | 43 | Thiosulfate sulfurtransferase/rhodanese-like domain-containing protein 2 OS=H |
| Q8N137 | 4 | 903 | 101,2 | 5,54 | 43 | Centrobin OS=Homo sapiens GN=CNTROB PE=1 SV=1 - [CNTRB_HUMAN] |
| Q9Y5N6 | 10 | 252 | 28,1 | 8,66 | 43 | Origin recognition complex subunit 6 OS=Homo sapiens GN=ORC6 PE=1 SV=1 - [O |
| O15321 | 9 | 606 | 68,8 | 7,17 | 43 | Transmembrane 9 superfamily member 1 OS=Homo sapiens GN=TM9SF1 PE=2 SV |
| Q8WY54 | 45 | 764 | 84,9 | 5,03 | 43 | Protein phosphatase 1E OS=Homo sapiens GN=PPM1E PE=1 SV=2 - [PPM1E_HUMA |
| Q13733 | 9 | 1029 | 114,1 | 6,64 | 43 | Sodium/potassium-transporting ATPase subunit alpha-4 OS=Homo sapiens GN=A |
| P01715 | 18 | 106 | 11,3 | 5,24 | 43 | Ig lambda chain V-IV region Bau OS=Homo sapiens PE=1 SV=1 - [LV401_HUMAN] |
| P06889 | 18 | 106 | 11,3 | 4,42 | 43 | Ig lambda chain V-IV region MOL OS=Homo sapiens PE=1 SV=1 - [LV405_HUMAN] |
| Q7RTX1 | 7 | 841 | 93,0 | 7,97 | 43 | Taste receptor type 1 member 1 OS=Homo sapiens GN=TAS1R1 PE=2 SV=1 - [TS1R |
| Q17RN3 | 3 | 349 | 37,3 | 7,18 | 43 | Protein FAM98C OS=Homo sapiens GN=FAM98C PE=2 SV=1 - [FA98C_HUMAN] |
| Q8TD55 | 16 | 490 | 53,3 | 5,43 | 43 | Pleckstrin homology domain-containing family O member 2 OS=Homo sapiens GI |
| O75888 | 3 | 250 | 27,4 | 9,63 | 43 | Tumor necrosis factor ligand superfamily member 13 OS=Homo sapiens GN=TNFS |
| Q9Y6C2 | 5 | 1016 | 106,6 | 5,15 | 43 | EMILIN-1 OS=Homo sapiens GN=EMILIN1 PE=1 SV=2 - [EMIL1_HUMAN] |
| P48357 | 4 | 1165 | 132,4 | 6,52 | 43 | Leptin receptor OS=Homo sapiens GN=LEPR PE=1 SV=2 - [LEPR_HUMAN] |
| Q14146 | 21 | 1524 | 170,4 | 7,31 | 43 | Unhealthy ribosome biogenesis protein 2 homolog OS=Homo sapiens GN=URB2 H |
| Q9BV36 | 3 | 600 | 65,9 | 6,07 | 43 | Melanophilin OS=Homo sapiens GN=MLPH PE=1 SV=1 - [MELPH_HUMAN] |
| Q86YP4 | 9 | 633 | 68,0 | 9,94 | 43 | Transcriptional repressor p66-alpha OS=Homo sapiens GN=GATAD2A PE=1 SV=1 - |
| O43148 | 34 | 476 | 54,8 | 6,61 | 43 | mRNA cap guanine-N7 methyltransferase OS=Homo sapiens GN=RNMT PE=1 SV=1 |
| Q9HCB6 | 12 | 807 | 90,9 | 6,11 | 43 | Spondin-1 OS=Homo sapiens GN=SPON1 PE=1 SV=2 - [SPON1_HUMAN] |
| O43615 | 8 | 452 | 51,3 | 8,32 | 43 | Mitochondrial import inner membrane translocase subunit TIM44 OS=Homo sapi |
| Q92556 | 3 | 727 | 83,8 | 6,28 | 43 | Engulfment and cell motility protein 1 OS=Homo sapiens GN=ELMO1 PE=1 SV=2 - |
| Q96NB3 | 6 | 372 | 42,0 | 5,31 | 43 | Zinc finger protein 830 OS=Homo sapiens GN=ZNF830 PE=1 SV=2 - [ZN830_HUMAN |
| Q96JP2 | 3 | 1530 | 167,0 | 8,41 | 43 | Putative myosin-XVB OS=Homo sapiens GN=MYO15B PE=5 SV=2 - [MY15B_HUMAI |
| Q68J44 | 16 | 220 | 25,3 | 6,04 | 43 | Dual specificity phosphatase DUPD1 OS=Homo sapiens GN=DUPD1 PE=2 SV=1 - [D |
| Q9NXN4 | 55 | 497 | 56,2 | 5,74 | 43 | Ganglioside-induced differentiation-associated protein 2 OS=Homo sapiens GN= |
| P14780 | 10 | 707 | 78,4 | 6,06 | 42 | Matrix metalloproteinase-9 OS=Homo sapiens GN=MMP9 PE=1 SV=3 - [MMP9_HU |
| Q8IYS0 | 14 | 662 | 76,0 | 7,24 | 42 | GRAM domain-containing protein 1C OS=Homo sapiens GN=GRAMD1C PE=2 SV=2 |
| P01699 | 3 | 111 | 11,5 | 5,29 | 42 | Ig lambda chain V-I region VOR OS=Homo sapiens PE=1 SV=1 - [LV101_HUMAN] |
| Q9NWN3 | 5 | 711 | 78,7 | 8 | 42 | F-box only protein 34 OS=Homo sapiens GN=FBXO34 PE=1 SV=2 - [FBX34_HUMAN |
| Q8NDY6 | 10 | 225 | 23,7 | 9,22 | 42 | Class E basic helix-loop-helix protein 23 OS=Homo sapiens GN=BHLHE23 PE=2 SV= |
| Q9H4K7 | 14 | 406 | 43,9 | 9,45 | 42 | GTP-binding protein 5 OS=Homo sapiens GN=GTPBP5 PE=2 SV=1 - [GTPB5_HUMAN |
| Q9P283 | 8 | 1151 | 125,8 | 7,65 | 42 | Semaphorin-5B OS=Homo sapiens GN=SEMA5B PE=2 SV=4 - [SEM5B_HUMAN] |
| P43490 | 34 | 491 | 55,5 | 7,15 | 42 | Nicotinamide phosphoribosyltransferase OS=Homo sapiens GN=NAMPT PE=1 SV= |
| Q9BY31 | 13 | 904 | 105,2 | 8,57 | 42 | Zinc finger protein 717 OS=Homo sapiens GN=ZNF717 PE=1 SV=2 - [ZN717_HUMAN |
| Q15842 | 7 | 424 | 47,9 | 9,26 | 42 | ATP-sensitive inward rectifier potassium channel 8 OS=Homo sapiens GN=KCNJ8 |
| O43299 | 3 | 807 | 88,5 | 7,01 | 42 | Uncharacterized protein KIAA0415 OS=Homo sapiens GN=KIAA0415 PE=2 SV=2 - [ |
| A6NM62 | 6 | 1247 | 140,7 | 7,91 | 42 | Leucine-rich repeat-containing protein 53 OS=Homo sapiens GN=LRRC53 PE=4 SV= |
| Q14671 | 6 | 1186 | 126,4 | 6,84 | 42 | Pumilio homolog 1 OS=Homo sapiens GN=PUM1 PE=1 SV=3 - [PUM1_HUMAN] |
| P07814 | 14 | 1512 | 170,5 | 7,33 | 42 | Bifunctional aminoacyl-tRNA synthetase OS=Homo sapiens GN=EPRS PE=1 SV=5 - |

| | | | | | | |
|---|---|---|---|---|---|---|
| Q8WVL7 | 12 | 239 | 27,3 | 5,15 | 42 | Ankyrin repeat domain-containing protein 49 OS=Homo sapiens GN=ANKRD49 PE |
| Q6ZNI0 | 6 | 430 | 49,3 | 8,68 | 42 | Beta-1,3-galactosyl-O-glycosyl-glycoprotein beta-1,6-N-acetylglucosaminyltransf |
| Q11203 | 19 | 375 | 42,1 | 8,98 | 42 | CMP-N-acetylneuraminate-beta-1,4-galactoside alpha-2,3-sialyltransferase OS=H |
| O00338 | 10 | 296 | 34,9 | 7,52 | 42 | Sulfotransferase 1C2 OS=Homo sapiens GN=SULT1C2 PE=1 SV=1 - [ST1C2_HUMAN |
| A6NMZ2 | 4 | 147 | 16,5 | 8,27 | 42 | Sentan OS=Homo sapiens GN=SNTN PE=2 SV=1 - [SNTAN_HUMAN] |
| Q9BV20 | 16 | 369 | 39,1 | 6,3 | 42 | Methylthioribose-1-phosphate isomerase OS=Homo sapiens GN=MRI1 PE=1 SV=1 |
| A6NEY8 | 3 | 169 | 18,6 | 6,25 | 42 | PrdX deacylase domain-containing protein 1 OS=Homo sapiens GN=PRDXDD1P PE |
| Q14CX7 | 24 | 972 | 112,2 | 6,64 | 42 | N-alpha-acetyltransferase 25, NatB auxiliary subunit OS=Homo sapiens GN=NAA2 |
| P29122 | 7 | 969 | 106,4 | 7,68 | 42 | Proprotein convertase subtilisin/kexin type 6 OS=Homo sapiens GN=PCSK6 PE=1 |
| O43674 | 8 | 189 | 21,7 | 9,63 | 42 | NADH dehydrogenase [ubiquinone] 1 beta subcomplex subunit 5, mitochondrial |
| Q9H5I5 | 10 | 2752 | 317,9 | 6,15 | 42 | Protein PIEZO2 OS=Homo sapiens GN=FAM38B PE=2 SV=2 - [PIEZ2_HUMAN] |
| O14544 | 12 | 535 | 59,5 | 7,25 | 42 | Suppressor of cytokine signaling 6 OS=Homo sapiens GN=SOCS6 PE=1 SV=2 - [SOC |
| Q9H4Z2 | 8 | 1342 | 144,8 | 6,42 | 42 | Zinc finger protein 335 OS=Homo sapiens GN=ZNF335 PE=1 SV=1 - [ZN335_HUMAN |
| P01743 | 2 | 117 | 12,9 | 8,92 | 42 | Ig heavy chain V-I region HG3 OS=Homo sapiens PE=4 SV=1 - [HV102_HUMAN] |
| Q6ZRR9 | 8 | 648 | 72,7 | 8,85 | 42 | Doublecortin domain-containing protein 5 OS=Homo sapiens GN=DCDC5 PE=2 SV |
| Q9Y2C2 | 12 | 406 | 47,6 | 8,69 | 42 | Uronyl 2-sulfotransferase OS=Homo sapiens GN=UST PE=2 SV=1 - [UST_HUMAN] |
| P42681 | 6 | 527 | 61,2 | 7,97 | 42 | Tyrosine-protein kinase TXK OS=Homo sapiens GN=TXK PE=1 SV=3 - [TXK_HUMAN |
| P83105 | 3 | 476 | 50,9 | 8,02 | 42 | Probable serine protease HTRA4 OS=Homo sapiens GN=HTRA4 PE=2 SV=1 - [HTRA |
| P01604 | 19 | 108 | 12,1 | 8,81 | 42 | Ig kappa chain V-I region Kue OS=Homo sapiens PE=1 SV=1 - [KV112_HUMAN] |
| Q86YQ8 | 21 | 564 | 63,1 | 5,96 | 41 | Copine-8 OS=Homo sapiens GN=CPNE8 PE=1 SV=2 - [CPNE8_HUMAN] |
| Q9UPP1 | 9 | 1060 | 117,8 | 8,72 | 41 | Histone lysine demethylase PHF8 OS=Homo sapiens GN=PHF8 PE=1 SV=3 - [PHF8_ |
| Q6PII3 | 15 | 467 | 53,9 | 6,33 | 41 | Uncharacterized protein C3orf19 OS=Homo sapiens GN=C3orf19 PE=2 SV=3 - [CC0 |
| P52740 | 5 | 706 | 80,6 | 8,4 | 41 | Zinc finger protein 132 OS=Homo sapiens GN=ZNF132 PE=2 SV=2 - [ZN132_HUMAN |
| Q15293 | 3 | 331 | 38,9 | 5 | 41 | Reticulocalbin-1 OS=Homo sapiens GN=RCN1 PE=1 SV=1 - [RCN1_HUMAN] |
| P01713 | 16 | 110 | 11,4 | 5,96 | 41 | Ig lambda chain V-II region NIG-58 OS=Homo sapiens PE=1 SV=1 - [LV210_HUMAN |
| P46952 | 36 | 286 | 32,5 | 5,88 | 41 | 3-hydroxyanthranilate 3,4-dioxygenase OS=Homo sapiens GN=HAAO PE=1 SV=2 - |
| Q2M3W8 | 16 | 571 | 65,8 | 8,9 | 41 | Zinc finger protein 181 OS=Homo sapiens GN=ZNF181 PE=2 SV=1 - [ZN181_HUMAN |
| Q9Y575 | 11 | 518 | 57,7 | 6,27 | 41 | Ankyrin repeat and SOCS box protein 3 OS=Homo sapiens GN=ASB3 PE=1 SV=1 - [A |
| O60884 | 7 | 412 | 45,7 | 6,48 | 41 | DnaJ homolog subfamily A member 2 OS=Homo sapiens GN=DNAJA2 PE=1 SV=1 - |
| Q92896 | 16 | 1179 | 134,5 | 6,9 | 41 | Golgi apparatus protein 1 OS=Homo sapiens GN=GLG1 PE=1 SV=2 - [GSLG1_HUMA |
| P32248 | 5 | 378 | 42,8 | 8,48 | 41 | C-C chemokine receptor type 7 OS=Homo sapiens GN=CCR7 PE=1 SV=2 - [CCR7_HU |
| Q8TBZ3 | 10 | 569 | 62,9 | 8 | 41 | WD repeat-containing protein 20 OS=Homo sapiens GN=WDR20 PE=1 SV=2 - [WDR |
| Q14134 | 9 | 588 | 65,8 | 7,15 | 41 | Tripartite motif-containing protein 29 OS=Homo sapiens GN=TRIM29 PE=1 SV=2 - |
| Q8IXM7 | 10 | 274 | 31,0 | 9,54 | 41 | Outer dense fiber protein 3-like protein 1 OS=Homo sapiens GN=ODF3L1 PE=2 SV |
| P11586 | 86 | 935 | 101,5 | 7,3 | 41 | C-1-tetrahydrofolate synthase, cytoplasmic OS=Homo sapiens GN=MTHFD1 PE=1 |
| Q99594 | 4 | 435 | 48,6 | 8,4 | 41 | Transcriptional enhancer factor TEF-5 (TEA domain family member 3) (TEAD-3) (D |
| Q6ZU11 | 4 | 926 | 104,4 | 8,88 | 41 | Uncharacterized protein FLJ44066 OS=Homo sapiens PE=1 SV=1 - [YD002_HUMAN] |
| P07864 | 40 | 332 | 36,3 | 7,46 | 41 | L-lactate dehydrogenase C chain OS=Homo sapiens GN=LDHC PE=2 SV=4 - [LDHC_ |
| Q8TC20 | 11 | 777 | 90,2 | 5,29 | 41 | Cancer-associated gene 1 protein OS=Homo sapiens GN=CAGE1 PE=2 SV=2 - [CAG |
| Q96A46 | 12 | 364 | 39,2 | 8,59 | 41 | Mitoferrin-2 OS=Homo sapiens GN=SLC25A28 PE=2 SV=1 - [MFRN2_HUMAN] |
| O76070 | 24 | 127 | 13,3 | 4,86 | 41 | Gamma-synuclein OS=Homo sapiens GN=SNCG PE=1 SV=2 - [SYUG_HUMAN] |
| P01603 | 15 | 108 | 11,9 | 8,85 | 41 | Ig kappa chain V-I region Ka OS=Homo sapiens PE=1 SV=1 - [KV111_HUMAN] |
| A6NJ16 | 7 | 123 | 13,6 | 9,6 | 41 | Putative V-set and immunoglobulin domain-containing protein 6 OS=Homo sapie |
| Q86WR0 | 118 | 208 | 24,5 | 6,8 | 41 | Coiled-coil domain-containing protein 25 OS=Homo sapiens GN=CCDC25 PE=1 SV |
| Q9BQ52 | 45 | 826 | 92,2 | 7,9 | 41 | Zinc phosphodiesterase ELAC protein 2 OS=Homo sapiens GN=ELAC2 PE=1 SV=2 - |
| Q16820 | 14 | 701 | 79,5 | 5,74 | 41 | Meprin A subunit beta OS=Homo sapiens GN=MEP1B PE=1 SV=3 - [MEP1B_HUMAN |
| Q6NUM6 | 23 | 668 | 76,9 | 6,27 | 41 | tRNA wybutosine-synthesizing protein 1 homolog B OS=Homo sapiens GN=TYW1 |
| Q96PE7 | 18 | 176 | 18,7 | 9,09 | 41 | Methylmalonyl-CoA epimerase, mitochondrial OS=Homo sapiens GN=MCEE PE=1 |
| O15403 | 16 | 523 | 57,4 | 7,81 | 41 | Monocarboxylate transporter 7 OS=Homo sapiens GN=SLC16A6 PE=1 SV=2 - [MOT |
| P0C2Y1 | 5 | 421 | 48,1 | 4,79 | 40 | Putative neuroblastoma breakpoint family member 7 OS=Homo sapiens GN=NBP |
| Q96T68 | 13 | 719 | 81,8 | 7,5 | 40 | Histone-lysine N-methyltransferase SETDB2 OS=Homo sapiens GN=SETDB2 PE=1 |
| P26196 | 6 | 483 | 54,4 | 8,66 | 40 | Probable ATP-dependent RNA helicase DDX6 (EC 3.6.1.-) (DEAD box protein 6) (A |
| Q13907 | 10 | 227 | 26,3 | 6,34 | 40 | Isopentenyl-diphosphate Delta-isomerase 1 OS=Homo sapiens GN=IDI1 PE=1 SV= |
| Q9NUS5 | 10 | 200 | 22,5 | 6,87 | 40 | Uncharacterized protein C20orf29 OS=Homo sapiens GN=C20orf29 PE=2 SV=1 - [C |
| Q5NE16 | 3 | 218 | 25,0 | 7,15 | 40 | Putative cathepsin L-like protein 3 OS=Homo sapiens GN=CTSL3 PE=5 SV=1 - [CAT |
| Q6UXR4 | 10 | 307 | 34,8 | 6,4 | 40 | Putative serpin A13 OS=Homo sapiens GN=SERPINA13 PE=5 SV=1 - [SPA13_HUMA |
| Q9NSE7 | 6 | 274 | 30,8 | 9,51 | 40 | Putative ATP-binding cassette sub-family C member 13 OS=Homo sapiens GN=AB |
| A4D263 | 4 | 438 | 49,6 | 8,48 | 40 | Uncharacterized protein C7orf72 OS=Homo sapiens GN=C7orf72 PE=4 SV=2 - [CG0 |
| Q9Y6K1 | 43 | 912 | 101,8 | 6,57 | 40 | DNA (cytosine-5)-methyltransferase 3A OS=Homo sapiens GN=DNMT3A PE=1 SV= |
| Q9BQI5 | 13 | 828 | 89,1 | 8,22 | 40 | SH3-containing GRB2-like protein 3-interacting protein 1 OS=Homo sapiens GN=S |
| P35475 | 6 | 653 | 72,6 | 9,14 | 40 | Alpha-L-iduronidase OS=Homo sapiens GN=IDUA PE=1 SV=2 - [IDUA_HUMAN] |
| Q16621 | 18 | 373 | 41,4 | 4,94 | 40 | Transcription factor NF-E2 45 kDa subunit OS=Homo sapiens GN=NFE2 PE=1 SV=1 |
| O75953 | 34 | 348 | 39,1 | 9,04 | 40 | DnaJ homolog subfamily B member 5 OS=Homo sapiens GN=DNAJB5 PE=2 SV=1 - |
| Q9HCH5 | 2 | 934 | 104,9 | 8 | 40 | Synaptotagmin-like protein 2 OS=Homo sapiens GN=SYTL2 PE=1 SV=3 - [SYTL2_HU |
| Q6ZT98 | 12 | 887 | 102,9 | 9,29 | 40 | Tubulin polyglutamylase TTLL7 OS=Homo sapiens GN=TTLL7 PE=2 SV=2 - [TTLL7_H |

| | | | | | | |
|---|---|---|---|---|---|---|
| O00299 | 1 | 241 | 26,9 | 5,17 | 40 | Chloride intracellular channel protein 1 OS=Homo sapiens GN=CLIC1 PE=1 SV=4 - |
| Q14576 | 35 | 367 | 39,5 | 9,28 | 40 | ELAV-like protein 3 OS=Homo sapiens GN=ELAVL3 PE=1 SV=3 - [ELAV3_HUMAN] |
| Q3SXY7 | 13 | 634 | 69,9 | 5,69 | 40 | Leucine-rich repeat, immunoglobulin-like domain and transmembrane domain-c |
| Q9H6E5 | 9 | 874 | 93,8 | 6,16 | 40 | Speckle targeted PIP5K1A-regulated poly(A) polymerase OS=Homo sapiens GN=T |
| Q8N475 | 5 | 847 | 95,7 | 5,95 | 40 | Follistatin-related protein 5 OS=Homo sapiens GN=FSTL5 PE=2 SV=2 - [FSTL5_HUM |
| Q5T699 | 3 | 396 | 45,7 | 5,62 | 40 | Putative uncharacterized protein C6orf183 OS=Homo sapiens GN=C6orf183 PE=5 S |
| P53004 | 6 | 296 | 33,4 | 6,44 | 40 | Biliverdin reductase A OS=Homo sapiens GN=BLVRA PE=1 SV=2 - [BIEA_HUMAN] |
| Q9BYX2 | 27 | 928 | 105,3 | 6,58 | 40 | TBC1 domain family member 2A OS=Homo sapiens GN=TBC1D2 PE=1 SV=3 - [TBD2 |
| O75185 | 29 | 946 | 103,1 | 5,66 | 40 | Calcium-transporting ATPase type 2C member 2 OS=Homo sapiens GN=ATP2C2 PE |
| O00339 | 2 | 956 | 106,8 | 6,19 | 40 | Matrilin-2 OS=Homo sapiens GN=MATN2 PE=1 SV=3 - [MATN2_HUMAN] |
| Q8N2K0 | 5 | 398 | 45,1 | 8,65 | 40 | Monoacylglycerol lipase ABHD12 OS=Homo sapiens GN=ABHD12 PE=2 SV=2 - [ABI |
| Q5T160 | 5 | 578 | 65,5 | 8,21 | 39 | Probable arginyl-tRNA synthetase, mitochondrial precursor (EC 6.1.1.19) (Arginin |
| P61576 | 8 | 105 | 11,7 | 9,92 | 39 | HERV-K_5q13.3 provirus Rec protein (HERV-K104 Rec protein) - Homo sapiens (Hu |
| Q8N3F9 | 7 | 429 | 47,0 | 7,42 | 39 | Integral membrane protein GPR137C OS=Homo sapiens GN=GPR137C PE=2 SV=2 - |
| O60888 | 5 | 179 | 19,1 | 5,5 | 39 | Protein CutA OS=Homo sapiens GN=CUTA PE=1 SV=2 - [CUTA_HUMAN] |
| Q96J88 | 2 | 318 | 36,8 | 9,89 | 39 | Epithelial-stromal interaction protein 1 OS=Homo sapiens GN=EPSTI1 PE=2 SV=2 - |
| Q8N393 | 5 | 782 | 89,8 | 9,13 | 39 | Zinc finger protein 786 OS=Homo sapiens GN=ZNF786 PE=2 SV=2 - [ZN786_HUMAN |
| P17174 | 3 | 413 | 46,2 | 7,01 | 39 | Aspartate aminotransferase, cytoplasmic OS=Homo sapiens GN=GOT1 PE=1 SV=3 |
| Q96BY7 | 33 | 2078 | 232,6 | 5,76 | 39 | Autophagy-related protein 2 homolog B OS=Homo sapiens GN=ATG2B PE=1 SV=5 |
| O43593 | 8 | 1189 | 127,4 | 7,08 | 39 | Protein hairless OS=Homo sapiens GN=HR PE=1 SV=5 - [HAIR_HUMAN] |
| P62257 | 9 | 183 | 20,6 | 4,67 | 39 | Ubiquitin-conjugating enzyme E2 H OS=Mus musculus GN=Ube2h PE=2 SV=1 - [UB |
| Q8N554 | 11 | 614 | 67,2 | 8,51 | 39 | Zinc finger protein 276 OS=Homo sapiens GN=ZNF276 PE=1 SV=4 - [ZN276_HUMAN |
| P42261 | 8 | 906 | 101,4 | 7,71 | 39 | Glutamate receptor 1 OS=Homo sapiens GN=GRIA1 PE=1 SV=2 - [GRIA1_HUMAN] |
| P98198 | 8 | 1209 | 137,4 | 7,01 | 39 | Probable phospholipid-transporting ATPase ID OS=Homo sapiens GN=ATP8B2 PE= |
| Q99941 | 73 | 703 | 76,7 | 6,27 | 39 | Cyclic AMP-dependent transcription factor ATF-6 beta OS=Homo sapiens GN=ATF |
| Q9C0B9 | 4 | 1178 | 125,9 | 7,01 | 39 | Zinc finger CCHC domain-containing protein 2 OS=Homo sapiens GN=ZCCHC2 PE= |
| Q9NV06 | 10 | 445 | 51,4 | 9,19 | 39 | DDB1- and CUL4-associated factor 13 OS=Homo sapiens GN=DCAF13 PE=1 SV=2 - [ |
| A6NKL6 | 3 | 621 | 63,9 | 10,08 | 39 | Transmembrane protein 200C OS=Homo sapiens GN=TMEM200C PE=2 SV=2 - [T20 |
| P40121 | 12 | 348 | 38,5 | 6,19 | 39 | Macrophage-capping protein OS=Homo sapiens GN=CAPG PE=1 SV=2 - [CAPG_HU |
| Q9UNN5 | 11 | 650 | 73,9 | 4,88 | 39 | FAS-associated factor 1 OS=Homo sapiens GN=FAF1 PE=1 SV=2 - [FAF1_HUMAN] |
| Q9BSC4 | 3 | 688 | 80,3 | 8,46 | 39 | Nucleolar protein 10 OS=Homo sapiens GN=NOL10 PE=1 SV=1 - [NOL10_HUMAN] |
| Q9NSI2 | 3 | 230 | 25,4 | 11,08 | 39 | Uncharacterized protein C21orf70 OS=Homo sapiens GN=C21orf70 PE=1 SV=2 - [CU |
| Q6W3E5 | 43 | 623 | 71,9 | 9,03 | 39 | Glycerophosphodiester phosphodiesterase domain-containing protein 4 OS=Hon |
| Q08211 | 2 | 1270 | 140,9 | 6,84 | 39 | ATP-dependent RNA helicase A OS=Homo sapiens GN=DHX9 PE=1 SV=4 - [DHX9_H |
| Q9Y6L7 | 9 | 1015 | 113,5 | 5,94 | 39 | Tolloid-like protein 2 OS=Homo sapiens GN=TLL2 PE=1 SV=1 - [TLL2_HUMAN] |
| Q9UJU3 | 3 | 913 | 105,8 | 8,27 | 39 | Zinc finger protein 112 homolog OS=Homo sapiens GN=ZFP112 PE=2 SV=2 - [ZF112 |
| Q9NZI7 | 34 | 540 | 60,5 | 6,35 | 39 | Upstream-binding protein 1 OS=Homo sapiens GN=UBP1 PE=2 SV=1 - [UBIP1_HUM |
| Q8IZU1 | 12 | 332 | 37,3 | 4,83 | 39 | Protein FAM9A OS=Homo sapiens GN=FAM9A PE=2 SV=1 - [FAM9A_HUMAN] |
| Q8N9Z2 | 8 | 235 | 26,2 | 11,71 | 39 | Uncharacterized protein FLJ36031 OS=Homo sapiens PE=2 SV=2 - [YG034_HUMAN] |
| Q96L42 | 7 | 1107 | 123,7 | 6,92 | 39 | Potassium voltage-gated channel subfamily H member 8 OS=Homo sapiens GN=K |
| P04438 | 7 | 147 | 16,3 | 7,09 | 39 | Ig heavy chain V-II region SESS OS=Homo sapiens PE=2 SV=1 - [HV208_HUMAN] |
| Q9BRG2 | 7 | 576 | 63,1 | 7,42 | 39 | SH2 domain-containing protein 3A OS=Homo sapiens GN=SH2D3A PE=1 SV=1 - [SH |
| Q9Y4B4 | 6 | 1467 | 162,7 | 6,09 | 39 | Helicase ARIP4 OS=Homo sapiens GN=RAD54L2 PE=1 SV=4 - [ARIP4_HUMAN] |
| Q15173 | 4 | 497 | 57,4 | 6,71 | 38 | Serine/threonine-protein phosphatase 2A 56 kDa regulatory subunit beta isoform |
| Q8WXD2 | 3 | 468 | 53,0 | 5,03 | 38 | Secretogranin-3 precursor (Secretogranin III) (SgIII) - Homo sapiens (Human) - [SC |
| Q92974 | 15 | 986 | 111,5 | 7,27 | 38 | Rho guanine nucleotide exchange factor 2 OS=Homo sapiens GN=ARHGEF2 PE=1 S |
| Q9UK59 | 3 | 544 | 61,5 | 5,47 | 38 | Lariat debranching enzyme OS=Homo sapiens GN=DBR1 PE=1 SV=2 - [DBR1_HUMA |
| P0C1H6 | 6 | 257 | 28,2 | 9,82 | 38 | Histone H2B type F-M OS=Homo sapiens GN=H2BFM PE=2 SV=1 - [H2BFM_HUMAN |
| Q92539 | 5 | 896 | 99,3 | 5,33 | 38 | Lipin-2 - Homo sapiens (Human) - [LPIN2_HUMAN] |
| Q9Y426 | 14 | 696 | 75,5 | 6,92 | 38 | C2 domain-containing protein 2 OS=Homo sapiens GN=C2CD2 PE=1 SV=2 - [CU025 |
| Q15858 | 9 | 1988 | 226,2 | 6,99 | 38 | Sodium channel protein type 9 subunit alpha OS=Homo sapiens GN=SCN9A PE=1 |
| Q9H0H3 | 3 | 589 | 65,9 | 6,57 | 38 | Ectoderm-neural cortex protein 2 OS=Homo sapiens GN=KLHL25 PE=2 SV=1 - [ENC |
| P09210 | 2 | 222 | 25,6 | 8,59 | 38 | Glutathione S-transferase A2 OS=Homo sapiens GN=GSTA2 PE=1 SV=4 - [GSTA2_H |
| P18077 | 6 | 110 | 12,5 | 11,06 | 38 | 60S ribosomal protein L35a - Homo sapiens (Human) - [RL35A_HUMAN] |
| P61009 | 43 | 180 | 20,3 | 8,62 | 38 | Signal peptidase complex subunit 3 OS=Homo sapiens GN=SPCS3 PE=1 SV=1 - [SP |
| P28336 | 25 | 390 | 43,4 | 8,66 | 38 | Neuromedin-B receptor OS=Homo sapiens GN=NMBR PE=2 SV=2 - [NMBR_HUMA |
| Q86XW9 | 1 | 330 | 36,8 | 4,89 | 38 | Thioredoxin domain-containing protein 6 OS=Homo sapiens GN=TXNDC6 PE=1 SV |
| P98082 | 54 | 770 | 82,4 | 5,53 | 38 | Disabled homolog 2 OS=Homo sapiens GN=DAB2 PE=1 SV=3 - [DAB2_HUMAN] |
| P56545 | 2 | 445 | 48,9 | 6,95 | 38 | C-terminal-binding protein 2 OS=Homo sapiens GN=CTBP2 PE=1 SV=1 - [CTBP2_H |
| O95461 | 29 | 756 | 88,0 | 7,84 | 38 | Glycosyltransferase-like protein LARGE1 OS=Homo sapiens GN=LARGE PE=1 SV=1 |
| Q9Y2F9 | 10 | 522 | 58,4 | 7,46 | 38 | BTB/POZ domain-containing protein 3 OS=Homo sapiens GN=BTBD3 PE=2 SV=1 - [ |
| Q15404 | 52 | 277 | 31,5 | 8,65 | 38 | Ras suppressor protein 1 OS=Homo sapiens GN=RSU1 PE=1 SV=3 - [RSU1_HUMAN] |
| Q9HCF6 | 101 | 1732 | 197,4 | 7,15 | 38 | Transient receptor potential cation channel subfamily M member 3 OS=Homo sap |
| Q5HYI8 | 35 | 236 | 26,4 | 7,11 | 38 | Rab-like protein 3 OS=Homo sapiens GN=RABL3 PE=1 SV=1 - [RABL3_HUMAN] |
| Q14435 | 34 | 633 | 72,6 | 7,99 | 38 | Polypeptide N-acetylgalactosaminyltransferase 3 OS=Homo sapiens GN=GALNT3 |

| | | | | | | |
|---|---|---|---|---|---|---|
| Q7L5D6 | 116 | 327 | 36,5 | 5,41 | 38 | Golgi to ER traffic protein 4 homolog OS=Homo sapiens GN=GET4 PE=1 SV=1 - [GE |
| P17544 | 21 | 494 | 52,9 | 8,65 | 38 | Cyclic AMP-dependent transcription factor ATF-7 OS=Homo sapiens GN=ATF7 PE= |
| Q9UHR6 | 4 | 403 | 42,9 | 5,99 | 38 | Zinc finger HIT domain-containing protein 2 OS=Homo sapiens GN=ZNHIT2 PE=1 S |
| P48058 | 4 | 902 | 100,8 | 8,1 | 38 | Glutamate receptor 4 OS=Homo sapiens GN=GRIA4 PE=2 SV=2 - [GRIA4_HUMAN] |
| Q5VSD8 | 43 | 79 | 8,2 | 9,74 | 38 | Putative uncharacterized protein LOC401522 OS=Homo sapiens PE=4 SV=2 - [YI02 |
| Q8ND61 | 8 | 904 | 101,2 | 9,13 | 38 | Uncharacterized protein C3orf20 OS=Homo sapiens GN=C3orf20 PE=1 SV=2 - [CC0 |
| Q14005 | 19 | 1332 | 141,7 | 8,06 | 38 | Pro-interleukin-16 OS=Homo sapiens GN=IL16 PE=1 SV=4 - [IL16_HUMAN] |
| P01708 | 3 | 109 | 11,5 | 7,87 | 38 | Ig lambda chain V-II region BUR OS=Homo sapiens PE=1 SV=1 - [LV205_HUMAN] |
| Q96RY5 | 2 | 1269 | 134,6 | 7,87 | 38 | Protein cramped-like OS=Homo sapiens GN=CRAMP1L PE=1 SV=3 - [CRML_HUMA |
| Q96I23 | 3 | 114 | 12,6 | 9,33 | 37 | Protein preY, mitochondrial OS=Homo sapiens GN=PREY PE=1 SV=1 - [PREY_HUM |
| P51160 | 23 | 858 | 99,1 | 5,72 | 37 | Cone cGMP-specific 3',5'-cyclic phosphodiesterase subunit alpha' OS=Homo sapie |
| P49917 | 9 | 911 | 103,9 | 7,96 | 37 | DNA ligase 4 OS=Homo sapiens GN=LIG4 PE=1 SV=2 - [DNLI4_HUMAN] |
| O76014 | 2 | 449 | 49,7 | 4,96 | 37 | Keratin, type I cuticular Ha7 OS=Homo sapiens GN=KRT37 PE=2 SV=3 - [KRT37_HU |
| Q9Y689 | 13 | 179 | 20,7 | 6,79 | 37 | ADP-ribosylation factor-like protein 5A OS=Homo sapiens GN=ARL5A PE=1 SV=1 - |
| Q9HCD5 | 10 | 579 | 65,5 | 9,6 | 37 | Nuclear receptor coactivator 5 OS=Homo sapiens GN=NCOA5 PE=1 SV=2 - [NCOA5 |
| O95785 | 10 | 1651 | 178,6 | 6,86 | 37 | Protein Wiz OS=Homo sapiens GN=WIZ PE=1 SV=2 - [WIZ_HUMAN] |
| Q9H0M4 | 7 | 648 | 72,0 | 7,53 | 37 | Zinc finger CW-type PWWP domain protein 1 OS=Homo sapiens GN=ZCWPW1 PE |
| Q15014 | 13 | 288 | 32,3 | 9,72 | 37 | Mortality factor 4-like protein 2 OS=Homo sapiens GN=MORF4L2 PE=1 SV=1 - [MO |
| Q9H4B6 | 8 | 383 | 44,6 | 9,09 | 37 | Protein salvador homolog 1 OS=Homo sapiens GN=SAV1 PE=1 SV=2 - [SAV1_HUM |
| Q6MZM9 | 14 | 219 | 22,7 | 4,87 | 37 | Uncharacterized protein C4orf40 OS=Homo sapiens GN=C4orf40 PE=1 SV=1 - [CD0 |
| Q8N201 | 14 | 2190 | 244,1 | 6,13 | 37 | Integrator complex subunit 1 OS=Homo sapiens GN=INTS1 PE=1 SV=2 - [INT1_HUM |
| Q99814 | 23 | 870 | 96,4 | 6,28 | 37 | Endothelial PAS domain-containing protein 1 OS=Homo sapiens GN=EPAS1 PE=1 S |
| Q9UBL0 | 3 | 812 | 89,1 | 6,95 | 37 | cAMP-regulated phosphoprotein 21 OS=Homo sapiens GN=ARPP21 PE=1 SV=2 - [A |
| P40818 | 1 | 1118 | 127,4 | 8,51 | 37 | Ubiquitin carboxyl-terminal hydrolase 8 OS=Homo sapiens GN=USP8 PE=1 SV=1 - |
| P10828 | 3 | 461 | 52,8 | 7,11 | 37 | Thyroid hormone receptor beta OS=Homo sapiens GN=THRB PE=1 SV=2 - [THB_HU |
| Q8N1Q8 | 27 | 247 | 27,7 | 7,72 | 37 | Thioesterase superfamily member 5 OS=Homo sapiens GN=THEM5 PE=2 SV=2 - [T |
| Q9P0W5 | 10 | 487 | 53,4 | 5,12 | 37 | Schwannomin-interacting protein 1 OS=Homo sapiens GN=SCHIP1 PE=1 SV=1 - [SC |
| Q96I99 | 6 | 432 | 46,5 | 6,39 | 37 | Succinyl-CoA ligase [GDP-forming] subunit beta, mitochondrial OS=Homo sapien |
| Q9Y662 | 12 | 390 | 43,3 | 9,63 | 37 | Heparan sulfate glucosamine 3-O-sulfotransferase 3B1 OS=Homo sapiens GN=HS |
| Q9UJZ1 | 2 | 356 | 38,5 | 7,39 | 37 | Stomatin-like protein 2 OS=Homo sapiens GN=STOML2 PE=1 SV=1 - [STML2_HUM |
| Q8NCU1 | 2 | 140 | 15,8 | 6,54 | 37 | Uncharacterized protein C14orf48 OS=Homo sapiens GN=C14orf48 PE=2 SV=1 - [CI |
| Q16665 | 23 | 826 | 92,6 | 5,33 | 37 | Hypoxia-inducible factor 1-alpha OS=Homo sapiens GN=HIF1A PE=1 SV=1 - [HIF1A |
| Q00872 | 4 | 1141 | 128,2 | 6,04 | 37 | Myosin-binding protein C, slow-type OS=Homo sapiens GN=MYBPC1 PE=1 SV=2 - |
| Q6ZN19 | 8 | 808 | 93,1 | 9,33 | 37 | Zinc finger protein 841 OS=Homo sapiens GN=ZNF841 PE=2 SV=1 - [ZN841_HUMAN |
| Q5HYM0 | 2 | 825 | 93,0 | 7,8 | 37 | Probable ribonuclease ZC3H12B OS=Homo sapiens GN=ZC3H12B PE=2 SV=2 - [ZC1 |
| Q70Z35 | 6 | 1606 | 182,5 | 7,44 | 37 | Phosphatidylinositol 3,4,5-trisphosphate-dependent Rac exchanger 2 protein OS |
| P33260 | 23 | 490 | 55,7 | 7,2 | 37 | Cytochrome P450 2C18 (EC 1.14.14.1) (CYPIIC18) (P450-6B/29C) - Homo sapiens (H |
| Q5TAH2 | 15 | 1124 | 129,0 | 6,92 | 37 | Sodium/hydrogen exchanger 11 OS=Homo sapiens GN=SLC9A11 PE=2 SV=1 - [S9A |
| O60911 | 3 | 334 | 37,3 | 8,76 | 37 | Cathepsin L2 OS=Homo sapiens GN=CTSL2 PE=1 SV=2 - [CATL2_HUMAN] |
| P16234 | 3 | 1089 | 122,6 | 5,17 | 37 | Alpha-type platelet-derived growth factor receptor OS=Homo sapiens GN=PDGFR |
| Q8TED0 | 4 | 518 | 58,4 | 9,11 | 37 | U3 small nucleolar RNA-associated protein 15 homolog OS=Homo sapiens GN=UT |
| Q8IVI9 | 2 | 506 | 57,6 | 8,97 | 37 | Nostrin OS=Homo sapiens GN=NOSTRIN PE=1 SV=2 - [NOSTN_HUMAN] |
| Q9H6S0 | 4 | 1430 | 160,1 | 8,4 | 37 | Probable ATP-dependent RNA helicase YTHDC2 OS=Homo sapiens GN=YTHDC2 PE |
| Q86Y26 | 22 | 1132 | 120,2 | 5,45 | 37 | Protein NUT OS=Homo sapiens GN=NUT PE=1 SV=2 - [NUT_HUMAN] |
| Q9NXB0 | 4 | 559 | 64,5 | 6,46 | 37 | Meckel syndrome type 1 protein OS=Homo sapiens GN=MKS1 PE=1 SV=2 - [MKS1_ |
| O94933 | 15 | 977 | 108,9 | 7,37 | 37 | SLIT and NTRK-like protein 3 OS=Homo sapiens GN=SLITRK3 PE=2 SV=2 - [SLIK3_HU |
| P38435 | 3 | 758 | 87,5 | 8,02 | 37 | Vitamin K-dependent gamma-carboxylase OS=Homo sapiens GN=GGCX PE=1 SV= |
| O60330 | 12 | 932 | 100,9 | 5,05 | 36 | Protocadherin gamma-A12 OS=Homo sapiens GN=PCDHGA12 PE=2 SV=1 - [PCDGC |
| P51948 | 11 | 309 | 35,8 | 6,09 | 36 | CDK-activating kinase assembly factor MAT1 OS=Homo sapiens GN=MNAT1 PE=1 |
| Q9Y6L6 | 7 | 691 | 76,4 | 8,57 | 36 | Solute carrier organic anion transporter family member 1B1 OS=Homo sapiens GN |
| Q8TEY5 | 15 | 395 | 43,4 | 5,43 | 36 | Cyclic AMP-responsive element-binding protein 3-like protein 4 OS=Homo sapie |
| P42566 | 9 | 896 | 98,6 | 4,64 | 36 | Epidermal growth factor receptor substrate 15 OS=Homo sapiens GN=EPS15 PE=1 |
| Q9P2M4 | 4 | 693 | 78,1 | 7,01 | 36 | TBC1 domain family member 14 OS=Homo sapiens GN=TBC1D14 PE=1 SV=3 - [TBC |
| O14672 | 5 | 748 | 84,1 | 7,77 | 36 | Disintegrin and metalloproteinase domain-containing protein 10 OS=Homo sapie |
| Q9NWX6 | 6 | 298 | 34,8 | 8 | 36 | Probable tRNA(His) guanylyltransferase OS=Homo sapiens GN=THG1L PE=1 SV=2 |
| O43542 | 107 | 346 | 37,8 | 8,48 | 36 | DNA-repair protein XRCC3 (X-ray repair cross-complementing protein 3) - Homo s |
| Q96PB1 | 8 | 797 | 91,6 | 8,82 | 36 | CAS1 domain-containing protein 1 OS=Homo sapiens GN=CASD1 PE=2 SV=1 - [CAS |
| Q86XG9 | 4 | 351 | 40,5 | 5,05 | 36 | Neuroblastoma breakpoint family member 5 OS=Homo sapiens GN=NBPF5 PE=2 S |
| P39023 | 7 | 403 | 46,1 | 10,18 | 36 | 60S ribosomal protein L3 OS=Homo sapiens GN=RPL3 PE=1 SV=2 - [RL3_HUMAN] |
| Q92674 | 33 | 756 | 86,7 | 8,76 | 36 | Centromere protein I OS=Homo sapiens GN=CENPI PE=1 SV=2 - [CENPI_HUMAN] |
| P01825 | 5 | 117 | 12,8 | 7,08 | 36 | Ig heavy chain V-II region NEWM OS=Homo sapiens PE=1 SV=1 - [HV207_HUMAN] |
| O75420 | 11 | 1035 | 114,5 | 5,39 | 36 | PERQ amino acid-rich with GYF domain-containing protein 1 OS=Homo sapiens GI |
| Q15650 | 10 | 581 | 66,1 | 7,85 | 36 | Activating signal cointegrator 1 OS=Homo sapiens GN=TRIP4 PE=1 SV=4 - [TRIP4_H |
| O60347 | 4 | 775 | 85,6 | 5,74 | 36 | TBC1 domain family member 12 OS=Homo sapiens GN=TBC1D12 PE=1 SV=3 - [TBC |
| Q5T7N3 | 3 | 995 | 107,3 | 5,27 | 36 | KN motif and ankyrin repeat domain-containing protein 4 OS=Homo sapiens GN= |

| | | | | | | |
|---|---|---|---|---|---|---|
| Q96GW9 | 9 | 593 | 66,5 | 8,09 | 36 | Methionyl-tRNA synthetase, mitochondrial OS=Homo sapiens GN=MARS2 PE=1 S |
| O95163 | 33 | 1332 | 150,2 | 5,94 | 36 | Elongator complex protein 1 OS=Homo sapiens GN=IKBKAP PE=1 SV=3 - [ELP1_HU |
| A6NNW6 | 2 | 628 | 68,8 | 6 | 36 | Enolase-like protein ENO4 OS=Homo sapiens GN=ENO4 PE=2 SV=2 - [ENO4_HUMA |
| Q14457 | 3 | 450 | 51,9 | 4,89 | 36 | Beclin-1 OS=Homo sapiens GN=BECN1 PE=1 SV=2 - [BECN1_HUMAN] |
| Q8WV83 | 17 | 523 | 58,8 | 9,26 | 36 | Solute carrier family 35 member F5 OS=Homo sapiens GN=SLC35F5 PE=2 SV=1 - [S |
| Q6ZMV7 | 4 | 388 | 45,1 | 6,68 | 36 | Leucine-, glutamate- and lysine-rich protein 1 OS=Homo sapiens GN=LEKR1 PE=2 |
| Q99965 | 4 | 735 | 82,4 | 6,15 | 36 | Disintegrin and metalloproteinase domain-containing protein 2 OS=Homo sapier |
| Q99543 | 8 | 621 | 72,0 | 8,7 | 36 | DnaJ homolog subfamily C member 2 OS=Homo sapiens GN=DNAJC2 PE=1 SV=4 - |
| P78412 | 16 | 446 | 48,2 | 6,02 | 36 | Iroquois-class homeodomain protein IRX-6 OS=Homo sapiens GN=IRX6 PE=2 SV=3 |
| O95755 | 6 | 333 | 36,3 | 7,85 | 36 | Ras-related protein Rab-36 OS=Homo sapiens GN=RAB36 PE=1 SV=2 - [RAB36_HUI |
| P51003 | 9 | 745 | 82,8 | 7,37 | 36 | Poly(A) polymerase alpha OS=Homo sapiens GN=PAPOLA PE=1 SV=4 - [PAPOA_HU |
| Q7Z7A4 | 3 | 578 | 64,9 | 9,35 | 36 | PX domain-containing protein kinase-like protein OS=Homo sapiens GN=PXK PE= |
| Q8N5H7 | 20 | 860 | 94,4 | 8,07 | 36 | SH2 domain-containing protein 3C OS=Homo sapiens GN=SH2D3C PE=1 SV=1 - [SH |
| P05783 | 2 | 430 | 48,0 | 5,45 | 36 | Keratin, type I cytoskeletal 18 OS=Homo sapiens GN=KRT18 PE=1 SV=2 - [K1C18_H |
| P11177 | 28 | 359 | 39,2 | 6,65 | 36 | Pyruvate dehydrogenase E1 component subunit beta, mitochondrial OS=Homo sa |
| A6NNL0 | 18 | 878 | 93,9 | 7,84 | 36 | Protein FAM22B OS=Homo sapiens GN=FAM22B PE=2 SV=2 - [FA22B_HUMAN] |
| Q8TEK3 | 8 | 1739 | 184,7 | 9,33 | 36 | Histone-lysine N-methyltransferase, H3 lysine-79 specific OS=Homo sapiens GN= |
| Q96S52 | 6 | 555 | 61,6 | 6,49 | 36 | GPI transamidase component PIG-S OS=Homo sapiens GN=PIGS PE=1 SV=3 - [PIGS |
| Q15345 | 3 | 812 | 88,6 | 8,38 | 36 | Leucine-rich repeat-containing protein 41 OS=Homo sapiens GN=LRRC41 PE=1 SV |
| O75600 | 2 | 419 | 45,3 | 8,05 | 36 | 2-amino-3-ketobutyrate coenzyme A ligase, mitochondrial OS=Homo sapiens GN |
| Q2M3V2 | 7 | 549 | 57,4 | 10,18 | 36 | Ankyrin repeat domain-containing protein 43 OS=Homo sapiens GN=ANKRD43 PE |
| Q5T1N1 | 16 | 836 | 92,8 | 6,81 | 36 | Protein AKNAD1 OS=Homo sapiens GN=AKNAD1 PE=2 SV=3 - [AKND1_HUMAN] |
| A8MX80 | 17 | 341 | 37,6 | 10,45 | 36 | Putative UPF0607 protein ENSP00000383144 OS=Homo sapiens PE=3 SV=2 - [YM01 |
| A6PVS8 | 12 | 624 | 73,6 | 9,72 | 36 | Leucine-rich repeat and IQ domain-containing protein 3 OS=Homo sapiens GN=LR |
| Q9BR76 | 15 | 489 | 54,2 | 5,88 | 36 | Coronin-1B OS=Homo sapiens GN=CORO1B PE=1 SV=1 - [COR1B_HUMAN] |
| O95672 | 4 | 775 | 87,7 | 7,03 | 36 | Endothelin-converting enzyme-like 1 OS=Homo sapiens GN=ECEL1 PE=2 SV=3 - [E |
| P51956 | 11 | 506 | 57,7 | 7,17 | 35 | Serine/threonine-protein kinase Nek3 OS=Homo sapiens GN=NEK3 PE=1 SV=2 - [N |
| P04808 | 8 | 185 | 21,1 | 8,69 | 35 | Prorelaxin H1 precursor [Contains: Relaxin B chain; Relaxin A chain] - Homo sapie |
| Q9H2A3 | 4 | 272 | 28,6 | 7,75 | 35 | Neurogenin-2 OS=Homo sapiens GN=NEUROG2 PE=1 SV=2 - [NGN2_HUMAN] |
| P84996 | 2 | 626 | 67,9 | 11,55 | 35 | Protein ALEX OS=Homo sapiens GN=GNAS PE=1 SV=1 - [ALEX_HUMAN] |
| Q5VYM1 | 2 | 1079 | 117,6 | 7,36 | 35 | Uncharacterized protein C9orf131 OS=Homo sapiens GN=C9orf131 PE=2 SV=3 - [CI |
| P22914 | 14 | 178 | 21,0 | 6,89 | 35 | Beta-crystallin S OS=Homo sapiens GN=CRYGS PE=1 SV=4 - [CRBS_HUMAN] |
| Q96S38 | 2 | 1066 | 118,6 | 4,87 | 35 | Ribosomal protein S6 kinase delta-1 OS=Homo sapiens GN=RPS6KC1 PE=1 SV=2 - |
| Q8WU58 | 41 | 562 | 59,6 | 9,23 | 35 | Uncharacterized protein C17orf63 OS=Homo sapiens GN=C17orf63 PE=1 SV=1 - [C |
| Q8TB36 | 16 | 358 | 41,3 | 8,34 | 35 | Ganglioside-induced differentiation-associated protein 1 OS=Homo sapiens GN= |
| Q5JPI3 | 69 | 329 | 37,5 | 6,47 | 35 | Uncharacterized protein C3orf38 OS=Homo sapiens GN=C3orf38 PE=2 SV=1 - [CC0 |
| O15079 | 3 | 494 | 53,5 | 5,6 | 35 | Syntaphilin OS=Homo sapiens GN=SNPH PE=1 SV=2 - [SNPH_HUMAN] |
| O95049 | 3 | 933 | 102,7 | 6,54 | 35 | Tight junction protein ZO-3 OS=Homo sapiens GN=TJP3 PE=1 SV=2 - [ZO3_HUMAN |
| Q13905 | 14 | 1077 | 120,5 | 5,92 | 35 | Rap guanine nucleotide exchange factor 1 OS=Homo sapiens GN=RAPGEF1 PE=1 S |
| A6NED2 | 28 | 376 | 40,1 | 5,27 | 35 | RCC1 domain-containing protein 1 OS=Homo sapiens GN=RCCD1 PE=1 SV=1 - [RCC |
| O15165 | 5 | 306 | 33,9 | 6,28 | 35 | Uncharacterized protein C18orf1 OS=Homo sapiens GN=C18orf1 PE=2 SV=1 - [CR0 |
| Q7RTS3 | 5 | 328 | 34,9 | 5,25 | 35 | Pancreas transcription factor 1 subunit alpha OS=Homo sapiens GN=PTF1A PE=1 S |
| Q6ZP65 | 4 | 573 | 64,8 | 5 | 35 | Bicaudal D-related protein 1 OS=Homo sapiens GN=CCDC64 PE=2 SV=2 - [BICR1_H |
| Q92764 | 3 | 455 | 50,3 | 4,91 | 35 | Keratin, type I cuticular Ha5 OS=Homo sapiens GN=KRT35 PE=1 SV=5 - [KRT35_HUI |
| Q14774 | 3 | 488 | 50,8 | 8,5 | 35 | H2.0-like homeobox protein OS=Homo sapiens GN=HLX PE=1 SV=3 - [HLX_HUMAN |
| Q9NTZ6 | 3 | 932 | 97,3 | 8,63 | 35 | RNA-binding protein 12 OS=Homo sapiens GN=RBM12 PE=1 SV=1 - [RBM12_HUMA |
| Q13425 | 2 | 540 | 57,9 | 8,82 | 35 | Beta-2-syntrophin (59 kDa dystrophin-associated protein A1 basic component 2) |
| A2RUR9 | 10 | 1427 | 165,0 | 5,36 | 35 | Coiled-coil domain-containing protein 144A OS=Homo sapiens GN=CCDC144A PE= |
| Q8N0U7 | 6 | 546 | 62,0 | 8,65 | 35 | Uncharacterized protein C1orf87 OS=Homo sapiens GN=C1orf87 PE=2 SV=1 - [CA0 |
| Q9NZL6 | 11 | 768 | 86,6 | 6,09 | 35 | Ral guanine nucleotide dissociation stimulator-like 1 OS=Homo sapiens GN=RGL1 |
| Q5JRM2 | 7 | 361 | 39,9 | 9,54 | 35 | Uncharacterized protein CXorf66 OS=Homo sapiens GN=CXorf66 PE=2 SV=1 - [CX0 |
| O14746 | 4 | 1132 | 126,9 | 10,52 | 35 | Telomerase reverse transcriptase OS=Homo sapiens GN=TERT PE=1 SV=1 - [TERT_ |
| Q9H6R7 | 23 | 721 | 79,1 | 6,7 | 35 | WD repeat-containing protein C2orf44 OS=Homo sapiens GN=C2orf44 PE=1 SV=1 |
| O75629 | 4 | 220 | 24,1 | 7,59 | 35 | Protein CREG1 OS=Homo sapiens GN=CREG1 PE=1 SV=1 - [CREG1_HUMAN] |
| Q9UP65 | 4 | 541 | 60,9 | 6,93 | 35 | Cytosolic phospholipase A2 gamma OS=Homo sapiens GN=PLA2G4C PE=1 SV=2 - [ |
| Q04609 | 6 | 750 | 84,3 | 6,98 | 35 | Glutamate carboxypeptidase 2 OS=Homo sapiens GN=FOLH1 PE=1 SV=1 - [FOLH1_ |
| Q9Y4K1 | 10 | 1723 | 188,6 | 5,86 | 35 | Absent in melanoma 1 protein OS=Homo sapiens GN=AIM1 PE=1 SV=3 - [AIM1_HU |
| Q9P032 | 4 | 175 | 20,3 | 8,82 | 35 | UPF0240 protein C6orf66 - Homo sapiens (Human) - [CF066_HUMAN] |
| Q7Z6J6 | 3 | 570 | 65,0 | 8,35 | 35 | FERM domain-containing protein 5 OS=Homo sapiens GN=FRMD5 PE=2 SV=1 - [FR |
| P35236 | 5 | 360 | 40,5 | 6,79 | 35 | Tyrosine-protein phosphatase non-receptor type 7 OS=Homo sapiens GN=PTPN7 |
| Q0ZLH3 | 9 | 352 | 39,9 | 9,01 | 35 | Pejvakin OS=Homo sapiens GN=PJVK PE=1 SV=1 - [PJVK_HUMAN] |
| Q99608 | 5 | 321 | 36,1 | 8,78 | 35 | Necdin OS=Homo sapiens GN=NDN PE=1 SV=1 - [NECD_HUMAN] |
| Q96AP4 | 6 | 578 | 65,9 | 6,49 | 35 | Zinc finger with UFM1-specific peptidase domain protein OS=Homo sapiens GN=Z |

**Appendix 3:** LC ESI MS identified Schirmer strip tear proteins (Funke et al. 2014)

| Accession | # Peptides | # AAs | MW [kDa] | calc. pI | Score | Description |
|---|---|---|---|---|---|---|
| P02788 | 7530 | 710 | 78,1 | 8,12 | 2196 | Lactotransferrin GN=LTF PE=1 SV=6 [TRFL] |
| P02768 | 1668 | 609 | 69,3 | 6,28 | 1721 | Serum albumin precursor [ALBU] |
| P04264 | 324 | 644 | 66,0 | 8,12 | 1525 | Keratin, type II cytoskeletal 1 GN=KRT1 PE=1 SV=6 [K2C1] |
| P13645 | 228 | 584 | 58,8 | 5,21 | 1365 | Keratin, type I cytoskeletal 10 GN=KRT10 PE=1 SV=6 [K1C10] |
| P06733 | 470 | 434 | 47,1 | 7,39 | 1134 | Alphaenolase (EC 4.2.1.11) (2phosphoDglycerate hydrolyase) (Nonneural enolase) ( |
| P25311 | 1276 | 298 | 34,2 | 6,05 | 1075 | Zinc alpha 2 glycoprotein GN=AZGP1 PE=1 SV=2 [ZA2G] |
| P98160 | 81 | 4391 | 468,5 | 6,51 | 1073 | Basement membranespecific heparan sulfate proteoglycan core protein GN=HSPG2 |
| P00352 | 174 | 501 | 54,8 | 6,73 | 1029 | Retinal dehydrogenase 1 GN=ALDH1A1 PE=1 SV=2 [AL1A1] |
| P01009 | 167 | 418 | 46,7 | 5,59 | 886 | Alpha1antitrypsin GN=SERPINA1 PE=1 SV=3 [A1AT] |
| P60709 | 434 | 375 | 41,7 | 5,48 | 878 | Actin, cytoplasmic 1 (Betaactin) [ACTB] |
| P01024 | 62 | 1663 | 187,0 | 6,40 | 776 | Complement C3 precursor [CO3] |
| Q8WZ42 | 265 | 34350 | 3813,7 | 6,35 | 765 | Titin GN=TTN PE=1 SV=4 [TITIN] |
| P04083 | 128 | 346 | 38,7 | 7,02 | 747 | Annexin A1 GN=ANXA1 PE=1 SV=2 [ANXA1] |
| P30740 | 108 | 379 | 42,7 | 6,28 | 747 | Leukocyte elastase inhibitor GN=SERPINB1 PE=1 SV=1 [ILEU] |
| P68032 | 291 | 377 | 42,0 | 5,39 | 727 | Actin, alpha cardiac muscle 1 (Alphacardiac actin) [ACTC] |
| P14618 | 62 | 531 | 57,9 | 7,84 | 666 | Pyruvate kinase isozymes M1/M2 (EC 2.7.1.40) (Pyruvate kinase muscle isozyme) (P |
| Q06830 | 111 | 199 | 22,1 | 8,13 | 654 | Peroxiredoxin1 (EC 1.11.1.15) (Thioredoxin peroxidase 2) (Thioredoxindependent p |
| P04792 | 183 | 205 | 22,8 | 6,40 | 646 | Heatshock protein beta1 (HspB1) (Heat shock 27 kDa protein) (HSP 27) (Stressrespor |
| P01833 | 446 | 764 | 83,2 | 5,74 | 641 | Polymeric immunoglobulin receptor GN=PIGR PE=1 SV=4 [PIGR] |
| Q9UGM3 | 206 | 2413 | 260,6 | 5,44 | 640 | Deleted in malignant brain tumors 1 protein GN=DMBT1 PE=1 SV=2 [DMBT1] |
| P31025 | 3987 | 176 | 19,2 | 5,58 | 603 | Lipocalin1 GN=LCN1 PE=1 SV=1 [LCN1] |
| P01876 | 1313 | 353 | 37,6 | 6,51 | 588 | Ig alpha1 chain C region GN=IGHA1 PE=1 SV=2 [IGHA1] |
| Q6S8J3 | 245 | 1075 | 121,3 | 6,20 | 553 | POTE ankyrin domain family member E GN=POTEE PE=1 SV=3 [POTEE] |
| P00738 | 67 | 406 | 45,2 | 6,58 | 550 | Haptoglobin GN=HP PE=1 SV=1 [HPT] |
| P30838 | 56 | 453 | 50,4 | 6,54 | 540 | Aldehyde dehydrogenase, dimeric NADPpreferring GN=ALDH3A1 PE=1 SV=3 [AL3A |
| A5A3E0 | 235 | 1075 | 121,4 | 6,20 | 535 | POTE ankyrin domain family member F GN=POTEF PE=1 SV=2 [POTEF] |
| P01877 | 1100 | 340 | 36,5 | 6,10 | 525 | Ig alpha2 chain C region GN=IGHA2 PE=1 SV=3 [IGHA2] |
| P07355 | 35 | 339 | 38,6 | 7,75 | 519 | Annexin A2 GN=ANXA2 PE=1 SV=2 [ANXA2] |
| P09211 | 161 | 210 | 23,3 | 5,64 | 516 | Glutathione Stransferase P GN=GSTP1 PE=1 SV=2 [GSTP1] |
| P02538 | 60 | 564 | 60,0 | 8,00 | 488 | Keratin, type II cytoskeletal 6A GN=KRT6A PE=1 SV=3 [K2C6A] |
| P12273 | 1635 | 146 | 16,6 | 8,05 | 487 | Prolactininducible protein GN=PIP PE=1 SV=1 [PIP] |
| P08758 | 31 | 320 | 35,9 | 5,05 | 473 | Annexin A5 GN=ANXA5 PE=1 SV=2 [ANXA5] |
| P00338 | 80 | 332 | 36,7 | 8,27 | 454 | Llactate dehydrogenase A chain GN=LDHA PE=1 SV=2 [LDHA] |
| P0CG38 | 206 | 1075 | 121,2 | 6,21 | 449 | POTE ankyrin domain family member I GN=POTEI PE=3 SV=1 [POTEI] |
| P02787 | 400 | 698 | 77,0 | 7,12 | 444 | Serotransferrin GN=TF PE=1 SV=3 [TRFE] |
| P01857 | 256 | 330 | 36,1 | 8,19 | 434 | Ig gamma1 chain C region [IGHG1] |
| P06702 | 271 | 114 | 13,2 | 6,13 | 432 | Protein S100A9 GN=S100A9 PE=1 SV=1 [S10A9] |
| P61626 | 3675 | 148 | 16,5 | 9,16 | 431 | Lysozyme C precursor (EC 3.2.1.17) (1,4betaNacetylmuramidase C) [LYSC] |
| Q9GZZ8 | 912 | 138 | 14,2 | 5,50 | 415 | Extracellular glycoprotein lacritin GN=LACRT PE=1 SV=1 [LACRT] |
| P10909 | 83 | 449 | 52,5 | 6,27 | 412 | Clusterin GN=CLU PE=1 SV=1 [CLUS] |
| P00450 | 61 | 1065 | 122,1 | 5,72 | 403 | Ceruloplasmin GN=CP PE=1 SV=1 [CERU] |
| P01623 | 67 | 109 | 11,7 | 8,91 | 381 | Ig kappa chain VIII region WOL PE=1 SV=1 [KV305] |
| P31947 | 103 | 248 | 27,8 | 4,74 | 373 | 1433 protein sigma GN=SFN PE=1 SV=1 [1433S] |
| P35908 | 73 | 639 | 65,4 | 8,00 | 372 | Keratin, type II cytoskeletal 2 epidermal GN=KRT2 PE=1 SV=2 [K22E] |
| P60174 | 34 | 286 | 30,8 | 5,92 | 367 | Triosephosphate isomerase GN=TPI1 PE=1 SV=3 [TPIS] |
| P20061 | 96 | 433 | 48,2 | 5,03 | 362 | Transcobalamin1 GN=TCN1 PE=1 SV=2 [TCO1] |
| P00558 | 52 | 417 | 44,6 | 8,10 | 357 | Phosphoglycerate kinase 1 (EC 2.7.2.3) (Primer recognition protein 2) (PRP 2) [PGK |
| P14550 | 32 | 325 | 36,5 | 6,79 | 343 | Alcohol dehydrogenase [NADP+] GN=AKR1A1 PE=1 SV=3 [AK1A1] |
| Q562R1 | 219 | 376 | 42,0 | 5,59 | 341 | Betaactinlike protein 2 GN=ACTBL2 PE=1 SV=2 [ACTBL] |
| P05109 | 234 | 93 | 10,8 | 7,03 | 337 | Protein S100A8 GN=S100A8 PE=1 SV=1 [S10A8] |
| Q13421 | 39 | 630 | 68,9 | 6,38 | 332 | Mesothelin GN=MSLN PE=1 SV=2 [MSLN] |
| P01036 | 254 | 141 | 16,2 | 5,02 | 329 | CystatinS precursor (Cystatin4) (Salivary acidic protein 1) (CystatinSAIII) [CYTS] |
| P63104 | 59 | 245 | 27,7 | 4,79 | 320 | 1433 protein zeta/delta GN=YWHAZ PE=1 SV=1 [1433Z] |
| P0CG05 | 460 | 106 | 11,3 | 7,24 | 311 | Ig lambda2 chain C regions GN=IGLC2 PE=1 SV=1 [LAC2] |
| P02533 | 63 | 472 | 51,5 | 5,16 | 308 | Keratin, type I cytoskeletal 14 GN=KRT14 PE=1 SV=4 [K1C14] |
| O75556 | 1021 | 95 | 10,9 | 5,78 | 301 | MammaglobinB GN=SCGB2A1 PE=1 SV=1 [SG2A1] |
| P01622 | 55 | 109 | 11,8 | 8,50 | 299 | Ig kappa chain VIII region Ti PE=1 SV=1 [KV304] |
| P40925 | 39 | 334 | 36,4 | 7,36 | 297 | Malate dehydrogenase, cytoplasmic GN=MDH1 PE=1 SV=4 [MDHC] |
| P30041 | 47 | 224 | 25,0 | 6,38 | 294 | Peroxiredoxin6 GN=PRDX6 PE=1 SV=3 [PRDX6] |
| P02763 | 54 | 201 | 23,5 | 5,02 | 284 | Alpha1acid glycoprotein 1 precursor (AGP 1) (Orosomucoid1) (OMD 1) [A1AG1] |
| P52209 | 30 | 483 | 53,1 | 7,23 | 282 | 6phosphogluconate dehydrogenase, decarboxylating GN=PGD PE=1 SV=3 [6PGD] |
| P06396 | 64 | 782 | 85,6 | 6,28 | 281 | Gelsolin GN=GSN PE=1 SV=1 [GELS] |
| P15924 | 4 | 2871 | 331,6 | 6,81 | 273 | Desmoplakin GN=DSP PE=1 SV=3 [DESP] |
| P68372 | 26 | 445 | 49,8 | 4,89 | 273 | Tubulin beta2C chain [TBB2C] |

| | | | | | | |
|---|---|---|---|---|---|---|
| P68104 | 31 | 462 | 50,1 | 9,01 | 271 | Elongation factor 1alpha 1 GN=EEF1A1 PE=1 SV=1 [EF1A1] |
| P01859 | 129 | 326 | 35,9 | 7,59 | 268 | Ig gamma2 chain C region GN=IGHG2 PE=1 SV=2 [IGHG2] |
| Q99935 | 242 | 248 | 27,2 | 10,42 | 262 | Prolinerich protein 1 GN=PROL1 PE=1 SV=2 [PROL1] |
| P62259 | 32 | 255 | 29,2 | 4,74 | 260 | 1433 protein epsilon (1433E) [1433E] |
| P26447 | 106 | 101 | 11,7 | 6,11 | 256 | Protein S100A4 GN=S100A4 PE=1 SV=1 [S10A4] |
| Q96KP4 | 24 | 475 | 52,8 | 5,97 | 254 | Cytosolic nonspecific dipeptidase (Glutamate carboxypeptidaselike protein 1) (CND |
| O95968 | 550 | 90 | 9,9 | 9,25 | 247 | Secretoglobin family 1D member 1 GN=SCGB1D1 PE=1 SV=1 [SG1D1] |
| P09104 | 99 | 434 | 47,2 | 5,03 | 247 | Gammaenolase (EC 4.2.1.11) (2phosphoDglycerate hydrolyase) (Neural enolase) (N |
| P40394 | 30 | 386 | 41,5 | 7,85 | 242 | Alcohol dehydrogenase class 4 mu/sigma chain GN=ADH7 PE=1 SV=2 [ADH7] |
| B9A064 | 216 | 214 | 23,0 | 8,84 | 233 | Immunoglobulin lambdalike polypeptide 5 GN=IGLL5 PE=2 SV=2 [IGLL5] |
| P02647 | 19 | 267 | 30,8 | 5,76 | 233 | Apolipoprotein AI precursor (ApoAI) (ApoAI) [Contains: Apolipoprotein AI(1242)] |
| P62987 | 21 | 128 | 14,7 | 9,83 | 232 | Ubiquitin60S ribosomal protein L40 GN=UBA52 PE=1 SV=2 [RL40] |
| Q15149 | 3 | 4684 | 531,5 | 5,96 | 231 | Plectin GN=PLEC PE=1 SV=3 [PLEC] |
| Q8NF91 | 37 | 8797 | 1010,4 | 5,53 | 230 | Nesprin1 GN=SYNE1 PE=1 SV=3 [SYNE1] |
| P61982 | 39 | 247 | 28,3 | 4,89 | 229 | 1433 protein gamma [1433G] |
| O00299 | 29 | 241 | 26,9 | 5,17 | 216 | Chloride intracellular channel protein 1 GN=CLIC1 PE=1 SV=4 [CLIC1] |
| P35527 | 13 | 623 | 62,0 | 5,24 | 212 | Keratin, type I cytoskeletal 9 GN=KRT9 PE=1 SV=3 [K1C9] |
| Q04695 | 57 | 432 | 48,1 | 5,02 | 211 | Keratin, type I cytoskeletal 17 GN=KRT17 PE=1 SV=2 [K1C17] |
| P09228 | 58 | 141 | 16,4 | 4,93 | 210 | CystatinSA GN=CST2 PE=1 SV=1 [CYTT] |
| P01834 | 476 | 106 | 11,6 | 5,87 | 193 | Ig kappa chain C region [KAC] |
| P07737 | 32 | 140 | 15,0 | 8,27 | 192 | Profilin1 GN=PFN1 PE=1 SV=2 [PROF1] |
| P01037 | 122 | 141 | 16,4 | 7,21 | 188 | CystatinSN GN=CST1 PE=1 SV=3 [CYTN] |
| Q8IVF4 | 129 | 4471 | 514,5 | 5,88 | 186 | Dynein heavy chain 10, axonemal GN=DNAH10 PE=1 SV=4 [DYH10] |
| O15078 | 39 | 2479 | 290,2 | 5,95 | 183 | Centrosomal protein of 290 kDa GN=CEP290 PE=1 SV=2 [CE290] |
| P12429 | 12 | 323 | 36,4 | 5,92 | 182 | Annexin A3 GN=ANXA3 PE=1 SV=3 [ANXA3] |
| P06703 | 30 | 90 | 10,2 | 5,48 | 178 | Protein S100A6 GN=S100A6 PE=1 SV=1 [S10A6] |
| P01766 | 87 | 120 | 13,2 | 6,57 | 178 | Ig heavy chain VIII region BRO PE=1 SV=1 [HV305] |
| Q5XKE5 | 25 | 535 | 57,8 | 7,20 | 176 | Keratin, type II cytoskeletal 79 GN=KRT79 PE=1 SV=2 [K2C79] |
| A7E2Y1 | 1 | 1941 | 221,3 | 6,01 | 174 | Myosin7B GN=MYH7B PE=2 SV=3 [MYH7B] |
| P02790 | 10 | 462 | 51,6 | 7,02 | 174 | Hemopexin precursor (Beta1Bglycoprotein) [HEMO] |
| P20929 | 1 | 6669 | 772,4 | 9,07 | 174 | Nebulin GN=NEB PE=1 SV=4 [NEBU] |
| P04745 | 10 | 511 | 57,7 | 6,93 | 173 | Alphaamylase 1 GN=AMY1A PE=1 SV=2 [AMY1] |
| P04080 | 15 | 98 | 11,1 | 7,56 | 173 | CystatinB GN=CSTB PE=1 SV=2 [CYTB] |
| P49454 | 2 | 3210 | 367,5 | 5,07 | 171 | Centromere protein F GN=CENPF PE=1 SV=2 [CENPF] |
| Q16378 | 1671 | 134 | 15,1 | 7,06 | 167 | Prolinerich protein 4 GN=PRR4 PE=1 SV=3 [PROL4] |
| P27348 | 84 | 245 | 27,7 | 4,78 | 164 | 1433 protein theta GN=YWHAQ PE=1 SV=1 [1433T] |
| P46100 | 54 | 2492 | 282,4 | 6,58 | 163 | Transcriptional regulator ATRX GN=ATRX PE=1 SV=5 [ATRX] |
| P01591 | 91 | 159 | 18,1 | 5,24 | 163 | Immunoglobulin J chain GN=IGJ PE=1 SV=4 [IGJ] |
| Q99996 | 35 | 3911 | 453,4 | 4,98 | 162 | Akinase anchor protein 9 (Protein kinase Aanchoring protein 9) (PRKA9) (Akinase ar |
| P01781 | 62 | 116 | 12,7 | 8,48 | 161 | Ig heavy chain VIII region GAL PE=1 SV=1 [HV320] |
| Q9UQE7 | 190 | 1217 | 141,5 | 7,18 | 159 | Structural maintenance of chromosomes protein 3 GN=SMC3 PE=1 SV=2 [SMC3] |
| Q8TD57 | 2 | 4116 | 470,5 | 6,43 | 159 | Dynein heavy chain 3, axonemal GN=DNAH3 PE=2 SV=1 [DYH3] |
| O95239 | 115 | 1232 | 139,8 | 6,27 | 158 | Chromosomeassociated kinesin KIF4A GN=KIF4A PE=1 SV=3 [KIF4A] |
| Q14643 | 83 | 2758 | 313,7 | 6,04 | 157 | Inositol 1,4,5trisphosphate receptor type 1 GN=ITPR1 PE=1 SV=2 [ITPR1] |
| Q9Y5Z4 | 6 | 205 | 22,9 | 4,63 | 156 | Hemebinding protein 2 GN=HEBP2 PE=1 SV=1 [HEBP2] |
| Q92736 | 101 | 4967 | 564,2 | 6,07 | 156 | Ryanodine receptor 2 GN=RYR2 PE=1 SV=3 [RYR2] |
| Q14789 | 4 | 3259 | 375,8 | 5,00 | 154 | Golgin subfamily B member 1 GN=GOLGB1 PE=1 SV=2 [GOGB1] |
| Q5VST9 | 9 | 7968 | 867,9 | 5,99 | 153 | Obscurin GN=OBSCN PE=1 SV=3 [OBSCN] |
| P19652 | 16 | 201 | 23,6 | 5,11 | 152 | Alpha1acid glycoprotein 2 GN=ORM2 PE=1 SV=2 [A1AG2] |
| Q02224 | 8 | 2701 | 316,2 | 5,64 | 151 | Centromereassociated protein E GN=CENPE PE=1 SV=2 [CENPE] |
| P04746 | 10 | 511 | 57,7 | 7,05 | 147 | Pancreatic alphaamylase GN=AMY2A PE=1 SV=2 [AMYP] |
| P01765 | 63 | 115 | 12,3 | 9,13 | 146 | Ig heavy chain VIII region TIL [HV304] |
| Q96T58 | 51 | 3664 | 402,0 | 7,64 | 145 | Msx2interacting protein GN=SPEN PE=1 SV=1 [MINT] |
| Q9UPN3 | 26 | 7388 | 837,8 | 5,39 | 145 | Microtubuleactin crosslinking factor 1, isoforms 1/2/3/5 GN=MACF1 PE=1 SV=4 [MA |
| Q8TDY2 | 20 | 1594 | 183,0 | 5,41 | 144 | RB1inducible coiledcoil protein 1 GN=RB1CC1 PE=1 SV=3 [RBCC1] |
| P19961 | 10 | 511 | 57,7 | 7,09 | 143 | Alphaamylase 2B GN=AMY2B PE=1 SV=1 [AMY2B] |
| Q5CZC0 | 1 | 6907 | 780,1 | 6,71 | 142 | Fibrous sheathinteracting protein 2 GN=FSIP2 PE=1 SV=4 [FSIP2] |
| Q14980 | 20 | 2115 | 238,1 | 5,78 | 141 | Nuclear mitotic apparatus protein 1 GN=NUMA1 PE=1 SV=2 [NUMA1] |
| Q9NQX4 | 31 | 1742 | 202,7 | 7,71 | 141 | MyosinVc GN=MYO5C PE=1 SV=2 [MYO5C] |
| P01597 | 38 | 108 | 11,7 | 9,36 | 140 | Ig kappa chain VI region DEE PE=1 SV=1 [KV105] |
| Q2M2I5 | 45 | 525 | 55,1 | 4,96 | 138 | Keratin, type I cytoskeletal 24 GN=KRT24 PE=1 SV=1 [K1C24] |
| Q9BV73 | 49 | 2442 | 281,0 | 5,02 | 138 | Centrosomeassociated protein CEP250 GN=CEP250 PE=1 SV=2 [CP250] |
| P18669 | 6 | 254 | 28,8 | 7,18 | 131 | Phosphoglycerate mutase 1 GN=PGAM1 PE=1 SV=2 [PGAM1] |
| O75037 | 49 | 1637 | 182,5 | 7,08 | 131 | Kinesinlike protein KIF21B GN=KIF21B PE=1 SV=2 [KI21B] |
| P47989 | 27 | 1333 | 146,3 | 7,66 | 130 | Xanthine dehydrogenase/oxidase GN=XDH PE=1 SV=4 [XDH] |

| | | | | | | |
|---|---|---|---|---|---|---|
| P35580 | 1 | 1976 | 228,9 | 5,54 | 129 | Myosin10 GN=MYH10 PE=1 SV=3 [MYH10] |
| P25054 | 12 | 2843 | 311,5 | 7,80 | 129 | Adenomatous polyposis coli protein GN=APC PE=1 SV=2 [APC] |
| P80748 | 9 | 111 | 11,9 | 5,08 | 128 | Ig lambda chain VIII region LOI PE=1 SV=1 [LV302] |
| P52895 | 8 | 323 | 36,7 | 7,49 | 127 | Aldoketo reductase family 1 member C2 GN=AKR1C2 PE=1 SV=3 [AK1C2] |
| Q7Z3Z0 | 26 | 450 | 49,3 | 5,08 | 125 | Keratin, type I cytoskeletal 25 GN=KRT25 PE=1 SV=1 [K1C25] |
| P06309 | 30 | 117 | 12,7 | 7,12 | 124 | Ig kappa chain VII region GM607 (Fragment) PE=4 SV=1 [KV205] |
| P04207 | 29 | 129 | 14,3 | 8,51 | 124 | Ig kappa chain VIII region CLL PE=1 SV=2 [KV308] |
| P46013 | 42 | 3256 | 358,5 | 9,45 | 123 | Antigen KI67 GN=MKI67 PE=1 SV=2 [KI67] |
| P04075 | 13 | 364 | 39,4 | 8,09 | 123 | Fructosebisphosphate aldolase A GN=ALDOA PE=1 SV=2 [ALDOA] |
| Q7Z794 | 26 | 578 | 61,9 | 5,99 | 122 | Keratin, type II cytoskeletal 1b GN=KRT77 PE=1 SV=3 [K2C1B] |
| Q04828 | 5 | 323 | 36,8 | 7,88 | 122 | Aldoketo reductase family 1 member C1 GN=AKR1C1 PE=1 SV=1 [AK1C1] |
| Q6ZR08 | 1 | 3092 | 356,7 | 6,19 | 120 | Dynein heavy chain 12, axonemal GN=DNAH12 PE=1 SV=2 [DYH12] |
| Q8TE73 | 29 | 4624 | 528,7 | 6,10 | 120 | Dynein heavy chain 5, axonemal GN=DNAH5 PE=1 SV=3 [DYH5] |
| Q15772 | 18 | 3267 | 354,1 | 8,51 | 119 | Striated muscle preferentially expressed protein kinase GN=SPEG PE=1 SV=4 [SPEG |
| Q15643 | 1 | 1979 | 227,4 | 5,26 | 118 | Thyroid receptorinteracting protein 11 GN=TRIP11 PE=1 SV=3 [TRIPB] |
| P15311 | 121 | 586 | 69,4 | 6,27 | 118 | Ezrin GN=EZR PE=1 SV=4 [EZRI] |
| Q8NEN9 | 292 | 1154 | 128,5 | 6,09 | 118 | PDZ domaincontaining protein 8 GN=PDZD8 PE=1 SV=1 [PDZD8] |
| O75417 | 14 | 2590 | 289,4 | 7,36 | 116 | DNA polymerase theta GN=POLQ PE=1 SV=2 [DPOLQ] |
| P13716 | 22 | 330 | 36,3 | 6,79 | 116 | Deltaaminolevulinic acid dehydratase GN=ALAD PE=1 SV=1 [HEM2] |
| P27797 | 7 | 417 | 48,1 | 4,44 | 115 | Calreticulin GN=CALR PE=1 SV=1 [CALR] |
| Q14008 | 54 | 2032 | 225,4 | 7,80 | 115 | Cytoskeletonassociated protein 5 GN=CKAP5 PE=1 SV=3 [CKAP5] |
| P47929 | 4 | 136 | 15,1 | 7,62 | 114 | Galectin7 GN=LGALS7 PE=1 SV=2 [LEG7] |
| Q01484 | 87 | 3957 | 433,4 | 5,14 | 114 | Ankyrin2 GN=ANK2 PE=1 SV=4 [ANK2] |
| A4UGR9 | 23 | 3374 | 382,1 | 6,38 | 114 | Xin actinbinding repeatcontaining protein 2 GN=XIRP2 PE=1 SV=2 [XIRP2] |
| Q92608 | 386 | 1830 | 211,8 | 6,87 | 114 | Dedicator of cytokinesis protein 2 GN=DOCK2 PE=1 SV=2 [DOCK2] |
| Q7Z460 | 31 | 1538 | 169,3 | 9,03 | 113 | CLIPassociating protein 1 GN=CLASP1 PE=1 SV=1 [CLAP1] |
| Q12955 | 17 | 4377 | 480,1 | 6,49 | 113 | Ankyrin3 GN=ANK3 PE=1 SV=3 [ANK3] |
| Q14683 | 32 | 1233 | 143,1 | 7,64 | 113 | Structural maintenance of chromosomes protein 1A GN=SMC1A PE=1 SV=2 [SMC1A |
| Q9UIG0 | 4 | 1483 | 170,8 | 8,48 | 113 | Tyrosineprotein kinase BAZ1B GN=BAZ1B PE=1 SV=2 [BAZ1B] |
| Q13439 | 19 | 2230 | 261,0 | 5,39 | 112 | Golgin subfamily A member 4 GN=GOLGA4 PE=1 SV=1 [GOGA4] |
| P21817 | 98 | 5038 | 564,8 | 5,30 | 112 | Ryanodine receptor 1 GN=RYR1 PE=1 SV=3 [RYR1] |
| Q2M1P5 | 18 | 1343 | 150,5 | 6,79 | 111 | Kinesinlike protein KIF7 GN=KIF7 PE=1 SV=2 [KIF7] |
| P0C6X7 | 154 | 7073 | 789,7 | 6,62 | 110 | Replicase polyprotein 1ab SARS coronavirus GN=rep PE=1 SV=1 [R1ABCVHSA] |
| P11717 | 55 | 2491 | 274,2 | 5,94 | 110 | Cationindependent mannose6phosphate receptor GN=IGF2R PE=1 SV=3 [MPRI] |
| Q8NCM8 | 426 | 4307 | 492,3 | 6,54 | 109 | Cytoplasmic dynein 2 heavy chain 1 GN=DYNC2H1 PE=1 SV=4 [DYHC2] |
| Q14004 | 16 | 1512 | 164,8 | 9,69 | 109 | Cyclindependent kinase 13 GN=CDK13 PE=1 SV=2 [CDK13] |
| Q03001 | 18 | 7570 | 860,1 | 5,25 | 109 | Dystonin GN=DST PE=1 SV=4 [DYST] |
| Q93008 | 28 | 2570 | 292,1 | 5,80 | 109 | Probable ubiquitin carboxylterminal hydrolase FAFX GN=USP9X PE=1 SV=3 [USP9X] |
| Q6N069 | 1 | 864 | 101,4 | 7,87 | 108 | Nalphaacetyltransferase 16, NatA auxiliary subunit GN=NAA16 PE=1 SV=2 [NAA16] |
| Q9P273 | 105 | 2699 | 300,8 | 6,42 | 107 | Teneurin3 GN=ODZ3 PE=2 SV=3 [TEN3] |
| Q8WXH0 | 18 | 6885 | 795,9 | 5,36 | 107 | Nesprin2 GN=SYNE2 PE=1 SV=3 [SYNE2] |
| Q9Y2W1 | 28 | 955 | 108,6 | 10,15 | 107 | Thyroid hormone receptorassociated protein 3 GN=THRAP3 PE=1 SV=2 [TR150] |
| Q9Y5S2 | 156 | 1711 | 194,2 | 6,37 | 106 | Serine/threonineprotein kinase MRCK beta GN=CDC42BPB PE=1 SV=2 [MRCKB] |
| P01764 | 57 | 117 | 12,6 | 8,28 | 105 | Ig heavy chain VIII region VH26 PE=1 SV=1 [HV303] |
| P01768 | 58 | 122 | 13,7 | 9,63 | 105 | Ig heavy chain VIII region CAM PE=1 SV=1 [HV307] |
| P78527 | 25 | 4128 | 468,8 | 7,12 | 105 | DNAdependent protein kinase catalytic subunit GN=PRKDC PE=1 SV=3 [PRKDC] |
| P06744 | 15 | 558 | 63,1 | 8,32 | 105 | Glucose6phosphate isomerase GN=GPI PE=1 SV=4 [G6PI] |
| Q8IVL1 | 10 | 2488 | 268,0 | 9,03 | 104 | Neuron navigator 2 GN=NAV2 PE=1 SV=3 [NAV2] |
| Q8WXG6 | 6 | 1647 | 183,2 | 6,04 | 104 | MAP kinaseactivating death domain protein GN=MADD PE=1 SV=2 [MADD] |
| P80303 | 10 | 420 | 50,2 | 5,12 | 104 | Nucleobindin2 GN=NUCB2 PE=1 SV=2 [NUCB2] |
| P12270 | 20 | 2363 | 267,1 | 5,02 | 103 | Nucleoprotein TPR GN=TPR PE=1 SV=3 [TPR] |
| Q5TBA9 | 17 | 3013 | 338,7 | 5,99 | 103 | Protein furry homolog GN=FRY PE=1 SV=1 [FRY] |
| Q4G0P3 | 23 | 5121 | 575,5 | 6,06 | 103 | Hydrocephalusinducing protein homolog GN=HYDIN PE=1 SV=3 [HYDIN] |
| Q8IUD2 | 21 | 1116 | 128,0 | 5,97 | 103 | ELKS/Rab6interacting/CAST family member 1 GN=ERC1 PE=1 SV=1 [RB6I2] |
| Q92817 | 58 | 2033 | 231,5 | 6,96 | 103 | Envoplakin GN=EVPL PE=1 SV=3 [EVPL] |
| Q6UB99 | 39 | 2663 | 297,7 | 7,11 | 103 | Ankyrin repeat domaincontaining protein 11 GN=ANKRD11 PE=1 SV=3 [ANR11] |
| Q6VAB6 | 15 | 950 | 107,6 | 8,69 | 103 | Kinase suppressor of Ras 2 GN=KSR2 PE=1 SV=2 [KSR2] |
| O14686 | 10 | 5537 | 593,0 | 5,58 | 102 | Histonelysine Nmethyltransferase MLL2 GN=MLL2 PE=1 SV=2 [MLL2] |
| Q8N3K9 | 1 | 4069 | 448,9 | 4,78 | 101 | Cardiomyopathyassociated protein 5 GN=CMYA5 PE=1 SV=3 [CMYA5] |
| A6QL64 | 18 | 1941 | 217,3 | 8,66 | 101 | Ankyrin repeat domaincontaining protein 36A GN=ANKRD36 PE=2 SV=3 [AN36A] |
| Q15413 | 68 | 4870 | 551,7 | 5,68 | 101 | Ryanodine receptor 3 GN=RYR3 PE=1 SV=3 [RYR3] |
| Q5VYS8 | 13 | 1495 | 171,1 | 6,83 | 100 | Terminal uridylyltransferase 7 GN=ZCCHC6 PE=1 SV=1 [TUT7] |
| P16591 | 10 | 822 | 94,6 | 7,14 | 100 | Protooncogene tyrosineprotein kinase FER (EC 2.7.10.2) (p94FER) (cFER) (Tyrosine k |
| Q12756 | 39 | 1690 | 190,9 | 6,21 | 100 | Kinesinlike protein KIF1A GN=KIF1A PE=2 SV=2 [KIF1A] |
| Q99880 | 21 | 126 | 13,9 | 10,32 | 99 | Histone H2B type 1L GN=HIST1H2BL PE=1 SV=3 [H2B1L] |

| | | | | | | |
|---|---|---|---|---|---|---|
| Q02880 | 34 | 1626 | 183,2 | 8,00 | 97 | DNA topoisomerase 2beta GN=TOP2B PE=1 SV=3 [TOP2B] |
| Q9HD33 | 13 | 250 | 29,4 | 10,37 | 97 | 39S ribosomal protein L47, mitochondrial GN=MRPL47 PE=1 SV=2 [RM47] |
| Q13098 | 384 | 491 | 55,5 | 6,74 | 97 | COP9 signalosome complex subunit 1 GN=GPS1 PE=1 SV=4 [CSN1] |
| O75747 | 394 | 1445 | 165,6 | 6,93 | 97 | Phosphatidylinositol4phosphate 3kinase C2 domaincontaining subunit gamma GN= |
| Q2VIQ3 | 68 | 1234 | 139,9 | 6,18 | 96 | Chromosomeassociated kinesin KIF4B GN=KIF4B PE=1 SV=2 [KIF4B] |
| Q9UFH2 | 162 | 4485 | 511,5 | 5,77 | 96 | Dynein heavy chain 17, axonemal GN=DNAH17 PE=2 SV=2 [DYH17] |
| Q96Q89 | 34 | 1820 | 210,5 | 5,67 | 96 | Kinesinlike protein KIF20B GN=KIF20B PE=1 SV=3 [KI20B] |
| P07339 | 37 | 412 | 44,5 | 6,54 | 95 | Cathepsin D GN=CTSD PE=1 SV=1 [CATD] |
| Q9UKN7 | 9 | 3530 | 395,0 | 9,17 | 95 | MyosinXV GN=MYO15A PE=1 SV=2 [MYO15] |
| O14578 | 57 | 2027 | 231,3 | 6,57 | 95 | Citron Rhointeracting kinase GN=CIT PE=1 SV=2 [CTRO] |
| Q9Y4I1 | 447 | 1855 | 215,3 | 8,48 | 95 | MyosinVa GN=MYO5A PE=1 SV=2 [MYO5A] |
| Q9NYC9 | 151 | 4486 | 511,6 | 5,91 | 95 | Dynein heavy chain 9, axonemal GN=DNAH9 PE=1 SV=3 [DYH9] |
| Q5VYK3 | 3 | 1845 | 204,2 | 7,12 | 94 | Proteasomeassociated protein ECM29 homolog GN=ECM29 PE=1 SV=2 [ECM29] |
| Q7Z6Z7 | 14 | 4374 | 481,6 | 5,22 | 94 | E3 ubiquitinprotein ligase HUWE1 GN=HUWE1 PE=1 SV=3 [HUWE1] |
| Q9UM54 | 17 | 1294 | 149,6 | 8,53 | 93 | MyosinVI GN=MYO6 PE=1 SV=4 [MYO6] |
| P35749 | 13 | 1972 | 227,2 | 5,50 | 93 | Myosin11 GN=MYH11 PE=1 SV=3 [MYH11] |
| Q14C86 | 38 | 1478 | 164,9 | 5,22 | 93 | GTPaseactivating protein and VPS9 domaincontaining protein 1 GN=GAPVD1 PE=1 S |
| Q96M86 | 9 | 4753 | 533,3 | 6,71 | 93 | Dynein heavy chain domaincontaining protein 1 GN=DNHD1 PE=1 SV=2 [DNHD1] |
| Q8WZ64 | 26 | 1704 | 193,3 | 7,39 | 93 | ArfGAP with RhoGAP domain, ANK repeat and PH domaincontaining protein 2 GN=A |
| Q96L93 | 3 | 1317 | 151,9 | 6,16 | 93 | Kinesinlike protein KIF16B GN=KIF16B PE=1 SV=2 [KI16B] |
| Q8IZT6 | 1 | 3477 | 409,5 | 10,45 | 92 | Abnormal spindlelike microcephalyassociated protein GN=ASPM PE=1 SV=2 [ASPM |
| Q5SZL2 | 26 | 805 | 91,8 | 6,33 | 92 | Coiledcoil domaincontaining protein C6orf204 GN=C6orf204 PE=2 SV=1 [CF204] |
| A6NNM3 | 73 | 1639 | 180,8 | 6,77 | 92 | RIMSbinding protein 3B GN=RIMBP3B PE=2 SV=3 [RIM3B] |
| Q8NCA5 | 69 | 519 | 55,4 | 9,03 | 92 | Protein FAM98A GN=FAM98A PE=1 SV=1 [FA98A] |
| Q9NS87 | 24 | 1388 | 160,1 | 6,00 | 92 | Kinesinlike protein KIF15 GN=KIF15 PE=1 SV=1 [KIF15] |
| Q63HN8 | 41 | 5207 | 591,0 | 6,48 | 92 | E3 ubiquitinprotein ligase RNF213 GN=RNF213 PE=1 SV=3 [RN213] |
| O43290 | 4 | 800 | 90,2 | 6,13 | 91 | U4/U6.U5 trisnRNPassociated protein 1 GN=SART1 PE=1 SV=1 [SNUT1] |
| O15083 | 18 | 957 | 110,5 | 6,99 | 91 | ERC protein 2 GN=ERC2 PE=1 SV=3 [ERC2] |
| P01625 | 4 | 114 | 12,6 | 7,93 | 90 | Ig kappa chain VIV region Len PE=1 SV=2 [KV402] |
| O15020 | 25 | 2390 | 271,2 | 6,11 | 90 | Spectrin beta chain, brain 2 GN=SPTBN2 PE=1 SV=3 [SPTN2] |
| B2RTY4 | 1 | 2548 | 292,5 | 8,88 | 90 | MyosinIXa GN=MYO9A PE=1 SV=2 [MYO9A] |
| A2VDJ0 | 18 | 1609 | 179,2 | 6,86 | 89 | Transmembrane protein 131like GN=KIAA0922 PE=1 SV=2 [T131L] |
| P06576 | 10 | 529 | 56,5 | 5,40 | 89 | ATP synthase subunit beta, mitochondrial GN=ATP5B PE=1 SV=3 [ATPB] |
| P31629 | 15 | 2446 | 268,9 | 6,96 | 88 | Transcription factor HIVEP2 GN=HIVEP2 PE=1 SV=2 [ZEP2] |
| P13533 | 16 | 1939 | 223,6 | 5,73 | 88 | Myosin6 GN=MYH6 PE=1 SV=5 [MYH6] |
| P05165 | 132 | 728 | 80,0 | 7,52 | 88 | PropionylCoA carboxylase alpha chain, mitochondrial GN=PCCA PE=1 SV=4 [PCCA] |
| P01767 | 52 | 115 | 12,4 | 9,25 | 88 | Ig heavy chain VIII region BUT PE=1 SV=1 [HV306] |
| Q9NQW8 | 15 | 809 | 92,1 | 7,93 | 88 | Cyclic nucleotidegated cation channel beta3 GN=CNGB3 PE=1 SV=2 [CNGB3] |
| P98161 | 178 | 4303 | 462,2 | 6,73 | 87 | Polycystin1 GN=PKD1 PE=1 SV=3 [PKD1] |
| Q9BZF9 | 9 | 1416 | 162,4 | 7,03 | 87 | Uveal autoantigen with coiledcoil domains and ankyrin repeats GN=UACA PE=1 SV= |
| O75122 | 28 | 1294 | 141,0 | 8,47 | 87 | CLIPassociating protein 2 GN=CLASP2 PE=1 SV=2 [CLAP2] |
| O60293 | 116 | 1989 | 226,2 | 8,13 | 87 | Zinc finger C3H1 domaincontaining protein GN=ZFC3H1 PE=1 SV=3 [ZC3H1] |
| Q96QB1 | 53 | 1528 | 170,5 | 6,40 | 87 | Rho GTPaseactivating protein 7 GN=DLC1 PE=1 SV=4 [RHG07] |
| Q8NFC6 | 13 | 3051 | 330,3 | 5,08 | 87 | Biorientation of chromosomes in cell division protein 1like GN=BOD1L PE=1 SV=2 [ |
| Q15652 | 17 | 2540 | 284,3 | 7,87 | 86 | Probable JmjC domaincontaining histone demethylation protein 2C GN=JMJD1C PE |
| Q92614 | 28 | 2054 | 233,0 | 6,30 | 86 | MyosinXVIIIa GN=MYO18A PE=1 SV=3 [MY18A] |
| Q9UQ35 | 19 | 2752 | 299,4 | 12,06 | 86 | Serine/arginine repetitive matrix protein 2 GN=SRRM2 PE=1 SV=2 [SRRM2] |
| P49792 | 59 | 3224 | 358,0 | 6,20 | 85 | E3 SUMOprotein ligase RanBP2 GN=RANBP2 PE=1 SV=2 [RBP2] |
| Q96DT5 | 69 | 4523 | 520,7 | 6,44 | 84 | Dynein heavy chain 11, axonemal GN=DNAH11 PE=1 SV=3 [DYH11] |
| Q14679 | 27 | 1199 | 133,3 | 8,85 | 84 | Tubulin polyglutamylase TTLL4 GN=TTLL4 PE=1 SV=2 [TTLL4] |
| Q9UN79 | 23 | 622 | 69,2 | 6,71 | 84 | Transcription factor SOX13 GN=SOX13 PE=1 SV=3 [SOX13] |
| P07951 | 8 | 284 | 32,8 | 4,70 | 84 | Tropomyosin beta chain (Tropomyosin 2) (Betatropomyosin) [TPM2] |
| A2RUB6 | 91 | 948 | 109,3 | 8,25 | 84 | Coiledcoil domaincontaining protein 66 GN=CCDC66 PE=1 SV=4 [CCD66] |
| Q96T17 | 62 | 732 | 81,9 | 8,84 | 84 | MAP7 domaincontaining protein 2 GN=MAP7D2 PE=1 SV=2 [MA7D2] |
| P30040 | 21 | 261 | 29,0 | 7,31 | 83 | Endoplasmic reticulum resident protein 29 GN=ERP29 PE=1 SV=4 [ERP29] |
| Q9NR99 | 46 | 2828 | 312,0 | 8,32 | 83 | Matrixremodelingassociated protein 5 GN=MXRA5 PE=2 SV=3 [MXRA5] |
| Q9Y283 | 17 | 1065 | 117,8 | 9,35 | 83 | Inversin GN=INVS PE=1 SV=2 [INVS] |
| Q5VU43 | 24 | 2346 | 264,9 | 5,44 | 83 | Myomegalin GN=PDE4DIP PE=1 SV=1 [MYOME] |
| Q0VDD8 | 5 | 3507 | 399,6 | 6,93 | 83 | Dynein heavy chain 14, axonemal GN=DNAH14 PE=2 SV=3 [DYH14] |
| Q86VI3 | 13 | 1631 | 184,6 | 7,65 | 83 | Ras GTPaseactivatinglike protein IQGAP3 GN=IQGAP3 PE=1 SV=2 [IQGA3] |
| Q96JB1 | 69 | 4490 | 514,3 | 6,32 | 83 | Dynein heavy chain 8, axonemal GN=DNAH8 PE=1 SV=2 [DYH8] |
| Q05D60 | 428 | 604 | 70,9 | 6,21 | 83 | Coiledcoil domaincontaining protein 67 GN=CCDC67 PE=2 SV=2 [CCD67] |
| Q7Z7A1 | 7 | 2325 | 268,7 | 5,55 | 82 | Centriolin GN=CEP110 PE=1 SV=2 [CE110] |
| P47895 | 17 | 512 | 56,1 | 7,25 | 82 | Aldehyde dehydrogenase family 1 member A3 GN=ALDH1A3 PE=1 SV=2 [AL1A3] |
| Q9H1J1 | 8 | 476 | 54,7 | 9,03 | 82 | Regulator of nonsense transcripts 3A GN=UPF3A PE=1 SV=1 [REN3A] |

| | | | | | | |
|---|---|---|---|---|---|---|
| Q7Z5Q5 | 76 | 900 | 100,2 | 8,29 | 82 | DNA polymerase nu GN=POLN PE=1 SV=2 [DPOLN] |
| P01624 | 27 | 109 | 11,9 | 8,94 | 82 | Ig kappa chain VIII region POM PE=1 SV=1 [KV306] |
| A4D1E1 | 1 | 1349 | 152,5 | 8,54 | 82 | Zinc finger protein 804B GN=ZNF804B PE=1 SV=2 [Z804B] |
| P05787 | 4 | 483 | 53,7 | 5,59 | 82 | Keratin, type II cytoskeletal 8 GN=KRT8 PE=1 SV=7 [K2C8] |
| Q07954 | 10 | 4544 | 504,3 | 5,39 | 81 | Prolowdensity lipoprotein receptorrelated protein 1 GN=LRP1 PE=1 SV=2 [LRP1] |
| Q96Q15 | 1 | 3661 | 410,2 | 6,46 | 81 | Serine/threonineprotein kinase SMG1 GN=SMG1 PE=1 SV=3 [SMG1] |
| P20742 | 11 | 1482 | 163,8 | 6,38 | 81 | Pregnancy zone protein GN=PZP PE=1 SV=4 [PZP] |
| P57071 | 47 | 1507 | 169,2 | 8,24 | 81 | PR domain zinc finger protein 15 GN=PRDM15 PE=2 SV=4 [PRD15] |
| Q8TDN4 | 1 | 633 | 67,6 | 9,17 | 81 | CDK5 and ABL1 enzyme substrate 1 GN=CABLES1 PE=1 SV=2 [CABL1] |
| Q86UK5 | 3 | 1308 | 147,9 | 6,96 | 81 | Limbin GN=EVC2 PE=1 SV=1 [LBN] |
| Q15811 | 14 | 1721 | 195,3 | 7,77 | 80 | Intersectin1 GN=ITSN1 PE=1 SV=3 [ITSN1] |
| P33151 | 19 | 784 | 87,5 | 5,43 | 79 | Cadherin5 GN=CDH5 PE=1 SV=5 [CADH5] |
| Q9H3R1 | 31 | 872 | 100,7 | 7,55 | 79 | Bifunctional heparan sulfate Ndeacetylase/Nsulfotransferase 4 GN=NDST4 PE=2 SV |
| Q96T21 | 70 | 854 | 95,4 | 8,12 | 79 | Selenocysteine insertion sequencebinding protein 2 GN=SECISBP2 PE=1 SV=2 [SEBI |
| Q6ZT98 | 8 | 887 | 102,9 | 9,29 | 79 | Tubulin polyglutamylase TTLL7 GN=TTLL7 PE=2 SV=2 [TTLL7] |
| Q15154 | 28 | 2024 | 228,4 | 5,02 | 78 | Pericentriolar material 1 protein GN=PCM1 PE=1 SV=4 [PCM1] |
| Q70CQ4 | 20 | 1352 | 146,6 | 9,22 | 78 | Ubiquitin carboxylterminal hydrolase 31 GN=USP31 PE=1 SV=2 [UBP31] |
| Q9NRZ9 | 97 | 838 | 97,0 | 7,93 | 78 | Lymphoidspecific helicase GN=HELLS PE=1 SV=1 [HELLS] |
| Q9NQ38 | 22 | 1064 | 120,6 | 8,06 | 78 | Serine protease inhibitor Kazaltype 5 GN=SPINK5 PE=1 SV=2 [ISK5] |
| P48634 | 15 | 2157 | 228,7 | 9,45 | 77 | Large prolinerich protein BAT2 GN=BAT2 PE=1 SV=3 [BAT2] |
| Q6ZU35 | 50 | 1233 | 136,7 | 5,60 | 77 | Uncharacterized protein KIAA1211 GN=KIAA1211 PE=1 SV=3 [K1211] |
| P78559 | 13 | 2803 | 305,3 | 4,92 | 77 | Microtubuleassociated protein 1A GN=MAP1A PE=1 SV=6 [MAP1A] |
| Q14722 | 10 | 419 | 46,5 | 8,94 | 77 | Voltagegated potassium channel subunit beta1 GN=KCNAB1 PE=2 SV=1 [KCAB1] |
| P54652 | 6 | 639 | 70,0 | 5,74 | 77 | Heat shockrelated 70 kDa protein 2 GN=HSPA2 PE=1 SV=1 [HSP72] |
| O15066 | 13 | 747 | 85,1 | 7,69 | 77 | Kinesinlike protein KIF3B GN=KIF3B PE=1 SV=1 [KIF3B] |
| O95071 | 20 | 2799 | 309,2 | 5,85 | 76 | E3 ubiquitinprotein ligase UBR5 GN=UBR5 PE=1 SV=2 [UBR5] |
| Q8TF72 | 21 | 1996 | 216,7 | 7,80 | 76 | Protein Shroom3 GN=SHROOM3 PE=1 SV=2 [SHRM3] |
| Q14566 | 7 | 821 | 92,8 | 5,41 | 76 | DNA replication licensing factor MCM6 GN=MCM6 PE=1 SV=1 [MCM6] |
| Q14966 | 10 | 1978 | 220,5 | 6,38 | 76 | Zinc finger protein 638 GN=ZNF638 PE=1 SV=2 [ZN638] |
| O43149 | 4 | 2961 | 330,9 | 5,95 | 76 | Zinc finger ZZtype and EFhand domaincontaining protein 1 GN=ZZEF1 PE=1 SV=6 [ZZ |
| P12883 | 18 | 1935 | 223,0 | 5,80 | 76 | Myosin7 GN=MYH7 PE=1 SV=5 [MYH7] |
| Q86UQ4 | 5 | 5058 | 575,8 | 6,46 | 75 | ATPbinding cassette subfamily A member 13 GN=ABCA13 PE=2 SV=3 [ABCAD] |
| Q9UPZ9 | 442 | 632 | 71,4 | 9,77 | 75 | Serine/threonineprotein kinase ICK GN=ICK PE=1 SV=1 [ICK] |
| Q5T200 | 11 | 1668 | 196,5 | 9,42 | 74 | Zinc finger CCCH domaincontaining protein 13 GN=ZC3H13 PE=1 SV=1 [ZC3HD] |
| Q8N2N9 | 9 | 1353 | 153,5 | 8,85 | 74 | Ankyrin repeat domaincontaining protein 36B GN=ANKRD36B PE=2 SV=4 [AN36B] |
| P07195 | 2 | 334 | 36,6 | 6,05 | 74 | Llactate dehydrogenase B chain (EC 1.1.1.27) (LDHB) (LDH heart subunit) (LDHH) (Re |
| Q5TAX3 | 28 | 1644 | 185,0 | 7,97 | 74 | Terminal uridylyltransferase 4 GN=ZCCHC11 PE=1 SV=3 [TUT4] |
| Q6ZUT3 | 28 | 714 | 81,6 | 7,90 | 74 | FERM domaincontaining protein 7 GN=FRMD7 PE=1 SV=1 [FRMD7] |
| Q5VZK9 | 28 | 1371 | 151,5 | 7,85 | 74 | Leucinerich repeatcontaining protein 16A GN=LRRC16A PE=1 SV=1 [LR16A] |
| Q5TCS8 | 10 | 1911 | 221,3 | 5,01 | 74 | Adenylate kinase domaincontaining protein 1 GN=AKD1 PE=1 SV=2 [AKD1] |
| Q5JR59 | 11 | 1369 | 150,1 | 6,68 | 74 | Microtubuleassociated tumor suppressor candidate 2 GN=MTUS2 PE=1 SV=3 [MTUS |
| Q9UBC5 | 8 | 1043 | 118,3 | 9,31 | 73 | MyosinIa GN=MYO1A PE=1 SV=1 [MYO1A] |
| Q9Y4D8 | 25 | 3996 | 439,1 | 6,19 | 73 | Probable E3 ubiquitinprotein ligase C12orf51 GN=C12orf51 PE=1 SV=5 [K0614] |
| Q6IPM2 | 2 | 695 | 77,3 | 9,07 | 73 | IQ domaincontaining protein E GN=IQCE PE=1 SV=2 [IQCE] |
| Q5JU85 | 24 | 1478 | 161,6 | 8,56 | 73 | IQ motif and SEC7 domaincontaining protein 2 GN=IQSEC2 PE=1 SV=1 [IQEC2] |
| Q14571 | 58 | 2701 | 307,9 | 6,43 | 73 | Inositol 1,4,5trisphosphate receptor type 2 GN=ITPR2 PE=1 SV=2 [ITPR2] |
| Q15147 | 63 | 1175 | 134,4 | 6,90 | 73 | 1phosphatidylinositol4,5bisphosphate phosphodiesterase beta4 GN=PLCB4 PE=1 SV |
| Q07864 | 60 | 2286 | 261,4 | 6,39 | 73 | DNA polymerase epsilon catalytic subunit A GN=POLE PE=1 SV=5 [DPOE1] |
| Q9Y4C0 | 22 | 1643 | 180,5 | 5,54 | 72 | Neurexin3alpha GN=NRXN3 PE=2 SV=4 [NRX3A] |
| O60449 | 6 | 1722 | 198,2 | 6,67 | 72 | Lymphocyte antigen 75 GN=LY75 PE=1 SV=3 [LY75] |
| P11142 | 6 | 646 | 70,9 | 5,52 | 72 | Heat shock cognate 71 kDa protein GN=HSPA8 PE=1 SV=1 [HSP7C] |
| P06313 | 26 | 133 | 14,6 | 6,58 | 72 | Ig kappa chain VIV region JI PE=4 SV=1 [KV403] |
| Q86WI1 | 79 | 4243 | 465,4 | 6,11 | 72 | FibrocystinL GN=PKHD1L1 PE=2 SV=2 [PKHL1] |
| Q13023 | 11 | 2319 | 256,6 | 5,01 | 72 | Akinase anchor protein 6 GN=AKAP6 PE=1 SV=3 [AKAP6] |
| Q8IWZ3 | 220 | 2542 | 269,3 | 5,73 | 72 | Ankyrin repeat and KH domaincontaining protein 1 GN=ANKHD1 PE=1 SV=1 [ANKH1 |
| Q8N9T8 | 18 | 709 | 83,2 | 5,17 | 72 | Protein KRI1 homolog GN=KRI1 PE=1 SV=2 [KRI1] |
| O60673 | 10 | 3130 | 352,6 | 8,47 | 72 | DNA polymerase zeta catalytic subunit GN=REV3L PE=1 SV=2 [DPOLZ] |
| O75185 | 52 | 946 | 103,1 | 5,66 | 72 | Calciumtransporting ATPase type 2C member 2 GN=ATP2C2 PE=1 SV=2 [AT2C2] |
| Q2LD37 | 1 | 5005 | 555,1 | 6,58 | 72 | Uncharacterized protein KIAA1109 GN=KIAA1109 PE=1 SV=2 [K1109] |
| Q99490 | 244 | 1192 | 124,6 | 9,89 | 71 | Centauringamma 1 (ARFGAP with GTPbinding proteinlike, ankyrin repeat and plecks |
| Q9NNX1 | 12 | 390 | 44,2 | 6,00 | 71 | Tuftelin GN=TUFT1 PE=2 SV=1 [TUFT1] |
| O95359 | 9 | 2948 | 309,2 | 4,79 | 71 | Transforming acidic coiledcoilcontaining protein 2 GN=TACC2 PE=1 SV=3 [TACC2] |
| Q7Z2W7 | 46 | 1104 | 127,6 | 7,24 | 71 | Transient receptor potential cation channel subfamily M member 8 GN=TRPM8 PE= |
| Q8NCU4 | 12 | 936 | 110,5 | 9,60 | 71 | Coiledcoil domaincontaining protein KIAA1407 GN=KIAA1407 PE=2 SV=1 [K1407] |
| Q70UQ0 | 19 | 350 | 39,3 | 9,17 | 71 | Inhibitor of nuclear factor kappaB kinaseinteracting protein GN=IKBIP PE=1 SV=1 [I |

| | | | | | | |
|---|---|---|---|---|---|---|
| Q86UP2 | 1 | 1357 | 156,2 | 5,64 | 70 | Kinectin GN=KTN1 PE=1 SV=1 [KTN1] |
| Q9UPV0 | 11 | 1460 | 164,2 | 5,36 | 70 | Centrosomal protein of 164 kDa GN=CEP164 PE=1 SV=3 [CE164] |
| P61164 | 35 | 376 | 42,6 | 6,64 | 70 | Alphacentractin GN=Actr1a PE=2 SV=1 [ACTZ] |
| Q86Y38 | 11 | 959 | 107,5 | 9,22 | 70 | Xylosyltransferase 1 GN=XYLT1 PE=1 SV=1 [XYLT1] |
| Q9HCD6 | 10 | 1990 | 219,5 | 8,07 | 70 | Protein TANC2 GN=TANC2 PE=1 SV=3 [TANC2] |
| Q8IUG5 | 21 | 2567 | 285,0 | 6,90 | 70 | MyosinXVIIIb GN=MYO18B PE=1 SV=1 [MY18B] |
| Q9HCC0 | 11 | 563 | 61,3 | 7,68 | 70 | MethylcrotonoylCoA carboxylase beta chain, mitochondrial GN=MCCC2 PE=1 SV=1 |
| Q86UR5 | 1 | 1692 | 189,0 | 9,66 | 70 | Regulating synaptic membrane exocytosis protein 1 GN=RIMS1 PE=1 SV=1 [RIMS1] |
| P07602 | 11 | 524 | 58,1 | 5,17 | 70 | Proactivator polypeptide GN=PSAP PE=1 SV=2 [SAP] |
| Q6AWC2 | 11 | 1192 | 133,8 | 5,53 | 70 | Protein WWC2 GN=WWC2 PE=1 SV=2 [WWC2] |
| Q9NZM3 | 9 | 1697 | 193,3 | 8,12 | 70 | Intersectin2 GN=ITSN2 PE=1 SV=3 [ITSN2] |
| O60237 | 2 | 982 | 110,3 | 5,67 | 70 | Protein phosphatase 1 regulatory subunit 12B GN=PPP1R12B PE=1 SV=2 [MYPT2] |
| Q8IV32 | 21 | 467 | 49,6 | 11,80 | 69 | Coiledcoil domaincontaining protein 71 GN=CCDC71 PE=2 SV=3 [CCD71] |
| Q13427 | 41 | 754 | 88,6 | 10,29 | 69 | Peptidylprolyl cistrans isomerase G GN=PPIG PE=1 SV=2 [PPIG] |
| Q14126 | 15 | 1118 | 122,2 | 5,24 | 69 | Desmoglein2 GN=DSG2 PE=1 SV=2 [DSG2] |
| P35251 | 9 | 1148 | 128,2 | 9,36 | 69 | Replication factor C subunit 1 GN=RFC1 PE=1 SV=4 [RFC1] |
| Q9H6T3 | 34 | 665 | 75,7 | 6,84 | 69 | RNA polymerase IIassociated protein 3 GN=RPAP3 PE=1 SV=2 [RPAP3] |
| P07384 | 1 | 714 | 81,8 | 5,67 | 69 | Calpain1 catalytic subunit GN=CAPN1 PE=1 SV=1 [CAN1] |
| Q6WRI0 | 65 | 2623 | 290,7 | 9,13 | 69 | Immunoglobulin superfamily member 10 GN=IGSF10 PE=1 SV=1 [IGS10] |
| Q5VVW2 | 2 | 1013 | 112,8 | 7,65 | 68 | GTPaseactivating Rap/RanGAP domainlike protein 3 GN=GARNL3 PE=1 SV=2 [GARL3 |
| Q6PGP7 | 15 | 1564 | 175,4 | 7,53 | 68 | Tetratricopeptide repeat protein 37 GN=TTC37 PE=1 SV=1 [TTC37] |
| Q8NBS3 | 10 | 891 | 99,5 | 7,68 | 68 | Sodium bicarbonate transporterlike protein 11 GN=SLC4A11 PE=1 SV=2 [S4A11] |
| P19237 | 61 | 187 | 21,7 | 9,58 | 68 | Troponin I, slow skeletal muscle GN=TNNI1 PE=1 SV=3 [TNNI1] |
| Q3SY84 | 13 | 523 | 57,3 | 6,61 | 68 | Keratin, type II cytoskeletal 71 GN=KRT71 PE=1 SV=3 [K2C71] |
| Q7Z7B0 | 5 | 1213 | 138,0 | 8,32 | 68 | FilaminAinteracting protein 1 GN=FILIP1 PE=1 SV=1 [FLIP1] |
| Q9ULU4 | 40 | 1186 | 131,6 | 7,20 | 68 | Protein kinase Cbinding protein 1 GN=ZMYND8 PE=1 SV=2 [PKCB1] |
| Q96L96 | 12 | 1907 | 201,1 | 7,58 | 67 | Alphaprotein kinase 3 GN=ALPK3 PE=2 SV=2 [ALPK3] |
| P06737 | 3 | 847 | 97,1 | 7,17 | 67 | Glycogen phosphorylase, liver form GN=PYGL PE=1 SV=4 [PYGL] |
| Q5VVJ2 | 435 | 828 | 95,0 | 5,53 | 67 | Histone H2A deubiquitinase MYSM1 GN=MYSM1 PE=1 SV=1 [MYSM1] |
| Q96M83 | 10 | 486 | 55,7 | 7,78 | 67 | Coiledcoil domaincontaining protein 7 GN=CCDC7 PE=2 SV=2 [CCDC7] |
| Q9NSB2 | 114 | 600 | 64,8 | 7,56 | 67 | Keratin, type II cuticular Hb4 GN=KRT84 PE=1 SV=2 [KRT84] |
| O95197 | 65 | 1032 | 112,5 | 4,96 | 66 | Reticulon3 GN=RTN3 PE=1 SV=2 [RTN3] |
| Q96N67 | 357 | 2140 | 242,4 | 6,80 | 66 | Dedicator of cytokinesis protein 7 GN=DOCK7 PE=1 SV=4 [DOCK7] |
| Q86SR1 | 44 | 603 | 68,9 | 8,59 | 66 | Polypeptide Nacetylgalactosaminyltransferase 10 GN=GALNT10 PE=1 SV=2 [GLT10] |
| O60333 | 30 | 1816 | 204,3 | 5,60 | 66 | Kinesinlike protein KIF1B GN=KIF1B PE=1 SV=5 [KIF1B] |
| P12955 | 13 | 493 | 54,5 | 6,00 | 66 | XaaPro dipeptidase GN=PEPD PE=1 SV=3 [PEPD] |
| O15042 | 52 | 1029 | 118,2 | 8,47 | 66 | U2associated protein SR140 GN=SR140 PE=1 SV=2 [SR140] |
| Q9BXX2 | 24 | 1392 | 157,9 | 6,35 | 66 | Ankyrin repeat domaincontaining protein 30B GN=ANKRD30B PE=2 SV=3 [AN30B] |
| Q86VF7 | 70 | 1730 | 197,0 | 9,20 | 66 | Nebulinrelatedanchoring protein GN=NRAP PE=2 SV=2 [NRAP] |
| Q08378 | 12 | 1498 | 167,3 | 5,44 | 66 | Golgin subfamily A member 3 GN=GOLGA3 PE=1 SV=2 [GOGA3] |
| Q9UHN6 | 29 | 1383 | 154,3 | 8,15 | 66 | Transmembrane protein 2 GN=TMEM2 PE=1 SV=1 [TMEM2] |
| Q9H4L7 | 122 | 1026 | 117,3 | 5,55 | 66 | SWI/SNFrelated matrixassociated actindependent regulator of chromatin subfamily |
| Q8NDM7 | 8 | 1665 | 191,9 | 5,99 | 66 | WD repeatcontaining protein C10orf79 GN=C10orf79 PE=2 SV=3 [CJ079] |
| O60281 | 17 | 2723 | 304,6 | 7,39 | 66 | Zinc finger protein 292 GN=ZNF292 PE=1 SV=3 [ZN292] |
| Q5KSL6 | 467 | 1271 | 141,7 | 5,53 | 66 | Diacylglycerol kinase kappa GN=DGKK PE=1 SV=1 [DGKK] |
| Q99575 | 4 | 1024 | 114,6 | 9,22 | 65 | Ribonucleases P/MRP protein subunit POP1 GN=POP1 PE=1 SV=2 [POP1] |
| A5PLK6 | 35 | 1076 | 125,6 | 9,01 | 65 | Regulator of Gprotein signaling proteinlike GN=RGSL1 PE=2 SV=1 [RGSL] |
| Q9UPW8 | 5 | 1703 | 192,9 | 5,35 | 65 | Protein unc13 homolog A GN=UNC13A PE=2 SV=4 [UN13A] |
| Q8TC20 | 1 | 777 | 90,2 | 5,29 | 65 | Cancerassociated gene 1 protein GN=CAGE1 PE=2 SV=2 [CAGE1] |
| Q92973 | 150 | 898 | 102,3 | 4,98 | 65 | Transportin1 GN=TNPO1 PE=1 SV=2 [TNPO1] |
| Q9BQ52 | 122 | 826 | 92,2 | 7,90 | 65 | Zinc phosphodiesterase ELAC protein 2 GN=ELAC2 PE=1 SV=2 [RNZ2] |
| Q8N4C6 | 19 | 2090 | 243,1 | 5,03 | 65 | Ninein GN=NIN PE=1 SV=4 [NIN] |
| P19174 | 66 | 1290 | 148,4 | 6,05 | 65 | 1phosphatidylinositol4,5bisphosphate phosphodiesterase gamma1 GN=PLCG1 PE= |
| Q5T2S8 | 28 | 1044 | 115,6 | 7,77 | 65 | Armadillo repeatcontaining protein 4 GN=ARMC4 PE=2 SV=1 [ARMC4] |
| Q96SI9 | 10 | 672 | 73,6 | 8,72 | 65 | Spermatid perinuclear RNAbinding protein GN=STRBP PE=1 SV=1 [STRBP] |
| Q9BYJ4 | 19 | 488 | 56,8 | 7,44 | 65 | Tripartite motifcontaining protein 34 GN=TRIM34 PE=1 SV=2 [TRI34] |
| Q86UP3 | 5 | 3567 | 393,5 | 6,37 | 65 | Zinc finger homeobox protein 4 GN=ZFHX4 PE=1 SV=1 [ZFHX4] |
| P20591 | 14 | 662 | 75,5 | 5,83 | 65 | Interferoninduced GTPbinding protein Mx1 GN=MX1 PE=1 SV=4 [MX1] |
| Q8NDI1 | 1 | 1231 | 139,9 | 5,35 | 65 | EH domainbinding protein 1 GN=EHBP1 PE=1 SV=3 [EHBP1] |
| Q96C24 | 3 | 671 | 76,0 | 8,98 | 64 | Synaptotagminlike protein 4 GN=SYTL4 PE=1 SV=2 [SYTL4] |
| P35712 | 22 | 828 | 91,9 | 7,78 | 64 | Transcription factor SOX6 GN=SOX6 PE=1 SV=3 [SOX6] |
| A6NKT7 | 55 | 1758 | 197,4 | 6,33 | 64 | RanBP2like and GRIP domaincontaining protein 3 GN=RGPD3 PE=2 SV=2 [RGPD3] |
| Q14678 | 12 | 1352 | 147,2 | 5,30 | 64 | KN motif and ankyrin repeat domaincontaining protein 1 GN=KANK1 PE=1 SV=3 [KA |
| Q6ZN28 | 17 | 852 | 96,6 | 6,90 | 64 | Metastasisassociated in colon cancer protein 1 GN=MACC1 PE=1 SV=2 [MACC1] |
| P52907 | 99 | 286 | 32,9 | 5,69 | 64 | Factincapping protein subunit alpha1 GN=CAPZA1 PE=1 SV=3 [CAZA1] |

| | | | | | | |
|---|---|---|---|---|---|---|
| Q9C099 | 8 | 1032 | 119,5 | 5,88 | 64 | Leucinerich repeat and coiledcoil domaincontaining protein 1 GN=LRRCC1 PE=2 SV= |
| P19013 | 15 | 534 | 57,2 | 6,61 | 64 | Keratin, type II cytoskeletal 4 GN=KRT4 PE=1 SV=4 [K2C4] |
| Q9HC62 | 72 | 589 | 67,8 | 9,48 | 64 | Sentrinspecific protease 2 GN=SENP2 PE=1 SV=3 [SENP2] |
| Q86TE4 | 363 | 346 | 38,9 | 8,73 | 64 | Leucine zipper protein 2 GN=LUZP2 PE=2 SV=2 [LUZP2] |
| Q8IYE0 | 24 | 955 | 112,7 | 8,48 | 64 | Coiledcoil domaincontaining protein 146 GN=CCDC146 PE=2 SV=2 [CC146] |
| P30613 | 15 | 574 | 61,8 | 7,74 | 63 | Pyruvate kinase isozymes R/L GN=PKLR PE=1 SV=2 [KPYR] |
| Q9P219 | 4 | 2028 | 228,1 | 6,23 | 63 | Protein Daple GN=CCDC88C PE=1 SV=3 [DAPLE] |
| Q68CJ6 | 48 | 796 | 91,1 | 8,63 | 63 | GTPase SLIPGC GN=C8orf80 PE=1 SV=3 [SLIP] |
| Q8IXZ2 | 1 | 948 | 101,9 | 10,95 | 63 | Zinc finger CCCH domaincontaining protein 3 GN=ZC3H3 PE=1 SV=3 [ZC3H3] |
| Q9BSK4 | 25 | 669 | 73,6 | 6,07 | 63 | Protein fem1 homolog A GN=FEM1A PE=1 SV=1 [FEM1A] |
| A2RUR9 | 10 | 1427 | 165,0 | 5,36 | 63 | Coiledcoil domaincontaining protein 144A GN=CCDC144A PE=1 SV=1 [C144A] |
| Q9C0C9 | 7 | 1292 | 141,2 | 5,12 | 63 | Ubiquitinconjugating enzyme E2 O GN=UBE2O PE=1 SV=3 [UBE2O] |
| Q8IWN7 | 29 | 2480 | 261,0 | 4,41 | 63 | Retinitis pigmentosa 1like 1 protein GN=RP1L1 PE=1 SV=4 [RP1L1] |
| Q6ZU80 | 1 | 1094 | 127,9 | 6,52 | 63 | Uncharacterized protein C14orf145 GN=C14orf145 PE=1 SV=2 [CN145] |
| Q15003 | 35 | 741 | 82,5 | 5,06 | 63 | Condensin complex subunit 2 GN=NCAPH PE=1 SV=3 [CND2] |
| Q86XP1 | 8 | 1220 | 134,8 | 6,54 | 63 | Diacylglycerol kinase eta (EC 2.7.1.107) (Diglyceride kinase eta) (DGKeta) (DAG kinas |
| O75460 | 17 | 977 | 109,7 | 6,42 | 63 | Serine/threonineprotein kinase/endoribonuclease IRE1 GN=ERN1 PE=1 SV=2 [ERN1 |
| O75096 | 11 | 1905 | 211,9 | 5,27 | 63 | Lowdensity lipoprotein receptorrelated protein 4 GN=LRP4 PE=1 SV=4 [LRP4] |
| Q99456 | 23 | 494 | 53,5 | 4,78 | 63 | Keratin, type I cytoskeletal 12 GN=KRT12 PE=1 SV=1 [K1C12] |
| O15021 | 1 | 2626 | 284,2 | 8,62 | 63 | Microtubuleassociated serine/threonineprotein kinase 4 GN=MAST4 PE=1 SV=3 [M |
| P35498 | 11 | 2009 | 228,8 | 5,81 | 62 | Sodium channel protein type 1 subunit alpha GN=SCN1A PE=1 SV=2 [SCN1A] |
| Q86VQ6 | 438 | 682 | 74,8 | 8,22 | 62 | Thioredoxin reductase 3 (Fragment) GN=TXNRD3 PE=1 SV=3 [TRXR3] |
| Q9P2D1 | 41 | 2997 | 335,7 | 6,34 | 62 | ChromodomainhelicaseDNAbinding protein 7 GN=CHD7 PE=1 SV=3 [CHD7] |
| Q99698 | 1 | 3801 | 428,9 | 6,61 | 62 | Lysosomaltrafficking regulator GN=LYST PE=1 SV=3 [LYST] |
| Q5THJ4 | 4 | 4387 | 491,5 | 6,58 | 62 | Vacuolar protein sortingassociated protein 13D GN=VPS13D PE=1 SV=1 [VP13D] |
| Q15560 | 6 | 299 | 33,6 | 9,13 | 62 | Transcription elongation factor A protein 2 GN=TCEA2 PE=1 SV=1 [TCEA2] |
| Q8IYW2 | 75 | 2715 | 303,3 | 7,36 | 62 | Tetratricopeptide repeat protein 40 GN=TTC40 PE=2 SV=3 [TTC40] |
| Q15858 | 9 | 1988 | 226,2 | 6,93 | 62 | Sodium channel protein type 9 subunit alpha GN=SCN9A PE=1 SV=3 [SCN9A] |
| P10632 | 38 | 490 | 55,8 | 8,50 | 62 | Cytochrome P450 2C8 GN=CYP2C8 PE=1 SV=2 [CP2C8] |
| P52948 | 16 | 1817 | 197,5 | 6,40 | 62 | Nuclear pore complex protein Nup98Nup96 GN=NUP98 PE=1 SV=4 [NUP98] |
| Q92667 | 95 | 903 | 97,3 | 4,94 | 62 | Akinase anchor protein 1, mitochondrial GN=AKAP1 PE=1 SV=1 [AKAP1] |
| Q96NB3 | 13 | 372 | 42,0 | 5,31 | 62 | Zinc finger protein 830 GN=ZNF830 PE=1 SV=2 [ZN830] |
| Q9H582 | 412 | 1327 | 149,5 | 8,16 | 62 | Zinc finger protein 644 GN=ZNF644 PE=1 SV=2 [ZN644] |
| P30046 | 2 | 118 | 12,7 | 7,30 | 62 | Ddopachrome decarboxylase GN=DDT PE=1 SV=3 [DOPD] |
| Q9BYB0 | 1 | 1741 | 186,2 | 9,03 | 62 | SH3 and multiple ankyrin repeat domains protein 3 GN=SHANK3 PE=1 SV=2 [SHAN3 |
| Q9ULD0 | 46 | 1010 | 114,4 | 6,65 | 62 | 2oxoglutarate dehydrogenaselike, mitochondrial GN=OGDHL PE=2 SV=3 [OGDHL] |
| Q8IY85 | 54 | 973 | 110,1 | 6,57 | 62 | EFhand domaincontaining protein C17orf57 GN=C17orf57 PE=2 SV=2 [CQ057] |
| O94913 | 6 | 1555 | 172,9 | 8,48 | 62 | PremRNA cleavage complex 2 protein Pcf11 GN=PCF11 PE=1 SV=3 [PCF11] |
| Q8IZF0 | 24 | 1738 | 200,2 | 8,68 | 61 | Sodium leak channel nonselective protein GN=NALCN PE=1 SV=1 [NALCN] |
| Q9NRG4 | 40 | 433 | 49,7 | 6,71 | 61 | SET and MYND domaincontaining protein 2 GN=SMYD2 PE=1 SV=2 [SMYD2] |
| B7ZAP0 | 8 | 253 | 29,0 | 5,33 | 61 | Rab GTPaseactivating protein 1like, isoform 10 GN=RABGAP1L PE=2 SV=1 [RBG10] |
| Q5TCY1 | 34 | 1321 | 142,6 | 5,60 | 61 | Tautubulin kinase 1 GN=TTBK1 PE=1 SV=2 [TTBK1] |
| Q5TB80 | 7 | 1403 | 161,8 | 5,47 | 61 | Protein QN1 homolog GN=KIAA1009 PE=1 SV=2 [QN1] |
| P46063 | 3 | 649 | 73,4 | 7,88 | 61 | ATPdependent DNA helicase Q1 GN=RECQL PE=1 SV=3 [RECQ1] |
| Q7RTX0 | 35 | 852 | 93,3 | 7,14 | 60 | Taste receptor type 1 member 3 GN=TAS1R3 PE=1 SV=2 [TS1R3] |
| Q8IV76 | 4 | 773 | 87,4 | 5,07 | 60 | PAS domaincontaining protein 1 GN=PASD1 PE=2 SV=1 [PASD1] |
| O60603 | 90 | 784 | 89,8 | 6,61 | 60 | Tolllike receptor 2 GN=TLR2 PE=1 SV=1 [TLR2] |
| Q96C45 | 1 | 1275 | 142,4 | 6,29 | 60 | Serine/threonineprotein kinase ULK4 GN=ULK4 PE=2 SV=2 [ULK4] |
| Q7Z478 | 7 | 1369 | 155,1 | 8,09 | 60 | ATPdependent RNA helicase DHX29 GN=DHX29 PE=1 SV=2 [DHX29] |
| Q6ZS81 | 5 | 3184 | 353,4 | 6,32 | 60 | WD repeat and FYVE domaincontaining protein 4 GN=WDFY4 PE=1 SV=3 [WDFY4] |
| Q6P3X8 | 18 | 592 | 68,0 | 8,54 | 60 | PiggyBac transposable elementderived protein 2 GN=PGBD2 PE=2 SV=1 [PGBD2] |
| Q5T0Z8 | 73 | 1188 | 124,0 | 9,45 | 60 | Uncharacterized protein C6orf132 GN=C6orf132 PE=1 SV=4 [CF132] |
| P15121 | 9 | 316 | 35,8 | 6,98 | 60 | Aldose reductase GN=AKR1B1 PE=1 SV=3 [ALDR] |
| Q9UPX8 | 8 | 1470 | 158,7 | 6,90 | 60 | SH3 and multiple ankyrin repeat domains protein 2 GN=SHANK2 PE=1 SV=3 [SHAN2 |
| Q13075 | 24 | 1403 | 159,5 | 5,99 | 60 | Baculoviral IAP repeatcontaining protein 1 GN=NAIP PE=1 SV=3 [BIRC1] |
| P01780 | 42 | 115 | 12,6 | 9,29 | 60 | Ig heavy chain VIII region JON [HV319] |
| Q8IZD9 | 109 | 2030 | 233,0 | 6,98 | 60 | Dedicator of cytokinesis protein 3 GN=DOCK3 PE=1 SV=1 [DOCK3] |
| P61161 | 23 | 394 | 44,7 | 6,74 | 60 | Actinrelated protein 2 GN=Actr2 PE=1 SV=1 [ARP2] |
| Q9ULW6 | 14 | 460 | 52,5 | 4,49 | 59 | Nucleosome assembly protein 1like 2 GN=NAP1L2 PE=2 SV=1 [NP1L2] |
| Q8N4A0 | 37 | 578 | 66,6 | 7,61 | 59 | Polypeptide Nacetylgalactosaminyltransferase 4 GN=GALNT4 PE=1 SV=2 [GALT4] |
| Q70CQ2 | 36 | 3546 | 404,0 | 5,82 | 59 | Ubiquitin carboxylterminal hydrolase 34 GN=USP34 PE=1 SV=2 [UBP34] |
| Q9Y2R2 | 36 | 807 | 91,6 | 7,59 | 59 | Tyrosineprotein phosphatase nonreceptor type 22 GN=PTPN22 PE=1 SV=2 [PTN22] |
| Q15911 | 4 | 3703 | 404,2 | 6,20 | 59 | Zinc finger homeobox protein 3 GN=ZFHX3 PE=1 SV=2 [ZFHX3] |
| P35579 | 4 | 1960 | 226,4 | 5,60 | 59 | Myosin9 GN=MYH9 PE=1 SV=4 [MYH9] |
| O94986 | 10 | 1654 | 189,0 | 5,44 | 59 | Centrosomal protein of 152 kDa GN=CEP152 PE=1 SV=3 [CE152] |

| | | | | | | |
|---|---|---|---|---|---|---|
| Q9UKK3 | 177 | 1724 | 192,5 | 5,66 | 59 | Poly [ADPribose] polymerase 4 GN=PARP4 PE=1 SV=3 [PARP4] |
| O75116 | 13 | 1388 | 160,8 | 6,02 | 59 | Rhoassociated protein kinase 2 GN=ROCK2 PE=1 SV=4 [ROCK2] |
| Q9HAP6 | 3 | 207 | 22,9 | 8,66 | 58 | Protein lin7 homolog B GN=LIN7B PE=1 SV=1 [LIN7B] |
| Q00013 | 1 | 466 | 52,3 | 7,37 | 58 | 55 kDa erythrocyte membrane protein GN=MPP1 PE=1 SV=2 [EM55] |
| Q9H0B6 | 16 | 622 | 68,9 | 7,15 | 58 | Kinesin light chain 2 GN=KLC2 PE=1 SV=1 [KLC2] |
| Q9Y2H5 | 20 | 1048 | 117,1 | 9,10 | 58 | Pleckstrin homology domaincontaining family A member 6 GN=PLEKHA6 PE=1 SV=4 |
| Q7Z3V4 | 2 | 1068 | 123,0 | 8,19 | 58 | Ubiquitinprotein ligase E3B GN=UBE3B PE=1 SV=3 [UBE3B] |
| O75145 | 14 | 1194 | 133,4 | 5,68 | 58 | Liprinalpha3 GN=PPFIA3 PE=1 SV=3 [LIPA3] |
| Q01973 | 18 | 937 | 104,2 | 7,17 | 58 | Tyrosineprotein kinase transmembrane receptor ROR1 GN=ROR1 PE=2 SV=2 [ROR1 |
| Q86UW7 | 7 | 1296 | 147,6 | 6,19 | 58 | Calciumdependent secretion activator 2 GN=CADPS2 PE=1 SV=2 [CAPS2] |
| P62331 | 1 | 175 | 20,1 | 8,95 | 58 | ADPribosylation factor 6 GN=Arf6 PE=1 SV=2 [ARF6] |
| P46952 | 133 | 286 | 32,5 | 5,88 | 58 | 3hydroxyanthranilate 3,4dioxygenase GN=HAAO PE=1 SV=2 [3HAO] |
| Q8TE56 | 2 | 1095 | 121,0 | 8,06 | 58 | A disintegrin and metalloproteinase with thrombospondin motifs 17 GN=ADAMTS1 |
| Q1MSJ5 | 22 | 1256 | 145,4 | 6,80 | 58 | Centrosome and spindle poleassociated protein 1 GN=CSPP1 PE=1 SV=4 [CSPP1] |
| Q969T7 | 80 | 292 | 33,5 | 6,68 | 58 | Cytosolic 5'nucleotidase IIIlike protein GN=NT5C3L PE=1 SV=3 [5NT3L] |
| Q5T5U3 | 4 | 1957 | 217,2 | 7,80 | 58 | Rho GTPaseactivating protein 21 GN=ARHGAP21 PE=1 SV=1 [RHG21] |
| Q2PPJ7 | 1 | 1873 | 210,6 | 6,07 | 57 | Ral GTPaseactivating protein subunit alpha2 GN=RALGAPA2 PE=1 SV=2 [RGPA2] |
| P08729 | 14 | 469 | 51,4 | 5,48 | 57 | Keratin, type II cytoskeletal 7 GN=KRT7 PE=1 SV=5 [K2C7] |
| Q67726 | 63 | 1436 | 163,8 | 6,92 | 57 | Nonstructural polyprotein 1AB astrovirus1 GN=ORF1 PE=3 SV=1 [NS1ABHASV1] |
| Q14289 | 16 | 1009 | 115,8 | 6,25 | 57 | Proteintyrosine kinase 2beta GN=PTK2B PE=1 SV=2 [FAK2] |
| Q5TAH2 | 168 | 1124 | 129,0 | 6,92 | 57 | Sodium/hydrogen exchanger 11 GN=SLC9A11 PE=2 SV=1 [S9A11] |
| Q8N9H9 | 190 | 656 | 69,7 | 5,43 | 57 | Uncharacterized protein C1orf127 GN=C1orf127 PE=2 SV=2 [CA127] |
| O60330 | 22 | 932 | 100,9 | 5,05 | 57 | Protocadherin gammaA12 GN=PCDHGA12 PE=2 SV=1 [PCDGC] |
| Q13535 | 177 | 2644 | 301,2 | 7,43 | 57 | Serine/threonineprotein kinase ATR GN=ATR PE=1 SV=3 [ATR] |
| Q13561 | 33 | 401 | 44,2 | 5,21 | 57 | Dynactin subunit 2 GN=DCTN2 PE=1 SV=4 [DCTN2] |
| Q9BQE9 | 1 | 202 | 22,2 | 4,75 | 56 | Bcell CLL/lymphoma 7 protein family member B GN=BCL7B PE=1 SV=1 [BCL7B] |
| P42694 | 21 | 1942 | 218,8 | 7,42 | 56 | Probable helicase with zinc finger domain GN=HELZ PE=1 SV=2 [HELZ] |
| Q711Q0 | 5 | 1435 | 156,4 | 6,38 | 56 | Uncharacterized protein C10orf71 GN=C10orf71 PE=2 SV=2 [CJ071] |
| Q2M1K9 | 1 | 1284 | 144,5 | 6,89 | 56 | Zinc finger protein 423 GN=ZNF423 PE=1 SV=1 [ZN423] |
| P20338 | 4 | 213 | 23,9 | 6,07 | 56 | Rasrelated protein Rab4A GN=RAB4A PE=1 SV=2 [RAB4A] |
| P61018 | 6 | 213 | 23,6 | 6,06 | 56 | Rasrelated protein Rab4B GN=RAB4B PE=1 SV=1 [RAB4B] |
| Q96SB3 | 19 | 815 | 89,1 | 4,97 | 56 | Neurabin2 GN=PPP1R9B PE=1 SV=2 [NEB2] |
| O14744 | 15 | 637 | 72,6 | 6,29 | 56 | Protein arginine Nmethyltransferase 5 GN=PRMT5 PE=1 SV=4 [ANM5] |
| Q9NRL2 | 12 | 1556 | 178,6 | 6,60 | 56 | Bromodomain adjacent to zinc finger domain protein 1A GN=BAZ1A PE=1 SV=2 [BA |
| P35670 | 19 | 1465 | 157,2 | 6,70 | 56 | Coppertransporting ATPase 2 GN=ATP7B PE=1 SV=4 [ATP7B] |
| Q96HP0 | 10 | 2047 | 229,4 | 6,74 | 56 | Dedicator of cytokinesis protein 6 GN=DOCK6 PE=1 SV=3 [DOCK6] |
| Q9ULV0 | 440 | 1848 | 213,5 | 7,20 | 56 | MyosinVb GN=MYO5B PE=1 SV=3 [MYO5B] |
| Q7Z6J4 | 436 | 655 | 74,8 | 6,93 | 56 | FYVE, RhoGEF and PH domaincontaining protein 2 GN=FGD2 PE=2 SV=1 [FGD2] |
| Q3ZCX4 | 61 | 644 | 74,3 | 8,22 | 56 | Zinc finger protein 568 GN=ZNF568 PE=2 SV=2 [ZN568] |
| Q9HAU0 | 12 | 1116 | 127,4 | 7,53 | 56 | Pleckstrin homology domaincontaining family A member 5 GN=PLEKHA5 PE=1 SV=1 |
| Q7RTW8 | 78 | 1153 | 128,5 | 5,82 | 56 | Otoancorin GN=OTOA PE=1 SV=1 [OTOAN] |
| Q09666 | 11 | 5890 | 628,7 | 6,15 | 55 | Neuroblast differentiationassociated protein AHNAK GN=AHNAK PE=1 SV=2 [AHNK |
| Q00536 | 8 | 496 | 55,7 | 7,62 | 55 | Cyclindependent kinase 16 GN=CDK16 PE=1 SV=1 [CDK16] |
| Q00526 | 5 | 305 | 35,0 | 8,79 | 55 | Cyclindependent kinase 3 GN=CDK3 PE=1 SV=1 [CDK3] |
| Q8NFT6 | 108 | 615 | 67,2 | 8,34 | 55 | Protein DBF4 homolog B GN=DBF4B PE=1 SV=1 [DBF4B] |
| Q7Z5J4 | 74 | 1906 | 203,2 | 8,79 | 55 | Retinoic acidinduced protein 1 GN=RAI1 PE=1 SV=2 [RAI1] |
| O95425 | 10 | 2214 | 247,6 | 6,98 | 55 | Supervillin GN=SVIL PE=1 SV=2 [SVIL] |
| P10412 | 9 | 219 | 21,9 | 11,03 | 55 | Histone H1.4 GN=HIST1H1E PE=1 SV=2 [H14] |
| Q9Y6K9 | 290 | 419 | 48,2 | 5,71 | 55 | NFkappaB essential modulator (NEMO) (NFkappaB essential modifier) (Inhibitor of |
| Q7Z6G8 | 21 | 1248 | 138,0 | 6,37 | 55 | Ankyrin repeat and sterile alpha motif domaincontaining protein 1B GN=ANKS1B PI |
| O95819 | 8 | 1239 | 142,0 | 7,46 | 55 | Mitogenactivated protein kinase kinase kinase kinase 4 GN=MAP4K4 PE=1 SV=2 [M |
| Q9BXJ9 | 445 | 866 | 101,2 | 7,42 | 55 | Nalphaacetyltransferase 15, NatA auxiliary subunit GN=NAA15 PE=1 SV=1 [NAA15] |
| Q9UHA4 | 1 | 124 | 13,6 | 7,34 | 55 | Ragulator complex protein LAMTOR3 GN=LAMTOR3 PE=1 SV=1 [LTOR3] |
| O75683 | 26 | 361 | 41,4 | 10,64 | 55 | Surfeit locus protein 6 GN=SURF6 PE=1 SV=3 [SURF6] |
| Q2VWP7 | 52 | 1150 | 127,0 | 7,59 | 55 | Protogenin GN=PRTG PE=2 SV=1 [PRTG] |
| Q9HD67 | 443 | 2058 | 237,2 | 6,21 | 54 | MyosinX GN=MYO10 PE=1 SV=3 [MYO10] |
| Q6ULP2 | 19 | 937 | 102,1 | 4,54 | 54 | Aftiphilin GN=AFTPH PE=1 SV=2 [AFTIN] |
| O00192 | 52 | 962 | 104,6 | 6,81 | 54 | Armadillo repeat protein deleted in velocardiofacial syndrome GN=ARVCF PE=1 SV |
| Q8IWG1 | 1 | 891 | 102,9 | 5,74 | 54 | WD repeatcontaining protein 63 GN=WDR63 PE=2 SV=1 [WDR63] |
| Q9BSV6 | 186 | 310 | 33,6 | 8,43 | 54 | tRNAsplicing endonuclease subunit Sen34 GN=TSEN34 PE=1 SV=1 [SEN34] |
| Q9BXT4 | 18 | 1180 | 131,9 | 6,34 | 54 | Tudor domaincontaining protein 1 GN=TDRD1 PE=1 SV=2 [TDRD1] |
| Q8IXQ6 | 1 | 854 | 96,3 | 7,91 | 54 | Poly [ADPribose] polymerase 9 GN=PARP9 PE=1 SV=2 [PARP9] |
| Q7Z494 | 89 | 1330 | 150,8 | 6,76 | 54 | Nephrocystin3 GN=NPHP3 PE=1 SV=1 [NPHP3] |
| Q14146 | 28 | 1524 | 170,4 | 7,31 | 54 | Unhealthy ribosome biogenesis protein 2 homolog GN=URB2 PE=1 SV=2 [URB2] |
| O43795 | 5 | 1136 | 131,9 | 9,38 | 54 | MyosinIb GN=MYO1B PE=1 SV=3 [MYO1B] |

| | | | | | | |
|---|---|---|---|---|---|---|
| Q9UPU5 | 42 | 2620 | 294,2 | 6,14 | 54 | Ubiquitin carboxylterminal hydrolase 24 GN=USP24 PE=1 SV=3 [UBP24] |
| P0DJD1 | 45 | 1756 | 197,2 | 6,20 | 54 | RANBP2like and GRIP domaincontaining protein 2 GN=RGPD2 PE=2 SV=1 [RGPD2] |
| Q8TC71 | 9 | 538 | 61,1 | 8,63 | 54 | Spermatogenesisassociated protein 18 GN=SPATA18 PE=1 SV=1 [SPT18] |
| P0C221 | 10 | 828 | 97,4 | 5,99 | 54 | Uncharacterized protein C14orf38 GN=C14orf38 PE=2 SV=1 [CN038] |
| Q8WVJ2 | 66 | 157 | 17,7 | 5,07 | 53 | NudC domaincontaining protein 2 GN=NUDCD2 PE=1 SV=1 [NUDC2] |
| Q9Y4E6 | 10 | 1490 | 163,7 | 6,92 | 53 | WD repeatcontaining protein 7 GN=WDR7 PE=2 SV=2 [WDR7] |
| Q96A58 | 1 | 199 | 22,6 | 7,37 | 53 | Rasrelated and estrogenregulated growth inhibitor GN=RERG PE=1 SV=1 [RERG] |
| P48547 | 2 | 511 | 57,9 | 6,58 | 53 | Potassium voltagegated channel subfamily C member 1 GN=KCNC1 PE=1 SV=1 [KCN |
| A0MZ66 | 9 | 631 | 71,6 | 5,33 | 53 | Shootin1 GN=KIAA1598 PE=1 SV=4 [SHOT1] |
| O94933 | 1 | 977 | 108,9 | 7,37 | 53 | SLIT and NTRKlike protein 3 GN=SLITRK3 PE=2 SV=2 [SLIK3] |
| Q96PY6 | 8 | 1258 | 142,7 | 5,94 | 53 | Serine/threonineprotein kinase Nek1 GN=NEK1 PE=1 SV=2 [NEK1] |
| Q13428 | 3 | 1488 | 152,0 | 9,04 | 53 | Treacle protein GN=TCOF1 PE=1 SV=3 [TCOF] |
| Q7Z7M9 | 36 | 940 | 106,2 | 9,47 | 53 | Polypeptide Nacetylgalactosaminyltransferase 5 GN=GALNT5 PE=1 SV=1 [GALT5] |
| Q13395 | 60 | 1621 | 181,6 | 7,05 | 53 | Probable methyltransferase TARBP1 GN=TARBP1 PE=1 SV=1 [TARB1] |
| Q9UF12 | 28 | 536 | 58,8 | 8,60 | 53 | Probable proline dehydrogenase 2 GN=PRODH2 PE=1 SV=1 [PROD2] |
| Q6P996 | 4 | 788 | 86,7 | 5,38 | 53 | Pyridoxaldependent decarboxylase domaincontaining protein 1 GN=PDXDC1 PE=1 S |
| Q5H9M0 | 16 | 696 | 79,0 | 4,97 | 53 | PWWP domaincontaining protein MUM1L1 GN=MUM1L1 PE=2 SV=1 [MUML1] |
| Q96J65 | 8 | 1359 | 152,2 | 8,35 | 53 | Multidrug resistanceassociated protein 9 GN=ABCC12 PE=1 SV=2 [MRP9] |
| Q8NHM5 | 70 | 1336 | 152,5 | 8,56 | 53 | Lysinespecific demethylase 2B GN=KDM2B PE=1 SV=1 [KDM2B] |
| P49917 | 8 | 911 | 103,9 | 7,96 | 52 | DNA ligase 4 GN=LIG4 PE=1 SV=2 [DNLI4] |
| Q8TBF8 | 3 | 368 | 42,4 | 8,92 | 52 | Protein FAM81A GN=FAM81A PE=2 SV=3 [FA81A] |
| Q9ULD4 | 12 | 1205 | 135,7 | 6,58 | 52 | Bromodomain and PHD fingercontaining protein 3 GN=BRPF3 PE=1 SV=2 [BRPF3] |
| Q9P2E9 | 21 | 1410 | 152,4 | 8,60 | 52 | Ribosomebinding protein 1 GN=RRBP1 PE=1 SV=4 [RRBP1] |
| Q9BRK4 | 9 | 669 | 72,7 | 6,51 | 52 | Leucine zipper putative tumor suppressor 2 GN=LZTS2 PE=1 SV=2 [LZTS2] |
| Q96S53 | 407 | 571 | 63,6 | 7,06 | 52 | Dual specificity testisspecific protein kinase 2 GN=TESK2 PE=2 SV=1 [TESK2] |
| Q14315 | 38 | 2725 | 290,8 | 5,97 | 52 | FilaminC GN=FLNC PE=1 SV=3 [FLNC] |
| Q03989 | 1 | 594 | 64,0 | 9,25 | 52 | ATrich interactive domaincontaining protein 5A GN=ARID5A PE=2 SV=2 [ARI5A] |
| Q13905 | 12 | 1077 | 120,5 | 5,92 | 52 | Rap guanine nucleotide exchange factor 1 GN=RAPGEF1 PE=1 SV=3 [RPGF1] |
| Q5THR3 | 6 | 1501 | 172,8 | 8,40 | 52 | EFhand calciumbinding domaincontaining protein 6 GN=EFCAB6 PE=1 SV=1 [EFCB6] |
| P57768 | 10 | 344 | 39,1 | 4,65 | 52 | Sorting nexin16 GN=SNX16 PE=1 SV=2 [SNX16] |
| Q5W0A0 | 6 | 696 | 81,6 | 4,75 | 52 | Protein FAM194B GN=FAM194B PE=2 SV=1 [F194B] |
| Q9NQG7 | 2 | 708 | 76,9 | 5,45 | 52 | HermanskyPudlak syndrome 4 protein GN=HPS4 PE=1 SV=2 [HPS4] |
| Q7Z6E9 | 23 | 1792 | 201,4 | 9,64 | 52 | E3 ubiquitinprotein ligase RBBP6 GN=RBBP6 PE=1 SV=1 [RBBP6] |
| Q9ULE3 | 53 | 1009 | 113,8 | 8,95 | 52 | DENN domaincontaining protein 2A GN=DENND2A PE=2 SV=4 [DEN2A] |
| Q14028 | 11 | 1251 | 139,6 | 4,81 | 52 | Cyclic nucleotidegated cation channel beta1 GN=CNGB1 PE=1 SV=2 [CNGB1] |
| Q4AC94 | 7 | 2353 | 260,2 | 7,12 | 52 | C2 domaincontaining protein 3 GN=C2CD3 PE=1 SV=4 [C2CD3] |
| Q99613 | 36 | 913 | 105,3 | 5,68 | 52 | Eukaryotic translation initiation factor 3 subunit C GN=EIF3C PE=1 SV=1 [EIF3C] |
| Q8NA56 | 13 | 475 | 55,0 | 5,71 | 52 | Tetratricopeptide repeat protein 29 GN=TTC29 PE=2 SV=2 [TTC29] |
| Q96RV3 | 15 | 2341 | 258,5 | 7,21 | 52 | Pecanexlike protein 1 GN=PCNX PE=2 SV=2 [PCX1] |
| Q01518 | 9 | 475 | 51,9 | 8,06 | 52 | Adenylyl cyclaseassociated protein 1 GN=CAP1 PE=1 SV=5 [CAP1] |
| Q9UKA4 | 8 | 1901 | 210,4 | 5,39 | 51 | Akinase anchor protein 11 GN=AKAP11 PE=1 SV=1 [AKA11] |
| P13611 | 1 | 3396 | 372,6 | 4,51 | 51 | Versican core protein GN=VCAN PE=1 SV=3 [CSPG2] |
| Q9HC36 | 79 | 420 | 47,0 | 8,73 | 51 | RNA methyltransferaselike protein 1 GN=RNMTL1 PE=1 SV=2 [RMTL1] |
| P55786 | 5 | 919 | 103,2 | 5,72 | 51 | Puromycinsensitive aminopeptidase GN=NPEPPS PE=1 SV=2 [PSA] |
| Q12965 | 8 | 1108 | 127,0 | 8,92 | 51 | MyosinIe GN=MYO1E PE=1 SV=2 [MYO1E] |
| O43150 | 23 | 1006 | 111,6 | 6,68 | 51 | ArfGAP with SH3 domain, ANK repeat and PH domaincontaining protein 2 GN=ASAP |
| Q13206 | 9 | 875 | 100,8 | 8,63 | 51 | Probable ATPdependent RNA helicase DDX10 GN=DDX10 PE=1 SV=2 [DDX10] |
| O14727 | 79 | 1248 | 141,7 | 6,40 | 51 | Apoptotic proteaseactivating factor 1 GN=APAF1 PE=1 SV=2 [APAF] |
| Q86SQ0 | 23 | 1253 | 142,1 | 7,43 | 51 | Pleckstrin homologylike domain family B member 2 GN=PHLDB2 PE=1 SV=2 [PHLB2 |
| O43566 | 329 | 566 | 61,4 | 8,19 | 51 | Regulator of Gprotein signaling 14 GN=RGS14 PE=1 SV=4 [RGS14] |
| P50995 | 60 | 505 | 54,4 | 7,65 | 51 | Annexin A11 GN=ANXA11 PE=1 SV=1 [ANX11] |
| Q5QJE6 | 348 | 756 | 84,4 | 6,16 | 51 | Deoxynucleotidyltransferase terminalinteracting protein 2 GN=DNTTIP2 PE=1 SV=2 |
| Q9H3S7 | 7 | 1636 | 178,9 | 6,92 | 51 | Tyrosineprotein phosphatase nonreceptor type 23 GN=PTPN23 PE=1 SV=1 [PTN23] |
| P01763 | 42 | 114 | 12,2 | 8,50 | 51 | Ig heavy chain VIII region WEA PE=1 SV=1 [HV302] |
| Q96L58 | 29 | 329 | 37,1 | 9,66 | 51 | Beta1,3galactosyltransferase 6 GN=B3GALT6 PE=2 SV=2 [B3GT6] |
| O95267 | 5 | 797 | 90,3 | 7,96 | 51 | RAS guanylreleasing protein 1 GN=RASGRP1 PE=1 SV=2 [GRP1] |
| Q6N022 | 19 | 2769 | 307,8 | 6,55 | 51 | Teneurin4 GN=ODZ4 PE=2 SV=2 [TEN4] |
| O94808 | 15 | 682 | 76,9 | 7,37 | 51 | Glucosaminefructose6phosphate aminotransferase [isomerizing] 2 GN=GFPT2 PE=1 |
| Q58F21 | 6 | 947 | 107,9 | 8,95 | 51 | Bromodomain testisspecific protein GN=BRDT PE=1 SV=4 [BRDT] |
| Q8N884 | 450 | 522 | 58,8 | 9,48 | 50 | Uncharacterized protein C6orf150 GN=C6orf150 PE=1 SV=2 [CF150] |
| O15055 | 22 | 1255 | 136,5 | 6,47 | 50 | Period circadian protein homolog 2 GN=PER2 PE=1 SV=2 [PER2] |
| Q9UBJ2 | 69 | 740 | 83,2 | 8,92 | 50 | ATPbinding cassette subfamily D member 2 GN=ABCD2 PE=1 SV=1 [ABCD2] |
| Q96CP6 | 1 | 724 | 80,6 | 6,74 | 50 | GRAM domaincontaining protein 1A GN=GRAMD1A PE=1 SV=2 [GRM1A] |
| Q8NEP3 | 5 | 725 | 80,0 | 4,67 | 50 | Leucinerich repeatcontaining protein 50 GN=LRRC50 PE=1 SV=5 [LRC50] |
| Q86YP4 | 14 | 633 | 68,0 | 9,94 | 50 | Transcriptional repressor p66alpha GN=GATAD2A PE=1 SV=1 [P66A] |

| | | | | | | |
|---|---|---|---|---|---|---|
| O43424 | 69 | 1007 | 113,3 | 6,07 | 50 | Glutamate receptor delta2 subunit GN=GRID2 PE=2 SV=2 [GRID2] |
| Q16236 | 56 | 605 | 67,8 | 4,78 | 50 | Nuclear factor erythroid 2related factor 2 GN=NFE2L2 PE=1 SV=3 [NF2L2] |
| P08237 | 20 | 780 | 85,1 | 7,99 | 50 | 6phosphofructokinase, muscle type GN=PFKM PE=1 SV=2 [K6PF] |
| P02786 | 1 | 760 | 84,8 | 6,61 | 50 | Transferrin receptor protein 1 GN=TFRC PE=1 SV=2 [TFR1] |
| A6NI56 | 14 | 674 | 76,0 | 8,38 | 50 | Coiledcoil domaincontaining protein 154 GN=CCDC154 PE=2 SV=4 [CC154] |
| P23634 | 12 | 1241 | 137,8 | 6,60 | 50 | Plasma membrane calciumtransporting ATPase 4 GN=ATP2B4 PE=1 SV=2 [AT2B4] |
| O00159 | 7 | 1063 | 121,6 | 9,41 | 50 | MyosinIc GN=MYO1C PE=1 SV=4 [MYO1C] |
| Q96JD6 | 3 | 320 | 36,6 | 7,49 | 50 | 1,5anhydroDfructose reductase GN=AKR1E2 PE=1 SV=2 [AKCL2] |
| Q05397 | 18 | 1052 | 119,2 | 6,62 | 50 | Focal adhesion kinase 1 GN=PTK2 PE=1 SV=2 [FAK1] |
| Q7Z745 | 5 | 1585 | 180,7 | 6,28 | 50 | HEAT repeatcontaining protein 7B2 GN=HEATR7B2 PE=2 SV=3 [HTRB2] |
| Q15561 | 21 | 434 | 48,3 | 7,33 | 50 | Transcriptional enhancer factor TEF3 GN=TEAD4 PE=1 SV=3 [TEAD4] |
| Q14203 | 16 | 1278 | 141,6 | 5,81 | 50 | Dynactin subunit 1 GN=DCTN1 PE=1 SV=3 [DCTN1] |
| Q8NHH1 | 7 | 538 | 58,0 | 9,20 | 50 | Tubulin polyglutamylase TTLL11 GN=TTLL11 PE=2 SV=1 [TTL11] |
| Q15021 | 8 | 1401 | 157,1 | 6,61 | 49 | Condensin complex subunit 1 GN=NCAPD2 PE=1 SV=3 [CND1] |
| Q92797 | 367 | 1274 | 141,1 | 6,13 | 49 | Symplekin GN=SYMPK PE=1 SV=2 [SYMPK] |
| B1AJZ9 | 4 | 1412 | 161,8 | 6,95 | 49 | Forkheadassociated domaincontaining protein 1 GN=FHAD1 PE=2 SV=2 [FHAD1] |
| Q9BXX0 | 4 | 1053 | 115,6 | 6,46 | 49 | EMILIN2 GN=EMILIN2 PE=1 SV=3 [EMIL2] |
| Q8WXK1 | 8 | 588 | 65,8 | 5,83 | 49 | Ankyrin repeat and SOCS box protein 15 GN=ASB15 PE=2 SV=3 [ASB15] |
| Q14511 | 10 | 834 | 92,8 | 6,70 | 49 | Enhancer of filamentation 1 GN=NEDD9 PE=1 SV=1 [CASL] |
| Q86VF2 | 8 | 1251 | 137,7 | 7,56 | 49 | Immunoglobulinlike and fibronectin type III domaincontaining protein 1 GN=IGFN1 |
| P35236 | 21 | 360 | 40,5 | 6,79 | 49 | Tyrosineprotein phosphatase nonreceptor type 7 GN=PTPN7 PE=1 SV=3 [PTN7] |
| Q02846 | 1 | 1103 | 120,0 | 7,44 | 49 | Retinal guanylyl cyclase 1 GN=GUCY2D PE=1 SV=2 [GUC2D] |
| Q8IZJ3 | 20 | 1885 | 206,6 | 6,42 | 49 | C3 and PZPlike alpha2macroglobulin domaincontaining protein 8 GN=CPAMD8 PE=1 |
| Q9H3U1 | 16 | 944 | 103,0 | 6,07 | 49 | Protein unc45 homolog A GN=UNC45A PE=1 SV=1 [UN45A] |
| Q96JP5 | 14 | 570 | 63,4 | 7,36 | 49 | E3 ubiquitinprotein ligase ZFP91 GN=ZFP91 PE=1 SV=1 [ZFP91] |
| Q9UH92 | 16 | 298 | 33,3 | 8,06 | 49 | Maxlike protein X GN=MLX PE=1 SV=2 [MLX] |
| P51451 | 18 | 505 | 57,7 | 7,87 | 49 | Tyrosineprotein kinase Blk GN=BLK PE=1 SV=3 [BLK] |
| Q8WYB5 | 13 | 2073 | 231,2 | 5,96 | 49 | Histone acetyltransferase MYST4 GN=MYST4 PE=1 SV=3 [MYST4] |
| Q9H4A3 | 15 | 2382 | 250,6 | 6,34 | 49 | Serine/threonineprotein kinase WNK1 GN=WNK1 PE=1 SV=2 [WNK1] |
| Q07866 | 14 | 573 | 65,3 | 6,20 | 49 | Kinesin light chain 1 GN=KLC1 PE=1 SV=2 [KLC1] |
| Q7L592 | 11 | 441 | 49,2 | 8,34 | 49 | Protein midA homolog, mitochondrial GN=C2orf56 PE=1 SV=1 [MIDA] |
| Q6UB98 | 1 | 2062 | 235,5 | 7,01 | 49 | Ankyrin repeat domaincontaining protein 12 GN=ANKRD12 PE=1 SV=3 [ANR12] |
| Q8IXK2 | 36 | 581 | 66,9 | 6,80 | 49 | Polypeptide Nacetylgalactosaminyltransferase 12 GN=GALNT12 PE=1 SV=3 [GLT12] |
| Q96L73 | 9 | 2696 | 296,5 | 8,03 | 49 | Histonelysine Nmethyltransferase, H3 lysine36 and H4 lysine20 specific GN=NSD1 P |
| P56945 | 11 | 870 | 93,3 | 5,67 | 48 | Breast cancer antiestrogen resistance protein 1 GN=BCAR1 PE=1 SV=2 [BCAR1] |
| P13612 | 26 | 1032 | 114,8 | 6,48 | 48 | Integrin alpha4 GN=ITGA4 PE=1 SV=3 [ITA4] |
| Q95460 | 16 | 341 | 39,3 | 6,30 | 48 | Major histocompatibility complex class Irelated gene protein GN=MR1 PE=1 SV=1 [ |
| A6NKG5 | 3 | 1359 | 155,1 | 5,20 | 48 | Retrotransposonlike protein 1 GN=RTL1 PE=2 SV=2 [RTL1] |
| Q9NW08 | 181 | 1133 | 127,7 | 8,50 | 48 | DNAdirected RNA polymerase III subunit RPC2 GN=POLR3B PE=1 SV=2 [RPC2] |
| Q8N371 | 339 | 416 | 47,2 | 5,80 | 48 | Lysinespecific demethylase 8 GN=JMJD5 PE=1 SV=1 [KDM8] |
| Q86Z14 | 25 | 1044 | 119,7 | 9,22 | 48 | Betaklotho GN=KLB PE=1 SV=1 [KLOTB] |
| P08582 | 363 | 738 | 80,2 | 5,94 | 48 | Melanotransferrin GN=MFI2 PE=1 SV=2 [TRFM] |
| O43639 | 91 | 380 | 42,9 | 6,95 | 48 | Cytoplasmic protein NCK2 GN=NCK2 PE=1 SV=2 [NCK2] |
| Q96N23 | 26 | 812 | 92,3 | 7,71 | 48 | Uncharacterized protein C12orf55 GN=C12orf55 PE=2 SV=2 [CL055] |
| O95185 | 34 | 931 | 103,1 | 6,10 | 48 | Netrin receptor UNC5C GN=UNC5C PE=1 SV=2 [UNC5C] |
| Q9UMW8 | 8 | 372 | 43,0 | 7,80 | 48 | Ubl carboxylterminal hydrolase 18 GN=USP18 PE=1 SV=1 [UBP18] |
| Q9BXT8 | 58 | 1623 | 184,5 | 5,40 | 48 | RING finger protein 17 GN=RNF17 PE=1 SV=3 [RNF17] |
| Q8TEL6 | 70 | 797 | 90,8 | 7,61 | 48 | Short transient receptor potential channel 4associated protein GN=TRPC4AP PE=1 S |
| Q9Y2I1 | 68 | 1504 | 166,5 | 5,14 | 48 | Nischarin GN=NISCH PE=1 SV=3 [NISCH] |
| Q9UKE5 | 6 | 1360 | 154,8 | 7,17 | 48 | TRAF2 and NCKinteracting protein kinase GN=TNIK PE=1 SV=1 [TNIK] |
| P23921 | 40 | 792 | 90,0 | 7,15 | 48 | Ribonucleosidediphosphate reductase large subunit GN=RRM1 PE=1 SV=1 [RIR1] |
| Q9BUQ8 | 12 | 820 | 95,5 | 9,55 | 48 | Probable ATPdependent RNA helicase DDX23 GN=DDX23 PE=1 SV=3 [DDX23] |
| P25705 | 11 | 553 | 59,7 | 9,13 | 47 | ATP synthase subunit alpha, mitochondrial GN=ATP5A1 PE=1 SV=1 [ATPA] |
| Q16820 | 20 | 701 | 79,5 | 5,74 | 47 | Meprin A subunit beta GN=MEP1B PE=1 SV=3 [MEP1B] |
| P01700 | 9 | 112 | 11,9 | 8,91 | 47 | Ig lambda chain VI region HA PE=1 SV=1 [LV102] |
| Q8NEB9 | 11 | 887 | 101,5 | 6,81 | 47 | Phosphatidylinositol 3kinase catalytic subunit type 3 GN=PIK3C3 PE=1 SV=1 [PK3C3 |
| Q6NT04 | 13 | 549 | 63,2 | 8,75 | 47 | Tigger transposable elementderived protein 7 GN=TIGD7 PE=2 SV=1 [TIGD7] |
| O94769 | 7 | 699 | 79,7 | 5,41 | 47 | Extracellular matrix protein 2 GN=ECM2 PE=2 SV=1 [ECM2] |
| Q4G0S7 | 14 | 254 | 30,0 | 9,06 | 47 | Coiledcoil domaincontaining protein 152 GN=CCDC152 PE=2 SV=3 [CC152] |
| P09131 | 3 | 477 | 50,3 | 7,77 | 47 | P3 protein GN=SLC10A3 PE=2 SV=1 [P3] |
| P13639 | 4 | 858 | 95,3 | 6,83 | 47 | Elongation factor 2 GN=EEF2 PE=1 SV=4 [EF2] |
| O94927 | 18 | 633 | 71,6 | 8,51 | 47 | HAUS augminlike complex subunit 5 GN=HAUS5 PE=1 SV=2 [HAUS5] |
| Q8NFP4 | 39 | 955 | 105,7 | 8,34 | 47 | MAM domaincontaining glycosylphosphatidylinositol anchor protein 1 GN=MDGA1 |
| Q9Y426 | 29 | 696 | 75,5 | 6,92 | 47 | C2 domaincontaining protein 2 GN=C2CD2 PE=1 SV=2 [CU025] |
| Q86SJ6 | 8 | 1040 | 113,8 | 4,56 | 47 | Desmoglein4 GN=DSG4 PE=1 SV=1 [DSG4] |

| | | | | | | |
|---|---|---|---|---|---|---|
| Q6PKG0 | 34 | 1096 | 123,4 | 8,82 | 47 | Larelated protein 1 GN=LARP1 PE=1 SV=2 [LARP1] |
| Q99590 | 10 | 1463 | 164,6 | 8,41 | 47 | Protein SCAF11 GN=SCAF11 PE=1 SV=2 [SCAFB] |
| Q13402 | 3 | 2215 | 254,2 | 8,56 | 47 | MyosinVIIa GN=MYO7A PE=1 SV=1 [MYO7A] |
| Q9Y6N6 | 21 | 1575 | 171,1 | 6,58 | 47 | Laminin subunit gamma3 GN=LAMC3 PE=2 SV=3 [LAMC3] |
| Q8NHV1 | 3 | 300 | 34,5 | 6,46 | 47 | GTPase IMAP family member 7 GN=GIMAP7 PE=2 SV=1 [GIMA7] |
| P22455 | 7 | 802 | 87,9 | 6,81 | 47 | Fibroblast growth factor receptor 4 GN=FGFR4 PE=1 SV=2 [FGFR4] |
| Q8IZU8 | 20 | 1212 | 139,1 | 8,32 | 47 | Dermatansulfate epimeraselike protein GN=DSEL PE=2 SV=2 [DSEL] |
| Q14832 | 4 | 879 | 98,8 | 7,66 | 46 | Metabotropic glutamate receptor 3 GN=GRM3 PE=2 SV=2 [GRM3] |
| Q9BV20 | 1 | 369 | 39,1 | 6,30 | 46 | Methylthioribose1phosphate isomerase GN=MRI1 PE=1 SV=1 [MTNA] |
| P82932 | 157 | 125 | 14,2 | 9,26 | 46 | Mitochondrial 28S ribosomal protein S6 (S6mt) (MRPS6) [RT06] |
| Q9NR16 | 20 | 1453 | 159,1 | 5,76 | 46 | Scavenger receptor cysteinerich type 1 protein M160 GN=CD163L1 PE=1 SV=2 [C163 |
| Q96BY6 | 9 | 2186 | 249,4 | 7,14 | 46 | Dedicator of cytokinesis protein 10 GN=DOCK10 PE=1 SV=3 [DOC10] |
| Q9H9J4 | 11 | 1324 | 145,3 | 8,63 | 46 | Ubiquitin carboxylterminal hydrolase 42 GN=USP42 PE=1 SV=3 [UBP42] |
| Q96AA8 | 56 | 810 | 94,9 | 6,16 | 46 | Uncharacterized protein KIAA0555 [K0555] |
| O75197 | 16 | 1615 | 179,0 | 5,34 | 46 | Lowdensity lipoprotein receptorrelated protein 5 GN=LRP5 PE=1 SV=2 [LRP5] |
| Q13424 | 29 | 505 | 53,9 | 6,80 | 46 | Alpha1syntrophin GN=SNTA1 PE=1 SV=1 [SNTA1] |
| P59045 | 14 | 1033 | 117,7 | 7,71 | 46 | NACHT, LRR and PYD domainscontaining protein 11 GN=NLRP11 PE=2 SV=2 [NAL11] |
| Q49AM1 | 14 | 385 | 44,4 | 8,97 | 46 | mTERF domaincontaining protein 3, mitochondrial GN=MTERFD3 PE=1 SV=2 [MTER |
| Q68CZ2 | 64 | 1445 | 155,2 | 6,81 | 46 | Tensin3 GN=TNS3 PE=1 SV=2 [TENS3] |
| Q92558 | 2 | 559 | 61,6 | 6,46 | 46 | WiskottAldrich syndrome protein family member 1 GN=WASF1 PE=1 SV=1 [WASF1] |
| P35711 | 19 | 763 | 84,0 | 6,60 | 46 | Transcription factor SOX5 GN=SOX5 PE=2 SV=3 [SOX5] |
| Q13733 | 14 | 1029 | 114,1 | 6,64 | 46 | Sodium/potassiumtransporting ATPase subunit alpha4 GN=ATP1A4 PE=1 SV=3 [AT1 |
| Q9Y4G8 | 14 | 1499 | 167,3 | 6,67 | 46 | Rap guanine nucleotide exchange factor 2 (Neural RAP guanine nucleotide exchang |
| P51160 | 1 | 858 | 99,1 | 5,72 | 46 | Cone cGMPspecific 3',5'cyclic phosphodiesterase subunit alpha' GN=PDE6C PE=1 SV |
| Q12934 | 9 | 665 | 74,5 | 5,14 | 46 | Filensin GN=BFSP1 PE=1 SV=3 [BFSP1] |
| Q9C0B5 | 36 | 715 | 77,5 | 9,01 | 46 | Probable palmitoyltransferase ZDHHC5 GN=ZDHHC5 PE=1 SV=2 [ZDHC5] |
| Q9BYX2 | 48 | 928 | 105,3 | 6,58 | 46 | TBC1 domain family member 2A GN=TBC1D2 PE=1 SV=3 [TBD2A] |
| Q9Y6D6 | 18 | 1849 | 208,6 | 5,85 | 46 | Brefeldin Ainhibited guanine nucleotideexchange protein 1 GN=ARFGEF1 PE=1 SV= |
| P01604 | 9 | 108 | 12,1 | 8,81 | 46 | Ig kappa chain VI region Kue PE=1 SV=1 [KV112] |
| Q9UEG4 | 42 | 869 | 96,6 | 7,93 | 46 | Zinc finger protein 629 GN=ZNF629 PE=2 SV=2 [ZN629] |
| Q8TDR2 | 34 | 534 | 58,0 | 9,74 | 46 | Serine/threonineprotein kinase 35 GN=STK35 PE=1 SV=2 [STK35] |
| Q6L8Q7 | 11 | 609 | 67,3 | 6,57 | 46 | 2',5'phosphodiesterase 12 GN=PDE12 PE=1 SV=2 [PDE12] |
| Q9NV06 | 16 | 445 | 51,4 | 9,19 | 46 | DDB1 and CUL4associated factor 13 GN=DCAF13 PE=1 SV=2 [DCA13] |
| Q96AX9 | 1 | 1013 | 109,9 | 8,44 | 45 | E3 ubiquitinprotein ligase MIB2 GN=MIB2 PE=1 SV=3 [MIB2] |
| O43299 | 4 | 807 | 88,5 | 7,01 | 45 | Uncharacterized protein KIAA0415 GN=KIAA0415 PE=2 SV=2 [K0415] |
| Q9ULT8 | 20 | 2610 | 289,2 | 5,35 | 45 | E3 ubiquitinprotein ligase HECTD1 GN=HECTD1 PE=1 SV=3 [HECD1] |
| Q9BZJ0 | 7 | 848 | 100,4 | 8,00 | 45 | Crooked necklike protein 1 GN=CRNKL1 PE=1 SV=4 [CRNL1] |
| Q38SD2 | 1 | 2015 | 225,2 | 6,68 | 45 | Leucinerich repeat serine/threonineprotein kinase 1 GN=LRRK1 PE=1 SV=3 [LRRK1] |
| P00480 | 56 | 354 | 39,9 | 8,63 | 45 | Ornithine carbamoyltransferase, mitochondrial precursor (EC 2.1.3.3) (OTCase) (Orr |
| Q12912 | 145 | 555 | 62,1 | 5,85 | 45 | Lymphoidrestricted membrane protein GN=LRMP PE=1 SV=3 [LRMP] |
| Q13017 | 4 | 1502 | 172,4 | 6,62 | 45 | Rho GTPaseactivating protein 5 GN=ARHGAP5 PE=1 SV=2 [RHG05] |
| P33992 | 10 | 734 | 82,2 | 8,37 | 45 | DNA replication licensing factor MCM5 GN=MCM5 PE=1 SV=5 [MCM5] |
| Q2M1Z3 | 3 | 1444 | 156,9 | 5,76 | 45 | Rho GTPaseactivating protein 31 GN=ARHGAP31 PE=1 SV=2 [RHG31] |
| Q8WXG9 | 9 | 6306 | 692,6 | 4,64 | 45 | Gprotein coupled receptor 98 GN=GPR98 PE=1 SV=2 [GPR98] |
| Q9NVE4 | 3 | 849 | 96,3 | 8,59 | 45 | Coiledcoil domaincontaining protein 87 GN=CCDC87 PE=2 SV=2 [CCD87] |
| Q9C0G6 | 15 | 4158 | 475,7 | 6,00 | 45 | Dynein heavy chain 6, axonemal GN=DNAH6 PE=1 SV=3 [DYH6] |
| Q9H8K7 | 7 | 445 | 49,2 | 6,25 | 45 | Uncharacterized protein C10orf88 GN=C10orf88 PE=2 SV=2 [CJ088] |
| P78562 | 12 | 749 | 86,4 | 8,76 | 45 | Phosphateregulating neutral endopeptidase GN=PHEX PE=1 SV=1 [PHEX] |
| Q13576 | 75 | 1575 | 180,5 | 5,64 | 45 | Ras GTPaseactivatinglike protein IQGAP2 GN=IQGAP2 PE=1 SV=4 [IQGA2] |
| O60522 | 10 | 2096 | 236,4 | 5,25 | 45 | Tudor domaincontaining protein 6 GN=TDRD6 PE=2 SV=2 [TDRD6] |
| P52888 | 14 | 689 | 78,8 | 6,05 | 45 | Thimet oligopeptidase GN=THOP1 PE=1 SV=2 [THOP1] |
| Q9NWM0 | 9 | 555 | 61,8 | 5,45 | 45 | Spermine oxidase GN=SMOX PE=1 SV=1 [SMOX] |
| Q9BYD6 | 24 | 325 | 36,9 | 8,78 | 45 | 39S ribosomal protein L1, mitochondrial GN=MRPL1 PE=1 SV=2 [RM01] |
| P14136 | 36 | 432 | 49,8 | 5,52 | 44 | Glial fibrillary acidic protein GN=GFAP PE=1 SV=1 [GFAP] |
| Q86SG4 | 1 | 172 | 20,4 | 9,83 | 44 | Dresden prostate carcinoma protein 2 GN=C15orf21 PE=2 SV=1 [DPCA2] |
| Q8WYN3 | 10 | 585 | 64,9 | 4,75 | 44 | Cysteine/serinerich nuclear protein 3 GN=CSRNP3 PE=1 SV=1 [CSRN3] |
| C9JTQ0 | 142 | 380 | 39,6 | 11,03 | 44 | Ankyrin repeat domaincontaining protein 63 GN=ANKRD63 PE=4 SV=1 [ANR63] |
| P14616 | 1 | 1297 | 143,6 | 6,47 | 44 | Insulin receptorrelated protein GN=INSRR PE=2 SV=2 [INSRR] |
| Q8WY54 | 16 | 764 | 84,9 | 5,03 | 44 | Protein phosphatase 1E GN=PPM1E PE=1 SV=2 [PPM1E] |
| Q99684 | 12 | 422 | 45,3 | 9,00 | 44 | Zinc finger protein Gfi1 GN=GFI1 PE=1 SV=2 [GFI1] |
| Q9H013 | 7 | 955 | 104,9 | 8,35 | 44 | Disintegrin and metalloproteinase domaincontaining protein 19 GN=ADAM19 PE=1 |
| Q7Z2Y8 | 18 | 2422 | 278,9 | 6,55 | 44 | Interferoninduced very large GTPase 1 GN=GVIN1 PE=2 SV=2 [GVIN1] |
| Q96A08 | 11 | 127 | 14,2 | 10,32 | 44 | Histone H2B type 1A GN=HIST1H2BA PE=1 SV=3 [H2B1A] |
| Q96CN5 | 6 | 670 | 75,9 | 6,23 | 44 | Leucinerich repeatcontaining protein 45 GN=LRRC45 PE=2 SV=1 [LRC45] |
| P55060 | 2 | 971 | 110,3 | 5,77 | 44 | Exportin2 GN=CSE1L PE=1 SV=3 [XPO2] |

| | | | | | | |
|---|---|---|---|---|---|---|
| P52746 | 11 | 1687 | 187,8 | 7,91 | 44 | Zinc finger protein 142 GN=ZNF142 PE=1 SV=4 [ZN142] |
| Q8NHY2 | 31 | 731 | 80,4 | 6,84 | 44 | E3 ubiquitinprotein ligase RFWD2 GN=RFWD2 PE=1 SV=1 [RFWD2] |
| Q9NVL8 | 12 | 296 | 34,7 | 9,28 | 44 | Uncharacterized protein C14orf105 GN=C14orf105 PE=2 SV=2 [CN105] |
| Q8WUM0 | 43 | 1156 | 128,9 | 5,10 | 44 | Nuclear pore complex protein Nup133 GN=NUP133 PE=1 SV=2 [NU133] |
| Q9ULV3 | 197 | 898 | 100,0 | 6,11 | 44 | Cip1interacting zinc finger protein GN=CIZ1 PE=1 SV=2 [CIZ1] |
| Q99608 | 13 | 321 | 36,1 | 8,78 | 44 | Necdin GN=NDN PE=1 SV=1 [NECD] |
| Q9Y2G9 | 3 | 1366 | 150,2 | 6,52 | 44 | Protein strawberry notch homolog 2 GN=SBNO2 PE=2 SV=3 [SBNO2] |
| Q92540 | 2 | 1137 | 127,2 | 8,72 | 44 | Protein SMG7 GN=SMG7 PE=1 SV=2 [SMG7] |
| O95219 | 328 | 450 | 51,9 | 5,99 | 43 | Sorting nexin4 GN=SNX4 PE=1 SV=1 [SNX4] |
| Q8N7X0 | 38 | 1667 | 189,6 | 8,31 | 43 | Calpain7like protein GN=C6orf103 PE=2 SV=3 [CAN7L] |
| Q14435 | 26 | 633 | 72,6 | 7,99 | 43 | Polypeptide Nacetylgalactosaminyltransferase 3 GN=GALNT3 PE=2 SV=2 [GALT3] |
| Q49MI3 | 93 | 558 | 62,6 | 8,27 | 43 | Ceramide kinaselike protein GN=CERKL PE=1 SV=1 [CERKL] |
| Q9Y4F4 | 368 | 1720 | 189,2 | 8,50 | 43 | Protein FAM179B GN=FAM179B PE=1 SV=4 [F179B] |
| Q8N6S4 | 1 | 541 | 60,8 | 6,93 | 43 | Ankyrin repeat domaincontaining protein 13C GN=ANKRD13C PE=2 SV=2 [AN13C] |
| Q9Y2D5 | 21 | 859 | 94,6 | 5,11 | 43 | Akinase anchor protein 2 GN=AKAP2 PE=1 SV=3 [AKAP2] |
| Q9Y697 | 7 | 457 | 50,2 | 8,31 | 43 | Cysteine desulfurase, mitochondrial GN=NFS1 PE=1 SV=3 [NFS1] |
| O76027 | 442 | 345 | 38,3 | 5,77 | 43 | Annexin A9 GN=ANXA9 PE=1 SV=3 [ANXA9] |
| O75161 | 16 | 1426 | 157,5 | 8,13 | 43 | Nephrocystin4 GN=NPHP4 PE=1 SV=2 [NPHP4] |
| P32926 | 8 | 999 | 107,5 | 5,00 | 43 | Desmoglein3 GN=DSG3 PE=1 SV=2 [DSG3] |
| P47756 | 2 | 277 | 31,3 | 5,59 | 43 | Factincapping protein subunit beta GN=CAPZB PE=1 SV=4 [CAPZB] |
| Q9NPF5 | 28 | 467 | 53,0 | 9,50 | 43 | DNA methyltransferase 1associated protein 1 GN=DMAP1 PE=1 SV=1 [DMAP1] |
| P56730 | 31 | 875 | 97,0 | 8,03 | 43 | Neurotrypsin GN=PRSS12 PE=2 SV=2 [NETR] |
| O95447 | 7 | 670 | 76,5 | 9,48 | 42 | Lebercilinlike protein GN=LCA5L PE=2 SV=1 [LCA5L] |
| Q96M91 | 9 | 514 | 61,8 | 8,90 | 42 | Coiledcoil domaincontaining protein 11 GN=CCDC11 PE=2 SV=2 [CCD11] |
| O75369 | 3 | 2602 | 278,0 | 5,73 | 42 | FilaminB GN=FLNB PE=1 SV=2 [FLNB] |
| O43526 | 29 | 872 | 95,8 | 9,23 | 42 | Potassium voltagegated channel subfamily KQT member 2 GN=KCNQ2 PE=1 SV=2 [ |
| Q0ZGT2 | 19 | 675 | 80,6 | 5,33 | 42 | Nexilin GN=NEXN PE=1 SV=1 [NEXN] |
| O00160 | 6 | 1098 | 124,8 | 9,11 | 42 | MyosinIf GN=MYO1F PE=1 SV=3 [MYO1F] |
| P30281 | 17 | 292 | 32,5 | 7,06 | 42 | G1/Sspecific cyclinD3 GN=CCND3 PE=1 SV=2 [CCND3] |
| P51523 | 43 | 738 | 85,4 | 8,78 | 42 | Zinc finger protein 84 (Zinc finger protein HPF2) [ZNF84] |
| Q6PIF6 | 9 | 2116 | 241,4 | 8,57 | 42 | MyosinVIIb GN=MYO7B PE=2 SV=2 [MYO7B] |
| Q9NZQ8 | 5 | 1165 | 131,4 | 6,77 | 42 | Transient receptor potential cation channel subfamily M member 5 GN=TRPM5 PE= |
| P17480 | 4 | 764 | 89,4 | 5,81 | 42 | Nucleolar transcription factor 1 GN=UBTF PE=1 SV=1 [UBF1] |
| Q9Y277 | 42 | 283 | 30,6 | 8,66 | 42 | Voltagedependent anionselective channel protein 3 GN=VDAC3 PE=1 SV=1 [VDAC3 |
| Q9BZF1 | 432 | 889 | 101,1 | 6,96 | 42 | Oxysterolbinding proteinrelated protein 8 GN=OSBPL8 PE=1 SV=3 [OSBL8] |
| Q96DR5 | 434 | 249 | 27,0 | 5,59 | 42 | Short palate, lung and nasal epithelium carcinomaassociated protein 2 GN=SPLUNC |
| Q8TBK2 | 18 | 473 | 53,2 | 5,34 | 42 | Nlysine methyltransferase SETD6 GN=SETD6 PE=1 SV=2 [SETD6] |
| P49910 | 1 | 485 | 55,7 | 7,17 | 42 | Zinc finger protein 165 GN=ZNF165 PE=1 SV=1 [ZN165] |
| Q8WVM7 | 1 | 1258 | 144,3 | 5,59 | 42 | Cohesin subunit SA1 GN=STAG1 PE=1 SV=3 [STAG1] |
| Q7Z736 | 8 | 793 | 85,3 | 7,83 | 42 | Pleckstrin homology domaincontaining family H member 3 GN=PLEKHH3 PE=1 SV=2 |
| Q6UWX4 | 19 | 724 | 80,7 | 9,01 | 42 | HHIPlike protein 2 GN=HHIPL2 PE=2 SV=1 [HIPL2] |
| P52272 | 1 | 730 | 77,5 | 8,70 | 42 | Heterogeneous nuclear ribonucleoprotein M GN=HNRNPM PE=1 SV=3 [HNRPM] |
| Q9UQN3 | 2 | 213 | 23,9 | 8,76 | 41 | Charged multivesicular body protein 2b GN=CHMP2B PE=1 SV=1 [CHM2B] |
| Q86X52 | 1 | 802 | 91,7 | 9,23 | 41 | Chondroitin sulfate synthase 1 GN=CHSY1 PE=1 SV=3 [CHSS1] |
| P17643 | 25 | 537 | 60,7 | 5,99 | 41 | 5,6dihydroxyindole2carboxylic acid oxidase GN=TYRP1 PE=1 SV=2 [TYRP1] |
| Q9HAU5 | 25 | 1272 | 147,7 | 5,69 | 41 | Regulator of nonsense transcripts 2 GN=UPF2 PE=1 SV=1 [RENT2] |
| Q96BQ5 | 5 | 260 | 30,8 | 9,20 | 41 | Coiledcoil domaincontaining protein 127 [CC127] |
| Q86V15 | 454 | 1759 | 189,9 | 7,03 | 41 | Zinc finger protein castor homolog 1 GN=CASZ1 PE=2 SV=4 [CASZ1] |
| Q99665 | 6 | 862 | 97,1 | 7,75 | 41 | Interleukin12 receptor beta2 chain precursor (IL12 receptor beta2) (IL12Rbeta2) [I |
| Q76NI1 | 23 | 1749 | 191,3 | 6,16 | 41 | Protein very KIND GN=KNDC1 PE=2 SV=2 [VKIND] |
| Q96EF6 | 59 | 278 | 31,5 | 8,10 | 41 | Fbox only protein 17 GN=FBXO17 PE=1 SV=1 [FBX17] |
| P23919 | 1 | 212 | 23,8 | 8,27 | 41 | Thymidylate kinase GN=DTYMK PE=1 SV=4 [KTHY] |
| Q16394 | 20 | 746 | 86,2 | 9,04 | 41 | Exostosin1 GN=EXT1 PE=1 SV=2 [EXT1] |
| Q70JA7 | 14 | 882 | 100,2 | 8,75 | 41 | Chondroitin sulfate synthase 3 GN=CHSY3 PE=1 SV=3 [CHSS3] |
| Q9HCS4 | 1 | 588 | 62,6 | 8,94 | 41 | Transcription factor 7like 1 GN=TCF7L1 PE=2 SV=1 [TF7L1] |
| Q96NH3 | 7 | 1257 | 144,7 | 6,74 | 41 | Protein broadminded GN=BROMI PE=2 SV=4 [BROMI] |
| P10253 | 1 | 952 | 105,3 | 6,00 | 41 | Lysosomal alphaglucosidase GN=GAA PE=1 SV=4 [LYAG] |
| P11678 | 8 | 715 | 81,0 | 10,29 | 41 | Eosinophil peroxidase GN=EPX PE=1 SV=2 [PERE] |
| Q8N8U2 | 93 | 506 | 56,5 | 8,79 | 41 | Chromodomain Ylike protein 2 GN=CDYL2 PE=2 SV=2 [CDYL2] |
| Q2Q1W2 | 12 | 868 | 93,3 | 7,61 | 41 | Tripartite motifcontaining protein 71 GN=TRIM71 PE=2 SV=1 [LIN41] |
| Q9UPN9 | 19 | 1127 | 122,5 | 6,67 | 40 | E3 ubiquitinprotein ligase TRIM33 GN=TRIM33 PE=1 SV=3 [TRI33] |
| Q14153 | 20 | 422 | 45,7 | 6,76 | 40 | Protein FAM53B GN=FAM53B PE=1 SV=2 [FA53B] |
| Q8IW52 | 10 | 837 | 94,3 | 7,80 | 40 | SLIT and NTRKlike protein 4 GN=SLITRK4 PE=2 SV=1 [SLIK4] |
| Q8NA47 | 119 | 563 | 66,2 | 9,06 | 40 | Coiledcoil domaincontaining protein 63 GN=CCDC63 PE=1 SV=1 [CCD63] |
| Q86TU7 | 17 | 594 | 67,2 | 5,96 | 40 | SET domaincontaining protein 3 GN=SETD3 PE=1 SV=1 [SETD3] |

| | | | | | | |
|---|---|---|---|---|---|---|
| O75127 | 27 | 700 | 78,8 | 8,59 | 40 | Pentatricopeptide repeatcontaining protein 1 GN=PTCD1 PE=1 SV=2 [PTCD1] |
| P17302 | 28 | 382 | 43,0 | 8,76 | 40 | Gap junction alpha1 protein GN=GJA1 PE=1 SV=2 [CXA1] |
| Q6UQ28 | 26 | 207 | 23,4 | 5,12 | 40 | Placentaexpressed transcript 1 protein GN=PLET1 PE=2 SV=2 [PLET1] |
| Q96CU9 | 1 | 486 | 53,8 | 7,78 | 40 | FADdependent oxidoreductase domaincontaining protein 1 GN=FOXRED1 PE=1 SV= |
| Q96J02 | 23 | 903 | 102,7 | 6,30 | 40 | E3 ubiquitinprotein ligase Itchy homolog GN=ITCH PE=1 SV=2 [ITCH] |
| P78316 | 25 | 857 | 97,6 | 7,58 | 40 | Nucleolar protein 14 GN=NOP14 PE=1 SV=3 [NOP14] |
| Q8TBR7 | 5 | 257 | 29,4 | 9,41 | 40 | Protein FAM57A GN=FAM57A PE=1 SV=2 [FA57A] |
| P16402 | 327 | 221 | 22,3 | 11,02 | 40 | Histone H1.3 GN=HIST1H1D PE=1 SV=2 [H13] |
| Q9NT68 | 70 | 2774 | 307,6 | 6,68 | 40 | Teneurin2 GN=ODZ2 PE=1 SV=3 [TEN2] |
| O43593 | 7 | 1189 | 127,4 | 7,08 | 40 | Protein hairless GN=HR PE=1 SV=5 [HAIR] |
| Q92538 | 4 | 1859 | 206,3 | 5,73 | 40 | Golgispecific brefeldin Aresistance guanine nucleotide exchange factor 1 GN=GBF1 |
| Q8WWZ4 | 4 | 1543 | 175,7 | 6,65 | 40 | ATPbinding cassette subfamily A member 10 GN=ABCA10 PE=1 SV=3 [ABCAA] |
| Q2M329 | 49 | 555 | 62,7 | 4,94 | 40 | Coiledcoil domaincontaining protein 96 GN=CCDC96 PE=2 SV=2 [CCD96] |
| P54756 | 71 | 1037 | 114,7 | 6,93 | 40 | Ephrin typeA receptor 5 GN=EPHA5 PE=1 SV=3 [EPHA5] |
| Q8N0X2 | 1 | 631 | 70,8 | 6,33 | 39 | Spermassociated antigen 16 protein GN=SPAG16 PE=2 SV=2 [SPG16] |
| P22352 | 5 | 226 | 25,5 | 8,13 | 39 | Glutathione peroxidase 3 GN=GPX3 PE=1 SV=2 [GPX3] |
| O15530 | 4 | 556 | 63,1 | 7,36 | 39 | 3phosphoinositidedependent protein kinase 1 GN=PDPK1 PE=1 SV=1 [PDPK1] |
| Q8NDZ2 | 1 | 872 | 96,8 | 6,62 | 39 | Uncharacterized protein C5orf25 GN=C5orf25 PE=1 SV=2 [CE025] |
| Q3SXZ7 | 41 | 439 | 51,4 | 8,76 | 39 | Probable tubulin polyglutamylase TTLL9 GN=TTLL9 PE=2 SV=3 [TTLL9] |
| Q96G75 | 288 | 393 | 44,4 | 6,61 | 39 | Protein RMD5 homolog B GN=RMND5B PE=2 SV=1 [RMD5B] |
| Q96BN8 | 24 | 352 | 40,2 | 5,47 | 39 | Protein FAM105B GN=FAM105B PE=1 SV=3 [F105B] |
| O60241 | 1 | 1585 | 172,5 | 7,42 | 39 | Brainspecific angiogenesis inhibitor 2 GN=BAI2 PE=2 SV=2 [BAI2] |
| Q00537 | 4 | 523 | 59,5 | 9,03 | 39 | Serine/threonineprotein kinase PCTAIRE2 (EC 2.7.11.22) (PCTAIREmotif protein kina |
| Q96QE3 | 16 | 1844 | 207,4 | 9,19 | 39 | ATPase family AAA domaincontaining protein 5 GN=ATAD5 PE=1 SV=4 [ATAD5] |
| P15884 | 12 | 667 | 71,3 | 7,01 | 39 | Transcription factor 4 GN=TCF4 PE=1 SV=3 [ITF2] |
| Q8WY91 | 27 | 577 | 62,9 | 9,28 | 39 | THAP domaincontaining protein 4 GN=THAP4 PE=1 SV=2 [THAP4] |
| Q5VYM1 | 5 | 1079 | 117,6 | 7,36 | 39 | Uncharacterized protein C9orf131 GN=C9orf131 PE=2 SV=3 [CI131] |
| Q96GW9 | 3 | 593 | 66,5 | 8,09 | 39 | MethionyltRNA synthetase, mitochondrial GN=MARS2 PE=1 SV=2 [SYMM] |
| Q6ZQW0 | 1 | 407 | 45,4 | 6,84 | 39 | Indoleamine 2,3dioxygenase 2 GN=IDO2 PE=1 SV=3 [I23O2] |
| Q86YE8 | 123 | 645 | 75,8 | 9,14 | 39 | Zinc finger protein 573 GN=ZNF573 PE=2 SV=3 [ZN573] |
| O00566 | 10 | 681 | 78,8 | 4,86 | 39 | U3 small nucleolar ribonucleoprotein protein MPP10 GN=MPHOSPH10 PE=1 SV=2 [ |
| Q8N239 | 124 | 644 | 70,6 | 5,60 | 39 | Kelchlike protein 34 GN=KLHL34 PE=2 SV=1 [KLH34] |
| Q9ULM3 | 13 | 1422 | 150,7 | 8,98 | 39 | YEATS domaincontaining protein 2 GN=YEATS2 PE=1 SV=2 [YETS2] |
| Q9BXW9 | 8 | 1471 | 166,4 | 6,24 | 39 | Fanconi anemia group D2 protein GN=FANCD2 PE=1 SV=1 [FACD2] |
| Q5TFE4 | 2 | 455 | 51,8 | 6,35 | 39 | 5'nucleotidase domaincontaining protein 1 GN=NT5DC1 PE=1 SV=1 [NT5D1] |
| Q17R98 | 8 | 1081 | 119,1 | 6,89 | 39 | Zinc finger protein 827 GN=ZNF827 PE=2 SV=1 [ZN827] |
| P07741 | 3 | 180 | 19,6 | 6,02 | 39 | Adenine phosphoribosyltransferase GN=APRT PE=1 SV=2 [APT] |
| Q9NYF0 | 17 | 836 | 90,1 | 8,69 | 38 | Dapper homolog 1 GN=DACT1 PE=2 SV=2 [DACT1] |
| Q96LP6 | 27 | 360 | 39,7 | 9,60 | 38 | Uncharacterized protein C12orf42 GN=C12orf42 PE=2 SV=2 [CL042] |
| Q99700 | 3 | 1313 | 140,2 | 9,57 | 38 | Ataxin2 GN=ATXN2 PE=1 SV=2 [ATX2] |
| Q9UKG1 | 15 | 709 | 79,6 | 5,41 | 38 | DCCinteracting protein 13alpha GN=APPL1 PE=1 SV=1 [DP13A] |
| Q9Y5H2 | 22 | 935 | 101,5 | 4,96 | 38 | Protocadherin gammaA11 GN=PCDHGA11 PE=1 SV=1 [PCDGB] |
| Q9BRD0 | 3 | 619 | 70,5 | 9,86 | 38 | BUD13 homolog GN=BUD13 PE=1 SV=1 [BUD13] |
| Q13615 | 10 | 1198 | 133,5 | 5,80 | 38 | Myotubularinrelated protein 3 GN=MTMR3 PE=1 SV=3 [MTMR3] |
| Q8N5C8 | 23 | 712 | 78,6 | 8,46 | 38 | TGFbetaactivated kinase 1 and MAP3K7binding protein 3 GN=TAB3 PE=1 SV=2 [TAB |
| B3KS81 | 3 | 715 | 80,3 | 12,06 | 38 | Serine/arginine repetitive matrix protein 5 GN=SRRM5 PE=2 SV=3 [SRRM5] |
| Q4W5G0 | 408 | 525 | 59,6 | 9,00 | 38 | Tigger transposable elementderived protein 2 GN=TIGD2 PE=2 SV=1 [TIGD2] |
| P53004 | 4 | 296 | 33,4 | 6,44 | 38 | Biliverdin reductase A GN=BLVRA PE=1 SV=2 [BIEA] |
| P19367 | 13 | 917 | 102,4 | 6,80 | 38 | Hexokinase1 (EC 2.7.1.1) (Hexokinase type I) (HK I) (Brain form hexokinase) [HXK1 |
| Q7Z7M0 | 19 | 2845 | 302,9 | 6,87 | 38 | Multiple epidermal growth factorlike domains protein 8 GN=MEGF8 PE=1 SV=2 [ME |
| Q5D862 | 9 | 2391 | 247,9 | 8,31 | 38 | Filaggrin2 GN=FLG2 PE=1 SV=1 [FILA2] |
| A6NJ16 | 4 | 123 | 13,6 | 9,60 | 38 | Putative Vset and immunoglobulin domaincontaining protein 6 GN=VSIG6 PE=5 SV= |
| Q969N2 | 8 | 578 | 65,7 | 8,38 | 38 | GPI transamidase component PIGT GN=PIGT PE=1 SV=1 [PIGT] |
| Q460N3 | 1 | 656 | 72,5 | 8,82 | 38 | Poly [ADPribose] polymerase 15 GN=PARP15 PE=1 SV=1 [PAR15] |
| Q8IZ20 | 1 | 524 | 56,9 | 8,69 | 38 | Zinc finger protein 683 GN=ZNF683 PE=2 SV=3 [ZN683] |
| Q8NF86 | 9 | 280 | 29,8 | 9,94 | 38 | Serine protease 33 GN=PRSS33 PE=1 SV=3 [PRS33] |
| Q8TCB7 | 26 | 284 | 33,2 | 6,19 | 38 | Methyltransferaselike protein 6 GN=METTL6 PE=2 SV=2 [METL6] |
| Q9H825 | 17 | 291 | 33,4 | 6,95 | 38 | Methyltransferaselike protein 8 GN=METTL8 PE=2 SV=2 [METL8] |
| Q68DN1 | 12 | 1984 | 224,2 | 10,08 | 38 | Uncharacterized protein C2orf16 GN=C2orf16 PE=1 SV=3 [CB016] |
| Q07001 | 2 | 517 | 58,9 | 6,55 | 38 | Acetylcholine receptor subunit delta GN=CHRND PE=1 SV=1 [ACHD] |
| Q7Z410 | 144 | 1059 | 113,9 | 8,07 | 38 | Transmembrane protease serine 9 GN=TMPRSS9 PE=1 SV=2 [TMPS9] |
| Q9BPX7 | 1 | 421 | 46,4 | 6,42 | 38 | UPF0415 protein C7orf25 GN=C7orf25 PE=1 SV=1 [CG025] |
| Q9C030 | 36 | 488 | 56,4 | 7,55 | 38 | Tripartite motifcontaining protein 6 GN=TRIM6 PE=1 SV=1 [TRIM6] |
| P11586 | 369 | 935 | 101,5 | 7,30 | 37 | C1tetrahydrofolate synthase, cytoplasmic GN=MTHFD1 PE=1 SV=3 [C1TC] |
| Q8N4C8 | 5 | 1332 | 149,7 | 7,85 | 37 | Misshapenlike kinase 1 GN=MINK1 PE=1 SV=2 [MINK1] |

| | | | | | | |
|---|---|---|---|---|---|---|
| P29590 | 5 | 882 | 97,5 | 6,21 | 37 | Protein PML GN=PML PE=1 SV=3 [PML] |
| Q9NQ75 | 2 | 786 | 87,1 | 7,08 | 37 | Cas scaffolding protein family member 4 GN=CASS4 PE=1 SV=2 [CASS4] |
| Q9P2D3 | 39 | 2071 | 224,2 | 7,17 | 37 | HEAT repeatcontaining protein 5B GN=HEATR5B PE=1 SV=2 [HTR5B] |
| P22304 | 26 | 550 | 61,8 | 5,45 | 37 | Iduronate 2sulfatase GN=IDS PE=1 SV=1 [IDS] |
| Q9BZE7 | 1 | 217 | 24,9 | 9,80 | 37 | UPF0193 protein EVG1 [EVG1] |
| A2VCL2 | 4 | 907 | 103,8 | 7,90 | 37 | Coiledcoil domaincontaining protein 162 GN=CCDC162P PE=2 SV=3 [CC162] |
| P20930 | 10 | 4061 | 434,9 | 9,25 | 37 | Filaggrin GN=FLG PE=1 SV=3 [FILA] |
| Q9BRX2 | 3 | 385 | 43,3 | 6,34 | 37 | Protein pelota homolog GN=PELO PE=1 SV=2 [PELO] |
| P21796 | 42 | 283 | 30,8 | 8,54 | 37 | Voltagedependent anionselective channel protein 1 GN=VDAC1 PE=1 SV=2 [VDAC1 |
| Q6IBS0 | 6 | 349 | 39,5 | 6,84 | 37 | Twinfilin2 GN=TWF2 PE=1 SV=2 [TWF2] |
| Q9BZ23 | 3 | 570 | 62,6 | 9,28 | 37 | Pantothenate kinase 2, mitochondrial GN=PANK2 PE=1 SV=3 [PANK2] |
| Q9P2E3 | 16 | 1918 | 220,1 | 7,30 | 37 | NFX1type zinc fingercontaining protein 1 GN=ZNFX1 PE=1 SV=2 [ZNFX1] |
| P41219 | 15 | 470 | 53,6 | 5,47 | 37 | Peripherin GN=PRPH PE=1 SV=2 [PERI] |
| Q658Y4 | 86 | 838 | 93,8 | 6,39 | 37 | Protein FAM91A1 GN=FAM91A1 PE=1 SV=3 [F91A1] |
| Q12840 | 1 | 1032 | 117,3 | 5,90 | 37 | Kinesin heavy chain isoform 5A GN=KIF5A PE=1 SV=2 [KIF5A] |
| Q9BZ95 | 3 | 1437 | 161,5 | 8,21 | 37 | Histonelysine Nmethyltransferase NSD3 GN=WHSC1L1 PE=1 SV=1 [NSD3] |
| Q9BQE4 | 10 | 189 | 21,2 | 9,70 | 37 | Selenoprotein S GN=SELS PE=1 SV=3 [SELS] |
| Q8IWV2 | 5 | 1026 | 113,4 | 7,47 | 37 | Contactin4 GN=CNTN4 PE=1 SV=1 [CNTN4] |
| Q9NRP7 | 23 | 1315 | 143,9 | 5,90 | 37 | Serine/threonineprotein kinase 36 GN=STK36 PE=1 SV=2 [STK36] |
| Q5JTD7 | 10 | 316 | 33,4 | 4,84 | 37 | Uncharacterized protein C6orf154 GN=C6orf154 PE=2 SV=1 [CF154] |
| Q8N187 | 123 | 725 | 80,6 | 5,69 | 37 | Amyotrophic lateral sclerosis 2 chromosomal region candidate gene 8 protein GN=A |
| P55345 | 3 | 433 | 49,0 | 5,17 | 37 | Protein arginine Nmethyltransferase 2 GN=PRMT2 PE=1 SV=1 [ANM2] |
| Q2VPB7 | 18 | 878 | 93,9 | 5,92 | 37 | AP5 complex subunit beta1 GN=AP5B1 PE=1 SV=4 [AP5B1] |
| Q9UQP3 | 6 | 1299 | 143,9 | 5,63 | 37 | TenascinN GN=TNN PE=1 SV=2 [TENN] |
| Q15291 | 24 | 538 | 59,1 | 5,10 | 36 | Retinoblastomabinding protein 5 GN=RBBP5 PE=1 SV=2 [RBBP5] |
| Q9NUS5 | 13 | 200 | 22,5 | 6,87 | 36 | Uncharacterized protein C20orf29 GN=C20orf29 PE=2 SV=1 [CT029] |
| Q92692 | 1 | 538 | 57,7 | 4,82 | 36 | Poliovirus receptorrelated protein 2 GN=PVRL2 PE=1 SV=1 [PVRL2] |
| Q8N3C0 | 10 | 2202 | 251,3 | 7,09 | 36 | Activating signal cointegrator 1 complex subunit 3 GN=ASCC3 PE=1 SV=3 [HELC1] |
| Q8TER5 | 3 | 1519 | 164,6 | 6,15 | 36 | Rho guanine nucleotide exchange factor 40 GN=ARHGEF40 PE=1 SV=3 [ARH40] |
| Q99715 | 30 | 3063 | 332,9 | 5,53 | 36 | Collagen alpha1(XII) chain GN=COL12A1 PE=1 SV=2 [COCA1] |
| Q96K76 | 1 | 1375 | 157,2 | 5,08 | 36 | Ubiquitin carboxylterminal hydrolase 47 GN=USP47 PE=1 SV=3 [UBP47] |
| Q9H6A9 | 10 | 2034 | 221,9 | 6,64 | 36 | Pecanexlike protein 3 GN=PCNXL3 PE=1 SV=2 [PCX3] |
| Q9NV72 | 25 | 465 | 53,8 | 9,22 | 36 | Zinc finger protein 701 GN=ZNF701 PE=2 SV=2 [ZN701] |
| P56645 | 1 | 1201 | 131,8 | 6,89 | 36 | Period circadian protein homolog 3 GN=PER3 PE=2 SV=4 [PER3] |
| O95271 | 9 | 1327 | 142,0 | 7,05 | 36 | Tankyrase1 GN=TNKS PE=1 SV=2 [TNKS1] |
| Q5VT99 | 3 | 294 | 32,1 | 4,97 | 36 | Leucinerich repeatcontaining protein 38 GN=LRRC38 PE=2 SV=1 [LRC38] |
| Q9Y2F9 | 7 | 522 | 58,4 | 7,46 | 36 | BTB/POZ domaincontaining protein 3 GN=BTBD3 PE=2 SV=1 [BTBD3] |
| Q06210 | 26 | 699 | 78,8 | 7,11 | 36 | Glucosaminefructose6phosphate aminotransferase [isomerizing] 1 GN=GFPT1 PE=1 |
| Q9UDX4 | 40 | 400 | 46,0 | 6,11 | 36 | SEC14like protein 3 GN=SEC14L3 PE=2 SV=1 [S14L3] |
| Q8N584 | 17 | 583 | 65,8 | 6,99 | 36 | Tetratricopeptide repeat protein 39C GN=TTC39C PE=1 SV=2 [TT39C] |
| Q9ULI0 | 30 | 1458 | 164,8 | 6,80 | 36 | ATPase family AAA domaincontaining protein 2B GN=ATAD2B PE=1 SV=3 [ATD2B] |
| Q8N201 | 28 | 2190 | 244,1 | 6,13 | 36 | Integrator complex subunit 1 GN=INTS1 PE=1 SV=2 [INT1] |
| Q9C0I3 | 15 | 900 | 99,4 | 7,83 | 36 | Protein FAM190A GN=FAM190A PE=2 SV=2 [F190A] |
| P05155 | 171 | 500 | 55,1 | 6,55 | 36 | Plasma protease C1 inhibitor GN=SERPING1 PE=1 SV=2 [IC1] |
| Q96PP8 | 5 | 586 | 66,6 | 5,55 | 36 | Guanylatebinding protein 5 GN=GBP5 PE=2 SV=1 [GBP5] |
| Q5W5X9 | 7 | 447 | 50,0 | 8,38 | 36 | Tetratricopeptide repeat protein 23 GN=TTC23 PE=2 SV=1 [TTC23] |
| Q96C03 | 5 | 454 | 49,2 | 5,12 | 36 | SmithMagenis syndrome chromosomal region candidate gene 7 protein GN=SMCR7 |
| Q9P283 | 21 | 1151 | 125,8 | 7,65 | 36 | Semaphorin5B GN=SEMA5B PE=2 SV=4 [SEM5B] |
| O00116 | 440 | 658 | 72,9 | 7,34 | 36 | Alkyldihydroxyacetonephosphate synthase, peroxisomal GN=AGPS PE=1 SV=1 [AD |
| Q6DN14 | 26 | 999 | 111,6 | 8,15 | 36 | Multiple C2 and transmembrane domaincontaining protein 1 GN=MCTP1 PE=2 SV=2 |
| Q8NCI6 | 2 | 653 | 74,8 | 8,95 | 36 | Betagalactosidase1like protein 3 GN=GLB1L3 PE=2 SV=3 [GLBL3] |
| Q15404 | 189 | 277 | 31,5 | 8,65 | 36 | Ras suppressor protein 1 GN=RSU1 PE=1 SV=3 [RSU1] |
| Q9NPZ5 | 36 | 323 | 36,9 | 10,62 | 36 | Galactosylgalactosylxylosylprotein 3betaglucuronosyltransferase 2 GN=B3GAT2 PE= |
| Q96FB5 | 1 | 475 | 52,9 | 7,97 | 36 | UPF0431 protein C1orf66 GN=C1orf66 PE=2 SV=2 [CA066] |
| Q6ZU65 | 8 | 1347 | 146,0 | 9,19 | 36 | Ubinuclein2 GN=UBN2 PE=1 SV=2 [UBN2] |
| P52735 | 8 | 878 | 101,2 | 7,08 | 36 | Guanine nucleotide exchange factor VAV2 GN=VAV2 PE=1 SV=2 [VAV2] |
| A6NEL2 | 8 | 793 | 85,7 | 9,60 | 36 | Ankyrin repeat domaincontaining protein 56 GN=ANKRD56 PE=2 SV=1 [ANR56] |
| Q15067 | 4 | 660 | 74,4 | 8,16 | 36 | Peroxisomal acylcoenzyme A oxidase 1 GN=ACOX1 PE=1 SV=3 [ACOX1] |
| Q49A17 | 6 | 601 | 69,7 | 7,46 | 36 | Polypeptide Nacetylgalactosaminyltransferaselike 6 GN=GALNTL6 PE=2 SV=2 [GLTL |
| Q63HK5 | 10 | 1081 | 118,5 | 7,25 | 36 | Teashirt homolog 3 GN=TSHZ3 PE=1 SV=2 [TSH3] |
| A8MZ36 | 32 | 301 | 33,9 | 6,20 | 36 | Envoplakinlike protein GN=EVPLL PE=2 SV=1 [EVPLL] |
| Q8N6V9 | 3 | 391 | 44,8 | 6,60 | 36 | Testisexpressed sequence 9 protein GN=TEX9 PE=2 SV=1 [TEX9] |
| Q9NQ87 | 440 | 328 | 35,1 | 10,68 | 36 | Hairy/enhancerofsplit related with YRPW motiflike protein GN=HEYL PE=2 SV=2 [HI |
| P12081 | 12 | 509 | 57,4 | 5,88 | 36 | HistidyltRNA synthetase, cytoplasmic GN=HARS PE=1 SV=2 [SYHC] |
| Q8IWR0 | 12 | 971 | 110,5 | 7,30 | 36 | Zinc finger CCCH domaincontaining protein 7A GN=ZC3H7A PE=1 SV=1 [Z3H7A] |

| | | | | | | |
|---|---|---|---|---|---|---|
| P33261 | 28 | 490 | 55,9 | 7,39 | 36 | Cytochrome P450 2C19 GN=CYP2C19 PE=1 SV=3 [CP2CJ] |
| Q93084 | 13 | 1043 | 113,9 | 5,57 | 36 | Sarcoplasmic/endoplasmic reticulum calcium ATPase 3 (EC 3.6.3.8) (Calcium pump 3 |
| Q11203 | 2 | 375 | 42,1 | 8,98 | 36 | CMPNacetylneuraminatebeta1,4galactoside alpha2,3sialyltransferase GN=ST3GAL3 |
| Q9NQ66 | 17 | 1216 | 138,5 | 6,23 | 35 | 1phosphatidylinositol4,5bisphosphate phosphodiesterase beta1 GN=PLCB1 PE=1 SV |
| P17544 | 53 | 494 | 52,9 | 8,65 | 35 | Cyclic AMPdependent transcription factor ATF7 GN=ATF7 PE=1 SV=2 [ATF7] |
| Q92805 | 16 | 767 | 88,1 | 5,27 | 35 | Golgin subfamily A member 1 GN=GOLGA1 PE=1 SV=3 [GOGA1] |
| Q5THK1 | 6 | 2151 | 237,2 | 6,33 | 35 | Uncharacterized protein C22orf30 GN=C22orf30 PE=1 SV=1 [CV030] |
| P48553 | 173 | 1259 | 142,1 | 6,04 | 35 | Trafficking protein particle complex subunit 10 GN=TRAPPC10 PE=1 SV=2 [TPC10] |
| P08069 | 1 | 1367 | 154,7 | 5,80 | 35 | Insulinlike growth factor 1 receptor GN=IGF1R PE=1 SV=1 [IGF1R] |
| Q92674 | 10 | 756 | 86,7 | 8,76 | 35 | Centromere protein I GN=CENPI PE=1 SV=2 [CENPI] |
| P16066 | 9 | 1061 | 118,8 | 6,64 | 35 | Atrial natriuretic peptide receptor 1 GN=NPR1 PE=1 SV=1 [ANPRA] |
| Q01581 | 223 | 520 | 57,3 | 5,41 | 35 | HydroxymethylglutarylCoA synthase, cytoplasmic (EC 2.3.3.10) (HMGCoA synthase) |
| O00330 | 1 | 501 | 54,1 | 8,66 | 35 | Pyruvate dehydrogenase protein X component, mitochondrial GN=PDHX PE=1 SV=3 |
| Q8IVG5 | 6 | 1584 | 184,4 | 8,02 | 35 | Sterile alpha motif domaincontaining protein 9like GN=SAMD9L PE=1 SV=2 [SAM9L |
| Q8NEM0 | 148 | 835 | 92,8 | 8,25 | 35 | Microcephalin GN=MCPH1 PE=1 SV=3 [MCPH1] |
| Q5JPI3 | 311 | 329 | 37,5 | 6,47 | 35 | Uncharacterized protein C3orf38 GN=C3orf38 PE=2 SV=1 [CC038] |
| Q9HC56 | 2 | 1237 | 136,0 | 5,47 | 35 | Protocadherin9 GN=PCDH9 PE=1 SV=2 [PCDH9] |
| Q6ZTR7 | 4 | 304 | 34,8 | 8,66 | 35 | Protein FAM92B GN=FAM92B PE=2 SV=1 [FA92B] |
| A7MCY6 | 2 | 615 | 67,7 | 5,86 | 35 | TANKbinding kinase 1binding protein 1 GN=TBKBP1 PE=1 SV=1 [TBKB1] |
| Q08999 | 18 | 1139 | 128,3 | 7,44 | 35 | Retinoblastomalike protein 2 GN=RBL2 PE=1 SV=3 [RBL2] |
| Q9H0I3 | 10 | 377 | 44,2 | 8,73 | 35 | Coiledcoil domaincontaining protein 113 GN=CCDC113 PE=2 SV=1 [CC113] |
| P33908 | 21 | 653 | 72,9 | 6,47 | 35 | Mannosyloligosaccharide 1,2alphamannosidase IA GN=MAN1A1 PE=1 SV=3 [MA1A1 |
| Q6ZRR7 | 2 | 1453 | 166,8 | 7,65 | 35 | Leucinerich repeatcontaining protein 9 GN=LRRC9 PE=2 SV=2 [LRRC9] |
| Q8N323 | 12 | 547 | 63,1 | 8,56 | 35 | Protein FAM55A GN=FAM55A PE=2 SV=2 [FA55A] |
| P14543 | 2 | 1247 | 136,3 | 5,29 | 35 | Nidogen1 GN=NID1 PE=1 SV=3 [NID1] |
| P83105 | 3 | 476 | 50,9 | 8,02 | 35 | Probable serine protease HTRA4 GN=HTRA4 PE=2 SV=1 [HTRA4] |
| Q9H307 | 163 | 717 | 81,6 | 7,14 | 35 | Pinin GN=PNN PE=1 SV=4 [PININ] |
| O15440 | 2 | 1437 | 160,6 | 8,66 | 35 | Multidrug resistanceassociated protein 5 GN=ABCC5 PE=1 SV=2 [MRP5] |
| Q8TCG2 | 56 | 481 | 54,7 | 5,97 | 35 | Phosphatidylinositol 4kinase type 2beta GN=PI4K2B PE=1 SV=1 [P4K2B] |
| Q9Y5P8 | 2 | 575 | 65,0 | 5,14 | 35 | Serine/threonineprotein phosphatase 2A regulatory subunit B'' subunit beta GN=PP |
| Q7Z553 | 3 | 956 | 107,4 | 7,20 | 35 | MAM domaincontaining glycosylphosphatidylinositol anchor protein 2 GN=MDGA2 |
| Q9HAW4 | 8 | 1339 | 151,0 | 4,82 | 35 | Claspin GN=CLSPN PE=1 SV=3 [CLSPN] |
| P61764 | 37 | 594 | 67,5 | 6,96 | 35 | Syntaxinbinding protein 1 GN=STXBP1 PE=1 SV=1 [STXB1] |
| O15068 | 239 | 1137 | 128,0 | 6,43 | 35 | Guanine nucleotide exchange factor DBS GN=MCF2L PE=1 SV=2 [MCF2L] |
| Q9Y5B9 | 57 | 1047 | 119,8 | 5,66 | 35 | FACT complex subunit SPT16 GN=SUPT16H PE=1 SV=1 [SP16H] |
| Q9ULH0 | 58 | 1771 | 196,4 | 6,62 | 35 | Kinase Dinteracting substrate of 220 kDa GN=KIDINS220 PE=1 SV=3 [KDIS] |
| Q8IX95 | 2 | 158 | 18,0 | 4,92 | 35 | Putative cutaneous Tcell lymphomaassociated antigen 3 GN=CTAGE3P PE=5 SV=1 [C |
| Q15008 | 7 | 389 | 45,5 | 5,62 | 35 | 26S proteasome nonATPase regulatory subunit 6 GN=PSMD6 PE=1 SV=1 [PSMD6] |
| Q9Y2Z2 | 2 | 717 | 79,9 | 8,31 | 35 | Protein MTO1 homolog, mitochondrial GN=MTO1 PE=1 SV=2 [MTO1] |
| Q9H6W3 | 4 | 641 | 71,0 | 6,46 | 35 | Lysinespecific demethylase NO66 GN=NO66 PE=1 SV=2 [NO66] |
| Q9H0I9 | 3 | 626 | 67,8 | 6,33 | 35 | Transketolaselike protein 2 GN=TKTL2 PE=1 SV=1 [TKTL2] |
| Q96C10 | 14 | 678 | 76,6 | 7,37 | 34 | Probable ATPdependent RNA helicase DHX58 GN=DHX58 PE=1 SV=1 [DHX58] |
| Q96ST2 | 7 | 819 | 91,9 | 4,69 | 34 | Protein IWS1 homolog GN=IWS1 PE=1 SV=2 [IWS1] |
| O14595 | 8 | 271 | 30,6 | 5,53 | 34 | Carboxyterminal domain RNA polymerase II polypeptide A small phosphatase 2 GN |
| Q9H3U7 | 18 | 446 | 49,6 | 8,46 | 34 | SPARCrelated modular calciumbinding protein 2 GN=SMOC2 PE=2 SV=2 [SMOC2] |
| Q13042 | 6 | 620 | 71,6 | 5,85 | 34 | Cell division cycle protein 16 homolog GN=CDC16 PE=1 SV=2 [CDC16] |
| P29475 | 5 | 1434 | 160,9 | 7,42 | 34 | Nitric oxide synthase, brain GN=NOS1 PE=1 SV=2 [NOS1] |
| P51948 | 21 | 309 | 35,8 | 6,09 | 34 | CDKactivating kinase assembly factor MAT1 GN=MNAT1 PE=1 SV=1 [MAT1] |
| Q15650 | 2 | 581 | 66,1 | 7,85 | 34 | Activating signal cointegrator 1 GN=TRIP4 PE=1 SV=4 [TRIP4] |
| Q7Z5J8 | 3 | 1434 | 161,9 | 8,10 | 34 | Ankyrin and armadillo repeatcontaining protein GN=ANKAR PE=2 SV=3 [ANKAR] |
| Q9H0A9 | 4 | 340 | 37,6 | 7,43 | 34 | Uncharacterized protein C21orf56 GN=C21orf56 PE=2 SV=3 [CU056] |
| Q9GZY0 | 13 | 626 | 71,6 | 7,64 | 34 | Nuclear RNA export factor 2 GN=NXF2 PE=1 SV=1 [NXF2] |
| Q8N556 | 23 | 730 | 80,7 | 8,68 | 34 | Actin filamentassociated protein 1 GN=AFAP1 PE=1 SV=2 [AFAP1] |
| P78333 | 11 | 572 | 63,7 | 6,81 | 34 | Glypican5 GN=GPC5 PE=1 SV=1 [GPC5] |
| Q6UWF7 | 10 | 544 | 62,2 | 8,85 | 34 | Protein FAM55D GN=FAM55D PE=2 SV=1 [FA55D] |
| P42766 | 7 | 123 | 14,5 | 11,05 | 34 | 60S ribosomal protein L35 GN=RPL35 PE=1 SV=2 [RL35] |
| Q9H324 | 1 | 1103 | 120,8 | 7,94 | 34 | A disintegrin and metalloproteinase with thrombospondin motifs 10 GN=ADAMTS1 |
| Q16665 | 18 | 826 | 92,6 | 5,33 | 34 | Hypoxiainducible factor 1alpha GN=HIF1A PE=1 SV=1 [HIF1A] |
| Q9H3G5 | 27 | 476 | 54,1 | 5,62 | 34 | Probable serine carboxypeptidase CPVL GN=CPVL PE=1 SV=2 [CPVL] |
| Q6W4X9 | 1 | 2439 | 256,9 | 7,39 | 34 | Mucin6 GN=MUC6 PE=1 SV=3 [MUC6] |
| Q9UPW6 | 211 | 733 | 82,5 | 6,90 | 34 | DNAbinding protein SATB2 GN=SATB2 PE=1 SV=2 [SATB2] |
| Q9NRL3 | 1 | 753 | 80,5 | 5,40 | 34 | Striatin4 GN=STRN4 PE=1 SV=2 [STRN4] |
| O75420 | 20 | 1035 | 114,5 | 5,39 | 34 | PERQ amino acidrich with GYF domaincontaining protein 1 GN=GIGYF1 PE=1 SV=2 [P |
| P59046 | 8 | 1061 | 120,1 | 6,99 | 34 | NACHT, LRR and PYD domainscontaining protein 12 GN=NLRP12 PE=2 SV=2 [NAL12] |
| Q9NRR4 | 13 | 1374 | 159,2 | 7,87 | 33 | Ribonuclease 3 GN=DROSHA PE=1 SV=2 [RNC] |

| | | | | | | |
|---|---|---|---|---|---|---|
| Q08828 | 11 | 1119 | 123,4 | 8,43 | 33 | Adenylate cyclase type 1 GN=ADCY1 PE=1 SV=2 [ADCY1] |
| Q96JJ6 | 17 | 628 | 65,8 | 6,81 | 33 | Junctophilin4 GN=JPH4 PE=1 SV=2 [JPH4] |
| P35228 | 6 | 1153 | 131,0 | 7,96 | 33 | Nitric oxide synthase, inducible GN=NOS2 PE=1 SV=2 [NOS2] |
| Q15262 | 9 | 1439 | 162,0 | 5,90 | 33 | Receptortype tyrosineprotein phosphatase kappa GN=PTPRK PE=1 SV=2 [PTPRK] |
| O14490 | 101 | 977 | 108,8 | 7,08 | 33 | Disks largeassociated protein 1 GN=DLGAP1 PE=1 SV=1 [DLGP1] |
| Q96QR8 | 4 | 312 | 33,2 | 5,43 | 33 | Transcriptional activator protein Purbeta GN=PURB PE=1 SV=3 [PURB] |
| Q9HCM3 | 37 | 1950 | 210,6 | 6,11 | 33 | UPF0606 protein KIAA1549 GN=KIAA1549 PE=1 SV=4 [K1549] |
| P29375 | 12 | 1690 | 192,0 | 6,49 | 33 | Lysinespecific demethylase 5A GN=KDM5A PE=1 SV=3 [KDM5A] |
| Q8WXA9 | 24 | 508 | 59,3 | 10,39 | 33 | Splicing regulatory glutamine/lysinerich protein 1 GN=SREK1 PE=1 SV=1 [SREK1] |
| O15117 | 2 | 783 | 85,3 | 6,48 | 33 | FYNbinding protein GN=FYB PE=1 SV=2 [FYB] |
| P30954 | 11 | 320 | 35,9 | 9,07 | 33 | Olfactory receptor 10J1 GN=OR10J1 PE=2 SV=2 [O10J1] |
| Q8IWB9 | 9 | 1127 | 125,2 | 6,01 | 33 | Testisexpressed sequence 2 protein GN=TEX2 PE=1 SV=2 [TEX2] |
| P20701 | 24 | 1170 | 128,7 | 5,63 | 33 | Integrin alphaL GN=ITGAL PE=1 SV=3 [ITAL] |
| Q9NNZ3 | 2 | 241 | 27,6 | 10,55 | 33 | DnaJ homolog subfamily C member 4 GN=DNAJC4 PE=2 SV=1 [DNJC4] |
| P42680 | 5 | 631 | 73,5 | 8,44 | 33 | Tyrosineprotein kinase Tec GN=TEC PE=1 SV=2 [TEC] |
| Q9UBD0 | 6 | 423 | 46,7 | 7,11 | 33 | Heat shock transcription factor, Xlinked GN=HSFX1 PE=1 SV=1 [HSFX1] |
| P00751 | 3 | 764 | 85,5 | 7,06 | 33 | Complement factor B GN=CFB PE=1 SV=2 [CFAB] |
| Q494X3 | 2 | 552 | 65,4 | 9,14 | 33 | Zinc finger protein 404 GN=ZNF404 PE=2 SV=1 [ZN404] |
| P11171 | 2 | 864 | 97,0 | 5,58 | 33 | Protein 4.1 GN=EPB41 PE=1 SV=4 [41] |
| Q1X8D7 | 6 | 754 | 83,8 | 7,15 | 33 | Leucinerich repeatcontaining protein 36 GN=LRRC36 PE=2 SV=2 [LRC36] |
| Q9Y238 | 4 | 1755 | 195,6 | 6,33 | 32 | Deleted in lung and esophageal cancer protein 1 GN=DLEC1 PE=2 SV=2 [DLEC1] |
| P22557 | 16 | 587 | 64,6 | 8,12 | 32 | 5aminolevulinate synthase, erythroidspecific, mitochondrial GN=ALAS2 PE=1 SV=2 |
| Q96ER9 | 6 | 411 | 45,8 | 8,19 | 32 | Coiledcoil domaincontaining protein 51 GN=CCDC51 PE=1 SV=2 [CCD51] |
| Q9GZQ6 | 4 | 430 | 47,8 | 9,41 | 32 | Neuropeptide FF receptor 1 GN=NPFFR1 PE=1 SV=1 [NPFF1] |
| Q8WYP5 | 3 | 2266 | 252,3 | 6,60 | 32 | Protein ELYS GN=AHCTF1 PE=1 SV=3 [ELYS] |
| Q9Y575 | 11 | 518 | 57,7 | 6,27 | 32 | Ankyrin repeat and SOCS box protein 3 GN=ASB3 PE=1 SV=1 [ASB3] |
| Q16795 | 8 | 377 | 42,5 | 9,80 | 32 | NADH dehydrogenase [ubiquinone] 1 alpha subcomplex subunit 9, mitochondrial p |
| Q10981 | 4 | 343 | 39,0 | 8,54 | 32 | Galactoside 2alphaLfucosyltransferase 2 GN=FUT2 PE=2 SV=1 [FUT2] |
| P21580 | 62 | 790 | 89,6 | 8,22 | 32 | Tumor necrosis factor alphainduced protein 3 GN=TNFAIP3 PE=1 SV=1 [TNAP3] |
| Q6WKZ4 | 5 | 1283 | 137,1 | 5,47 | 32 | Rab11 familyinteracting protein 1 GN=RAB11FIP1 PE=1 SV=2 [RFIP1] |
| P49750 | 24 | 1951 | 219,8 | 6,57 | 32 | YLP motifcontaining protein 1 GN=YLPM1 PE=1 SV=3 [YLPM1] |
| Q6NUQ1 | 22 | 792 | 90,6 | 5,45 | 32 | RAD50interacting protein 1 GN=RINT1 PE=1 SV=1 [RINT1] |
| Q14191 | 3 | 1432 | 162,4 | 6,34 | 32 | Werner syndrome ATPdependent helicase GN=WRN PE=1 SV=2 [WRN] |
| P17661 | 8 | 470 | 53,5 | 5,27 | 32 | Desmin GN=DES PE=1 SV=3 [DESM] |
| O75146 | 4 | 1068 | 119,3 | 6,67 | 32 | Huntingtininteracting protein 1related protein GN=HIP1R PE=1 SV=2 [HIP1R] |
| Q2WGJ6 | 2 | 581 | 65,5 | 7,93 | 32 | Kelchlike protein 38 GN=KLHL38 PE=2 SV=3 [KLH38] |
| O00294 | 7 | 542 | 60,6 | 9,47 | 32 | Tubbyrelated protein 1 GN=TULP1 PE=1 SV=3 [TULP1] |
| O43148 | 29 | 476 | 54,8 | 6,61 | 32 | mRNA cap guanineN7 methyltransferase GN=RNMT PE=1 SV=1 [MCES] |
| O76039 | 5 | 1030 | 115,5 | 9,54 | 32 | Cyclindependent kinaselike 5 GN=CDKL5 PE=1 SV=1 [CDKL5] |
| Q92974 | 23 | 986 | 111,5 | 7,27 | 32 | Rho guanine nucleotide exchange factor 2 GN=ARHGEF2 PE=1 SV=4 [ARHG2] |
| Q9H0B3 | 3 | 1180 | 127,6 | 10,23 | 32 | Uncharacterized protein KIAA1683 GN=KIAA1683 PE=1 SV=1 [K1683] |
| Q9Y2G1 | 108 | 1151 | 124,3 | 7,44 | 32 | Myelin gene regulatory factor GN=MRF PE=1 SV=3 [MRF] |
| Q99714 | 12 | 261 | 26,9 | 7,78 | 32 | 3hydroxyacylCoA dehydrogenase type2 GN=HSD17B10 PE=1 SV=3 [HCD2] |
| O43283 | 7 | 966 | 108,2 | 6,49 | 32 | Mitogenactivated protein kinase kinase kinase 13 GN=MAP3K13 PE=1 SV=1 [M3K13 |
| Q9H3R5 | 3 | 247 | 28,5 | 5,29 | 32 | Centromere protein H (CENPH) (Interphase centromere complex protein 35) [CEN |
| Q9UJC3 | 11 | 728 | 84,6 | 5,15 | 32 | Protein Hook homolog 1 GN=HOOK1 PE=1 SV=2 [HOOK1] |
| Q96T51 | 2 | 708 | 79,8 | 5,74 | 32 | RUN and FYVE domaincontaining protein 1 GN=RUFY1 PE=1 SV=2 [RUFY1] |
| Q8N998 | 3 | 374 | 43,8 | 5,36 | 31 | Coiledcoil domaincontaining protein 89 GN=CCDC89 PE=2 SV=1 [CCD89] |
| O60244 | 3 | 1454 | 160,5 | 8,73 | 31 | Mediator of RNA polymerase II transcription subunit 14 GN=MED14 PE=1 SV=2 [MEI |
| Q99988 | 1 | 308 | 34,1 | 9,66 | 31 | Growth/differentiation factor 15 GN=GDF15 PE=1 SV=3 [GDF15] |
| Q5SRN2 | 4 | 563 | 61,6 | 9,25 | 31 | Uncharacterized protein C6orf10 GN=C6orf10 PE=1 SV=3 [CF010] |
| P49760 | 3 | 499 | 60,1 | 9,66 | 31 | Dual specificity protein kinase CLK2 GN=CLK2 PE=1 SV=1 [CLK2] |
| Q5FYB1 | 5 | 569 | 64,0 | 8,62 | 31 | Arylsulfatase I GN=ARSI PE=1 SV=1 [ARSI] |
| Q96G42 | 6 | 594 | 63,3 | 9,00 | 31 | Kelch domaincontaining protein 7B GN=KLHDC7B PE=2 SV=2 [KLD7B] |
| Q99729 | 6 | 332 | 36,2 | 8,21 | 31 | Heterogeneous nuclear ribonucleoprotein A/B GN=HNRNPAB PE=1 SV=2 [ROAA] |
| Q9HCE9 | 17 | 1232 | 135,9 | 5,82 | 31 | Anoctamin8 GN=ANO8 PE=2 SV=3 [ANO8] |
| Q5T7V8 | 2 | 394 | 45,0 | 7,08 | 31 | RAB6interacting golgin GN=GORAB PE=1 SV=1 [GORAB] |
| P17213 | 3 | 487 | 53,9 | 9,38 | 31 | Bactericidal permeabilityincreasing protein GN=BPI PE=1 SV=4 [BPI] |
| Q9UNN5 | 17 | 650 | 73,9 | 4,88 | 31 | FASassociated factor 1 GN=FAF1 PE=1 SV=2 [FAF1] |
| Q9Y3E1 | 67 | 203 | 22,6 | 7,99 | 31 | Hepatomaderived growth factorrelated protein 3 GN=HDGFRP3 PE=1 SV=1 [HDGR3 |
| A4FU01 | 4 | 709 | 79,5 | 7,03 | 31 | Myotubularinrelated protein 11 GN=MTMR11 PE=2 SV=2 [MTMRB] |
| Q05195 | 24 | 221 | 25,2 | 8,53 | 31 | Max dimerization protein 1 GN=MXD1 PE=1 SV=1 [MAD1] |
| Q494V2 | 198 | 611 | 71,1 | 7,11 | 30 | Coiledcoil domaincontaining protein 37 GN=CCDC37 PE=1 SV=1 [CCD37] |
| P19823 | 5 | 946 | 106,4 | 6,86 | 30 | Interalphatrypsin inhibitor heavy chain H2 GN=ITIH2 PE=1 SV=2 [ITIH2] |
| O43913 | 8 | 435 | 50,3 | 7,74 | 30 | Origin recognition complex subunit 5 GN=ORC5 PE=1 SV=1 [ORC5] |

**Appendix 4:** LC ESI MS identified NHC-IOBA cell proteins.

| Accession | #Peptides | # AAs | MW [kDa] | calc. pI | Score | Description |
|---|---|---|---|---|---|---|
| P07900 | 1111 | 732 | 84,6 | 5,02 | 17236 | Heat shock protein HSP 90-alpha GN=HSP90AA1 PE=1 SV=5 |
| A2Q0Z1 | 874 | 646 | 70,9 | 5,52 | 16909 | Heat shock cognate 71 kDa protein GN=HSPA8 PE=2 SV=1 |
| P08238 | 1102 | 724 | 83,2 | 5,03 | 16858 | Heat shock protein HSP 90-beta GN=HSP90AB1 PE=1 SV=4 |
| P60712 | 1063 | 375 | 41,7 | 5,48 | 15447 | Actin, cytoplasmic 1 GN=ACTB PE=1 SV=1 |
| P06733 | 904 | 434 | 47,1 | 7,39 | 15161 | Alpha-enolase GN=ENO1 PE=1 SV=2 |
| P14618 | 809 | 531 | 57,9 | 7,84 | 14932 | Pyruvate kinase isozymes M1/M2 GN=PKM2 PE=1 SV=4 |
| Q2KJD0 | 635 | 444 | 49,6 | 4,89 | 13736 | Tubulin beta-5 chain GN=TUBB5 PE=2 SV=1 |
| P31327 | 1057 | 1500 | 164,8 | 6,74 | 13385 | Carbamoyl-phosphate synthase [ammonia], mitochondrial GN=CPS1 PE=1 SV=2 |
| P11021 | 662 | 654 | 72,3 | 5,16 | 12923 | 78 kDa glucose-regulated protein GN=HSPA5 PE=1 SV=2 |
| Q3MHM5 | 606 | 445 | 49,8 | 4,89 | 12793 | Tubulin beta-4B chain GN=TUBB4B PE=2 SV=1 |
| P07355 | 760 | 339 | 38,6 | 7,75 | 12539 | Annexin A2 GN=ANXA2 PE=1 SV=2 |
| P21333 | 1072 | 2647 | 280,6 | 6,06 | 12012 | Filamin-A GN=FLNA PE=1 SV=4 |
| P68103 | 898 | 462 | 50,1 | 9,01 | 11679 | Elongation factor 1-alpha 1 GN=EEF1A1 PE=2 SV=1 |
| P04406 | 695 | 335 | 36,0 | 8,46 | 11605 | Glyceraldehyde-3-phosphate dehydrogenase GN=GAPDH PE=1 SV=3 |
| Q3ZC07 | 823 | 377 | 42,0 | 5,39 | 11333 | Actin, alpha cardiac muscle 1 GN=ACTC1 PE=2 SV=1 |
| P62739 | 758 | 377 | 42,0 | 5,39 | 10443 | Actin, aortic smooth muscle GN=ACTA2 PE=1 SV=1 |
| Q13885 | 478 | 445 | 49,9 | 4,89 | 10178 | Tubulin beta-2A chain GN=TUBB2A PE=1 SV=1 |
| Q2T9S0 | 450 | 450 | 50,4 | 4,93 | 10153 | Tubulin beta-3 chain GN=TUBB3 PE=2 SV=1 |
| P81947 | 701 | 451 | 50,1 | 5,06 | 9968 | Tubulin alpha-1B chain PE=1 SV=2 |
| P63258 | 626 | 375 | 41,8 | 5,48 | 9606 | Actin, cytoplasmic 2 GN=ACTG1 PE=1 SV=1 |
| Q32PH8 | 650 | 463 | 50,4 | 9,03 | 9574 | Elongation factor 1-alpha 2 GN=EEF1A2 PE=2 SV=1 |
| Q06830 | 780 | 199 | 22,1 | 8,13 | 9544 | Peroxiredoxin-1 GN=PRDX1 PE=1 SV=1 |
| O75369 | 847 | 2602 | 278,0 | 5,73 | 9474 | Filamin-B GN=FLNB PE=1 SV=2 |
| P08107 | 500 | 641 | 70,0 | 5,66 | 9053 | Heat shock 70 kDa protein 1A/1B GN=HSPA1A PE=1 SV=5 |
| P04264 | 650 | 644 | 66,0 | 8,12 | 8972 | Keratin, type II cytoskeletal 1 GN=KRT1 PE=1 SV=6 |
| A6NMY6 | 567 | 339 | 38,6 | 6,95 | 8312 | Putative annexin A2-like protein GN=ANXA2P2 PE=5 SV=2 |
| P68362 | 648 | 451 | 50,1 | 5,06 | 8271 | Tubulin alpha-1A chain OS=Cricetulus griseus GN=TUBA1A PE=2 SV=1 |
| P54652 | 448 | 639 | 70,0 | 5,74 | 7852 | Heat shock-related 70 kDa protein 2 GN=HSPA2 PE=1 SV=1 |
| P00558 | 564 | 417 | 44,6 | 8,10 | 7648 | Phosphoglycerate kinase 1 GN=PGK1 PE=1 SV=3 |
| Q3ZBU7 | 429 | 444 | 49,6 | 4,88 | 7498 | Tubulin beta-4A chain GN=TUBB4A PE=2 SV=1 |
| P38646 | 386 | 679 | 73,6 | 6,16 | 7254 | Stress-70 protein, mitochondrial GN=HSPA9 PE=1 SV=2 |
| P81948 | 513 | 448 | 49,9 | 5,06 | 6852 | Tubulin alpha-4A chain GN=TUBA4A PE=1 SV=2 |
| P08670 | 412 | 466 | 53,6 | 5,12 | 6846 | Vimentin GN=VIM PE=1 SV=4 |
| P04083 | 282 | 346 | 38,7 | 7,02 | 6596 | Annexin A1 GN=ANXA1 PE=1 SV=2 |
| Q09666 | 1140 | 5890 | 628,7 | 6,15 | 6396 | Neuroblast differentiation-associated protein AHNAK GN=AHNAK PE=1 SV=2 |
| P22314 | 383 | 1058 | 117,8 | 5,76 | 6353 | Ubiquitin-like modifier-activating enzyme 1 GN=UBA1 PE=1 SV=3 |
| Q6S8J3 | 456 | 1075 | 121,3 | 6,20 | 6331 | POTE ankyrin domain family member E GN=POTEE PE=1 SV=3 |
| P34931 | 306 | 641 | 70,3 | 6,02 | 6284 | Heat shock 70 kDa protein 1-like GN=HSPA1L PE=1 SV=2 |
| A5A3E0 | 425 | 1075 | 121,4 | 6,20 | 6266 | POTE ankyrin domain family member F GN=POTEF PE=1 SV=2 |
| P07195 | 446 | 334 | 36,6 | 6,05 | 6193 | L-lactate dehydrogenase B chain GN=LDHB PE=1 SV=2 |
| P60174 | 293 | 286 | 30,8 | 5,92 | 5602 | Triosephosphate isomerase GN=TPI1 PE=1 SV=3 |
| P07737 | 264 | 140 | 15,0 | 8,27 | 5594 | Profilin-1 GN=PFN1 PE=1 SV=2 |
| P10809 | 405 | 573 | 61,0 | 5,87 | 5582 | 60 kDa heat shock protein, mitochondrial GN=HSPD1 PE=1 SV=2 |
| Q6B856 | 219 | 445 | 49,9 | 4,89 | 5580 | Tubulin beta-2B chain GN=TUBB2B PE=1 SV=2 |
| P06744 | 331 | 558 | 63,1 | 8,32 | 5578 | Glucose-6-phosphate isomerase GN=GPI PE=1 SV=4 |
| P06576 | 269 | 529 | 56,5 | 5,40 | 5405 | ATP synthase subunit beta, mitochondrial GN=ATP5B PE=1 SV=3 |
| P08758 | 338 | 320 | 35,9 | 5,05 | 5291 | Annexin A5 GN=ANXA5 PE=1 SV=2 |
| P09211 | 179 | 210 | 23,3 | 5,64 | 5286 | Glutathione S-transferase P GN=GSTP1 PE=1 SV=2 |
| P46940 | 411 | 1657 | 189,1 | 6,48 | 5207 | Ras GTPase-activating-like protein IQGAP1 GN=IQGAP1 PE=1 SV=1 |
| P00338 | 439 | 332 | 36,7 | 8,27 | 5121 | L-lactate dehydrogenase A chain GN=LDHA PE=1 SV=2 |
| Q562R1 | 468 | 376 | 42,0 | 5,59 | 5088 | Beta-actin-like protein 2 GN=ACTBL2 PE=1 SV=2 |
| P17066 | 261 | 643 | 71,0 | 6,14 | 5043 | Heat shock 70 kDa protein 6 GN=HSPA6 PE=1 SV=2 |
| Q13748 | 460 | 450 | 49,9 | 5,10 | 5037 | Tubulin alpha-3C/D chain GN=TUBA3C PE=1 SV=3 |
| P32119 | 384 | 198 | 21,9 | 5,97 | 4946 | Peroxiredoxin-2 GN=PRDX2 PE=1 SV=5 |
| Q6PEY2 | 405 | 450 | 49,8 | 5,14 | 4876 | Tubulin alpha-3E chain GN=TUBA3E PE=1 SV=2 |
| P37802 | 260 | 199 | 22,4 | 8,25 | 4871 | Transgelin-2 GN=TAGLN2 PE=1 SV=3 |
| P62938 | 500 | 165 | 18,0 | 7,81 | 4726 | Peptidyl-prolyl cis-trans isomerase A OS=Chlorocebus aethiops GN=PPIA PE=2 SV=2 |
| P13639 | 409 | 858 | 95,3 | 6,83 | 4618 | Elongation factor 2 GN=EEF2 PE=1 SV=4 |
| P13645 | 319 | 584 | 58,8 | 5,21 | 4601 | Keratin, type I cytoskeletal 10 GN=KRT10 PE=1 SV=6 |
| Q58FF7 | 428 | 597 | 68,3 | 4,79 | 4411 | Putative heat shock protein HSP 90-beta-3 GN=HSP90AB3P PE=5 SV=1 |
| Q5E9B5 | 335 | 376 | 41,8 | 5,48 | 4399 | Actin, gamma-enteric smooth muscle GN=ACTG2 PE=2 SV=1 |
| P14625 | 353 | 803 | 92,4 | 4,84 | 4209 | Endoplasmin GN=HSP90B1 PE=1 SV=1 |
| Q9BUF5 | 271 | 446 | 49,8 | 4,88 | 4182 | Tubulin beta-6 chain GN=TUBB6 PE=1 SV=1 |
| Q9BYX7 | 256 | 375 | 42,0 | 6,33 | 4143 | Putative beta-actin-like protein 3 GN=POTEKP PE=5 SV=1 |

| | | | | | | |
|---|---|---|---|---|---|---|
| P23284 | 397 | 216 | 23,7 | 9,41 | 4139 | Peptidyl-prolyl cis-trans isomerase B GN=PPIB PE=1 SV=2 |
| Q9NY65 | 310 | 449 | 50,1 | 5,06 | 4114 | Tubulin alpha-8 chain GN=TUBA8 PE=1 SV=1 |
| P09104 | 163 | 434 | 47,2 | 5,03 | 4082 | Gamma-enolase GN=ENO2 PE=1 SV=3 |
| P0CG38 | 387 | 1075 | 121,2 | 6,21 | 3941 | POTE ankyrin domain family member I GN=POTEI PE=3 SV=1 |
| Q58FF8 | 315 | 381 | 44,3 | 4,84 | 3906 | Putative heat shock protein HSP 90-beta 2 GN=HSP90AB2P PE=1 SV=2 |
| Q3SZ54 | 176 | 406 | 46,1 | 5,48 | 3837 | Eukaryotic initiation factor 4A-I GN=EIF4A1 PE=2 SV=1 |
| P62259 | 315 | 255 | 29,2 | 4,74 | 3577 | 14-3-3 protein epsilon GN=Ywhae PE=1 SV=1 |
| Q12931 | 144 | 704 | 80,1 | 8,21 | 3460 | Heat shock protein 75 kDa, mitochondrial GN=TRAP1 PE=1 SV=3 |
| P49327 | 296 | 2511 | 273,3 | 6,44 | 3405 | Fatty acid synthase GN=FASN PE=1 SV=3 |
| Q00610 | 299 | 1675 | 191,5 | 5,69 | 3382 | Clathrin heavy chain 1 GN=CLTC PE=1 SV=5 |
| P07205 | 221 | 417 | 44,8 | 8,54 | 3317 | Phosphoglycerate kinase 2 GN=PGK2 PE=1 SV=3 |
| Q13162 | 305 | 271 | 30,5 | 6,29 | 3295 | Peroxiredoxin-4 GN=PRDX4 PE=1 SV=1 |
| Q14568 | 252 | 343 | 39,3 | 4,65 | 3240 | Putative heat shock protein HSP 90-alpha A2 GN=HSP90AA2 PE=1 SV=2 |
| P13929 | 112 | 434 | 46,9 | 7,71 | 3236 | Beta-enolase GN=ENO3 PE=1 SV=4 |
| P04075 | 276 | 364 | 39,4 | 8,09 | 3229 | Fructose-bisphosphate aldolase A GN=ALDOA PE=1 SV=2 |
| P0CG39 | 328 | 1038 | 117,3 | 5,97 | 3152 | POTE ankyrin domain family member J GN=POTEJ PE=3 SV=1 |
| Q3ZCM7 | 237 | 444 | 49,7 | 4,89 | 3109 | Tubulin beta-8 chain GN=TUBB8 PE=1 SV=2 |
| Q3SZ65 | 129 | 407 | 46,4 | 5,48 | 3011 | Eukaryotic initiation factor 4A-II GN=EIF4A2 PE=2 SV=1 |
| P61603 | 209 | 102 | 10,9 | 8,92 | 2974 | 10 kDa heat shock protein, mitochondrial GN=HSPE1 PE=3 SV=2 |
| P48741 | 136 | 367 | 40,2 | 7,87 | 2873 | Putative heat shock 70 kDa protein 7 GN=HSPA7 PE=5 SV=2 |
| P35908 | 228 | 639 | 65,4 | 8,00 | 2835 | Keratin, type II cytoskeletal 2 epidermal GN=KRT2 PE=1 SV=2 |
| P23528 | 233 | 166 | 18,5 | 8,09 | 2800 | Cofilin-1 GN=CFL1 PE=1 SV=3 |
| Q58FG1 | 129 | 418 | 47,7 | 5,19 | 2763 | Putative heat shock protein HSP 90-alpha A4 GN=HSP90AA4P PE=5 SV=1 |
| P26038 | 237 | 577 | 67,8 | 6,40 | 2740 | Moesin GN=MSN PE=1 SV=3 |
| P31946 | 304 | 246 | 28,1 | 4,83 | 2721 | 14-3-3 protein beta/alpha GN=YWHAB PE=1 SV=3 |
| Q01105 | 194 | 290 | 33,5 | 4,32 | 2713 | Protein SET GN=SET PE=1 SV=3 |
| P30086 | 110 | 187 | 21,0 | 7,53 | 2673 | Phosphatidylethanolamine-binding protein 1 GN=PEBP1 PE=1 SV=3 |
| A6NNZ2 | 215 | 444 | 49,5 | 4,86 | 2663 | Tubulin beta-8 chain B PE=1 SV=1 |
| P63103 | 239 | 245 | 27,7 | 4,79 | 2645 | 14-3-3 protein zeta/delta GN=YWHAZ PE=1 SV=1 |
| P30041 | 271 | 224 | 25,0 | 6,38 | 2630 | Peroxiredoxin-6 GN=PRDX6 PE=1 SV=3 |
| P29401 | 346 | 623 | 67,8 | 7,66 | 2602 | Transketolase GN=TKT PE=1 SV=3 |
| P40926 | 102 | 338 | 35,5 | 8,68 | 2571 | Malate dehydrogenase, mitochondrial GN=MDH2 PE=1 SV=3 |
| P27797 | 184 | 417 | 48,1 | 4,44 | 2541 | Calreticulin GN=CALR PE=1 SV=1 |
| P05141 | 194 | 298 | 32,8 | 9,69 | 2463 | ADP/ATP translocase 2 GN=SLC25A5 PE=1 SV=7 |
| P05387 | 104 | 115 | 11,7 | 4,54 | 2352 | 60S acidic ribosomal protein P2 GN=RPLP2 PE=1 SV=1 |
| P50990 | 155 | 548 | 59,6 | 5,60 | 2339 | T-complex protein 1 subunit theta GN=CCT8 PE=1 SV=4 |
| Q99867 | 181 | 434 | 48,4 | 5,26 | 2329 | Putative tubulin beta-4q chain GN=TUBB4Q PE=5 SV=1 |
| P15531 | 241 | 152 | 17,1 | 6,19 | 2312 | Nucleoside diphosphate kinase A GN=NME1 PE=1 SV=1 |
| P27824 | 124 | 592 | 67,5 | 4,60 | 2272 | Calnexin GN=CANX PE=1 SV=2 |
| P25705 | 167 | 553 | 59,7 | 9,13 | 2257 | ATP synthase subunit alpha, mitochondrial GN=ATP5A1 PE=1 SV=1 |
| P16152 | 76 | 277 | 30,4 | 8,32 | 2237 | Carbonyl reductase [NADPH] 1 GN=CBR1 PE=1 SV=3 |
| P62984 | 211 | 128 | 14,7 | 9,83 | 2235 | Ubiquitin-60S ribosomal protein L40 GN=Uba52 PE=1 SV=2 |
| P08195 | 244 | 630 | 68,0 | 5,01 | 2226 | 4F2 cell-surface antigen heavy chain GN=SLC3A2 PE=1 SV=3 |
| P10599 | 125 | 105 | 11,7 | 4,92 | 2225 | Thioredoxin GN=TXN PE=1 SV=3 |
| Q3SZI4 | 225 | 245 | 27,7 | 4,78 | 2147 | 14-3-3 protein theta GN=YWHAQ PE=2 SV=1 |
| P29692 | 80 | 281 | 31,1 | 5,01 | 2144 | Elongation factor 1-delta GN=EEF1D PE=1 SV=5 |
| P78371 | 90 | 535 | 57,5 | 6,46 | 2144 | T-complex protein 1 subunit beta GN=CCT2 PE=1 SV=4 |
| P19338 | 221 | 710 | 76,6 | 4,70 | 2108 | Nucleolin GN=NCL PE=1 SV=3 |
| P26641 | 195 | 437 | 50,1 | 6,67 | 2076 | Elongation factor 1-gamma GN=EEF1G PE=1 SV=3 |
| Q148F1 | 129 | 166 | 18,7 | 7,88 | 2048 | Cofilin-2 GN=CFL2 PE=2 SV=1 |
| Q7Z794 | 100 | 578 | 61,9 | 5,99 | 1998 | Keratin, type II cytoskeletal 1b GN=KRT77 PE=1 SV=3 |
| P12956 | 154 | 609 | 69,8 | 6,64 | 1997 | X-ray repair cross-complementing protein 6 GN=XRCC6 PE=1 SV=2 |
| P30044 | 139 | 214 | 22,1 | 8,70 | 1995 | Peroxiredoxin-5, mitochondrial GN=PRDX5 PE=1 SV=4 |
| P55060 | 198 | 971 | 110,3 | 5,77 | 1993 | Exportin-2 GN=CSE1L PE=1 SV=3 |
| P12236 | 158 | 298 | 32,8 | 9,74 | 1991 | ADP/ATP translocase 3 GN=SLC25A6 PE=1 SV=4 |
| P24534 | 93 | 225 | 24,7 | 4,67 | 1980 | Elongation factor 1-beta GN=EEF1B2 PE=1 SV=3 |
| P12277 | 152 | 381 | 42,6 | 5,59 | 1978 | Creatine kinase B-type GN=CKB PE=1 SV=1 |
| P30101 | 164 | 505 | 56,7 | 6,35 | 1978 | Protein disulfide-isomerase A3 GN=PDIA3 PE=1 SV=4 |
| P49368 | 121 | 545 | 60,5 | 6,49 | 1962 | T-complex protein 1 subunit gamma GN=CCT3 PE=1 SV=4 |
| P31948 | 259 | 543 | 62,6 | 6,80 | 1959 | Stress-induced-phosphoprotein 1 GN=STIP1 PE=1 SV=1 |
| P67936 | 196 | 248 | 28,5 | 4,69 | 1921 | Tropomyosin alpha-4 chain GN=TPM4 PE=1 SV=3 |
| P13797 | 199 | 630 | 70,8 | 5,60 | 1910 | Plastin-3 GN=PLS3 PE=1 SV=4 |
| P02786 | 153 | 760 | 84,8 | 6,61 | 1908 | Transferrin receptor protein 1 GN=TFRC PE=1 SV=2 |
| Q9H853 | 82 | 241 | 27,5 | 7,83 | 1888 | Putative tubulin-like protein alpha-4B GN=TUBA4B PE=5 SV=2 |
| Q9H4B7 | 160 | 451 | 50,3 | 5,17 | 1883 | Tubulin beta-1 chain GN=TUBB1 PE=1 SV=1 |

| | | | | | | |
|---|---|---|---|---|---|---|
| P22392 | 242 | 152 | 17,3 | 8,41 | 1851 | Nucleoside diphosphate kinase B GN=NME2 PE=1 SV=1 |
| P35241 | 138 | 583 | 68,5 | 6,37 | 1850 | Radixin GN=RDX PE=1 SV=1 |
| Q14974 | 111 | 876 | 97,1 | 4,78 | 1838 | Importin subunit beta-1 GN=KPNB1 PE=1 SV=2 |
| P18669 | 161 | 254 | 28,8 | 7,18 | 1825 | Phosphoglycerate mutase 1 GN=PGAM1 PE=1 SV=2 |
| P78527 | 237 | 4128 | 468,8 | 7,12 | 1811 | DNA-dependent protein kinase catalytic subunit GN=PRKDC PE=1 SV=3 |
| P50395 | 124 | 445 | 50,6 | 6,47 | 1808 | Rab GDP dissociation inhibitor beta GN=GDI2 PE=1 SV=2 |
| P61982 | 221 | 247 | 28,3 | 4,89 | 1786 | 14-3-3 protein gamma GN=Ywhag PE=1 SV=2 |
| P61205 | 141 | 181 | 20,6 | 7,43 | 1781 | ADP-ribosylation factor 3 GN=Arf3 PE=2 SV=2 |
| P84078 | 133 | 181 | 20,7 | 6,80 | 1780 | ADP-ribosylation factor 1 GN=Arf1 PE=1 SV=2 |
| P15311 | 140 | 586 | 69,4 | 6,27 | 1741 | Ezrin GN=EZR PE=1 SV=4 |
| P22234 | 111 | 425 | 47,0 | 7,23 | 1718 | Multifunctional protein ADE2 GN=PAICS PE=1 SV=3 |
| P52209 | 64 | 483 | 53,1 | 7,23 | 1715 | 6-phosphogluconate dehydrogenase, decarboxylating GN=PGD PE=1 SV=3 |
| Q99832 | 88 | 543 | 59,3 | 7,65 | 1689 | T-complex protein 1 subunit eta GN=CCT7 PE=1 SV=2 |
| Q58FG0 | 150 | 334 | 38,7 | 6,57 | 1684 | Putative heat shock protein HSP 90-alpha A5 GN=HSP90AA5P PE=1 SV=1 |
| P05023 | 104 | 1023 | 112,8 | 5,49 | 1666 | Sodium/potassium-transporting ATPase subunit alpha-1 GN=ATP1A1 PE=1 SV=1 |
| P30048 | 93 | 256 | 27,7 | 7,78 | 1652 | Thioredoxin-dependent peroxide reductase, mitochondrial GN=PRDX3 PE=1 SV=3 |
| Q14204 | 219 | 4646 | 532,1 | 6,40 | 1651 | Cytoplasmic dynein 1 heavy chain 1 GN=DYNC1H1 PE=1 SV=5 |
| P07237 | 225 | 508 | 57,1 | 4,87 | 1629 | Protein disulfide-isomerase GN=P4HB PE=1 SV=3 |
| P12429 | 95 | 323 | 36,4 | 5,92 | 1622 | Annexin A3 GN=ANXA3 PE=1 SV=3 |
| P23526 | 116 | 432 | 47,7 | 6,34 | 1617 | Adenosylhomocysteinase GN=AHCY PE=1 SV=4 |
| P62827 | 180 | 216 | 24,4 | 7,49 | 1584 | GTP-binding nuclear protein Ran GN=Ran PE=1 SV=3 |
| P60661 | 105 | 151 | 16,9 | 4,65 | 1571 | Myosin light polypeptide 6 GN=MYL6 PE=2 SV=2 |
| O14818 | 94 | 248 | 27,9 | 8,46 | 1528 | Proteasome subunit alpha type-7 GN=PSMA7 PE=1 SV=1 |
| P31947 | 212 | 248 | 27,8 | 4,74 | 1518 | 14-3-3 protein sigma GN=SFN PE=1 SV=1 |
| P53675 | 102 | 1640 | 186,9 | 5,85 | 1493 | Clathrin heavy chain 2 GN=CLTCL1 PE=1 SV=2 |
| P00441 | 112 | 154 | 15,9 | 6,13 | 1492 | Superoxide dismutase [Cu-Zn] GN=SOD1 PE=1 SV=2 |
| P02538 | 127 | 564 | 60,0 | 8,00 | 1481 | Keratin, type II cytoskeletal 6A GN=KRT6A PE=1 SV=3 |
| P08865 | 71 | 295 | 32,8 | 4,87 | 1454 | 40S ribosomal protein SA GN=RPSA PE=1 SV=4 |
| O14737 | 54 | 125 | 14,3 | 6,04 | 1444 | Programmed cell death protein 5 GN=PDCD5 PE=1 SV=3 |
| O75828 | 37 | 277 | 30,8 | 6,18 | 1431 | Carbonyl reductase [NADPH] 3 GN=CBR3 PE=1 SV=3 |
| P05388 | 92 | 317 | 34,3 | 5,97 | 1415 | 60S acidic ribosomal protein P0 GN=RPLP0 PE=1 SV=1 |
| Q07021 | 68 | 282 | 31,3 | 4,84 | 1406 | Complement component 1 Q subcomponent-binding protein, mitochondrial GN=C1C |
| P63242 | 135 | 154 | 16,8 | 5,24 | 1400 | Eukaryotic translation initiation factor 5A-1 GN=Eif5a PE=1 SV=2 |
| P04259 | 122 | 564 | 60,0 | 8,00 | 1396 | Keratin, type II cytoskeletal 6B GN=KRT6B PE=1 SV=5 |
| Q3T0C7 | 169 | 149 | 17,3 | 5,97 | 1380 | Stathmin GN=STMN1 PE=2 SV=3 |
| P12235 | 106 | 298 | 33,0 | 9,76 | 1374 | ADP/ATP translocase 1 GN=SLC25A4 PE=1 SV=4 |
| Q99714 | 99 | 261 | 26,9 | 7,78 | 1366 | 3-hydroxyacyl-CoA dehydrogenase type-2 GN=HSD17B10 PE=1 SV=3 |
| Q15084 | 67 | 440 | 48,1 | 5,08 | 1360 | Protein disulfide-isomerase A6 GN=PDIA6 PE=1 SV=1 |
| P26639 | 146 | 723 | 83,4 | 6,67 | 1352 | Threonine--tRNA ligase, cytoplasmic GN=TARS PE=1 SV=3 |
| P61979 | 106 | 463 | 50,9 | 5,54 | 1343 | Heterogeneous nuclear ribonucleoprotein K GN=Hnrnpk PE=1 SV=1 |
| P36952 | 115 | 375 | 42,1 | 6,05 | 1343 | Serpin B5 GN=SERPINB5 PE=1 SV=2 |
| P18206 | 172 | 1134 | 123,7 | 5,66 | 1327 | Vinculin GN=VCL PE=1 SV=4 |
| O60361 | 154 | 137 | 15,5 | 8,57 | 1318 | Putative nucleoside diphosphate kinase GN=NME2P1 PE=5 SV=1 |
| O43707 | 118 | 911 | 104,8 | 5,44 | 1315 | Alpha-actinin-4 GN=ACTN4 PE=1 SV=2 |
| Q3T169 | 105 | 243 | 26,7 | 9,66 | 1315 | 40S ribosomal protein S3 GN=RPS3 PE=2 SV=1 |
| P30040 | 105 | 261 | 29,0 | 7,31 | 1314 | Endoplasmic reticulum resident protein 29 GN=ERP29 PE=1 SV=4 |
| P61284 | 88 | 165 | 17,8 | 9,42 | 1299 | 60S ribosomal protein L12 GN=RPL12 PE=2 SV=1 |
| Q8BGY2 | 107 | 153 | 16,8 | 5,58 | 1295 | Eukaryotic translation initiation factor 5A-2 GN=Eif5a2 PE=2 SV=3 |
| Q13765 | 30 | 215 | 23,4 | 4,56 | 1291 | Nascent polypeptide-associated complex subunit alpha GN=NACA PE=1 SV=1 |
| Q6IS14 | 104 | 154 | 16,8 | 5,00 | 1284 | Eukaryotic translation initiation factor 5A-1-like GN=EIF5AL1 PE=1 SV=2 |
| Q9CXW4 | 82 | 178 | 20,2 | 9,60 | 1284 | 60S ribosomal protein L11 GN=Rpl11 PE=1 SV=4 |
| Q8NHW5 | 75 | 317 | 34,3 | 5,55 | 1276 | 60S acidic ribosomal protein P0-like GN=RPLP0P6 PE=5 SV=1 |
| P23921 | 74 | 792 | 90,0 | 7,15 | 1247 | Ribonucleoside-diphosphate reductase large subunit GN=RRM1 PE=1 SV=1 |
| P07741 | 100 | 180 | 19,6 | 6,02 | 1223 | Adenine phosphoribosyltransferase GN=APRT PE=1 SV=2 |
| O00299 | 71 | 241 | 26,9 | 5,17 | 1217 | Chloride intracellular channel protein 1 GN=CLIC1 PE=1 SV=4 |
| Q04917 | 182 | 246 | 28,2 | 4,84 | 1202 | 14-3-3 protein eta GN=YWHAH PE=1 SV=4 |
| Q58FF6 | 168 | 505 | 58,2 | 4,73 | 1198 | Putative heat shock protein HSP 90-beta 4 GN=HSP90AB4P PE=5 SV=1 |
| P04843 | 116 | 607 | 68,5 | 6,38 | 1195 | Dolichyl-diphosphooligosaccharide--protein glycosyltransferase subunit 1 GN=RPN1 |
| P09382 | 100 | 135 | 14,7 | 5,50 | 1191 | Galectin-1 GN=LGALS1 PE=1 SV=2 |
| P62992 | 118 | 156 | 18,0 | 9,64 | 1191 | Ubiquitin-40S ribosomal protein S27a GN=RPS27A PE=1 SV=2 |
| P30613 | 115 | 574 | 61,8 | 7,74 | 1182 | Pyruvate kinase isozymes R/L GN=PKLR PE=1 SV=2 |
| P62204 | 71 | 149 | 16,8 | 4,22 | 1180 | Calmodulin GN=Calm1 PE=1 SV=2 |
| Q92688 | 97 | 251 | 28,8 | 4,06 | 1174 | Acidic leucine-rich nuclear phosphoprotein 32 family member B GN=ANP32B PE=1 SV |
| P06748 | 136 | 294 | 32,6 | 4,78 | 1172 | Nucleophosmin GN=NPM1 PE=1 SV=2 |
| P11586 | 125 | 935 | 101,5 | 7,30 | 1166 | C-1-tetrahydrofolate synthase, cytoplasmic GN=MTHFD1 PE=1 SV=3 |

| | | | | | | |
|---|---|---|---|---|---|---|
| P31939 | 109 | 592 | 64,6 | 6,71 | 1152 | Bifunctional purine biosynthesis protein PURH GN=ATIC PE=1 SV=3 |
| O35129 | 114 | 299 | 33,3 | 9,83 | 1146 | Prohibitin-2 GN=Phb2 PE=1 SV=1 |
| P05787 | 94 | 483 | 53,7 | 5,59 | 1130 | Keratin, type II cytoskeletal 8 GN=KRT8 PE=1 SV=7 |
| O95373 | 105 | 1038 | 119,4 | 4,82 | 1129 | Importin-7 GN=IPO7 PE=1 SV=1 |
| Q14697 | 172 | 944 | 106,8 | 6,14 | 1126 | Neutral alpha-glucosidase AB GN=GANAB PE=1 SV=3 |
| Q9Z2U1 | 106 | 241 | 26,4 | 4,79 | 1119 | Proteasome subunit alpha type-5 GN=Psma5 PE=1 SV=1 |
| P14131 | 90 | 146 | 16,4 | 10,21 | 1112 | 40S ribosomal protein S16 GN=Rps16 PE=2 SV=4 |
| P48643 | 98 | 541 | 59,6 | 5,66 | 1110 | T-complex protein 1 subunit epsilon GN=CCT5 PE=1 SV=1 |
| P07910 | 65 | 306 | 33,6 | 5,08 | 1110 | Heterogeneous nuclear ribonucleoproteins C1/C2 GN=HNRNPC PE=1 SV=4 |
| P34932 | 93 | 840 | 94,3 | 5,19 | 1108 | Heat shock 70 kDa protein 4 GN=HSPA4 PE=1 SV=4 |
| O60506 | 72 | 623 | 69,6 | 8,59 | 1106 | Heterogeneous nuclear ribonucleoprotein Q GN=SYNCRIP PE=1 SV=2 |
| Q14315 | 116 | 2725 | 290,8 | 5,97 | 1103 | Filamin-C GN=FLNC PE=1 SV=3 |
| P07951 | 116 | 284 | 32,8 | 4,70 | 1098 | Tropomyosin beta chain GN=TPM2 PE=1 SV=1 |
| P35579 | 119 | 1960 | 226,4 | 5,60 | 1094 | Myosin-9 GN=MYH9 PE=1 SV=4 |
| P17987 | 123 | 556 | 60,3 | 6,11 | 1085 | T-complex protein 1 subunit alpha GN=TCP1 PE=1 SV=1 |
| P13647 | 102 | 590 | 62,3 | 7,74 | 1083 | Keratin, type II cytoskeletal 5 GN=KRT5 PE=1 SV=3 |
| A6NL28 | 50 | 223 | 26,3 | 4,51 | 1080 | Putative tropomyosin alpha-3 chain-like protein PE=5 SV=2 |
| P31949 | 94 | 105 | 11,7 | 7,12 | 1071 | Protein S100-A11 GN=S100A11 PE=1 SV=2 |
| P04080 | 104 | 98 | 11,1 | 7,56 | 1056 | Cystatin-B GN=CSTB PE=1 SV=2 |
| P62821 | 94 | 205 | 22,7 | 6,21 | 1047 | Ras-related protein Rab-1A GN=Rab1A PE=1 SV=3 |
| P12268 | 72 | 514 | 55,8 | 6,90 | 1046 | Inosine-5'-monophosphate dehydrogenase 2 GN=IMPDH2 PE=1 SV=2 |
| Q9H0C2 | 46 | 315 | 35,0 | 9,89 | 1046 | ADP/ATP translocase 4 GN=SLC25A31 PE=1 SV=1 |
| P52565 | 51 | 204 | 23,2 | 5,11 | 1039 | Rho GDP-dissociation inhibitor 1 GN=ARHGDIA PE=1 SV=3 |
| Q9Y2T3 | 78 | 454 | 51,0 | 5,68 | 1035 | Guanine deaminase GN=GDA PE=1 SV=1 |
| P49748 | 84 | 655 | 70,3 | 8,75 | 1016 | Very long-chain specific acyl-CoA dehydrogenase, mitochondrial GN=ACADVL PE=1 S |
| P55072 | 130 | 806 | 89,3 | 5,26 | 1002 | Transitional endoplasmic reticulum ATPase GN=VCP PE=1 SV=4 |
| P06703 | 175 | 90 | 10,2 | 5,48 | 988 | Protein S100-A6 GN=S100A6 PE=1 SV=1 |
| P53999 | 102 | 127 | 14,4 | 9,60 | 980 | Activated RNA polymerase II transcriptional coactivator p15 GN=SUB1 PE=1 SV=3 |
| P61007 | 79 | 207 | 23,7 | 9,07 | 980 | Ras-related protein Rab-8A OS=Canis familiaris GN=RAB8A PE=2 SV=1 |
| P27105 | 51 | 288 | 31,7 | 7,88 | 979 | Erythrocyte band 7 integral membrane protein GN=STOM PE=1 SV=3 |
| P50993 | 44 | 1020 | 112,2 | 5,66 | 978 | Sodium/potassium-transporting ATPase subunit alpha-2 GN=ATP1A2 PE=1 SV=1 |
| P13637 | 41 | 1013 | 111,7 | 5,38 | 975 | Sodium/potassium-transporting ATPase subunit alpha-3 GN=ATP1A3 PE=1 SV=3 |
| Q8TAA3 | 55 | 256 | 28,5 | 8,98 | 971 | Proteasome subunit alpha type-7-like GN=PSMA8 PE=1 SV=3 |
| P60900 | 52 | 246 | 27,4 | 6,76 | 971 | Proteasome subunit alpha type-6 GN=PSMA6 PE=1 SV=1 |
| Q5KR47 | 113 | 284 | 32,8 | 4,72 | 971 | Tropomyosin alpha-3 chain GN=TPM3 PE=2 SV=1 |
| P14314 | 56 | 528 | 59,4 | 4,41 | 963 | Glucosidase 2 subunit beta GN=PRKCSH PE=1 SV=2 |
| P12814 | 75 | 892 | 103,0 | 5,41 | 942 | Alpha-actinin-1 GN=ACTN1 PE=1 SV=2 |
| P25815 | 61 | 95 | 10,4 | 4,88 | 927 | Protein S100-P GN=S100P PE=1 SV=2 |
| Q32PD5 | 106 | 145 | 16,1 | 10,32 | 926 | 40S ribosomal protein S19 GN=RPS19 PE=2 SV=3 |
| P00505 | 32 | 430 | 47,5 | 9,01 | 908 | Aspartate aminotransferase, mitochondrial GN=GOT2 PE=1 SV=3 |
| Q3ZCF3 | 53 | 163 | 18,6 | 4,54 | 904 | S-phase kinase-associated protein 1 GN=SKP1 PE=2 SV=1 |
| P18124 | 82 | 248 | 29,2 | 10,65 | 899 | 60S ribosomal protein L7 GN=RPL7 PE=1 SV=1 |
| P40227 | 83 | 531 | 58,0 | 6,68 | 882 | T-complex protein 1 subunit zeta GN=CCT6A PE=1 SV=3 |
| Q15293 | 27 | 331 | 38,9 | 5,00 | 881 | Reticulocalbin-1 GN=RCN1 PE=1 SV=1 |
| P12004 | 76 | 261 | 28,8 | 4,69 | 881 | Proliferating cell nuclear antigen GN=PCNA PE=1 SV=1 |
| P09493 | 91 | 284 | 32,7 | 4,74 | 879 | Tropomyosin alpha-1 chain GN=TPM1 PE=1 SV=2 |
| P02533 | 122 | 472 | 51,5 | 5,16 | 878 | Keratin, type I cytoskeletal 14 GN=KRT14 PE=1 SV=4 |
| Q3T0F4 | 74 | 165 | 18,9 | 10,15 | 867 | 40S ribosomal protein S10 GN=RPS10 PE=2 SV=1 |
| O43175 | 72 | 533 | 56,6 | 6,71 | 866 | D-3-phosphoglycerate dehydrogenase GN=PHGDH PE=1 SV=4 |
| P35268 | 56 | 128 | 14,8 | 9,19 | 855 | 60S ribosomal protein L22 GN=RPL22 PE=1 SV=2 |
| P15259 | 99 | 253 | 28,7 | 8,88 | 852 | Phosphoglycerate mutase 2 GN=PGAM2 PE=1 SV=3 |
| P50991 | 91 | 539 | 57,9 | 7,83 | 850 | T-complex protein 1 subunit delta GN=CCT4 PE=1 SV=4 |
| Q9H0U4 | 82 | 201 | 22,2 | 5,73 | 850 | Ras-related protein Rab-1B GN=RAB1B PE=1 SV=1 |
| P51150 | 59 | 207 | 23,5 | 6,70 | 844 | Ras-related protein Rab-7a GN=Rab7a PE=1 SV=2 |
| Q5E958 | 56 | 208 | 24,2 | 10,32 | 832 | 40S ribosomal protein S8 GN=RPS8 PE=2 SV=3 |
| O95678 | 72 | 551 | 59,5 | 7,74 | 831 | Keratin, type II cytoskeletal 75 GN=KRT75 PE=1 SV=2 |
| P33316 | 51 | 252 | 26,5 | 9,36 | 830 | Deoxyuridine 5'-triphosphate nucleotidohydrolase, mitochondrial GN=DUT PE=1 SV= |
| Q3T0F7 | 27 | 118 | 12,9 | 5,52 | 829 | Myotrophin GN=MTPN PE=1 SV=3 |
| P61286 | 104 | 636 | 70,6 | 9,50 | 829 | Polyadenylate-binding protein 1 GN=PABPC1 PE=2 SV=1 |
| P48668 | 63 | 564 | 60,0 | 8,00 | 817 | Keratin, type II cytoskeletal 6C GN=KRT6C PE=1 SV=3 |
| O00410 | 97 | 1097 | 123,5 | 4,94 | 815 | Importin-5 GN=IPO5 PE=1 SV=4 |
| P49736 | 69 | 904 | 101,8 | 5,52 | 808 | DNA replication licensing factor MCM2 GN=MCM2 PE=1 SV=4 |
| Q08211 | 94 | 1270 | 140,9 | 6,84 | 807 | ATP-dependent RNA helicase A GN=DHX9 PE=1 SV=4 |
| P68040 | 57 | 317 | 35,1 | 7,69 | 799 | Guanine nucleotide-binding protein subunit beta-2-like 1 GN=Gnb2l1 PE=1 SV=3 |
| P05783 | 52 | 430 | 48,0 | 5,45 | 788 | Keratin, type I cytoskeletal 18 GN=KRT18 PE=1 SV=2 |

| | | | | | | |
|---|---|---|---|---|---|---|
| P28074 | 46 | 263 | 28,5 | 6,92 | 788 | Proteasome subunit beta type-5 GN=PSMB5 PE=1 SV=3 |
| Q04837 | 34 | 148 | 17,2 | 9,60 | 772 | Single-stranded DNA-binding protein, mitochondrial GN=SSBP1 PE=1 SV=1 |
| P61027 | 56 | 200 | 22,5 | 8,38 | 767 | Ras-related protein Rab-10 GN=Rab10 PE=1 SV=1 |
| P00491 | 61 | 289 | 32,1 | 6,95 | 762 | Purine nucleoside phosphorylase GN=PNP PE=1 SV=2 |
| Q969H8 | 68 | 173 | 18,8 | 6,68 | 758 | UPF0556 protein C19orf10 GN=C19orf10 PE=1 SV=1 |
| Q07020 | 49 | 188 | 21,6 | 11,72 | 756 | 60S ribosomal protein L18 GN=RPL18 PE=1 SV=2 |
| Q91V41 | 54 | 215 | 23,9 | 6,21 | 744 | Ras-related protein Rab-14 GN=Rab14 PE=1 SV=3 |
| O43776 | 61 | 548 | 62,9 | 6,25 | 740 | Asparagine--tRNA ligase, cytoplasmic GN=NARS PE=1 SV=1 |
| Q56K14 | 32 | 114 | 11,5 | 4,32 | 739 | 60S acidic ribosomal protein P1 GN=RPLP1 PE=3 SV=1 |
| P78417 | 99 | 241 | 27,5 | 6,60 | 738 | Glutathione S-transferase omega-1 GN=GSTO1 PE=1 SV=2 |
| P38919 | 42 | 411 | 46,8 | 6,73 | 738 | Eukaryotic initiation factor 4A-III GN=EIF4A3 PE=1 SV=4 |
| P62264 | 45 | 151 | 16,3 | 10,05 | 737 | 40S ribosomal protein S14 GN=Rps14 PE=2 SV=3 |
| Q92930 | 61 | 207 | 23,6 | 9,07 | 724 | Ras-related protein Rab-8B GN=RAB8B PE=1 SV=2 |
| Q02790 | 96 | 459 | 51,8 | 5,43 | 721 | Peptidyl-prolyl cis-trans isomerase FKBP4 GN=FKBP4 PE=1 SV=3 |
| P59190 | 53 | 212 | 24,4 | 5,71 | 719 | Ras-related protein Rab-15 GN=RAB15 PE=1 SV=1 |
| Q6PHN9 | 57 | 201 | 23,0 | 8,29 | 719 | Ras-related protein Rab-35 GN=Rab35 PE=1 SV=1 |
| Q5XKE5 | 64 | 535 | 57,8 | 7,20 | 716 | Keratin, type II cytoskeletal 79 GN=KRT79 PE=1 SV=2 |
| P08729 | 63 | 469 | 51,4 | 5,48 | 706 | Keratin, type II cytoskeletal 7 GN=KRT7 PE=1 SV=5 |
| Q3T165 | 57 | 272 | 29,8 | 5,76 | 703 | Prohibitin GN=PHB PE=2 SV=1 |
| P62852 | 70 | 125 | 13,7 | 10,11 | 703 | 40S ribosomal protein S25 GN=Rps25 PE=2 SV=1 |
| P62702 | 87 | 263 | 29,6 | 10,15 | 703 | 40S ribosomal protein S4, X isoform GN=Rps4x PE=2 SV=2 |
| P13693 | 41 | 172 | 19,6 | 4,93 | 698 | Translationally-controlled tumor protein GN=TPT1 PE=1 SV=1 |
| P16442 | 355 | 354 | 40,9 | 8,98 | 698 | Histo-blood group ABO system transferase GN=ABO PE=1 SV=2 |
| Q9NPC6 | 350 | 264 | 29,9 | 8,25 | 698 | Myozenin-2 GN=MYOZ2 PE=1 SV=1 |
| Q6DD88 | 39 | 541 | 60,5 | 5,66 | 688 | Atlastin-3 GN=ATL3 PE=1 SV=1 |
| P30049 | 23 | 168 | 17,5 | 5,49 | 681 | ATP synthase subunit delta, mitochondrial GN=ATP5D PE=1 SV=2 |
| P53396 | 89 | 1101 | 120,8 | 7,33 | 677 | ATP-citrate synthase GN=ACLY PE=1 SV=3 |
| P18085 | 77 | 180 | 20,5 | 7,14 | 673 | ADP-ribosylation factor 4 GN=ARF4 PE=1 SV=3 |
| P60902 | 89 | 97 | 11,2 | 7,37 | 673 | Protein S100-A10 GN=S100A10 PE=1 SV=2 |
| O43399 | 45 | 206 | 22,2 | 5,36 | 670 | Tumor protein D54 GN=TPD52L2 PE=1 SV=2 |
| P52292 | 39 | 529 | 57,8 | 5,40 | 669 | Importin subunit alpha-2 GN=KPNA2 PE=1 SV=1 |
| P56192 | 41 | 900 | 101,1 | 6,16 | 665 | Methionine--tRNA ligase, cytoplasmic GN=MARS PE=1 SV=2 |
| P62270 | 93 | 152 | 17,7 | 10,99 | 663 | 40S ribosomal protein S18 GN=Rps18 PE=1 SV=3 |
| P30046 | 68 | 118 | 12,7 | 7,30 | 660 | D-dopachrome decarboxylase GN=DDT PE=1 SV=3 |
| P42704 | 86 | 1394 | 157,8 | 6,13 | 654 | Leucine-rich PPR motif-containing protein, mitochondrial GN=LRPPRC PE=1 SV=3 |
| Q60972 | 16 | 425 | 47,6 | 4,89 | 654 | Histone-binding protein RBBP4 GN=Rbbp4 PE=1 SV=5 |
| P00492 | 45 | 218 | 24,6 | 6,68 | 652 | Hypoxanthine-guanine phosphoribosyltransferase GN=HPRT1 PE=1 SV=2 |
| Q6PDM2 | 67 | 248 | 27,7 | 10,36 | 650 | Serine/arginine-rich splicing factor 1 GN=Srsf1 PE=1 SV=3 |
| P39687 | 75 | 249 | 28,6 | 4,09 | 649 | Acidic leucine-rich nuclear phosphoprotein 32 family member A GN=ANP32A PE=1 SV |
| P37108 | 29 | 136 | 14,6 | 10,04 | 649 | Signal recognition particle 14 kDa protein GN=SRP14 PE=1 SV=2 |
| P07814 | 91 | 1512 | 170,5 | 7,33 | 644 | Bifunctional glutamate/proline--tRNA ligase GN=EPRS PE=1 SV=5 |
| Q92928 | 54 | 201 | 22,0 | 5,43 | 643 | Putative Ras-related protein Rab-1C GN=RAB1C PE=5 SV=2 |
| P21796 | 46 | 283 | 30,8 | 8,54 | 636 | Voltage-dependent anion-selective channel protein 1 GN=VDAC1 PE=1 SV=2 |
| Q99497 | 116 | 189 | 19,9 | 6,79 | 633 | Protein DJ-1 GN=PARK7 PE=1 SV=2 |
| P08779 | 96 | 473 | 51,2 | 5,05 | 633 | Keratin, type I cytoskeletal 16 GN=KRT16 PE=1 SV=4 |
| Q96FW1 | 25 | 271 | 31,3 | 4,94 | 632 | Ubiquitin thioesterase OTUB1 GN=OTUB1 PE=1 SV=2 |
| P84084 | 77 | 180 | 20,5 | 6,79 | 630 | ADP-ribosylation factor 5 GN=Arf5 PE=2 SV=2 |
| Q02878 | 58 | 288 | 32,7 | 10,58 | 620 | 60S ribosomal protein L6 GN=RPL6 PE=1 SV=3 |
| P22102 | 48 | 1010 | 107,7 | 6,70 | 614 | Trifunctional purine biosynthetic protein adenosine-3 GN=GART PE=1 SV=1 |
| P61087 | 33 | 200 | 22,4 | 5,44 | 613 | Ubiquitin-conjugating enzyme E2 K GN=Ube2k PE=1 SV=3 |
| O14980 | 64 | 1071 | 123,3 | 6,06 | 612 | Exportin-1 GN=XPO1 PE=1 SV=1 |
| Q9UKK9 | 36 | 219 | 24,3 | 4,94 | 609 | ADP-sugar pyrophosphatase GN=NUDT5 PE=1 SV=1 |
| P17931 | 56 | 250 | 26,1 | 8,56 | 608 | Galectin-3 GN=LGALS3 PE=1 SV=5 |
| O14684 | 65 | 152 | 17,1 | 9,50 | 603 | Prostaglandin E synthase GN=PTGES PE=1 SV=2 |
| Q99733 | 41 | 375 | 42,8 | 4,69 | 597 | Nucleosome assembly protein 1-like 4 GN=NAP1L4 PE=1 SV=1 |
| Q9BSJ8 | 51 | 1104 | 122,8 | 5,83 | 595 | Extended synaptotagmin-1 GN=ESYT1 PE=1 SV=1 |
| Q9Y266 | 44 | 331 | 38,2 | 5,38 | 594 | Nuclear migration protein nudC GN=NUDC PE=1 SV=1 |
| P46777 | 52 | 297 | 34,3 | 9,72 | 585 | 60S ribosomal protein L5 GN=RPL5 PE=1 SV=3 |
| P49755 | 36 | 219 | 25,0 | 7,44 | 581 | Transmembrane emp24 domain-containing protein 10 GN=TMED10 PE=1 SV=2 |
| P54819 | 48 | 239 | 26,5 | 7,81 | 574 | Adenylate kinase 2, mitochondrial GN=AK2 PE=1 SV=2 |
| P55854 | 29 | 103 | 11,6 | 5,49 | 568 | Small ubiquitin-related modifier 3 GN=SUMO3 PE=1 SV=2 |
| P57088 | 21 | 247 | 28,0 | 9,70 | 566 | Transmembrane protein 33 GN=TMEM33 PE=1 SV=2 |
| P62245 | 53 | 130 | 14,8 | 10,13 | 562 | 40S ribosomal protein S15a GN=Rps15a PE=2 SV=2 |
| P42126 | 23 | 302 | 32,8 | 8,54 | 561 | Enoyl-CoA delta isomerase 1, mitochondrial GN=ECI1 PE=1 SV=1 |
| P61018 | 27 | 213 | 23,6 | 6,06 | 557 | Ras-related protein Rab-4B GN=RAB4B PE=1 SV=1 |

| | | | | | | |
|---|---|---|---|---|---|---|
| P61294 | 29 | 208 | 23,4 | 5,53 | 557 | Ras-related protein Rab-6B GN=Rab6b PE=1 SV=1 |
| Q9H082 | 31 | 229 | 25,7 | 7,18 | 557 | Ras-related protein Rab-33B GN=RAB33B PE=1 SV=1 |
| Q8N0Y7 | 72 | 254 | 28,8 | 6,65 | 553 | Probable phosphoglycerate mutase 4 GN=PGAM4 PE=1 SV=1 |
| Q99829 | 62 | 537 | 59,0 | 5,83 | 549 | Copine-1 GN=CPNE1 PE=1 SV=1 |
| Q9Y230 | 23 | 463 | 51,1 | 5,64 | 546 | RuvB-like 2 GN=RUVBL2 PE=1 SV=3 |
| P61290 | 50 | 254 | 29,5 | 5,95 | 545 | Proteasome activator complex subunit 3 GN=Psme3 PE=1 SV=1 |
| P49411 | 30 | 452 | 49,5 | 7,61 | 544 | Elongation factor Tu, mitochondrial GN=TUFM PE=1 SV=2 |
| P55209 | 34 | 391 | 45,3 | 4,46 | 538 | Nucleosome assembly protein 1-like 1 GN=NAP1L1 PE=1 SV=1 |
| P67809 | 21 | 324 | 35,9 | 9,88 | 538 | Nuclease-sensitive element-binding protein 1 GN=YBX1 PE=1 SV=3 |
| Q01650 | 33 | 507 | 55,0 | 7,72 | 535 | Large neutral amino acids transporter small subunit 1 GN=SLC7A5 PE=1 SV=2 |
| P14174 | 14 | 115 | 12,5 | 7,88 | 534 | Macrophage migration inhibitory factor GN=MIF PE=1 SV=4 |
| A7MBJ5 | 70 | 1230 | 136,3 | 5,78 | 532 | Cullin-associated NEDD8-dissociated protein 1 GN=CAND1 PE=2 SV=1 |
| P62751 | 52 | 156 | 17,7 | 10,45 | 531 | 60S ribosomal protein L23a GN=Rpl23a PE=1 SV=1 |
| P55821 | 92 | 179 | 20,8 | 8,32 | 529 | Stathmin-2 GN=Stmn2 PE=1 SV=1 |
| Q13263 | 48 | 835 | 88,5 | 5,77 | 527 | Transcription intermediary factor 1-beta GN=TRIM28 PE=1 SV=5 |
| Q13011 | 60 | 328 | 35,8 | 8,00 | 526 | Delta(3,5)-Delta(2,4)-dienoyl-CoA isomerase, mitochondrial GN=ECH1 PE=1 SV=2 |
| P62301 | 322 | 151 | 17,2 | 10,54 | 523 | 40S ribosomal protein S13 GN=Rps13 PE=1 SV=2 |
| B0CM99 | 93 | 215 | 24,9 | 5,74 | 522 | High mobility group protein B1 OS=Callithrix jacchus GN=HMGB1 PE=3 SV=1 |
| Q9BZK3 | 14 | 213 | 23,3 | 4,59 | 522 | Putative nascent polypeptide-associated complex subunit alpha-like protein GN=NA |
| P37837 | 47 | 337 | 37,5 | 6,81 | 521 | Transaldolase GN=TALDO1 PE=1 SV=2 |
| P26640 | 38 | 1264 | 140,4 | 7,59 | 521 | Valine--tRNA ligase GN=VARS PE=1 SV=4 |
| P47755 | 26 | 286 | 32,9 | 5,85 | 515 | F-actin-capping protein subunit alpha-2 GN=CAPZA2 PE=1 SV=3 |
| P08559 | 30 | 390 | 43,3 | 8,06 | 514 | Pyruvate dehydrogenase E1 component subunit alpha, somatic form, mitochondrial |
| P80723 | 52 | 227 | 22,7 | 4,63 | 513 | Brain acid soluble protein 1 GN=BASP1 PE=1 SV=2 |
| Q14651 | 54 | 629 | 70,2 | 5,41 | 511 | Plastin-1 GN=PLS1 PE=1 SV=2 |
| P62858 | 27 | 69 | 7,8 | 10,70 | 511 | 40S ribosomal protein S28 GN=Rps28 PE=2 SV=1 |
| P48047 | 40 | 213 | 23,3 | 9,96 | 509 | ATP synthase subunit O, mitochondrial GN=ATP5O PE=1 SV=1 |
| P27695 | 31 | 318 | 35,5 | 8,12 | 508 | DNA-(apurinic or apyrimidinic site) lyase GN=APEX1 PE=1 SV=2 |
| P40925 | 52 | 334 | 36,4 | 7,36 | 508 | Malate dehydrogenase, cytoplasmic GN=MDH1 PE=1 SV=4 |
| Q9NQ39 | 20 | 176 | 20,1 | 10,13 | 505 | Putative 40S ribosomal protein S10-like GN=RPS10P5 PE=5 SV=1 |
| A6H769 | 65 | 194 | 22,1 | 10,10 | 505 | 40S ribosomal protein S7 GN=RPS7 PE=2 SV=1 |
| Q15758 | 48 | 541 | 56,6 | 5,48 | 504 | Neutral amino acid transporter B(0) GN=SLC1A5 PE=1 SV=2 |
| Q3T0Y5 | 30 | 234 | 25,9 | 7,43 | 502 | Proteasome subunit alpha type-2 GN=PSMA2 PE=1 SV=3 |
| P00966 | 59 | 412 | 46,5 | 8,02 | 502 | Argininosuccinate synthase GN=ASS1 PE=1 SV=2 |
| Q5E9E6 | 63 | 217 | 24,8 | 9,94 | 498 | 60S ribosomal protein L10a GN=RPL10A PE=2 SV=3 |
| P62900 | 50 | 125 | 14,5 | 10,54 | 495 | 60S ribosomal protein L31 GN=Rpl31 PE=2 SV=1 |
| P13010 | 68 | 732 | 82,7 | 5,81 | 491 | X-ray repair cross-complementing protein 5 GN=XRCC5 PE=1 SV=3 |
| P00568 | 42 | 194 | 21,6 | 8,63 | 490 | Adenylate kinase isoenzyme 1 GN=AK1 PE=1 SV=3 |
| A6NHG4 | 50 | 134 | 14,2 | 6,29 | 481 | D-dopachrome decarboxylase-like protein GN=DDTL PE=2 SV=1 |
| Q7Z3Y7 | 67 | 464 | 50,5 | 5,47 | 480 | Keratin, type I cytoskeletal 28 GN=KRT28 PE=1 SV=2 |
| P14649 | 23 | 208 | 22,7 | 5,73 | 477 | Myosin light chain 6B GN=MYL6B PE=1 SV=1 |
| Q96QK1 | 38 | 796 | 91,6 | 5,49 | 476 | Vacuolar protein sorting-associated protein 35 GN=VPS35 PE=1 SV=2 |
| P52597 | 44 | 415 | 45,6 | 5,58 | 467 | Heterogeneous nuclear ribonucleoprotein F GN=HNRNPF PE=1 SV=3 |
| P49721 | 41 | 201 | 22,8 | 7,02 | 462 | Proteasome subunit beta type-2 GN=PSMB2 PE=1 SV=1 |
| Q13310 | 33 | 644 | 70,7 | 9,26 | 462 | Polyadenylate-binding protein 4 GN=PABPC4 PE=1 SV=1 |
| Q14103 | 32 | 355 | 38,4 | 7,81 | 461 | Heterogeneous nuclear ribonucleoprotein D0 GN=HNRNPD PE=1 SV=1 |
| P05455 | 25 | 408 | 46,8 | 7,12 | 461 | Lupus La protein GN=SSB PE=1 SV=2 |
| O75964 | 34 | 103 | 11,4 | 9,64 | 461 | ATP synthase subunit g, mitochondrial GN=ATP5L PE=1 SV=3 |
| A6NHL2 | 76 | 446 | 49,9 | 6,05 | 453 | Tubulin alpha chain-like 3 GN=TUBAL3 PE=1 SV=2 |
| P30153 | 73 | 589 | 65,3 | 5,11 | 453 | Serine/threonine-protein phosphatase 2A 65 kDa regulatory subunit A alpha isoform |
| Q15181 | 60 | 289 | 32,6 | 5,86 | 451 | Inorganic pyrophosphatase GN=PPA1 PE=1 SV=2 |
| P20674 | 47 | 150 | 16,8 | 6,79 | 450 | Cytochrome c oxidase subunit 5A, mitochondrial GN=COX5A PE=1 SV=2 |
| O75396 | 17 | 215 | 24,6 | 6,92 | 449 | Vesicle-trafficking protein SEC22b GN=SEC22B PE=1 SV=4 |
| Q6ZWN5 | 93 | 194 | 22,6 | 10,65 | 449 | 40S ribosomal protein S9 GN=Rps9 PE=2 SV=3 |
| P35609 | 30 | 894 | 103,8 | 5,45 | 446 | Alpha-actinin-2 GN=ACTN2 PE=1 SV=1 |
| P61956 | 26 | 95 | 10,8 | 5,50 | 445 | Small ubiquitin-related modifier 2 GN=SUMO2 PE=1 SV=2 |
| P24752 | 19 | 427 | 45,2 | 8,85 | 444 | Acetyl-CoA acetyltransferase, mitochondrial GN=ACAT1 PE=1 SV=1 |
| O00231 | 28 | 422 | 47,4 | 6,48 | 444 | 26S proteasome non-ATPase regulatory subunit 11 GN=PSMD11 PE=1 SV=3 |
| P61105 | 33 | 212 | 23,5 | 6,54 | 443 | Ras-related protein Rab-2A OS=Canis familiaris GN=RAB2A PE=1 SV=1 |
| O75340 | 37 | 191 | 21,9 | 5,40 | 438 | Programmed cell death protein 6 GN=PDCD6 PE=1 SV=1 |
| Q7Z3Z0 | 52 | 450 | 49,3 | 5,08 | 437 | Keratin, type I cytoskeletal 25 GN=KRT25 PE=1 SV=1 |
| P63010 | 25 | 937 | 104,5 | 5,38 | 436 | AP-2 complex subunit beta GN=AP2B1 PE=1 SV=1 |
| Q10567 | 22 | 949 | 104,6 | 5,06 | 434 | AP-1 complex subunit beta-1 GN=AP1B1 PE=1 SV=2 |
| Q9BYC2 | 30 | 517 | 56,1 | 7,14 | 432 | Succinyl-CoA:3-ketoacid coenzyme A transferase 2, mitochondrial GN=OXCT2 PE=2 SV |
| Q01813 | 31 | 784 | 85,5 | 7,55 | 432 | 6-phosphofructokinase type C GN=PFKP PE=1 SV=2 |

| | | | | | | |
|---|---|---|---|---|---|---|
| P51148 | 38 | 216 | 23,5 | 8,41 | 431 | Ras-related protein Rab-5C GN=RAB5C PE=1 SV=2 |
| Q6WUX8 | 43 | 105 | 11,7 | 9,57 | 429 | Cytochrome c OS=Gorilla gorilla gorilla GN=CYCS PE=3 SV=3 |
| O43598 | 17 | 174 | 19,1 | 5,05 | 429 | Deoxyribonucleoside 5'-monophosphate N-glycosidase GN=RCL PE=1 SV=1 |
| Q9NR45 | 33 | 359 | 40,3 | 6,74 | 427 | Sialic acid synthase GN=NANS PE=1 SV=2 |
| P47897 | 44 | 775 | 87,7 | 7,15 | 425 | Glutamine--tRNA ligase GN=QARS PE=1 SV=1 |
| P29803 | 17 | 388 | 42,9 | 8,46 | 424 | Pyruvate dehydrogenase E1 component subunit alpha, testis-specific form, mitochon |
| Q32P51 | 30 | 320 | 34,2 | 9,00 | 422 | Heterogeneous nuclear ribonucleoprotein A1-like 2 GN=HNRNPA1L2 PE=2 SV=2 |
| Q3T0E7 | 21 | 330 | 37,5 | 6,33 | 422 | Serine/threonine-protein phosphatase PP1-alpha catalytic subunit GN=PPP1CA PE=2 |
| Q9H3K6 | 21 | 86 | 10,1 | 6,52 | 419 | BolA-like protein 2 GN=BOLA2 PE=1 SV=1 |
| P07954 | 29 | 510 | 54,6 | 8,76 | 419 | Fumarate hydratase, mitochondrial GN=FH PE=1 SV=3 |
| P31040 | 38 | 664 | 72,6 | 7,39 | 419 | Succinate dehydrogenase [ubiquinone] flavoprotein subunit, mitochondrial GN=SDH |
| P11177 | 26 | 359 | 39,2 | 6,65 | 417 | Pyruvate dehydrogenase E1 component subunit beta, mitochondrial GN=PDHB PE=1 S |
| P16989 | 12 | 372 | 40,1 | 9,77 | 414 | DNA-binding protein A GN=CSDA PE=1 SV=4 |
| Q9Y2T7 | 10 | 364 | 38,5 | 10,80 | 414 | Y-box-binding protein 2 GN=YBX2 PE=1 SV=2 |
| Q9NQP4 | 17 | 134 | 15,3 | 4,53 | 414 | Prefoldin subunit 4 GN=PFDN4 PE=1 SV=1 |
| O43143 | 29 | 795 | 90,9 | 7,46 | 414 | Putative pre-mRNA-splicing factor ATP-dependent RNA helicase DHX15 GN=DHX15 P |
| P50213 | 18 | 366 | 39,6 | 6,92 | 414 | Isocitrate dehydrogenase [NAD] subunit alpha, mitochondrial GN=IDH3A PE=1 SV=1 |
| Q9BVC6 | 29 | 243 | 26,2 | 10,48 | 411 | Transmembrane protein 109 GN=TMEM109 PE=1 SV=1 |
| O43242 | 36 | 534 | 60,9 | 8,44 | 411 | 26S proteasome non-ATPase regulatory subunit 3 GN=PSMD3 PE=1 SV=2 |
| P33991 | 46 | 863 | 96,5 | 6,74 | 407 | DNA replication licensing factor MCM4 GN=MCM4 PE=1 SV=5 |
| P55884 | 38 | 814 | 92,4 | 5,00 | 406 | Eukaryotic translation initiation factor 3 subunit B GN=EIF3B PE=1 SV=3 |
| Q16658 | 14 | 493 | 54,5 | 7,24 | 406 | Fascin GN=FSCN1 PE=1 SV=3 |
| P60867 | 38 | 119 | 13,4 | 9,94 | 406 | 40S ribosomal protein S20 GN=Rps20 PE=1 SV=1 |
| Q15561 | 64 | 434 | 48,3 | 7,33 | 402 | Transcriptional enhancer factor TEF-3 GN=TEAD4 PE=1 SV=3 |
| Q08043 | 38 | 901 | 103,2 | 5,52 | 400 | Alpha-actinin-3 GN=ACTN3 PE=1 SV=2 |
| P49720 | 35 | 205 | 22,9 | 6,55 | 397 | Proteasome subunit beta type-3 GN=PSMB3 PE=1 SV=2 |
| P60766 | 40 | 191 | 21,2 | 6,55 | 397 | Cell division control protein 42 homolog GN=Cdc42 PE=1 SV=2 |
| P35749 | 34 | 1972 | 227,2 | 5,50 | 397 | Myosin-11 GN=MYH11 PE=1 SV=3 |
| Q99584 | 46 | 98 | 11,5 | 6,16 | 396 | Protein S100-A13 GN=S100A13 PE=1 SV=1 |
| Q9CXY6 | 14 | 390 | 43,0 | 5,26 | 395 | Interleukin enhancer-binding factor 2 GN=Ilf2 PE=1 SV=1 |
| P31943 | 38 | 449 | 49,2 | 6,30 | 394 | Heterogeneous nuclear ribonucleoprotein H GN=HNRNPH1 PE=1 SV=4 |
| P54709 | 18 | 279 | 31,5 | 8,35 | 392 | Sodium/potassium-transporting ATPase subunit beta-3 GN=ATP1B3 PE=1 SV=1 |
| P62492 | 40 | 216 | 24,4 | 6,57 | 389 | Ras-related protein Rab-11A GN=Rab11a PE=1 SV=3 |
| O60812 | 25 | 293 | 32,1 | 5,06 | 389 | Heterogeneous nuclear ribonucleoprotein C-like 1 GN=HNRNPCL1 PE=1 SV=1 |
| P17661 | 83 | 470 | 53,5 | 5,27 | 388 | Desmin GN=DES PE=1 SV=3 |
| Q13620 | 33 | 913 | 103,9 | 7,37 | 387 | Cullin-4B GN=CUL4B PE=1 SV=4 |
| P62424 | 38 | 266 | 30,0 | 10,61 | 386 | 60S ribosomal protein L7a GN=RPL7A PE=1 SV=2 |
| O60888 | 21 | 179 | 19,1 | 5,50 | 385 | Protein CutA GN=CUTA PE=1 SV=2 |
| P36578 | 67 | 427 | 47,7 | 11,06 | 384 | 60S ribosomal protein L4 GN=RPL4 PE=1 SV=5 |
| Q9Y265 | 29 | 456 | 50,2 | 6,42 | 382 | RuvB-like 1 GN=RUVBL1 PE=1 SV=1 |
| P25685 | 40 | 340 | 38,0 | 8,63 | 382 | DnaJ homolog subfamily B member 1 GN=DNAJB1 PE=1 SV=4 |
| Q9Y490 | 72 | 2541 | 269,6 | 6,07 | 379 | Talin-1 GN=TLN1 PE=1 SV=3 |
| Q13185 | 19 | 183 | 20,8 | 5,33 | 378 | Chromobox protein homolog 3 GN=CBX3 PE=1 SV=4 |
| Q9H361 | 61 | 631 | 70,0 | 9,67 | 375 | Polyadenylate-binding protein 3 GN=PABPC3 PE=1 SV=2 |
| Q9UNM6 | 19 | 376 | 42,9 | 5,81 | 375 | 26S proteasome non-ATPase regulatory subunit 13 GN=PSMD13 PE=1 SV=2 |
| Q9Y262 | 37 | 564 | 66,7 | 6,34 | 374 | Eukaryotic translation initiation factor 3 subunit L GN=EIF3L PE=1 SV=1 |
| P14927 | 21 | 111 | 13,5 | 8,78 | 373 | Cytochrome b-c1 complex subunit 7 GN=UQCRB PE=1 SV=2 |
| P13798 | 11 | 732 | 81,2 | 5,48 | 372 | Acylamino-acid-releasing enzyme GN=APEH PE=1 SV=4 |
| P23381 | 8 | 471 | 53,1 | 6,23 | 370 | Tryptophan--tRNA ligase, cytoplasmic GN=WARS PE=1 SV=2 |
| P38117 | 63 | 255 | 27,8 | 8,10 | 368 | Electron transfer flavoprotein subunit beta GN=ETFB PE=1 SV=3 |
| P50914 | 21 | 215 | 23,4 | 10,93 | 366 | 60S ribosomal protein L14 GN=RPL14 PE=1 SV=4 |
| P13073 | 44 | 169 | 19,6 | 9,51 | 366 | Cytochrome c oxidase subunit 4 isoform 1, mitochondrial GN=COX4I1 PE=1 SV=1 |
| Q00688 | 37 | 224 | 25,2 | 9,28 | 365 | Peptidyl-prolyl cis-trans isomerase FKBP3 GN=FKBP3 PE=1 SV=1 |
| Q3THE2 | 15 | 172 | 19,8 | 4,84 | 364 | Myosin regulatory light chain 12B GN=Myl12b PE=1 SV=2 |
| Q04760 | 35 | 184 | 20,8 | 5,31 | 359 | Lactoylglutathione lyase GN=GLO1 PE=1 SV=4 |
| Q9BYZ2 | 21 | 381 | 41,9 | 8,65 | 358 | L-lactate dehydrogenase A-like 6B GN=LDHAL6B PE=1 SV=3 |
| Q9H254 | 49 | 2564 | 288,8 | 6,01 | 358 | Spectrin beta chain, brain 3 GN=SPTBN4 PE=1 SV=2 |
| Q96TA1 | 40 | 746 | 84,1 | 6,19 | 357 | Niban-like protein 1 GN=FAM129B PE=1 SV=3 |
| P62849 | 17 | 133 | 15,4 | 10,78 | 356 | 40S ribosomal protein S24 GN=Rps24 PE=1 SV=1 |
| B2RPK0 | 43 | 211 | 24,2 | 6,21 | 356 | Putative high mobility group protein B1-like 1 GN=HMGB1P1 PE=5 SV=1 |
| Q9UI30 | 16 | 125 | 14,2 | 5,26 | 355 | tRNA methyltransferase 112 homolog GN=TRMT112 PE=1 SV=1 |
| Q06323 | 23 | 249 | 28,7 | 6,02 | 355 | Proteasome activator complex subunit 1 GN=PSME1 PE=1 SV=1 |
| P17655 | 34 | 700 | 79,9 | 4,98 | 354 | Calpain-2 catalytic subunit GN=CAPN2 PE=1 SV=6 |
| Q9NZ01 | 38 | 308 | 36,0 | 9,45 | 351 | Trans-2,3-enoyl-CoA reductase GN=TECR PE=1 SV=1 |
| P28347 | 32 | 426 | 47,9 | 8,15 | 351 | Transcriptional enhancer factor TEF-1 GN=TEAD1 PE=1 SV=2 |

| | | | | | | |
|---|---|---|---|---|---|---|
| Q76I81 | 49 | 132 | 14,5 | 7,21 | 350 | 40S ribosomal protein S12 GN=RPS12 PE=2 SV=1 |
| P13804 | 28 | 333 | 35,1 | 8,38 | 349 | Electron transfer flavoprotein subunit alpha, mitochondrial GN=ETFA PE=1 SV=1 |
| Q13283 | 25 | 466 | 52,1 | 5,52 | 349 | Ras GTPase-activating protein-binding protein 1 GN=G3BP1 PE=1 SV=1 |
| P32969 | 46 | 192 | 21,8 | 9,95 | 347 | 60S ribosomal protein L9 GN=RPL9 PE=1 SV=1 |
| Q04695 | 70 | 432 | 48,1 | 5,02 | 345 | Keratin, type I cytoskeletal 17 GN=KRT17 PE=1 SV=2 |
| Q9UI15 | 10 | 199 | 22,5 | 7,33 | 345 | Transgelin-3 GN=TAGLN3 PE=1 SV=2 |
| O75874 | 16 | 414 | 46,6 | 7,01 | 343 | Isocitrate dehydrogenase [NADP] cytoplasmic GN=IDH1 PE=1 SV=2 |
| Q8BMJ3 | 44 | 144 | 16,5 | 5,24 | 343 | Eukaryotic translation initiation factor 1A, X-chromosomal GN=Eif1ax PE=2 SV=3 |
| Q16719 | 30 | 465 | 52,3 | 7,03 | 338 | Kynureninase GN=KYNU PE=1 SV=1 |
| P35237 | 21 | 376 | 42,6 | 5,27 | 338 | Serpin B6 GN=SERPINB6 PE=1 SV=3 |
| P06454 | 18 | 111 | 12,2 | 3,78 | 337 | Prothymosin alpha GN=PTMA PE=1 SV=2 |
| Q02413 | 29 | 1049 | 113,7 | 5,03 | 336 | Desmoglein-1 GN=DSG1 PE=1 SV=2 |
| Q09019 | 31 | 674 | 70,4 | 7,24 | 336 | Dystrophia myotonica WD repeat-containing protein GN=DMWD PE=1 SV=3 |
| Q04941 | 29 | 152 | 16,7 | 7,24 | 335 | Proteolipid protein 2 GN=PLP2 PE=1 SV=1 |
| P10620 | 10 | 155 | 17,6 | 9,39 | 333 | Microsomal glutathione S-transferase 1 GN=MGST1 PE=1 SV=1 |
| P19012 | 62 | 456 | 49,2 | 4,77 | 333 | Keratin, type I cytoskeletal 15 GN=KRT15 PE=1 SV=3 |
| Q9Y536 | 112 | 164 | 18,2 | 9,22 | 332 | Peptidyl-prolyl cis-trans isomerase A-like 4A/B/C GN=PPIAL4A PE=1 SV=1 |
| P35527 | 85 | 623 | 62,0 | 5,24 | 331 | Keratin, type I cytoskeletal 9 GN=KRT9 PE=1 SV=3 |
| P36871 | 19 | 562 | 61,4 | 6,76 | 331 | Phosphoglucomutase-1 GN=PGM1 PE=1 SV=3 |
| P51571 | 17 | 173 | 19,0 | 6,15 | 331 | Translocon-associated protein subunit delta GN=SSR4 PE=1 SV=1 |
| P61222 | 34 | 599 | 67,3 | 8,34 | 330 | ATP-binding cassette sub-family E member 1 GN=Abce1 PE=2 SV=1 |
| O95831 | 36 | 613 | 66,9 | 8,95 | 327 | Apoptosis-inducing factor 1, mitochondrial GN=AIFM1 PE=1 SV=1 |
| Q58FF3 | 47 | 399 | 45,8 | 5,26 | 326 | Putative endoplasmin-like protein GN=HSP90B2P PE=5 SV=1 |
| P30084 | 42 | 290 | 31,4 | 8,07 | 326 | Enoyl-CoA hydratase, mitochondrial GN=ECHS1 PE=1 SV=4 |
| P09874 | 24 | 1014 | 113,0 | 8,88 | 326 | Poly [ADP-ribose] polymerase 1 GN=PARP1 PE=1 SV=4 |
| P25788 | 47 | 255 | 28,4 | 5,33 | 325 | Proteasome subunit alpha type-3 GN=PSMA3 PE=1 SV=2 |
| Q0P5D0 | 85 | 177 | 19,2 | 8,07 | 323 | Peptidyl-prolyl cis-trans isomerase H GN=PPIH PE=2 SV=1 |
| P40429 | 61 | 203 | 23,6 | 10,93 | 322 | 60S ribosomal protein L13a GN=RPL13A PE=1 SV=2 |
| P27708 | 69 | 2225 | 242,8 | 6,46 | 321 | CAD protein GN=CAD PE=1 SV=3 |
| P51858 | 34 | 240 | 26,8 | 4,73 | 321 | Hepatoma-derived growth factor GN=HDGF PE=1 SV=1 |
| Q13451 | 21 | 457 | 51,2 | 5,90 | 320 | Peptidyl-prolyl cis-trans isomerase FKBP5 GN=FKBP5 PE=1 SV=2 |
| P62267 | 20 | 143 | 15,8 | 10,49 | 320 | 40S ribosomal protein S23 GN=Rps23 PE=2 SV=3 |
| P45877 | 76 | 212 | 22,7 | 8,40 | 319 | Peptidyl-prolyl cis-trans isomerase C GN=PPIC PE=1 SV=1 |
| O95747 | 12 | 527 | 58,0 | 6,43 | 318 | Serine/threonine-protein kinase OSR1 GN=OXSR1 PE=1 SV=1 |
| P20648 | 18 | 1035 | 114,0 | 5,81 | 318 | Potassium-transporting ATPase alpha chain 1 GN=ATP4A PE=2 SV=5 |
| P13796 | 39 | 627 | 70,2 | 5,43 | 317 | Plastin-2 GN=LCP1 PE=1 SV=6 |
| Q5VT79 | 16 | 327 | 36,8 | 5,63 | 314 | Annexin A8-like protein 2 GN=ANXA8L2 PE=2 SV=1 |
| Q92973 | 51 | 898 | 102,3 | 4,98 | 313 | Transportin-1 GN=TNPO1 PE=1 SV=2 |
| O00116 | 17 | 658 | 72,9 | 7,34 | 311 | Alkyldihydroxyacetonephosphate synthase, peroxisomal GN=AGPS PE=1 SV=1 |
| Q9NTK5 | 10 | 396 | 44,7 | 7,81 | 310 | Obg-like ATPase 1 GN=OLA1 PE=1 SV=2 |
| Q9BQ67 | 8 | 446 | 49,4 | 4,92 | 310 | Glutamate-rich WD repeat-containing protein 1 GN=GRWD1 PE=1 SV=1 |
| Q9UQ80 | 34 | 394 | 43,8 | 6,55 | 309 | Proliferation-associated protein 2G4 GN=PA2G4 PE=1 SV=3 |
| Q96A49 | 12 | 352 | 39,9 | 4,53 | 309 | Synapse-associated protein 1 GN=SYAP1 PE=1 SV=1 |
| P15880 | 76 | 293 | 31,3 | 10,24 | 308 | 40S ribosomal protein S2 GN=RPS2 PE=1 SV=2 |
| P13928 | 23 | 327 | 36,9 | 5,78 | 308 | Annexin A8 GN=ANXA8 PE=1 SV=3 |
| P49589 | 14 | 748 | 85,4 | 6,76 | 306 | Cysteine--tRNA ligase, cytoplasmic GN=CARS PE=1 SV=3 |
| P05198 | 28 | 315 | 36,1 | 5,08 | 306 | Eukaryotic translation initiation factor 2 subunit 1 GN=EIF2S1 PE=1 SV=3 |
| Q15645 | 20 | 432 | 48,5 | 6,09 | 306 | Pachytene checkpoint protein 2 homolog GN=TRIP13 PE=1 SV=2 |
| Q15366 | 25 | 365 | 38,6 | 6,79 | 306 | Poly(rC)-binding protein 2 GN=PCBP2 PE=1 SV=1 |
| Q7Z406 | 35 | 1995 | 227,7 | 5,60 | 303 | Myosin-14 GN=MYH14 PE=1 SV=2 |
| Q00325 | 37 | 362 | 40,1 | 9,38 | 301 | Phosphate carrier protein, mitochondrial GN=SLC25A3 PE=1 SV=2 |
| P41252 | 59 | 1262 | 144,4 | 6,15 | 301 | Isoleucine--tRNA ligase, cytoplasmic GN=IARS PE=1 SV=2 |
| Q14964 | 19 | 217 | 25,0 | 7,65 | 300 | Ras-related protein Rab-39A GN=RAB39A PE=2 SV=2 |
| P51153 | 25 | 203 | 22,8 | 9,19 | 300 | Ras-related protein Rab-13 GN=RAB13 PE=1 SV=1 |
| Q6EEV6 | 17 | 95 | 10,7 | 7,18 | 298 | Small ubiquitin-related modifier 4 GN=SUMO4 PE=1 SV=2 |
| O60763 | 19 | 962 | 107,8 | 4,91 | 298 | General vesicular transport factor p115 GN=USO1 PE=1 SV=2 |
| P17174 | 32 | 413 | 46,2 | 7,01 | 296 | Aspartate aminotransferase, cytoplasmic GN=GOT1 PE=1 SV=3 |
| Q14126 | 37 | 1118 | 122,2 | 5,24 | 295 | Desmoglein-2 GN=DSG2 PE=1 SV=2 |
| Q9BRA2 | 30 | 123 | 13,9 | 5,52 | 292 | Thioredoxin domain-containing protein 17 GN=TXNDC17 PE=1 SV=1 |
| Q6NZI2 | 11 | 390 | 43,4 | 5,60 | 291 | Polymerase I and transcript release factor GN=PTRF PE=1 SV=1 |
| O00429 | 20 | 736 | 81,8 | 6,81 | 288 | Dynamin-1-like protein GN=DNM1L PE=1 SV=2 |
| Q96AE4 | 18 | 644 | 67,5 | 7,61 | 288 | Far upstream element-binding protein 1 GN=FUBP1 PE=1 SV=3 |
| Q5E9D5 | 32 | 165 | 18,5 | 7,85 | 288 | Destrin GN=DSTN PE=2 SV=3 |
| P20962 | 24 | 102 | 11,5 | 4,16 | 287 | Parathymosin GN=PTMS PE=1 SV=2 |
| P09972 | 58 | 364 | 39,4 | 6,87 | 287 | Fructose-bisphosphate aldolase C GN=ALDOC PE=1 SV=2 |

| | | | | | | |
|---|---|---|---|---|---|---|
| P25786 | 27 | 263 | 29,5 | 6,61 | 286 | Proteasome subunit alpha type-1 GN=PSMA1 PE=1 SV=1 |
| Q8NCW5 | 29 | 288 | 31,7 | 7,66 | 286 | Apolipoprotein A-I-binding protein GN=APOA1BP PE=1 SV=2 |
| Q9CZM2 | 27 | 204 | 24,1 | 11,62 | 283 | 60S ribosomal protein L15 GN=Rpl15 PE=2 SV=4 |
| Q3T0W9 | 18 | 196 | 23,5 | 11,47 | 281 | 60S ribosomal protein L19 GN=RPL19 PE=2 SV=1 |
| Q14116 | 32 | 193 | 22,3 | 4,67 | 280 | Interleukin-18 GN=IL18 PE=1 SV=1 |
| O14595 | 25 | 271 | 30,6 | 5,53 | 280 | Carboxy-terminal domain RNA polymerase II polypeptide A small phosphatase 2 GN= |
| P63221 | 17 | 83 | 9,1 | 8,50 | 279 | 40S ribosomal protein S21 OS=Sus scrofa GN=RPS21 PE=3 SV=1 |
| P24666 | 21 | 158 | 18,0 | 6,74 | 279 | Low molecular weight phosphotyrosine protein phosphatase GN=ACP1 PE=1 SV=3 |
| P43487 | 21 | 201 | 23,3 | 5,29 | 278 | Ran-specific GTPase-activating protein GN=RANBP1 PE=1 SV=1 |
| P38606 | 16 | 617 | 68,3 | 5,52 | 277 | V-type proton ATPase catalytic subunit A GN=ATP6V1A PE=1 SV=2 |
| O00159 | 28 | 1063 | 121,6 | 9,41 | 277 | Unconventional myosin-Ic GN=MYO1C PE=1 SV=4 |
| Q3T035 | 15 | 178 | 20,5 | 8,59 | 276 | Actin-related protein 2/3 complex subunit 3 GN=ARPC3 PE=1 SV=3 |
| P02794 | 15 | 183 | 21,2 | 5,55 | 275 | Ferritin heavy chain GN=FTH1 PE=1 SV=2 |
| P61358 | 33 | 136 | 15,8 | 10,56 | 274 | 60S ribosomal protein L27 GN=Rpl27 PE=2 SV=2 |
| Q9H4A4 | 11 | 650 | 72,5 | 5,74 | 273 | Aminopeptidase B GN=RNPEP PE=1 SV=2 |
| P04908 | 24 | 130 | 14,1 | 11,05 | 273 | Histone H2A type 1-B/E GN=HIST1H2AB PE=1 SV=2 |
| Q96CT7 | 12 | 223 | 25,8 | 9,54 | 272 | Coiled-coil domain-containing protein 124 GN=CCDC124 PE=1 SV=1 |
| Q9NZ45 | 10 | 108 | 12,2 | 9,09 | 271 | CDGSH iron-sulfur domain-containing protein 1 GN=CISD1 PE=1 SV=1 |
| P55809 | 22 | 520 | 56,1 | 7,46 | 271 | Succinyl-CoA:3-ketoacid coenzyme A transferase 1, mitochondrial GN=OXCT1 PE=1 SV |
| P17812 | 9 | 591 | 66,6 | 6,46 | 271 | CTP synthase 1 GN=CTPS1 PE=1 SV=2 |
| P09525 | 36 | 319 | 35,9 | 6,13 | 269 | Annexin A4 GN=ANXA4 PE=1 SV=4 |
| P07108 | 21 | 87 | 10,0 | 6,57 | 269 | Acyl-CoA-binding protein GN=DBI PE=1 SV=2 |
| Q9Y617 | 57 | 370 | 40,4 | 7,66 | 269 | Phosphoserine aminotransferase GN=PSAT1 PE=1 SV=2 |
| Q9Y2B0 | 17 | 182 | 20,6 | 4,92 | 269 | Protein canopy homolog 2 GN=CNPY2 PE=1 SV=1 |
| Q13619 | 18 | 759 | 87,6 | 8,13 | 268 | Cullin-4A GN=CUL4A PE=1 SV=3 |
| Q3ZCK9 | 15 | 261 | 29,5 | 7,72 | 268 | Proteasome subunit alpha type-4 GN=PSMA4 PE=1 SV=1 |
| P06737 | 39 | 847 | 97,1 | 7,17 | 266 | Glycogen phosphorylase, liver form GN=PYGL PE=1 SV=4 |
| O00764 | 6 | 312 | 35,1 | 6,13 | 266 | Pyridoxal kinase GN=PDXK PE=1 SV=1 |
| Q9NQG5 | 18 | 326 | 36,9 | 5,97 | 266 | Regulation of nuclear pre-mRNA domain-containing protein 1B GN=RPRD1B PE=1 SV= |
| Q15785 | 16 | 309 | 34,5 | 8,98 | 266 | Mitochondrial import receptor subunit TOM34 GN=TOMM34 PE=1 SV=2 |
| P26373 | 62 | 211 | 24,2 | 11,65 | 266 | 60S ribosomal protein L13 GN=RPL13 PE=1 SV=4 |
| P33993 | 33 | 719 | 81,3 | 6,46 | 265 | DNA replication licensing factor MCM7 GN=MCM7 PE=1 SV=4 |
| Q9UNL2 | 10 | 185 | 21,1 | 9,61 | 265 | Translocon-associated protein subunit gamma GN=SSR3 PE=1 SV=1 |
| O95292 | 20 | 243 | 27,2 | 7,30 | 264 | Vesicle-associated membrane protein-associated protein B/C GN=VAPB PE=1 SV=3 |
| P55327 | 20 | 224 | 24,3 | 4,83 | 263 | Tumor protein D52 GN=TPD52 PE=1 SV=2 |
| Q08J23 | 31 | 767 | 86,4 | 6,77 | 263 | tRNA (cytosine(34)-C(5))-methyltransferase GN=NSUN2 PE=1 SV=2 |
| P21266 | 23 | 225 | 26,5 | 5,54 | 261 | Glutathione S-transferase Mu 3 GN=GSTM3 PE=1 SV=3 |
| P14324 | 41 | 419 | 48,2 | 6,15 | 261 | Farnesyl pyrophosphate synthase GN=FDPS PE=1 SV=4 |
| P11413 | 27 | 515 | 59,2 | 6,84 | 261 | Glucose-6-phosphate 1-dehydrogenase GN=G6PD PE=1 SV=4 |
| Q9Y6C9 | 16 | 303 | 33,3 | 7,97 | 259 | Mitochondrial carrier homolog 2 GN=MTCH2 PE=1 SV=1 |
| Q16576 | 9 | 425 | 47,8 | 5,05 | 258 | Histone-binding protein RBBP7 GN=RBBP7 PE=1 SV=1 |
| P20290 | 20 | 206 | 22,2 | 9,38 | 257 | Transcription factor BTF3 GN=BTF3 PE=1 SV=1 |
| P83917 | 10 | 185 | 21,4 | 4,93 | 257 | Chromobox protein homolog 1 GN=Cbx1 PE=1 SV=1 |
| P41250 | 24 | 739 | 83,1 | 7,03 | 257 | Glycyl-tRNA synthetase GN=GARS PE=1 SV=3 |
| P39748 | 16 | 380 | 42,6 | 8,62 | 256 | Flap endonuclease 1 GN=FEN1 PE=1 SV=1 |
| Q13838 | 25 | 428 | 49,0 | 5,67 | 256 | Spliceosome RNA helicase DDX39B GN=DDX39B PE=1 SV=1 |
| Q16836 | 30 | 314 | 34,3 | 8,85 | 256 | Hydroxyacyl-coenzyme A dehydrogenase, mitochondrial GN=HADH PE=1 SV=3 |
| P04181 | 30 | 439 | 48,5 | 7,03 | 255 | Ornithine aminotransferase, mitochondrial GN=OAT PE=1 SV=1 |
| P61021 | 17 | 215 | 23,7 | 8,13 | 255 | Ras-related protein Rab-5B GN=Rab5b PE=1 SV=1 |
| P17980 | 30 | 439 | 49,2 | 5,24 | 255 | 26S protease regulatory subunit 6A GN=PSMC3 PE=1 SV=3 |
| O75347 | 32 | 108 | 12,8 | 5,29 | 255 | Tubulin-specific chaperone A GN=TBCA PE=1 SV=3 |
| Q96IX5 | 7 | 58 | 6,5 | 9,76 | 254 | Up-regulated during skeletal muscle growth protein 5 GN=USMG5 PE=1 SV=1 |
| Q3SZ52 | 39 | 147 | 16,5 | 7,93 | 254 | Ubiquitin-conjugating enzyme E2 variant 1 GN=UBE2V1 PE=2 SV=1 |
| Q9UHV9 | 16 | 154 | 16,6 | 6,58 | 253 | Prefoldin subunit 2 GN=PFDN2 PE=1 SV=1 |
| P17858 | 13 | 780 | 85,0 | 7,50 | 253 | 6-phosphofructokinase, liver type GN=PFKL PE=1 SV=6 |
| O76021 | 19 | 490 | 54,9 | 10,13 | 252 | Ribosomal L1 domain-containing protein 1 GN=RSL1D1 PE=1 SV=3 |
| Q3SZ43 | 29 | 145 | 16,4 | 8,09 | 251 | Ubiquitin-conjugating enzyme E2 variant 2 GN=UBE2V2 PE=2 SV=3 |
| P33992 | 24 | 734 | 82,2 | 8,37 | 250 | DNA replication licensing factor MCM5 GN=MCM5 PE=1 SV=5 |
| P56134 | 18 | 94 | 10,9 | 9,67 | 250 | ATP synthase subunit f, mitochondrial GN=ATP5J2 PE=1 SV=3 |
| Q16543 | 13 | 378 | 44,4 | 5,25 | 247 | Hsp90 co-chaperone Cdc37 GN=CDC37 PE=1 SV=1 |
| O95716 | 17 | 219 | 24,3 | 4,93 | 246 | Ras-related protein Rab-3D GN=RAB3D PE=1 SV=1 |
| Q13423 | 35 | 1086 | 113,8 | 8,09 | 246 | NAD(P) transhydrogenase, mitochondrial GN=NNT PE=1 SV=3 |
| P41091 | 39 | 472 | 51,1 | 8,40 | 246 | Eukaryotic translation initiation factor 2 subunit 3 GN=EIF2S3 PE=1 SV=3 |
| Q6ZVH7 | 32 | 1005 | 108,1 | 6,47 | 245 | Espin-like protein GN=ESPNL PE=1 SV=3 |
| Q9UN86 | 15 | 482 | 54,1 | 5,55 | 244 | Ras GTPase-activating protein-binding protein 2 GN=G3BP2 PE=1 SV=2 |

| | | | | | | |
|---|---|---|---|---|---|---|
| P13646 | 31 | 458 | 49,6 | 4,96 | 244 | Keratin, type I cytoskeletal 13 GN=KRT13 PE=1 SV=4 |
| Q8WUD1 | 16 | 216 | 24,2 | 7,83 | 243 | Ras-related protein Rab-2B GN=RAB2B PE=1 SV=1 |
| P20339 | 22 | 215 | 23,6 | 8,15 | 243 | Ras-related protein Rab-5A GN=RAB5A PE=1 SV=2 |
| Q9HC84 | 46 | 5762 | 596,0 | 6,64 | 242 | Mucin-5B GN=MUC5B PE=1 SV=3 |
| Q9UL46 | 19 | 239 | 27,4 | 5,73 | 240 | Proteasome activator complex subunit 2 GN=PSME2 PE=1 SV=4 |
| P60335 | 16 | 356 | 37,5 | 7,09 | 240 | Poly(rC)-binding protein 1 GN=Pcbp1 PE=1 SV=1 |
| Q5XTY7 | 17 | 184 | 21,4 | 10,17 | 238 | 60S ribosomal protein L17 OS=Felis catus GN=RPL17 PE=2 SV=3 |
| Q96FQ6 | 12 | 103 | 11,8 | 6,79 | 237 | Protein S100-A16 GN=S100A16 PE=1 SV=1 |
| Q9HAV0 | 20 | 340 | 37,5 | 6,00 | 235 | Guanine nucleotide-binding protein subunit beta-4 GN=GNB4 PE=1 SV=3 |
| O14949 | 11 | 82 | 9,9 | 10,08 | 235 | Cytochrome b-c1 complex subunit 8 GN=UQCRQ PE=1 SV=4 |
| Q6NVV1 | 17 | 102 | 12,1 | 10,76 | 233 | Putative 60S ribosomal protein L13a-like MGC87657 PE=5 SV=1 |
| Q12965 | 12 | 1108 | 127,0 | 8,92 | 233 | Unconventional myosin-Ie GN=MYO1E PE=1 SV=2 |
| P61164 | 35 | 376 | 42,6 | 6,64 | 233 | Alpha-centractin GN=Actr1a PE=2 SV=1 |
| P68433 | 60 | 136 | 15,4 | 11,12 | 232 | Histone H3.1 GN=Hist1h3a PE=1 SV=2 |
| Q86WQ0 | 16 | 139 | 15,9 | 6,16 | 229 | Nuclear receptor 2C2-associated protein GN=NR2C2AP PE=1 SV=1 |
| P49419 | 18 | 539 | 58,5 | 7,99 | 229 | Alpha-aminoadipic semialdehyde dehydrogenase GN=ALDH7A1 PE=1 SV=5 |
| Q9Y2Q3 | 9 | 226 | 25,5 | 8,41 | 227 | Glutathione S-transferase kappa 1 GN=GSTK1 PE=1 SV=3 |
| P61009 | 192 | 180 | 20,3 | 8,62 | 227 | Signal peptidase complex subunit 3 GN=SPCS3 PE=1 SV=1 |
| P55010 | 7 | 431 | 49,2 | 5,58 | 226 | Eukaryotic translation initiation factor 5 GN=EIF5 PE=1 SV=2 |
| Q92598 | 21 | 858 | 96,8 | 5,39 | 225 | Heat shock protein 105 kDa GN=HSPH1 PE=1 SV=1 |
| P54577 | 21 | 528 | 59,1 | 7,05 | 224 | Tyrosyl-tRNA synthetase, cytoplasmic GN=YARS PE=1 SV=4 |
| Q15562 | 19 | 447 | 49,2 | 6,47 | 224 | Transcriptional enhancer factor TEF-4 GN=TEAD2 PE=1 SV=2 |
| Q7L2H7 | 15 | 374 | 42,5 | 5,63 | 223 | Eukaryotic translation initiation factor 3 subunit M GN=EIF3M PE=1 SV=1 |
| Q9Y5L4 | 11 | 95 | 10,5 | 8,18 | 223 | Mitochondrial import inner membrane translocase subunit Tim13 GN=TIMM13 PE=1 S |
| P13667 | 23 | 645 | 72,9 | 5,07 | 223 | Protein disulfide-isomerase A4 GN=PDIA4 PE=1 SV=2 |
| Q13347 | 44 | 325 | 36,5 | 5,64 | 223 | Eukaryotic translation initiation factor 3 subunit I GN=EIF3I PE=1 SV=1 |
| P30085 | 18 | 196 | 22,2 | 5,57 | 222 | UMP-CMP kinase GN=CMPK1 PE=1 SV=3 |
| P39023 | 16 | 403 | 46,1 | 10,18 | 221 | 60S ribosomal protein L3 GN=RPL3 PE=1 SV=2 |
| Q9H2P0 | 33 | 1102 | 123,5 | 7,34 | 221 | Activity-dependent neuroprotector homeobox protein GN=ADNP PE=1 SV=1 |
| O14787 | 28 | 897 | 101,3 | 5,01 | 221 | Transportin-2 GN=TNPO2 PE=1 SV=3 |
| P62281 | 41 | 158 | 18,4 | 10,30 | 220 | 40S ribosomal protein S11 GN=Rps11 PE=2 SV=3 |
| P36957 | 28 | 453 | 48,7 | 8,95 | 220 | Dihydrolipoyllysine-residue succinyltransferase component of 2-oxoglutarate dehydı |
| Q15008 | 17 | 389 | 45,5 | 5,62 | 220 | 26S proteasome non-ATPase regulatory subunit 6 GN=PSMD6 PE=1 SV=1 |
| P05062 | 27 | 364 | 39,4 | 7,87 | 219 | Fructose-bisphosphate aldolase B GN=ALDOB PE=1 SV=2 |
| O15357 | 31 | 1258 | 138,5 | 6,54 | 219 | Phosphatidylinositol 3,4,5-trisphosphate 5-phosphatase 2 GN=INPPL1 PE=1 SV=2 |
| O76064 | 20 | 485 | 55,5 | 7,33 | 219 | E3 ubiquitin-protein ligase RNF8 GN=RNF8 PE=1 SV=1 |
| P35557 | 23 | 465 | 52,2 | 5,20 | 219 | Glucokinase GN=GCK PE=1 SV=1 |
| Q12829 | 20 | 278 | 30,9 | 9,61 | 219 | Ras-related protein Rab-40B GN=RAB40B PE=2 SV=1 |
| Q8IUM7 | 20 | 802 | 87,1 | 4,64 | 219 | Neuronal PAS domain-containing protein 4 GN=NPAS4 PE=1 SV=1 |
| Q8TE56 | 19 | 1095 | 121,0 | 8,06 | 219 | A disintegrin and metalloproteinase with thrombospondin motifs 17 GN=ADAMTS17 |
| Q8WXH6 | 21 | 277 | 31,1 | 9,32 | 219 | Ras-related protein Rab-40A GN=RAB40A PE=2 SV=2 |
| Q99571 | 25 | 388 | 43,3 | 7,99 | 219 | P2X purinoceptor 4 GN=P2RX4 PE=1 SV=2 |
| Q6IQ22 | 11 | 244 | 27,2 | 8,41 | 219 | Ras-related protein Rab-12 GN=RAB12 PE=1 SV=3 |
| P53621 | 28 | 1224 | 138,3 | 7,66 | 219 | Coatomer subunit alpha GN=COPA PE=1 SV=2 |
| Q9Y3F4 | 10 | 350 | 38,4 | 5,12 | 218 | Serine-threonine kinase receptor-associated protein GN=STRAP PE=1 SV=1 |
| P52907 | 13 | 286 | 32,9 | 5,69 | 218 | F-actin-capping protein subunit alpha-1 GN=CAPZA1 PE=1 SV=3 |
| P28663 | 13 | 298 | 33,5 | 5,47 | 217 | Beta-soluble NSF attachment protein GN=Napb PE=1 SV=2 |
| Q8CGP0 | 53 | 126 | 13,9 | 10,32 | 217 | Histone H2B type 3-B GN=Hist3h2bb PE=1 SV=3 |
| P57053 | 57 | 126 | 13,9 | 10,37 | 217 | Histone H2B type F-S GN=H2BFS PE=1 SV=2 |
| O43423 | 22 | 234 | 26,7 | 4,21 | 216 | Acidic leucine-rich nuclear phosphoprotein 32 family member C GN=ANP32C PE=2 SV |
| P35580 | 41 | 1976 | 228,9 | 5,54 | 214 | Myosin-10 GN=MYH10 PE=1 SV=3 |
| P35754 | 12 | 106 | 11,8 | 8,09 | 214 | Glutaredoxin-1 GN=GLRX PE=1 SV=2 |
| Q00839 | 22 | 825 | 90,5 | 6,00 | 214 | Heterogeneous nuclear ribonucleoprotein U GN=HNRNPU PE=1 SV=6 |
| O14979 | 37 | 420 | 46,4 | 9,57 | 213 | Heterogeneous nuclear ribonucleoprotein D-like GN=HNRPDL PE=1 SV=3 |
| P62942 | 18 | 108 | 11,9 | 8,16 | 212 | Peptidyl-prolyl cis-trans isomerase FKBP1A GN=FKBP1A PE=1 SV=2 |
| P48444 | 9 | 511 | 57,2 | 6,21 | 212 | Coatomer subunit delta GN=ARCN1 PE=1 SV=1 |
| P62996 | 15 | 288 | 33,6 | 11,25 | 212 | Transformer-2 protein homolog beta GN=Tra2b PE=1 SV=1 |
| O43324 | 11 | 174 | 19,8 | 8,54 | 211 | Eukaryotic translation elongation factor 1 epsilon-1 GN=EEF1E1 PE=1 SV=1 |
| P49588 | 18 | 968 | 106,7 | 5,53 | 211 | Alanine--tRNA ligase, cytoplasmic GN=AARS PE=1 SV=2 |
| P21291 | 11 | 193 | 20,6 | 8,57 | 211 | Cysteine and glycine-rich protein 1 GN=CSRP1 PE=1 SV=3 |
| P15121 | 22 | 316 | 35,8 | 6,98 | 210 | Aldose reductase GN=AKR1B1 PE=1 SV=3 |
| P11216 | 31 | 843 | 96,6 | 6,86 | 210 | Glycogen phosphorylase, brain form GN=PYGB PE=1 SV=5 |
| O14579 | 24 | 308 | 34,5 | 5,12 | 210 | Coatomer subunit epsilon GN=COPE PE=1 SV=3 |
| Q99536 | 10 | 393 | 41,9 | 6,29 | 209 | Synaptic vesicle membrane protein VAT-1 homolog GN=VAT1 PE=1 SV=2 |
| P43307 | 13 | 286 | 32,2 | 4,49 | 209 | Translocon-associated protein subunit alpha GN=SSR1 PE=1 SV=3 |

| | | | | | | |
|---|---|---|---|---|---|---|
| P62806 | 48 | 103 | 11,4 | 11,36 | 209 | Histone H4 GN=Hist1h4a PE=1 SV=2 |
| P42771 | 20 | 156 | 16,5 | 5,81 | 208 | Cyclin-dependent kinase inhibitor 2A, isoforms 1/2/3 GN=CDKN2A PE=1 SV=2 |
| O00148 | 13 | 427 | 49,1 | 5,68 | 208 | ATP-dependent RNA helicase DDX39A GN=DDX39A PE=1 SV=2 |
| P31942 | 7 | 346 | 36,9 | 6,87 | 208 | Heterogeneous nuclear ribonucleoprotein H3 GN=HNRNPH3 PE=1 SV=2 |
| Q8N9W4 | 52 | 650 | 79,3 | 5,54 | 208 | Golgin subfamily A member 6-like protein 2 GN=GOLGA6L2 PE=2 SV=2 |
| P16402 | 317 | 221 | 22,3 | 11,02 | 208 | Histone H1.3 GN=HIST1H1D PE=1 SV=2 |
| Q14257 | 23 | 317 | 36,9 | 4,40 | 206 | Reticulocalbin-2 GN=RCN2 PE=1 SV=1 |
| Q2VIR3 | 34 | 472 | 51,2 | 8,40 | 206 | Putative eukaryotic translation initiation factor 2 subunit 3-like protein GN=EIF2S3L P |
| Q01546 | 33 | 638 | 65,8 | 8,12 | 205 | Keratin, type II cytoskeletal 2 oral GN=KRT76 PE=1 SV=2 |
| P00367 | 22 | 558 | 61,4 | 7,80 | 205 | Glutamate dehydrogenase 1, mitochondrial GN=GLUD1 PE=1 SV=2 |
| P14550 | 21 | 325 | 36,5 | 6,79 | 204 | Alcohol dehydrogenase [NADP(+)] GN=AKR1A1 PE=1 SV=3 |
| P26599 | 33 | 531 | 57,2 | 9,17 | 204 | Polypyrimidine tract-binding protein 1 GN=PTBP1 PE=1 SV=1 |
| P59999 | 13 | 168 | 19,7 | 8,43 | 204 | Actin-related protein 2/3 complex subunit 4 GN=Arpc4 PE=1 SV=3 |
| P62192 | 22 | 440 | 49,2 | 6,21 | 204 | 26S protease regulatory subunit 4 GN=Psmc1 PE=1 SV=1 |
| Q02818 | 30 | 461 | 53,8 | 5,25 | 203 | Nucleobindin-1 GN=NUCB1 PE=1 SV=4 |
| P21980 | 20 | 687 | 77,3 | 5,22 | 201 | Protein-glutamine gamma-glutamyltransferase 2 GN=TGM2 PE=1 SV=2 |
| P50502 | 9 | 369 | 41,3 | 5,27 | 200 | Hsc70-interacting protein GN=ST13 PE=1 SV=2 |
| Q13057 | 12 | 564 | 62,3 | 6,99 | 198 | Bifunctional coenzyme A synthase GN=COASY PE=1 SV=4 |
| Q04446 | 14 | 702 | 80,4 | 6,32 | 198 | 1,4-alpha-glucan-branching enzyme GN=GBE1 PE=1 SV=3 |
| Q8NEB9 | 44 | 887 | 101,5 | 6,81 | 197 | Phosphatidylinositol 3-kinase catalytic subunit type 3 GN=PIK3C3 PE=1 SV=1 |
| P46778 | 13 | 160 | 18,6 | 10,49 | 197 | 60S ribosomal protein L21 GN=RPL21 PE=1 SV=2 |
| O75122 | 186 | 1294 | 141,0 | 8,47 | 197 | CLIP-associating protein 2 GN=CLASP2 PE=1 SV=2 |
| Q86YS6 | 10 | 212 | 23,3 | 5,64 | 197 | Ras-related protein Rab-43 GN=RAB43 PE=1 SV=1 |
| A6NDJ8 | 12 | 181 | 20,2 | 6,54 | 197 | Putative Rab-43-like protein ENSP00000330714 PE=5 SV=3 |
| P20340 | 10 | 208 | 23,6 | 5,54 | 197 | Ras-related protein Rab-6A GN=RAB6A PE=1 SV=3 |
| Q96JK9 | 29 | 1134 | 121,7 | 7,52 | 197 | Mastermind-like protein 3 GN=MAML3 PE=1 SV=3 |
| O00160 | 7 | 1098 | 124,8 | 9,11 | 196 | Unconventional myosin-If GN=MYO1F PE=1 SV=3 |
| Q862I1 | 25 | 157 | 17,8 | 11,25 | 196 | 60S ribosomal protein L24 GN=RPL24 PE=2 SV=2 |
| O15020 | 71 | 2390 | 271,2 | 6,11 | 196 | Spectrin beta chain, brain 2 GN=SPTBN2 PE=1 SV=3 |
| P84104 | 17 | 164 | 19,3 | 11,65 | 195 | Serine/arginine-rich splicing factor 3 GN=Srsf3 PE=1 SV=1 |
| Q3MIP1 | 43 | 535 | 58,4 | 9,42 | 195 | Inositol 1,4,5-trisphosphate receptor-interacting protein-like 2 GN=ITPRIPL2 PE=2 SV= |
| Q96DG6 | 25 | 245 | 28,0 | 7,18 | 195 | Carboxymethylenebutenolidase homolog GN=CMBL PE=1 SV=1 |
| P56537 | 27 | 245 | 26,6 | 4,68 | 194 | Eukaryotic translation initiation factor 6 GN=EIF6 PE=1 SV=1 |
| P15927 | 13 | 270 | 29,2 | 6,15 | 194 | Replication protein A 32 kDa subunit GN=RPA2 PE=1 SV=1 |
| O00264 | 14 | 195 | 21,7 | 4,70 | 193 | Membrane-associated progesterone receptor component 1 GN=PGRMC1 PE=1 SV=3 |
| P61247 | 29 | 264 | 29,9 | 9,73 | 193 | 40S ribosomal protein S3a GN=RPS3A PE=1 SV=2 |
| A6PW82 | 21 | 633 | 72,0 | 6,09 | 193 | Putative uncharacterized protein CXorf30 GN=CXorf30 PE=2 SV=2 |
| Q86WR0 | 292 | 208 | 24,5 | 6,80 | 193 | Coiled-coil domain-containing protein 25 GN=CCDC25 PE=1 SV=2 |
| P31150 | 35 | 447 | 50,6 | 5,14 | 192 | Rab GDP dissociation inhibitor alpha GN=GDI1 PE=1 SV=2 |
| Q9H7Z7 | 6 | 377 | 41,9 | 9,16 | 192 | Prostaglandin E synthase 2 GN=PTGES2 PE=1 SV=1 |
| P08174 | 23 | 381 | 41,4 | 7,59 | 192 | Complement decay-accelerating factor GN=CD55 PE=1 SV=4 |
| Q16629 | 18 | 238 | 27,4 | 11,82 | 192 | Serine/arginine-rich splicing factor 7 GN=SRSF7 PE=1 SV=1 |
| Q8WZ42 | 323 | 34350 | 3813,8 | 6,34 | 192 | Titin GN=TTN PE=1 SV=3 |
| Q15691 | 37 | 268 | 30,0 | 5,14 | 191 | Microtubule-associated protein RP/EB family member 1 GN=MAPRE1 PE=1 SV=3 |
| Q09161 | 29 | 790 | 91,8 | 6,43 | 191 | Nuclear cap-binding protein subunit 1 GN=NCBP1 PE=1 SV=1 |
| O15173 | 19 | 223 | 23,8 | 4,88 | 191 | Membrane-associated progesterone receptor component 2 GN=PGRMC2 PE=1 SV=1 |
| Q32LA7 | 53 | 128 | 13,5 | 10,58 | 190 | Histone H2A.V GN=H2AFV PE=2 SV=3 |
| Q92945 | 17 | 711 | 73,1 | 7,30 | 190 | Far upstream element-binding protein 2 GN=KHSRP PE=1 SV=4 |
| P20618 | 20 | 241 | 26,5 | 8,13 | 189 | Proteasome subunit beta type-1 GN=PSMB1 PE=1 SV=2 |
| P08727 | 45 | 400 | 44,1 | 5,14 | 189 | Keratin, type I cytoskeletal 19 GN=KRT19 PE=1 SV=4 |
| Q99460 | 22 | 953 | 105,8 | 5,39 | 189 | 26S proteasome non-ATPase regulatory subunit 1 GN=PSMD1 PE=1 SV=2 |
| Q9CQC6 | 59 | 419 | 48,0 | 5,92 | 188 | Basic leucine zipper and W2 domain-containing protein 1 GN=Bzw1 PE=1 SV=1 |
| A6NIZ1 | 12 | 184 | 20,9 | 5,48 | 187 | Ras-related protein Rap-1b-like protein PE=2 SV=1 |
| P62835 | 14 | 184 | 21,0 | 6,67 | 187 | Ras-related protein Rap-1A GN=Rap1a PE=2 SV=1 |
| O15067 | 41 | 1338 | 144,6 | 5,76 | 187 | Phosphoribosylformylglycinamidine synthase GN=PFAS PE=1 SV=4 |
| P40673 | 43 | 209 | 24,0 | 7,81 | 187 | High mobility group protein B2 GN=HMGB2 PE=1 SV=3 |
| Q9NYA3 | 39 | 693 | 79,9 | 5,41 | 186 | Golgin subfamily A member 6A GN=GOLGA6A PE=1 SV=3 |
| Q01082 | 45 | 2364 | 274,4 | 5,57 | 186 | Spectrin beta chain, brain 1 GN=SPTBN1 PE=1 SV=2 |
| P07196 | 27 | 543 | 61,5 | 4,65 | 186 | Neurofilament light polypeptide GN=NEFL PE=1 SV=3 |
| P07197 | 36 | 916 | 102,4 | 4,91 | 186 | Neurofilament medium polypeptide GN=NEFM PE=1 SV=3 |
| P12036 | 45 | 1026 | 112,4 | 6,18 | 186 | Neurofilament heavy polypeptide GN=NEFH PE=1 SV=4 |
| Q16352 | 27 | 499 | 55,4 | 5,40 | 186 | Alpha-internexin GN=INA PE=1 SV=2 |
| P80303 | 32 | 420 | 50,2 | 5,12 | 186 | Nucleobindin-2 GN=NUCB2 PE=1 SV=2 |
| Q9H009 | 5 | 215 | 23,2 | 4,73 | 185 | Nascent polypeptide-associated complex subunit alpha-2 GN=NACA2 PE=1 SV=1 |
| Q15019 | 9 | 361 | 41,5 | 6,60 | 185 | Septin-2 GN=SEPT2 PE=1 SV=1 |

| | | | | | | |
|---|---|---|---|---|---|---|
| A2RTX5 | 37 | 802 | 92,6 | 6,05 | 185 | Probable threonine--tRNA ligase 2, cytoplasmic GN=TARSL2 PE=1 SV=1 |
| P27482 | 16 | 149 | 16,9 | 4,42 | 184 | Calmodulin-like protein 3 GN=CALML3 PE=1 SV=2 |
| P22695 | 12 | 453 | 48,4 | 8,63 | 184 | Cytochrome b-c1 complex subunit 2, mitochondrial GN=UQCRC2 PE=1 SV=3 |
| Q96L21 | 18 | 214 | 24,5 | 10,01 | 183 | 60S ribosomal protein L10-like GN=RPL10L PE=1 SV=3 |
| Q9H444 | 6 | 224 | 24,9 | 4,82 | 183 | Charged multivesicular body protein 4b GN=CHMP4B PE=1 SV=1 |
| Q92526 | 29 | 530 | 57,8 | 7,24 | 183 | T-complex protein 1 subunit zeta-2 GN=CCT6B PE=1 SV=5 |
| Q7Z3Y8 | 29 | 459 | 49,8 | 5,05 | 183 | Keratin, type I cytoskeletal 27 GN=KRT27 PE=1 SV=2 |
| P68401 | 17 | 229 | 25,6 | 5,92 | 183 | Platelet-activating factor acetylhydrolase IB subunit beta GN=PAFAH1B2 PE=1 SV=1 |
| Q9NP97 | 12 | 96 | 10,9 | 7,25 | 182 | Dynein light chain roadblock-type 1 GN=DYNLRB1 PE=1 SV=3 |
| Q8NF37 | 7 | 534 | 59,1 | 6,02 | 182 | Lysophosphatidylcholine acyltransferase 1 GN=LPCAT1 PE=1 SV=2 |
| P62276 | 25 | 56 | 6,7 | 10,13 | 181 | 40S ribosomal protein S29 GN=RPS29 PE=3 SV=2 |
| Q12791 | 36 | 1236 | 137,5 | 7,06 | 181 | Calcium-activated potassium channel subunit alpha-1 GN=KCNMA1 PE=1 SV=2 |
| O00154 | 16 | 380 | 41,8 | 8,54 | 181 | Cytosolic acyl coenzyme A thioester hydrolase GN=ACOT7 PE=1 SV=3 |
| Q15843 | 22 | 81 | 9,1 | 8,43 | 180 | NEDD8 GN=NEDD8 PE=1 SV=1 |
| Q99798 | 193 | 780 | 85,4 | 7,61 | 180 | Aconitate hydratase, mitochondrial GN=ACO2 PE=1 SV=2 |
| O75947 | 27 | 161 | 18,5 | 5,30 | 179 | ATP synthase subunit d, mitochondrial GN=ATP5H PE=1 SV=3 |
| Q9NR31 | 24 | 198 | 22,4 | 6,68 | 179 | GTP-binding protein SAR1a GN=SAR1A PE=1 SV=1 |
| Q6ZMW3 | 35 | 1958 | 217,8 | 7,44 | 179 | Echinoderm microtubule-associated protein-like 6 GN=EML6 PE=2 SV=2 |
| Q9UMY4 | 8 | 172 | 19,7 | 7,87 | 178 | Sorting nexin-12 GN=SNX12 PE=1 SV=3 |
| P54105 | 6 | 237 | 26,2 | 4,11 | 178 | Methylosome subunit pICln GN=CLNS1A PE=1 SV=1 |
| P54136 | 25 | 660 | 75,3 | 6,68 | 177 | Arginyl-tRNA synthetase, cytoplasmic GN=RARS PE=1 SV=2 |
| P55795 | 9 | 449 | 49,2 | 6,30 | 177 | Heterogeneous nuclear ribonucleoprotein H2 GN=HNRNPH2 PE=1 SV=1 |
| P30043 | 6 | 206 | 22,1 | 7,65 | 176 | Flavin reductase (NADPH) GN=BLVRB PE=1 SV=3 |
| Q9Y5M8 | 6 | 271 | 29,7 | 9,04 | 176 | Signal recognition particle receptor subunit beta GN=SRPRB PE=1 SV=3 |
| Q13061 | 27 | 729 | 81,5 | 9,42 | 176 | Triadin GN=TRDN PE=1 SV=4 |
| Q9H169 | 20 | 189 | 22,1 | 5,99 | 175 | Stathmin-4 GN=STMN4 PE=2 SV=1 |
| O43390 | 12 | 633 | 70,9 | 8,13 | 175 | Heterogeneous nuclear ribonucleoprotein R GN=HNRNPR PE=1 SV=1 |
| Q96RP9 | 16 | 751 | 83,4 | 7,01 | 175 | Elongation factor G, mitochondrial GN=GFM1 PE=1 SV=2 |
| Q6P1F6 | 13 | 447 | 51,7 | 6,20 | 175 | Serine/threonine-protein phosphatase 2A 55 kDa regulatory subunit B alpha isoform |
| Q9UHY7 | 15 | 261 | 28,9 | 4,78 | 175 | Enolase-phosphatase E1 GN=ENOPH1 PE=1 SV=1 |
| O75694 | 45 | 1391 | 155,1 | 6,16 | 174 | Nuclear pore complex protein Nup155 GN=NUP155 PE=1 SV=1 |
| Q9HC38 | 19 | 313 | 34,8 | 5,60 | 174 | Glyoxalase domain-containing protein 4 GN=GLOD4 PE=1 SV=1 |
| Q02218 | 35 | 1023 | 115,9 | 6,86 | 174 | 2-oxoglutarate dehydrogenase, mitochondrial GN=OGDH PE=1 SV=3 |
| Q96EK6 | 11 | 184 | 20,7 | 7,99 | 174 | Glucosamine 6-phosphate N-acetyltransferase GN=GNPNAT1 PE=1 SV=1 |
| Q9BTP7 | 14 | 215 | 23,9 | 9,19 | 174 | Fanconi anemia-associated protein of 24 kDa GN=FAAP24 PE=1 SV=2 |
| Q16643 | 7 | 649 | 71,4 | 4,45 | 173 | Drebrin GN=DBN1 PE=1 SV=4 |
| O60762 | 34 | 260 | 29,6 | 9,57 | 173 | Dolichol-phosphate mannosyltransferase GN=DPM1 PE=1 SV=1 |
| O60664 | 8 | 434 | 47,0 | 5,44 | 172 | Perilipin-3 GN=PLIN3 PE=1 SV=3 |
| Q8NF91 | 125 | 8797 | 1010,4 | 5,53 | 172 | Nesprin-1 GN=SYNE1 PE=1 SV=3 |
| P52815 | 17 | 198 | 21,3 | 8,87 | 171 | 39S ribosomal protein L12, mitochondrial GN=MRPL12 PE=1 SV=2 |
| Q7Z3Y9 | 21 | 468 | 51,9 | 4,92 | 171 | Keratin, type I cytoskeletal 26 GN=KRT26 PE=1 SV=2 |
| Q9NUJ1 | 16 | 306 | 33,9 | 8,57 | 171 | Abhydrolase domain-containing protein 10, mitochondrial GN=ABHD10 PE=1 SV=1 |
| P18077 | 26 | 110 | 12,5 | 11,06 | 170 | 60S ribosomal protein L35a GN=RPL35A PE=1 SV=2 |
| P06493 | 11 | 297 | 34,1 | 8,40 | 169 | Cyclin-dependent kinase 1 GN=CDK1 PE=1 SV=3 |
| Q99613 | 30 | 913 | 105,3 | 5,68 | 168 | Eukaryotic translation initiation factor 3 subunit C GN=EIF3C PE=1 SV=1 |
| P21281 | 6 | 511 | 56,5 | 5,81 | 168 | V-type proton ATPase subunit B, brain isoform GN=ATP6V1B2 PE=1 SV=3 |
| Q9Y224 | 12 | 244 | 28,1 | 6,65 | 168 | UPF0568 protein C14orf166 GN=C14orf166 PE=1 SV=1 |
| P61161 | 31 | 394 | 44,7 | 6,74 | 168 | Actin-related protein 2 GN=Actr2 PE=1 SV=1 |
| Q16401 | 6 | 504 | 56,2 | 5,48 | 168 | 26S proteasome non-ATPase regulatory subunit 5 GN=PSMD5 PE=1 SV=3 |
| P62715 | 10 | 309 | 35,6 | 5,43 | 167 | Serine/threonine-protein phosphatase 2A catalytic subunit beta isoform GN=Ppp2cb |
| P54886 | 9 | 795 | 87,2 | 7,12 | 167 | Delta-1-pyrroline-5-carboxylate synthase GN=ALDH18A1 PE=1 SV=2 |
| P11279 | 10 | 417 | 44,9 | 8,75 | 167 | Lysosome-associated membrane glycoprotein 1 GN=LAMP1 PE=1 SV=3 |
| Q7Z3V4 | 39 | 1068 | 123,0 | 8,19 | 166 | Ubiquitin-protein ligase E3B GN=UBE3B PE=1 SV=3 |
| P14616 | 36 | 1297 | 143,6 | 6,47 | 166 | Insulin receptor-related protein GN=INSRR PE=1 SV=2 |
| Q921L3 | 14 | 188 | 21,2 | 9,74 | 166 | Transmembrane and coiled-coil domain-containing protein 1 GN=Tmco1 PE=2 SV=1 |
| P24539 | 17 | 256 | 28,9 | 9,36 | 166 | ATP synthase subunit b, mitochondrial GN=ATP5F1 PE=1 SV=2 |
| P21397 | 16 | 527 | 59,6 | 7,85 | 166 | Amine oxidase [flavin-containing] A GN=MAOA PE=1 SV=1 |
| P04792 | 14 | 205 | 22,8 | 6,40 | 166 | Heat shock protein beta-1 GN=HSPB1 PE=1 SV=2 |
| Q9CXU9 | 9 | 113 | 12,8 | 7,37 | 165 | Eukaryotic translation initiation factor 1b GN=Eif1b PE=2 SV=2 |
| O75167 | 34 | 634 | 69,7 | 8,16 | 165 | Phosphatase and actin regulator 2 GN=PHACTR2 PE=1 SV=2 |
| P19623 | 13 | 302 | 33,8 | 5,49 | 165 | Spermidine synthase GN=SRM PE=1 SV=1 |
| O95571 | 10 | 254 | 27,9 | 6,83 | 164 | Protein ETHE1, mitochondrial GN=ETHE1 PE=1 SV=2 |
| Q15149 | 168 | 4684 | 531,5 | 5,96 | 164 | Plectin GN=PLEC PE=1 SV=3 |
| Q13907 | 9 | 227 | 26,3 | 6,34 | 163 | Isopentenyl-diphosphate Delta-isomerase 1 GN=IDI1 PE=1 SV=2 |
| Q6ZMR3 | 19 | 332 | 36,5 | 6,99 | 163 | L-lactate dehydrogenase A-like 6A GN=LDHAL6A PE=2 SV=1 |

| | | | | | | |
|---|---|---|---|---|---|---|
| Q13442 | 25 | 181 | 20,6 | 8,87 | 163 | 28 kDa heat- and acid-stable phosphoprotein GN=PDAP1 PE=1 SV=1 |
| O35593 | 44 | 310 | 34,6 | 6,52 | 163 | 26S proteasome non-ATPase regulatory subunit 14 GN=Psmd14 PE=1 SV=2 |
| Q15046 | 20 | 597 | 68,0 | 6,35 | 162 | Lysyl-tRNA synthetase GN=KARS PE=1 SV=3 |
| O60701 | 13 | 494 | 55,0 | 7,12 | 162 | UDP-glucose 6-dehydrogenase GN=UGDH PE=1 SV=1 |
| Q3MHP2 | 16 | 218 | 24,5 | 5,94 | 162 | Ras-related protein Rab-11B GN=RAB11B PE=2 SV=3 |
| P14866 | 11 | 589 | 64,1 | 8,22 | 161 | Heterogeneous nuclear ribonucleoprotein L GN=HNRNPL PE=1 SV=2 |
| P50995 | 24 | 505 | 54,4 | 7,65 | 161 | Annexin A11 GN=ANXA11 PE=1 SV=1 |
| O95336 | 18 | 258 | 27,5 | 6,05 | 160 | 6-phosphogluconolactonase GN=PGLS PE=1 SV=2 |
| P34897 | 13 | 504 | 56,0 | 8,53 | 160 | Serine hydroxymethyltransferase, mitochondrial GN=SHMT2 PE=1 SV=3 |
| P12035 | 25 | 628 | 64,4 | 6,48 | 160 | Keratin, type II cytoskeletal 3 GN=KRT3 PE=1 SV=3 |
| P30154 | 23 | 601 | 66,2 | 4,94 | 159 | Serine/threonine-protein phosphatase 2A 65 kDa regulatory subunit A beta isoform ( |
| P34896 | 6 | 483 | 53,0 | 7,71 | 159 | Serine hydroxymethyltransferase, cytosolic GN=SHMT1 PE=1 SV=1 |
| Q6ZWV3 | 10 | 214 | 24,6 | 10,08 | 159 | 60S ribosomal protein L10 GN=Rpl10 PE=2 SV=3 |
| Q12912 | 358 | 555 | 62,1 | 5,85 | 159 | Lymphoid-restricted membrane protein GN=LRMP PE=1 SV=3 |
| Q8NC51 | 10 | 408 | 44,9 | 8,65 | 158 | Plasminogen activator inhibitor 1 RNA-binding protein GN=SERBP1 PE=1 SV=2 |
| P04818 | 19 | 313 | 35,7 | 7,01 | 158 | Thymidylate synthase GN=TYMS PE=1 SV=3 |
| P61255 | 32 | 145 | 17,2 | 10,55 | 158 | 60S ribosomal protein L26 GN=Rpl26 PE=2 SV=1 |
| Q9NQ38 | 78 | 1064 | 120,6 | 8,06 | 157 | Serine protease inhibitor Kazal-type 5 GN=SPINK5 PE=1 SV=2 |
| Q3ZCL8 | 18 | 93 | 10,4 | 4,93 | 157 | SH3 domain-binding glutamic acid-rich-like protein 3 GN=SH3BGRL3 PE=3 SV=1 |
| Q14914 | 16 | 329 | 35,8 | 8,29 | 156 | Prostaglandin reductase 1 GN=PTGR1 PE=1 SV=2 |
| Q68CJ6 | 41 | 796 | 91,1 | 8,63 | 155 | GTPase SLIP-GC GN=C8orf80 PE=1 SV=3 |
| O75531 | 8 | 89 | 10,1 | 6,09 | 155 | Barrier-to-autointegration factor GN=BANF1 PE=1 SV=1 |
| Q8NBS9 | 28 | 432 | 47,6 | 5,97 | 155 | Thioredoxin domain-containing protein 5 GN=TXNDC5 PE=1 SV=2 |
| Q07812 | 6 | 192 | 21,2 | 5,22 | 155 | Apoptosis regulator BAX GN=BAX PE=1 SV=1 |
| P22061 | 14 | 227 | 24,6 | 7,21 | 155 | Protein-L-isoaspartate(D-aspartate) O-methyltransferase GN=PCMT1 PE=1 SV=4 |
| P62880 | 14 | 340 | 37,3 | 6,00 | 154 | Guanine nucleotide-binding protein G(I)/G(S)/G(T) subunit beta-2 GN=Gnb2 PE=1 SV= |
| P40121 | 9 | 348 | 38,5 | 6,19 | 154 | Macrophage-capping protein GN=CAPG PE=1 SV=2 |
| P22090 | 13 | 263 | 29,4 | 10,24 | 154 | 40S ribosomal protein S4, Y isoform 1 GN=RPS4Y1 PE=2 SV=2 |
| Q8TD47 | 22 | 263 | 29,3 | 10,08 | 154 | 40S ribosomal protein S4, Y isoform 2 GN=RPS4Y2 PE=1 SV=3 |
| Q96P16 | 6 | 312 | 35,7 | 7,55 | 154 | Regulation of nuclear pre-mRNA domain-containing protein 1A GN=RPRD1A PE=1 SV= |
| Q3T003 | 21 | 176 | 20,7 | 10,71 | 153 | 60S ribosomal protein L18a GN=RPL18A PE=2 SV=1 |
| Q15029 | 37 | 972 | 109,4 | 5,00 | 153 | 116 kDa U5 small nuclear ribonucleoprotein component GN=EFTUD2 PE=1 SV=1 |
| Q53GQ0 | 14 | 312 | 34,3 | 9,32 | 152 | Estradiol 17-beta-dehydrogenase 12 GN=HSD17B12 PE=1 SV=2 |
| P17844 | 7 | 614 | 69,1 | 8,92 | 151 | Probable ATP-dependent RNA helicase DDX5 GN=DDX5 PE=1 SV=1 |
| P41219 | 56 | 470 | 53,6 | 5,47 | 151 | Peripherin GN=PRPH PE=1 SV=2 |
| Q5TID7 | 70 | 509 | 60,1 | 5,91 | 151 | Uncharacterized protein C1orf114 GN=C1orf114 PE=2 SV=1 |
| Q9BYJ4 | 59 | 488 | 56,8 | 7,44 | 151 | Tripartite motif-containing protein 34 GN=TRIM34 PE=1 SV=2 |
| Q96QV6 | 31 | 131 | 14,2 | 10,86 | 151 | Histone H2A type 1-A GN=HIST1H2AA PE=1 SV=3 |
| Q99877 | 42 | 126 | 13,9 | 10,32 | 151 | Histone H2B type 1-N GN=HIST1H2BN PE=1 SV=3 |
| O94986 | 49 | 1654 | 189,0 | 5,44 | 151 | Centrosomal protein of 152 kDa GN=CEP152 PE=1 SV=3 |
| Q96J02 | 25 | 903 | 102,7 | 6,30 | 151 | E3 ubiquitin-protein ligase Itchy homolog GN=ITCH PE=1 SV=2 |
| Q92841 | 10 | 650 | 72,3 | 8,59 | 150 | Probable ATP-dependent RNA helicase DDX17 GN=DDX17 PE=1 SV=1 |
| P43490 | 4 | 491 | 55,5 | 7,15 | 150 | Nicotinamide phosphoribosyltransferase GN=NAMPT PE=1 SV=1 |
| O95340 | 10 | 614 | 69,5 | 8,03 | 150 | Bifunctional 3'-phosphoadenosine 5'-phosphosulfate synthase 2 GN=PAPSS2 PE=1 SV |
| Q5THR3 | 21 | 1501 | 172,8 | 8,40 | 150 | EF-hand calcium-binding domain-containing protein 6 GN=EFCAB6 PE=1 SV=1 |
| Q92540 | 28 | 1137 | 127,2 | 8,72 | 150 | Protein SMG7 GN=SMG7 PE=1 SV=2 |
| P48552 | 30 | 1158 | 126,9 | 8,18 | 150 | Nuclear receptor-interacting protein 1 GN=NRIP1 PE=1 SV=2 |
| Q86XW9 | 15 | 330 | 36,8 | 4,89 | 149 | Thioredoxin domain-containing protein 6 GN=NME9 PE=1 SV=1 |
| P46779 | 12 | 137 | 15,7 | 12,02 | 149 | 60S ribosomal protein L28 GN=RPL28 PE=1 SV=3 |
| Q96MM6 | 18 | 686 | 75,6 | 8,53 | 149 | Heat shock 70 kDa protein 12B GN=HSPA12B PE=1 SV=2 |
| P00540 | 53 | 346 | 37,8 | 8,91 | 149 | Proto-oncogene serine/threonine-protein kinase mos GN=MOS PE=2 SV=1 |
| Q9HCB6 | 10 | 807 | 90,9 | 6,11 | 149 | Spondin-1 GN=SPON1 PE=1 SV=2 |
| P06899 | 37 | 126 | 13,9 | 10,32 | 149 | Histone H2B type 1-J GN=HIST1H2BJ PE=1 SV=3 |
| P28070 | 33 | 264 | 29,2 | 5,97 | 149 | Proteasome subunit beta type-4 GN=PSMB4 PE=1 SV=4 |
| Q07960 | 24 | 439 | 50,4 | 6,29 | 148 | Rho GTPase-activating protein 1 GN=ARHGAP1 PE=1 SV=1 |
| Q3ZBF7 | 22 | 160 | 18,7 | 4,54 | 148 | Prostaglandin E synthase 3 GN=PTGES3 PE=1 SV=1 |
| P36542 | 13 | 298 | 33,0 | 9,22 | 147 | ATP synthase subunit gamma, mitochondrial GN=ATP5C1 PE=1 SV=1 |
| P45880 | 13 | 294 | 31,5 | 7,56 | 147 | Voltage-dependent anion-selective channel protein 2 GN=VDAC2 PE=1 SV=2 |
| Q4LE39 | 59 | 1312 | 147,7 | 5,12 | 147 | AT-rich interactive domain-containing protein 4B GN=ARID4B PE=1 SV=2 |
| P15374 | 23 | 230 | 26,2 | 4,92 | 147 | Ubiquitin carboxyl-terminal hydrolase isozyme L3 GN=UCHL3 PE=1 SV=1 |
| Q66LE6 | 18 | 453 | 52,0 | 6,39 | 147 | Serine/threonine-protein phosphatase 2A 55 kDa regulatory subunit B delta isoform |
| A7E2Y1 | 46 | 1941 | 221,3 | 6,01 | 147 | Myosin-7B GN=MYH7B PE=2 SV=3 |
| O60518 | 23 | 1105 | 124,6 | 5,01 | 147 | Ran-binding protein 6 GN=RANBP6 PE=1 SV=2 |
| P16070 | 8 | 742 | 81,5 | 5,33 | 146 | CD44 antigen GN=CD44 PE=1 SV=3 |
| Q8IWB6 | 41 | 1497 | 167,8 | 5,15 | 146 | Inactive serine/threonine-protein kinase TEX14 GN=TEX14 PE=1 SV=2 |

| | | | | | | |
|---|---|---|---|---|---|---|
| Q8WXX0 | 62 | 4024 | 460,9 | 6,00 | 146 | Dynein heavy chain 7, axonemal GN=DNAH7 PE=1 SV=2 |
| Q10471 | 14 | 571 | 64,7 | 8,35 | 145 | Polypeptide N-acetylgalactosaminyltransferase 2 GN=GALNT2 PE=1 SV=1 |
| P62141 | 9 | 327 | 37,2 | 6,19 | 145 | Serine/threonine-protein phosphatase PP1-beta catalytic subunit GN=Ppp1cb PE=1 S |
| O00232 | 7 | 456 | 52,9 | 7,65 | 144 | 26S proteasome non-ATPase regulatory subunit 12 GN=PSMD12 PE=1 SV=3 |
| Q92882 | 8 | 214 | 23,8 | 5,68 | 144 | Osteoclast-stimulating factor 1 GN=OSTF1 PE=1 SV=2 |
| O75489 | 21 | 264 | 30,2 | 7,50 | 144 | NADH dehydrogenase [ubiquinone] iron-sulfur protein 3, mitochondrial GN=NDUFS3 |
| P10412 | 26 | 219 | 21,9 | 11,03 | 144 | Histone H1.4 GN=HIST1H1E PE=1 SV=2 |
| Q14232 | 12 | 305 | 33,7 | 7,33 | 144 | Translation initiation factor eIF-2B subunit alpha GN=EIF2B1 PE=1 SV=1 |
| Q9BZZ5 | 9 | 524 | 59,0 | 7,34 | 144 | Apoptosis inhibitor 5 GN=API5 PE=1 SV=3 |
| P42766 | 38 | 123 | 14,5 | 11,05 | 144 | 60S ribosomal protein L35 GN=RPL35 PE=1 SV=2 |
| P32926 | 15 | 999 | 107,5 | 5,00 | 143 | Desmoglein-3 GN=DSG3 PE=1 SV=2 |
| Q9Y6B6 | 14 | 198 | 22,4 | 6,11 | 143 | GTP-binding protein SAR1b GN=SAR1B PE=1 SV=1 |
| P15313 | 3 | 513 | 56,8 | 5,66 | 143 | V-type proton ATPase subunit B, kidney isoform GN=ATP6V1B1 PE=1 SV=3 |
| Q9H871 | 14 | 391 | 44,0 | 6,06 | 143 | Protein RMD5 homolog A GN=RMND5A PE=1 SV=1 |
| A2A2Y4 | 21 | 597 | 68,7 | 6,39 | 143 | FERM domain-containing protein 3 GN=FRMD3 PE=2 SV=1 |
| P52888 | 11 | 689 | 78,8 | 6,05 | 143 | Thimet oligopeptidase GN=THOP1 PE=1 SV=2 |
| Q14258 | 8 | 630 | 70,9 | 8,09 | 143 | E3 ubiquitin/ISG15 ligase TRIM25 GN=TRIM25 PE=1 SV=2 |
| P08243 | 10 | 561 | 64,3 | 6,86 | 142 | Asparagine synthetase [glutamine-hydrolyzing] GN=ASNS PE=1 SV=4 |
| Q8N531 | 21 | 539 | 58,6 | 9,29 | 142 | F-box/LRR-repeat protein 6 GN=FBXL6 PE=2 SV=1 |
| Q9HCE9 | 30 | 1232 | 135,9 | 5,82 | 142 | Anoctamin-8 GN=ANO8 PE=2 SV=3 |
| Q96KB5 | 9 | 322 | 36,1 | 5,12 | 142 | Lymphokine-activated killer T-cell-originated protein kinase GN=PBK PE=1 SV=3 |
| Q9NSE4 | 32 | 1012 | 113,7 | 7,20 | 142 | Isoleucyl-tRNA synthetase, mitochondrial GN=IARS2 PE=1 SV=2 |
| Q02880 | 28 | 1626 | 183,2 | 8,00 | 142 | DNA topoisomerase 2-beta GN=TOP2B PE=1 SV=3 |
| Q3T0V7 | 11 | 148 | 16,4 | 9,95 | 142 | Endothelial differentiation-related factor 1 GN=EDF1 PE=2 SV=1 |
| Q16555 | 18 | 572 | 62,3 | 6,38 | 141 | Dihydropyrimidinase-related protein 2 GN=DPYSL2 PE=1 SV=1 |
| P09651 | 8 | 372 | 38,7 | 9,13 | 141 | Heterogeneous nuclear ribonucleoprotein A1 GN=HNRNPA1 PE=1 SV=5 |
| P46776 | 20 | 148 | 16,6 | 11,00 | 141 | 60S ribosomal protein L27a GN=RPL27A PE=1 SV=2 |
| P62331 | 21 | 175 | 20,1 | 8,95 | 140 | ADP-ribosylation factor 6 GN=Arf6 PE=1 SV=2 |
| Q9P2J5 | 16 | 1176 | 134,4 | 7,30 | 140 | Leucine--tRNA ligase, cytoplasmic GN=LARS PE=1 SV=2 |
| Q9UNS2 | 31 | 423 | 47,8 | 6,65 | 140 | COP9 signalosome complex subunit 3 GN=COPS3 PE=1 SV=3 |
| O95197 | 10 | 1032 | 112,5 | 4,96 | 140 | Reticulon-3 GN=RTN3 PE=1 SV=2 |
| P68399 | 7 | 391 | 45,1 | 7,74 | 140 | Casein kinase II subunit alpha GN=CSNK2A1 PE=1 SV=1 |
| Q4VXU2 | 28 | 614 | 68,3 | 8,87 | 140 | Polyadenylate-binding protein 1-like GN=PABPC1L PE=2 SV=1 |
| P28072 | 14 | 239 | 25,3 | 4,92 | 139 | Proteasome subunit beta type-6 GN=PSMB6 PE=1 SV=4 |
| P63163 | 26 | 240 | 24,6 | 11,19 | 139 | Small nuclear ribonucleoprotein-associated protein N GN=Snrpn PE=2 SV=1 |
| Q8NE71 | 14 | 845 | 95,9 | 6,80 | 139 | ATP-binding cassette sub-family F member 1 GN=ABCF1 PE=1 SV=2 |
| P11498 | 37 | 1178 | 129,6 | 6,84 | 139 | Pyruvate carboxylase, mitochondrial GN=PC PE=1 SV=2 |
| P30203 | 18 | 668 | 71,8 | 4,92 | 139 | T-cell differentiation antigen CD6 GN=CD6 PE=1 SV=3 |
| P62320 | 9 | 126 | 13,9 | 10,32 | 139 | Small nuclear ribonucleoprotein Sm D3 GN=Snrpd3 PE=1 SV=1 |
| Q15370 | 12 | 118 | 13,1 | 4,88 | 138 | Transcription elongation factor B polypeptide 2 GN=TCEB2 PE=1 SV=1 |
| Q7KZF4 | 18 | 910 | 101,9 | 7,17 | 137 | Staphylococcal nuclease domain-containing protein 1 GN=SND1 PE=1 SV=1 |
| Q9Y678 | 10 | 874 | 97,7 | 5,47 | 137 | Coatomer subunit gamma-1 GN=COPG1 PE=1 SV=1 |
| Q16795 | 16 | 377 | 42,5 | 9,80 | 137 | NADH dehydrogenase [ubiquinone] 1 alpha subcomplex subunit 9, mitochondrial GN |
| Q4G0N4 | 18 | 442 | 49,4 | 8,18 | 137 | NAD kinase domain-containing protein 1 GN=NADKD1 PE=1 SV=2 |
| Q6BDS2 | 19 | 1440 | 159,4 | 6,14 | 137 | UHRF1-binding protein 1 GN=UHRF1BP1 PE=1 SV=1 |
| Q8IX03 | 22 | 1113 | 125,2 | 5,85 | 137 | Protein KIBRA GN=WWC1 PE=1 SV=1 |
| O15381 | 21 | 856 | 95,0 | 6,48 | 137 | Nuclear valosin-containing protein-like GN=NVL PE=1 SV=1 |
| P43003 | 24 | 542 | 59,5 | 8,41 | 137 | Excitatory amino acid transporter 1 GN=SLC1A3 PE=1 SV=1 |
| Q13608 | 24 | 980 | 104,0 | 6,34 | 137 | Peroxisome assembly factor 2 GN=PEX6 PE=1 SV=2 |
| Q15056 | 8 | 248 | 27,4 | 7,23 | 136 | Eukaryotic translation initiation factor 4H GN=EIF4H PE=1 SV=5 |
| Q9UMX0 | 4 | 589 | 62,5 | 5,11 | 136 | Ubiquilin-1 GN=UBQLN1 PE=1 SV=2 |
| Q9Y285 | 10 | 508 | 57,5 | 7,80 | 136 | Phenylalanine--tRNA ligase alpha subunit GN=FARSA PE=1 SV=3 |
| P84244 | 34 | 136 | 15,3 | 11,27 | 135 | Histone H3.3 GN=H3f3a PE=1 SV=2 |
| Q92616 | 24 | 2671 | 292,6 | 7,47 | 135 | Translational activator GCN1 GN=GCN1L1 PE=1 SV=6 |
| A8MW92 | 7 | 1017 | 114,9 | 6,83 | 135 | PHD finger protein 20-like protein 1 GN=PHF20L1 PE=1 SV=2 |
| Q14152 | 23 | 1382 | 166,5 | 6,79 | 135 | Eukaryotic translation initiation factor 3 subunit A GN=EIF3A PE=1 SV=1 |
| P19013 | 27 | 534 | 57,2 | 6,61 | 135 | Keratin, type II cytoskeletal 4 GN=KRT4 PE=1 SV=4 |
| Q3MHP5 | 9 | 367 | 40,5 | 8,90 | 135 | Developmentally-regulated GTP-binding protein 1 GN=DRG1 PE=2 SV=1 |
| Q9BTT0 | 7 | 268 | 30,7 | 3,85 | 134 | Acidic leucine-rich nuclear phosphoprotein 32 family member E GN=ANP32E PE=1 SV |
| Q16531 | 23 | 1140 | 126,9 | 5,26 | 134 | DNA damage-binding protein 1 GN=DDB1 PE=1 SV=1 |
| P46926 | 7 | 289 | 32,6 | 6,92 | 134 | Glucosamine-6-phosphate isomerase 1 GN=GNPDA1 PE=1 SV=1 |
| Q99627 | 7 | 209 | 23,2 | 5,38 | 133 | COP9 signalosome complex subunit 8 GN=COPS8 PE=1 SV=1 |
| Q96A08 | 27 | 127 | 14,2 | 10,32 | 133 | Histone H2B type 1-A GN=HIST1H2BA PE=1 SV=3 |
| Q08050 | 227 | 763 | 84,2 | 7,91 | 133 | Forkhead box protein M1 GN=FOXM1 PE=1 SV=3 |
| Q9UHX3 | 226 | 823 | 90,4 | 6,87 | 133 | EGF-like module-containing mucin-like hormone receptor-like 2 GN=EMR2 PE=1 SV=2 |

| | | | | | | |
|---|---|---|---|---|---|---|
| Q9UBW8 | 12 | 275 | 30,3 | 8,22 | 133 | COP9 signalosome complex subunit 7a GN=COPS7A PE=1 SV=1 |
| Q9NRC6 | 67 | 3674 | 416,6 | 6,67 | 132 | Spectrin beta chain, brain 4 GN=SPTBN5 PE=1 SV=1 |
| Q80X95 | 38 | 313 | 36,5 | 7,72 | 132 | Ras-related GTP-binding protein A GN=Rraga PE=2 SV=1 |
| O76003 | 10 | 335 | 37,4 | 5,39 | 131 | Glutaredoxin-3 GN=GLRX3 PE=1 SV=2 |
| Q96P70 | 9 | 1041 | 115,9 | 4,81 | 131 | Importin-9 GN=IPO9 PE=1 SV=3 |
| O14744 | 12 | 637 | 72,6 | 6,29 | 131 | Protein arginine N-methyltransferase 5 GN=PRMT5 PE=1 SV=4 |
| O95235 | 41 | 890 | 100,2 | 6,92 | 131 | Kinesin-like protein KIF20A GN=KIF20A PE=1 SV=1 |
| P62855 | 18 | 115 | 13,0 | 11,00 | 131 | 40S ribosomal protein S26 GN=Rps26 PE=2 SV=3 |
| Q8NBJ5 | 8 | 622 | 71,6 | 7,31 | 130 | Procollagen galactosyltransferase 1 GN=GLT25D1 PE=1 SV=1 |
| P63210 | 12 | 74 | 8,5 | 4,82 | 130 | Guanine nucleotide-binding protein G(T) subunit gamma-T1 OS=Canis familiaris GN=G |
| Q4VNC0 | 14 | 1218 | 137,2 | 7,90 | 130 | Probable cation-transporting ATPase 13A5 GN=ATP13A5 PE=2 SV=1 |
| Q9UPN3 | 99 | 7388 | 837,8 | 5,39 | 130 | Microtubule-actin cross-linking factor 1, isoforms 1/2/3/5 GN=MACF1 PE=1 SV=4 |
| P78386 | 19 | 507 | 55,8 | 6,55 | 130 | Keratin, type II cuticular Hb5 GN=KRT85 PE=1 SV=1 |
| Q7Z6Z7 | 20 | 4374 | 481,6 | 5,22 | 130 | E3 ubiquitin-protein ligase HUWE1 GN=HUWE1 PE=1 SV=3 |
| Q8TF09 | 6 | 96 | 10,8 | 7,50 | 129 | Dynein light chain roadblock-type 2 GN=DYNLRB2 PE=1 SV=1 |
| P27338 | 23 | 520 | 58,7 | 7,50 | 129 | Amine oxidase [flavin-containing] B GN=MAOB PE=1 SV=3 |
| Q8WUM4 | 18 | 868 | 96,0 | 6,52 | 129 | Programmed cell death 6-interacting protein GN=PDCD6IP PE=1 SV=1 |
| Q15652 | 68 | 2540 | 284,3 | 7,87 | 129 | Probable JmjC domain-containing histone demethylation protein 2C GN=JMJD1C PE= |
| Q8IZP2 | 4 | 240 | 27,4 | 5,08 | 129 | Putative protein FAM10A4 GN=ST13P4 PE=5 SV=1 |
| Q8IWV8 | 20 | 1755 | 200,4 | 6,24 | 128 | E3 ubiquitin-protein ligase UBR2 GN=UBR2 PE=1 SV=1 |
| Q9HAV7 | 10 | 217 | 24,3 | 8,12 | 128 | GrpE protein homolog 1, mitochondrial GN=GRPEL1 PE=1 SV=2 |
| Q9Y2V2 | 8 | 147 | 15,9 | 8,21 | 128 | Calcium-regulated heat stable protein 1 GN=CARHSP1 PE=1 SV=2 |
| O95757 | 13 | 839 | 94,5 | 5,88 | 128 | Heat shock 70 kDa protein 4L GN=HSPA4L PE=1 SV=3 |
| P51812 | 16 | 740 | 83,7 | 6,89 | 128 | Ribosomal protein S6 kinase alpha-3 GN=RPS6KA3 PE=1 SV=1 |
| Q9BRP0 | 23 | 275 | 30,4 | 8,75 | 128 | Transcription factor Ovo-like 2 GN=OVOL2 PE=2 SV=1 |
| Q92905 | 14 | 334 | 37,6 | 6,54 | 127 | COP9 signalosome complex subunit 5 GN=COPS5 PE=1 SV=4 |
| Q04637 | 19 | 1599 | 175,4 | 5,33 | 127 | Eukaryotic translation initiation factor 4 gamma 1 GN=EIF4G1 PE=1 SV=4 |
| Q96QB1 | 36 | 1528 | 170,5 | 6,40 | 126 | Rho GTPase-activating protein 7 GN=DLC1 PE=1 SV=4 |
| Q12792 | 19 | 350 | 40,3 | 6,96 | 126 | Twinfilin-1 GN=TWF1 PE=1 SV=3 |
| P36405 | 13 | 182 | 20,4 | 7,24 | 126 | ADP-ribosylation factor-like protein 3 GN=ARL3 PE=1 SV=2 |
| Q14847 | 20 | 261 | 29,7 | 7,05 | 126 | LIM and SH3 domain protein 1 GN=LASP1 PE=1 SV=2 |
| Q14135 | 26 | 290 | 30,9 | 8,22 | 126 | Transcription cofactor vestigial-like protein 4 GN=VGLL4 PE=1 SV=4 |
| Q8IYT4 | 23 | 538 | 61,2 | 7,56 | 126 | Katanin p60 ATPase-containing subunit A-like 2 GN=KATNAL2 PE=2 SV=3 |
| P54727 | 30 | 409 | 43,1 | 4,84 | 125 | UV excision repair protein RAD23 homolog B GN=RAD23B PE=1 SV=1 |
| P23497 | 25 | 879 | 100,4 | 8,22 | 125 | Nuclear autoantigen Sp-100 GN=SP100 PE=1 SV=3 |
| Q9BVV6 | 214 | 1533 | 169,2 | 5,54 | 125 | Uncharacterized protein KIAA0586 GN=KIAA0586 PE=1 SV=4 |
| O43313 | 14 | 823 | 88,3 | 5,16 | 125 | ATM interactor GN=ATMIN PE=1 SV=2 |
| Q9UIJ7 | 10 | 227 | 25,5 | 9,16 | 124 | GTP:AMP phosphotransferase, mitochondrial GN=AK3 PE=1 SV=4 |
| Q6ZWY9 | 17 | 126 | 13,9 | 10,32 | 124 | Histone H2B type 1-C/E/G GN=Hist1h2bc PE=1 SV=3 |
| Q9Y277 | 11 | 283 | 30,6 | 8,66 | 124 | Voltage-dependent anion-selective channel protein 3 GN=VDAC3 PE=1 SV=1 |
| P10515 | 8 | 647 | 69,0 | 7,84 | 123 | Dihydrolipoyllysine-residue acetyltransferase component of pyruvate dehydrogenas |
| Q7Z2Z2 | 16 | 1120 | 125,3 | 5,91 | 123 | Elongation factor Tu GTP-binding domain-containing protein 1 GN=EFTUD1 PE=1 SV=2 |
| P31689 | 12 | 397 | 44,8 | 7,08 | 123 | DnaJ homolog subfamily A member 1 GN=DNAJA1 PE=1 SV=2 |
| Q9HAV4 | 14 | 1204 | 136,2 | 5,80 | 123 | Exportin-5 GN=XPO5 PE=1 SV=1 |
| Q02539 | 11 | 215 | 21,8 | 10,99 | 123 | Histone H1.1 GN=HIST1H1A PE=1 SV=3 |
| Q9H2U2 | 24 | 334 | 37,9 | 7,39 | 123 | Inorganic pyrophosphatase 2, mitochondrial GN=PPA2 PE=1 SV=2 |
| P30419 | 11 | 496 | 56,8 | 7,80 | 123 | Glycylpeptide N-tetradecanoyltransferase 1 GN=NMT1 PE=1 SV=2 |
| P07384 | 10 | 714 | 81,8 | 5,67 | 122 | Calpain-1 catalytic subunit GN=CAPN1 PE=1 SV=1 |
| O95996 | 28 | 2303 | 243,8 | 8,82 | 122 | Adenomatous polyposis coli protein 2 GN=APC2 PE=1 SV=1 |
| P10619 | 11 | 480 | 54,4 | 6,61 | 122 | Lysosomal protective protein GN=CTSA PE=1 SV=2 |
| P55786 | 8 | 919 | 103,2 | 5,72 | 122 | Puromycin-sensitive aminopeptidase GN=NPEPPS PE=1 SV=2 |
| O14793 | 44 | 375 | 42,7 | 6,76 | 122 | Growth/differentiation factor 8 GN=MSTN PE=1 SV=1 |
| Q9BPX3 | 61 | 1015 | 114,3 | 5,59 | 122 | Condensin complex subunit 3 GN=NCAPG PE=1 SV=1 |
| O95470 | 38 | 568 | 63,5 | 9,16 | 122 | Sphingosine-1-phosphate lyase 1 GN=SGPL1 PE=1 SV=3 |
| Q14566 | 296 | 821 | 92,8 | 5,41 | 121 | DNA replication licensing factor MCM6 GN=MCM6 PE=1 SV=1 |
| Q92900 | 18 | 1129 | 124,3 | 6,61 | 121 | Regulator of nonsense transcripts 1 GN=UPF1 PE=1 SV=2 |
| Q16881 | 5 | 649 | 70,9 | 7,39 | 121 | Thioredoxin reductase 1, cytoplasmic GN=TXNRD1 PE=1 SV=3 |
| P50416 | 15 | 773 | 88,3 | 8,65 | 120 | Carnitine O-palmitoyltransferase 1, liver isoform GN=CPT1A PE=1 SV=2 |
| P47756 | 16 | 277 | 31,3 | 5,59 | 120 | F-actin-capping protein subunit beta GN=CAPZB PE=1 SV=4 |
| P43243 | 11 | 847 | 94,6 | 6,25 | 120 | Matrin-3 GN=MATR3 PE=1 SV=2 |
| Q01518 | 24 | 475 | 51,9 | 8,06 | 120 | Adenylyl cyclase-associated protein 1 GN=CAP1 PE=1 SV=5 |
| P49902 | 7 | 561 | 64,9 | 6,14 | 120 | Cytosolic purine 5'-nucleotidase GN=NT5C2 PE=1 SV=1 |
| Q5VST9 | 57 | 7968 | 867,9 | 5,99 | 117 | Obscurin GN=OBSCN PE=1 SV=3 |
| Q9Y2L1 | 19 | 958 | 108,9 | 7,14 | 117 | Exosome complex exonuclease RRP44 GN=DIS3 PE=1 SV=2 |
| P26885 | 9 | 142 | 15,6 | 9,13 | 116 | Peptidyl-prolyl cis-trans isomerase FKBP2 GN=FKBP2 PE=1 SV=2 |

| | | | | | | |
|---|---|---|---|---|---|---|
| P62830 | 13 | 140 | 14,9 | 10,51 | 116 | 60S ribosomal protein L23 GN=Rpl23 PE=1 SV=1 |
| Q9P2D7 | 70 | 4330 | 493,6 | 5,94 | 116 | Dynein heavy chain 1, axonemal GN=DNAH1 PE=1 SV=4 |
| Q9HB71 | 36 | 228 | 26,2 | 8,25 | 116 | Calcyclin-binding protein GN=CACYBP PE=1 SV=2 |
| O14907 | 4 | 124 | 13,7 | 8,48 | 115 | Tax1-binding protein 3 GN=TAX1BP3 PE=1 SV=2 |
| Q86TD4 | 21 | 932 | 100,7 | 4,40 | 115 | Sarcalumenin GN=SRL PE=2 SV=2 |
| Q86W28 | 12 | 1048 | 119,4 | 7,96 | 115 | NACHT, LRR and PYD domains-containing protein 8 GN=NLRP8 PE=2 SV=2 |
| Q96CX6 | 14 | 371 | 40,6 | 6,84 | 115 | Leucine-rich repeat-containing protein 58 GN=LRRC58 PE=1 SV=2 |
| Q9D5T0 | 19 | 361 | 40,7 | 6,90 | 115 | ATPase family AAA domain-containing protein 1 GN=Atad1 PE=1 SV=1 |
| Q9Y2H5 | 20 | 1048 | 117,1 | 9,10 | 115 | Pleckstrin homology domain-containing family A member 6 GN=PLEKHA6 PE=1 SV=4 |
| Q9Y4W6 | 21 | 797 | 88,5 | 8,66 | 115 | AFG3-like protein 2 GN=AFG3L2 PE=1 SV=2 |
| P15170 | 10 | 499 | 55,7 | 5,62 | 114 | Eukaryotic peptide chain release factor GTP-binding subunit ERF3A GN=GSPT1 PE=1 S |
| Q15436 | 7 | 765 | 86,1 | 7,08 | 114 | Protein transport protein Sec23A GN=SEC23A PE=1 SV=2 |
| Q9UPY8 | 12 | 281 | 32,0 | 5,54 | 114 | Microtubule-associated protein RP/EB family member 3 GN=MAPRE3 PE=1 SV=1 |
| Q9UBF2 | 7 | 871 | 97,6 | 5,81 | 114 | Coatomer subunit gamma-2 GN=COPG2 PE=1 SV=1 |
| P04632 | 31 | 268 | 28,3 | 5,20 | 114 | Calpain small subunit 1 GN=CAPNS1 PE=1 SV=1 |
| O75569 | 32 | 313 | 34,4 | 8,41 | 114 | Interferon-inducible double stranded RNA-dependent protein kinase activator A GN |
| P61089 | 12 | 152 | 17,1 | 6,57 | 114 | Ubiquitin-conjugating enzyme E2 N GN=Ube2n PE=1 SV=1 |
| O00625 | 7 | 290 | 32,1 | 6,92 | 113 | Pirin GN=PIR PE=1 SV=1 |
| P58107 | 18 | 5090 | 555,3 | 5,60 | 113 | Epiplakin GN=EPPK1 PE=1 SV=2 |
| Q6NXT2 | 39 | 135 | 15,2 | 11,11 | 112 | Histone H3.3C GN=H3F3C PE=1 SV=3 |
| P54920 | 7 | 295 | 33,2 | 5,36 | 111 | Alpha-soluble NSF attachment protein GN=NAPA PE=1 SV=3 |
| P61971 | 21 | 127 | 14,5 | 5,38 | 111 | Nuclear transport factor 2 GN=Nutf2 PE=2 SV=1 |
| O95456 | 4 | 288 | 32,8 | 7,17 | 111 | Proteasome assembly chaperone 1 GN=PSMG1 PE=1 SV=1 |
| Q86U38 | 7 | 636 | 69,4 | 7,28 | 111 | Pumilio domain-containing protein C14orf21 GN=C14orf21 PE=1 SV=1 |
| Q96AC1 | 15 | 680 | 77,8 | 6,70 | 110 | Fermitin family homolog 2 GN=FERMT2 PE=1 SV=1 |
| Q86UD5 | 15 | 537 | 57,5 | 6,71 | 110 | Mitochondrial sodium/hydrogen exchanger 9B2 GN=SLC9B2 PE=1 SV=2 |
| P49257 | 16 | 510 | 57,5 | 6,77 | 110 | Protein ERGIC-53 GN=LMAN1 PE=1 SV=2 |
| Q13155 | 33 | 320 | 35,3 | 8,22 | 110 | Aminoacyl tRNA synthase complex-interacting multifunctional protein 2 GN=AIMP2 P |
| P20336 | 5 | 220 | 25,0 | 5,03 | 109 | Ras-related protein Rab-3A GN=RAB3A PE=1 SV=1 |
| P20338 | 7 | 213 | 23,9 | 6,07 | 109 | Ras-related protein Rab-4A GN=RAB4A PE=1 SV=2 |
| Q923S9 | 6 | 203 | 23,0 | 4,97 | 109 | Ras-related protein Rab-30 GN=Rab30 PE=2 SV=1 |
| Q96AX2 | 6 | 223 | 24,8 | 6,35 | 109 | Ras-related protein Rab-37 GN=RAB37 PE=1 SV=3 |
| Q9HCK1 | 43 | 2354 | 265,5 | 6,16 | 109 | DBF4-type zinc finger-containing protein 2 GN=ZDBF2 PE=1 SV=3 |
| Q9NWY4 | 31 | 346 | 39,4 | 6,80 | 109 | UPF0609 protein C4orf27 GN=C4orf27 PE=1 SV=2 |
| Q9Y483 | 61 | 593 | 67,1 | 8,72 | 109 | Metal-response element-binding transcription factor 2 GN=MTF2 PE=1 SV=2 |
| Q96M27 | 122 | 445 | 46,7 | 5,83 | 109 | Protein PRRC1 GN=PRRC1 PE=1 SV=1 |
| Q5VTH9 | 12 | 848 | 94,5 | 5,76 | 109 | WD repeat-containing protein 78 GN=WDR78 PE=2 SV=1 |
| Q8N3K9 | 32 | 4069 | 448,9 | 4,78 | 109 | Cardiomyopathy-associated protein 5 GN=CMYA5 PE=1 SV=3 |
| A2BFH1 | 30 | 164 | 18,2 | 9,06 | 108 | Peptidyl-prolyl cis-trans isomerase A-like 4G GN=PPIAL4G PE=2 SV=1 |
| Q9C0A0 | 46 | 1308 | 145,2 | 6,68 | 108 | Contactin-associated protein-like 4 GN=CNTNAP4 PE=1 SV=3 |
| P67810 | 7 | 179 | 20,6 | 9,48 | 108 | Signal peptidase complex catalytic subunit SEC11A GN=SEC11A PE=2 SV=1 |
| P22626 | 8 | 353 | 37,4 | 8,95 | 108 | Heterogeneous nuclear ribonucleoproteins A2/B1 GN=HNRNPA2B1 PE=1 SV=2 |
| O15247 | 46 | 247 | 28,3 | 5,59 | 108 | Chloride intracellular channel protein 2 GN=CLIC2 PE=1 SV=3 |
| P48637 | 3 | 474 | 52,4 | 5,92 | 108 | Glutathione synthetase GN=GSS PE=1 SV=1 |
| Q8TDQ7 | 6 | 276 | 31,1 | 6,95 | 107 | Glucosamine-6-phosphate isomerase 2 GN=GNPDA2 PE=1 SV=1 |
| P33176 | 22 | 963 | 109,6 | 6,51 | 107 | Kinesin-1 heavy chain GN=KIF5B PE=1 SV=1 |
| Q12840 | 6 | 1032 | 117,3 | 5,90 | 107 | Kinesin heavy chain isoform 5A GN=KIF5A PE=1 SV=2 |
| Q8NEZ5 | 9 | 403 | 44,5 | 7,03 | 107 | F-box only protein 22 GN=FBXO22 PE=1 SV=1 |
| Q969N2 | 15 | 578 | 65,7 | 8,38 | 107 | GPI transamidase component PIG-T GN=PIGT PE=1 SV=1 |
| Q9NX40 | 7 | 245 | 27,6 | 7,49 | 107 | OCIA domain-containing protein 1 GN=OCIAD1 PE=1 SV=1 |
| Q9UPU5 | 38 | 2620 | 294,2 | 6,14 | 107 | Ubiquitin carboxyl-terminal hydrolase 24 GN=USP24 PE=1 SV=3 |
| Q86XS8 | 27 | 419 | 46,4 | 8,87 | 107 | E3 ubiquitin-protein ligase RNF130 GN=RNF130 PE=1 SV=1 |
| Q9NTG1 | 51 | 2253 | 255,3 | 9,11 | 107 | Polycystic kidney disease and receptor for egg jelly-related protein GN=PKDREJ PE=2 |
| Q9NXE8 | 48 | 425 | 49,6 | 10,18 | 107 | Pre-mRNA-splicing factor CWC25 homolog GN=CWC25 PE=1 SV=1 |
| Q9Y603 | 36 | 341 | 39,0 | 8,03 | 107 | Transcription factor ETV7 GN=ETV7 PE=1 SV=1 |
| P28482 | 30 | 360 | 41,4 | 6,98 | 107 | Mitogen-activated protein kinase 1 GN=MAPK1 PE=1 SV=3 |
| P46108 | 4 | 304 | 33,8 | 5,55 | 107 | Adapter molecule crk GN=CRK PE=1 SV=2 |
| P49458 | 8 | 86 | 10,1 | 7,97 | 107 | Signal recognition particle 9 kDa protein GN=SRP9 PE=1 SV=2 |
| O14879 | 12 | 490 | 55,9 | 5,20 | 107 | Interferon-induced protein with tetratricopeptide repeats 3 GN=IFIT3 PE=1 SV=1 |
| P20073 | 18 | 488 | 52,7 | 5,68 | 106 | Annexin A7 GN=ANXA7 PE=1 SV=3 |
| P53618 | 6 | 953 | 107,1 | 6,05 | 106 | Coatomer subunit beta GN=COPB1 PE=1 SV=3 |
| Q92888 | 29 | 912 | 102,4 | 5,66 | 105 | Rho guanine nucleotide exchange factor 1 GN=ARHGEF1 PE=1 SV=2 |
| P08574 | 24 | 325 | 35,4 | 9,00 | 105 | Cytochrome c1, heme protein, mitochondrial GN=CYC1 PE=1 SV=3 |
| P10635 | 16 | 497 | 55,7 | 7,25 | 105 | Cytochrome P450 2D6 GN=CYP2D6 PE=1 SV=2 |
| P16403 | 17 | 213 | 21,4 | 10,93 | 105 | Histone H1.2 GN=HIST1H1C PE=1 SV=2 |

| | | | | | | |
|---|---|---|---|---|---|---|
| Q9Y6K8 | 10 | 562 | 63,3 | 5,07 | 105 | Adenylate kinase isoenzyme 5 GN=AK5 PE=1 SV=2 |
| Q86Y46 | 12 | 540 | 58,9 | 7,23 | 105 | Keratin, type II cytoskeletal 73 GN=KRT73 PE=1 SV=1 |
| Q9NSB2 | 12 | 600 | 64,8 | 7,56 | 105 | Keratin, type II cuticular Hb4 GN=KRT84 PE=1 SV=2 |
| P69905 | 21 | 142 | 15,2 | 8,68 | 104 | Hemoglobin subunit alpha GN=HBA1 PE=1 SV=2 |
| Q08380 | 16 | 585 | 65,3 | 5,27 | 104 | Galectin-3-binding protein GN=LGALS3BP PE=1 SV=1 |
| Q8WXH0 | 94 | 6885 | 795,9 | 5,36 | 103 | Nesprin-2 GN=SYNE2 PE=1 SV=3 |
| O15371 | 31 | 548 | 63,9 | 6,05 | 103 | Eukaryotic translation initiation factor 3 subunit D GN=EIF3D PE=1 SV=1 |
| Q8WXI9 | 26 | 593 | 65,2 | 9,70 | 103 | Transcriptional repressor p66-beta GN=GATAD2B PE=1 SV=1 |
| Q02952 | 9 | 1782 | 191,4 | 4,41 | 102 | A-kinase anchor protein 12 GN=AKAP12 PE=1 SV=4 |
| P14406 | 3 | 83 | 9,4 | 9,76 | 102 | Cytochrome c oxidase subunit 7A2, mitochondrial GN=COX7A2 PE=1 SV=1 |
| P31153 | 24 | 395 | 43,6 | 6,48 | 102 | S-adenosylmethionine synthase isoform type-2 GN=MAT2A PE=1 SV=1 |
| P04899 | 13 | 355 | 40,4 | 5,54 | 102 | Guanine nucleotide-binding protein G(i) subunit alpha-2 GN=GNAI2 PE=1 SV=3 |
| Q9UG01 | 27 | 1749 | 197,5 | 6,13 | 102 | Intraflagellar transport protein 172 homolog GN=IFT172 PE=1 SV=2 |
| Q14201 | 28 | 252 | 29,1 | 8,95 | 102 | Protein BTG3 GN=BTG3 PE=2 SV=3 |
| A0AVT1 | 12 | 1052 | 117,9 | 6,14 | 102 | Ubiquitin-like modifier-activating enzyme 6 GN=UBA6 PE=1 SV=1 |
| O75665 | 29 | 1012 | 116,6 | 6,10 | 102 | Oral-facial-digital syndrome 1 protein GN=OFD1 PE=1 SV=1 |
| P10854 | 15 | 126 | 13,9 | 10,32 | 101 | Histone H2B type 1-M GN=Hist1h2bm PE=1 SV=2 |
| O75312 | 3 | 459 | 50,9 | 4,73 | 101 | Zinc finger protein ZPR1 GN=ZNF259 PE=1 SV=1 |
| P50454 | 7 | 418 | 46,4 | 8,69 | 101 | Serpin H1 GN=SERPINH1 PE=1 SV=2 |
| P42765 | 14 | 397 | 41,9 | 8,09 | 101 | 3-ketoacyl-CoA thiolase, mitochondrial GN=ACAA2 PE=1 SV=2 |
| O60831 | 3 | 178 | 19,2 | 9,19 | 100 | PRA1 family protein 2 GN=PRAF2 PE=1 SV=1 |
| Q96AG4 | 17 | 307 | 34,9 | 9,57 | 100 | Leucine-rich repeat-containing protein 59 GN=LRRC59 PE=1 SV=1 |
| O75096 | 65 | 1905 | 211,9 | 5,27 | 100 | Low-density lipoprotein receptor-related protein 4 GN=LRP4 PE=1 SV=4 |
| Q8N1G4 | 3 | 583 | 63,4 | 8,28 | 99 | Leucine-rich repeat-containing protein 47 GN=LRRC47 PE=1 SV=1 |
| P62334 | 7 | 389 | 44,1 | 7,49 | 99 | 26S protease regulatory subunit 10B GN=Psmc6 PE=1 SV=1 |
| P46379 | 7 | 1132 | 119,3 | 5,60 | 99 | Large proline-rich protein BAG6 GN=BAG6 PE=1 SV=2 |
| O00193 | 3 | 183 | 20,3 | 4,72 | 99 | Small acidic protein GN=SMAP PE=1 SV=1 |
| P07332 | 24 | 822 | 93,4 | 6,73 | 99 | Tyrosine-protein kinase Fes/Fps GN=FES PE=1 SV=3 |
| P09110 | 9 | 424 | 44,3 | 8,44 | 99 | 3-ketoacyl-CoA thiolase, peroxisomal GN=ACAA1 PE=1 SV=2 |
| Q9Y547 | 6 | 144 | 16,3 | 5,03 | 99 | Heat shock protein beta-11 GN=HSPB11 PE=1 SV=1 |
| Q15555 | 10 | 327 | 37,0 | 5,57 | 99 | Microtubule-associated protein RP/EB family member 2 GN=MAPRE2 PE=1 SV=1 |
| Q05B71 | 9 | 135 | 15,3 | 9,61 | 99 | CDGSH iron-sulfur domain-containing protein 2 GN=CISD2 PE=2 SV=1 |
| Q969U7 | 13 | 264 | 29,4 | 6,98 | 99 | Proteasome assembly chaperone 2 GN=PSMG2 PE=1 SV=1 |
| P61769 | 13 | 119 | 13,7 | 6,52 | 98 | Beta-2-microglobulin GN=B2M PE=1 SV=1 |
| O60678 | 10 | 531 | 59,8 | 5,35 | 98 | Protein arginine N-methyltransferase 3 GN=PRMT3 PE=1 SV=3 |
| Q9H611 | 15 | 641 | 69,8 | 9,72 | 98 | ATP-dependent DNA helicase PIF1 GN=PIF1 PE=1 SV=2 |
| P54578 | 5 | 494 | 56,0 | 5,30 | 98 | Ubiquitin carboxyl-terminal hydrolase 14 GN=USP14 PE=1 SV=3 |
| O43488 | 3 | 359 | 39,6 | 7,17 | 98 | Aflatoxin B1 aldehyde reductase member 2 GN=AKR7A2 PE=1 SV=3 |
| Q8TF17 | 8 | 1288 | 144,7 | 6,37 | 98 | SH3 domain and tetratricopeptide repeat-containing protein 2 GN=SH3TC2 PE=1 SV=2 |
| Q9UPP2 | 11 | 1182 | 127,5 | 6,51 | 98 | IQ motif and SEC7 domain-containing protein 3 GN=IQSEC3 PE=2 SV=3 |
| Q15233 | 23 | 471 | 54,2 | 8,95 | 98 | Non-POU domain-containing octamer-binding protein GN=NONO PE=1 SV=4 |
| Q8TDN4 | 22 | 633 | 67,6 | 9,17 | 98 | CDK5 and ABL1 enzyme substrate 1 GN=CABLES1 PE=1 SV=2 |
| Q9NR09 | 55 | 4857 | 529,9 | 6,05 | 97 | Baculoviral IAP repeat-containing protein 6 GN=BIRC6 PE=1 SV=2 |
| P08912 | 21 | 532 | 60,0 | 9,28 | 97 | Muscarinic acetylcholine receptor M5 GN=CHRM5 PE=2 SV=2 |
| O95881 | 16 | 172 | 19,2 | 5,40 | 97 | Thioredoxin domain-containing protein 12 GN=TXNDC12 PE=1 SV=1 |
| P35270 | 2 | 261 | 28,0 | 8,05 | 97 | Sepiapterin reductase GN=SPR PE=1 SV=1 |
| Q08945 | 42 | 709 | 81,0 | 6,87 | 97 | FACT complex subunit SSRP1 GN=SSRP1 PE=1 SV=1 |
| P50552 | 2 | 380 | 39,8 | 8,94 | 96 | Vasodilator-stimulated phosphoprotein GN=VASP PE=1 SV=3 |
| P49915 | 29 | 693 | 76,7 | 6,87 | 96 | GMP synthase [glutamine-hydrolyzing] GN=GMPS PE=1 SV=1 |
| Q9BTF0 | 45 | 503 | 56,4 | 7,81 | 96 | THUMP domain-containing protein 2 GN=THUMPD2 PE=2 SV=2 |
| P31350 | 7 | 389 | 44,8 | 5,38 | 96 | Ribonucleoside-diphosphate reductase subunit M2 GN=RRM2 PE=1 SV=1 |
| Q7Z4S6 | 44 | 1674 | 187,1 | 6,42 | 96 | Kinesin-like protein KIF21A GN=KIF21A PE=1 SV=2 |
| Q2M2I5 | 15 | 525 | 55,1 | 4,96 | 96 | Keratin, type I cytoskeletal 24 GN=KRT24 PE=1 SV=1 |
| Q8N196 | 15 | 739 | 74,5 | 4,96 | 95 | Homeobox protein SIX5 GN=SIX5 PE=1 SV=3 |
| P51686 | 12 | 369 | 42,0 | 8,19 | 95 | C-C chemokine receptor type 9 GN=CCR9 PE=1 SV=2 |
| Q15772 | 48 | 3267 | 354,1 | 8,51 | 95 | Striated muscle preferentially expressed protein kinase GN=SPEG PE=1 SV=4 |
| Q96IY1 | 32 | 281 | 32,1 | 6,79 | 95 | Kinetochore-associated protein NSL1 homolog GN=NSL1 PE=1 SV=3 |
| P36776 | 19 | 959 | 106,4 | 6,39 | 95 | Lon protease homolog, mitochondrial GN=LONP1 PE=1 SV=2 |
| P10244 | 13 | 700 | 78,7 | 6,87 | 94 | Myb-related protein B GN=MYBL2 PE=1 SV=1 |
| Q8NI35 | 23 | 1801 | 196,2 | 4,94 | 94 | InaD-like protein GN=INADL PE=1 SV=3 |
| P62889 | 13 | 115 | 12,8 | 9,63 | 94 | 60S ribosomal protein L30 GN=Rpl30 PE=2 SV=2 |
| O75390 | 11 | 466 | 51,7 | 8,32 | 94 | Citrate synthase, mitochondrial GN=CS PE=1 SV=2 |
| Q6TFL3 | 29 | 1326 | 152,7 | 6,81 | 94 | Coiled-coil domain-containing protein 171 GN=CCDC171 PE=2 SV=1 |
| Q15631 | 12 | 228 | 26,2 | 6,44 | 94 | Translin GN=TSN PE=1 SV=1 |
| O75083 | 2 | 606 | 66,2 | 6,65 | 94 | WD repeat-containing protein 1 GN=WDR1 PE=1 SV=4 |

| | | | | | | |
|---|---|---|---|---|---|---|
| O14967 | 12 | 610 | 70,0 | 4,69 | 94 | Calmegin GN=CLGN PE=1 SV=1 |
| Q5VWN6 | 99 | 2430 | 268,7 | 5,90 | 94 | Protein FAM208B GN=FAM208B PE=1 SV=1 |
| Q15393 | 8 | 1217 | 135,5 | 5,26 | 93 | Splicing factor 3B subunit 3 GN=SF3B3 PE=1 SV=4 |
| Q01831 | 11 | 940 | 105,9 | 8,90 | 93 | DNA repair protein complementing XP-C cells GN=XPC PE=1 SV=4 |
| Q62093 | 3 | 221 | 25,5 | 11,85 | 93 | Serine/arginine-rich splicing factor 2 GN=Srsf2 PE=1 SV=4 |
| O60551 | 5 | 498 | 56,9 | 7,58 | 93 | Glycylpeptide N-tetradecanoyltransferase 2 GN=NMT2 PE=1 SV=1 |
| Q9NRE1 | 9 | 261 | 29,7 | 6,47 | 93 | Matrix metalloproteinase-26 GN=MMP26 PE=2 SV=2 |
| Q5T013 | 22 | 277 | 30,4 | 5,50 | 92 | Putative hydroxypyruvate isomerase GN=HYI PE=2 SV=2 |
| Q9UBU9 | 30 | 619 | 70,1 | 8,51 | 92 | Nuclear RNA export factor 1 GN=NXF1 PE=1 SV=1 |
| Q9D7G0 | 11 | 318 | 34,8 | 6,98 | 92 | Ribose-phosphate pyrophosphokinase 1 GN=Prps1 PE=1 SV=4 |
| O75449 | 13 | 491 | 55,9 | 6,90 | 92 | Katanin p60 ATPase-containing subunit A1 GN=KATNA1 PE=1 SV=1 |
| Q96G03 | 7 | 612 | 68,2 | 6,73 | 92 | Phosphoglucomutase-2 GN=PGM2 PE=1 SV=4 |
| Q13393 | 27 | 1074 | 124,1 | 8,78 | 92 | Phospholipase D1 GN=PLD1 PE=1 SV=1 |
| Q14203 | 30 | 1278 | 141,6 | 5,81 | 91 | Dynactin subunit 1 GN=DCTN1 PE=1 SV=3 |
| Q9Y4C1 | 32 | 1321 | 147,2 | 8,07 | 91 | Lysine-specific demethylase 3A GN=KDM3A PE=1 SV=4 |
| Q9UK76 | 6 | 154 | 16,0 | 5,60 | 91 | Hematological and neurological expressed 1 protein GN=HN1 PE=1 SV=3 |
| P62754 | 17 | 249 | 28,7 | 10,84 | 91 | 40S ribosomal protein S6 GN=Rps6 PE=1 SV=1 |
| P13521 | 19 | 617 | 70,9 | 4,75 | 91 | Secretogranin-2 GN=SCG2 PE=1 SV=2 |
| O14556 | 18 | 408 | 44,5 | 8,19 | 91 | Glyceraldehyde-3-phosphate dehydrogenase, testis-specific GN=GAPDHS PE=1 SV=2 |
| P13611 | 17 | 3396 | 372,6 | 4,51 | 91 | Versican core protein GN=VCAN PE=1 SV=3 |
| Q03001 | 55 | 7570 | 860,1 | 5,25 | 91 | Dystonin GN=DST PE=1 SV=4 |
| A4FU69 | 28 | 1503 | 173,3 | 5,85 | 90 | EF-hand calcium-binding domain-containing protein 5 GN=EFCAB5 PE=1 SV=2 |
| Q9NY33 | 5 | 737 | 82,5 | 5,10 | 90 | Dipeptidyl peptidase 3 GN=DPP3 PE=1 SV=2 |
| P63001 | 24 | 192 | 21,4 | 8,50 | 90 | Ras-related C3 botulinum toxin substrate 1 GN=Rac1 PE=1 SV=1 |
| O43169 | 3 | 146 | 16,3 | 4,97 | 90 | Cytochrome b5 type B GN=CYB5B PE=1 SV=2 |
| O60239 | 8 | 455 | 50,4 | 4,97 | 90 | SH3 domain-binding protein 5 GN=SH3BP5 PE=1 SV=2 |
| Q70HW3 | 8 | 274 | 29,4 | 9,35 | 90 | S-adenosylmethionine mitochondrial carrier protein GN=SLC25A26 PE=2 SV=1 |
| Q8IZS8 | 8 | 1091 | 122,9 | 5,78 | 90 | Voltage-dependent calcium channel subunit alpha-2/delta-3 GN=CACNA2D3 PE=1 SV |
| Q15437 | 8 | 767 | 86,4 | 6,89 | 90 | Protein transport protein Sec23B GN=SEC23B PE=1 SV=2 |
| P98161 | 29 | 4303 | 462,2 | 6,73 | 90 | Polycystin-1 GN=PKD1 PE=1 SV=3 |
| Q5TDP6 | 8 | 509 | 57,2 | 6,35 | 90 | Lengsin GN=LGSN PE=1 SV=1 |
| Q7RTS7 | 15 | 529 | 57,8 | 7,71 | 90 | Keratin, type II cytoskeletal 74 GN=KRT74 PE=1 SV=2 |
| Q8IZS6 | 3 | 198 | 23,2 | 9,33 | 90 | Tctex1 domain-containing protein 3 GN=TCTE3 PE=1 SV=1 |
| Q96EX2 | 3 | 444 | 48,9 | 7,84 | 90 | RING finger and transmembrane domain-containing protein 2 GN=RNFT2 PE=2 SV=2 |
| O95568 | 18 | 372 | 42,1 | 6,76 | 90 | Histidine protein methyltransferase 1 homolog GN=METTL18 PE=1 SV=1 |
| P56470 | 18 | 323 | 35,9 | 9,16 | 90 | Galectin-4 GN=LGALS4 PE=1 SV=1 |
| Q8N5S1 | 20 | 370 | 40,8 | 9,22 | 90 | Solute carrier family 25 member 41 GN=SLC25A41 PE=2 SV=2 |
| Q8WWI1 | 32 | 1683 | 192,6 | 8,09 | 90 | LIM domain only protein 7 GN=LMO7 PE=1 SV=3 |
| Q9BQL6 | 10 | 677 | 77,4 | 6,28 | 89 | Fermitin family homolog 1 GN=FERMT1 PE=1 SV=1 |
| P12955 | 2 | 493 | 54,5 | 6,00 | 89 | Xaa-Pro dipeptidase GN=PEPD PE=1 SV=3 |
| Q13126 | 7 | 283 | 31,2 | 7,18 | 89 | S-methyl-5'-thioadenosine phosphorylase GN=MTAP PE=1 SV=2 |
| Q56UQ5 | 9 | 140 | 15,8 | 6,19 | 89 | TPT1-like protein PE=1 SV=1 |
| Q3T030 | 3 | 418 | 47,3 | 5,21 | 89 | 26S protease regulatory subunit 6B GN=PSMC4 PE=2 SV=1 |
| Q7Z5L2 | 27 | 792 | 87,8 | 5,12 | 88 | Growth inhibition and differentiation-related protein 88 GN=GIDRP88 PE=2 SV=2 |
| Q5K651 | 27 | 1589 | 184,2 | 7,83 | 88 | Sterile alpha motif domain-containing protein 9 GN=SAMD9 PE=1 SV=1 |
| Q6RI45 | 34 | 1802 | 203,5 | 7,84 | 88 | Bromodomain and WD repeat-containing protein 3 GN=BRWD3 PE=1 SV=2 |
| Q8WWQ0 | 25 | 1821 | 206,6 | 8,85 | 88 | PH-interacting protein GN=PHIP PE=1 SV=2 |
| Q9Y696 | 26 | 253 | 28,8 | 5,59 | 88 | Chloride intracellular channel protein 4 GN=CLIC4 PE=1 SV=4 |
| O14983 | 30 | 1001 | 110,2 | 5,16 | 88 | Sarcoplasmic/endoplasmic reticulum calcium ATPase 1 GN=ATP2A1 PE=1 SV=1 |
| O75955 | 31 | 427 | 47,3 | 7,49 | 88 | Flotillin-1 GN=FLOT1 PE=1 SV=3 |
| P30679 | 27 | 374 | 43,5 | 8,51 | 88 | Guanine nucleotide-binding protein subunit alpha-15 GN=GNA15 PE=2 SV=2 |
| P60879 | 43 | 206 | 23,3 | 4,77 | 88 | Synaptosomal-associated protein 25 GN=Snap25 PE=1 SV=1 |
| Q14254 | 31 | 428 | 47,0 | 5,25 | 88 | Flotillin-2 GN=FLOT2 PE=1 SV=2 |
| Q2TAC6 | 29 | 998 | 111,3 | 8,69 | 88 | Kinesin-like protein KIF19 GN=KIF19 PE=2 SV=2 |
| O00151 | 7 | 329 | 36,0 | 7,02 | 88 | PDZ and LIM domain protein 1 GN=PDLIM1 PE=1 SV=4 |
| O14529 | 33 | 1486 | 161,6 | 5,48 | 88 | Homeobox protein cut-like 2 GN=CUX2 PE=1 SV=4 |
| Q8NGY6 | 17 | 317 | 35,7 | 8,82 | 88 | Olfactory receptor 6N2 GN=OR6N2 PE=1 SV=1 |
| Q8BWY3 | 4 | 437 | 49,0 | 5,71 | 88 | Eukaryotic peptide chain release factor subunit 1 GN=Etf1 PE=1 SV=4 |
| Q8NDA8 | 32 | 1641 | 181,1 | 6,89 | 88 | HEAT repeat-containing protein 7A GN=HEATR7A PE=1 SV=3 |
| Q8NGT2 | 11 | 312 | 34,7 | 8,51 | 87 | Olfactory receptor 13J1 GN=OR13J1 PE=2 SV=1 |
| Q9NVE4 | 245 | 849 | 96,3 | 8,59 | 87 | Coiled-coil domain-containing protein 87 GN=CCDC87 PE=2 SV=2 |
| P15559 | 14 | 274 | 30,8 | 8,88 | 87 | NAD(P)H dehydrogenase [quinone] 1 GN=NQO1 PE=1 SV=1 |
| O00443 | 39 | 1686 | 190,6 | 8,02 | 87 | Phosphatidylinositol-4-phosphate 3-kinase C2 domain-containing subunit alpha GN= |
| P26368 | 9 | 475 | 53,5 | 9,09 | 87 | Splicing factor U2AF 65 kDa subunit GN=U2AF2 PE=1 SV=4 |
| P13674 | 21 | 534 | 61,0 | 6,01 | 86 | Prolyl 4-hydroxylase subunit alpha-1 GN=P4HA1 PE=1 SV=2 |

| | | | | | | |
|---|---|---|---|---|---|---|
| Q6AWC2 | 60 | 1192 | 133,8 | 5,53 | 86 | Protein WWC2 GN=WWC2 PE=1 SV=2 |
| Q9NZM1 | 14 | 2061 | 234,6 | 6,18 | 86 | Myoferlin GN=MYOF PE=1 SV=1 |
| Q96JM2 | 47 | 2506 | 284,5 | 7,58 | 86 | Zinc finger protein 462 GN=ZNF462 PE=1 SV=3 |
| P07602 | 41 | 524 | 58,1 | 5,17 | 86 | Proactivator polypeptide GN=PSAP PE=1 SV=2 |
| Q15323 | 13 | 416 | 47,2 | 4,88 | 85 | Keratin, type I cuticular Ha1 GN=KRT31 PE=2 SV=3 |
| O95816 | 8 | 211 | 23,8 | 6,70 | 85 | BAG family molecular chaperone regulator 2 GN=BAG2 PE=1 SV=1 |
| O14645 | 29 | 258 | 29,6 | 8,50 | 85 | Axonemal dynein light intermediate polypeptide 1 GN=DNALI1 PE=2 SV=2 |
| Q96F24 | 29 | 287 | 32,4 | 5,87 | 85 | Nuclear receptor-binding factor 2 GN=NRBF2 PE=1 SV=1 |
| Q9NZQ7 | 30 | 290 | 33,3 | 7,23 | 85 | Programmed cell death 1 ligand 1 GN=CD274 PE=1 SV=1 |
| Q9Y6Y8 | 10 | 1000 | 111,0 | 5,54 | 85 | SEC23-interacting protein GN=SEC23IP PE=1 SV=1 |
| P16401 | 6 | 226 | 22,6 | 10,92 | 85 | Histone H1.5 GN=HIST1H1B PE=1 SV=3 |
| P46063 | 8 | 649 | 73,4 | 7,88 | 85 | ATP-dependent DNA helicase Q1 GN=RECQL PE=1 SV=3 |
| P61082 | 18 | 183 | 20,9 | 7,69 | 85 | NEDD8-conjugating enzyme Ubc12 GN=Ube2m PE=2 SV=1 |
| Q61411 | 3 | 189 | 21,3 | 5,31 | 85 | GTPase HRas GN=Hras1 PE=1 SV=2 |
| Q5VYK3 | 12 | 1845 | 204,2 | 7,12 | 84 | Proteasome-associated protein ECM29 homolog GN=ECM29 PE=1 SV=2 |
| Q14019 | 4 | 142 | 15,9 | 5,67 | 84 | Coactosin-like protein GN=COTL1 PE=1 SV=3 |
| O43847 | 9 | 1150 | 131,5 | 5,00 | 84 | Nardilysin GN=NRD1 PE=1 SV=2 |
| Q99615 | 7 | 494 | 56,4 | 6,96 | 84 | DnaJ homolog subfamily C member 7 GN=DNAJC7 PE=1 SV=2 |
| P62317 | 16 | 118 | 13,5 | 9,91 | 84 | Small nuclear ribonucleoprotein Sm D2 GN=Snrpd2 PE=2 SV=1 |
| P22492 | 8 | 207 | 22,0 | 11,71 | 84 | Histone H1t GN=HIST1H1T PE=1 SV=4 |
| Q9Y237 | 3 | 131 | 13,8 | 9,77 | 84 | Peptidyl-prolyl cis-trans isomerase NIMA-interacting 4 GN=PIN4 PE=1 SV=1 |
| P20042 | 3 | 333 | 38,4 | 5,80 | 83 | Eukaryotic translation initiation factor 2 subunit 2 GN=EIF2S2 PE=1 SV=2 |
| Q9BPU6 | 15 | 564 | 61,4 | 7,20 | 83 | Dihydropyrimidinase-related protein 5 GN=DPYSL5 PE=1 SV=1 |
| Q96NI8 | 27 | 536 | 62,3 | 8,28 | 83 | Zinc finger protein 570 GN=ZNF570 PE=2 SV=1 |
| Q9NQH7 | 27 | 507 | 57,0 | 6,83 | 83 | Probable Xaa-Pro aminopeptidase 3 GN=XPNPEP3 PE=1 SV=1 |
| Q2VPB7 | 14 | 821 | 87,8 | 5,99 | 83 | Uncharacterized protein DKFZp761E198 GN=PP1030 PE=1 SV=3 |
| P35613 | 17 | 385 | 42,2 | 5,66 | 83 | Basigin GN=BSG PE=1 SV=2 |
| Q29RF7 | 10 | 1337 | 150,7 | 7,91 | 83 | Sister chromatid cohesion protein PDS5 homolog A GN=PDS5A PE=1 SV=1 |
| Q9UJZ1 | 22 | 356 | 38,5 | 7,39 | 83 | Stomatin-like protein 2 GN=STOML2 PE=1 SV=1 |
| Q9UMD9 | 20 | 1497 | 150,3 | 8,79 | 82 | Collagen alpha-1(XVII) chain GN=COL17A1 PE=1 SV=3 |
| Q9NPJ3 | 7 | 140 | 15,0 | 9,14 | 82 | Acyl-coenzyme A thioesterase 13 GN=ACOT13 PE=1 SV=1 |
| P47914 | 5 | 159 | 17,7 | 11,66 | 82 | 60S ribosomal protein L29 GN=RPL29 PE=1 SV=2 |
| Q9NVD7 | 17 | 372 | 42,2 | 5,95 | 82 | Alpha-parvin GN=PARVA PE=1 SV=1 |
| Q0MQA1 | 4 | 116 | 13,5 | 5,99 | 82 | NADH dehydrogenase [ubiquinone] 1 alpha subcomplex subunit 5 OS=Gorilla gorilla g |
| Q9BRL6 | 9 | 282 | 32,3 | 11,72 | 82 | Serine/arginine-rich splicing factor 8 GN=SRSF8 PE=1 SV=1 |
| Q8WUI4 | 29 | 952 | 102,9 | 7,58 | 82 | Histone deacetylase 7 GN=HDAC7 PE=1 SV=2 |
| Q99JI6 | 6 | 184 | 20,8 | 5,78 | 82 | Ras-related protein Rap-1b GN=Rap1b PE=2 SV=2 |
| P09960 | 11 | 611 | 69,2 | 6,18 | 82 | Leukotriene A-4 hydrolase GN=LTA4H PE=1 SV=2 |
| Q01581 | 2 | 520 | 57,3 | 5,41 | 82 | Hydroxymethylglutaryl-CoA synthase, cytoplasmic GN=HMGCS1 PE=1 SV=2 |
| Q96QD8 | 3 | 506 | 56,0 | 8,00 | 82 | Sodium-coupled neutral amino acid transporter 2 GN=SLC38A2 PE=1 SV=2 |
| O95394 | 9 | 542 | 59,8 | 6,25 | 82 | Phosphoacetylglucosamine mutase GN=PGM3 PE=1 SV=1 |
| Q9BY32 | 4 | 194 | 21,4 | 5,66 | 81 | Inosine triphosphate pyrophosphatase GN=ITPA PE=1 SV=2 |
| Q92508 | 30 | 2521 | 286,6 | 7,47 | 81 | Piezo-type mechanosensitive ion channel component 1 GN=PIEZO1 PE=1 SV=4 |
| Q13561 | 10 | 401 | 44,2 | 5,21 | 81 | Dynactin subunit 2 GN=DCTN2 PE=1 SV=4 |
| Q7LBE3 | 6 | 791 | 86,9 | 8,22 | 81 | Solute carrier family 26 member 9 GN=SLC26A9 PE=2 SV=1 |
| Q7Z2Z1 | 32 | 1910 | 210,7 | 8,78 | 81 | Treslin GN=TICRR PE=1 SV=2 |
| Q8TF05 | 11 | 950 | 106,9 | 4,77 | 81 | Serine/threonine-protein phosphatase 4 regulatory subunit 1 GN=PPP4R1 PE=1 SV=1 |
| Q96BR1 | 13 | 496 | 57,1 | 6,93 | 81 | Serine/threonine-protein kinase Sgk3 GN=SGK3 PE=1 SV=1 |
| Q9HBY8 | 8 | 427 | 47,6 | 7,46 | 81 | Serine/threonine-protein kinase Sgk2 GN=SGK2 PE=1 SV=1 |
| Q9P1A2 | 14 | 438 | 49,5 | 5,44 | 81 | Putative serine/threonine-protein phosphatase 4 regulatory subunit 1-like GN=PPP4 |
| O75844 | 14 | 475 | 54,8 | 7,49 | 81 | CAAX prenyl protease 1 homolog GN=ZMPSTE24 PE=1 SV=2 |
| P58743 | 36 | 744 | 81,2 | 6,29 | 81 | Prestin GN=SLC26A5 PE=2 SV=1 |
| P07339 | 4 | 412 | 44,5 | 6,54 | 81 | Cathepsin D GN=CTSD PE=1 SV=1 |
| P83882 | 15 | 106 | 12,4 | 10,58 | 80 | 60S ribosomal protein L36a GN=Rpl36a PE=3 SV=2 |
| P48059 | 10 | 325 | 37,2 | 8,05 | 80 | LIM and senescent cell antigen-like-containing domain protein 1 GN=LIMS1 PE=1 SV= |
| A4D1E1 | 43 | 1349 | 152,5 | 8,54 | 80 | Zinc finger protein 804B GN=ZNF804B PE=1 SV=2 |
| Q2TVT4 | 101 | 97 | 11,1 | 8,76 | 79 | Putative keratinocyte growth factor-like protein 1 GN=KGFLP1 PE=5 SV=1 |
| O00303 | 4 | 357 | 37,5 | 5,45 | 79 | Eukaryotic translation initiation factor 3 subunit F GN=EIF3F PE=1 SV=1 |
| P39656 | 5 | 456 | 50,8 | 6,55 | 79 | Dolichyl-diphosphooligosaccharide--protein glycosyltransferase 48 kDa subunit GN=D |
| Q15125 | 7 | 230 | 26,3 | 7,90 | 79 | 3-beta-hydroxysteroid-Delta(8),Delta(7)-isomerase GN=EBP PE=1 SV=3 |
| Q96L46 | 22 | 248 | 27,6 | 5,73 | 79 | Calpain small subunit 2 GN=CAPNS2 PE=2 SV=2 |
| Q86SI9 | 16 | 138 | 15,1 | 11,41 | 79 | Protein CEI GN=C5orf38 PE=2 SV=1 |
| Q9Y3E0 | 8 | 138 | 15,4 | 10,36 | 79 | Vesicle transport protein GOT1B GN=GOLT1B PE=1 SV=1 |
| P29966 | 3 | 332 | 31,5 | 4,45 | 79 | Myristoylated alanine-rich C-kinase substrate GN=MARCKS PE=1 SV=4 |
| Q9BXJ9 | 8 | 866 | 101,2 | 7,42 | 79 | N-alpha-acetyltransferase 15, NatA auxiliary subunit GN=NAA15 PE=1 SV=1 |

| | | | | | | |
|---|---|---|---|---|---|---|
| P33778 | 10 | 126 | 13,9 | 10,32 | 79 | Histone H2B type 1-B GN=HIST1H2BB PE=1 SV=2 |
| Q9H845 | 7 | 621 | 68,7 | 7,96 | 79 | Acyl-CoA dehydrogenase family member 9, mitochondrial GN=ACAD9 PE=1 SV=1 |
| Q9BV73 | 48 | 2442 | 281,0 | 5,02 | 78 | Centrosome-associated protein CEP250 GN=CEP250 PE=1 SV=2 |
| Q6ZNQ3 | 17 | 347 | 39,6 | 8,57 | 78 | Leucine-rich repeat-containing protein 69 GN=LRRC69 PE=2 SV=2 |
| Q9Y2K7 | 21 | 1162 | 132,7 | 7,58 | 78 | Lysine-specific demethylase 2A GN=KDM2A PE=1 SV=3 |
| Q16740 | 6 | 277 | 30,2 | 8,09 | 78 | Putative ATP-dependent Clp protease proteolytic subunit, mitochondrial GN=CLPP P |
| Q86TM3 | 9 | 631 | 71,1 | 9,07 | 78 | Probable ATP-dependent RNA helicase DDX53 GN=DDX53 PE=1 SV=3 |
| P21580 | 25 | 790 | 89,6 | 8,22 | 77 | Tumor necrosis factor alpha-induced protein 3 GN=TNFAIP3 PE=1 SV=1 |
| Q13200 | 11 | 908 | 100,1 | 5,20 | 77 | 26S proteasome non-ATPase regulatory subunit 2 GN=PSMD2 PE=1 SV=3 |
| Q2PPJ7 | 34 | 1873 | 210,6 | 6,07 | 77 | Ral GTPase-activating protein subunit alpha-2 GN=RALGAPA2 PE=1 SV=2 |
| Q8TDM6 | 32 | 1919 | 213,7 | 7,42 | 77 | Disks large homolog 5 GN=DLG5 PE=1 SV=4 |
| P15328 | 27 | 257 | 29,8 | 7,97 | 77 | Folate receptor alpha GN=FOLR1 PE=1 SV=3 |
| O15511 | 12 | 151 | 16,3 | 5,67 | 77 | Actin-related protein 2/3 complex subunit 5 GN=ARPC5 PE=1 SV=3 |
| O75822 | 5 | 258 | 29,0 | 4,83 | 77 | Eukaryotic translation initiation factor 3 subunit J GN=EIF3J PE=1 SV=2 |
| Q6NSJ2 | 19 | 640 | 71,9 | 6,57 | 77 | Pleckstrin homology-like domain family B member 3 GN=PHLDB3 PE=2 SV=3 |
| Q9Y566 | 15 | 2161 | 224,8 | 8,15 | 77 | SH3 and multiple ankyrin repeat domains protein 1 GN=SHANK1 PE=1 SV=2 |
| Q9Y6E2 | 27 | 419 | 48,1 | 6,68 | 77 | Basic leucine zipper and W2 domain-containing protein 2 GN=BZW2 PE=1 SV=1 |
| Q96M86 | 44 | 4753 | 533,3 | 6,71 | 77 | Dynein heavy chain domain-containing protein 1 GN=DNHD1 PE=1 SV=2 |
| Q99959 | 24 | 881 | 97,4 | 9,33 | 77 | Plakophilin-2 GN=PKP2 PE=1 SV=2 |
| Q9ULW6 | 22 | 460 | 52,5 | 4,49 | 77 | Nucleosome assembly protein 1-like 2 GN=NAP1L2 PE=2 SV=1 |
| Q86UK5 | 39 | 1308 | 147,9 | 6,96 | 77 | Limbin GN=EVC2 PE=1 SV=1 |
| Q9NXH8 | 9 | 423 | 46,9 | 9,94 | 76 | Torsin family protein C9orf167 GN=C9orf167 PE=1 SV=2 |
| P49454 | 61 | 3210 | 367,5 | 5,07 | 76 | Centromere protein F GN=CENPF PE=1 SV=2 |
| O15034 | 23 | 1052 | 116,0 | 5,30 | 76 | RIMS-binding protein 2 GN=RIMBP2 PE=1 SV=3 |
| P10072 | 22 | 659 | 75,1 | 9,25 | 76 | Krueppel-related zinc finger protein 1 GN=HKR1 PE=2 SV=4 |
| P53350 | 23 | 603 | 68,2 | 8,91 | 76 | Serine/threonine-protein kinase PLK1 GN=PLK1 PE=1 SV=1 |
| Q9P055 | 12 | 326 | 36,7 | 7,93 | 75 | JNK1/MAPK8-associated membrane protein GN=JKAMP PE=2 SV=2 |
| Q5E988 | 8 | 204 | 22,9 | 9,72 | 75 | 40S ribosomal protein S5 GN=RPS5 PE=2 SV=3 |
| Q9H4Y5 | 12 | 243 | 28,2 | 7,56 | 75 | Glutathione S-transferase omega-2 GN=GSTO2 PE=2 SV=1 |
| Q6PGP7 | 40 | 1564 | 175,4 | 7,53 | 75 | Tetratricopeptide repeat protein 37 GN=TTC37 PE=1 SV=1 |
| Q0MQC2 | 12 | 156 | 17,4 | 4,93 | 75 | Acyl carrier protein, mitochondrial OS=Gorilla gorilla gorilla GN=NDUFAB1 PE=2 SV=1 |
| A4GXA9 | 26 | 379 | 41,2 | 6,89 | 75 | Probable crossover junction endonuclease EME2 GN=EME2 PE=1 SV=2 |
| P78344 | 33 | 907 | 102,3 | 7,14 | 75 | Eukaryotic translation initiation factor 4 gamma 2 GN=EIF4G2 PE=1 SV=1 |
| P02768 | 5 | 609 | 69,3 | 6,28 | 75 | Serum albumin GN=ALB PE=1 SV=2 |
| O60244 | 18 | 1454 | 160,5 | 8,73 | 75 | Mediator of RNA polymerase II transcription subunit 14 GN=MED14 PE=1 SV=2 |
| O94888 | 11 | 489 | 54,8 | 5,16 | 75 | UBX domain-containing protein 7 GN=UBXN7 PE=1 SV=2 |
| Q04323 | 3 | 297 | 33,3 | 5,25 | 75 | UBX domain-containing protein 1 GN=UBXN1 PE=1 SV=2 |
| Q9Y3A6 | 2 | 229 | 26,0 | 4,84 | 75 | Transmembrane emp24 domain-containing protein 5 GN=TMED5 PE=1 SV=1 |
| Q8WW22 | 15 | 397 | 44,8 | 7,59 | 74 | DnaJ homolog subfamily A member 4 GN=DNAJA4 PE=1 SV=1 |
| P30414 | 22 | 1462 | 165,6 | 9,99 | 74 | NK-tumor recognition protein GN=NKTR PE=1 SV=2 |
| P62918 | 16 | 257 | 28,0 | 11,03 | 74 | 60S ribosomal protein L8 GN=Rpl8 PE=2 SV=2 |
| O60281 | 40 | 2723 | 304,6 | 7,39 | 74 | Zinc finger protein 292 GN=ZNF292 PE=1 SV=3 |
| Q8IVL1 | 31 | 2488 | 268,0 | 9,03 | 74 | Neuron navigator 2 GN=NAV2 PE=1 SV=3 |
| O60673 | 43 | 3130 | 352,6 | 8,47 | 74 | DNA polymerase zeta catalytic subunit GN=REV3L PE=1 SV=2 |
| O95382 | 31 | 1288 | 142,5 | 7,11 | 74 | Mitogen-activated protein kinase kinase kinase 6 GN=MAP3K6 PE=1 SV=3 |
| O95905 | 16 | 644 | 72,7 | 4,87 | 74 | Protein SGT1 GN=ECD PE=1 SV=1 |
| P33764 | 14 | 101 | 11,7 | 4,78 | 74 | Protein S100-A3 GN=S100A3 PE=1 SV=1 |
| P51654 | 15 | 580 | 65,5 | 6,37 | 74 | Glypican-3 GN=GPC3 PE=1 SV=1 |
| Q7Z478 | 25 | 1369 | 155,1 | 8,09 | 74 | ATP-dependent RNA helicase DHX29 GN=DHX29 PE=1 SV=2 |
| Q8NFT6 | 16 | 615 | 67,2 | 8,34 | 74 | Protein DBF4 homolog B GN=DBF4B PE=1 SV=1 |
| Q8TBF8 | 23 | 368 | 42,4 | 8,92 | 74 | Protein FAM81A GN=FAM81A PE=2 SV=3 |
| Q9Y2R2 | 15 | 807 | 91,6 | 7,59 | 74 | Tyrosine-protein phosphatase non-receptor type 22 GN=PTPN22 PE=1 SV=2 |
| P10155 | 3 | 538 | 60,6 | 8,03 | 74 | 60 kDa SS-A/Ro ribonucleoprotein GN=TROVE2 PE=1 SV=2 |
| O43196 | 20 | 834 | 92,8 | 6,37 | 74 | MutS protein homolog 5 GN=MSH5 PE=1 SV=1 |
| O75037 | 34 | 1637 | 182,5 | 7,08 | 74 | Kinesin-like protein KIF21B GN=KIF21B PE=1 SV=2 |
| Q96NT1 | 15 | 182 | 19,6 | 4,21 | 74 | Nucleosome assembly protein 1-like 5 GN=NAP1L5 PE=2 SV=1 |
| Q9NYQ8 | 18 | 4349 | 479,0 | 5,16 | 74 | Protocadherin Fat 2 GN=FAT2 PE=1 SV=2 |
| P51659 | 2 | 736 | 79,6 | 8,84 | 74 | Peroxisomal multifunctional enzyme type 2 GN=HSD17B4 PE=1 SV=3 |
| O00391 | 16 | 747 | 82,5 | 8,92 | 73 | Sulfhydryl oxidase 1 GN=QSOX1 PE=1 SV=3 |
| O94921 | 24 | 469 | 53,0 | 8,92 | 73 | Cyclin-dependent kinase 14 GN=CDK14 PE=1 SV=3 |
| Q13232 | 12 | 169 | 19,0 | 7,84 | 73 | Nucleoside diphosphate kinase 3 GN=NME3 PE=1 SV=2 |
| Q16671 | 13 | 573 | 62,7 | 5,81 | 73 | Anti-Muellerian hormone type-2 receptor GN=AMHR2 PE=1 SV=1 |
| Q59H18 | 28 | 835 | 92,8 | 6,74 | 73 | Serine/threonine-protein kinase TNNI3K GN=TNNI3K PE=1 SV=3 |
| Q92772 | 14 | 493 | 56,0 | 8,21 | 73 | Cyclin-dependent kinase-like 2 GN=CDKL2 PE=2 SV=1 |
| Q9BXT8 | 19 | 1623 | 184,5 | 5,40 | 73 | RING finger protein 17 GN=RNF17 PE=1 SV=3 |

| | | | | | | |
|---|---|---|---|---|---|---|
| Q9H093 | 16 | 628 | 69,6 | 8,87 | 73 | NUAK family SNF1-like kinase 2 GN=NUAK2 PE=1 SV=1 |
| O94913 | 45 | 1555 | 172,9 | 8,48 | 73 | Pre-mRNA cleavage complex 2 protein Pcf11 GN=PCF11 PE=1 SV=3 |
| P19367 | 3 | 917 | 102,4 | 6,80 | 73 | Hexokinase-1 GN=HK1 PE=1 SV=3 |
| Q9P209 | 15 | 647 | 71,7 | 6,52 | 73 | Centrosomal protein of 72 kDa GN=CEP72 PE=1 SV=2 |
| P16520 | 17 | 340 | 37,2 | 5,67 | 73 | Guanine nucleotide-binding protein G(I)/G(S)/G(T) subunit beta-3 GN=GNB3 PE=1 SV |
| Q12907 | 12 | 356 | 40,2 | 6,95 | 73 | Vesicular integral-membrane protein VIP36 GN=LMAN2 PE=1 SV=1 |
| Q13535 | 29 | 2644 | 301,2 | 7,43 | 73 | Serine/threonine-protein kinase ATR GN=ATR PE=1 SV=3 |
| Q8NFI4 | 3 | 369 | 41,4 | 5,05 | 73 | Putative protein FAM10A5 GN=ST13P5 PE=5 SV=1 |
| Q96DM3 | 5 | 657 | 74,9 | 7,83 | 73 | Uncharacterized protein C18orf8 GN=C18orf8 PE=1 SV=2 |
| Q9Y3R5 | 37 | 2298 | 258,1 | 6,29 | 73 | Protein dopey-2 GN=DOPEY2 PE=1 SV=5 |
| A6NCI4 | 28 | 1184 | 133,9 | 8,46 | 73 | von Willebrand factor A domain-containing protein 3A GN=VWA3A PE=2 SV=3 |
| Q8IY92 | 18 | 1834 | 199,9 | 6,06 | 73 | Structure-specific endonuclease subunit SLX4 GN=SLX4 PE=1 SV=3 |
| Q07889 | 16 | 1333 | 152,4 | 6,84 | 73 | Son of sevenless homolog 1 GN=SOS1 PE=1 SV=1 |
| Q14571 | 51 | 2701 | 307,9 | 6,43 | 73 | Inositol 1,4,5-trisphosphate receptor type 2 GN=ITPR2 PE=1 SV=2 |
| Q9P2N5 | 22 | 1060 | 118,6 | 9,19 | 72 | RNA-binding protein 27 GN=RBM27 PE=1 SV=2 |
| Q8TAT6 | 2 | 608 | 68,1 | 6,38 | 72 | Nuclear protein localization protein 4 homolog GN=NPLOC4 PE=1 SV=3 |
| A7E2F4 | 23 | 631 | 70,1 | 6,24 | 72 | Golgin subfamily A member 8A GN=GOLGA8A PE=1 SV=3 |
| Q02978 | 6 | 314 | 34,0 | 9,91 | 72 | Mitochondrial 2-oxoglutarate/malate carrier protein GN=SLC25A11 PE=1 SV=3 |
| P78345 | 27 | 283 | 31,8 | 9,92 | 72 | Ribonuclease P protein subunit p38 GN=RPP38 PE=1 SV=2 |
| Q6P587 | 5 | 224 | 24,8 | 7,39 | 72 | Acylpyruvase FAHD1, mitochondrial GN=FAHD1 PE=1 SV=2 |
| Q96C19 | 11 | 240 | 26,7 | 5,20 | 72 | EF-hand domain-containing protein D2 GN=EFHD2 PE=1 SV=1 |
| Q9BUP0 | 8 | 239 | 26,9 | 5,39 | 72 | EF-hand domain-containing protein D1 GN=EFHD1 PE=1 SV=1 |
| P24941 | 13 | 298 | 33,9 | 8,68 | 72 | Cyclin-dependent kinase 2 GN=CDK2 PE=1 SV=2 |
| Q96DF8 | 17 | 476 | 52,5 | 7,56 | 72 | Protein DGCR14 GN=DGCR14 PE=1 SV=1 |
| Q13576 | 34 | 1575 | 180,5 | 5,64 | 72 | Ras GTPase-activating-like protein IQGAP2 GN=IQGAP2 PE=1 SV=4 |
| O14986 | 10 | 540 | 61,0 | 6,86 | 72 | Phosphatidylinositol-4-phosphate 5-kinase type-1 beta GN=PIP5K1B PE=1 SV=2 |
| O15455 | 12 | 904 | 103,8 | 7,18 | 72 | Toll-like receptor 3 GN=TLR3 PE=1 SV=1 |
| P05412 | 9 | 331 | 35,7 | 8,76 | 72 | Transcription factor AP-1 GN=JUN PE=1 SV=2 |
| P28340 | 14 | 1107 | 123,6 | 7,03 | 72 | DNA polymerase delta catalytic subunit GN=POLD1 PE=1 SV=2 |
| P43268 | 11 | 484 | 53,9 | 5,52 | 72 | ETS translocation variant 4 GN=ETV4 PE=1 SV=3 |
| P60508 | 8 | 538 | 59,5 | 8,85 | 72 | HERV-FRD_6p24.1 provirus ancestral Env polyprotein GN=ERVFRD-1 PE=1 SV=1 |
| Q14142 | 15 | 442 | 49,7 | 7,87 | 72 | Tripartite motif-containing protein 14 GN=TRIM14 PE=2 SV=2 |
| Q75QN2 | 11 | 995 | 113,0 | 7,05 | 72 | Integrator complex subunit 8 GN=INTS8 PE=1 SV=1 |
| Q86Y91 | 12 | 864 | 94,2 | 8,79 | 72 | Kinesin-like protein KIF18B GN=KIF18B PE=1 SV=3 |
| Q9NTI5 | 31 | 1447 | 164,6 | 8,47 | 72 | Sister chromatid cohesion protein PDS5 homolog B GN=PDS5B PE=1 SV=1 |
| Q9Y261 | 10 | 457 | 48,3 | 8,69 | 72 | Hepatocyte nuclear factor 3-beta GN=FOXA2 PE=1 SV=1 |
| Q8IWE2 | 4 | 563 | 60,7 | 4,68 | 72 | Protein NOXP20 GN=FAM114A1 PE=1 SV=2 |
| Q00526 | 22 | 305 | 35,0 | 8,79 | 72 | Cyclin-dependent kinase 3 GN=CDK3 PE=1 SV=1 |
| P49773 | 6 | 126 | 13,8 | 6,95 | 71 | Histidine triad nucleotide-binding protein 1 GN=HINT1 PE=1 SV=2 |
| O95684 | 13 | 399 | 43,0 | 4,81 | 71 | FGFR1 oncogene partner GN=FGFR1OP PE=1 SV=1 |
| Q8NA56 | 13 | 475 | 55,0 | 5,71 | 71 | Tetratricopeptide repeat protein 29 GN=TTC29 PE=2 SV=2 |
| Q8NEY4 | 9 | 427 | 48,7 | 6,14 | 71 | V-type proton ATPase subunit C 2 GN=ATP6V1C2 PE=2 SV=2 |
| Q96BY7 | 22 | 2078 | 232,6 | 5,76 | 71 | Autophagy-related protein 2 homolog B GN=ATG2B PE=1 SV=5 |
| O60282 | 12 | 957 | 109,4 | 6,19 | 71 | Kinesin heavy chain isoform 5C GN=KIF5C PE=1 SV=1 |
| P16870 | 4 | 476 | 53,1 | 5,14 | 71 | Carboxypeptidase E GN=CPE PE=1 SV=1 |
| P55265 | 40 | 1226 | 136,0 | 8,65 | 71 | Double-stranded RNA-specific adenosine deaminase GN=ADAR PE=1 SV=4 |
| P25205 | 4 | 808 | 90,9 | 5,77 | 71 | DNA replication licensing factor MCM3 GN=MCM3 PE=1 SV=3 |
| Q7Z6P3 | 26 | 723 | 77,6 | 4,92 | 71 | Ras-related protein Rab-44 GN=RAB44 PE=3 SV=3 |
| Q9H3S7 | 29 | 1636 | 178,9 | 6,92 | 71 | Tyrosine-protein phosphatase non-receptor type 23 GN=PTPN23 PE=1 SV=1 |
| Q9ULH7 | 21 | 1088 | 118,1 | 6,28 | 71 | MKL/myocardin-like protein 2 GN=MKL2 PE=1 SV=3 |
| Q9BZG1 | 11 | 259 | 29,0 | 7,88 | 71 | Ras-related protein Rab-34 GN=RAB34 PE=1 SV=1 |
| Q9NYY8 | 21 | 710 | 81,4 | 8,05 | 71 | FAST kinase domain-containing protein 2 GN=FASTKD2 PE=1 SV=1 |
| Q9P0L0 | 2 | 249 | 27,9 | 8,62 | 71 | Vesicle-associated membrane protein-associated protein A GN=VAPA PE=1 SV=3 |
| Q6YN16 | 6 | 418 | 45,4 | 7,99 | 70 | Hydroxysteroid dehydrogenase-like protein 2 GN=HSDL2 PE=1 SV=1 |
| P61157 | 3 | 418 | 47,3 | 5,88 | 70 | Actin-related protein 3 GN=ACTR3 PE=1 SV=3 |
| O14827 | 21 | 1237 | 140,7 | 7,53 | 70 | Ras-specific guanine nucleotide-releasing factor 2 GN=RASGRF2 PE=1 SV=2 |
| O95279 | 8 | 499 | 55,1 | 6,74 | 70 | Potassium channel subfamily K member 5 GN=KCNK5 PE=1 SV=1 |
| Q2TB10 | 7 | 664 | 75,2 | 9,47 | 70 | Zinc finger protein 800 GN=ZNF800 PE=1 SV=1 |
| Q8WYA1 | 9 | 636 | 70,8 | 7,37 | 70 | Aryl hydrocarbon receptor nuclear translocator-like protein 2 GN=ARNTL2 PE=1 SV=2 |
| Q96NY7 | 10 | 704 | 73,0 | 4,37 | 70 | Chloride intracellular channel protein 6 GN=CLIC6 PE=2 SV=3 |
| Q9BX26 | 23 | 1530 | 175,5 | 8,85 | 70 | Synaptonemal complex protein 2 GN=SYCP2 PE=2 SV=2 |
| Q9H6X5 | 7 | 657 | 71,3 | 5,78 | 70 | Uncharacterized protein C19orf44 GN=C19orf44 PE=2 SV=1 |
| Q9UJW0 | 5 | 460 | 52,3 | 7,34 | 70 | Dynactin subunit 4 GN=DCTN4 PE=1 SV=1 |
| Q15102 | 11 | 231 | 25,7 | 6,84 | 70 | Platelet-activating factor acetylhydrolase IB subunit gamma GN=PAFAH1B3 PE=1 SV= |
| Q969F9 | 10 | 1004 | 113,7 | 6,43 | 70 | Hermansky-Pudlak syndrome 3 protein GN=HPS3 PE=1 SV=1 |

| | | | | | | |
|---|---|---|---|---|---|---|
| Q13641 | 8 | 420 | 46,0 | 6,83 | 70 | Trophoblast glycoprotein GN=TPBG PE=1 SV=1 |
| P11766 | 6 | 374 | 39,7 | 7,49 | 70 | Alcohol dehydrogenase class-3 GN=ADH5 PE=1 SV=4 |
| O95714 | 52 | 4834 | 526,9 | 6,28 | 70 | E3 ubiquitin-protein ligase HERC2 GN=HERC2 PE=1 SV=2 |
| P36543 | 5 | 226 | 26,1 | 8,00 | 70 | V-type proton ATPase subunit E 1 GN=ATP6V1E1 PE=1 SV=1 |
| P36404 | 4 | 184 | 20,9 | 6,34 | 70 | ADP-ribosylation factor-like protein 2 GN=ARL2 PE=1 SV=4 |
| Q92995 | 2 | 863 | 97,3 | 5,53 | 70 | Ubiquitin carboxyl-terminal hydrolase 13 GN=USP13 PE=1 SV=2 |
| P40939 | 7 | 763 | 82,9 | 9,04 | 70 | Trifunctional enzyme subunit alpha, mitochondrial GN=HADHA PE=1 SV=2 |
| Q99873 | 3 | 361 | 41,5 | 5,43 | 70 | Protein arginine N-methyltransferase 1 GN=PRMT1 PE=1 SV=2 |
| Q9NRG9 | 8 | 546 | 59,5 | 7,50 | 70 | Aladin GN=AAAS PE=1 SV=1 |
| Q6ZR08 | 28 | 3092 | 356,7 | 6,19 | 69 | Dynein heavy chain 12, axonemal GN=DNAH12 PE=1 SV=2 |
| P04183 | 3 | 234 | 25,5 | 8,51 | 69 | Thymidine kinase, cytosolic GN=TK1 PE=1 SV=2 |
| Q29RI6 | 28 | 341 | 39,8 | 6,89 | 69 | Calcium-binding protein 39 GN=CAB39 PE=2 SV=1 |
| O60610 | 6 | 1272 | 141,3 | 5,41 | 69 | Protein diaphanous homolog 1 GN=DIAPH1 PE=1 SV=2 |
| Q9Y3U8 | 3 | 105 | 12,2 | 11,59 | 69 | 60S ribosomal protein L36 GN=RPL36 PE=1 SV=3 |
| P00403 | 12 | 227 | 25,5 | 4,82 | 69 | Cytochrome c oxidase subunit 2 GN=MT-CO2 PE=1 SV=1 |
| P54845 | 22 | 237 | 25,9 | 7,88 | 69 | Neural retina-specific leucine zipper protein GN=NRL PE=1 SV=1 |
| Q9UNX3 | 18 | 145 | 17,2 | 10,55 | 69 | 60S ribosomal protein L26-like 1 GN=RPL26L1 PE=1 SV=1 |
| Q13642 | 7 | 323 | 36,2 | 8,97 | 69 | Four and a half LIM domains protein 1 GN=FHL1 PE=1 SV=4 |
| P05109 | 8 | 93 | 10,8 | 7,03 | 69 | Protein S100-A8 GN=S100A8 PE=1 SV=1 |
| Q8NGA1 | 14 | 313 | 34,8 | 8,91 | 69 | Olfactory receptor 1M1 GN=OR1M1 PE=2 SV=1 |
| P09622 | 3 | 509 | 54,1 | 7,85 | 69 | Dihydrolipoyl dehydrogenase, mitochondrial GN=DLD PE=1 SV=2 |
| P0C221 | 27 | 828 | 97,4 | 5,99 | 69 | Uncharacterized protein C14orf38 GN=C14orf38 PE=2 SV=1 |
| Q96PK2 | 123 | 5938 | 669,7 | 5,30 | 68 | Microtubule-actin cross-linking factor 1, isoform 4 GN=MACF1 PE=1 SV=2 |
| Q6PKX4 | 353 | 331 | 38,3 | 8,48 | 68 | Docking protein 6 GN=DOK6 PE=1 SV=1 |
| Q5T6S3 | 16 | 580 | 65,5 | 8,84 | 68 | PHD finger protein 19 GN=PHF19 PE=1 SV=1 |
| P85298 | 14 | 464 | 53,5 | 9,41 | 68 | Rho GTPase-activating protein 8 GN=ARHGAP8 PE=1 SV=1 |
| Q8IUE6 | 19 | 130 | 14,0 | 10,89 | 68 | Histone H2A type 2-B GN=HIST2H2AB PE=1 SV=3 |
| P29144 | 2 | 1249 | 138,3 | 6,32 | 68 | Tripeptidyl-peptidase 2 GN=TPP2 PE=1 SV=4 |
| Q5T1N1 | 41 | 836 | 92,8 | 6,81 | 68 | Protein AKNAD1 GN=AKNAD1 PE=2 SV=3 |
| Q8NGX9 | 25 | 317 | 35,8 | 8,44 | 68 | Olfactory receptor 6P1 GN=OR6P1 PE=2 SV=1 |
| Q9P2P1 | 31 | 1898 | 208,2 | 8,02 | 68 | Protein NYNRIN GN=NYNRIN PE=1 SV=3 |
| Q8TCT9 | 7 | 377 | 41,5 | 6,43 | 68 | Minor histocompatibility antigen H13 GN=HM13 PE=1 SV=1 |
| Q9UKV3 | 24 | 1341 | 151,8 | 6,43 | 68 | Apoptotic chromatin condensation inducer in the nucleus GN=ACIN1 PE=1 SV=2 |
| P49366 | 7 | 369 | 40,9 | 5,36 | 68 | Deoxyhypusine synthase GN=DHPS PE=1 SV=1 |
| P20839 | 19 | 514 | 55,4 | 6,90 | 68 | Inosine-5'-monophosphate dehydrogenase 1 GN=IMPDH1 PE=1 SV=2 |
| O75368 | 3 | 114 | 12,8 | 5,25 | 67 | SH3 domain-binding glutamic acid-rich-like protein GN=SH3BGRL PE=1 SV=1 |
| O94817 | 16 | 140 | 15,1 | 5,10 | 67 | Ubiquitin-like protein ATG12 GN=ATG12 PE=1 SV=1 |
| Q8TDB6 | 20 | 740 | 83,5 | 8,06 | 67 | E3 ubiquitin-protein ligase DTX3L GN=DTX3L PE=1 SV=1 |
| P11532 | 70 | 3685 | 426,5 | 5,88 | 67 | Dystrophin GN=DMD PE=1 SV=3 |
| Q15717 | 7 | 326 | 36,1 | 9,17 | 67 | ELAV-like protein 1 GN=ELAVL1 PE=1 SV=2 |
| Q99575 | 58 | 1024 | 114,6 | 9,22 | 67 | Ribonucleases P/MRP protein subunit POP1 GN=POP1 PE=1 SV=2 |
| Q3LXA3 | 2 | 575 | 58,9 | 7,49 | 67 | Bifunctional ATP-dependent dihydroxyacetone kinase/FAD-AMP lyase (cyclizing) GN |
| Q7Z5Q5 | 45 | 900 | 100,2 | 8,29 | 67 | DNA polymerase nu GN=POLN PE=1 SV=2 |
| Q5JWR5 | 34 | 2465 | 277,2 | 6,29 | 67 | Protein dopey-1 GN=DOPEY1 PE=1 SV=1 |
| Q68CQ4 | 34 | 756 | 87,0 | 5,88 | 67 | Digestive organ expansion factor homolog GN=DIEXF PE=1 SV=2 |
| Q9Y5K8 | 17 | 247 | 28,2 | 9,36 | 67 | V-type proton ATPase subunit D GN=ATP6V1D PE=1 SV=1 |
| Q2TAZ0 | 20 | 1938 | 212,7 | 5,88 | 67 | Autophagy-related protein 2 homolog A GN=ATG2A PE=1 SV=3 |
| Q96Q15 | 56 | 3661 | 410,2 | 6,46 | 67 | Serine/threonine-protein kinase SMG1 GN=SMG1 PE=1 SV=3 |
| Q15011 | 13 | 391 | 43,7 | 5,25 | 67 | Homocysteine-responsive endoplasmic reticulum-resident ubiquitin-like domain me |
| Q8IVF5 | 32 | 1701 | 190,0 | 7,21 | 67 | T-lymphoma invasion and metastasis-inducing protein 2 GN=TIAM2 PE=2 SV=4 |
| P04070 | 3 | 461 | 52,0 | 6,28 | 66 | Vitamin K-dependent protein C GN=PROC PE=1 SV=1 |
| Q14832 | 13 | 879 | 98,8 | 7,66 | 66 | Metabotropic glutamate receptor 3 GN=GRM3 PE=1 SV=2 |
| Q68DA7 | 9 | 1419 | 157,5 | 8,44 | 66 | Formin-1 GN=FMN1 PE=1 SV=3 |
| P45974 | 7 | 858 | 95,7 | 5,03 | 66 | Ubiquitin carboxyl-terminal hydrolase 5 GN=USP5 PE=1 SV=2 |
| Q9BPX5 | 3 | 153 | 16,9 | 6,60 | 66 | Actin-related protein 2/3 complex subunit 5-like protein GN=ARPC5L PE=1 SV=1 |
| Q86SJ6 | 6 | 1040 | 113,8 | 4,56 | 66 | Desmoglein-4 GN=DSG4 PE=1 SV=1 |
| A6NC57 | 36 | 917 | 106,4 | 6,67 | 66 | Ankyrin repeat domain-containing protein 62 GN=ANKRD62 PE=2 SV=4 |
| Q07864 | 10 | 2286 | 261,4 | 6,39 | 66 | DNA polymerase epsilon catalytic subunit A GN=POLE PE=1 SV=5 |
| Q9H3U1 | 33 | 944 | 103,0 | 6,07 | 66 | Protein unc-45 homolog A GN=UNC45A PE=1 SV=1 |
| A6NKT7 | 61 | 1758 | 197,4 | 6,33 | 66 | RanBP2-like and GRIP domain-containing protein 3 GN=RGPD3 PE=2 SV=2 |
| O14715 | 37 | 1765 | 198,9 | 6,49 | 66 | RANBP2-like and GRIP domain-containing protein 8 GN=RGPD8 PE=1 SV=2 |
| P49792 | 49 | 3224 | 358,0 | 6,20 | 66 | E3 SUMO-protein ligase RanBP2 GN=RANBP2 PE=1 SV=2 |
| Q68DN6 | 48 | 1748 | 196,5 | 6,10 | 66 | RANBP2-like and GRIP domain-containing protein 1/2 GN=RGPD1 PE=1 SV=2 |
| Q7Z3J3 | 58 | 1758 | 197,2 | 6,27 | 66 | RanBP2-like and GRIP domain-containing protein 4 GN=RGPD4 PE=2 SV=3 |
| Q99666 | 36 | 1765 | 198,8 | 6,42 | 66 | RANBP2-like and GRIP domain-containing protein 5/6 GN=RGPD5 PE=1 SV=3 |

| | | | | | | |
|---|---|---|---|---|---|---|
| Q86XX4 | 34 | 4007 | 442,6 | 5,59 | 66 | Extracellular matrix protein FRAS1 GN=FRAS1 PE=2 SV=1 |
| Q1KMD3 | 5 | 747 | 85,1 | 4,91 | 66 | Heterogeneous nuclear ribonucleoprotein U-like protein 2 GN=HNRNPUL2 PE=1 SV=1 |
| Q9UBQ0 | 3 | 182 | 20,5 | 6,79 | 66 | Vacuolar protein sorting-associated protein 29 GN=VPS29 PE=1 SV=1 |
| P51956 | 14 | 506 | 57,7 | 7,17 | 66 | Serine/threonine-protein kinase Nek3 GN=NEK3 PE=1 SV=2 |
| Q9H0K1 | 32 | 926 | 103,8 | 6,02 | 66 | Serine/threonine-protein kinase SIK2 GN=SIK2 PE=1 SV=1 |
| Q13637 | 10 | 225 | 25,0 | 6,54 | 66 | Ras-related protein Rab-32 GN=RAB32 PE=1 SV=3 |
| P81605 | 12 | 110 | 11,3 | 6,54 | 65 | Dermcidin GN=DCD PE=1 SV=2 |
| P61758 | 3 | 197 | 22,6 | 7,11 | 65 | Prefoldin subunit 3 GN=VBP1 PE=1 SV=3 |
| P43246 | 3 | 934 | 104,7 | 5,77 | 65 | DNA mismatch repair protein Msh2 GN=MSH2 PE=1 SV=1 |
| Q9UQ90 | 8 | 795 | 88,2 | 8,69 | 65 | Paraplegin GN=SPG7 PE=1 SV=2 |
| Q08257 | 9 | 329 | 35,2 | 8,44 | 65 | Quinone oxidoreductase GN=CRYZ PE=1 SV=1 |
| P48751 | 23 | 1232 | 135,7 | 6,44 | 65 | Anion exchange protein 3 GN=SLC4A3 PE=1 SV=2 |
| Q93009 | 17 | 1102 | 128,2 | 5,55 | 65 | Ubiquitin carboxyl-terminal hydrolase 7 GN=USP7 PE=1 SV=2 |
| Q9BSL1 | 26 | 405 | 45,3 | 4,92 | 65 | Ubiquitin-associated domain-containing protein 1 GN=UBAC1 PE=1 SV=1 |
| Q9N2K0 | 9 | 584 | 64,3 | 8,25 | 65 | HERV-H_2q24.3 provirus ancestral Env polyprotein PE=2 SV=1 |
| Q5VV41 | 14 | 709 | 80,1 | 7,36 | 65 | Rho guanine nucleotide exchange factor 16 GN=ARHGEF16 PE=1 SV=1 |
| Q9C0B7 | 12 | 1094 | 120,7 | 6,11 | 65 | Transmembrane and coiled-coil domain-containing protein 7 GN=TMCO7 PE=2 SV=2 |
| P16591 | 13 | 822 | 94,6 | 7,14 | 65 | Tyrosine-protein kinase Fer GN=FER PE=1 SV=2 |
| Q9ULM3 | 10 | 1422 | 150,7 | 8,98 | 65 | YEATS domain-containing protein 2 GN=YEATS2 PE=1 SV=2 |
| Q9NS73 | 22 | 344 | 39,3 | 7,24 | 64 | MAP3K12-binding inhibitory protein 1 GN=MBIP PE=1 SV=2 |
| P60229 | 11 | 445 | 52,2 | 6,04 | 64 | Eukaryotic translation initiation factor 3 subunit E GN=Eif3e PE=1 SV=1 |
| Q9HCM7 | 40 | 1045 | 110,8 | 9,67 | 64 | Fibrosin-1-like protein GN=FBRSL1 PE=1 SV=4 |
| Q9H9A6 | 29 | 602 | 68,2 | 6,43 | 64 | Leucine-rich repeat-containing protein 40 GN=LRRC40 PE=1 SV=1 |
| P53384 | 7 | 320 | 34,5 | 5,33 | 64 | Cytosolic Fe-S cluster assembly factor NUBP1 GN=NUBP1 PE=1 SV=2 |
| O43615 | 2 | 452 | 51,3 | 8,32 | 64 | Mitochondrial import inner membrane translocase subunit TIM44 GN=TIMM44 PE=1 S |
| Q9UBQ7 | 2 | 328 | 35,6 | 7,39 | 63 | Glyoxylate reductase/hydroxypyruvate reductase GN=GRHPR PE=1 SV=1 |
| Q8IVV2 | 11 | 1947 | 221,8 | 5,38 | 63 | Lipoxygenase homology domain-containing protein 1 GN=LOXHD1 PE=2 SV=3 |
| Q15024 | 5 | 291 | 31,8 | 5,19 | 63 | Exosome complex component RRP42 GN=EXOSC7 PE=1 SV=3 |
| P49895 | 8 | 249 | 28,9 | 8,69 | 63 | Type I iodothyronine deiodinase GN=DIO1 PE=2 SV=3 |
| Q9UBV8 | 4 | 284 | 30,4 | 6,54 | 63 | Peflin GN=PEF1 PE=1 SV=1 |
| Q13867 | 3 | 455 | 52,5 | 6,27 | 63 | Bleomycin hydrolase GN=BLMH PE=1 SV=1 |
| Q9UIA9 | 11 | 1087 | 123,8 | 6,32 | 63 | Exportin-7 GN=XPO7 PE=1 SV=3 |
| Q9H582 | 23 | 1327 | 149,5 | 8,16 | 63 | Zinc finger protein 644 GN=ZNF644 PE=1 SV=2 |
| Q13526 | 2 | 163 | 18,2 | 8,82 | 62 | Peptidyl-prolyl cis-trans isomerase NIMA-interacting 1 GN=PIN1 PE=1 SV=1 |
| Q9HC10 | 22 | 1997 | 226,6 | 5,69 | 62 | Otoferlin GN=OTOF PE=1 SV=3 |
| Q3SY84 | 12 | 523 | 57,3 | 6,61 | 62 | Keratin, type II cytoskeletal 71 GN=KRT71 PE=1 SV=3 |
| P46060 | 2 | 587 | 63,5 | 4,68 | 62 | Ran GTPase-activating protein 1 GN=RANGAP1 PE=1 SV=1 |
| P22307 | 6 | 547 | 59,0 | 6,89 | 62 | Non-specific lipid-transfer protein GN=SCP2 PE=1 SV=2 |
| Q8WVX9 | 27 | 515 | 59,3 | 9,17 | 61 | Fatty acyl-CoA reductase 1 GN=FAR1 PE=1 SV=1 |
| Q9H936 | 14 | 323 | 34,4 | 9,29 | 61 | Mitochondrial glutamate carrier 1 GN=SLC25A22 PE=1 SV=1 |
| O00571 | 2 | 662 | 73,2 | 7,18 | 61 | ATP-dependent RNA helicase DDX3X GN=DDX3X PE=1 SV=3 |
| P56385 | 2 | 69 | 7,9 | 9,35 | 61 | ATP synthase subunit e, mitochondrial GN=ATP5I PE=1 SV=2 |
| Q3ZCA2 | 5 | 227 | 26,2 | 8,82 | 61 | Cleavage and polyadenylation specificity factor subunit 5 GN=NUDT21 PE=2 SV=1 |
| Q9NZL4 | 2 | 362 | 39,4 | 5,21 | 61 | Hsp70-binding protein 1 GN=HSPBP1 PE=1 SV=1 |
| P62196 | 4 | 406 | 45,6 | 7,55 | 60 | 26S protease regulatory subunit 8 GN=Psmc5 PE=1 SV=1 |
| Q9NQR4 | 4 | 276 | 30,6 | 7,21 | 60 | Omega-amidase NIT2 GN=NIT2 PE=1 SV=1 |
| Q15797 | 38 | 465 | 52,2 | 7,31 | 60 | Mothers against decapentaplegic homolog 1 GN=SMAD1 PE=1 SV=1 |
| Q8NEJ9 | 22 | 315 | 35,9 | 9,57 | 60 | Neuroguidin GN=NGDN PE=1 SV=1 |
| B2RSH2 | 3 | 354 | 40,3 | 5,97 | 60 | Guanine nucleotide-binding protein G(i) subunit alpha-1 GN=Gnai1 PE=2 SV=1 |
| P09471 | 5 | 354 | 40,0 | 5,53 | 60 | Guanine nucleotide-binding protein G(o) subunit alpha GN=GNAO1 PE=1 SV=4 |
| Q03113 | 4 | 381 | 44,3 | 9,83 | 60 | Guanine nucleotide-binding protein subunit alpha-12 GN=GNA12 PE=1 SV=4 |
| Q14344 | 9 | 377 | 44,0 | 8,00 | 60 | Guanine nucleotide-binding protein subunit alpha-13 GN=GNA13 PE=1 SV=2 |
| O95782 | 3 | 977 | 107,5 | 7,03 | 60 | AP-2 complex subunit alpha-1 GN=AP2A1 PE=1 SV=3 |
| Q38SD2 | 22 | 2015 | 225,2 | 6,68 | 59 | Leucine-rich repeat serine/threonine-protein kinase 1 GN=LRRK1 PE=1 SV=3 |
| Q9Y2Z9 | 19 | 468 | 50,8 | 7,30 | 59 | Ubiquinone biosynthesis monooxygenase COQ6 GN=COQ6 PE=1 SV=2 |
| Q99729 | 5 | 332 | 36,2 | 8,21 | 59 | Heterogeneous nuclear ribonucleoprotein A/B GN=HNRNPAB PE=1 SV=2 |
| Q9NQC3 | 5 | 1192 | 129,9 | 4,50 | 59 | Reticulon-4 GN=RTN4 PE=1 SV=2 |
| Q5JQF8 | 3 | 200 | 22,8 | 9,10 | 59 | Polyadenylate-binding protein 1-like 2 GN=PABPC1L2A PE=1 SV=1 |
| O95239 | 109 | 1232 | 139,8 | 6,27 | 59 | Chromosome-associated kinesin KIF4A GN=KIF4A PE=1 SV=3 |
| Q2VIQ3 | 107 | 1234 | 139,9 | 6,18 | 59 | Chromosome-associated kinesin KIF4B GN=KIF4B PE=1 SV=2 |
| P10301 | 9 | 218 | 23,5 | 6,93 | 58 | Ras-related protein R-Ras GN=RRAS PE=1 SV=1 |
| P04844 | 8 | 631 | 69,2 | 5,69 | 58 | Dolichyl-diphosphooligosaccharide--protein glycosyltransferase subunit 2 GN=RPN2 |
| Q13523 | 31 | 1007 | 116,9 | 10,26 | 58 | Serine/threonine-protein kinase PRP4 homolog GN=PRPF4B PE=1 SV=3 |
| P10606 | 4 | 129 | 13,7 | 8,81 | 57 | Cytochrome c oxidase subunit 5B, mitochondrial GN=COX5B PE=1 SV=2 |
| Q9UBT2 | 3 | 640 | 71,2 | 5,29 | 57 | SUMO-activating enzyme subunit 2 GN=UBA2 PE=1 SV=2 |

| | | | | | | |
|---|---|---|---|---|---|---|
| P24844 | 18 | 172 | 19,8 | 4,92 | 57 | Myosin regulatory light polypeptide 9 GN=MYL9 PE=1 SV=4 |
| Q9Y5L0 | 5 | 923 | 104,1 | 5,57 | 57 | Transportin-3 GN=TNPO3 PE=1 SV=3 |
| Q96K30 | 6 | 269 | 28,6 | 11,08 | 56 | RBPJ-interacting and tubulin-associated protein GN=RITA PE=1 SV=1 |
| Q1RMH8 | 1 | 162 | 18,8 | 8,66 | 56 | Sorting nexin-3 GN=SNX3 PE=2 SV=3 |
| P30520 | 8 | 456 | 50,1 | 6,55 | 55 | Adenylosuccinate synthetase isozyme 2 GN=ADSS PE=1 SV=3 |
| Q8IYD1 | 14 | 628 | 68,8 | 5,43 | 54 | Eukaryotic peptide chain release factor GTP-binding subunit ERF3B GN=GSPT2 PE=1 S |
| Q9Y4L1 | 10 | 999 | 111,3 | 5,22 | 54 | Hypoxia up-regulated protein 1 GN=HYOU1 PE=1 SV=1 |
| P52788 | 5 | 366 | 41,2 | 5,02 | 54 | Spermine synthase GN=SMS PE=1 SV=2 |
| Q9P0S9 | 1 | 112 | 11,6 | 9,88 | 54 | Transmembrane protein 14C GN=TMEM14C PE=1 SV=1 |
| P25325 | 2 | 297 | 33,2 | 6,60 | 54 | 3-mercaptopyruvate sulfurtransferase GN=MPST PE=1 SV=3 |
| O95399 | 4 | 124 | 14,3 | 7,80 | 53 | Urotensin-2 GN=UTS2 PE=1 SV=1 |
| Q99456 | 24 | 494 | 53,5 | 4,78 | 52 | Keratin, type I cytoskeletal 12 GN=KRT12 PE=1 SV=1 |
| O43432 | 10 | 1585 | 176,5 | 5,38 | 52 | Eukaryotic translation initiation factor 4 gamma 3 GN=EIF4G3 PE=1 SV=2 |
| P21399 | 5 | 889 | 98,3 | 6,68 | 52 | Cytoplasmic aconitate hydratase GN=ACO1 PE=1 SV=3 |
| Q96M42 | 8 | 142 | 15,2 | 8,00 | 52 | Putative uncharacterized protein encoded by LINC00479 GN=LINC00479 PE=5 SV=2 |
| P30566 | 3 | 484 | 54,9 | 7,11 | 52 | Adenylosuccinate lyase GN=ADSL PE=1 SV=2 |
| P21912 | 26 | 280 | 31,6 | 8,76 | 51 | Succinate dehydrogenase [ubiquinone] iron-sulfur subunit, mitochondrial GN=SDHB |
| O60437 | 44 | 1756 | 204,6 | 5,60 | 51 | Periplakin GN=PPL PE=1 SV=4 |
| P63280 | 3 | 158 | 18,0 | 8,66 | 51 | SUMO-conjugating enzyme UBC9 GN=Ube2i PE=1 SV=1 |
| P11217 | 10 | 842 | 97,0 | 7,03 | 51 | Glycogen phosphorylase, muscle form GN=PYGM PE=1 SV=6 |
| P02489 | 3 | 173 | 19,9 | 6,20 | 50 | Alpha-crystallin A chain GN=CRYAA PE=1 SV=2 |
| P43320 | 1 | 205 | 23,4 | 7,01 | 50 | Beta-crystallin B2 GN=CRYBB2 PE=1 SV=2 |
| O60925 | 4 | 122 | 14,2 | 6,81 | 49 | Prefoldin subunit 1 GN=PFDN1 PE=1 SV=2 |
| P11172 | 3 | 480 | 52,2 | 7,24 | 49 | Uridine 5'-monophosphate synthase GN=UMPS PE=1 SV=1 |
| Q9UBQ5 | 6 | 218 | 25,0 | 4,93 | 49 | Eukaryotic translation initiation factor 3 subunit K GN=EIF3K PE=1 SV=1 |
| Q6ZWH5 | 9 | 1172 | 133,1 | 6,80 | 48 | Serine/threonine-protein kinase Nek10 GN=NEK10 PE=2 SV=2 |
| P16615 | 4 | 1042 | 114,7 | 5,34 | 48 | Sarcoplasmic/endoplasmic reticulum calcium ATPase 2 GN=ATP2A2 PE=1 SV=1 |
| P02545 | 1 | 664 | 74,1 | 7,02 | 48 | Prelamin-A/C GN=LMNA PE=1 SV=1 |
| Q9UNH7 | 4 | 406 | 46,6 | 6,16 | 48 | Sorting nexin-6 GN=SNX6 PE=1 SV=1 |
| P10768 | 5 | 282 | 31,4 | 7,02 | 48 | S-formylglutathione hydrolase GN=ESD PE=1 SV=2 |
| P16083 | 1 | 231 | 25,9 | 6,29 | 48 | Ribosyldihydronicotinamide dehydrogenase [quinone] GN=NQO2 PE=1 SV=5 |
| Q9Y5F7 | 2 | 938 | 101,2 | 5,35 | 48 | Protocadherin gamma-C4 GN=PCDHGC4 PE=1 SV=1 |
| P49591 | 9 | 514 | 58,7 | 6,43 | 48 | Seryl-tRNA synthetase, cytoplasmic GN=SARS PE=1 SV=3 |
| Q9H4M9 | 4 | 534 | 60,6 | 6,83 | 47 | EH domain-containing protein 1 GN=EHD1 PE=1 SV=2 |
| Q9NTN9 | 3 | 838 | 91,4 | 7,84 | 47 | Semaphorin-4G GN=SEMA4G PE=2 SV=1 |
| P68037 | 4 | 154 | 17,9 | 8,51 | 47 | Ubiquitin-conjugating enzyme E2 L3 GN=Ube2l3 PE=2 SV=1 |
| O60884 | 2 | 412 | 45,7 | 6,48 | 47 | DnaJ homolog subfamily A member 2 GN=DNAJA2 PE=1 SV=1 |
| O94979 | 50 | 1220 | 132,9 | 6,89 | 47 | Protein transport protein Sec31A GN=SEC31A PE=1 SV=3 |
| Q14CN4 | 9 | 511 | 55,8 | 6,89 | 47 | Keratin, type II cytoskeletal 72 GN=KRT72 PE=1 SV=2 |
| Q9BU89 | 2 | 302 | 32,9 | 4,83 | 47 | Deoxyhypusine hydroxylase GN=DOHH PE=1 SV=1 |
| P52272 | 2 | 730 | 77,5 | 8,70 | 46 | Heterogeneous nuclear ribonucleoprotein M GN=HNRNPM PE=1 SV=3 |
| O14966 | 17 | 203 | 23,1 | 7,18 | 45 | Ras-related protein Rab-7L1 GN=RAB7L1 PE=1 SV=1 |
| P35462 | 5 | 400 | 44,2 | 8,94 | 45 | D(3) dopamine receptor GN=DRD3 PE=1 SV=2 |
| P04179 | 2 | 222 | 24,7 | 8,25 | 45 | Superoxide dismutase [Mn], mitochondrial GN=SOD2 PE=1 SV=2 |
| Q16222 | 2 | 522 | 58,7 | 6,33 | 45 | UDP-N-acetylhexosamine pyrophosphorylase GN=UAP1 PE=1 SV=3 |
| Q7L014 | 25 | 1031 | 117,3 | 9,29 | 45 | Probable ATP-dependent RNA helicase DDX46 GN=DDX46 PE=1 SV=2 |
| Q13257 | 2 | 205 | 23,5 | 5,08 | 45 | Mitotic spindle assembly checkpoint protein MAD2A GN=MAD2L1 PE=1 SV=1 |
| Q16650 | 14 | 682 | 74,0 | 7,33 | 44 | T-box brain protein 1 GN=TBR1 PE=1 SV=1 |
| P51665 | 1 | 324 | 37,0 | 6,77 | 44 | 26S proteasome non-ATPase regulatory subunit 7 GN=PSMD7 PE=1 SV=2 |
| Q96PD4 | 4 | 163 | 18,0 | 8,90 | 44 | Interleukin-17F GN=IL17F PE=1 SV=3 |
| P62874 | 1 | 340 | 37,4 | 6,00 | 44 | Guanine nucleotide-binding protein G(I)/G(S)/G(T) subunit beta-1 GN=Gnb1 PE=1 SV= |
| Q9C0K3 | 1 | 210 | 23,7 | 5,58 | 44 | Actin-related protein 3C GN=ACTR3C PE=2 SV=1 |
| A6NNC1 | 15 | 897 | 94,0 | 10,26 | 44 | Putative POM121-like protein 1-like PE=5 SV=3 |
| P51531 | 9 | 1590 | 181,2 | 7,20 | 44 | Probable global transcription activator SNF2L2 GN=SMARCA2 PE=1 SV=2 |
| O15523 | 1 | 660 | 73,1 | 7,55 | 44 | ATP-dependent RNA helicase DDX3Y GN=DDX3Y PE=1 SV=2 |
| Q13148 | 3 | 414 | 44,7 | 6,19 | 43 | TAR DNA-binding protein 43 GN=TARDBP PE=1 SV=1 |
| P47929 | 3 | 136 | 15,1 | 7,62 | 43 | Galectin-7 GN=LGALS7 PE=1 SV=2 |
| Q70J99 | 8 | 1090 | 123,2 | 6,65 | 42 | Protein unc-13 homolog D GN=UNC13D PE=1 SV=1 |
| P57729 | 2 | 211 | 23,7 | 7,77 | 42 | Ras-related protein Rab-38 GN=RAB38 PE=1 SV=1 |
| Q6P1M9 | 13 | 558 | 62,3 | 8,73 | 42 | Armadillo repeat-containing X-linked protein 5 GN=ARMCX5 PE=2 SV=1 |
| P00387 | 1 | 301 | 34,2 | 7,59 | 42 | NADH-cytochrome b5 reductase 3 GN=CYB5R3 PE=1 SV=3 |
| Q9UHD9 | 4 | 624 | 65,7 | 5,22 | 41 | Ubiquilin-2 GN=UBQLN2 PE=1 SV=2 |
| Q86TJ2 | 12 | 420 | 48,4 | 7,83 | 41 | Transcriptional adapter 2-beta GN=TADA2B PE=1 SV=2 |
| Q9H7B2 | 1 | 306 | 35,6 | 9,99 | 41 | Ribosome production factor 2 homolog GN=RPF2 PE=1 SV=2 |
| P51451 | 9 | 505 | 57,7 | 7,87 | 41 | Tyrosine-protein kinase Blk GN=BLK PE=1 SV=3 |

| | | | | | | |
|---|---|---|---|---|---|---|
| P61924 | 4 | 177 | 20,2 | 4,81 | 41 | Coatomer subunit zeta-1 GN=Copz1 PE=2 SV=1 |
| Q9BWW9 | 4 | 433 | 47,0 | 9,31 | 41 | Apolipoprotein L5 GN=APOL5 PE=1 SV=1 |
| P23786 | 3 | 658 | 73,7 | 8,18 | 41 | Carnitine O-palmitoyltransferase 2, mitochondrial GN=CPT2 PE=1 SV=2 |
| Q8TDN6 | 3 | 353 | 41,4 | 9,92 | 40 | Ribosome biogenesis protein BRX1 homolog GN=BRIX1 PE=1 SV=2 |
| Q8TEX9 | 2 | 1081 | 118,6 | 4,96 | 40 | Importin-4 GN=IPO4 PE=1 SV=2 |
| Q16822 | 3 | 640 | 70,7 | 7,62 | 40 | Phosphoenolpyruvate carboxykinase [GTP], mitochondrial GN=PCK2 PE=1 SV=3 |
| Q53S58 | 10 | 311 | 33,7 | 9,61 | 40 | Transmembrane protein 177 GN=TMEM177 PE=2 SV=1 |
| Q9P0U1 | 4 | 55 | 6,2 | 10,29 | 40 | Mitochondrial import receptor subunit TOM7 homolog GN=TOMM7 PE=1 SV=1 |
| Q8NBT2 | 3 | 197 | 22,4 | 4,70 | 40 | Kinetochore protein Spc24 GN=SPC24 PE=1 SV=1 |
| P06702 | 6 | 114 | 13,2 | 6,13 | 40 | Protein S100-A9 GN=S100A9 PE=1 SV=1 |
| Q96RT7 | 6 | 1819 | 200,4 | 6,32 | 40 | Gamma-tubulin complex component 6 GN=TUBGCP6 PE=1 SV=3 |
| Q14980 | 15 | 2115 | 238,1 | 5,78 | 40 | Nuclear mitotic apparatus protein 1 GN=NUMA1 PE=1 SV=2 |
| P29992 | 12 | 359 | 42,1 | 5,69 | 40 | Guanine nucleotide-binding protein subunit alpha-11 GN=GNA11 PE=1 SV=2 |
| P35251 | 19 | 1148 | 128,2 | 9,36 | 40 | Replication factor C subunit 1 GN=RFC1 PE=1 SV=4 |
| P11908 | 5 | 318 | 34,7 | 6,61 | 39 | Ribose-phosphate pyrophosphokinase 2 GN=PRPS2 PE=1 SV=2 |
| P21108 | 5 | 318 | 34,8 | 6,35 | 39 | Ribose-phosphate pyrophosphokinase 3 GN=PRPS1L1 PE=1 SV=2 |
| O60218 | 5 | 316 | 36,0 | 7,84 | 39 | Aldo-keto reductase family 1 member B10 GN=AKR1B10 PE=1 SV=2 |
| Q8WYA6 | 38 | 563 | 65,1 | 5,05 | 39 | Beta-catenin-like protein 1 GN=CTNNBL1 PE=1 SV=1 |
| Q9NXG2 | 6 | 353 | 39,3 | 7,88 | 39 | THUMP domain-containing protein 1 GN=THUMPD1 PE=1 SV=2 |
| P49448 | 3 | 558 | 61,4 | 8,46 | 39 | Glutamate dehydrogenase 2, mitochondrial GN=GLUD2 PE=1 SV=2 |
| Q14558 | 3 | 356 | 39,4 | 7,20 | 39 | Phosphoribosyl pyrophosphate synthase-associated protein 1 GN=PRPSAP1 PE=1 SV= |
| O00273 | 18 | 331 | 36,5 | 4,79 | 39 | DNA fragmentation factor subunit alpha GN=DFFA PE=1 SV=1 |
| Q7L1S5 | 8 | 443 | 52,0 | 9,38 | 39 | Carbohydrate sulfotransferase 9 GN=CHST9 PE=2 SV=2 |
| P33947 | 5 | 212 | 24,4 | 8,72 | 39 | ER lumen protein retaining receptor 2 GN=KDELR2 PE=1 SV=1 |
| P12524 | 1 | 364 | 40,3 | 5,66 | 39 | Protein L-Myc-1 GN=MYCL1 PE=1 SV=2 |
| O14764 | 8 | 452 | 50,7 | 8,54 | 39 | Gamma-aminobutyric acid receptor subunit delta GN=GABRD PE=1 SV=2 |
| Q5D0E6 | 6 | 543 | 59,3 | 7,42 | 39 | DALR anticodon-binding domain-containing protein 3 GN=DALRD3 PE=2 SV=2 |
| Q8IVF2 | 48 | 5795 | 616,2 | 5,36 | 39 | Protein AHNAK2 GN=AHNAK2 PE=1 SV=2 |
| P62315 | 2 | 119 | 13,3 | 11,56 | 39 | Small nuclear ribonucleoprotein Sm D1 GN=Snrpd1 PE=2 SV=1 |
| Q14C86 | 11 | 1478 | 164,9 | 5,22 | 39 | GTPase-activating protein and VPS9 domain-containing protein 1 GN=GAPVD1 PE=1 S |
| Q9NP72 | 11 | 206 | 23,0 | 5,24 | 39 | Ras-related protein Rab-18 GN=RAB18 PE=1 SV=1 |
| Q5TZA2 | 6 | 2017 | 228,4 | 5,50 | 39 | Rootletin GN=CROCC PE=1 SV=1 |
| Q9HD20 | 26 | 1204 | 132,9 | 8,13 | 39 | Probable cation-transporting ATPase 13A1 GN=ATP13A1 PE=1 SV=2 |
| C9J1S8 | 8 | 452 | 52,5 | 8,37 | 39 | Tripartite motif-containing protein 49-like protein 1 GN=TRIM49L1 PE=2 SV=1 |
| P0CI26 | 3 | 452 | 52,9 | 7,46 | 39 | Tripartite motif-containing protein 49-like protein 2 GN=TRIM49L2 PE=2 SV=1 |
| P40145 | 7 | 1251 | 140,0 | 6,99 | 39 | Adenylate cyclase type 8 GN=ADCY8 PE=1 SV=1 |
| Q15035 | 2 | 370 | 43,3 | 9,22 | 39 | Translocating chain-associated membrane protein 2 GN=TRAM2 PE=1 SV=1 |
| Q63HK5 | 17 | 1081 | 118,5 | 7,25 | 39 | Teashirt homolog 3 GN=TSHZ3 PE=1 SV=2 |
| Q6ZRF7 | 2 | 136 | 15,5 | 10,23 | 39 | Putative zinc finger protein 818 GN=ZNF818P PE=5 SV=1 |
| Q6ZSZ6 | 10 | 1077 | 117,8 | 7,06 | 39 | Teashirt homolog 1 GN=TSHZ1 PE=2 SV=2 |
| Q86YA3 | 18 | 1062 | 119,3 | 5,02 | 39 | Uncharacterized protein C4orf21 GN=C4orf21 PE=1 SV=2 |
| Q9NRE2 | 3 | 1034 | 114,9 | 7,83 | 39 | Teashirt homolog 2 GN=TSHZ2 PE=1 SV=3 |
| P35637 | 8 | 526 | 53,4 | 9,36 | 39 | RNA-binding protein FUS GN=FUS PE=1 SV=1 |
| Q86SQ0 | 12 | 1253 | 142,1 | 7,43 | 39 | Pleckstrin homology-like domain family B member 2 GN=PHLDB2 PE=1 SV=2 |
| Q13085 | 6 | 2346 | 265,4 | 6,37 | 39 | Acetyl-CoA carboxylase 1 GN=ACACA PE=1 SV=2 |
| Q9NUQ9 | 5 | 324 | 36,7 | 6,06 | 39 | Protein FAM49B GN=FAM49B PE=1 SV=1 |
| Q86SE5 | 14 | 291 | 32,3 | 7,93 | 39 | RNA-binding Raly-like protein GN=RALYL PE=2 SV=2 |
| Q9UKM9 | 7 | 306 | 32,4 | 9,17 | 39 | RNA-binding protein Raly GN=RALY PE=1 SV=1 |
| Q9P1Q0 | 4 | 977 | 110,5 | 6,55 | 38 | Vacuolar protein sorting-associated protein 54 GN=VPS54 PE=1 SV=2 |
| P40261 | 1 | 264 | 29,6 | 5,74 | 38 | Nicotinamide N-methyltransferase GN=NNMT PE=1 SV=1 |
| Q9NZ52 | 3 | 723 | 78,3 | 5,58 | 38 | ADP-ribosylation factor-binding protein GGA3 GN=GGA3 PE=1 SV=1 |
| Q9UJY5 | 1 | 639 | 70,3 | 5,29 | 38 | ADP-ribosylation factor-binding protein GGA1 GN=GGA1 PE=1 SV=1 |
| Q68DK2 | 6 | 2539 | 284,4 | 6,39 | 38 | Zinc finger FYVE domain-containing protein 26 GN=ZFYVE26 PE=1 SV=3 |
| Q96NW7 | 7 | 1537 | 172,5 | 6,81 | 38 | Leucine-rich repeat-containing protein 7 GN=LRRC7 PE=1 SV=1 |
| Q5U649 | 22 | 245 | 27,6 | 7,96 | 38 | Uncharacterized protein C12orf60 GN=C12orf60 PE=2 SV=2 |
| Q15418 | 7 | 735 | 82,7 | 7,83 | 38 | Ribosomal protein S6 kinase alpha-1 GN=RPS6KA1 PE=1 SV=2 |
| Q5JTZ9 | 17 | 985 | 107,3 | 6,27 | 38 | Alanine--tRNA ligase, mitochondrial GN=AARS2 PE=1 SV=1 |
| Q13144 | 2 | 721 | 80,3 | 5,08 | 38 | Translation initiation factor eIF-2B subunit epsilon GN=EIF2B5 PE=1 SV=3 |
| Q8IUZ0 | 19 | 686 | 78,8 | 7,87 | 38 | Leucine-rich repeat-containing protein 49 GN=LRRC49 PE=2 SV=2 |
| Q5HYI8 | 1 | 236 | 26,4 | 7,11 | 38 | Rab-like protein 3 GN=RABL3 PE=1 SV=1 |
| P49643 | 1 | 509 | 58,8 | 7,91 | 38 | DNA primase large subunit GN=PRIM2 PE=1 SV=2 |
| Q8ND04 | 8 | 991 | 109,6 | 7,68 | 38 | Protein SMG8 GN=SMG8 PE=1 SV=1 |
| Q9NVF7 | 4 | 368 | 41,1 | 9,55 | 38 | F-box only protein 28 GN=FBXO28 PE=1 SV=1 |
| Q9Y2G5 | 31 | 429 | 49,9 | 6,60 | 38 | GDP-fucose protein O-fucosyltransferase 2 GN=POFUT2 PE=2 SV=3 |
| Q9NRA8 | 33 | 985 | 108,1 | 8,32 | 38 | Eukaryotic translation initiation factor 4E transporter GN=EIF4ENIF1 PE=1 SV=2 |

| | | | | | | |
|---|---|---|---|---|---|---|
| Q9Y5C1 | 8 | 460 | 53,6 | 6,70 | 38 | Angiopoietin-related protein 3 GN=ANGPTL3 PE=1 SV=1 |
| P36639 | 12 | 197 | 22,5 | 5,27 | 38 | 7,8-dihydro-8-oxoguanine triphosphatase GN=NUDT1 PE=1 SV=3 |
| Q9H4A6 | 5 | 298 | 33,8 | 6,44 | 37 | Golgi phosphoprotein 3 GN=GOLPH3 PE=1 SV=1 |
| P61202 | 4 | 443 | 51,6 | 5,53 | 37 | COP9 signalosome complex subunit 2 GN=Cops2 PE=1 SV=1 |
| Q63HQ2 | 11 | 1017 | 111,2 | 7,40 | 37 | Pikachurin GN=EGFLAM PE=1 SV=2 |
| Q93033 | 8 | 1021 | 115,0 | 6,96 | 37 | Immunoglobulin superfamily member 2 GN=CD101 PE=1 SV=2 |
| Q02809 | 1 | 727 | 83,5 | 6,95 | 37 | Procollagen-lysine,2-oxoglutarate 5-dioxygenase 1 GN=PLOD1 PE=1 SV=2 |
| Q9P0X4 | 8 | 2223 | 244,9 | 6,54 | 37 | Voltage-dependent T-type calcium channel subunit alpha-1I GN=CACNA1I PE=1 SV=1 |
| Q5E9F9 | 2 | 433 | 48,6 | 5,95 | 37 | 26S protease regulatory subunit 7 GN=PSMC2 PE=2 SV=3 |
| Q14498 | 2 | 530 | 59,3 | 10,10 | 37 | RNA-binding protein 39 GN=RBM39 PE=1 SV=2 |
| P83105 | 23 | 476 | 50,9 | 8,02 | 37 | Serine protease HTRA4 GN=HTRA4 PE=2 SV=1 |
| Q00266 | 16 | 395 | 43,6 | 6,29 | 37 | S-adenosylmethionine synthase isoform type-1 GN=MAT1A PE=1 SV=2 |
| Q674X7 | 21 | 775 | 86,3 | 7,03 | 37 | Kazrin GN=KAZN PE=1 SV=2 |
| Q8WUY3 | 38 | 3088 | 340,4 | 4,45 | 37 | Protein prune homolog 2 GN=PRUNE2 PE=1 SV=3 |
| O60344 | 14 | 883 | 99,7 | 5,10 | 37 | Endothelin-converting enzyme 2 GN=ECE2 PE=1 SV=4 |
| P05937 | 25 | 261 | 30,0 | 4,83 | 37 | Calbindin GN=CALB1 PE=1 SV=2 |
| P23508 | 23 | 829 | 93,0 | 5,52 | 37 | Colorectal mutant cancer protein GN=MCC PE=1 SV=2 |
| Q05655 | 21 | 676 | 77,5 | 7,75 | 37 | Protein kinase C delta type GN=PRKCD PE=1 SV=2 |
| Q6JEL2 | 16 | 608 | 68,9 | 5,68 | 37 | Kelch-like protein 10 GN=KLHL10 PE=2 SV=1 |
| Q9Y274 | 15 | 331 | 38,2 | 9,00 | 37 | Type 2 lactosamine alpha-2,3-sialyltransferase GN=ST3GAL6 PE=1 SV=1 |
| Q14012 | 10 | 370 | 41,3 | 5,29 | 37 | Calcium/calmodulin-dependent protein kinase type 1 GN=CAMK1 PE=1 SV=1 |
| O95626 | 5 | 131 | 14,8 | 5,02 | 37 | Acidic leucine-rich nuclear phosphoprotein 32 family member D GN=ANP32D PE=1 SV |
| P00846 | 2 | 226 | 24,8 | 10,10 | 37 | ATP synthase subunit a GN=MT-ATP6 PE=1 SV=1 |
| O43868 | 2 | 658 | 71,9 | 7,94 | 37 | Sodium/nucleoside cotransporter 2 GN=SLC28A2 PE=2 SV=2 |
| Q08AD1 | 12 | 1489 | 168,0 | 6,80 | 37 | Calmodulin-regulated spectrin-associated protein 2 GN=CAMSAP2 PE=1 SV=3 |
| Q10713 | 20 | 525 | 58,2 | 6,92 | 37 | Mitochondrial-processing peptidase subunit alpha GN=PMPCA PE=1 SV=2 |
| P35244 | 2 | 121 | 13,6 | 5,08 | 37 | Replication protein A 14 kDa subunit GN=RPA3 PE=1 SV=1 |
| Q5VT25 | 29 | 1732 | 197,2 | 6,58 | 37 | Serine/threonine-protein kinase MRCK alpha GN=CDC42BPA PE=1 SV=1 |
| Q86SQ7 | 13 | 713 | 82,6 | 5,81 | 37 | Serologically defined colon cancer antigen 8 GN=SDCCAG8 PE=1 SV=1 |
| Q8IV03 | 11 | 231 | 24,6 | 5,14 | 37 | Leucine rich adaptor protein 1-like GN=LURAP1L PE=2 SV=2 |
| Q9P2R7 | 22 | 463 | 50,3 | 7,42 | 37 | Succinyl-CoA ligase [ADP-forming] subunit beta, mitochondrial GN=SUCLA2 PE=1 SV= |
| A6NDN3 | 19 | 693 | 79,9 | 5,50 | 37 | Putative golgin subfamily A member 6B GN=GOLGA6B PE=5 SV=3 |
| Q9BT78 | 9 | 406 | 46,2 | 5,83 | 37 | COP9 signalosome complex subunit 4 GN=COPS4 PE=1 SV=1 |
| P13473 | 3 | 410 | 44,9 | 5,63 | 37 | Lysosome-associated membrane glycoprotein 2 GN=LAMP2 PE=1 SV=2 |
| Q8WVT3 | 8 | 735 | 79,3 | 4,91 | 37 | Trafficking protein particle complex subunit 12 GN=TRAPPC12 PE=1 SV=3 |
| O14530 | 5 | 226 | 26,5 | 5,88 | 36 | Thioredoxin domain-containing protein 9 GN=TXNDC9 PE=1 SV=2 |
| Q9Y3I0 | 21 | 505 | 55,2 | 7,23 | 36 | tRNA-splicing ligase RtcB homolog GN=C22orf28 PE=1 SV=1 |
| P19525 | 4 | 551 | 62,1 | 8,40 | 36 | Interferon-induced, double-stranded RNA-activated protein kinase GN=EIF2AK2 PE= |
| Q9NQW7 | 2 | 623 | 69,9 | 5,67 | 36 | Xaa-Pro aminopeptidase 1 GN=XPNPEP1 PE=1 SV=3 |
| Q13243 | 19 | 272 | 31,2 | 11,59 | 36 | Serine/arginine-rich splicing factor 5 GN=SRSF5 PE=1 SV=1 |
| Q16533 | 24 | 368 | 43,0 | 9,51 | 36 | snRNA-activating protein complex subunit 1 GN=SNAPC1 PE=1 SV=1 |
| Q6P5Q4 | 4 | 547 | 61,6 | 5,78 | 36 | Leiomodin-2 GN=LMOD2 PE=2 SV=2 |
| O94760 | 5 | 285 | 31,1 | 5,81 | 36 | N(G),N(G)-dimethylarginine dimethylaminohydrolase 1 GN=DDAH1 PE=1 SV=3 |
| O00483 | 2 | 81 | 9,4 | 9,38 | 36 | NADH dehydrogenase [ubiquinone] 1 alpha subcomplex subunit 4 GN=NDUFA4 PE=1 |
| A8K979 | 9 | 691 | 77,4 | 8,90 | 36 | ERI1 exoribonuclease 2 GN=ERI2 PE=2 SV=2 |
| A8MTJ3 | 2 | 354 | 40,3 | 6,01 | 36 | Guanine nucleotide-binding protein G(t) subunit alpha-3 GN=GNAT3 PE=2 SV=2 |
| P08754 | 2 | 354 | 40,5 | 5,69 | 36 | Guanine nucleotide-binding protein G(k) subunit alpha GN=GNAI3 PE=1 SV=3 |
| P11488 | 3 | 350 | 40,0 | 5,62 | 36 | Guanine nucleotide-binding protein G(t) subunit alpha-1 GN=GNAT1 PE=1 SV=5 |
| P38405 | 6 | 381 | 44,3 | 6,65 | 36 | Guanine nucleotide-binding protein G(olf) subunit alpha GN=GNAL PE=1 SV=1 |
| Q5JWF2 | 7 | 1037 | 111,0 | 5,03 | 36 | Guanine nucleotide-binding protein G(s) subunit alpha isoforms XLas GN=GNAS PE=1 |
| P12273 | 1 | 146 | 16,6 | 8,05 | 36 | Prolactin-inducible protein GN=PIP PE=1 SV=1 |
| P56199 | 4 | 1179 | 130,8 | 6,29 | 36 | Integrin alpha-1 GN=ITGA1 PE=1 SV=2 |
| Q9NYL9 | 1 | 352 | 39,6 | 5,19 | 36 | Tropomodulin-3 GN=TMOD3 PE=1 SV=1 |
| Q7L576 | 6 | 1253 | 145,1 | 6,90 | 36 | Cytoplasmic FMR1-interacting protein 1 GN=CYFIP1 PE=1 SV=1 |
| Q12797 | 5 | 758 | 85,8 | 5,01 | 36 | Aspartyl/asparaginyl beta-hydroxylase GN=ASPH PE=1 SV=3 |
| Q96CN4 | 38 | 794 | 91,3 | 5,34 | 36 | EVI5-like protein GN=EVI5L PE=1 SV=1 |
| P62911 | 2 | 135 | 15,8 | 11,33 | 36 | 60S ribosomal protein L32 GN=Rpl32 PE=2 SV=2 |
| Q96HE7 | 1 | 468 | 54,4 | 5,68 | 36 | ERO1-like protein alpha GN=ERO1L PE=1 SV=2 |
| O35900 | 1 | 95 | 10,8 | 6,52 | 36 | U6 snRNA-associated Sm-like protein LSm2 GN=Lsm2 PE=2 SV=1 |
| Q96AY3 | 3 | 582 | 64,2 | 5,62 | 36 | Peptidyl-prolyl cis-trans isomerase FKBP10 GN=FKBP10 PE=1 SV=1 |
| O95758 | 8 | 552 | 59,7 | 9,04 | 35 | Regulator of differentiation 1 GN=ROD1 PE=1 SV=2 |
| Q9UKA9 | 11 | 531 | 57,5 | 8,66 | 35 | Polypyrimidine tract-binding protein 2 GN=PTBP2 PE=1 SV=1 |
| O43345 | 21 | 1167 | 134,3 | 9,07 | 35 | Zinc finger protein 208 GN=ZNF208 PE=2 SV=1 |
| Q5JUK3 | 2 | 1230 | 138,3 | 7,52 | 35 | Potassium channel subfamily T member 1 GN=KCNT1 PE=2 SV=2 |
| Q7L5N1 | 3 | 327 | 36,1 | 5,73 | 35 | COP9 signalosome complex subunit 6 GN=COPS6 PE=1 SV=1 |

| | | | | | | |
|---|---|---|---|---|---|---|
| Q32MQ0 | 8 | 723 | 77,3 | 8,18 | 35 | Zinc finger protein 750 GN=ZNF750 PE=1 SV=1 |
| Q9UPQ0 | 12 | 1083 | 121,8 | 6,47 | 35 | LIM and calponin homology domains-containing protein 1 GN=LIMCH1 PE=1 SV=4 |
| P52926 | 1 | 109 | 11,8 | 10,62 | 35 | High mobility group protein HMGI-C GN=HMGA2 PE=1 SV=1 |
| Q8NG31 | 84 | 2342 | 265,2 | 5,47 | 35 | Protein CASC5 GN=CASC5 PE=1 SV=3 |
| P62862 | 3 | 59 | 6,6 | 12,15 | 35 | 40S ribosomal protein S30 GN=Fau PE=3 SV=1 |
| O75208 | 1 | 318 | 35,5 | 5,94 | 35 | Ubiquinone biosynthesis protein COQ9, mitochondrial GN=COQ9 PE=1 SV=1 |
| O75131 | 13 | 537 | 60,1 | 5,85 | 35 | Copine-3 GN=CPNE3 PE=1 SV=1 |
| Q96FN4 | 8 | 548 | 61,2 | 6,07 | 35 | Copine-2 GN=CPNE2 PE=1 SV=3 |

# 14 Eidesstattliche Erklärung

„Hiermit versichere ich, dass ich die vorliegende Arbeit selbstständig verfasst habe. Zur Anfertigung wurden keine anderen als die angegebenen Hilfsmittel verwendet. Die Stellen, die aus anderen Werken wörtlich oder sinngemäß entnommen wurden, sind als solche kenntlich gemacht. Ich versichere weiterhin, dass diese Arbeit in gleicher oder ähnlicher Form noch keiner anderen Prüfungsbehörde vorgelegen hat."

Mainz, den 15.09.2014

Mainz, September 15th 2014